PROCEEDINGS OF THE

SYMPOSIUM

ON

WELDING, BONDING, AND FASTENING

Sponsored By
National Aeronautics and Space Administration
George Washington University
and
The American Society for Metals

MAY 30-31, JUNE 1, 1972 The Williamsburg Colony Williamsburg, Virginia

Compiled By
Bland A. Stein and Dr. John D. Buckley
NASA - Langley Research Center
Hampton, Virginia

SELECTED JOINING TECHNIQUES

The fabrication of advanced complex structures such as those employed in modern transportation vehicles require the use of numerous joints differing widely in nature. Thus it is only appropriate that the session on Selected Joining Techniques encompass a large portion of the joining spectrum. Processes such as weld-bonding, weld-brazing and brazing can be employed to fabricate cost effective and structural efficient hardware using thin-gage materials while electron beam and laser welding can be used to advantage for joining a variety of heavier gage materials. It is therefore the intention of this session to provide information on joining processes which, if judiciously selected, can be used to meet the requirement of todays and tomorrows structures.

Thomas 2. Bales

FOREWORD

The theme of the Symposium on Welding, Bonding, and Fastening was the achievement of lighter, more reliable joining systems by combining the best in new and existing technologies. In the past, many of those directly involved with joining of structural elements often felt that consideration of the capabilities and limitations of joints either came too late or were not adequate during design phases. It is now being recognized that as new materials and structural concepts are developed, joining techniques that are reliable, structurally efficient, and cost effective must be developed concurrently or the potential of the new concepts will not be fulfilled in service. Another past limitation was the type of symposium or conference related to joining technology; these were often limited to one class of joining such as welding or adhesive bonding, or subclasses of them. A significant area of concern within the joining disciplines continues to be the transfer of new and emerging technology.

As the abstract design on the front of these proceedings indicates, the planners of this Symposium believe that the key issue in joining today is the interrelationship of three key technologies: welding, adhesive bonding, and mechanical fastening. The most promising new techniques appear to be combinations of these to produce new joining systems which emerge from and draw on the experience of established technology.

Thus, this Symposium consisted of sessions where the joining methods, combinations of them, and nondestructive evaluation and quality assurance were emphasized. These proceedings are intended to present to the specialist and the manager an overview of recent developments in these disciplines and in various industries. Perhaps more importantly, an overview of new developments in other disciplines which compete for the same joining application is also presented. New joining methods combining two disciplines, such as weld-bonding and weld-brazing are featured.

We would again like to thank all those who participated in or served on the administrative staff of the Symposium on Welding, Bonding, and Fastening. Its success was due to their diligent efforts.

Bland A. Stein

General Chairman

John D. Buckley

Technical Program Chairman

Hampton, Virginia, December 1972

TABLE OF CONTENTS

PRESE	NTATIONS	PAGE
\mathcal{A} .	"Selected Joining Techniques on Overview"	
	T. T. Bales and D. M. Royster NASA Langley Research Center	
	Hampton, Virginia	1 🗸
/z.	"Spot-Weld Bonding on the Blackhawk TM Helicopter" M. J. Salkind Sikorsky Aircraft Division United Aircraft Corporation Stratford, Connecticut	2 ′
<u>3</u> .	"Electron Beam Welding of Aircraft Structures" R. H. Witt Grumman Aerospace Corporation	_
	Bethpage, New York	8 /
· 4.	"The Effect of Weld Stresses on Weld Quality" R. A. Chihoski Martin Marietta Aerospace Denver, Colorado	43
<u>_</u> 5.	"Titanium Honeycomb Structure" R. A. Davis, S. D. Elrod, and D. T. Lovell The Boeing Company Seattle, Washington	65
<i>√</i> 6.	"The Effects of High-Temperature Brazing and Thermal Cycling of the Mechanical Properties of Hastelloy X" D. L. Dicus and J. D. Buckley NASA Langley Research Center Hampton, Virginia	86 V
√ 7•	"Development of the Weldbond Process for Joining Titanuium" D. Fields Lockheed-Georgia Company Marietta, Georgia	109 🗸
8.	"Weld-Brazing - A New Joining Process" T. T. Bales, D. M. Royster, and W. E. Arnold, Jr. NASA Langley Research Center Hampton, Virginia	127

9/	"Thin-Film Diffusion Brazing of Titanium Alloys" E. B. Mekens Northrop Corporation		,
/	Hawthorne, California	149	
10.	"High Power Laser Welding" C. M. Banas United Aircraft Research Laboratories East Hortford Connections	182	
	East Hartford, Connecticut	102	
11.	"Adhesive Bonding Session on Overview" J. E. McCarty The Boeing Company		/
	Seattle, Washington	204	•
_12.	"Adhesive Bonding and the Use of Corrosion Resistant Primers"		
	R. R. Hockridge and H. G. Thibault Re-Entry and Environmental Systems Division		
	General Electric Company Philadelphia, Pennsylvania	206	
13.	"Residual Thermal Stress Control in Composite Reinforced Metal Structures" J. B. Kelly and R. R. June		
	The Boeing Company Seattle, Washington	222	6
14.	"Bonding of Reusable Surface Insulation With Low Density Silicon Foams"		
	A. A. Hiltz, R. R. Hockridge, and F. P. Curtis Re-Entry and Environmental Systems Division		
	General Electric Company	-1.0	
/	Philadelphia, Pennsylvania	248	
15.	"Design of Bonded Joints in Composite Materials" N. Corvelli		
7	Grumman Aerospace Corporation Bethpage, New York	276	w/
16.	"Adhesive and the ATS Satellite" F. E. Hancock		
	Advanced Manufacturing Technology Martin Marietta Corporation		
	Orlando, Florida	280	f

25.	"Welding Techniques" C. R. Manning Ceramic Engineering Department	
	North Carolina State University Raleigh, North Carolina	443 /
26.	"Factors Affecting the Strength of Multipass Low-Alloy Steel Weld Metal" B. M. Kratz	
/	AIRCO Welding Products Murray Hill, New Jersey	444 /
27.	"Extended Electrode Technique" V. D. Schaper and A. Pollack Naval Ship Research and Development Center	/
	Annapolis, Maryland	479
28.	"Electroslag and Electroslag Welding" H. C. Campbell Arcos Corporation	/
/	Philadelphia, Pennsylvania	507
29.	"Advanced Fusion Welding Processes, Solid State Joining and a Successful Marriage" F. R. Miller	
1 -	Air Force Materials Laboratory Wright-Patterson Air Force Base, Ohio	526
30.	"Submerged Arc Welding of Heavy Plate" R. A. Wilson The Lincoln Electric Company	,
,	Cleveland, Ohio	572
31.	"Electroslag Welding of 75 to 100 Ton Ingots" C. R. Manning	
e.	North Carolina State University Raleigh, North Carolina	591
32.	"Nondestructive Evaluation Overview" R. C. Stinebring	
	Re-Entry and Environmental Systems Division General Electric Company	/
	Philadelphia, Pennsylvania	606



127.	"Unique Joining Techniques Overview" R. E. Monroe	•
	Battelle Columbus Laboratories Columbus, Ohio	288
18.	"Stress Wave Riveting" B. P. Lefteris	<i>y</i>
/	Research Department Grummann Aerospace Corporation	000
1 70	Bethpage, New York	289
19.	K. C. Dullea, Jr. Space Division	
	North American Rockwell Downey, California	303
50.	"Small-Scale Explosive Seam Welding" L. J. Bement	•
	NASA Langley Research Center Hampton, Virginia	323 /
ź1.	"Diffusion Bonding of IN718 to VM350 Grade Maraging Steel"	
	S. R. Crosby, R. R. Biederman, and C. C. Reynolds Worcester Polytechnic Institute Worcester, Massachusetts	358
. 22.	"Modern Automotive Joining Techniques Overview"))U
5	P. Wynblatt Ford Motor Company	ý.
	Dearborn, Michigan	385 /
/23.	"Diffusion Bonding and its Application to Manufacturing"	
	W. M. Spurgeon Bendix Research Laboratories Southfield, Michigan	386
24.	"Ultrapulse Welding: A New Technique" D. G. Anderson	
	The Quanta Welding Company Troy, Michigan	421

Ç.

33.	"Special Nondestructive Techniques for Evaluating Space Shuttle Surface Insulation" R. C. Stinebring
/	Re-Entry and Environmental Systems Division General Electric Company Philadelphia, Pennsylvania
<u></u>	"Mossbauer Effect and its Applications in Materials Research" J. J. Singh
	NASA Langley Research Center Hampton, Virginia
35.	"Mechanical Fastening Overview" Jack B. Levy
	Corporate Consulting Service General Electric Company Schenectady, New York
36.	"Trends in Mechanical Fasteners" Jack B. Levy
	Corporate Consulting Service General Electric Company Schenectady, New York
37.	"Titanium Fasteners" J. L. Phillips
	Commercial Airplane Group The Boeing Company Seattle, Washington
38.	"Fastening on the F-14A for Cost Effective Fatigue Resistance" B. H. Beal
/	Grumman Aerospace Corporation Bethpage, New York
39.	"The ALCOA Ram Fastener-A Reuseable Blend Rivet" W. J. Dewalt
	Alcoa Research Laboratories New Kensington, Pennsylvania
40.	"Mechanical Fasteners for 1800° F and Above" T. A. Roach
	Standard Press Steel Company Jenkintown, Pennsylvania







SYMPOSIUM

ON

WELDING, BONDING, AND FASTENING

May 30-31, June 1, 1972

Sponsored by

National Aeronautics and Space Administration

George Washington University

and

The American Society for Metals

Williamsburg, Virginia

THE NATIONAL AERONAUTICS AND SPACE ADMINISTRATION

GEORGE WASHINGTON UNIVERSITY

and

THE AMERICAN SOCIETY FOR METALS

Presents a Symposium on

WELDING, BONDING, AND FASTENING

This Symposium provides a forum for the presentation of technical data pertinent to new joining methods and existing techniques relating to cost effectiveness. The major theme of the Symposium is "Achievement of Lighter More Reliable Joining Systems by Combining the Best Technologies of the Transportation and Construction Industries."

DATES AND PLACE

Tuesday, Wednesday, and Thursday — May 30—June 1, 1972 The Williamsburg Colony — Route 60 Bypass Williamsburg, Virginia 23185

SYMPOSIUM OFFICIALS

General Chairman

Mr. Bland A. Stein NASA Langley Research Center Hampton, Virginia

General Cochairman

Dr. Harold Leibowitz George Washington University Washington, D.C.

Technical Program Chairman

n *Dr. John Buckley* NASA Langley Research Center Hampton, Virginia

Administrative Chairman

Mr. Edward T. Maher NASA Langley Research Center Hampton, Virginia

LADIES PROGRAM — A special tour of Williamsburg will be provided for ladies who might be coming to the Symposium with their husbands. Ladies are also cordially invited to attend the Social Hour and Banquet on Wednesday, May 31, 1972. Cost for the Social Hour and Banquet will be \$13,00.

PROGRAM

TUESDAY, MAY 30, 1972

9:00 a.m.

INTRODUCTORY REMARKS AND ANNOUNCEMENTS

Mr. Bland A. Stein, General Cochairman

WELCOME EXTENDED ON BEHALF OF THE
AMERICAN SOCIETY OF METALS Dr. R. F. Decker
Assistant Director, Paul D. Merica Research Laboratory
The International Nickel Company, Inc.

WELCOME EXTENDED ON BEHALF OF THE NATIONAL AERONAUTICS AND SPACE ADMINISTRATION Dr. John E. Duberg Associate Director, Langley Research Center

TUESDAY, MAY 30, 1972

a.m.

CONCURRENT SESSIONS

SESSION NO. 1

Selected Joining Techniques

COCHAIRMEN Mr. T. T. Bales and Mr. Dick M. Royster
Manufacturing Technology Section
NASA Langley Research Center, Hampton, Virginia

- "Weldbonding Sheetmetal Structures" F. R. Sullivan Lockheed Missiles and Space Company Sunnyvale, California
- 2. "Spot Weld Bonding on the BlackhawkTM Helicopter"

 M. J. Salkind
 Sikorsky Aircraft Division, United Aircraft Corp.
 Stratford, Connecticut
- 3. "Electron Beam Welding of Aircraft Structures"
 R. W. Witt
 Grumman Aerospace Corp.
 Bethpage, New York
- 4. "Electron Beam Welding of High Strength Thermal Resistant Components" G. J. Langford General Dynamics, Convair Division San Diego, California
- 5. "Effect of Weld Stresses on Weld Quality"

R. Chihoski Martin Marietta Corp. Denver, Colorado

SESSION NO. 2

Adhesive Bonding

CHAIRMAN

Head, Advanced Structural Concepts and Stress Methods
and Allowables

The Boeing Company
Seattle, Washington

SESSION NO. 2 - Concluded

- 1. "Adhesive Bonding and the Use of Corrosion Resistant
 Primers" R. R. Hockridge and H. Thibault
 General Electric Company
 Valley Forge Space Center, Pennsylvania
- "Residual Thermal Stress Control in Composite Reinforced Metal Structures"
 R. R. June and J. B. Kelly Commercial Airplane Group, The Boeing Company Seattle, Washington
- "Bonding of Reusable Surface Insulation With Low Density Silicone Foams"
 A. A. Hiltz, R. R. Hockridge, and F. P. Curtis General Electric Company Valley Forge Space Center, Pennsylvania
- 4. "Design of Bonded Joints in Composite Materials"

 N. Corvelli

 Grumman Aerospace Corp.

 Bethpage, New York

TUESDAY, MAY 30, 1972

1:00 p.m.

SESSION NO. 3

Unique Joining Techniques

CHAIRMAN

R. Monroe
Chief Joining Technology
Battelle Columbus Laboratory
Columbus, Ohio

- 1. "Stress Wave Riveting" B. P. Leftheris
 Grumman Aerospace Corp.
 Bethpage, New York
- 2. "The Bi-Composite Transition Joint" K. C. Dullea North American Rockwell Space Division Downey, California
- 3. "Small Scale Explosive Seam Welding"

 L. J. Bement

 NASA Langley Research Center, Hampton, Virginia
- 4. "Diffusion Bonding of IN 718 to 350 Grade Maraging Steel" R. B. Biederman Worcester Polytechnic Institute Worcester, Massachusetts
- 5. "Application of Explosive Welding"

 V. D. Linse and M. Ryan

 Battelle Columbus Laboratory

 Columbus, Ohio

SESSION NO. 4 Modern Automotive Joining Techniques

CHAIRMAN

P. Wynblatt
Research Scientist
Scientific Research Staff
Ford Motor Company
Dearborn, Michigan

- 1. "Laser Welding of Low Carbon Steel"

 R. E. Bisaro, D. J. Schantz, and E. Baarden

 Ford Motor Company

 Dearborn, Michigan
- 2. "Diffusion Bonding and Its Application to Manufacture" W. M. Spurgeon Bendix Research Laboratories Southfield, Michigan
- 3. "Inertia Welding A Reliable and Economic Metal Joining Process" M. R. Calton and C. D. Weiss Production Technology, Inc. Peoria, Illinois
- 4. "Ultra Pulse Welding: A New Joining Technique"

 D. G. Anderson

 Quanta Welding Company

 Troy, Michigan
- 5. "Fluxless Vacuum Brazing of Aluminum"

 H. R. Wiltig, O. W. Swaeg, and R. E. Heise
 Philco Ford Corp.
 Refrigeration Products Div.
 Connorville, Indiana

WEDNESDAY, MAY 31, 1972

9:00 a.m.

SESSION NO. 5

Selected Joining Techniques II

CHAIRMEN

T. T. Bales and D. M. Royster
Manufacturing Technology Section
NASA Langley Research Center
Hampton, Virginia

- 2. "The Effects of High Temperature Brazing and Thermal Cycling on the Mechanical Properties of Hastelloy X" D. L. Dicus and J. D. Buckley NASA Langley Research Center Hampton, Virginia
- 3. "Joining Titanium Using the Weldbond Process"

 D. Fields

 Lockheed-Georgia Company

 Marietta, Georgia

- "Weld-Brazing" T. T. Bales, D. M. Royster, and W. E. Arnold NASA Langley Research Center Hampton, Virginia
- "Thin-Film Diffusion-Brazing of Titanium Alloys"
 E. B. Mikus 5. Northrop Norair Hawthorne, California
- "High Power Laser Welding" -C. M. Banas 6. United Aircraft Research Laboratories East Hartford, Connecticut

SESSION NO. 6

Welding Techniques

C. R. Manning CHAIRMAN Associate Professor, Dept. of Materials Eng. North Carolina State University Raleigh, North Carolina

- 1. "Welding of High Strength Steels" -B. M. Krantz **Airco Welding Products** Murray Hill, New Jersey
- 2. "The Extended Electrode Technique for Welding" V. D. Schaper Department of the Navy Naval Ship Research and Development Laboratory Annapolis, Maryland
- 3. "Electroslag and Electroslag Welding" H. C. Campbell Arcos Corp. Philadelphia, Pennslyvania
- "Advanced Fusion Welding Processes, Solid State Joining and a Successful Marriage" -F. Miller Department of the Air Force Wright-Patterson Air Force Base, Ohio
- 5. "Automatic Arc Welding" -R. A. Wilson Lincoln Electric Company Cleveland, Ohio
- "A New Method of Welding Heavy Ingots by Electro-6. slag Remelting" -C. R. Manning Department of Materials Eng. North Carolina State University Raleigh, North Carolina

WEDNESDAY, MAY 31, 1972

1:00 p.m.

Tours of Langley Research Center and Newport News Shipbuilding and Dry Dock Company.

WEDNESDAY, MAY 31, 1972

6:30 p.m.

Social Hour and Banquet, Jamestown Room, Williamsburg Colony.

Mr. Thomas J. Kelly Speaker: Vice President and Deputy Director Space Shuttle Program, Grumman Aerospace Corp. Bethpage, New York

Subject: "Space Shuttle - Our Next Step in Space"

THURSDAY, JUNE 1, 1972

9:00 a.m.

SESSION NO. 7

Nondestruction Evaluation

CHAIRMAN R. Stinebring Staff Consultant, Nondestructive Engineering General Electric Company

Philadelphia, Pennsylvania

- "Special Nondestructive Techniques for Evaluating 1. Space Shuttle Surface Insulation" — R. Stinebring
 General Electric Company Reentry and Environmental Systems Div. Philadelphia, Pennsylvania
- "The Application of Holography for Materials Evalu-2. T. V. Roszhart and J. R. Bohn ation" Systems Group of TRW, Inc. Redondo Beach, California
- 3. "Application of Holography to Quality Assurance" J. P. Waters United Aircraft Research Laboratories East Hartford, Connecticut
- "Mossbauer Effect and Application in Materials Research" -J. J. Singh NASA Langley Research Center Hampton, Virginia

SESSION NO. 8

Mechanical Fastening

CHAIRMAN J. Levv Corporate Consultant on Mechanical Parts General Electric Company Schenectady, New York

- "Trends in Mechanical Fasteners" -J. B. Levy General Electric Company Schenectady, New York
- 2. "Titanium Fasteners" -J. L. Phillips Commercial Airplane Group, The Boeing Co. Seattle, Washington
- "Preload Loss in Bolted Joint Due to Vibration"
 R. J. Finkelston 3. Standard Pressed Steel Co. Jenkintown, Pennsylvania
- "Fastening on the F-14 for Cost Effective Fatigue Resistance" B. Beal Grumman Aerospace Corp. Bethpage, New York
- 5. "The Alcoa Ram Fastener - A Reusable Blind Rivet" W. J. Dewalt New Kensington, Pennsylvania
- "Fasteners for 1800° F and Above" 6.

Thomas A. Roach Standard Pressed Steel Co. Jenkintown, Pennsylvania



SYMPOSIUM ON WELDING, BONDING, AND FASTENING May 1972 - Williamsburg, Virginia

ATTENDANCE LIST

Mr. Benjamin J. Aleck Advanced Development Grumman Aerospace Corporation Bethpage, NY 11714

Mr. David G. Anderson Director, R & D Quanta Welding Company 1463 Premier Street Troy, MI 48084

Mr. S. T. Andrews Stress Engineer The Boeing Company Vertol Division P.O. Box 16858 Philadelphia, PA 19142

Mr. Thomas T. Bales
Mail Stop 188A
National Aeronautics and
Space Administration
Langley Research Center
Hampton, VA 23365

Mr. Conrad M. Banas Senior Research Engineer United Aircraft Research Labs. United Aircraft Corporation 400 Main Street East Hartford, CT 06108

Mr. Roland Barone Materials Engineer Fairchild Industries, Inc. Republic Division Farmingdale, NY 11735

Mr. Robert M. Baucom
Mail Stop 188A
National Aeronautics and
Space Administration
Langley Research Center
Hampton, VA 23365

Mr. Bernard H. Beal Fastener Specialist Grumman Aerospace Corporation Plant 35 Bethpage, NY 11714

Mr. Laurence J. Bement Mail Stop 498 National Aeronautics and Space Administration Langley Research Center Hampton, VA 23365

Professor Ronald R. Biederman Worcester Polytechnic Institute Worcester, MA 01609

Mr. Jack R. Bohn Manager, Materials Technology TRW Systems One Space Park, 2210/01 Redondo Beach, CA 90278

Mr. Troy G. Brooks
Mail Stop 216
National Aeronautics and
Space Administration
Langley Research Center
Hampton, VA 23365

Mr. Briscoe B. Brown
Mail Stop 335
National Aeronautics and
Space Administration
Langley Research Center
Hampton, VA 23365

Dr. John D. Buckley
Mail Stop 206
National Aeronautics and
Space Administration
Langley Research Center
Hampton, VA 23365

Mr. Marion R. Calton Staff Metallurgist Production Technology, Inc. Peoria, IL 61601 Mr. Hallock C. Campbell Director, Research and Technology ARCOS Corporation 1500 50th Street P.O. Box 5531 Philadelphia, PA 19143

Mr. Arthur G. Capaccio
Business Manager
Grumman Aerospace Corporation
Department 838, Plant 35
Bethpage, NY 11714

Mr. Russell A. Chihoski G0934, Head of Welding Res. Martin Marietta Corporation Box 179 Denver, CO 80201

Mr. Nicholas Corvelli Structural Mechanics Engineer Grumman Aerospace Corporation Plant ^5, Department 589 Bethpage, Long Island, NY 11714

Mr. Stephen R. Crosby Graduate Student Worcester Polytechnic Institute Worcester, MA 01609

Mr. Edward A. Crossley, Jr. Mail Stop 315
National Aeronautics and Space Administration
Langley Research Center
Hampton, VA 23365

Mr. Walter J. Dale
Mail Stop 205
National Aeronautics and
Space Administration
Langley Research Center
Hampton, VA 23365

Mr. John G. Davis, Jr.
Mail Stop 188A
National Aeronautics and
Space Administration
Langley Research Center
Hampton, VA 23365

Mr. Robert A. Davis Chief, New Materials Technology The Boeing Company Box 3707 Seattle, WA 98124

Mr. Jerry W. Deaton
Mail Stop 188A
National Aeronautics and
Space Administration
Langley Research Center
Hampton, VA 23365

Dr. R. F. Decker
Assistant Manager
The International Nickel Company, Inc.
Paul D. Merica Research Lab.
Sterling Forest
Suffern, NY 10901

Mr. Ralph G. Dermott Director, Technology Division American Society for Metals Metals Park, OH 44073

Mr. William R. DeShazor Mail Stop 159 National Aeronautics and Space Administration Langley Research Center Hampton, VA 23365

Mr. William J. Dewalt Research Engineer Alcoa Research Laboratories P.O. Box 772 New Kensington, PA 15068

Mr. Walter S. DeWolf Senior Engineer Specialist Philco-Ford 3900 Welsh Road Willow Grove, PA 19090

Mr. H. Benson Dexter
Mail Stop 188A
National Aeronautics and
Space Administration
Langley Research Center
Hampton, VA 23365

Mr. Dennis L. Dicus
Mail Stop 206
National Aeronautics and
Space Administration
Langley Research Center
Hampton, VA 23365

Dr. John E. Duberg
Mail Stop 103
National Aeronautics and
Space Administration
Langley Research Center
Hampton, VA 23365

Mr. Kenneth C. Dullea, Jr.
Member of the Technical Staff
North American Rockwell Corporation
Space Division
12214 Lakewood Boulevard
Mail Code: FB80
Downey, CA 90241

Mr. Ch rles P. Eichelberger, Jr.
Mail Stop 334
National Aeronautics and
Space Administration
Langley Research Center
Hampton, VA 23365

Mr. J as E. Enghauser Supervisor, Metallurgical Dev. DELCO Moraine Division General Motors Corporation 1420 Wisconsin Boulevard Dayton, OH 45402

Mr. Victor J. Erdeman Senior Engineer Eastern Air Lines, Inc. Power Plant Engineering Miami International Airport Miami, FL 33148

Mr. Dallas Fields D/42-11, Zone 102 MFG Research Eng. Sr. Lockheed Georgia Company Lockheed Aircraft Corporation 86 S. Cobb Drive Marietta, GA 30060 Mr. Robert J. Finkelston Mechanical Research Engineer Standard Pressed Steel Company Jenkintown, PA 19046

Mr. Philip H. Glaude
Mail Stop 205
National Aeronautics and
Space Administration
Langley Research Center
Hampton, VA 23365

Mr. Sheldon Glucksman
Project Engineer
American Airlines
Maintenance and Engineering Center
3800 N. Mingo Road
Tulsa, OK 74151

Dr. Ross L. Goble
Mail Stop 184
National Aeronautics and
Space Administration
Langley Research Center
Hampton, VA 23365

Mr. Robert E. Grandle
Mail Stop 239
National Aeronautics and
Space Administration
Langley Research Center
Hampton, VA 23365

Mr. Frank E. Hancock Senior Materials Engineer Martin Martietta Corporation Box 5837 Orlando, FL 32805

Mr. Carl Hanson
Local Representative
McDonnell Douglas Corporation
2013 Cunningham Drive
Hampton, VA 23366

Mr. Kenneth D. Hedgepeth Mail Stop 237 National Aeronautics and Space Administration Langley Research Center Hampton, VA 23365 Mr. Robert Heise Chief Metallurgist Philco-Ford State Road 1 Connersville, IN 47331

Mr. Harry K. Herr Project Director Reynolds Metals Company P.O. Box 27003 Richmond, VA 23261

Mr. Harvey W. Herring
Mail Stop 188A
National Aeronautics and
Space Administration
Langley Research Center
Hampton, VA 23365

Mr. Ralph R. Hockridge Supv. Engineer General Electric Company - RESD VFSTC RV V-7026 P.O. Box 8555 Philadelphia, PA 19101

Mr. Edward L. Hoffman
Mail Stop 188A
N rional Aeronautics and
Space Administration
Langley Research Center
Hampton, VA 23365

Mr. Kenneth H. Holko
Mail Stop 105-1
National Aeronautics and
Space Administration
Lewis Research Center
2100 Brookpark Road
Cleveland, OH 44135

Mr. Leon B. Holt
Mail Stop 199
National Aeronautics and
Space Administration
Langley Research Center
Hampton, VA 23365

Mr. George W. Ivey, Jr. Mail Stop 317 National Aeronautics and Space Administration Langley Research Center Hampton, VA 23365

Mr. Charles E. Johnson Mail Stop 205 National Aeronautics and Space Administration Langley Research Center Hampton, VA 23365

Mr. Larry E. Jones Quality Control Engineer Newport News Shipbuilding and Dry Dock Company Washington Avenue Newport News, VA 23607

Mr. Reid June The Boeing Company Box 3707 Seattle, WA 98124

Mr. W. R. Kanne, Jr. Metallurgist
E. I. DuPont Company
Savannah River Plant
Aiken, SC 29801

Mr. Fred W. Kear Aircraft Project Engineer Piedmont Airlines Smith Reynolds Airport Winston Salem, NC 27101

Mr. Robert E. Keith Associate Professor Pennsylvania State University Department of Industrial Engineering 207 Hammond Building University Park, PA 16802

Mr. Thomas P. Kelly
Mail Stop 205
National Aeronautics and
Space Administration
Langley Research Center
Hampton, VA 23365

Mr. Cecil E. Kirby
Mail Stop 317
National Aeronautics and
Space Administration
Langley Research Center
Hampton, VA 23365

Dr. Boris M. Krantz Manager, Metallurgical Dev. AIRCO Welding Products Murray Hill, NJ 07971

Mr. Gerald J. Langford Group Engineer Convair Aerospace San Di 30, CA 91112

Mr. Ashby G. Lawson
Mail Stop 216
National Aeronautics and
Space Administration
angl∈ Research Center
Hampte, VA 23365

Mr. Basil P. Leftheris Research Grumman Aerospace Corporation Bethpage, NY 11714

Mr. Lawrence Levine
Director, Langley Operations
Grumman Aerospace Corporation
11 Towne Square Drive
Newport News, VA 23607

Mr. Jack B. Levy Consultant, Parts and Finishes General Electric Company 1 River Road, Building 36-413 Schenectady, NY 12345 Dean Harold Liebowitz
Dean of School of Engineering
George Washington University
Washington, DC 20006

Mr. Chester C. Linkenhoker, Jr. Welding Instructor Peninsula VO-Tech 50th and E Streets Hampton, VA 23361

Mr. Vonne D. Linse Senior Research Engineer Battelle Columbus Laboratories 505 King Avenue Columbus, OH 43201

Mr. W. Barry Lisagor Mail Stop 188A National Aeronautics and Space Administration Langley Research Center Hampton, VA 23365

Mr. Robert T. Magee
Mail Stop 159
National Aeronautics and
Space Administration
Langley Research Center
Hampton, VA 23365

Mr. Edward T. Maher Mail Stop 115 National Aeronautics and Space Administration Langley Research Center Hampton, VA 23365

Mr. Joseph Maltz Code RWM National Aeronautics and Space Administration Washington, DC 20456

Professor Charles R. Manning North Carolina State University 210 Page Hall Raleigh, NC 27607 Mr. James R. Mansfield Manager, Product Marketing Hamilton-Standard Windsor Locks, CT 06096

Mr. Eldon E. Mathauser
Mail Stop 188A
National Aeronautics and
Space Administration
Langley Research Center
Hampton, VA 23365

Mr. John E. McCarty The Boeing Company Renton, WA 98055

Mr. A. R. McMillan Section Engineer General Motors, Manufacturing Staff General Motors Technical Center Warren, MI 48094

Mr. D. L. Mehl Lab. Associate IBM 740 New Circle Road Lexington, KY 40507

Mr. Ernie B. Mikus Manage, Materials Research Northrop Corporation 3901 West Broadway Hawthorne, CA 90250

Mr. Frederick R. Miller Senior Project Manager A. F. Materials Lab. Manufacturing Technology Division (AFML/LTP) Wright-Patterson AFB, OH 45433

Mr. Robert E. Monroe Chief, Joining Technology Division Battelle Columbus Labs. 505 King Avenue Columbus, OH 43201 Mr. Lester J. Noble Materiel Treatment Specialist Naval Ship Engineering Center NAVSECPHILADIV 6765 Navy Department, Building 633 Philadelphia, PA 19112

Mr. Carl R. Osman
Research Engineer
Newport News Shipbuilding
and Dry Dock Company
Materials Engineering Department 007
Newport News, VA 23607

Dr. William A. Owczarski
Technical Supervisor
Materials Engineering and
Research Lab.
Pratt & Whitney Aircraft
Division of United Aircraft Corporation
400 Main Street
East Hartford, CT 06108

Mr. Joseph L. Phillips
Research Engineer
Manufacturing Research, Comm.
Airplane Group
The Boeing Company
Seattle, WA 98124

Mr. James E. Pleasants
Mail Stop 334
National Aeronautics and
Space Administration
Langley Research Center
Hampton, VA 23365

Mr. Edwin H. Polk Engineer LTV Aerospace Corporation 3221 N. Armistead Avenue Hampton, VA 23366

Mr. Richard A. Pride
Mail Stop 188A
National Aeronautics and
Space Administration
Langley Research Center
Hampton, VA 23365

Mr. Donald J. Progar
Mail Stop 226
National Aeronautics and
Space Administration
Langley Research Center
Hampton, VA 23365

Mr. Thomas A. Roach Manager, Materials Research Standard Pressed Steel Company Highland Avenue Jenkintown, PA 19046

Mr. Terry Roszhart Program Manager TRW Systems One Space Park Rędondo Beach, CA 90278

Mr. Dick M. Royster
Mail Stop 188A
National Aeronautics and
Space Administration
Langley Research Center
Hampton, VA 23365

Mr. Carl E. Rucker
Mail Stop 239
Notion of Aeronautics and Space Administration
Langley Research Center
Hampton, VA 23365

Mr. Donald R. Rummler
Mail Stop 188A
National Aeronautics and
Space Administration
Langley Research Center
Hampton, VA 23365

Dr. Michael J. Salkind Chief, Structures and Materials Sikorsky Aircraft Division of United Aircraft Corporation Stratford, CT 06470 Mr. Vincent D. Schaper Metallurgist Department of the Navy Naval Ship R & D Center/ANAA Code 2821 Annapolis, MD 21402

Dr. Jag J. Singh
Mail Stop 235
National Aeronautics and
Space Administration
Langley Research Center
Hampton, VA 23365

Dr. William M. Spurgeon Manager, Materials and Processes Department Bendix Research Labs. Bendix Center Southfield, MI 48076

Mr. Bland A. Stein
Mail Stop 188A
National Aeronautics and
Space Administration
Langley Research Center
Hampton, VA 23365

Mr. R. C. Stinebring Consulting Engineer General Electric Philadelphia, PA 19101

Mr. Victor Strautman
Manager, Process Tech. Lab.
AVCO Corporation
Lycoming Division
500 South Main Street
Stratford, CT 06497

Mr. Fletcher R. Sullivan Research Specialist Manufacturing Research Lockheed Missiles and Space Company, Inc. P.O. Box 504 Sunnyvale, CA 94088 Mr. Ian Taylor Research Engineer ITT, ALCAN International, Ltd. Research Centre Kingston P.O. Box 830C Kingston, Ontario, Canada

Mr. Lewis B. Thurston, Jr. Mail Stop 188A
National Aeronautics and
Space Administration
Langley Research Center
Hampton, VA 23365

Mr. Charles C. Troha

Program Manager - Titanium Technology
Department of Transportation
Federal Aviation Agency - AST-100
800 Independence Avenue, S.W.
Washington, DC 20591

Mr. G. B. Wadsworth
Group Engineer
Metals and Standards
The Boeing Company
Materials Technology/Metals
and Standards
3801 South Oliver, M/S K16-39
Wichita, KS 67210

Mr. George D. Ware
Mail Stop 251
National Aeronautics and
Space Administration
Langley Research Center
Hampton, VA 23365

Mr. James P. Waters Senior Research Engineer United Aircraft Research Lab. East Hartford, CT 06601

Mr. Granville L. Webb Mail Stop 159 National Aeronautics and Space Administration Langley Research Center Hampton, VA 23365 Mr. Stuart Weiss Senior Manufacturing R&D Engineer Hamilton Standard Division of United Aircraft Corporation Mail Stop No. 1-1-12 Windsor Locks, CT 06096

Mr. Jack Wert Program Manager, Aluminum Brazing ABAR Corporation 905 Pennsylvania Boulevard Feasterville, PA 19047

Mr. John K. White Westinghouse Research Pittsburgh, PA 15235

Mr. Gregory R. Wichorek Mail Stop 188A National Aeronautics and Space Administration Langley Research Center Hampton, VA 23365

Mr. Thomas L. Wilkinson Senior Development Engineer Reynolds Metals Company 1519 Summit Avenue Richmond, VA 23218

Mr. L. Edward Williams
Mail Stop 159
National Aeronautics and
Space Administration
Langley Research Center
Hampton, VA 23365

Mr. R. A. Wilson Vice President, Application Engineer Lincoln Electric Company 22801 Saint Clair Avenue Cleveland, OH 44106

Mr. Robert H. Witt Group Leader Grumman Aerospace Corporation Plant 12, Department 447 Bethpage, NY 11714 Dr. James S. Wolf Associate Professor - Mat. Engr. Clemson University College of Engineering - DIS Clemson, SC 29631

James F. Wood
Director of Engineering
Piedmont Airllines
Smith Reynolds Airport
Winston Salem, NC 27101

Mr. Paul Wynblatt Research Scientist Ford Motor Company P.O. Box 2053 Dearborn, MI 48121

Mr. Daniel S. Zamborsky Corporate Metallurgist The Warner & Swasey Company Cleveland Turning Machine Division 5701 Carnegie Avenue Cleveland, OH 44103

N74 30923

SPOT-WELD BONDING ON THE BLACKHAWK TM HELICOPTER

by

Michael J. Salkind, PhD. Chief, Structures and Materials

Sikorsky Aircraft Division of United Aircraft Corporation Stratford, Connecticut 06602

NASA, GWU, ASM SYMPOSIUM ON WELDING, BONDING AND FASTENING Williamsburg, Virginia

May 1972

The Sikorsky S-67 BlackhawkTM attack helicopter utilizes spot-weld bonding for stringer to skin attachment on more than 5 per cent of its surface area. The aircraft, seen in Figure 1, was first flown in 1970 and presently holds the absolute speed record for a helicopter. It is the first American aircraft to utilize spot-weld bonding, although the process has been used for some years in the USSR for the AN-24 and the AN-22 aircraft (Reference (1)). In addition, spot-weld bonding (also known as glue-welding, weld-bonding, and glue spot-welding) has been extensively investigated by Lockheed Aircraft under Air Force Materials Labs' sponsorship for fuselage structures and is used in production for missile tankage (References (2) and (3)). The process consists of applying adhesive on the surfaces to be joined, spot welding through the adhesive, then curing the adhesive.

Prior to incorporation into production on the S-67 in 1970, Sikorsky spent eight years developing and evaluating spot-weld bonding on 6061, 2024, and 7075 aluminum alloy components. Techniques were developed for joining two, three, and four layers of material which ranged in thickness from 0.020 to 0.110 inches. Materials of differing thicknesses were also joined.

The adhesives which were evaluated included FM-1000 film, XB-66 film, Epon 6 paste, AF-6 film, and 2214 paste. The film adhesives were found to be impractical because spot welds could not be made consistently. This was due to a large extent to the carrier. Both paste adhesives were successful, but 2214 was chosen for the S-67 because of its higher strength.

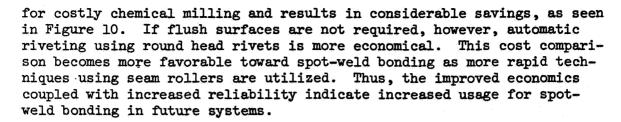
Prior to cleaning, the assemblies were prefit to assure good bonding contact between details. As the surface preparation for spot welding is different from that for adhesive bonding, it was necessary to determine which was the more critical. Because the spot-weld quality is highly dependent on the surface eletrical resistance, it was determined that the surface preparation would be determined primarily by the requirements for spot welding. The process used for Alclad aluminum sheet is depicted in Figure 2 with that for bare aluminum sheet being somewhat modified. The adhesive was applied to a thickness of 0.004 inches by using either an impregnated felt roller or by using a squeegee with tape dams of the appropriate thickness as is depicted in Figure 3. The parts were then assembled using Clico clips and spot welded as seen in Figure 4. After spot welding, the tape was removed and the adhesive oven cured.

Extensive testing was conducted using both coupons and panels in tension, shear, combined shear-compression, and fatigue in order to qualify the process. The static tensile strength, depicted in Figure 5, is considerably higher than that of the riveted construction which it replaced. It should be noted that the primary contributor to the increased strength is the adhesive bond, not the spot-weld, as comparative tests of riveted-bonded and spot-welded construction seen in Figure 5 indicate. The fatigue behavior of spot-weld bonded coupons compared with other constructions is summarized in Figure 6. Note that although spot-welding alone is poor in fatigue, the adhesive bond substantially improves this behavior.

An additional advantage of spot-weld bonding over conventional riveting was noted during combined shear-compression testing of panels. Because the panel skin is stabilized over the whole bonded area, there is less area of unsupported skin between stringers. This allows much higher loads to be achieved before skin buckling occurs.

The application of spot-weld bonding on the S-67 is seen in Figure 1. The process was limited to those applications shown because it was introduced late in the development of that aircraft. Nearly flat panels, such as the access door seen in Figure 7, the pilot's canopy glare shield, and several fairings were readily fabricated using spotweld bonding. More complex structures such as the vertical stabilizer trailing edge seen in Figure 8 and leading edge seen in Figure 9 required unique tooling to accomplish the spot welds.

In addition to the improved properties afforded by spot-weld bonding, a major motivation for developing the process was cost reduction. For structures having light gage skins, where there is a requirement for a flush aerodynamic surface, thicker gages are often used to accommodate countersinking, and the majority of the skin area is chemically milled to the required thickness. For such applications, spot-weld bonding of the required finished thickness precludes the requirement



REFERENCES

- 1.) A. Dobler, H. Koenigsberg, and D. Van Winkle, <u>SAE Journal</u>, Vol. 78, No. 3, Mar. 1970, pp. 56-61.
- 2.) F. Ridgeway, American Machinist, April 20, 1970, pp. 92-94.
- 3.) F. Sullivan, G. Faulkner, and F. Clauss, <u>Materials Eng.</u>, Jan. 1971, pp. 14-15.

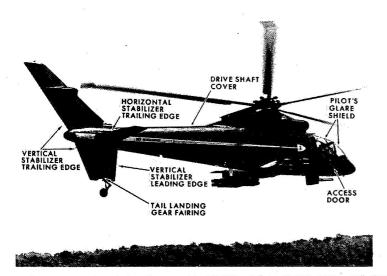


FIGURE 1. APPLICATIONS OF SPOT-WELD BONDING ON THE S-67 BLACKHAWK $^{\mathrm{TM}}$ ATTACK HELICOPTER

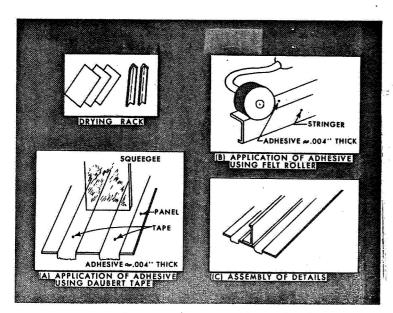


FIGURE 3. ADHESIVE APPLICATION

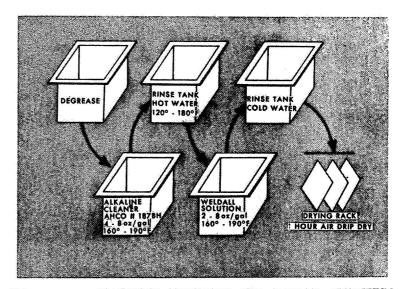


FIGURE 2. CLEANING SEQUENCE FOR ALCLAD ALUMINUM

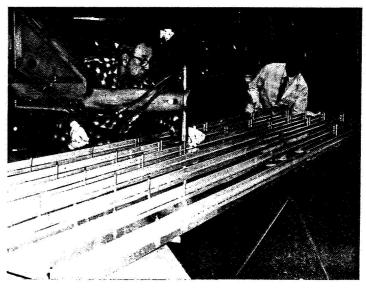


FIGURE 4. SPOT WELDING AFTER APPLICATION OF UNCURED ADHESIVE



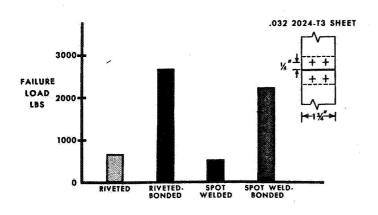


FIGURE 5. STATIC TENSION TESTS OF COUPONS

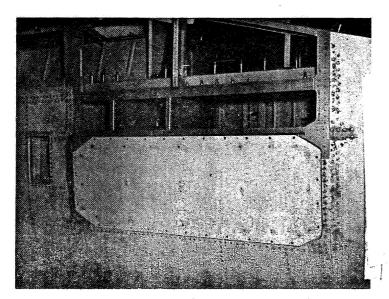


FIGURE 7. ELECTRONIC COMPARTMENT ACCESS DOOR

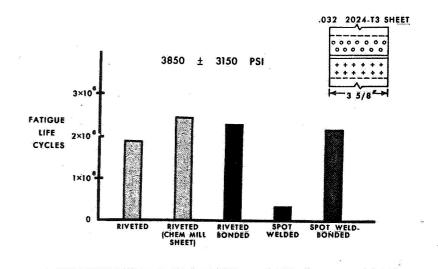


FIGURE 6. TENSION-TENSION FATIGUE TESTS OF COUPONS

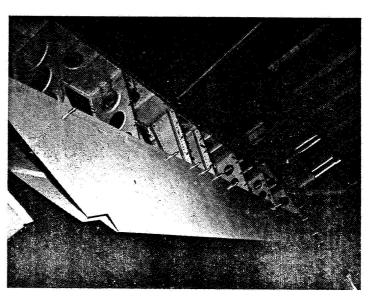


FIGURE 8. VERTICAL STABILIZER TRAILING EDGE

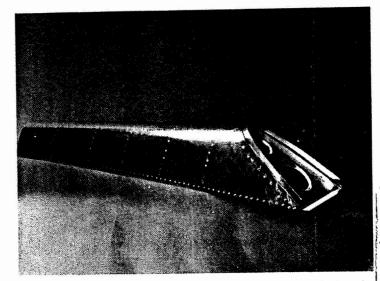


FIGURE 9. VERTICAL STABILIZER LEADING EDGE

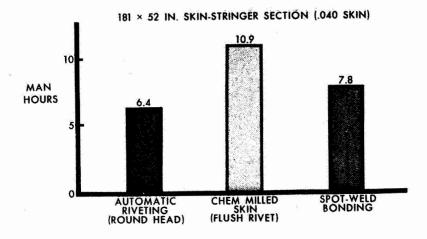


FIGURE 10. COST COMPARISON OF SPOT-WELD BONDING WITH RIVETING

'N74 30924

Electron Beam Welding of Aircraft Structures

by

R. H. Witt

Grumman Aerospace Corporation

Presented At
Symposium On Welding,
Bonding and Fastening
May 30, 1972

Sponsored By
National Aeronautics And Space Administration
George Washington University
and
American Society For Metals

Williamsburg, Virginia

"Electron Beam Welding Of Aircraft Structures"

By

R.H. Witt

Grumman Aerospace Corporation

Requirements for advanced aircraft have led to more extensive use of titanium alloys and the resultant search for joining processes which can produce lightweight, high-strength airframe structures efficiently. As a result, electron beam (EB) welding has been investigated and found to be particularly suited for certain types of primary structure. For example, Ti-6Al-4V rotor hubs were successfully EB welded for the Cheyenne helicopter several years ago at the Solar Division of International Harvester Company. Production of the vehicle is awaiting the results of trials now in progress. Recently, Grumman selected EB welding as a production method for the F-14A Navy Air Superiority Fighter Aircraft and starting in 1969 established it as a major production process for fabricating titanium components. The following F-14A components are now being EB welded in production and are mainly annealed Ti-6Al-4V except for the upper wing cover which is annealed Ti-6Al-6V-2Sn.

- o F-14A Wing Center Section Box (Figure 1, 22 feet long, 70 butt welds)
- o F-14A Lower and Upper Wing Covers joined to Wing Pivot Fitting Assemblies (Figure 2, two alloys)

Grumman also recently participated in EB welding the first two center wing boxes for the March 2 Messerschmidt Multi-Roll Combat Aircraft (MRCA). Messerschmidt (Munich, Germany) is presently tooling up to employ the method developed for production runs.

In the case of the F-14A, it is estimated that use of EB welding for the Center Wing Box saves over 1500 pounds of titanium per aircraft relative to alternate designs considered. This result fits the stated major theme of this Symposium which is "Achievement of Lighter, More Reliable Joint Systems." The paper will cover Criteria for Selection of Welding Processes, the Grumman EB Welding Facility, Development Work on EB Welding Titanium Alloys, F-14A Production and Sliding Seal Electron Beam (SSEB) Welding.

Criteria For Welding Process Selection

Grumman's decision in 1968 to purchase production EB welding equipment and establish an Electron Beam Welding Center was a significant factor in winning the F-14 program. The decision resulted from a consideration of various processes for production of titanium parts which make up 24 percent by weight of the F-14A airframe structure (Figure 3). The wing structure makes up the majority of the titanium used. Originally two large chambers were purchased and installed and made operational in 1969. The facility was increased to over a 10 million dollar investment in 1971 when a third large chamber was purchased, installed and made operational toward the end of the year. These facilities are discussed further later.

The following is a brief discussion of the primary advantages of EB welding that were particularly important in making this momentous decision which has resulted in establishing the largest known EB welding facility in the free world.

EB welding is defined in the Welding Handbook as "a fusion-joining process in which the workpiece is bombarded with a dense stream of high-velocity electrons, and virtually all of the kinetic energy (energy of motion) of the electrons is transformed into heat on impact." A deep-fused area of high depth-to-width ratio is caused by the electron beam drilling a hole by melting and vaporizing the metal bombarded by the fast-moving (half the speed of light) electrons. As the beam moves along the weld seam, the molten metal flows together by capillary action to form the weld.

Perhaps one can better get an idea of the amount of heat generated by a stream of electrons by thinking of an x-ray tube in which a tungsten or molybdenum target is bombarded by electrons to produce x-rays. In many x-ray tubes, water or oil is circulated in the interior of the hollow anode to cool the target. Sometimes, metal fins are adequate to dissipate heat to the air by convection. When the rating of the tube is exceeded or the fluid supply is cut off, however, the target invariably melts.

The amount of heat generated in an x-ray tube operating at a potential difference of 100 KV with a power input of 0.5 KW will heat the anode to 1800° C (3272°F) in one minute of operation. This would result in melting steel or titanium in that amount of time with an unfocused electron beam.



The period of time to melt such materials can be shortened significantly if the electron beam is focused to a smaller spot resulting in a smaller diameter, higher energy density spot and the resultant drilling action of the electron beam mentioned above. This is essentially what happens in an electron beam welding gun to produce continuous welds at high speed. Simple calculations of heat input and theoretical temperature rise using very conservative estimates of beam spot diameter show that temperatures greater than 8000° F per second are readily produced using between 20-30 KW of power input.

The above considerations indicate why simple butt welds in titanium considerably greater than 0.125 inch thick can be readily produced by EB welding in contrast to most arc welding processes where 0.125 inch is the limit for single-pass welding. This is depicted rather strikingly in Figure 4 where the two-inch-thick GTA weld shown required over fifty weld passes to complete and a V-groove had to be machined in order to deposit filler metal in the joint to obtain full penetration levels. The narrow EB weld shown in Figure 4 was made in the same thickness of Ti-6Al-4V with no groove machined in the simple square butt joint prior to welding; no filler metal was required either. Excessive distortion and hardness increases were noted in the GTA weld whereas the EB weld showed no distortion, less shrinkage across the weld and uniform hardness with no hardening.

Electron beam welding, then, is essentially a mechanized fusion welding process performed in a vacuum chamber where the pressure is reduced to 1 x 10⁻¹⁴ torr or less. Electrons emitted from a filament (Ta or W) are focused and accelerated by an EB gun equipped with a focusing coil and applied potential difference. The stream of high-velocity electrons strikes the workpiece and heat is generated producing welds as described above. Welds can be made with the gun positioned at any angle -- horizontal, vertical or oblique. The gun and/or workpiece move during the welding operation and joints from foil thicknesses up to three inches can be butt welded in a single pass.

Before choosing electron beam welding as the process for the F-14A, gastungsten-arc and plasma-arc welding were also considered as potential candidates. All three processes provide equivalent tensile joint efficiencies, but EB welding is the only one that provides almost 100 percent joint efficiency in fatigue for annealed Ti-6Al-4V titanium alloy weldments having thicknesses between 3/8 inch and 2 1/4 inches as per F-14A requirements. Figure 5 presents

EB and GTA welding fatigue data which shows that EB welding is superior in fatigue when reinforcement is removed by machining. Later work on plasma-arc welds also showed fatigue improvement over GTA welds, but this process has a limit of single-pass welding efficiently up to 3/8 to 1/2 inch thickness at best. These facts, coupled with the fact that inert gas shielding is not always effective in making long welds in titanium and contamination (e.g., alpha case) can readily occur, weighed the selection strongly toward the EB welding process. Gas shielding and welding in corners of a wing box are not considered to be easily accomplished consistently with high quality either. The following summarizes major considerations of advantages that EB welding offers at this time for fabricating airframe structures:

- Narrow weld bead (single pass)
- High depth-to-width ratio (can be varied to optimum)
- Small heat-affected zone (HAZ)
- Grain growth minimized
- Extremely pure atmosphere no contamination (orders of magnitude better than base metal vacuum melting conditions)
- Shrinkage and distortion control excellent
- Static and dynamic mechanical weld properties improved (joint efficiency near 100%)
- Minimized or no machining of weld grooves
- Thicknesses from foil gages to plate weldable with same gun
- High welding speeds from 20 ipm to over 100 ipm available
- Welding operation is mechanized

Of course, there are two sides to every coin and EB welding is no exception. Before making the decision to use this process, it was necessary to determine that the application was still justifiable despite the following potential limitations:

- High initial cost of equipment
- Defects can occur, e.g., arc-outs, cold shuts, lack of fusion . . .
- Precise fitup is required with small diameter (less than 0.1 inch)
 electron beam, which can result in machining problems especially for long welds
- Difficult-to-weld materials with high vapor pressure
- Vacuum chamber required limits part size



- Magnetic materials can deflect the electron beam
- X-rays are generated above 35 Kv accelerating voltage
- Vapors deposit on optical reflecting and refracting surfaces (mirrors, lens, etc.)
- Repairs costly, if parts must be refixtured in the chamber

After considering the above, it was still justifiable to use EB welding to obtain significant weight savings on the F-14A center wing box. This is part of the reason for the F-14A being one of the few modern aircraft to be built in such a short time and still not overrun initial weight predictions—a fact that is not too often mentioned in the media.

Grumman EB Welding Facility

When one considers the types of electron beam welding equipment that has been marketed, it has been the general rule to classify them as low, medium, and high-voltage types. Basically, the three classes of machines give the following power rating ranges:

Type	Max. Accelerating	Max. Beam	Beam Power, kw	
	Voltage, kv	Current, ma		
Low Voltage	30	500-1000	15-30	
Medium Voltage	60	500-1000	30–60	
High	150	100	2-15	

Below is a checklist of requirements that are considered to be desirable in the airframe industry, and the general rating for each type of machine is included. From this comparison, it is fairly obvious why the medium voltage type of machine is presently considered to have the edge.

		,	
Machine Requirement	Low Volt.	Medium Volt.	High Volt.
Weld 2 1/2 in. Thick Ti and Steel	No	Yes	Yes
Movable Gun (Inside Chamber)	Yes	Yes	No
Regular Bead Widths For Airframe Tolerances	Yes	Yes	?
Beam Deflection Available	Yes	Yes	Yes
Beam Oscillation Available	Yes **	Yes	Yes
Automatic Seam Tracking	Yes	Yes	Yes
Short Pump Down Time To lxl0-4 Torr	Yes	Yes	Yes
Size of Chamber	Part Size	Part Size	2x Part Size*
Wire Feed	Yes	Yes	Possible

^{*}Depends on Length of Weld Joint

A primary requirement for making a part such as the center wing box is to have a movable gun which will keep the size of the chamber at a minimum. With a stationary EB gun, the 22-foot-long wing box would require a chamber about 35 feet long by 25 feet wide or more. With a movable EB gun, welding is presently accomplished in a chamber approximately 25 feet long by 9 feet wide. Therefore, medium voltage equipment was selected by Grumman in 1968 when the decision to use EB welding was originally made.

Essentially, three generations of EB guns for medium voltage equipment have been produced and it is noteworthy that each generation has different welding characteristics. Inclusion of TV camera optics in the EB gun body has influenced the beam character significantly in the latest production equipment produced since 1968. The first two generations of guns were produced from 1959 - 1968 and were primarily used in R&D or limited production work. The third generation is typified by the machines that are installed in the Grumman Electron Beam Welding Facility, Bethpage, N.Y., the largest facility of this kind in the world that is actually in production. Figure 6 shows the layout of the self-contained production facility which includes controlled areas for welding, quality assurance, machining, heat treating, chemical cleaning, and forming operations.

Grumman placed an order for two of the largest EB production welding chambers in existence in 1968. They were installed in 1969 and have been in production since late 1969. These machines were considered necessary because new airframe designs in titanium alloys call for large parts and more operational flexibility than is available with most existing equipment. One machine is designed as a "clam-shell" type and is 388 inches long, 126 inches wide, and 96 inches high with 360 degree accessibility to the mechanisms and fixturing (Figure 7). The bed plate carries all the tooling and pumping equipment. The shell can be opened in clam-shell fashion to completely expose the fixturing. All fixturing, checking, etc., can be accomplished in place. One of the other chambers, called a "tunnel" type, has a rectangular cross-section 108 inches wide by 132 inches high with a length of 302 inches (Figure 8). Two end-opening doors permit tooling on tracks to be passed through the chamber for in-line production with multiple tools. A third chamber of the tunnel type was installed late in 1971. The chamber size is $362 \times 108 \times 132$ inches.

Each chamber is provided with gantry mechanisms that give degrees of freedom for the electron beam gun: X, Y, Z, A, and B. Gun mobility is controlled by servo systems. The linear motions available for each machine (Figures 9 and 10) are:

Axis	Clam-Shell Machine	Tunnel #1 Machine	Tunnel #2 Machine
X	310"	248"	315"
Y	82"	70"	70"
Z .	12"	54"	53"

With the flexibility provided by these machines, long assemblies of various heights can be welded. Types of parts that can be considered are wing panels, box sections and wing spars. Both of these machines are designed to pump to the vacuum level required ($\langle 1 \times 10^{-4} \text{ torr} \rangle$) in less than 20 minutes. Welding speeds of up to 100 inches per minute are available. The electron gun is rated at 30 kw (60 kv @ 500 ma) for each machine. Designs of the gantries allow the addition of another gun in each chamber, if required. Other features of the equipment include magnetic beam focusing, beam oscillation, beam deflection, and a closed circuit TV system for viewing

and locating the weld joint. A digital readout device informs the operator of the exact location of the gun at all times. Automatic wire feeder and seam tracking mechanisms are also available.

Development Work on Titanium

A large amount of electron-beam welding test work has been completed during the past five years at Grumman. A small EB welding chamber (54" x 50" x 54") was used for most of the early work since 1967. In the titanium field, we have EB welded commercially pure titanium, Ti-6Al-4V, Ti-6Al-6V-2Sn, Ti-8Al-1Mo-1V, Ti-6Al-2Cb-1Ta-8Mo, and Ti-5Al-2.5V. Until recently, it was thought that the most difficult to weld of the titanium alloys was Ti-6Al-6V-2Sn. Although the welds looked good visually, low ductility and fatigue properties limited the use of this alloy for EB welding, particularly in thin gages. Work at Grumman on heavier gages (around 0.5-inch thick) has indicated that weld-line microporosity sometimes caused reduced fatigue properties in this alloy. To eliminate this tendency, it was necessary to employ acid (HNO₃-HF) cleaning consistently as per GSS Specification #7015, Method 3. Proper postweld stress-relief at 1250°F for four hours has also produced ductility and adequate fatigue and fracture toughness for future design considerations.

Butt weld parameters have been developed for Ti-6Al-4V titanium alloy for many thicknesses over the range of 0.16 inch through 2.0 inches. Tensile, fatigue, flaw growth, and fracture toughness tests have been conducted on 1/4, 1/2, and 1-inch welded plate. The electron beam welding program includes welds prepared with and without the use of filler wire, as well as single and multiple pass welds. In all cases, the static weld joint efficiency has been 100%. While this is an indication of high quality welding, it is not meant to infer that designs are based on full properties in the weld. Hundreds of mechanical tests on electron beam welds have been performed.

Specimen testing has been supplemented by testing of prototype components. Two 50-inch-long specimens, simulating welded longerons or stiffened wing skin designs, have successfully passed a modified 12,000-flight-hour spectrum-fatigue test with the weld bead intact. A Ti-6Al-4V diagonal tension beam (Figure 12) have also been electron beam welded. The diagonal tension beam specimen employed relatively light gage materials in the range of 0.16 inch in thickness, and was about 2 ft x 4 ft in size. The 250-pound carry-through structure employed heavier material (up to 1-7/8 thick) and measured 12 x 14 x 52 inches.

A 1-7/8-inch-thick, electron beam weld was designed to carry primary tension loads. This weld joined a beta-processed plate to a press diffusion bonded laminate and was machined flush. The simulated wing center box structure successfully completed a 12,000-hour spectrum without failure. The initial net stress was set at 80,000 psi for 120 blocks. Each block, representing 100-hour life, consisted of the following:

No. of Load Applications	Load (% of Limit)	Nominal Stress (ksi)	
330	69	55.2	
110	84.5	69.6	
28	100	80	
6	115	92	

The test was continued after increasing the limit stress to 90,000 psi. At this stress level the failure occurred in the base metal after 24 blocks.

EB studies were also conducted as a part of the beta forging and precision forging evaluation programs. Two forgings were joined at an end flange to form a center rib as shown in Figure 13. F-14 spectrum fatigue testing of this item was satisfactorily completed. This development contributed to the diversification and optimization of the designs for rib and frame structures on the F-14.

F-14 Production

Experience with F-14A EB welding includes design, fabrication and successful static and flight testing of an all-welded center wing box and outer wing covers EB welded to the required pivot fittings. All of the material is annealed Ti-6Al-4V plate and forgings except for the upper wing cover/pivot assembly which is annealed Ti-6Al-6V-2Sn alloy.

As a result of the successful fabrication and test evaluation of the electron beam welded torque box, a full-scale box was designed for the F-l4. Figure 14 shows the weld land configuration that was used to weld the straight butt welds (89 in number when the first boxes were fabricated). Extensive test work showed that by using scribed witness lines on top and root-side of each joint, missed joints and other defects could be readily identified, even prior to radiographic examination. Other efforts were directed toward parametric studies on various gages to establish optimum

weld bead shapes and widths. A relatively parallel-sided weld of uniform width was developed. Minimum weld widths of 0.070 - 0.080 inch were made to assure that internal missed seams were not encountered in production welding. The witness lines on top and root side of the weld help to locate the position of the weld bead relative to the original joint. It is required that at least 0.015 inch of weld be measurable on each side of the joint for acceptance.

The results of fatigue and fracture toughness tests were established to finalize the design of the box. Reweld studies were accomplished to determine the effect of rewelding on mechanical properties as well. It was found that seven rewelds were not detrimental so that various defects can be EB repaired. The fatigue studies showed that fatigue properties were reduced by leaving the weld reinforcement intact or by eliminating stress relief after welding. Essentially 100% fatigue efficiency is obtained when reinforcement is removed and a stress relief at 1200° F for 4 hours is utilized after welding. Lower stress relief temperatures reduce efficiency. Fracture toughness requirements call for a $K_{\rm IC}$ of 70.0 for base metal and a minimum of 37.5 for electron beam welded plate. Fatigue flaw growth tests were also run to establish critical flaw sizes for twice the spectrum fatigue life of the aircraft.

The center wing box is essentially manufactured in modular construction from four basic boxes (Figure 15). Starting at the left end of the box, there is a L.H. outboard module, L.H. inboard module, R.H. inboard module and R.H. outboard module. Each module is initially fabricated from its own bottom plate, side plates, end plates and rib stiffeners. The top of the box is welded on last, so that initial module joining includes inboard-to-outboard modules. The left side of the box is then joined to the right side at the midpoint transverse centerline. The top covers are then sequentially installed. Since forgings have become available, the number of welds have been reduced to 70. Of these, 52 welds are greater than one-inch thick and eight are greater than 1.9-inch thick. The smallest gage is 0.580-inch thick. It takes 25 setups to fabricate each wing center-section. All electron beam welds employ start and stop tabs integrally attached to the part, where possible, to avoid defects associated with starting and stopping of the weld. Integral tabs are essential, particularly



for deep welds, to assure proper solidification and prevention of bursts near the finish-end of the welds.

The operational sequence for production weldments is:

1. Prefit

- 9. X-ray inspection
- 2. Apply witness lines
- 10. Ultrasonic inspection

3. Clean

ll. Clean

4. Setup

12. Stress relieve

5. EB weld

- 13. Descale
- 6. Visual inspection
- 14. Penetrant inspection
- 7. Witness line inspection
- 15. Clean

8. Machine weld

Upper and lower wing covers are fabricated using essentially the same procedures. However, the wing plank is hot formed to a moderate curvature prior to welding. The initial weld in a typical wing cover is a relatively short one joining the pivot section to an actuator piece on the inboard wing cover (Figure 2). After removal of end tabs and final machining, the inboard cover is welded to the outboard cover. Figure 16 shows this weld being made and the related tooling required.

To date over 30 wing center boxes and many sets of wing covers have been EB welded and accepted by quality assurance for flight and test articles.

Sliding Seal Electron Beam (SSEB) Welding

An Air Force-sponsored program (Contract F33(615)-70-C-1806) at Grumman is directed toward generation of performance data, determination of the functional capability of a Government-owned SSEB welding system, and demonstration of a capability to weld large aerospace structures (Figure 17).

This program commenced in August 1970 and will be completed this year. Straight butt welds in the downhand position have been produced in annealed Ti-6Al-4V and 2014-T6 aluminum alloys for thicknesses up to one inch thick and HY-130 steel up to 1/2 inch thick. Some bead-on-plate welds have demonstrated capability to weld two-inch-thick aluminum and 1 1/2-inch-thick titanium for lengths up to two feet. On the basis of power input, it is probably possible to weld 1/2 to one inch additional thickness with this equipment. F. R. Miller of AFML is the Air Force Manager for this program.

To make an SSEB weld at the present time, it is first required to make a GTA seal-pass weld approximately 0.050 inch deep to prevent vacuum leakage when SSEB welding. Following this, the part is immediately transferred to the SSEB welding fixture which has double 0-ring seals (Figure 18). The backing pump is turned on and the small backup chamber pumped to below 50 microns of mercury. The welding head equipped with double-ring seals (Figure 19) is positioned on top of the GTA sealed weld plate and pumped down to a vacuum around one micron of mercury. The weld is then made with a full-penetration SSEB weld pass. Figure 20 shows typical microstructures of SSEB welds in various thicknesses of Ti-6Al-4V up to one inch thick. The higher pressure of the SSEB vacuum compared to the chamber "hard vacuum" appears to result in less spatter and generally smoother underbead configurations.

SSEB welded tensile properties are summarized in Table I together with weld parameters employed for weldments 1/4 to one inch thick. The parameters including welding speed are similar to those used in "hard vacuum" chambers for the same gages of material and near 100% tensile joint efficiencies and good elongation are obtained. Unnotched fatigue efficiencies of 100% were obtained at a stress ratio of ± 0.1 and fracture toughness (± 0.0) of 39.0 for SSEB resulted with plate having ± 0.0 for 55.4.

The final phase of the program is an evaluation of SSEB butt welding as it might be used to manufacture a simulated stiffened titanium wing skin for an aerospace structure. Figure 21 shows a section of an SSEB welded panel with the SSEB weld transverse to the length of the panel. A fatigue test specimen machined from the weldment is also shown in the figure. This weld was made by building up the weld area as indicated in Figure 22 using titanium rib blocks to produce a constant weld depth. These blocks were machined out after welding. The panels are now being spectrum fatigue tested.

Such a structure might be employed in producing wing planks for future aerospace vehicles where parts are too large to be welded in existing EB chambers. These parts might run from 35 to 70 feet in length or more. Usually it is proposed to EB weld such a structure by joining narrow, stiffened extruded sections longitudinally parallel to the stiffeners along the length of the skin. Such an approach would not be economically practical at this time for the following reasons:

Long length (20 to 50 feet) welds in multiple stringers would require costly machining and fitup practices, inspection of long lengths of weld, and would be difficult to repair. If, for example, ten stiffeners were required per plank, 200-500 feet of joint would have to be machined, fitted-up carefully and ultimately inspected by radiography and ultrasonics. Using transverse weldments, it is possible to keep the total weld length down to 15 to 30 feet per plank, resulting in much less cost and time.

Depending on the ultimate design of the stiffeners and the weld location, it may not at all be possible to apply SSEB welding to longitudinal joints. Also, the present equipment has a maximum stroke of six feet when the gun is moved in the downhand position and five feet in the vertical position. This makes it mandatory to move the part which has not been developed for this equipment to date.

Another area in which the SSEB welding process may be readily adaptable is in welding large cylinders and tankage. However, considerable development will be required before such uses become practical. Any weldment that would require post-heat-treatment (e.g., solutioning, annealing and stress relieving) first requires that large heat-treat facilities be made available to handle 20 to 40-foot-diameter tanks.

Conclusions

From the foregoing discussion it is evident that EB production welding has come a long way since the early 60's. To one who has been involved in EB welding in the aerospace industry since 1958, it is with great satisfaction that these results can now be presented.

The future of electron beam welding such reactive alloys as titanium is very promising. As designers and stress people get more familiar with the structural efficiencies attainable in strength and weight savings, other companies and industries will invest in EB welding equipment for primary structures. Coincident with the development of large vacuum chambers with movable EB guns and large, precision tooling, non-destructive inspection methods have been improved to the extent that quality can be consistently controlled even in deep structural welds. Further development of out-of-chamber methods such as SSEB welding should enhance versatility and extend potential application areas to larger parts than can now be efficiently welded.

TABLE I ANNEALED Ti-6A1-4V WELDED TENSILE PROPERTIES

THICK., IN.	UTS/JE*	YS/JE*	ELONG/JE*
1/4	143.2/ 99.6	138.3/ 98.2	9.7/80.7
1/2 Trans	138.5/100.0	134.1/ 99.7	11.8/87.5
1/2 Long.	144.9/105.3	140.7/102.8	12.3/80.6
3/4	139.5/101.2	138.0/101.9	10.3/77.5
l Trans	159.1/113.5	146.4/107.9	9.3/66.4
l Long	144.1/ 99.2	137.7/ 97.2	11.0/82.7

THICK.,	BEAM VOLT., KV	BEAM CURR, MA	WELDING SPEED, IPM	HEAT INPUT, KJ/IN.
1/4	40	180	60	7.2
1/2	45	270	50	14.6
3/4	50	300	50	18.0
1	50	330	45	22.0

^{*} UTS - Ultimate Tensile Strength YS - Yield Tensile Strength

ELONG-Elongation

JE - Joint Efficiency

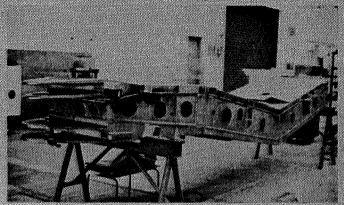


Figure 1. F-14A Wing Center Section Box

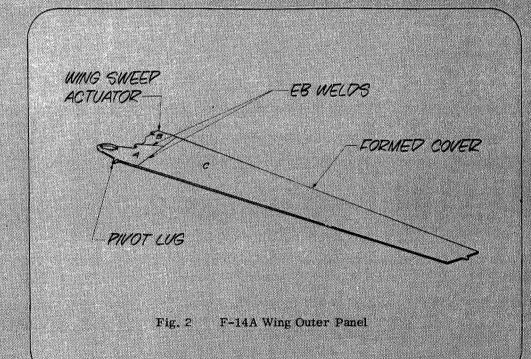
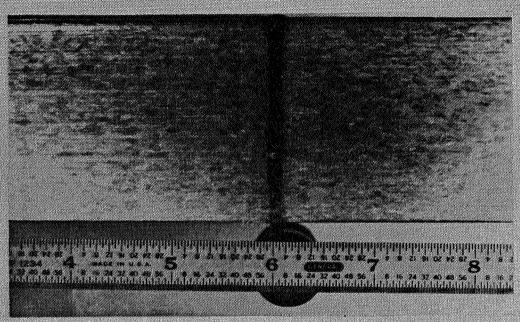
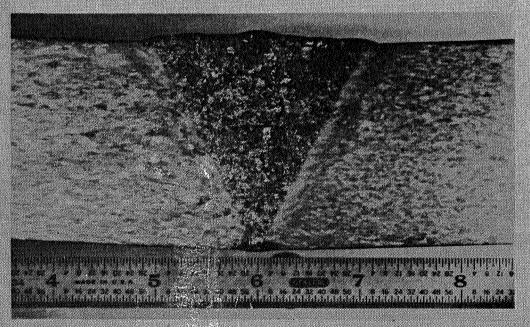




Figure 3. F-14A Structural Components



a. EB Weld



b. GTA Weld

Figure 4. Welds in Two-Inch-Thick Ti-6Al-4V Titanium Alloy Plate (1.3X MAG)

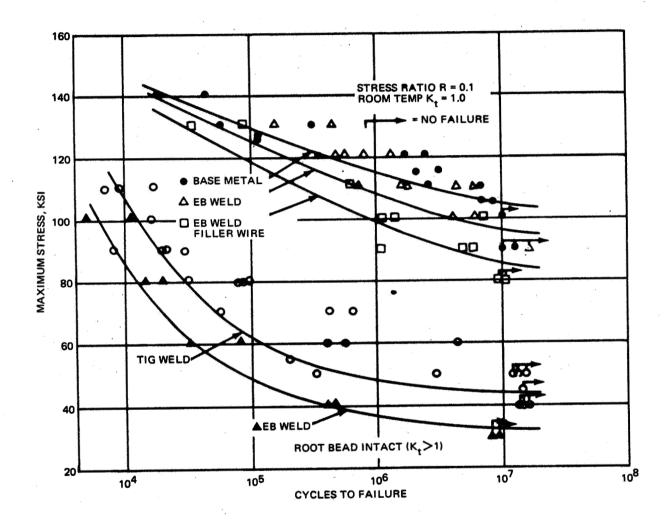


Figure 5. EB and GTA Fatigue Data

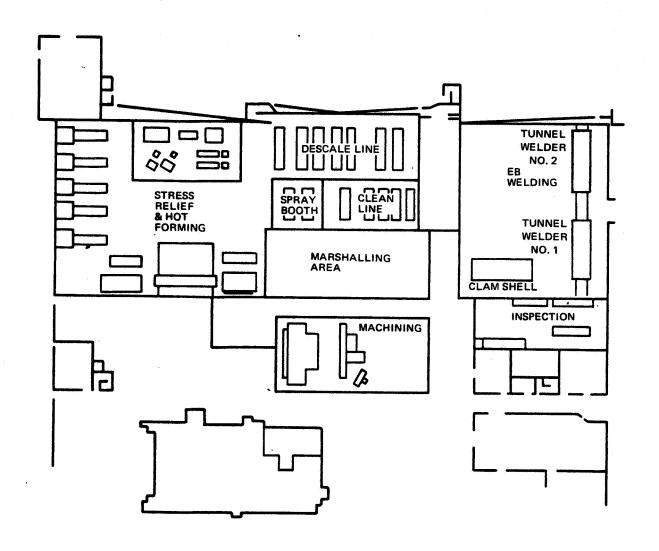
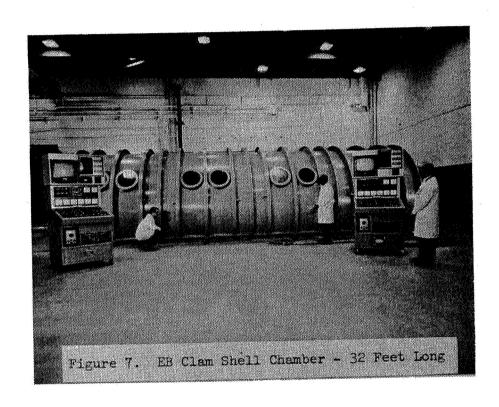
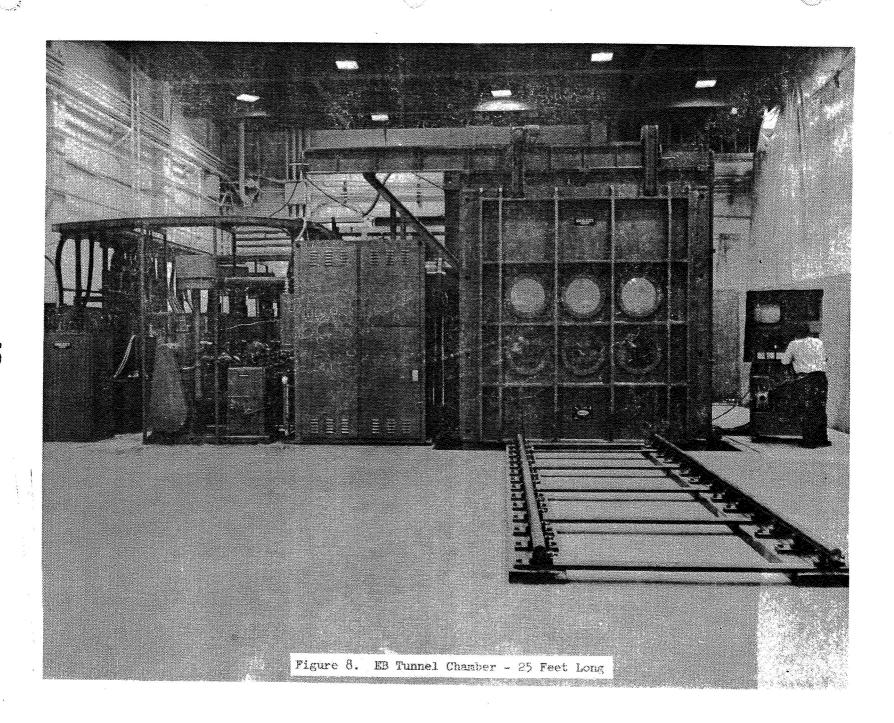


Figure 6 Electron Beam Welding and Related Facilities - Plant 2





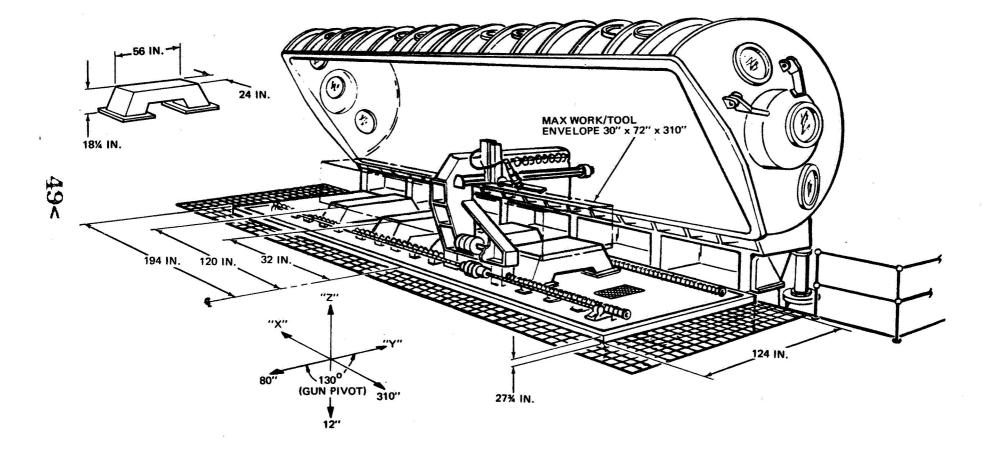


Figure 9 EB Clam-Shell Chamber - 388 x 124 x 96 Inches

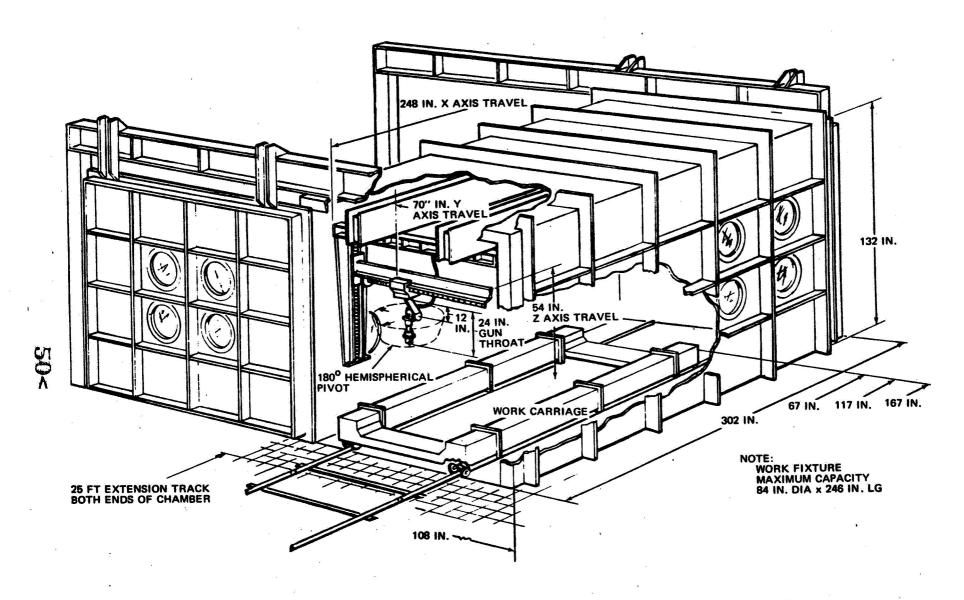


Figure 10 Rectangular EB Chamber - 302 x 108 x 132 Inches

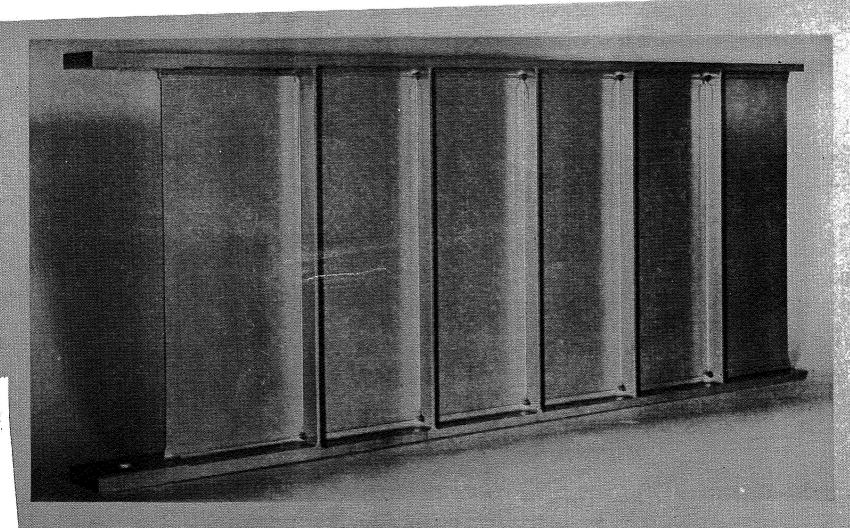
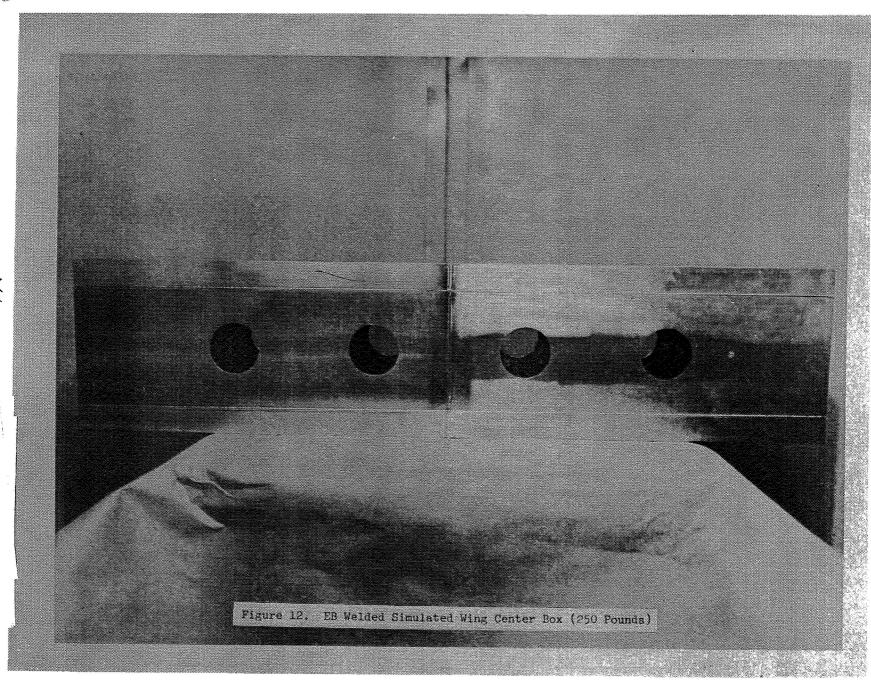
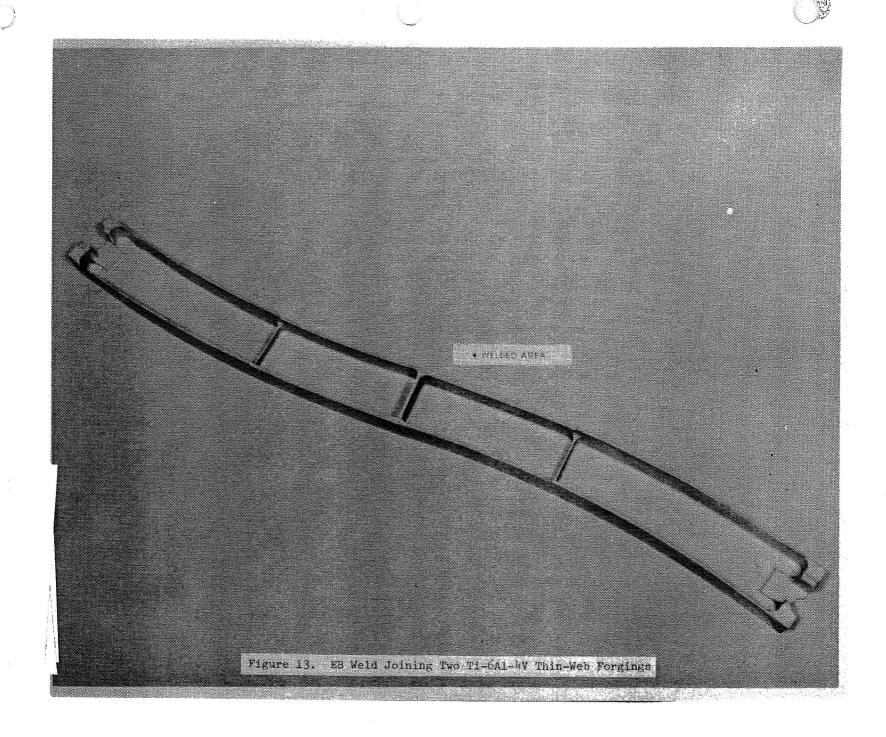
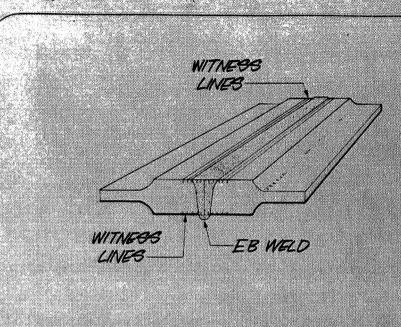


Figure 11. T1-6A1-4V EB Welded Diagonal Tension Beam









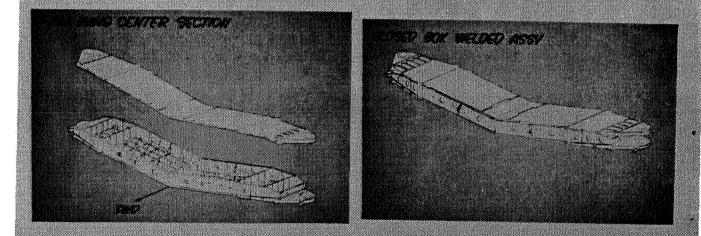


Figure 15. Schematic Representations of F-14A Wing Center Section

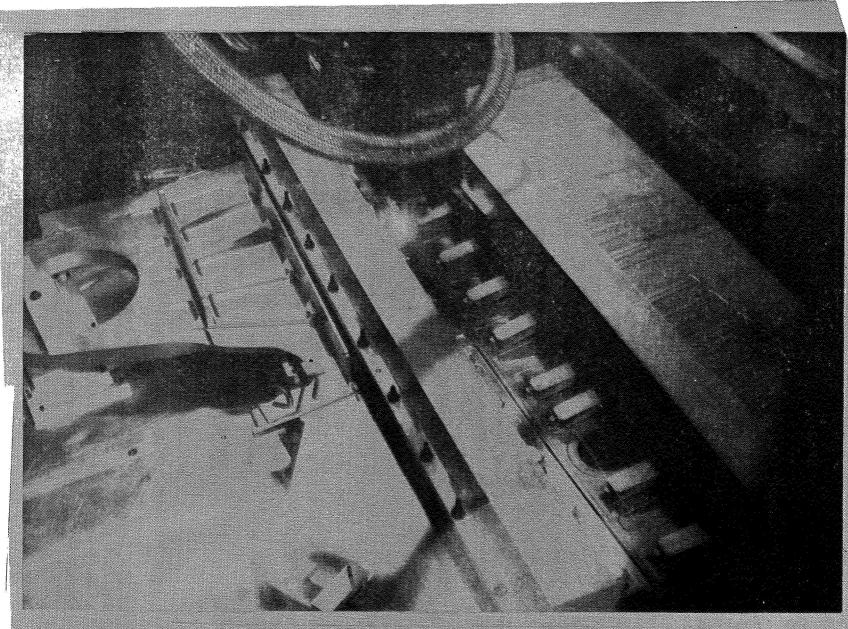
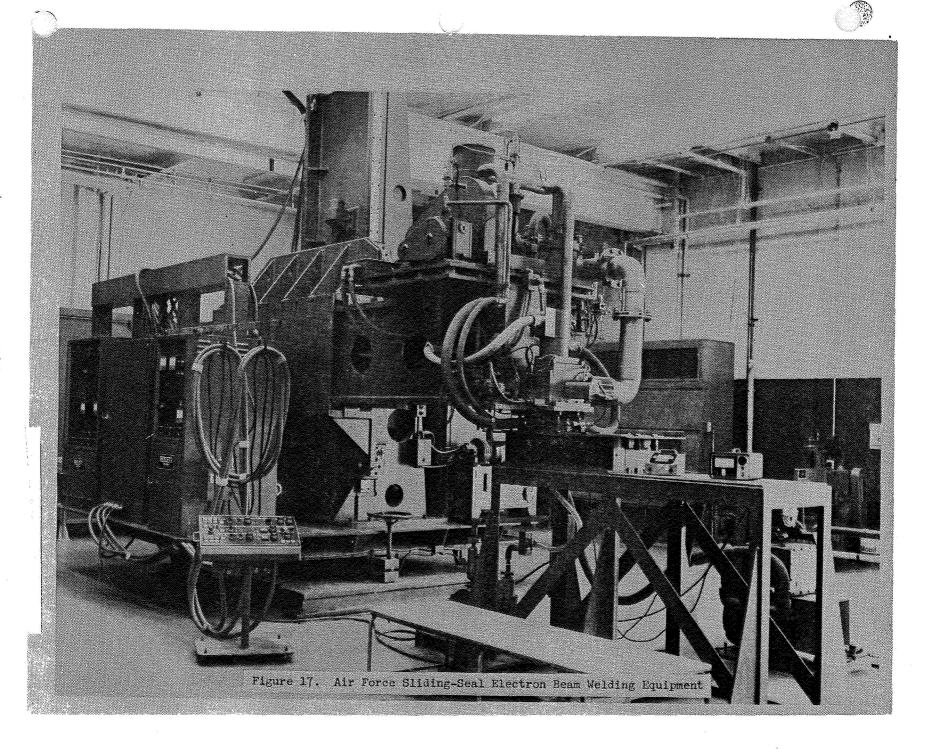
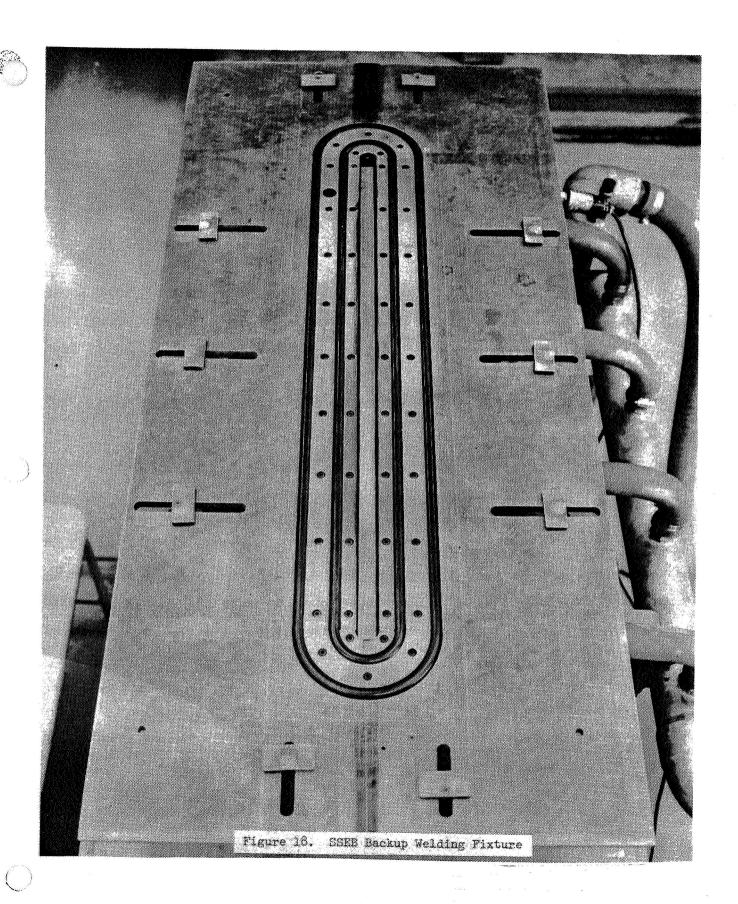
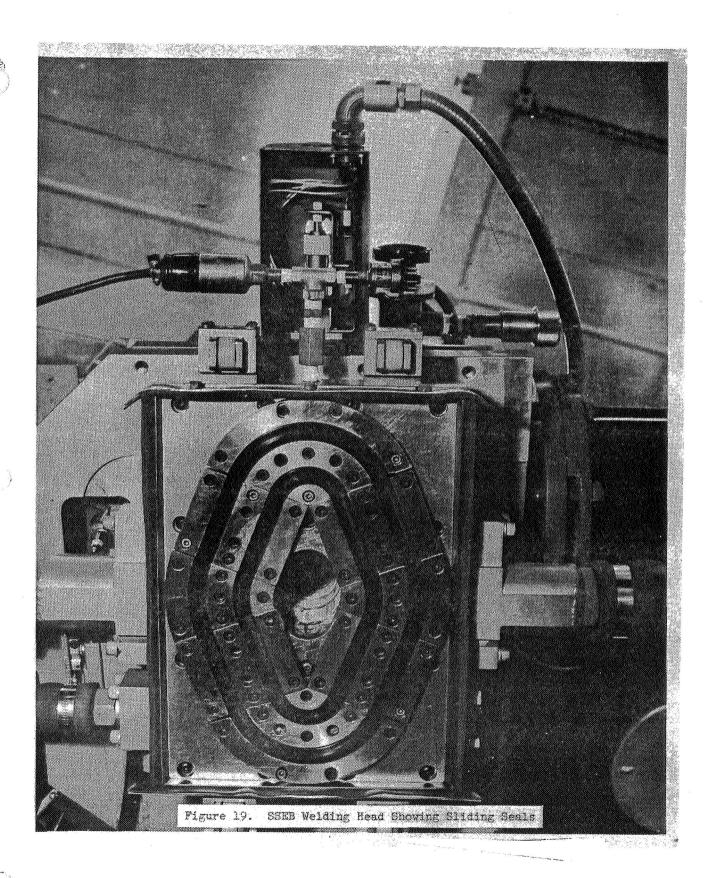
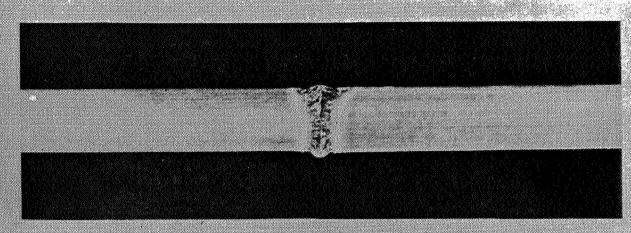


Figure 16. EB Welding of Inboard Pivot/Actuator to Outboard Wing Cover

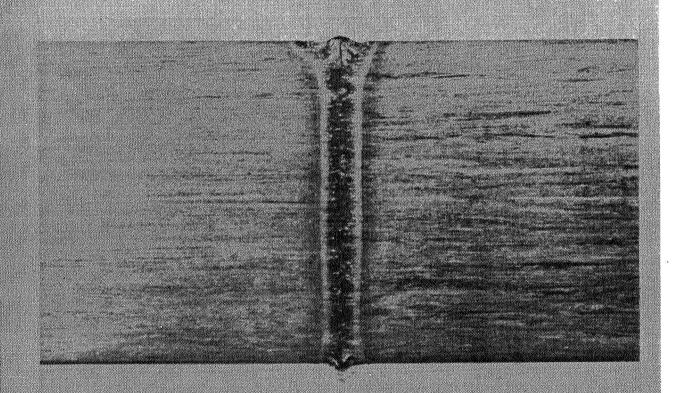






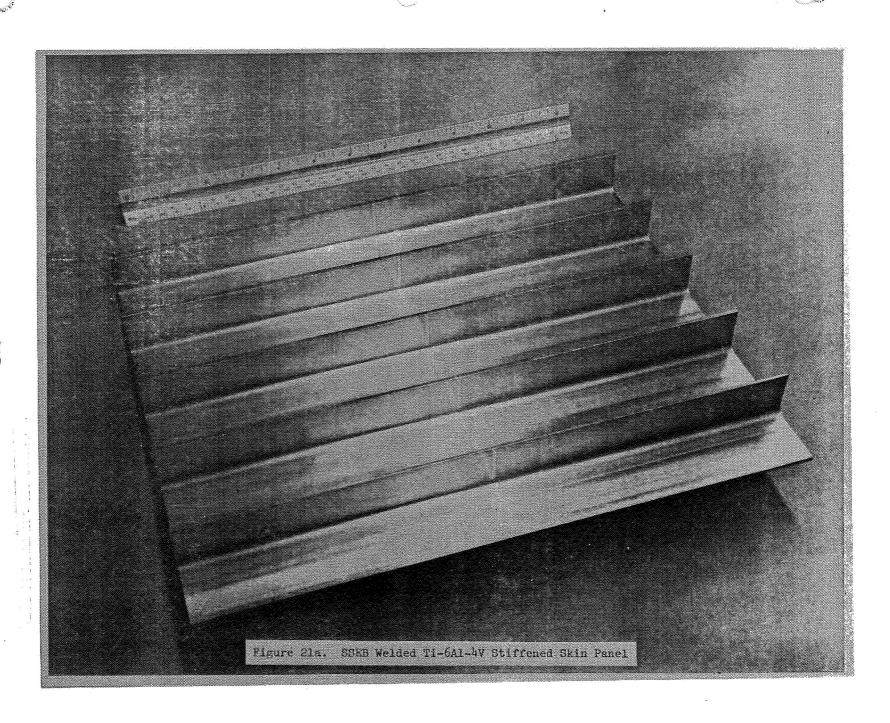


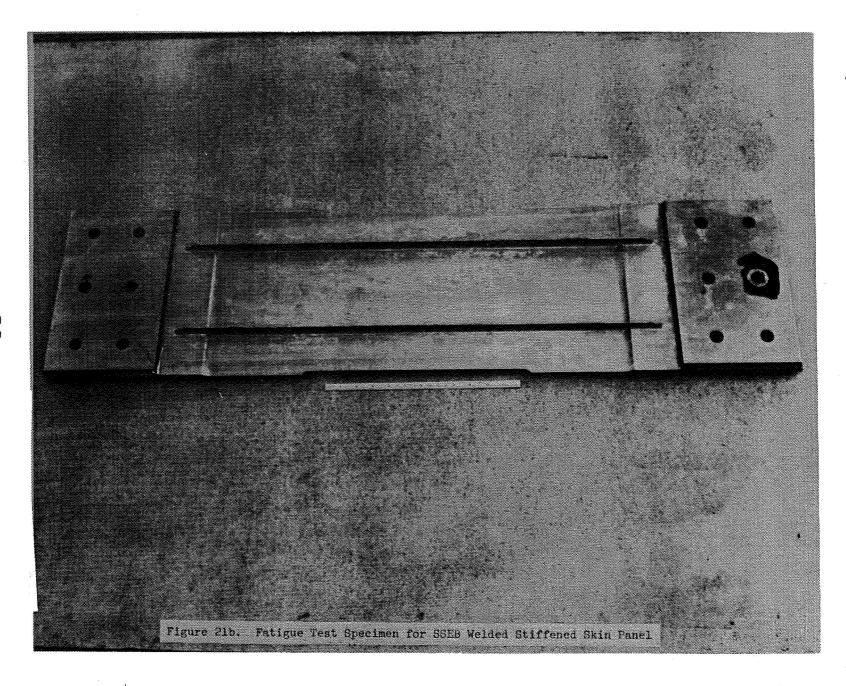
a. 1/4-Inch-Thick (2X MAG)

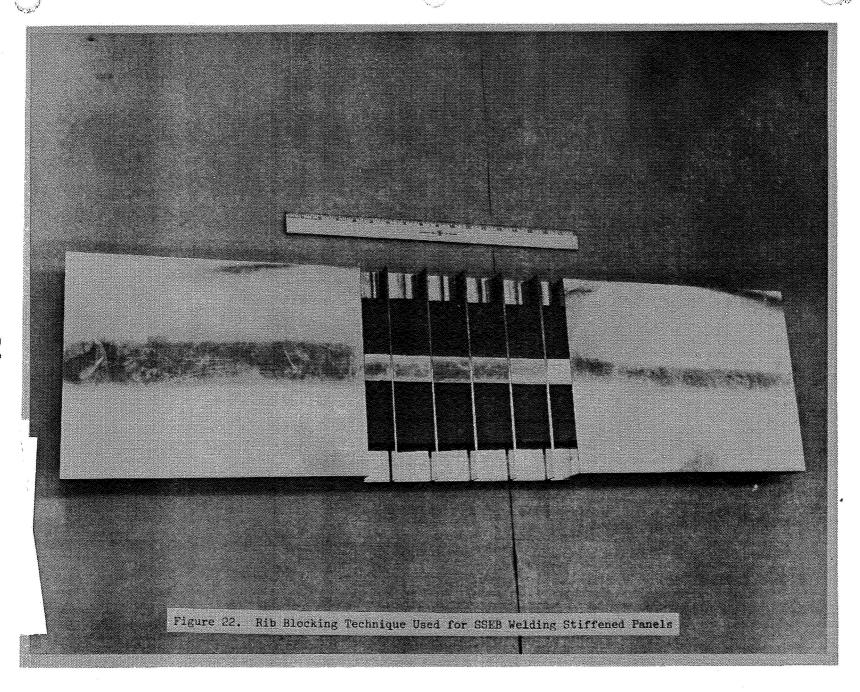


b. One-Inch-Thick (2X MAG)

Figure 20. Typical Macrostructures of SSEB Welds in Ti-6Al-kV







N74 30925

THE EFFECT OF WELD STRESSES ON WELD QUALITY

R. A. Chihoski Head of Welding Research

ADVANCED MANUFACTURING TECHNOLOGY
MARTIN MARIETTA AEROSPACE
DENVER DIVISION

INTRODUCTION:

A narrow heat source raises the temperature of a spot on a solid piece of material like metal. The high temperature of the spot decreases with distance from the spot. This is true whether the heat source is an arc, a flame, an electron beam, a plasma jet, a laser beam, or any other source of intense, narrowly defined heat. As soon as the heat spot moves, the thermal slope on the forward side becomes steeper, while the trailing side stretches out behind it. This can be seen in the two examples in Fig. 1, where temperature is shown as altitude on a three-dimensional plot.

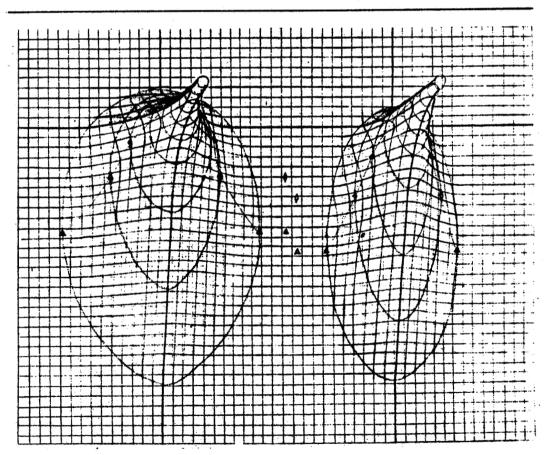


Figure 1 - A slow weld (left) on 2014 T6 aluminum compared to a fast weld shows three notable differences on the isothermal maps: (1) broader flatter gradients, (2) greater temperature rise ahead of the heat source, and (3) less lagging by the heated system.

Advantage is taken, in this discussion, of comparing the qualities of slow welding (6 inch per min.) with fast welding (20 inch per min.). Several, simple differences of <u>degree</u> are visible as the speed of the moving heat increases: (1) The sides of the faster become narrower and more steeply sloped; (2) The bow wave of heat, i.e. the temperature rise over an area preceding the heat source, becomes lower, shorter, and narrower; (3) The general mass heating lags the source more, as suggested by the swept-back lines that mark the points of peaking temperature. This signifies lagging by a kind of thermal-expansion center of gravity.

The isotherms illustrated here (the ellipsoidal topographic lines) can be found by experiments or by calculation; but only calculated curves such as these can describe conditions smoothly right up to the puddle edge. It was the growth of strips defined under these isotherms that led to the understanding of the patterns to be described.

The theoretical construction followed by some experiments precipitated an image of a coherent pattern of stress fields around a weld arc moving on metal sheet. A series of subsequent experiments reinforced the sense of the fields operating where expected. evidence points toward stresses imposed across the center line (transverse to the weld line) but changing several times. First, compression ahead of the puddle gives two effects: a force pushing the plates apart and plastic upset just before the puddle. General heating of material on both sides of the puddle pushes the material without resistance into the puddle. This is responsible for subsequent shrink and for the bead thickening. Tension appears across the mushy zone as expected. Compression can be found at higher weld speeds just behind that because of a lag in the area's gross expansion aside of the heat source. It has two effects: a plastic forging effect on the just-cast aluminum, and a holding of the sides apart that can increase the tensile strain of the last stressed zone which comes essentially from the shrinking of local area in the center of the surrounding greater expanse of rigid material. Longitudinal stresses are simpler, but they still add significantly to bead thickening and thereby to transverse shrink and residual stresses.

These stress events can have their intensity and extent changed coherently with changes in the simple and most available instruments: weld speed, hold down, gaps, tacks, and others.

The work started on theoretical grounds and moved as far as simple theoretical rigor could take it then shifted to a deductive and reasoning system to uncover the location and order of the various fields of stress. At the end, a variety of experiments added up to some proofs that the identified stresses existed and in the order described.

The work was originally undertaken to determine the reason for cracking in the 2014 welds. The simple pattern to be described and illustrated provides the rationale behind the varying stresses in other alloys as well. It appears to provide a simple format for the seemingly confusing deformations-and-stresses interplay on any material experiencing a moving point heat source.

METHOD OF EXPERIMENT:

The isotherms in Fig. 1 were calculated and drawn for a 6 inch per min. moving heat source and the 20 inch per min. heat source, with the heat input in each case sufficient to make a fused zone 0.8 inch of an inch wide (The detailed paper covering much of this development can be found in Ref. 5). Strip models were built as shown in Fig. 2 which in effect sum the volume increase under each area increment of heated aluminum. The growth of the horizontal (longitudinal) strips are expanded to the rear. The vertical (transverse) strips are increased so as to project expansion over the centerline of travel.

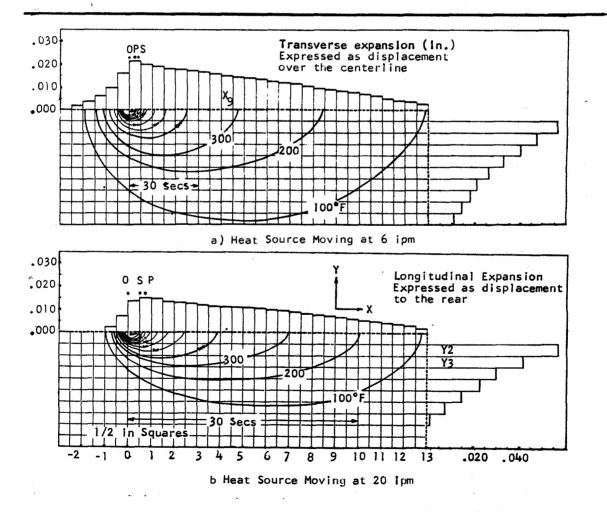


Figure 2 - Calculated isotherms and strip expansions caused by moving point heat source, moving at 6 or 20 ipm, with heat sufficient to each case to produce a 0.8 in. wide bead in 0.250 in. thick aluminum alloy. Note how Peak expansion on the faster weld has come to lay behind the solidus.

The first categorical difference between slow welding and fast welding is evident. Because of the more trailing isotherms in the faster weld, the peak of the integrated expansion appears to have fallen behind the solidus. The effect of this, however, is more clearly shown in Fig. 3 where a rule change is made at the point marking the solidus. The L₁ line marks the profile of transverse expansion, and should in its way mark the creation of stresses.



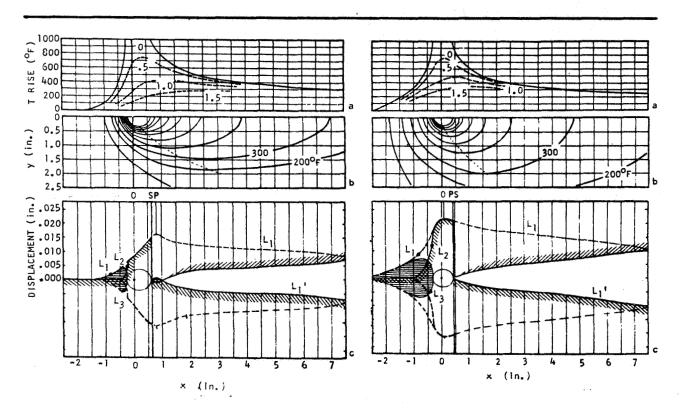


Figure 3 - Note how the changes in transvers expansion after the solidus in the fast weld (left) may create compression and upset.

Ahead of the puddle this obviously means compression and expansion that should push two plates apart. This is clearly very much larger on the slow weld that has a large bow wave of heat. Soon the puddle will absorb all of the material that intrudes into it from the sides and without back pressure or stress resistance. But with solidification at the back of the puddle, changes in strip length will again produce stresses instead of uninhibited movements of material. Now it can be seen clearly, if the L1 profile is transferred to the L1' position, that height of strips changes after solidification must result in compression where the vertical strips intrude and tension where they retreat. The fast weld then experiences compression and upset before the general recession. The slow weld (on the right)

has its strips receding from some point starting inside the puddle, which is the conventional view of weld cracking. The illustrated after-gaps can exist in fact or in the form of tension concentrated toward their forward end. This ended the more rigorous mathematical and physical description of events acting across the travel centerline.

The effort to understand the meaning of this information and the many anamolies appearing in the laboratory and the shop nourished the next phase of this investigation that attempted to complete the pattern and interpret welding experiences. The final results are summarized figuratively in Fig. 4.

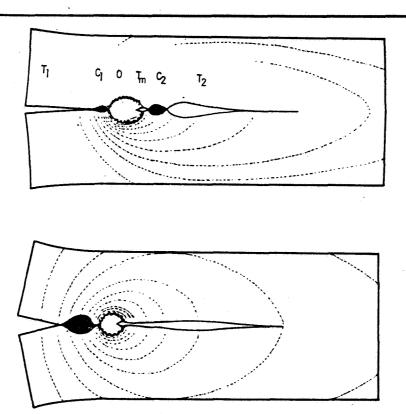


Figure 4 - Five transverse stresses may operate on the centerline of a weld, as marked on the fast aluminum weld above. With slower welding one compression field disappears and the two aft tensions coalesce.

A variety of experiments, (noted in reference 2 & 5) were studied for their relation to the mathematical and graphical expressions of Fig. 3. They consisted of specimens on which distortion or shrink or strain was measured as a moving heat source traversed the length of the part. The welding produced very graphic illustrations of the forces at play in certain locations. The changes in strain or

in geometry of these specimens was consistent but it had heretofore eluded explanation. With the laying out of the characteristic stress pattern, the strange behavior of specimens did indeed fall coherently into place, and thereby became some proof of the validity of the revealed pattern.

DISCUSSION:

The Character of Stresses Around a Moving Heat Source

Proof of the following stress status will be avoided in this paper for the sake of brevity and because the theme to be emphasized here will be the effect of these stresses on weld quality. It is most important though to set the pattern firmly in mind. The basic pattern of forces acting on the center line is most completely illustrated by the fast weld in Fig. 5. The bow wave of heat preceding the puddle tends to push two plates apart at C1. This creates tension or a gap ahead of it, in reaction. The puddle can bear no stress at all. The liquid to solid phase change in the mushy zone does create an operating tension (Tm). But after the

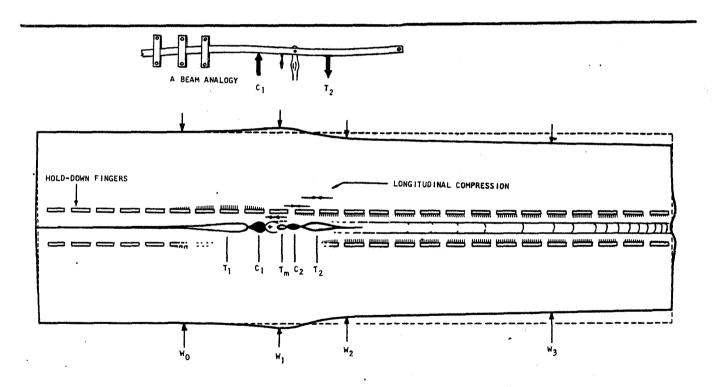


Figure 5 - In a steady state fast weld on aluminum alloy it should be possible to find the work pieces spread (T_1) because of the push-apart force (C_1) caused by the temperature rise and swelling ahead of the arc. After the arc, effects combine to give transverse tension (T_m) , compression (C_2) , and a general recessional tension (T_2) . But longitudinal compression is found alongside the arc and lagging at points further from the centerline. Several shop-available instruments can be used to reduce or reproportion these stresses.

solidus the expanding outer isotherms tend to push material toward the centerline so as to more than make up for the shrinking value at the centerline. This creates a compression. But soon the general recession, that is shrinkage over a wide area, soon requires tension across the whole specimen. The rigidity of the outer area prevents this tension from being satisfied by an inward bending of material. This reaction alone indicates the necessity of making weld specimens out of wide parts when an experiment's purpose is parameter optimization or weld strength or stress determination. It is clear that narrow specimen plates will deflect outward and inward as the heat wave passes and they will never allow great stresses, normal stresses, to rise across the centerline.

The existence of longitudinal stresses is simpler to understand. They are in fact peaks of compression which occur at the peaks of temperature rise in each horizontal strip. It is important however to note that the longitudinal as well as transverse compression vectors cause an transverse extrusion of material into the soft plastic-and-liquid puddle area sink as it passes. This causes greater bead thickening, weld shrinkage, and residual stress than simple (transverse) calculation will predict.

Now some illustrations of how this train of stress events operates in common situations will serve to set the pattern in mind and to introduce ideas of how these stresses affect weld quality.

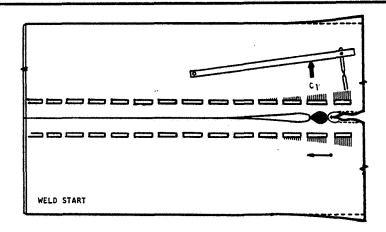


Figure 6 - The normal push-apart force (C_1) of the advance heating exerts an extraordinary stress on the short length of weld which exists at the onset of welding. This applies no matter where on the piece the weld is started. Strong hold-downs and those extending far to the rear inhibit the motion of the parts and so reduce this tendency.

Wherever a weld starts, (Figure 6) the bow wave of heat that precedes it, although of ordinary magnitude, has the power to render the initially short length of material behind it. C1 then can push two

plates apart sufficiently to tear a short length of weld that may be complete. Tacks are usually sufficient to preclude the beginning of this kind of event.

In contrast (Fig. 7) as the heat source approaches the <u>end</u> of a piece of material, the heat wave preceding the puddle grows to extraordinary proportions when the dam formed by the end of the metal prevents the heat from running forward into wide areas.

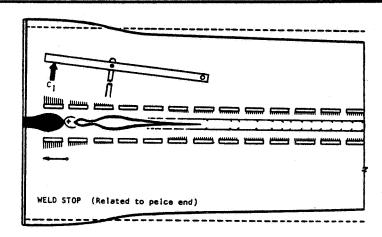


Figure 7 - As the heat in advance of the arc approaches the end of the work piece it can no longer run forward so it builds up higher and over a wider area. This gives C_1 an extraordinary push-apart force that stretches the after puddle area to an unusual degree resulting in cracks near the end or in diminished weld shrinkage.

This causes an extraordinary growth of temperature and expansion (which means the C1 force reaches an extraordinary peak). When this occurs, it produces an extraordinary tensile strain and sometimes cracks after the puddle. This unusual event is manifested also as a flare in the width of the work as illustrated. When C1 becomes very hot as the puddle moves more towards the end, it becomes plastic and diminishes as a force. If the weld is terminated near the end, extraordinary tension will ultimately grow across this upset region. A bridging tack may aggravate instead of cure this problem. It should be noted here that there is a part widening at the start of a weld caused by stretching of the aft material and also at the terminus of a weld caused by stretching of some distance of aft material. These do increase the width of the specimen in these locations. If the weld represents the longitudinal joint on a tank, it creates a flare on both ends of the cylinder. If the weld start and termination point are not consistent and the trimoff cut is not consistent tanks produced with the same weld parameters will appear to be highly variable in diameter. But in fact the span between these end transition situations is very constant in its weld shrinkage and tank diameter, from point to point in a tank, and tank to tank in production.

In the case of a circumferential weld around a tank or tube no end of the material is reached, but rather a tie-on to the previous weld is made. When the heat source comes upon a tack or the prior weld as it does in the circumferential weld of a tank or tube (Fig. 8), something else happens. Ordinarily the C₁ force pushing plates apart creates a small gap ahead of the heat. But when the system approaches a prior weld gapping cannot occur. C₁ then grows as a force because of the failure to spread and flex its members. This force puts extraordinary stress on the end of the approached weld or tack. Often the force can crack the prior weld. Furthermore as the puddle approaches the rigid bridge the upset at C₁ increases and then the extraordinary upset area experiences extraordinary tensile strain when the heat passes on. This extraordinary strain can turn to cracks in that location.

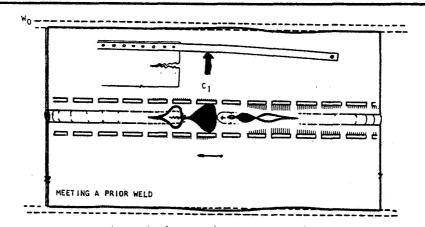


Figure 8 - The rigidity of the prior weld causes the normal forward expansion (C₁) to give extraordinary effects: (1) the push apart force may become high enough to split the prior weld, and (2) the upset in the plastic zone grows larger to require an extraordinary shrink in that location when the heat source moves on.

In the previous three illustrations, it can be seen that the force of C_1 has had undesirable effects on the after-puddle material. That force of C_1 can be diminished by the filing of a gap into the butt lines where C_1 's force must be decreased. Instead of the members being spread by the arrival of C_1 at the critical point they will remain unflexed as C_1 only fills some space with its swelling.

Cracks are undoubtedly due to tensile stress of the wrong magnitude occuring at the wrong temperature. Since some of the tension after the puddle is due to the forces exerted ahead of the puddle, any device for reducing this tension ahead of the puddle, could cause an alloy that has post-puddle cracking problems to do better. So

it seems conceivable that welding on a gap such as shown in Fig. 9 would keep down the magnitude of C_1 and thereby keep down the magnitude of T_2 . Welding onto the right size gap can create just the right T_2 conditions by adjusting C_1 to a specific magnitude. In this way it may be possible to successfully join an alloy which is unweldable because it always cracks under normal shrinkage strains.

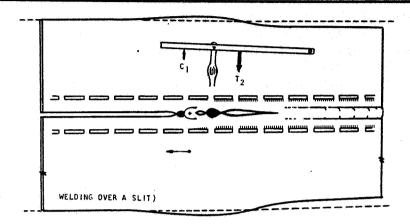


Figure 9 - The normal push-apart force (C_1) is diminished when the forward swelling moves only into a gap. This reduces net tension in the after puddle areas diminishing certain forms of cracking.

Changing Welding Stresses

There are many ordinary instruments for producing extraordinarily successful results such as welding the unweldable or as easily welding the difficult-to-weld. Introducing a local gap to compensate for a local problem is one instrument. A specific constant gap or tapered gaps are others. The difference between a closing gap and an opening gap is remarkable. Welding into a closing gap greatly raises and shifts forward the general after-tension. Welding into an opening gap has the opposite effect. This suggests that generalizations on residual stresses are tenuous, no matter how carefully the ex post facto material is scribed and sliced on the laboratory bench, when such vital conditions as gap, travel speed, and the others are not specified.

Of course, the instrument of change most vital and most easily altered is travel speed. At a very slow speed tensile strain across the solidus and the most sensitive after areas is great and usually damaging. Increasing the speed tends to move the tension aft further from the liquid into hot short regions. By

gradually increasing weld speed the maximum tension can be made to act across positions farther and farther after the solidus. It can be seen that this tension can be placed deliberately over a selected temperature-structure or it can be moved off of a particularly sensitive point. Indeed it always should be.

There is evidence on the 2014 aluminum alloy that damaging stress diminishes from 6 ipm to 13 ipm to rise again with higher speeds. It may be that at first the tension is moved back beneficially from a most sensitive hot short region but that with faster speeds the magnitude of peak-tension-stress, rising, becomes so great that it imposes damaging strain even on the later sturdier metallurgical structures.

In connection with this, the exotic attempts to influence stresses and structures by point heating or cooling must take into account the coherent thermal-and-stress geography of the part lest they sink into a sea of contradictory results.

For example, the effect of moderately heating and expanding C_2 would be deleterious by increasing the tensile stress imposed at T_2 . Yet by either moving the concentrated heating .6 inch back on to T_2 to relieve tension or by increasing the heat to turn C_1 plastic reducing its push-apart strength gives opposite salutary results. Similarly, cooling after the weld can produce harmful or salutary results depending on its location within an inch. The coherent pattern is vital to predicting the consequences of heat added or subtracted from point on a part surface.

In almost every case hold-downs -their force, position, and chilling quality - are not appreciated for their effect on the puddle, the solidifying weld, and the integrity of the post weld structures. Yet it is clear now that a row of hold-down fingers such as in Figure 5 (or in Figures 6, 7, 8 and 9) can have first order importance on the stress balances (nicely exemplified by the beam-lever analogies that are shown). A heavy hold-down force by the fingers of Figure 5 will counter the push-apart force C1 puts on the plates and thereby reduce the aft tension ordinarily imposed. On the other hand too much force causes the expansion of C1 to convert mainly into centerband upset. And then after the puddle passes when general shrink requires the material to go back out then the more thickened bead may split instead of stretch. closeness of the hold-down line to the weld edge also influences the see-saw balance of the prime actors, C1 and T2, and the other three also, since it tends to isolate the volume changes and stresses that lie between the hold-down lines from those outside. If nominal status is unrestrained material then the most abnormal situation has heavy hold-downs very close to the bead edge. Neither is optimum for that lies under a certain travel speed with fingers of a specific load placed at just the right position between zero and infinite distance from the weld. Inept choices increase warpage, cracks, porosity, and the need for more variation in parameter values in the course of the weld.

The degree of heat that shunts into the hold-down line produces effects similar to the mechanical restraints. They are especially significant when the alloy welded is of low thermal conductivity and the hold-down material is high. Since the heat sinks in the hold-down line there is little temperature rise or expansion beyond the lines. Any of the inwardly directed effects (good or bad), produced by the usual expansion in the outlying areas, are missing.

A philosophical point should be made here. These are significant influences, but complicated because of the multi-weighted balance that exists. Yet they cannot be ignored, because these instruments are commonly acting. There is too great a likelihood that they are by chance being misused to cause trouble. They should be rationally used to ward off trouble. Since these devices form every welding situation, it behooves every technician to become their master. All that needs to be acquired for this is understanding.

The theme carried through the last few paragraphs has dwelt on how to use the conditions that influence welds to diminish the level of defects that may be a norm. In other words by recognizing the importance of these conditions and choosing their value wisely the threshold of success can be shifted. The usual instruments for bringing this about —better tools, more precise power sources, more cooperative alloys; all well worked subjects— are not part of this discussion. The specific instruments discussed here, although varied, are all related to one common frame of reference: their push and pull ahead of, over, and behind the heat source. So little of the tortuous experience of the material is visible that this field has not received its proper ranking in importance, and its position may be prime. Certainly aluminum welds suggest this more emphatically.

Welding Stresses and Weld Quality

Consider now a theme that has a different slant. Instead of looking to shifting the thresholds in order to lower stresses and diminish average defect incidences examine for a while some unfortunate symptoms that dot a welded product. Many of these anomalies can be explained by tracing back across the territory of the dynamic-stress logic to find their cause.

It was during some pre-activation experiments of a large vertical aluminum welding fixture that it was found that the population of almost every kind of weld defect increased close to a gap dimension change. Cracks, porosity, lack-of-penetration, burn-thru, and distortion showed distinguishable rises in population in areas within 5 inches of gap changes. The explanation reveals one of the most interesting and significant sources of those problems, and also uncovers the relevance of the stress factor.

Starting with Fig. 9 imagine the weld progressing on a gap of a constant 0.010 inches. A natural balance exists between the largest forces of C1 pushing the plates apart and T2 pulling them together. To is naturally under a tensile strain and yielding, to an extent, to it. The minor loads of Tm and C2 are acting in there also. Tm is being stretched without much resistance considering its temperature. The balance is producing a nice and straight weld. Now the arc approaches a place where the gap changes to 0.006 inches in one quarter inch of run. Suddenly the plates are pushed apart almost 0.004 inch, the after-puddle material is abruptly stretched and if it cannot strain gracefully then it cracks between the weakest planes to relieve the tension. Furthermore it seems reasonable, (and as good a suggestion as any) to think that such a tension on the mushy zone could precipitate a tension-relieving-porosity which might not appear otherwise. An array of strain gages parallel to a weld has shown this transverse tension after the puddle as a spike on a record when the arc came to the point on a long tapered gap where the gap changed from opening at the rate of 0.001 inch per inch to closing at 0.001 inch per inch.

Consider how many times the gap changes, so insignificantly from a dimensional point of view, on an edge hand filed for machine welding. These little geometric but large dynamic activities occur on a machine weld when no change is made to any of the machine settings. But look at such a weld. In spite of constant parameters held to within $\pm 2\%$ of set values bead face and root width and height variations may vary commonly to 20% of nominal without an apparent reason. In the extreme the following may be found in the vicinity

- (1) A crack, porosity;
- (2) Bead crown thinout sometimes accompanying overpenetration even burnthru;
- (3) Bead crown rise accompanying lack of penetration; and
- (4) A crack and porosity.

If they should all appear the conditions would appear one after the other in the order shown counting in the direction of weld travel Why?

- (1) The crack and porosity after the puddle occur because the plates are pushed apart by the instant rise in the force of C_1 . (like Fig. 7).
- (2) The liquid of the puddle is stretched at the same time causing it to drop and have a thinned bottom. This drops the arc and causes overheating.

- (3) With 0.500 inch more of arc travel the rigid extraordinary C₁ collapses plastically (as it rises through 600°F). It upsets and the centerband ahead of the puddle thickens

 The arc then requires up to 15% more current just to maintain a constant root penetration. If current is not increased lack of penetration will occur and the weld crown will rise and narrow.
- (4) The last tension occurs because the abnormal upset occurring at the gap closing will, after the puddle passes, turn into an abnormal tensile strain.

The magnitude of the events in this train is increased mainly when the gap rate of change is high, that is when the rise over run is high. For example a 0.004 inch reduction in gap that occurs in 0.200 inch is more serious then 0.010 closure in one inch. It is not 0.004 inch of metal mass to be melted that requires change. It is the instantaneous separating of the parts by that much. stress events and their visible manifestations are exagerrated when a gap opens, then must close, and when the change is momentary. The rise and fall of anomalous stresses is bad enough when the weld controls are fixed but the problem is compounded and magnified when the operator reacts. The thinout of puddle caused by a closing gap does require a reduction in welding current which an alert welder may provide. But within an inch, when the arc enters the heavy upset, the requirement is extraordinary heat. He usually reacts late to the signs and provides the extra heat when it is not necessary and not wanted.

Optimum Welding Conditions

A quick change in travel, in weld current, in part thickness, in filler metal buildup, in hold-down conditions, or tacks will generate nearly the same train of anomalies. It is interesting to note that these conditions are seemingly so unrelated to one another in kind. So much that those that have been studied have been examined in isolated investigations. But when each is translated into forces exerted around the heat source in combination with the temperature of the material there appears a very important, heretofore unappreciated, common ground or language, one that requires each of those conditions to take into account its effect with the others thru this common channel. Without a fair sensitivity to effect of others on the force-and-stress balance any conclusions about any one's effect on cracks, residual stresses, distortion, even or weld parameters, do not have the general applicability they ought to have, or may seem to have. This is not to say that a conclusion about residual stresses or some other quality for a 10 ipm nominally proportioned weld are invalid. But the reservation is about how generally true the conclusion of such an experiment is. At what rate will the results change if travel speed, bead height, or hold down location change?

Certainly a slowly made weld has stresses formed quite differently from a fast made weld. Even tests of certain locations that appear to be different only in degree between slow and fast are not revealing the sizably different experiences of the micro-structures. Certainly a narrow specimen does not experience the high peak of stresses that a wide specimen does, and it should not carry the same degree of residual stresses in the same fine and critical locations (35% of the stresses in the fast welds may be due to plastic extrusion from longitudinal compression vectors). Surely now, a weld specimen with no butt line gaps must be used only reservedly to predict stresses on a filed field weld.

The sometimes-microcracks and sometimes-porosity have not quite been explained by physical or chemical thermodynamics. Is it at all possible to almost pull porosity out of the solidifying mushy-zone? This is different then from solidifying castings in which hydrogen pores push their way into being. If that were possible is there a detectable shape or pore size-frequency distribution or a mechanical property difference between two "expost facto" specimens that at first appear alike but were produced by different routes? Then the conclusions drawn from one should not apply to the other or others.

There is to be found scatter in reported test results, lack of reinforcement by conclusions of different test programs, and so many departures from assumed trends that the different reactions from supposedly standard conditions beg for explanations. remedy to apply immediately is to specify in all work the value of all conditions especially the heavily instrumental ones discussed here. Test results are often portrayed as "the change of A with a change of B" sometimes with different levels of C, the fact is that the change of A occurs in different degrees for each change in B, C, D, E, etc. Then C, D, E, etc. values must be part of documentation. The entire relationship must look like an n dimensional game of Tic-Tack-Toe. Too frequently other conditions or dimensions (even travel speed) have been thought of as having little influence on A vs B conclusions. Since the nature of the matter is like an "n" dimensional matrix any new information has to be identified by the conclusion and the right address, which is the value of all the relevant conditions. By that, as positions are filled in time a picture will take shape.

Another parallel remedy is to regard dynamic stress and those conditions that can effect it as probably important and set out to measure the effect of change. For example, put a strain gage near a weld. Make a weld and record the change. Change the value of one condition twelve times (like travel speed from 4 ipm to 26 ipm). Then: is the condition significant? If so, one plane in the matrix is defined, i.e. the weight of condition T changes on quality A can be sensibly appreciated or depreciated. By these remedial processes the isolated bits of data may be gradually hung together in the right order.

There are two other regimes, new ones, by which measured coherency may be acquired. The cost of either can be much less in the long run than the early jig saw puzzling suggested by the two prior systems that try to relate isolated experiments.



But first, it is interesting to recognize that a good welder or technician has probably not missed the significance of the important instruments. And his approach is good optimization even without a vision of the subject stress pattern. He will run a weld at one speed, then run one faster. If differences are discernible, and also good he will try a faster speed. If they are bad he will try a lower speed. He will try again and again until he finds one speed that produces better results than the next lower or next higher; or until the results are good enough; or until he has run out of time or money and must use what he has. He may try the 'same routine with finger hold-down location; and then with the other conditions he has seen to be important. Of course the valuable advantages to be found in reiterating (like doing travel again later) is a level of effort usually omitted. For him an understanding of the stress-characteristic patterns should help emphasize neglected instruments and make optimum hunting a little more rational.

But on a more sophisticated level, it would be more than useful to have an experimental technique or a computer technique that gave a topographic map of stresses or of strains for a given set of conditions. Note that the key qualification in the prior paragraph was the "if discernable". In practice a change of 2 ipm in travel may change the porosity rate from 21 per 1000 inches to 19, but this is hardly observable by a technician or credible in a practical number of laboratory specimens. So if it can be established and agreed that tensile strain on mushy or plastic or firmer aluminum of a given temperature is bad then an effort to create a system to expose the strain at all points on the part for any selected set of conditions would really be priceless.

Here is how a system should be used. Select a set of values for typical welding conditions (travel = 10 ipm, hold-down = 100 pounds per inch at one inch from the weld edge; etc.). Make a weld with this setting observing and recording the strain action. Print a three dimensional plot of strain around the heat source. Change the value of the condition being studied make another weld and draw up another plot. After several changes, the several plots (like the array in Figure 10) can be studied to see if the subject condition has a significant effect on the magnitude and position of the critical strains. And if it does, which value minimizes that strain and which does increase it. Similarly each other notable condition can be changed in order to determine (1) the relevance of the condition to strain and (2) the particular condition value associated with minimum strain. Note that optimum travel speed might be found in 12 welds, finger hold down optimum in 16. number of welds required to find the optimum set is not large considering the many feet of welding now made to statistically verify small effects.

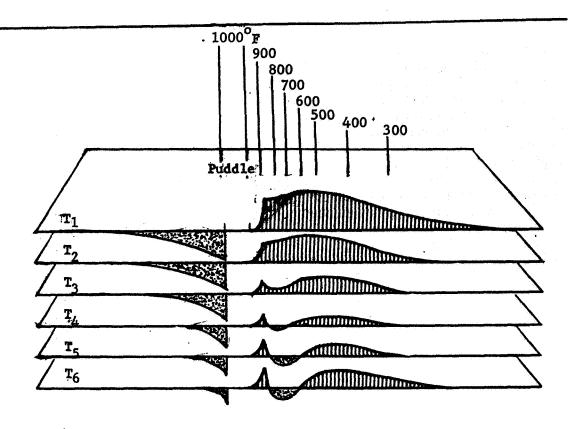


Figure 10 - Here is a simple example of how tensile strain across the centerline might be represented for welds made at six different travel speeds. This is a center section thru the strain map with transverse stretch plotted upward from the no-strain plane. In this, the value of T4 would probably identify the optimum weld speed. The same kind of array could be made for other significant weld conditions. This kind of information can be quite useful to a metallurgist who is concerned about the strain being suffered by a structure at a given temperature.

Considering the number of welding condition permutations waiting to be examined the measurement-and-observational system should not be the factor to impede progress. To be practical and to let the limit on progress lay with the setup-and-weld repititions the observational system must be almost photographic. With all the welding work to be done hours spent to measure strain in each incremental area of each specimen is inappropriate. Several systems hold potential for "seeing" strain all around a weld. Holography, for example, is one kind of candidate. For those offices whose interest lies in raising the level of industrial science and in making technology felt in the shop it seems that there is hardly a more worthy project than discovering or developing such an observational system. Welders complete millions of tons of work every month in one of the most basic of American industries.

Progress in Welding Science

It seems that past and present research is highly compartmentalized and especially when handled by metallurgists it deals with welds after-the-fact. It is a surprise that the dynamic responses of masses under particular heating, i.e. welding, has received such scant attention. Perhaps shrinkage tensions and residual stresses had seemed to adequately define the regime.

Where should welding science go now? It is proposed, somewhat presumptiously, that the door that <u>must</u> be passed is one that exposes stresses and strains experienced around the weld during <u>welding</u>. Metallographic conclusions and mechanical temperature-strain or stress tests based on assumed experiences by specimen areas, must be called into question until the experience of an increment by a weld can be documented. What really was its stress and strain? Figure 11 provides an example of the pertinence of this question.

Tension is customarily assumed to draw on the solidified bead and the weld-wrought transition structures right from solidification. But this appears to be valid only for the slower welds in aluminum. The faster welds may experience a severe biaxial compressions in the same points after the puddle. Incongruences in the collected body of research on the subject of strengths, fatigue life, and void geometries cannot be dismissed as experimental error. Metallographic and physical tests and organization must relate to the true experiences. Prior assumptions are called into question.

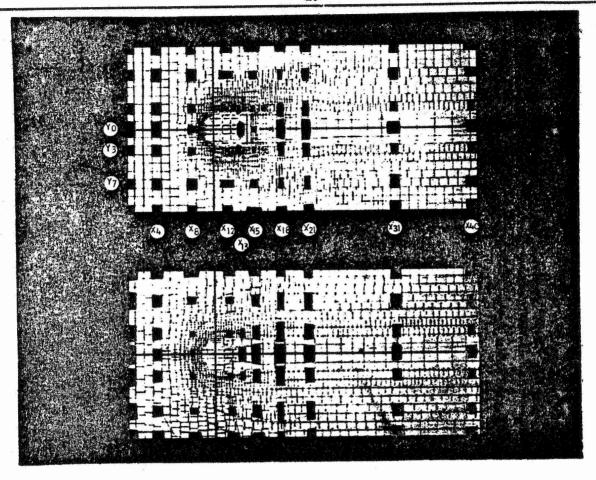


Figure 11 - The experience of a spot on the surface of a weld cannot be safely assumed. Moreso any assumption about the experience cannot be simply transferred to all other welds in the alloy. The gridding here (another possible form of strain expression) represents compression or tension in two axes by shortening or stretching the unit squares. The black tiles symbolize the immediate experience of the increment at the given location. The cast-to-wrought transition zone (lying under Y3) may experience in the fast weld (upper) biaxial compression at X15 when it is plastic but a strong transverse tension immediately after when it is short (X18). By contrast the same zone on a slow weld only experiences increasing transverse tension, first on plastic material then on firmer material.

Definition and measurement of actual in opera stresses and strains is a path that must be tread in efforts to further organize independent revelations and make basic researches more pertinent. How else will the great problem of weld parameter optimization be solved? The optimum sought may be the highest strength from an alloy or it can be minimum defects under given conditions. Vaster numbers of permuted and redundant experiments cannot promise the ultimate answers. But just putting an effective system into being should have wide and obvious effects on insights.

About the candidate system: (1) It should be experimental and (2) it should be turned easily into an efficient instrument for answering practical questions. Outside of benefits flowing thru science and a general improved comprehension of events the value of a system to metal fabricators will depend on (1) how much insight it can provide to pattern peaks and shifts for changed conditions in typical alloys and (2) how often it can be called on to solve particular shop problems (which are solved now by craftsmen not scientists).

Of course to be most useful the developed system cannot use a year to make and a year to test one weld. The cost of finding the one right welding parameter for a selected alloy should be low enough to be paid for by the savings to come from the right choice. There are a number of operations valuable enough to pay for answers to those kinds of questions. But the simpler the system is the more problems there are eligible to be economically answered.

Again, the only door to this seems to be welding experiments with an efficient observational system. Solve the problem of exposing strains easily, and energies can be used extracting meaning from graphic data instead of spent pulling data out of parts. This strain portrayal system must be experimental. Certainly the ultimate way to answer a parameter, tooling, alloy, or configuration problem is to punch a set of conditions into a computer with a developed program and letting it draw a map in minutes. Change a condition value and get the next map. But several comments deserve to be made.

First, the experimental mapping system, proven, and trusted must come first. Computer mapping is the door after this. Computer programs are so complicated and require so many assumed boundary conditions that they must be treated with some suspicion until they are verified by a trusted reference system which will have to come by proven experimental system. They must never be used until they produce the same pictures as experimental evidence. Second, some of the formulations or data that are now a fragment of the larger computer program should, and can, be taken from experimentally discovered information rather than pure mathematical

roots. The difficult roots may have questionable applicability or be questionable in their complexity. Third, the only practical reason for pursuing a mathematical program is that ultimately the cost-and-time saved in making a valid run on a set of conditions will be less than that of an experimental run. When a strain picture can be drawn in minutes the program work is justified.

If this eventually becomes true then many more applications will be able to afford the cost of optimization: (1) shops may ask frequently for the optimum weld schedule and for application, (2) they may ask for a report on the likely advantage of more expensive tool, (3) a metal company may ask for the reactions of a continuum of alloy variations to a variety of weld conditions and thereby really design a strong and weldable alloy, (4) perhaps ultimately a handbook of strain maps may be printed for each key alloy and used like navigation tables by a technician to determine the best combination of conditions to use to make a given weld. The possibilities are beautiful to consider.

CONCLUSIONS:

The subject of stress and strain fields around a moving heat source is neither too complicated to organize into a coherent visible system nor so simple that residual stresses can be used to describe weld area experiences.

Five stresses act across the weld line in turn as an arc passes. Their proportions and positions are considerably altered by weld parameter or condition changes.

These pushes and pulls effect the metallurgical character and integity of the weld area even when there is no apparent difference between after-the-fact examples.

Comprehension of the stress pattern and its manipulation with shop instruments are easily within the capabilities of the weld technician or welder.

But <u>peak</u> optimization including the greater number of weld conditions awaits an experimental method for "seeing" strains.

Ultimately the computer may be used to replace the experimental system, but it seems it should be only after it has proved (1) equal to the experiment and (2) quicker to execute.

With the completion of each of these stages in turn the advantages to knowledge and to accomplishment will be multiplied, because more questions will be eligible for consideration and solution.

REFERENCES

- 1. Chihoski, R. A., "The Characteristic of Stress Fields Around a Weld Arc Moving an Aluminum Sheet" paper given at AWS National Fall meeting Houston Texas Oct. 1967.
- 2. Gott, C; Clover, F; & Rudy, J; "Metal Movement and Mismatch in Aluminum Welds" Welding Journal Res Supl 47 (8), Aug 1968.
- Clover, F. R. & Chihoski, R. A. "New Generation of Weld Tooling Goes Vertical" Welding Journal 49 (10) Oct. 1970.
- 4. Chihoski, R. A., "Understanding Weld Cracking in Aluminum Sheet" Welding Journal 51 (1) Jan. 1972.
- 5. Chihoski, R. A., "The Character of Stress Fields Around a Weld Arc Moving on Aluminum Sheet" Welding Journal Res Supl 51 (1) Jan. 1972.



N74 30926

TITANIUM HONEYCOMB STRUCTURE

By R. A. Davis, S. D. Elrod, and D. T. Lovell

INTRODUCITON AND BACKGROUND

During initial engineering design studies for a commercial supersonic transport, titanium was shown to provide the lowest weight structure to carry a given payload. A summary of this data compared to aluminum and stainless steel is shown in Figure 1. The lowest structural weight has a favorable impact on the operating economics of a commercial transport airplane. As design refinements occurred based on aerodynamic, propulsion, pressure loads, flutter, and range / payload developments, a mach. 2.7 fixed wing titanium airplane evolved.

The major impact of this final configuration on structures and materials technology was to require development of a titanium honeycomb sandwich system for wing cover panels. There were basically three technical reasons for a sandwich structure. First, spanwise and chordwise and loadings (Figure 2) were generally low and sandwich material provided the most efficient structure. Second, flutter testing showed that high wing stiffness was required and again sandwich structure was most efficient. Third, liquid fuel was carried in direct contact with the wing structure in integral fuel tanks and sandwich structure provided thermal insulation for the fuel.

Figure 3 shows the temperature profile for the prototype supersonic transport. Generally the basic structure would be operating at 450°F with some local areas reaching peaks of 500°F under special flight conditions. For the basic wing sandwich material the maximum operating temperature would be 450°F. Figure 4 shows the major structural concepts planned for construction of the prototype aircraft. Titanium honeycomb sandwich applications were also expanded to the power plant pod and empennage structure for improved structural efficiency. Additionally, resistance to relatively high senic levels (160 dB) was required in portions of the empennage structure and honeycomb sandwich met this requirement. Titanium honeycomb sandwich was not planned for the

most highly loaded center section of the wing nor the relatively deep (up to 11 inches) wedge structure on both leading and trailing edges of wing and tail structure of the prototype airplane because process development could not be carried out in time to meet the planned prototype manufacturing schedule.

PROCESS DEVELOPMENT

The criteria of concern in development of a brazed titanium system involved three major areas; (1) metallurgical compatibility, (2) manufacturing feasibility, and (3) design viability. Process development, although concerned primarily with metallurgical parameters, had to consider concurrently both manufacturing and design aspects.

The initial step was to assess and selectively test brazing alloy systems for compatibility with titanium, for processing parameters, and for preliminary strength properties. Table 1 shows a summary of the various brazing alloy systems and their pertinent characteristics. As a result of this assessment, the aluminum base alloys were selected for further evaluation and subsequently aluminum alloy 3003 was chosen as the best alloy. This choice was based on brazing temperature range, foil availability, flatwise tensile strength and corrosion resistance.

A primary concern was the formation of any embrittling effects as a result of the formation of titanium aluminide (TiAl₃) during the brazing cycle. The brazing cycle temperature envelope was developed to limit titanium aluminide formation by restricting the holding time above $1175^{\circ}F$ to one hour maximum. With this control, an aluminide layer of .0003 inches maximum is formed. This thin layer has no noticeable effect on static properties of the basic titanium 6A1-4V face sheet alloy. Fatigue properties may be reduced by approximately 20%, however, due to difficulties in specimen preparation, the available data are inconclusive. Figure 5 shows the final high temperature portion of the braze cycle envelope used for process control.

85<

Another major concern was galvanic coupling effects resulting from exposing aluminum and titanium to a corrosive environment. From a theoretical standpoint based on single electrode potentials of the two alloys, aluminum should preferentially corrode when in contact with titanium. Extensive accelerated laboratory testing and commercial airline fleet exposure showed that no galvanic accelerated corrosion effects occurred. Figure 6 shows an unprotected honeycomb sandwich panel installed on the mud flap of a Boeing 727 model airplane for service evaluation. Approximately three years of airline service exposure have been carried out with no corrosive attack occurring.

Although all corrosion testing indicated that galvanic acceleration would not be a problem, a conservative approach was taken by stipulating that non-perforated core would be used exclusively. With this approach each individual cell cavity would be hermetically sealed and any progression of moisture through a panel would have to progress a cell at a time.

In 1969 at the time of initiation of development of brazed titanium honeycomb sandwich, the state-of-the-art structural sandwich system which existed was bilver brazed Fi 13-7mo stainless steel. This system had been used extensively on the B70 supersonic bomber. A comparison of the stainless steel and titanium honeycomb sandwich processes is shown in Table 2. Several items are note-worthy. First the brazing temperature of the titanium system is much lower and this fact simplifies both tooling and heat source requirements. Secondly, the titanium system requires no post brazing thermal cycle. Finally, a generous amount of aluminum braze alloy is used during the process to produce a .030" fillet at the core to face sheet junction. With the standard .002" thick one-quarter inch cell size and optimum braze conditions, this amount of braze alloy provides enough strength to break the 3A1-2.5V core foil during a flatwise tensile test.

MECHANICAL PROPERTIES

As process development progressed, firm requirements were developed for basic honeycomb panel strength. The standard honeycomb core consisted of .002"

thick one-quarter inch cell produced from 3A1-2.5V foil (density = 5 pounds per cubic foot). Cell walls were corrugated for added stiffness. Static mechanical properties were developed for the basic honeycomb panels from tests of flatwise tension, flatwise compression, plate shear, beam shear, and edgewise compression specimens. Figure 7 contains a summary of the mechanical property data.

In addition, creep behavior was of concern and a simple single cell tubular test specimen was developed for evaluation. This specimen permitted easy mechanical loading for data gathering. The data were later confirmed using standard 2 inch square honeycomb sandwich specimens. Figure 8 contains a summary of both single cell and multiple cell test specimens for both 450° F and 600° F. All test fractures that occurred were of a stress rupture nature. No perceptible creep occurred with any of the test specimens.

DESIGN DEVELOPMENT

Basic panel strength requirements could be met with five pound per cubic foot core. At load transfer areas however, where mechanical fasteners were used to fasten panels to spars and ribs, higher density core was used. This high density core provided both increased resistance to environmental effects at panel edges as well as capability to withstand fastener loads. Table 3 shows an approximate distribution of the various types of core planned for use on the supersonic transport prototype. Edge designs utilizing the higher density core are schematically shown in Figure 9.

NDT

One of the major developments involved utilization of appropriate non-destructive testing techniques to ascertain that brazed panel quality was acceptable. Figure 10 shows schematically the techniques utilized to determine panel quality. The eddy current scan technique would be applied 100% to each panel to check for the proper distribution of the aluminum braze alloy within the panel. Radiographic inspection was used selectively to determine node flow, shear tie integrity and the extent of core crushing



if any. The Ultrasonic C-Scan technique was used 100% on each panel to determine braze alloy fillet size and the location of any sheet-to-core voids. Figure 11 shows an ultrasonic trace representing three levels of fillet size.

SCALE-UP

Although many fine ideas can be satisfactorily demonstrated in the laboratory, the final proof of acceptability for aerospace structural usage consists of full scale hardware fabrication and testing. Concurrent with the design phase of the prototype program, a major effort was devoted to building three foot by twenty foot panels representative of both wing and empennage designs. The philosophy behind this approach is that there are generally technical problems encountered with fabrication of full scale hardware that are not revealed in small scale fabrication. This fact was also true with this aluminum brazed system. Considerable effort was expended in tooling development, temperature control, retort purging, panel restraint, core machining and non-destructive testing.

The simplified tooling concept used for face sheet forming and panel brazing is shown in Figure 12. This concept was devised to minimize production costs of the process. In fact masonite side walls were found to be acceptable as side wall retainers for the braze fixture. Figure 13 shows a successfully completed 20 foot wing panel.

SUMMARY

At the time of the SST cancellation, the development and evaluation of the system was essentially complete for the planned applications. Design criteria and properties were established. Subsequent extensive testing has shown that neither corrosion nor creep rupture would be a problem for the proposed applications. Process and material specifications and quality acceptance criteria and inspection methods were established as demonstrated by the successful fabrication of 3' x 20' production wing panel. At the present time, further development work sponsored by the Department of Transportation is underway to extend the process for broader applications such as more highly loaded structure, wedge configurations, and acoustic panels.

TABLE 1

BRAZE ALLOY SYSTEM COMPARISONS

ALLOY SYSTEM	CHARACTERISTICS					
	COST	BRAZE TEMPERATURE	CORROSION RESISTANCE	STRENGTH	METALLURGICAL COMPATIBILITY	
Silver Base (Ag, Ag-Al)	High	Moderate	Poor	High	Good	
Noble Metals (Au, Pd)	(Very High)	High	Good	High	Good	
TI-Gu-Ni	High	High	Excellent	High	Embrittling	
Ti-Zr-Be	High	High	Excellent	High	Embrittling	
Copper Base	Low	High	Good (if Diffused)	High	Embrittling	
Al	Low	Low	Good	Moderate	Good	

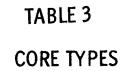
TABLE 2

COMPARISON - STAINLESS STEEL & TITANIUM H/C SANDWICH

ITEM	PH 15-7 Mo/Ag	Ti-6AI-4V/AI	
Braze Temperature	1900 ⁰ F	1250 ⁰ F	
Faying Surface Joints	Us ed	Not Used	
Intercell Hermetic Seal	No	Yes	
Post Braze Heat Treatment	Required	Not Required	
Braze Alloy Cost	High	Low	
Braze Alloy Quantity	Small	Large	
Fillet Size	.010 inch	.030 inch	
Quality	Moderate	High	
Corrosion Resistance	Fair	Good	
Fl atwi se Tensile Strength	900 psi	1500 psi	

90





DESIGNATION	CELL SIZE Inch	WALL THICKNESS Inch	DENS ITY lbs/cu.ft.	SST % USAGE
4-20	1/4	.002	4. 9	70
4-30	1/4	. 003	7.3	12
2-20	1/8	.002	9, 3	10
2-30	1/8	.003	14.0	3
2-60*	1/8	.006	28, 5	5 .

^{*} Ti-6AI-4V - All Others Ti-3AI-2.5V

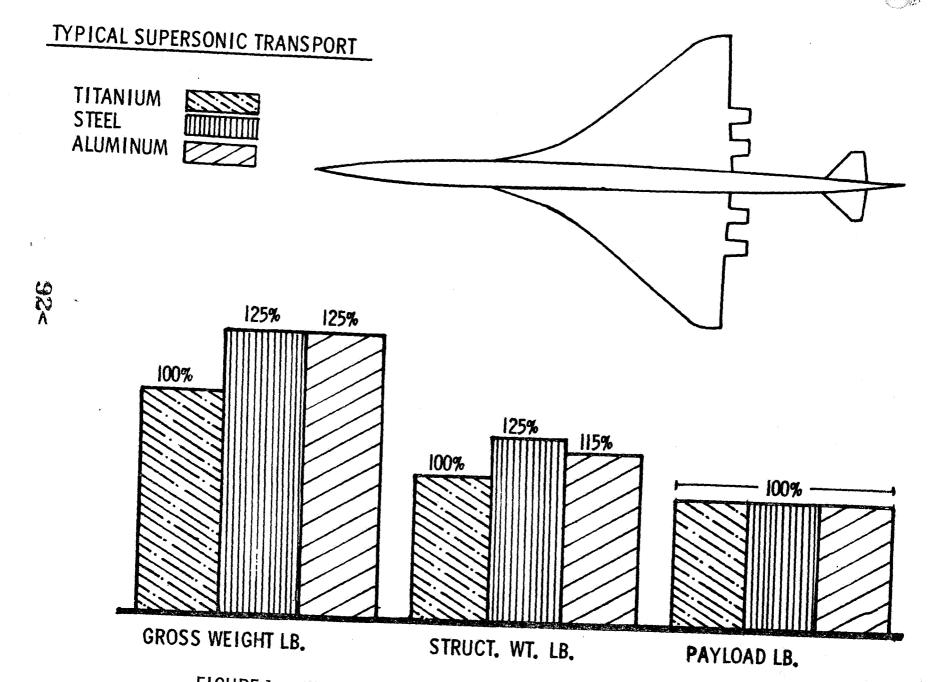


FIGURE 1 WEIGHT COMPARISON FOR DIFFERENT STRUCTURAL METALS

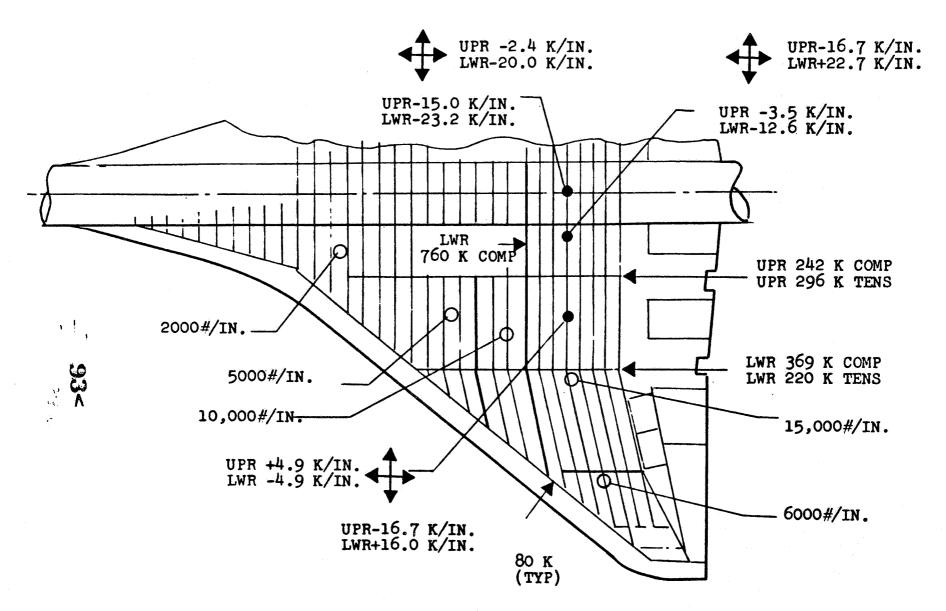


FIGURE 2 TYPICAL WING END LOADS

FIGURE 3 SST SURFACE TEMPERATURE, OF.

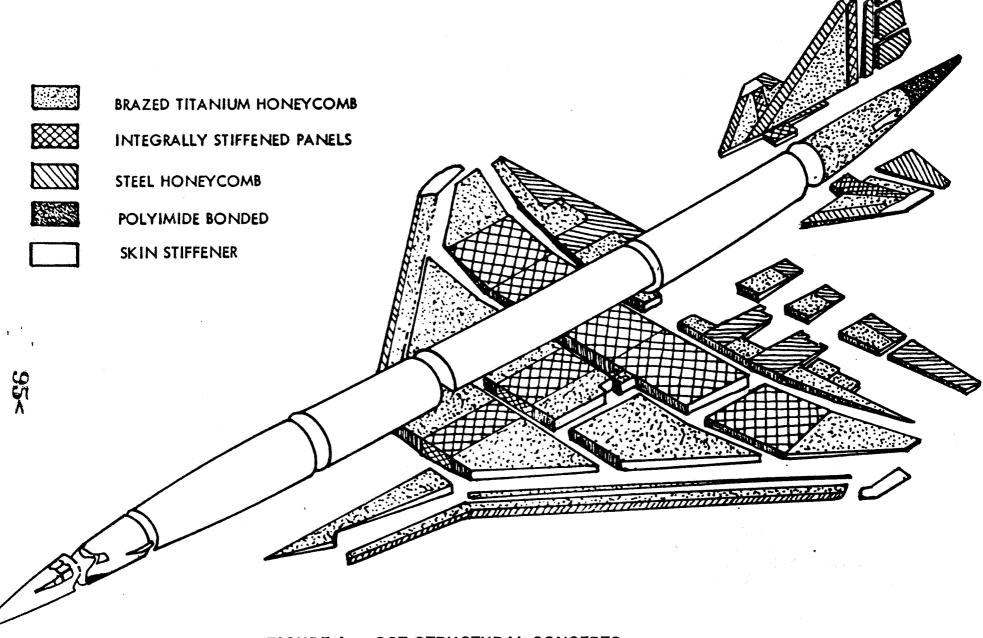


FIGURE 4 SST STRUCTURAL CONCEPTS

に の A

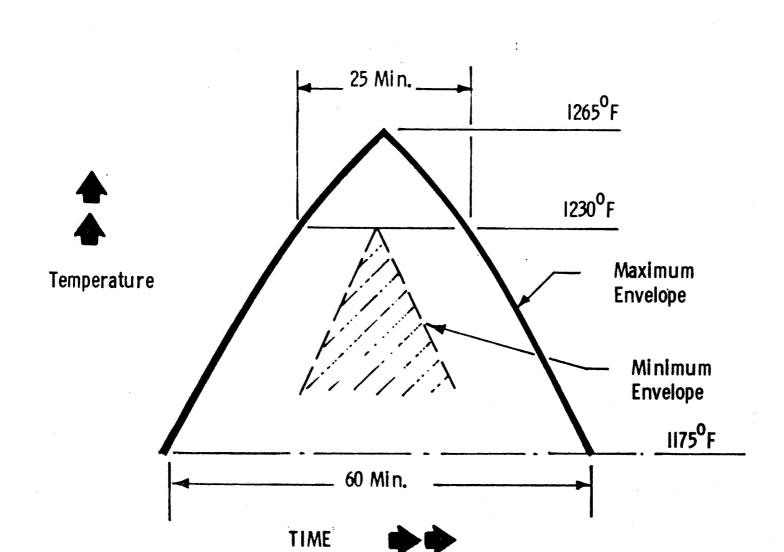


FIGURE 5 BRAZE CYCLE ENVELOPE

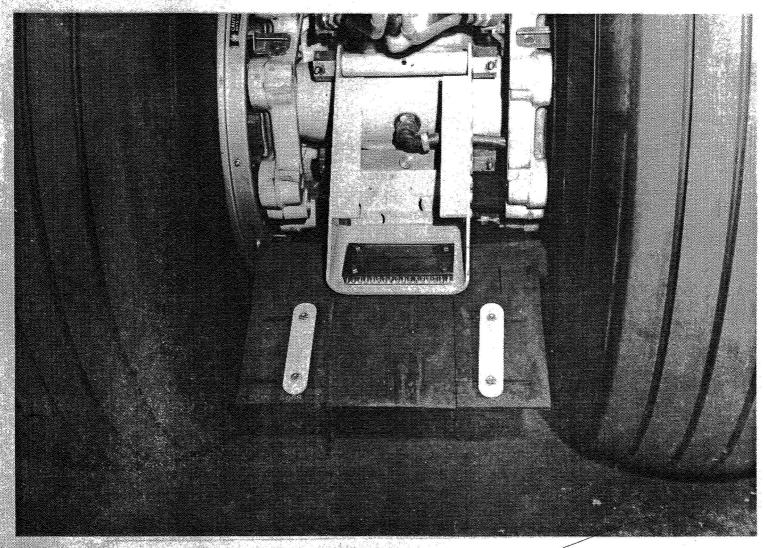


FIGURE 6 727 LANDING GEAR CORROSION TEST INSTALLATION

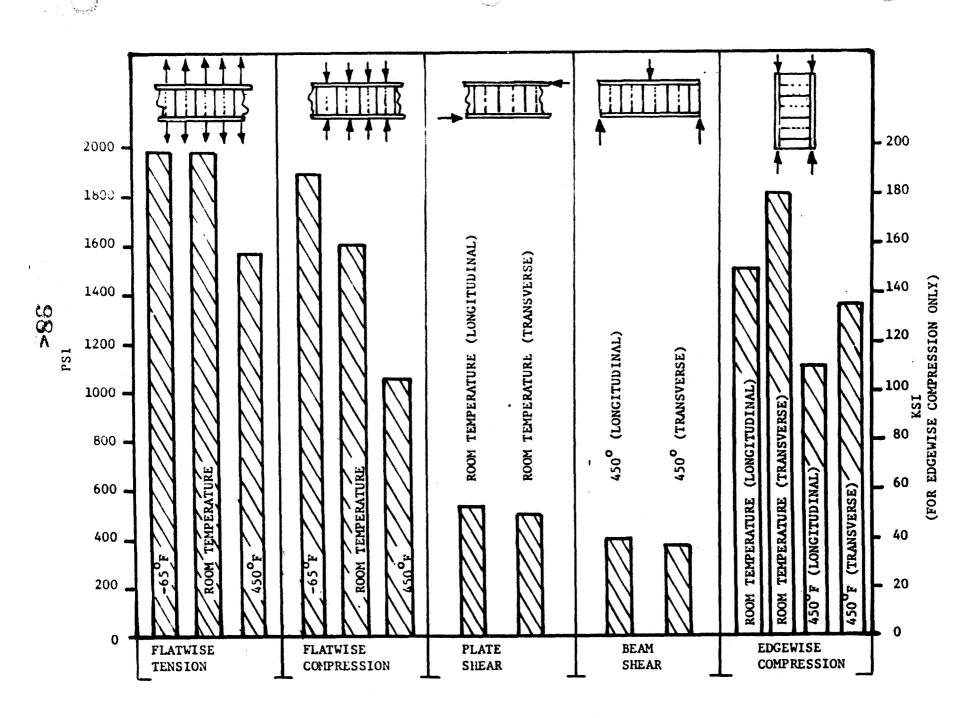


FIGURE 7 AVERAGE STRENGTH OF HONEYCOMB PANELS WITH 4-20 CORE

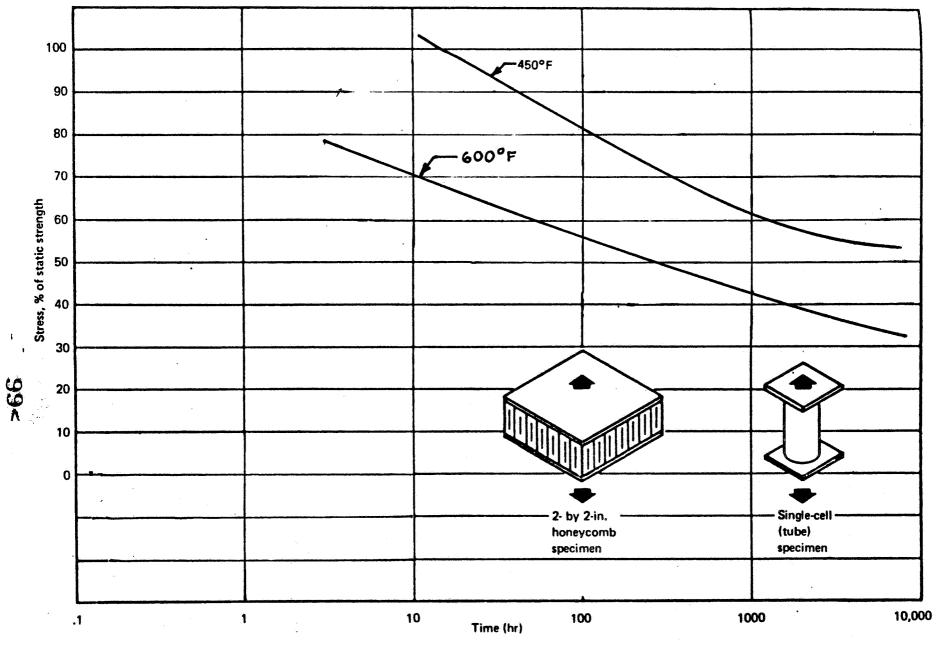
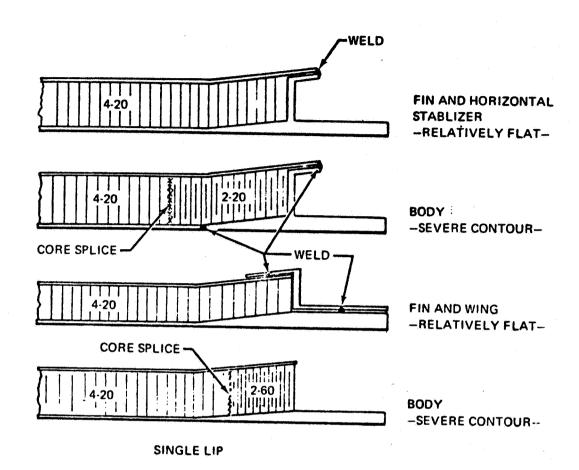


FIGURE 8 STRESS -RUPTURE STRENGTH





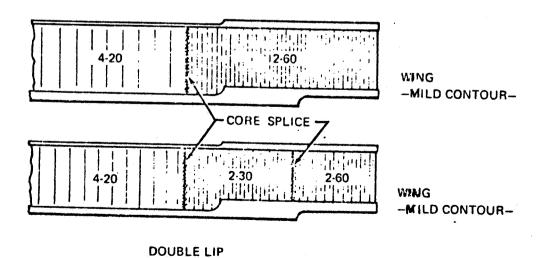


FIGURE 9 TYPICAL EDGE DESIGNS
100<

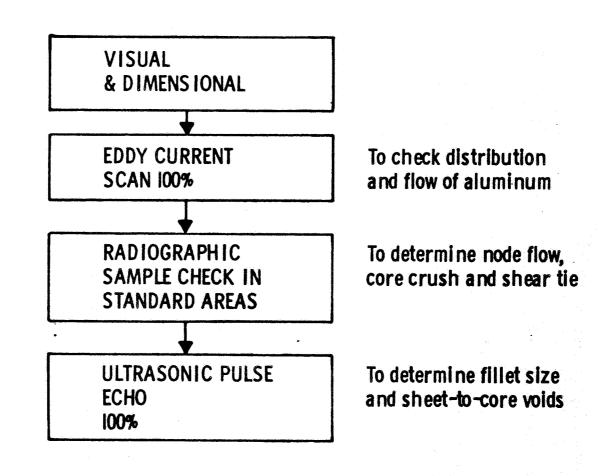


FIGURE 10 NON DESTRUCTIVE TESTING

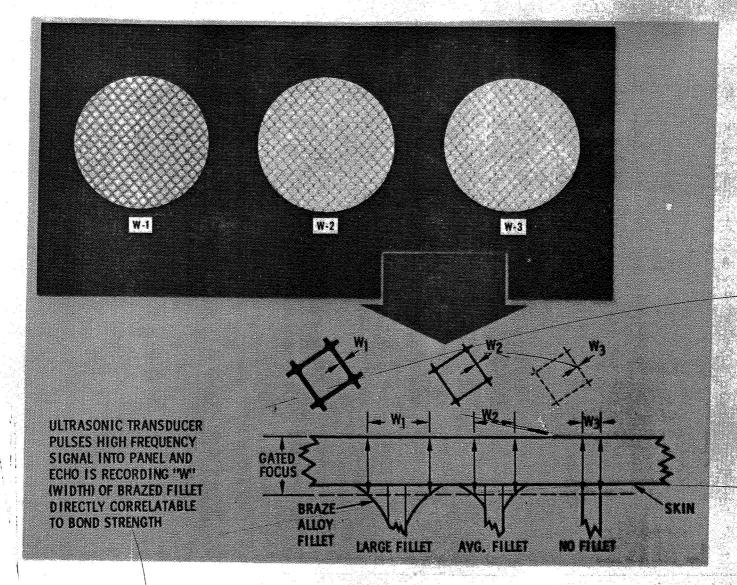


FIGURE 11 ULTRASONIC INSPECTION FOR BRAZING OF CORE TO SKIN

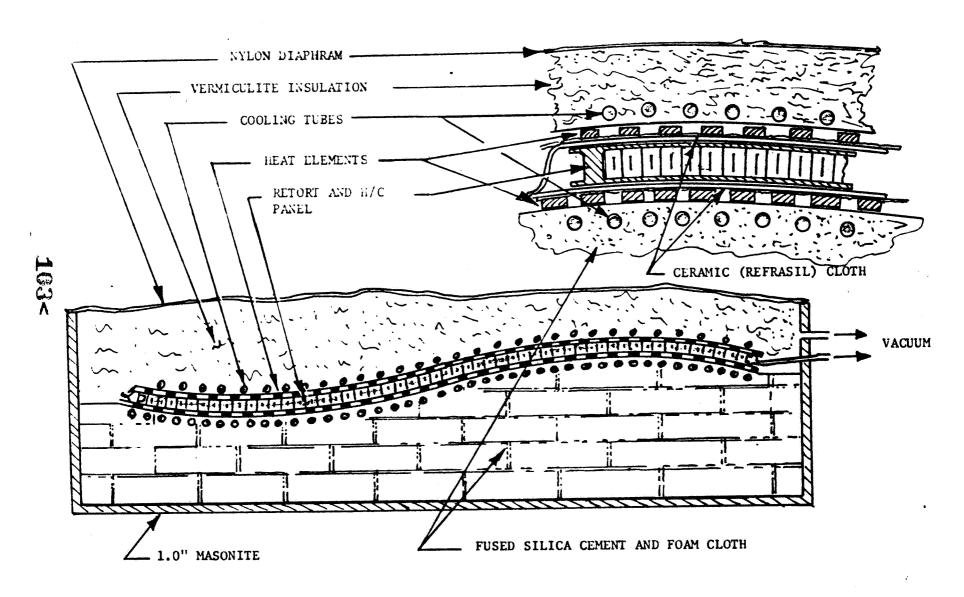


FIGURE 12 SOFT TOP BRAZE TOOL

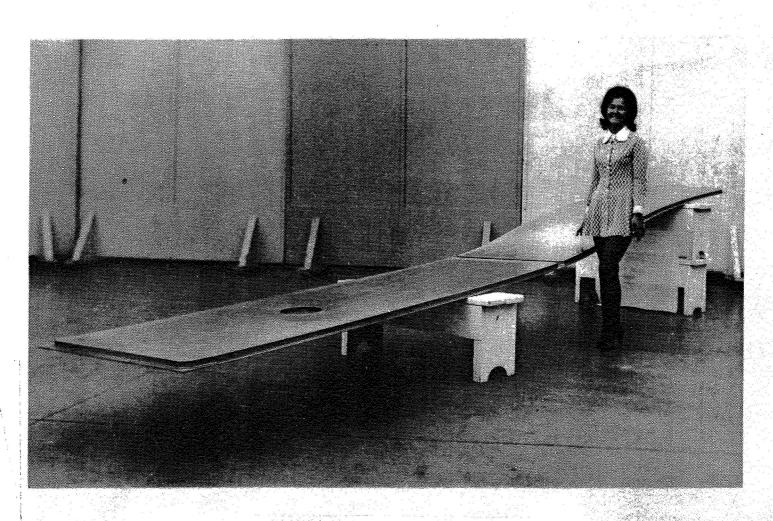


FIGURE 13 3' x 20' WING PANEL

7 N74 30927

THE EFFECTS OF HIGH-TEMPERATURE BRAZING AND THERMAL CYCLING ON THE MECHANICAL PROPERTIES OF HASTELLOY X

Dennis L. Dicus and Dr. John D. Buckley

NASA Langley Research Center Hampton, Virginia

Presented at the Symposium on Welding, Bonding, and Fastening

Williamsburg, Virginia May 30-June 1, 1972

THE EFFECTS OF HIGH-TEMPERATURE BRAZING AND THERMAL CYCLING

ON THE MECHANICAL PROPERTIES OF HASTELLOY X

Dennis L. Dicus and Dr. John D. Buckley

NASA Langley Research Center Hampton, Virginia

ABSTRACT

Data are presented on the effects of brazing alloy, brazing operation, thermal cycling, and combinations of these on the yield strength, elongation, tensile strength, and fatigue life of thin gage Hastelloy X. These data show that brazing at $1461~\rm K~(2170^{\circ}~F)$ with a Ni-Pd-Au alloy and subsequent exposure to 200 service thermal cycles between 533 and $1144~\rm K~(500^{\circ}~and~1600^{\circ}~F)$ resulted in reduction of as much as 39 percent in yield strength, 33 percent in elongation, 14 percent in tensile strength, and 26 percent in fatigue limit of Hastelloy X, as compared to as-received materials. These property losses were primarily caused by the brazing operation rather than the subsequent service thermal cycles.

INTRODUCTION

High-temperature brazing is a commonly used joining process in the aerospace industry (refs. 1, 2, and 3). Complex structures like heat exchangers are frequently built using a step brazing technique that allows successive parts to be joined, one or two at a time with successively lower melting point brazing alloys (refs. 2 and 4).

A step-brazing process was employed in the fabrication of the regeneratively cooled Hypersonic Research Engine (ref. 5). Test models of the engine's cooling structure, which is made of Hastelloy X,* failed during burst tests at stress values much lower than predicted by the known mechanical properties of the metal. In addition, other models of this same structure failed prematurely during thermal cycling under stress (ref. 6). A research program was undertaken at NASA Langley Research Center to assess the probable cause of the apparent degradation of the properties of Hastelloy X. The objective of this study was to determine the effects of (1) brazing alloy, (2) brazing operation, and (3) simulated engine operating cycles (hereinafter referred to as service thermal cycles) on the fatigue and mechanical properties of Hastelloy X.

^{*}Nickel-based superalloy manufactured by Union Carbide Corporation.

MATERIALS AND SPECIMENS



Table I shows the chemical composition of the base metal and brazing alloys used in this study. Table II shows the melting temperature range of the two brazing alloys used, Palniro 1* and Palniro 4.* The melting temperature range of Palniro 1 is lower than that of Palniro 4 allowing the use of these alloys in a step-brazing process.

Figures 1(a) and 1(b) show the bare metal and as-brazed tensile test specimen configurations. Bare metal and as-brazed fatigue test specimen configurations are shown in figures 2(a) and 2(b). All specimens were cut from sheet material and machined to final size.

Figure 3 shows the specimen configuration used to study interactions between the base metal and the brazing alloy. Longitudinal sections were cut from specimens of this type after brazing and mounted for metallographic and electron microprobe analysis. Transverse and longitudinal sections were cut from tensile specimens after testing and mounted for metallographic examination. Fracture surfaces of the tensile specimens were analyzed using a scanning electron microscope.

EQUIPMENT AND PROCEDURES

Prior to brazing, specimens were deburred and cleaned by the following method: degreased with trichloroethylene, dipped in alkaline solution, rinsed with tap water, rubbed with pumice, descaled by immersion in an acid (30 percent nitric, 15 percent hydrofloric, 55 percent water) bath for 15 minutes, rinsed with tap water, and hot-air dried. Tensile tests on cleaned specimens showed this cleaning procedure had no detrimental effects on Hastelloy X. After cleaning, a 76.2 µm (0.003 in.) thick strip of brazing alloy was tack spot welded to the tensile and fatigue specimens. On the tensile specimens, the brazing alloy strip covered the length of the test section, and on the fatigue specimens it covered a 5.1 cm (2 in.) section in the middle of the specimen. (See figs. 1(b) and 2(b).) Chromel-alumel thermocouples were tack welded to the specimens just outside of the test section for temperature control and monitoring during brazing. The specimens were placed on an alumina-coated carbon block and inserted into a vacuum furnace in the horizontal plane. The brazing heat cycles for both the Palniro 1 and Palniro 4 brazing alloys are described in Table III and illustrated in figure 4. The two brazing operations are quite similar with the Palniro 1 operation involving a lower maximum temperature and a shorter total time than that used for Palniro 4. After brazing, the tensile and fatigue specimens were hand-sanded and polished to reduce the thickness of the brazing alloy to approximately 25.4 µm (0.001 in.), final machined, and deburred.

^{*}Manufactured by Western Gold and Platinum Company.

Specimens to be exposed to service thermal cycling were again instrumented with thermocouples, mounted on a transite block, and lightly clamped to prevent distortion during heating. Figure 5 illustrates the service thermal cycling procedure which was accomplished by radiant heating in air with a tungsten filament quartz lamp bank coupled to a specimen temperature controller. Prior to the first cycle the specimens were preheated to 977 K (1300° F) in 180 seconds (3 minutes) and cooled by airblast to 533 K (500° F). These specimens were then cycled 200 times between 533 and 1144 K (500° and 1600° F). Each cycle lasted 80 seconds and included a 20-second hold at the high temperature. The specimens were cooled from 1144 to 533 K (1600° to 500° F) by airblast.

Two series of tensile tests were conducted in the air at room temperature. An initial screening series covering the material conditions shown in the table below was conducted without strain measurement to determine ultimate tensile strength and to identify conditions that should be examined in the fatigue tests and another series of tensile tests. These initial screening tests were conducted at a strain rate of 0.02 per minute.

Material Conditions Examined in Initial Screening Tensile Tests

- 1. As-received
- 2. As-brazed with Palniro 1
- 3. As-brazed with Palniro l and service thermal cycled
- 4. As-brazed with Palniro 4
- 5. As-brazed with Palniro 4 and service thermal cycled
- 6. As-exposed to Palniro 4 brazing heat cycle (no braze alloy used)
- 7. As-exposed to Palniro 4 brazing heat cycle (no braze alloy used) and service thermal cycled
- 8. As service thermal cycled (no braze alloy used)

The second series of tensile tests was conducted at strain rates of 0.002 per minute and 0.08 per minute before and after yielding, respectively. Tensile strain for this test series was measured by a strain gage extensometer with a 5.1 cm (2 in.) gage length.

Constant amplitude fatigue tests were conducted in subresonant-type axial load fatigue machines operated at a frequency of 30 Hz (ref. 7). Load was sensed by a weigh-bar in series with the gripped specimen. A wire strain gage bridge cemented to the weigh-bar supplied the load signal to an oscilloscope

used to monitor the cyclic load. The machines were calibrated periodically to maintain a loading accuracy of $\pm 88N$ (± 20 lb).



DISCUSSION OF RESULTS

The results of the initial screening tensile tests are summarized in figure 6. Eight different parent metal conditions were examined with a minimum of five tests each. These data indicate that Palniro 1 brazing and/or the service thermal cycling had virtually no effect on the ultimate tensile strength of Hastelloy X. However, the four conditions involving the Palniro 4 brazing operation each caused about a 6 percent reduction in ultimate tensile strength. Since this reduction occurred in both brazed specimens and unbrazed specimens subjected to the Palniro 4 heat cycle, it appears that the brazing heat cycle is primarily responsible for the reduction in ultimate tensile strength.

Metallographic studies were conducted on sections cut from brazing alloy-base metal interaction specimens (fig. 3) to observe the effects of the brazing operation on Hastelloy X. Figures 7(a), 7(b), and 7(c), respectively, show the virgin base metal, the base metal after brazing with Palniro 1, and the base metal after brazing with Palniro 4. The Palniro 1 and Palniro 4 brazing operations resulted in grains which were 1.2 and 6 times larger than as-received grains, respectively.

Figure 8 illustrates the effects of the step-brazing procedure involving successive brazing operations with Palniro 4 and Palniro 1. The microstructure resulting from the first step, brazing with Palniro 4, is shown in figure 8(a). The result of step 2, brazing with Palniro 1, is illustrated in figure 8(b). In figure 8(b) the base metal above the brazing alloy has experienced both brazing cycles and shows no further grain growth over figure 8(a). The base metal below the brazing alloy has experienced only the lower maximum temperature, Palniro 1 brazing cycle.

Sections cut from these interaction specimens were subjected to electron microprobe analysis. Considerable dissolution of the nickel in the base metal adjacent to the brazing alloy interface occurred during the brazing operation. Migration of the nickel into the brazing alloy was indicated by higher nickel content present in the brazing alloy. In addition, microsegregation of the gold in the brazing alloy was also indicated.* This dissolution and migration of the nickel apparently had no effect on the ultimate tensile strength of the metal, however, since the tensile strength of the brazed specimens and of the unbrazed specimens subjected to the Palniro 4 heat cycle was about the same. (See fig. 6.)

Additional tensile and fatigue tests were performed on Hastelloy X in the following conditions: as-received, as-brazed with Palniro 4, and as-brazed and service thermal cycled. Figure 9 shows typical stress-strain diagrams for

^{*}Analysis performed by W. Barry Lisagor, NASA Langley Research Center.

the conditions just described. A summary of the tensile test results is shown in table IV. These data show that the Palniro 4 brazing operation results in a 6 percent decrease in ultimate tensile strength, a 35 percent decrease in yield strength, and a greater than one-third reduction in elongation to failure. Specimens subjected to service thermal cycling after brazing showed only small changes in these properties as compared to the changes resulting from the brazing operation.

Due to the unusual finding that both the yield strength and the elongation to failure decreased as a result of the Palniro 4 brazing operation, sections were cut from the as-tested specimens for metallographic examination, and the fracture surfaces were studied with a scanning electron microscope. A photomicrograph of the as-received base metal before tensile testing is shown in figure 10(a). Figures 10(b) through 10(d) show photomicrographs typical of the as-received, as-brazed with Palniro 4, and as-brazed and service thermal cycled specimens after testing. These photomicrographs showed grain growth similar to that shown in figure 7. Figures 11(a) through 11(c) show typical fracture surfaces of the as-received, as-brazed with Palniro 4, and as-brazed and service thermal cycled specimens. Intergranular fracture occurred in the two specimens exposed to the brazing operation, whereas intragranular fracture occurred in the as-received specimen. This intergranular cracking occurred only in specimens which were actually brazed with Palniro 4 (i.e., not in specimens subjected to the Palniro 4 heating cycle alone). Consequently, selective embrittlement of the grain boundaries promoted by the thermochemical reaction of the Hastelloy X with the brazing alloy appears to have occurred. In addition, the fracture surfaces within the grains of the specimens exposed to brazing had a ductile appearance.

The grain growth resulting from the Palniro 4 brazing operation normally would indicate an annealing phenomenon associated with the high brazing temperature. The metal within the grains remained ductile. This annealing would account for the observed reduction in ultimate tensile strength and yield strength. The intergranular failute apparent in the fracture surfaces of the brazed specimens indicates embrittling, which would account for the reduction in elongation to failure.

Figure 12 presents the results of constant amplitude fatigue tests on specimens exposed to the same brazing and service thermal cycling conditions as the tensile specimens. The specimens brazed with Palniro 4 exhibited a fatigue limit (the maximum stress that will not cause fracture in 10^7 stress cycles) or $386~\rm{MN/m^2}$ (56 KSI) as compared to $469~\rm{MN/m^2}$ (68 KSI) for the asreceived specimens. Those specimens brazed and service thermal cycled had a fatigue limit of $345~\rm{MN/m^2}$ (50 KSI). These results are consistent with the tensile test results in that the brazing operation caused most of the observed degradation of the mechanical properties of Hastelloy X and that service thermal cycling had only a small additional effect.

CONCLUDING REMARKS

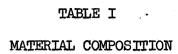
The results of these studies into the effects of brazing alloy, brazing operation, and service thermal cycling on the mechanical properties of Hastelloy X are as follows:

- 1. The Palniro 1 brazing operation apparently had little or no effect on the mechanical properties of Hastelloy X.
- 2. The Palniro 4 brazing operation, however, decreased the ultimate tensile strength by 6 percent, lowered the yield strength by 35 percent, and decreased the elongation to failure of Hastelloy X by more than one-third. These effects were probably caused by both the higher brazing temperature and a thermochemical reaction of the brazing alloy with the base metal. The lower ultimate tensile strength and yield strength were probably caused by the brazing temperature while the lower elongation to failure was apparently due to selective embritlement of the grain boundaries resulting from a thermochemical reaction. In addition, the Palniro 4 brazing operation caused an 18 percent reduction in the fatigue limit of Hastelloy X.
- 3. The effect of service thermal cycling on the mechanical properties of Hastelloy X was much less significant than the effect of the Palniro 1 brazing operation. Two hundred thermal cycles between 533 and 1144 K (500° and 1600° F) caused further but smaller reductions in ultimate tensile strength, yield strength, and fatigue limit of 8 percent, 1 percent, and 8 percent, respectively.

REFERENCES

- 1. Vagi, J. J.; Monroe, R. E.; Evans, R. M.; and Martin, D. C.: Joining of Nickel and Nickel-Base Alloys. NASA TM X-53447, 1966.
- 2. Cremer, George D.; and Long, John V.: Brazing Bonanza Brazing of Aero-Space Materials. ASM Technical Report No. C7-10.9, 1967.
- 3. Beuyukian, C. S.: Fluxless Brazing of Apollo Coldplate Development and Production. Welding Journal, vol. 47, Sept. 1968, pp. 710-719.
- 4. Demogenes, C.; et al.: Fabrication and Structural Evaluation for Regeneratively Cooled Panels. NASA CR-1651, March 1971.
- 5. Buchmann, O. A.: Hypersonic Research Engine Project, Phase IIA, Item No. 55-7.01, Structures and Cooling Development Interim Technical Data Report, 3 Feb.-3 May 1967. NASA CR-66997, May 12, 1967.
- 6. Deckmann, G.: Hypersonic Research Engine Project, Phase IIA, Structures and Cooling Development Interim Technical Data Report No. 3, 3 Aug.-2 Nov. 1967, NASA CR-66996, Dec. 4, 1967.

7. Grover, H. J.; Hyler, W. S.; Kuhn, Paul; Landers, Charles B.; and Howell, F. M.: Axial-Load Fatigue Properties of 24S-T and 75S-T Aluminum Alloy as Determined in Several Laboratories. NACA Rept. 1190, 1954. (Supersedes NACA TN 2928.)



		Element												
Material	Cr	W	Fc	C	Si	Со	Ni	Mn	Мо	P	ន	Au	Pđ	
Hastelloy X*	22.14	0.47	18.09	0.08	0.39	1.85	Bal	0.27	8.76	0.016	0.005			
Palniro 1**							25					50	25	
Palniro 4**							36					30	34	

TABLE II MELTING TEMPERATURE RANGE OF BRAZING ALLOYS

Brazing alloy	Sol K	idus (F)	Liq K	uidus (F)
Palniro 1	1375	(2016)	1394	(2050)
Palniro 4	1408	(2075)	1442	(2136)

^{*}Union Carbide Corporation.

**Western Gold and Platinum Company.



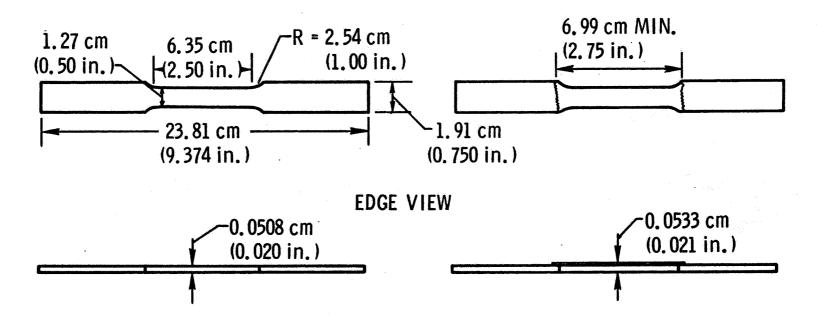
BRAZING PROCEDURES

Step	Palniro l	Palniro 4
1	Evacuate furnace to 0.13 N/m ² (10 ⁻³ torr)	Evacuate furnace to 0.13 N/m ² (10 ⁻³ torr)
2	Raise specimen temperature to 1222 K (1740° F) in about 2 hours	Raise specimen temperature to 1255 K (1800° F) in about 2-3/4 hours
3	Hold specimen temperature at 1222 K (1740°F) for 15 minutes	Hold specimen temperature at 1255 K (1800°F) for 15 minutes
14	Raise specimen temperature to 1405 K (2070°F) and hold there for 5 minutes	Raise specimen temperature to 1461 K (2170° F) and hold there for 5 minutes
5	Cool specimen to 1033 K (1400°F) in 45 minutes	Cool specimen to 1033 K (1400° F) in 1 hour
6	Cut off furnace power and flood chamber with dry argon to a pressure of 20.7 kN/m (3 psi) above ambient	Cut off furnace power and flood chamber with dry argon to a pressure of 20.7 kN/m ² (3 psi) above ambient
7	Remove specimen from furnace after cooling to 366 K (200°F)	Remove specimen from furnace after cooling to 366 K (200°F)

TABLE IV RESULTS OF TENSILE TESTS ON HASTELLOY $\mathbf X$

Material condition	I .	strength ent offset) (KSI)	Ultimat MN/m ²	e strength	Elongation to failure, percent
As-received	503.0	(73.0)	850.2	(123.4)	38.2
Brazed with Palniro 4	325.9	(47.3)	795.8	(115.5)	24.8
Brazed with Palniro 4 and service thermal cycled	305.9	(44.4)	729.7	(105.9)	26.1

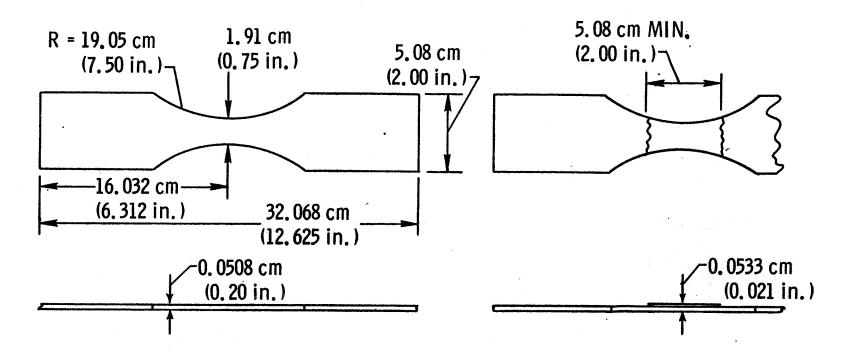
TOP VIEW



(a) Bare metal specimen.

(b) Brazed specimen with braze overlay. (Dimensions not shown are same as figure (a).)

Figure 1.- Tensile test specimen configurations.



(a) Bare metal specimen.

(b) Brazed specimen with braze overlay. (Dimensions not shown are the same as for figure (a).)

Figure 2.- Fatigue test specimen configurations.

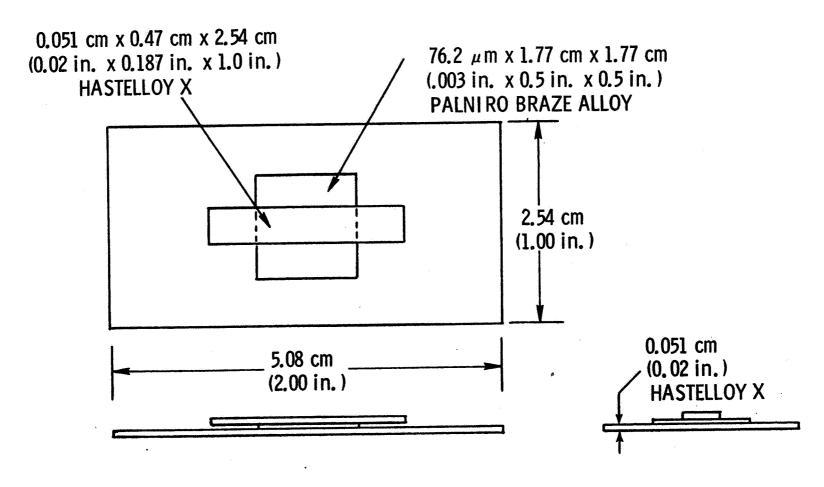


Figure 3. - Brazing alloy-base metal interaction specimen.

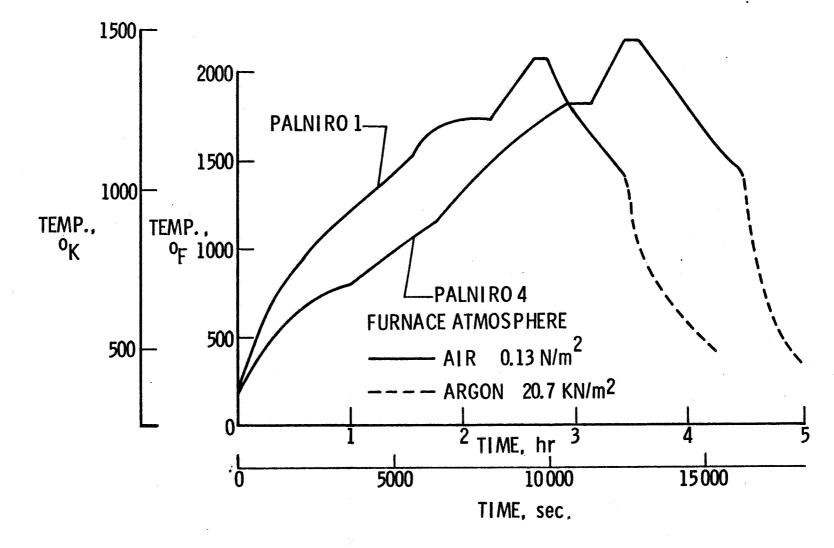


Figure 4.- Brazing heat cycles.

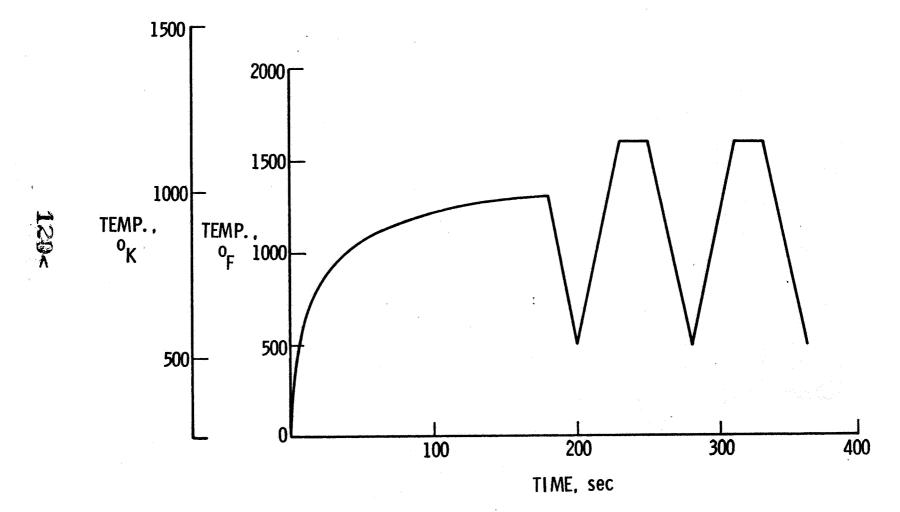


Figure 5.- Service thermal cycle.

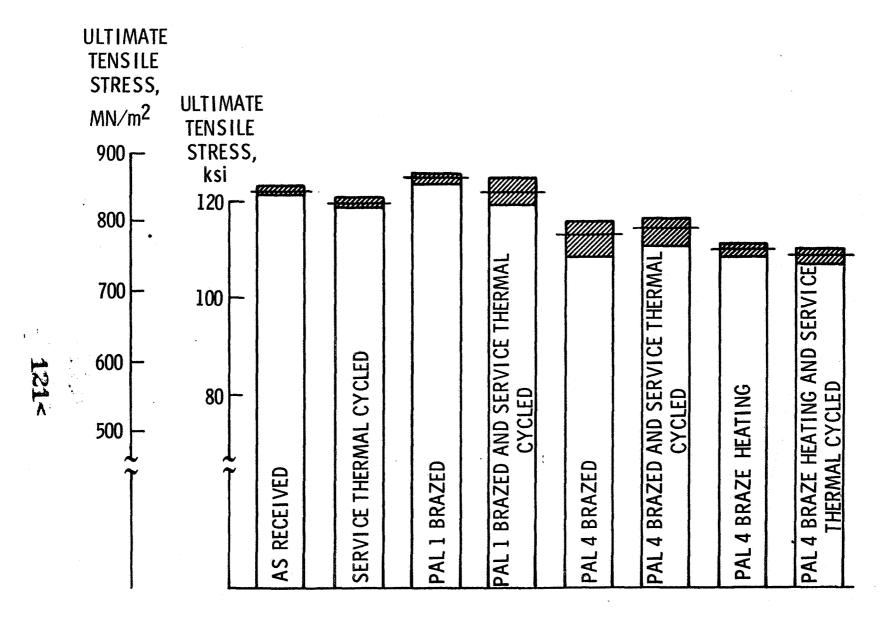
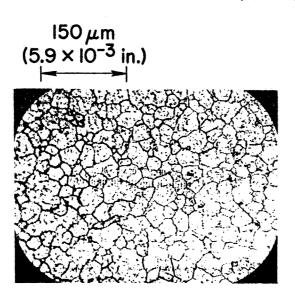


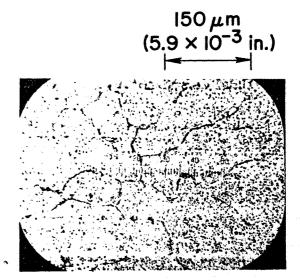
Figure 6.- Initial screening tensile tests on Hastelloy X.



(a) Virgin Hastelloy X.



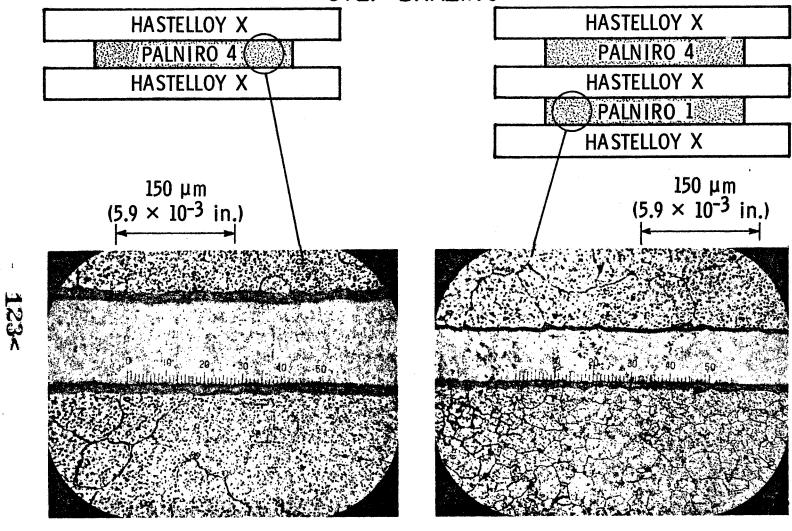
(b) After brazing with Palniro 1.



(c) After brazing with Palniro 4.

Figure 7.- Photomicrographs of virgin and as-brazed Hastelloy X.

HASTELLOY X-BRAZING ALLOY JOINTS ILLUSTRATING STEP BRAZING



(a) Step 1, brazed with Palniro 4.

(b) Step 2, brazed with Palniro 1.

Figure 8.- Photomicrographs of Hastelloy X - brazing alloy joints illustrating the effects of step-brazing.

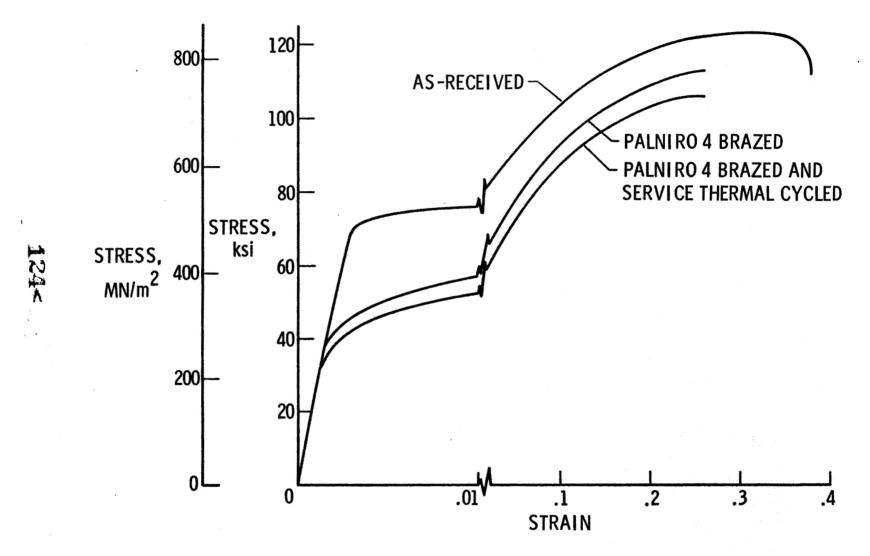
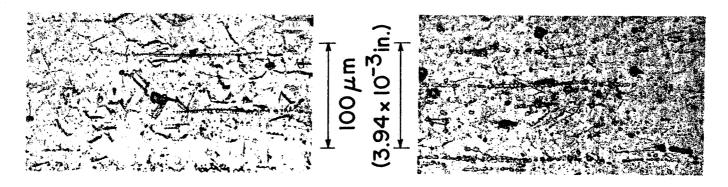
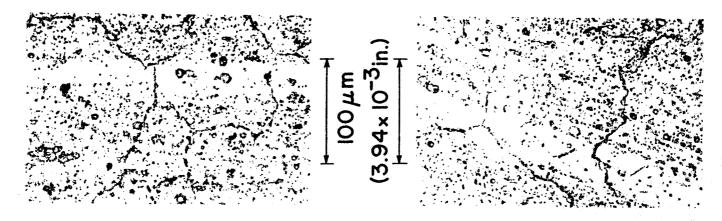


Figure 9.- Typical stress-strain diagrams for Hastelloy X.

HASTELLOY X BEFORE AND AFTER TENSILE TESTING



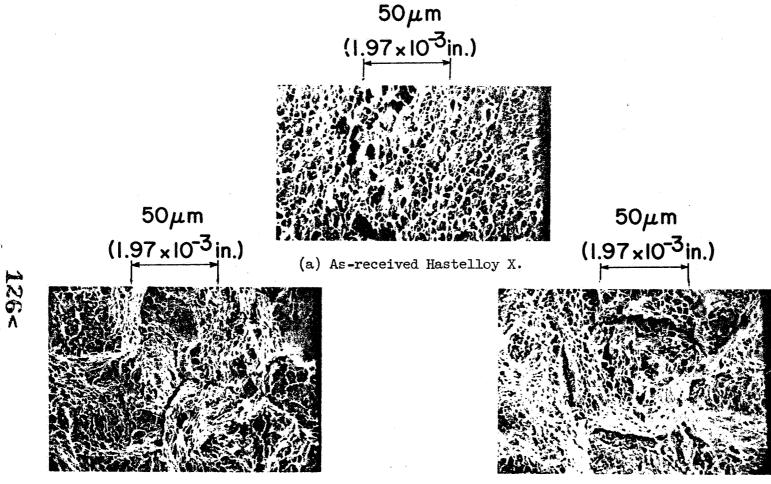
- (a) As-received Hastelloy X, before testing.
- (b) As-received Hastelloy X after tensile testing.



- (c) Hastelloy X as-brazed with Palniro 4.
- (d) Hastelloy X as-brazed and service thermal cycled.

Figure 10. - Photomicrographs of Hastelloy X before and after tensile testing.

TYPICAL HASTELLOY X FRACTURE SURFACES



- (b) Hastelloy X as-brazed with Palniro 4.
- (c) Hastelloy X as-brazed and service thermal cycled.

Figure 11. - Typical Hastelloy X fracture surfaces.

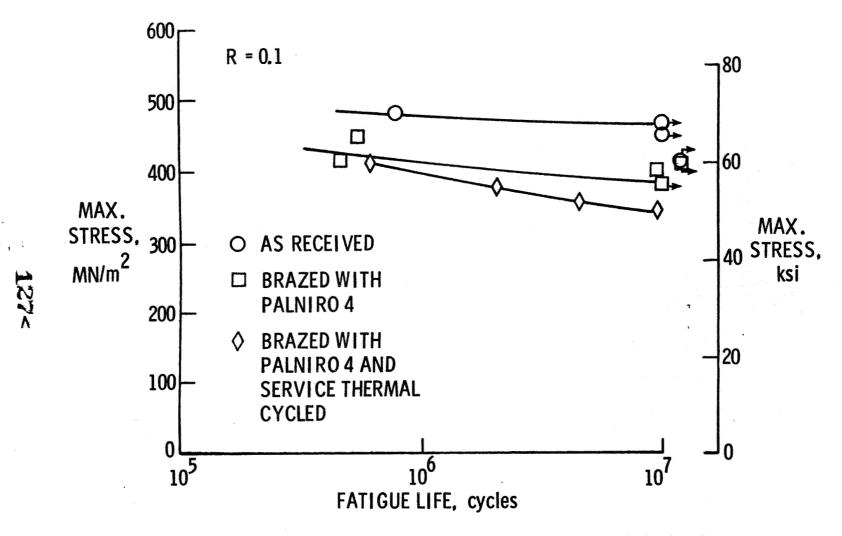


Figure 12.- Results of room temperature fatigue tests on Hastelloy X.

'N74 30928

DEVELOPMENT OF THE WELDBOND PROCESS FOR JOINING TITANIUM

ABSTRACT

This paper presents a digest of work performed under Contract F33615-71-C-1099 for the Fabrication Branch, Manufacturing Technology Division, AFML, Air Force Systems Command, Wright Patterson Air Force Base, Ohio. Data discussed within the scope of this paper resulted primarily from this program which established the basic parameters for joining titanium alloy using the resistance spot weld-adhesive bonding (Weldbonding process).

The writer wishes to gratefully acknowledge the technical and administrative efforts of Mr. Fredrick R. Miller, Air Force Manager for the Weldbond Program, and Mr. Gail E. Eichelman, Acting Chief, Metals Branch, AFML. The efforts of both Mr. Miller and Mr. Eichelman have contributed greatly to the advancement of Weldbonding from a specimen stage to a full scale production process.

INTRODUCTION

Beginning in 1965, experimental work at Lockheed-Georgia Company in resistance welding through high strength structural adhesives produced a process whereby exceptionally high mechanical strength properties could be obtained in aircraft joints fabricated from aluminum alloys. Continued work with adhesive formulations, and continued improvement in welding techniques further advanced the repeatability of the process to a point where large scale test structures could be produced.

In July, 1969, the Fabrication Branch, Manufacturing Technology Division, Air Force Materials Laboratory awarded a contract to Lockheed-Georgia Company - for the purpose of building and testing a full scale aluminum aircraft fuselage section joined by the spot weld-adhesive bonding (Weldbonding) process.

Results from the successful completion of the program encouraged the continued development of a weldbonding technology that would encompass other materials and other conditions.

Many military aircraft operate under conditions of stress and temperature that are beyond the design limits of aluminum alloy, regardless of the type joint fastening system used. Development and utilization of the weldbonding process in titanium alloys would greatly increase the usefulness of the weldbonding process for the military customer.

The overall objective of the program discussed herein was to further advance manufacturing methods related processes of weldbond in high strength, heat and corrosion resistant alloys.

In order to establish basic joint static strength criteria for weldbonded titanium joints at room and elevated temperatures and to establish weldability using various adhesives, the following program objectives were outlined:

1. Select an adhesive for optimum compatibility with weldbonding of titanium alloy.

- 2. Establish resistance spotweld schedules and obtain certifications of weldbond joints to meet minimum requirements of MIL Specification MIL-W-6858C.
- 3. Fabricate and join single and multiple spot lap and butt shear joints to establish basic static strength of weldbonded joints in titanium 6A1-4V alloy.
- 4. Compare static strength of multiple and single row weldbond joints with conventional resistance spot weld joints, and to similar specimens joined by mechanical fasteners and by structural adhesive bonding.
- 5. Record and document data related to weldability of titanium using high temperature type adhesives and compare joint strength at room and elevated temperature.

MATERIALS

TITANIUM

Titanium sheet material type 6Al-4V in the solution treated condition in thicknesses of 0.045" and 0.063" was used in one series of tests during this program. Thitanium sheet material type 6Al-4V in the annealed condition in thicknesses of 0.020" and 0.025" was used in other tests during this program.

MECHANICAL FASTENERS

The following mechanical fasteners were used to join specimens made during this program:

- 1. 5/32" diameter Hilok Universal head, stock No. STSAF004-05-02.
- 2. 5/32" diameter Hilok Flush head, stock No. STSAF015D05IN02.
- 3. 5/32" diameter Hilok nut, stock No. STSAE007-05.

ADHESIVES

The following adhesives were selected from several candidate adhesives and were used to join the specimens tested during this program:

- 1. 3M Company Adhesive EC3419. The adhesive is a one part, 100% solids thermosetting heavy liquid. The adhesive is light grey in color.

 The adhesive base is a modified epoxy resin. Recommended cure procedure for optimum results is 350°F for 60 minutes.
- 2. 3M Company Adhesive type EC2214 Hi-Flex. The adhesive is a one part, 100% solids, thermosetting liquid adhesive. The color is light grey. Recommended cure temperature is 250°F for 60 minutes.

EQUIPMENT

WELDING EQUIPMENT

A Sciaky, three phase, variable pressure resistance spot welder shown in Figure 1 was used to join all welded and weldbonded tensile specimens

tested during this program. The welder is rated at 150 KVA and is equipped with turret heads and automatic electrode dressers.

TESTING EQUIPMENT

A Tinius Olsen testing machine shown in Figure 2 was used throughout the program. The machine is rated at 60,000 pound capacity and has a test accuracy of two percent of indicated load. The testing machine was equipped with an Olsen Atcotran recorder, a model S-1 Electronic Extensometer, and a type D-2 Deflectometer. The testing machine was also equipped with a Marshall Electric Furnance, serial number 6510742, for an elevated temperature testing range 78°F to 1800°F.

DESIGN OF TEST PARAMETERS

TEST DESIGN LOGIC

Design of test parameters for evaluation of static strength of weldbond joints in titanium alloy required that first consideration be given to probable use of the developed process. Since a high percentage of titanium used in military aircraft would involve areas either exposed to high stress and/or elevated temperatures, strength at elevated temperatures would have to be given prime consideration. Where titanium would be used in structures not exposed to elevated temperature, generally the choice would be made because of better strength to weight advantages of titanium as

compared to aluminum or other alloys. Joint thickness ratios were selected in this program with strength/weight considerations paramount.



Realistic evaluation of weldbonded joints in titanium required that whereever possible weldbond joint strength would be compared directly to strength
of other type joints. Joints were designed utilizing spot welds only,
mechanical fasteners only, mechanical fasteners with adhesive, and structural
adhesive bond only. Joint configurations, joint overlap, and joint thickness
were kept identical in order to obtain a direct strength comparison at room
and elevated temperatures.

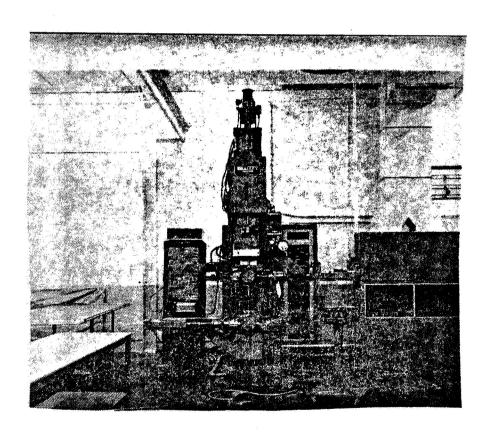


FIGURE 1 - SCIAKY THREE PHASE, VARIABLE PRESSURE, TURRET HEAD
WELDER USED TO WELDBOND TITANIUM

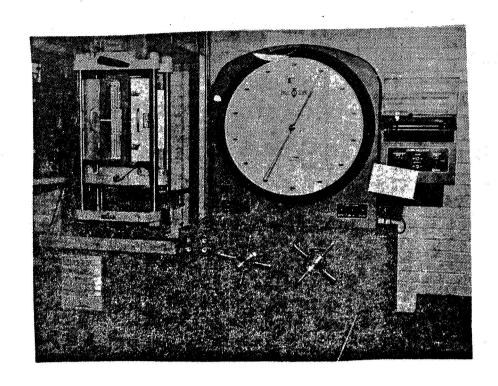


FIGURE 2 - TINIUS-OLSEN TENSILE TEST MACHINE

TEST SPECIMEN DESIGN

Typical test specimen design for multispot, double row weldbond and fastener bond joints is shown in Figures 3 through 5. Elevated temperature test specimens were of the same essential configuration except they were made 18 inches long in order to allow for heating of the specimen within the specimen gage length during testing.

WELD SCHEDULE DEVELOPMENT

WELD SCHEDULES

In order to obtain weldbond titanium joint strength data that could be compared qualitatively and quantitatively with other joining processes, basic welding schedules were needed. Machine schedule setups were made to establish adhesive weldability, correct spot weld nugget diameter and penetration, and other criteria as required by Military Specification MIL-W-6858C. It was necessary to vary weld schedule setups as various types of adhesives were tested. Weld current and weld pressure settings were found to differ with variation in adhesive type and/or viscosity.

WELD CERTIFICATION

Weld certifications were obtained for the following joint combinations tested within the scope of this program.

- 1. Titanium type 6Al-4V in the annealed condition, 0.025" thick weldbonded to titanium 6Al-4V in the solution treated condition, 0.063" thick.
- 2. Titanium type 6Al-4V in the solution treated condition, 0.045" thick weldbonded to titanium type 6Al-4V in the solution treated condition, 0.063" thick.
- 3. Titanium AMS4900 (Commercially Pure) 0.025" thick weldbonded to titanium 6Al-4V in the solution treated condition, 0.063" thick.



Weld certifications met Class A requirements for Group C, (titanium) alloys, MIL-W-6858C, Welding, Resistance Spot and Seam. Some difficulty was encountered in obtaining certified schedules in the commercially pure titanium to type 6Al-4V joints. This difficulty was due primarily to the difference in welding characteristics of the two alloys and not to the effect of adhesive at the joint interface.

CLEANING PROCEDURES

Preliminary cleaning and welding tests were made at the beginning of this program to determine if resistance welding could be accomplished in titanium that had been chemically cleaned for structural metal bonding. All attempts were unsuccessful as measured by standard weld certification requirements of MIL-W-6858C. It was determined that the passivation treatment (immersion in Trisodium Phospate (Na₃PO₄) used prior to bonding inhibited the passage of welding current during the welding operation and caused highly erratic weld quality.

Since high strength bonds could be achieved on parts cleaned for resistance welding, (except for passivation the two cleaning processes were essentially the same), all weldbonding accomplished within the scope of this program was done on parts cleaned by the chemical process used for resistance welding.

ADRESIVE SELECTION

ADHESIVE WELDABILITY

Adhesive weldability as discussed herein relates to the compatibility and/or incompatibility of the adhesive with the resistance welding process, and conversely, the effect of the welding process on the adhesive. First requirement of any adhesive candidate for the weld through process of weldbonding is that the adhesive have the capability of being moved under pressure of the welding electrodes in order for metal to metal contact to occur at the joint interface.

A second requirement for an adhesive candidate was that the heat resulting from the spot weld would cause only limited detrimental effect on the strength of the bond. The strength of the bond in titanium alloy joints, the adhesive and/or cohesive failure characteristics of the adhesive all entered into the final selection of the adhesive.

Final selection of the adhesives used during this program was based on overall weldbond properties at room and elevated temperatures as related to titanium weldbond joint strength.

ADHESIVE SCREENING AND SELECTION

A listing of the adhesives screened for use during this program and results of the screening are detailed as follows.



- 1. 3M Company epoxy adhesive type XA3919 is a roll coatable paste adhesive. XA3919 is a temperature resistant, 70% solids version of AF130 adhesive film. XA3919 exhibited adequate weldability and fair strength at 350°F temperature, but showed poor lap shear strength at room temperature.
- 2. 3M Company epoxy type XA3410 is a one part, 100% solids, thermosetting liquid adhesive advertised as being resistant to temperatures up to 350°F. XA3410 exhibited fair weldability, but showed low strength at all temperatures.
- 3. 3M Company adhesive XA3435 is a one part, 100% solids, thermosetting liquid advertised as offering superior strength up to and including 350°F temperature. XA3435 showed good weldability but exhibited only fair strength at all temperatures.
- 4. 3M Company adhesive type EC3419 is a one part, 100% solids, thermosetting heavy liquid advertised as having exceptionally high strength properties from -40 to 350°F. This adhesive exhibited excellent weldability on titanium alloy 6A1-4V and showed fair to good strength at elevated temperature and at room temperature. EC3419 was one of the adhesives selected for use during this program.
- 5. 3M Company adhesive type EC2214 Hi-Flex is a paste epoxy adhesive with filler designed for use from -40 to 250°F. This adhesive exhibited excellent weldability and showed cohesive type failures both at room and elevated temperature. Room temperature shear strength in titanium

joints was superior to all others tested. EC2214 was selected for use in this program.

6. Eysol Corporation adhesive ADX347 and ADX373, and Whittaker Corporation adhesive X6800 were also subjected to preliminary tests in titanium joints but exhibited adhesive failures with low lap shear strength at room temperature.

FABRICATION AND JOINING OF SPECIMENS

Specimens used for preliminary evaluation of adhesives were finger panel type. These specimens were stamped from titanium sheet stock and are of the type normally used for process control tensile testing as required by Military Specification MIL-W-6858C and Federal Specification MMM-132.

Specimens used to obtain the final test results were sheared from titanium sheet and machined to the configurations shown in Figure 3.

TEST PROCEDURES

TENSILE TESTS

Room temperature static tensile tests were performed on the Tinius-Olsen tensile testing machine shown in Figure 2. Test load pounds were all within a range of 500 to 12,000 pounds which allowed a test machine accuracy of two percent of indicated load.

139<

Load deflection curves were obtained for each of the tests. Ultimate strength, yield strength, and percent elongation were obtained for each specimen. Yield strength was determined using the 0.2% offset method.

Figures 3 through 5 show joint description and static shear strength of the specimens tested during this program.

Elevated temperature static tensile tests were made on the Tinius-Olsen testing machine using the Marshall specimen furnace as shown in Figure 2. Welded, weldbonded, adhesive bonded, mechanically fastened, and mechanically fastened and bonded specimens were subjected to various temperatures under load to failure. Static shear strength and mechanical properties of the joints at different temperature levels are shown in Figures 3 through 5.

FIGURE 3 - STATIC SHEAR

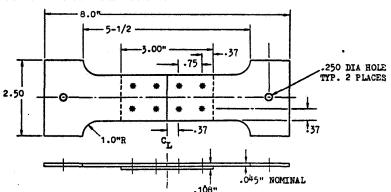
STRENGTH, BUTT SHEAR

DOUBLE ROW, MULTISPOT

WELDBOND, 0.045" TO

0.063"

SPEC NO.	TIDIH		EDGE DIST.	FAST DIA.	LOAD LBS.				JOINT PROC.	JOINT TYPE		Joint Comb.	PITCH IN.
18-1 18-2 18-3 18-4 18-5 18-6 18-7 18-8 18-9 18-10	1.50	1.50			11100 11150 10950 10740 10830 11080 10850 10730 10720 10930	4955 4866 4773 4813 4924 4822 4768 4764 4857		2214	WB	BSDR MS	N.E.	.045 TO .063	.75
18A-1 18A-2 18A-3 18A-4 18A-5		1.50	•37	None	10070 9490	4417	200° 200° 325°	2214	WB	BSDR	N.E.	.045 TO .063	•75





SPEC NO.	WIDTH IN.	OVER LAP IN.	EDGE DIST.	FAST FIA.	LOAD LBS.	LBS ₂	TEST TEMP (°F)		JOINT PROC.		PAIL MODE	JOINT COMB.	PITCH IN.
20-1 20-2 20-3 20-4 20-5 20-6 20-7 20-8 20-9	1.50	1.50	•37 At	5/ 32 FLUSH HEAD	7685 7750 7120 7440 8050 <u>7350</u>		RT	None	Past Hi- Lok	esdr MF	HEAD SHEAR	.045 TO .063	•75
20A-1	1.50	1.50	-37	⁵ / ₃₂	6630		150*	2214	Fast Hi-	BSDR	HEAD SHEAR	.045	•75
20A-2				FLUSH	6750		200*	F2214	Lok	MF	SHEAR FAST	.063	
20A-3				HEAD	6895		200•	None		MP	SHEAR FAST		
20A-4					5865		325 •	2214		MP	PAST SHEAR		
20A-5			,		6940		325•	None		MF	FAST SHEAR		

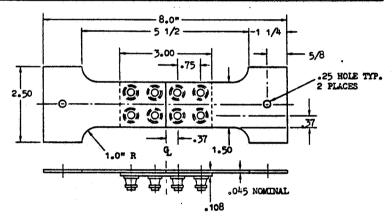


FIGURE 4 - STATIC SHEAR STRENGTH, BUTT SHEAR DOUBLE
ROW, MULTIPLE FASTENER, 0.045" TO 0.063"

SPEC NO.	WIDIH IN.		EDGE DIST.	FAST DIA.	LOAD	LBS ₂	TEST TEMP (°F)	ADHE SIVE	JOINT PROC.	JOINT TYPE		JOINT COMB.	PITCH IN.
24-1 24-2 24-3 24-4 24-5 24-6 24-7 24-8 24-9 24-10	1.50	1.50		None Prage	5700 7500 6900 4230 6230 5240 6460 6030 6220	2533 3333 3066 1880 2768 2328 2871 2680 2764		2214	Bond	BSSB	SHEAR	.045 TO .063	None
24A-1 24A-2 24A-3 24A-4 24A-5	1.50	1.50	None	None	3520	1564 1395	2000	2214	Bond	BSSB	SHEAR	.045 20 .063	None

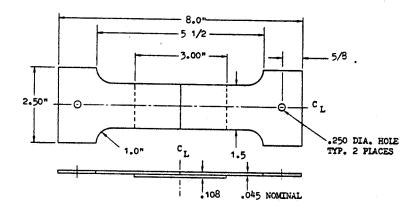


FIGURE 5 - STATIC SHEAR STRENGTH, BUTT SHEAR STRUCTURAL
BOND, DOUBLE ROW MULTIPLE SPOT EQUIVALENT
0.045" TO 0.063"

PEEL TESTS

In order to test the combined strength of both the bond and the spot weld, peel specimens typical of those shown in Figure 6 were tested in a peel test fixture at room temperature.

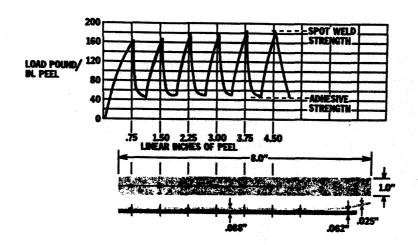


FIGURE 6 - DIAGRAM SHOWING TYPICAL PEEL STRENGTH
OF WELDBONDED JOINTS IN TITANIUM

TEST RESULTS ANALYSIS

ROOM AND ELEVATED TEMPERATURE TEST RESULTS

Comparative strength of the different joining methods is shown in Figures 7 and 8. Strength of the joints is plotted in ultimate load pounds versus temperature in order to obtain a direct strength comparison of the various joining techniques.

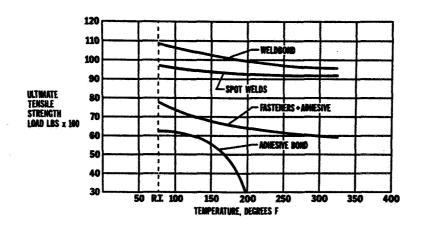


FIGURE 7 - COMPARATIVE JOINT STRENGTH, BUTT SHEAR
DOUBLE ROW, 0.045" TO 0.063" TITANIUM

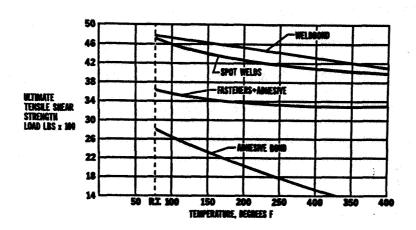


FIGURE 8 - COMPARATIVE JOINT STRENGTH, BUTT SHEAR SINGLE ROW, 0.025" TO 0.063" TITANIUM

Weldbond joints show a superior strength at room temperature in all joint types tested. The double row, and double row multiple spot type joint showed the greatest superiority in weldbond strength as compared to other joining methods.

Spot-welds were inferior only to the weldbond joint at room temperature in all categories tested. Mechanical fasteners plus adhesive showed the third highest strength properties at room temperature in all joint categories except in the single row, 0.045 to 0.065 condition. Structural adhesive bond joints were inferior to all other type joints tested at room temperature.

Weldbond strength at elevated temperatures varied not only with the temperature but also as a function of the type adhesive used and the type of joint design used. As shown in Figure 7 and Figure 8, weldbond joint type double row, multiple spot, exhibited a definite strength superiority from room temperature through 325°F.

Weldbond joints and/or spot-weld joints were superior in strength in all categories from room temperature to 400°F as compared to other joining methods. The structural adhesive bond joints made with EC2214 Hi Flex adhesive lost approximately 50% of their effective strength at 200°F. The structural adhesive bonded joints made with EC3419 retained approximately 50% of their strength at 325°F.

DISCUSSION

High quality resistance spot-welds meeting the requirements of Military Specification MIL-W-6858C were produced when welding through epoxy adhesive on titanium alloys. No special machine modifications were required for weldbonding titanium alloys.

Weldbond joints were produced that were consistently stronger than those of either mechanical fasteners, structural adhesive bonds, or mechanical fasteners with adhesive at the joint interface. Weldbond joints and/or spot weld joints showed superior strength at all temperature ranges as compared to other joints tested.

Adhesives having a strength above 3000 psi at 400°F need to be developed for weldbonding in order to achieve optimum joint efficiency in titanium alloys at elevated temperatures.

The combined peel strength of spot welds and adhesive bond joints was approximately five times greater than that of a bond joint alone.

N74 30929

WELD-BRAZING - A NEW JOINING PROCESS

Ву

Thomas T. Bales, Dick M. Royster, and Winfrey E. Arnold, Jr.

NASA - Langley Research Center

Presented at Symposium on Welding, Bonding, and Fastening

Sponsored By
National Aeronautics and Space Administration
George Washington University
The American Society for Metals

Williamsburg, Virginia May 30-June 1, 1972

WELD-BRAZING - A NEW JOINING PROCESS

By

Thomas T. Bales, Dick M. Royster, and Winfrey E. Arnold, Jr.

SUMMARY

A joining process designated weld-brazing which combines resistance spot welding and brazing has been developed. Resistance spot welding is used to position and align the parts as well as to establish a suitable faying surface gap for brazing. Fabrication is then completed by capillary flow of the braze alloy into the joint. The process has been used successfully to fabricate Ti-6A1-4V titanium alloy joints using 3003 aluminum braze alloy and should be applicable to other metal-braze systems.

Test results obtained on single overlap and hat-stiffened structural specimens show that weld-brazed joints are superior in tensile shear, stress rupture, fatigue, and buckling than joints fabricated by spotwelding or brazing. Another attractive feature of the process is that the brazed joint is hermetically sealed by the braze material which should eliminate many of the sealing problems encountered in riveted or spotwelded structures. The ease of fabrication associated with the weld-brazing process could well make it cost effective on a production basis compared with more conventional techniques in addition to the improved joint characteristics observed.

WELD-BRAZING - A NEW JOINING PROCESS

By

Thomas T. Bales, Dick M. Royster, and Winfrey E. Arnold, Jr.

INTRODUCTION

Recent interest has been generated in the combined use of resistance spotwelding and epoxy bonding (weld-bonding) as an effective means of fabricating aerospace structures. In a study sponsored by the Air Force Materials Laboratory (ref. 1), weld-bonding was used to fabricate aluminum alloy structures having mechanical properties vastly superior to similar panels fabricated by conventional methods. The interest in weldbonding as an effective manufacturing process prompted NASA-Langley to investigate its applicability to some of their current and future programs. A study was undertaken at NASA-Langley to investigate weld-bonding as a potential joining method in the fabrication of titanium structures. However, since titanium structures are considered for use at temperatures which exceed the capability of current epoxy systems, a higher temperature adhesive was desired. The idea of substituting a braze alloy for the adhesive to extend the temperature capabilities was conceived and a program was therefore initiated to evaluate the process designated as WELD-BRAZING. The material used in the study was mill annealed Ti-6Al-4V titanium alloy sheet and the braze alloy was 3003 aluminum. The study consisted of the fabrication of single overlap specimens which were tested at room and elevated temperatures, and the fabrication of hat-stiffened panels which were tested in compression at room temperature.

Weld-brazed joints were examined metallurgically to verify adequate flow of the braze and absence of porosity. This paper reports the results obtained in this study.



PROCESS DEVELOPMENT

In the development of the weld-brazing process, which combined the use of resistance spotwelding and brazing, two primary approaches were investigated. One was designated the prepunched foil approach (figure 1) and the other the capillary flow approach (figure 2). Both of these approaches were developed together and both proved to be successful joining methods.

In the prepunched foil approach, the foil was punched (see Figure 1) so that the diameter of the holes was larger than the diameter of the intended spotweld nugget. This was done in order to prevent excessive reaction of the parent material with the braze alloy in the vicinity of the spotweld. Single overlap specimens fabricated in this manner showed that expansion of the weld nugget caused the faying surface gap to be approximately 0.002-inch greater than the thickness of the braze foils being used. It was therefore necessary that the width of the braze foil be greater than the overlap in order to have a sufficient volume of braze alloy to adequately fill the gap resulting from welding. Specimens were heated to 1250°F in vacuum to accomplish the brazing cycle.

In the capillary flow approach (see figure 2) the titanium strips are first chemically cleaned and then joined by conventional spot-welding techniques. Nugget expansion during welding produced a faying surface



gap which could be varied from 0.002-inch to 0.006-inch by varying the welding parameters. Following welding, the braze foil was positioned at the edge of the overlap and the assembly was heated to the brazing temperature of 1250°F in vacuum as in the prepunched approach. Upon melting the braze alloy was drawn into the gap by capillary action. Ultrasonic and metallographic inspection of the joint indicated that the gap was filled completely.

Both approaches produced satisfactory joints that were hermetically sealed. In the prepunched foil approach, the positioning of the punched foil and the welding electrodes, without the aid of precise positioning equipment made the process somewhat difficult for application to the fabrication of structural parts. However, there could be certain applications where the braze would not flow into the faying surface gap and the prepunched foil approach would be the better joining method. Weld-brazed joints were fabricated with relative ease by the capillary flow approach, and it was for this reason that this approach was used to fabricate the test specimens used in the test program.

SPECIMENS AND TEST PROCEDURES

The weld-brazing process, using the capillary flow approach, was used to fabricate single overlap specimens and hat-stiffened panels. These specimens were then tested to evaluate the mechanical properties of weld-brazed joints. The parent material used was annealed 0.050-inch thick Ti-6Al-4V titanium alloy and the braze alloy employed throughout

the study was 0.004-inch thick 3003 aluminum alloy. The Ti-6Al-4V parts were thoroughly cleaned before weld-brazing as outlined in reference 2.



Specimens

Single overlap specimens. - The configurations of the single overlap specimens are shown on figure 3. Specimens were fabricated by spotwelding, brazing, and weld-brazing. The overlap on all specimens was approximately 3/8-inch and was selected to insure determination of joint characteristics. The specimen on the right of the figure was used for determining the tensile shear and stress rupture properties of the joints. End tabs were spotwelded to the specimens to prevent end failure during testing. The longer specimen shown in the figure was used for determining the fatigue properties of the joints. The weld spacing on the spotwelded only and weld-brazed specimens was 1 inch. All brazing operations were accomplished in a vacuum furnace at a temperature of 1250°F and a pressure of 10⁻⁵ torr for 10 minutes

Hat-stiffened panels. - The panel configuration used in the program is shown on figure 4. Panels having a maximum width to thickness ratio of 25 were fabricated by brazing only, riveting only, spotwelding only, and weld brazing. The panels fabricated by brazing only were first spotwelded at the ends and in the center to eliminate fixturing. The riveted panels were fabricated using 0.16-inch diameter flush-head stainless steel rivets and a rivet spacing of 1/2-inch. For comparative purposes, the spacing of the spotwelds in the spotwelded only and weld-brazed panels were also 1/2-inch. The weld-brazed and brazed only panels

were fabricated using the same brazing parameters as for the single overlap specimens.

The need for spotwelding the brazed panels, as mentioned above, resulted from difficulties associated with attempts to fabricate specimens by brazing alone. Attempts to maintain alinement of the hat stringer on the face sheet and to establish the optimum gap for brazing were found to be very difficult unless elaborate fixtures were used. A slight twist in the stiffener during fabrication resulted in braze thicknesses ranging from 0.003 to 0.020-inch. Therefore, to eliminate the need for fixturing, the brazed only panels were fabricated by spotwelding the stiffener to the face sheet at each end and in the center. The braze alloy was then placed along the edge of the overlap and fabrication was completed in the same manner as the weld-brazed panels. Thus, the brazed only panels were actually fabricated by weld-brazing using widely spaced spotwelds.

Test Procedures

Tensile shear test. - The tensile shear tests of single overlap specimens were conducted at ambient temperature, 350°F and 550°F at a constant load rate of 2000 lb/min using a 100 kip capacity hydraulic testing machine. Heating of the specimens tested at elevated temperature was accomplished using a resistance-wound furnace mounted in the testing machine.

Stress-rupture tests. - Stress rupture tests were conducted using single overlap specimens. The specimens were loaded in conventional creep testing machines, equipped with tube furnaces, to various percentages of

the elevated temperature static tensile shear strength. The loading was applied shortly after reaching test temperature and the times to rupture were obtained from digital elapsed-test-time indicators that stopped automatically when the specimens ruptured.

Fatigue tests. - Constant-amplitude fatigue tests (R=0.05) were conducted in subresonant-type axial load fatigue machines (reference 3). Load was sensed by a weigh-bar in series with the specimen and grips. A wire strain-gage bridge cemented to the weigh-bar supplied a load signal to an oscilloscope which was used to monitor cyclic loading. Operating frequency was 1800 cycles per minute.

Panel tests. - the hat-stiffened structural panels were tested in compression using a 300-kip-capacity hydraulic testing machine. The edges of the specimens were supported with knife edges positioned 1/4 of an inch from the edge. Foil strain gages were attached at the centers of the stiffener and face sheet and were used to measure local strains. Relative motion between the upper and lower heads of the testing machine was measured using linear variable differential transformers. Data were recorded every 10 seconds to local instability and at an increased rate of every second from local instability to maximum load. All tests were conducted at a load rate of 12,000 lbs/min.

RESULTS AND DISCUSSION

Single Overlap Specimens

<u>Tensile-shear</u>. - The tensile shear results obtained at room temperature, 350°F and 550°F are presented on figure 5 for specimens



fabricated by spotwelding, brazing, and weld-brazing where maximum load is plotted against test temperature. The data points are the average of 6 tests with the data spread indicated. The tensile shear properties of the weld-brazed specimens are shown to be greater than those of the brazed or spotwelded specimens and are approximately equal to the sum of the values shown for the spotwelded and brazed specimens. The strength of the weld-brazed specimens apparently decrease linearly with increasing temperature, and at 550°F the specimens were capable of carrying a load which was 85 percent of the value obtained at room temperature. The strength of the brazed specimens decreases in a similar fashion, and the spread in the data indicates that the brazing process was much more difficult to control. At a temperature of 550°F, the average strength of the brazed specimens was equal to approximately 80 percent of the room temperature strength. Although both the weld-brazed and brazed specimens experienced a decrease in strength at 550°F, the decrease compared to room temperature strength was proportionally less for the weld-brazed specimens. The differences in the percentages noted for the weld-brazed specimens might be attributed to the fact that the strength of the spotwelds were not temperature dependent.

<u>Stress-rupture</u>. - The stress-rupture properties at 350°F and 550°F for single overlap specimens fabricated by spotwelding, brazing, and weld-brazing are shown on figure 6. At 550°F for a 500-hour life, the weld-brazed specimens appear capable of carrying more than twice as much load as the brazed specimens and approximately 15 percent more load

than the spotwelded specimens. Although both the weld-brazed and brazed specimens exhibited substantial decreases in load carrying ability at 550°F compared to 350°F, the decrease noted for the weld-brazed specimens was proportinally less, probably because of the contribution from the spotwelds. Based on these results and those obtained from the tensile shear test, it would seem possible to tailor the elevated temperature properties of a weld-brazed joint by varying the number of spotwelds present. Although the strength contribution of the braze decreases with increasing temperature, it should be sufficient to redistribute the stress in the joint so that the stresses in the spotwelds are reduced.

Fatigue. - The room temperature fatigue data obtained from the single overlap specimens are shown on figure 7. Note that the fatigue strengths of the brazed and weld-brazed specimens are approximately equal and that the strengths are approximately three times as great as the strength of the spotwelded specimens for a life of 200,000 cycles. Failure of the brazed and weld-brazed specimens occurred in the joint for stress levels resulting in failure in less than about 50,000 cycles while failure of the gross section occurred for the specimens having a fatigue life greater than about 50,000 cycles. The reason for the change in failure mode was attributed to specimen configuration.

Hat-Stiffened Panels

The hat-stiffened panels fabricated by the various methods were tested in compression, and the results obtained are presented on figure 8. Data are shown for three panels tested for each joining process. The load carrying ability of the brazed and weld-brazed panels are shown to be similar and substantially greater than that of the panels fabricated



by spotwelding or riveting. The maximum load of the weld-brazed panels was approximately 59 kips compared to 38 kips for the riveted panel or an increase in load carrying capability of 55 percent. A similar increase was also noted for the loads at which face sheet wrinkling or buckling occurred for the weld-brazed panels compared to the riveted specimens. The increase in load carrying ability of the weld-brazed and brazed panels is attributed to an increased panel stiffeness resulting from the continuous bond between the stiffener and face sheet as compared to the point attachment inherent with spotwelded and riveted specimens. However, since the specimens were of the same configuration, a structure fabricated by weld-brazing should provide a reasonable weight savings for buckling design considerations.

Metallographic Investigation

Metallographic specimens were prepared using conventional polishing and etching techniques. Typical cross-sections of a weld-brazed joint taken from a compression panel are shown on figure 9. The upper portion of the figure depicts the joint and provides evidence that the faying surface gap is adequately filled by brazing. The braze alloy which was placed adjacent to the flange of the stiffener is shown to have penetrated completely through the joint to form a generous fillet between the inner surface of the stiffener and the face sheet.

The photomicrograph on the lower portion of figure 9 provides further verification of adequate braze penetration, at least to the weld nugget.

A good metallurgical bond is shown to exist between the braze and all adjoining titanium surfaces although there is some evidence of the

formation of titanium aluminide. However, the formation of the intermetallic to the extent shown was not detrimental to the properties studied.



CONCLUDING REMARKS

The results obtained indicate that weld-brazing is a fabrication process capable of producing joints having superior ambient and elevated temperature properties compared to similar joints produced by brazing only or spotwelding only. Tailoring of the properties may also be possible by varying the extent of the overlap and the number of spotwelds. Weldbrazing may also eliminate many of the sealing problems encountered in spotwelded and riveted structures because the process results in a hermetically sealed joint. The ease of fabrication associated with the weld-brazing process could well make it cost effective on a production basis compared with more conventional techniques in addition to the improved joint characteristics observed. Although the process has only been used to join Ti-6Al-4V titanium alloy 3003 aluminum braze, weldbrazing should also be adaptable to any material system where both brazing and spotwelding techniques are viable methods for joining. Candidate systems include nickel-base superalloy and refractory metal structures as well as the fabrication of structures using more conventional material such as mild steel.



REFERENCES

- 1. Fields, Dallas: Resistance Spot Weld-Adhesive Bonding Process. Technical Report AFML-TR-70-227, November 1970.
- 2. Heimerl, George J.; Baucom, Robert M.; Manning, Charles R.; and Braski, David N.: Stability of Four Titanium-Alloy and Four Stainless Steel Sheet Materials After Exposures Up to 22,000 Hours at 550°F (561°K). NASA TN D-2607, 1965.
- 3. Grover, H. J.; Hyler, W. S.; Kuhn, Paul; Landers, Charles B.; and Howell, F. M.: Axial-Load Fatigue Properties of 245-T and 755-T Aluminum Alloy as Determined in Several Laboratories. NACA Report 1190, 1954. (Supersedes NACA TN 2928.)

c

(c) Weld-Brazed

FIGURE 1. WELD-BRAZING WITH PRE-PUNCHED FOIL.

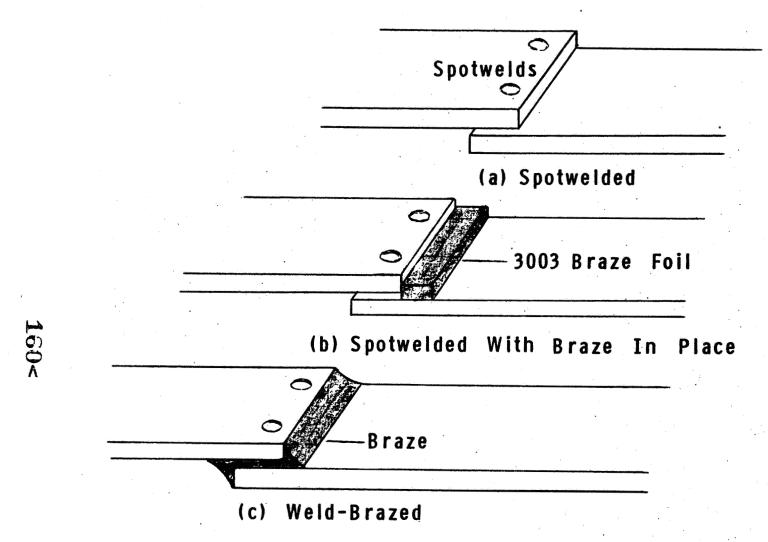


FIGURE 2. - WELD-BRAZING WITH CAPILLARY FLOW.

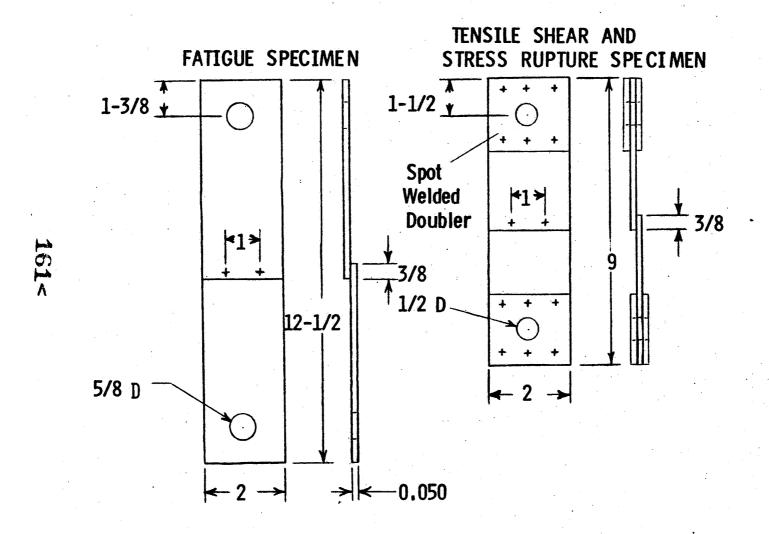


FIGURE 3. - SINGLE-OVERLAP TEST SPECIMENS; DIMENSIONS IN INCHES.

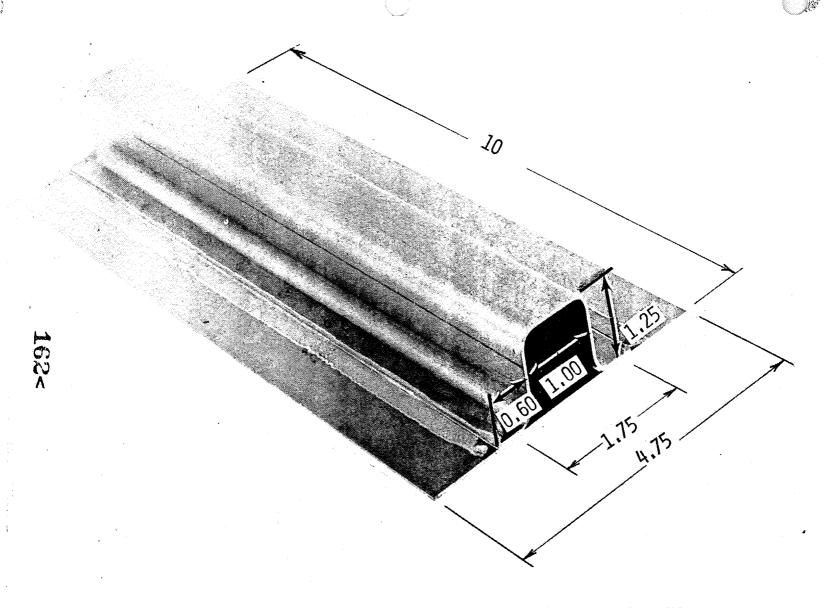


FIGURE 4. - HAT-STIFFENED COMPRESSION PANEL; DIMENSIONS IN INCHES.

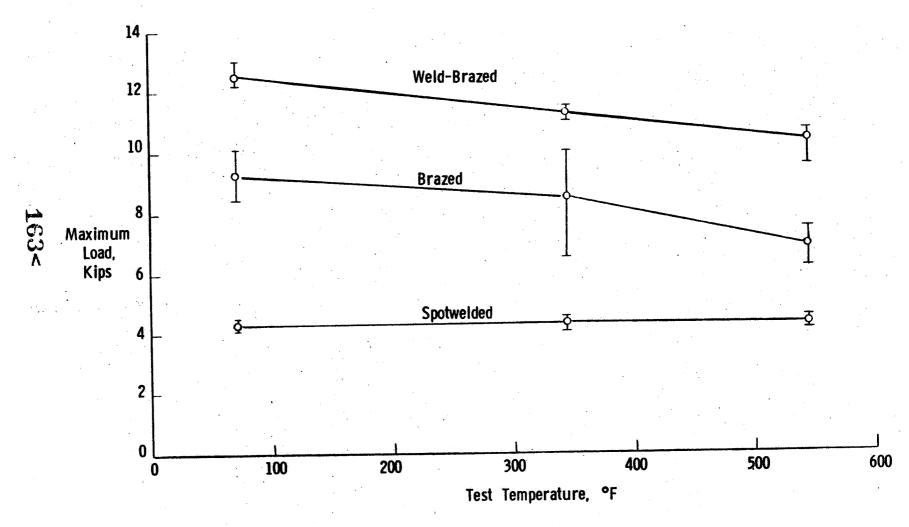


FIGURE 5. - SINGLE-OVERLAP TENSILE-SHEAR DATA.

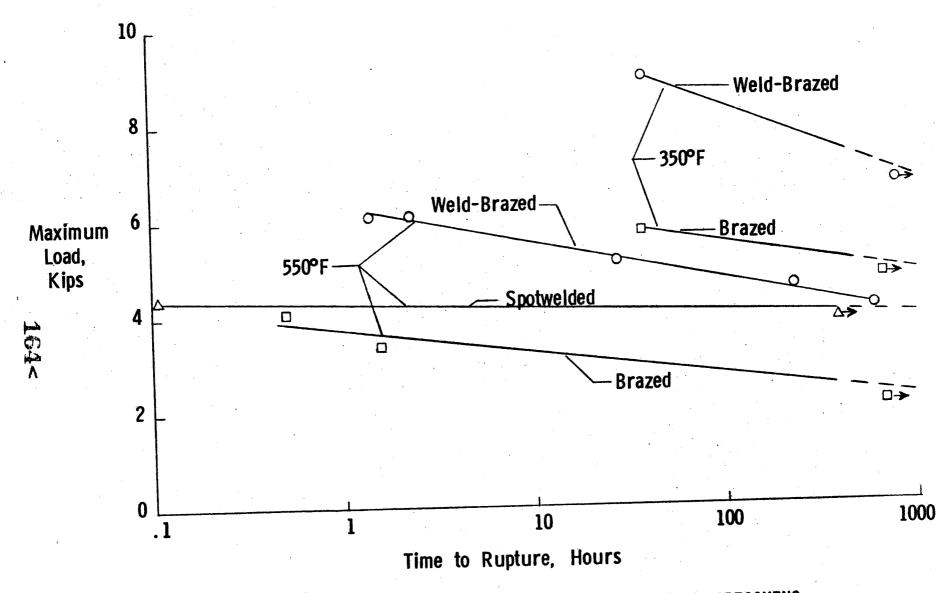


FIGURE 6. - TIME TO STRESS RUPTURE OF SINGLE-OVERLAP SPECIMENS.

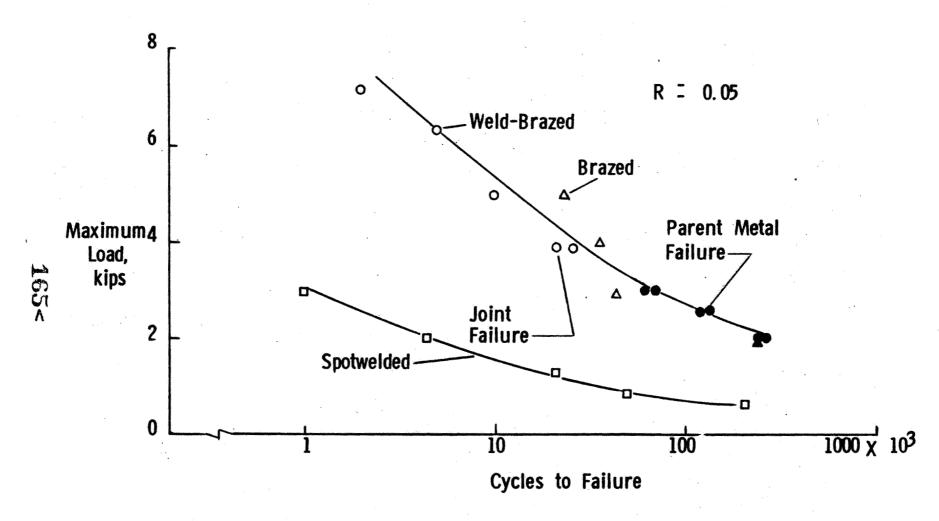


FIGURE 7. - RESULTS OF FATIGUE TESTS ON SINGLE-OVERLAP SPECIMENS.

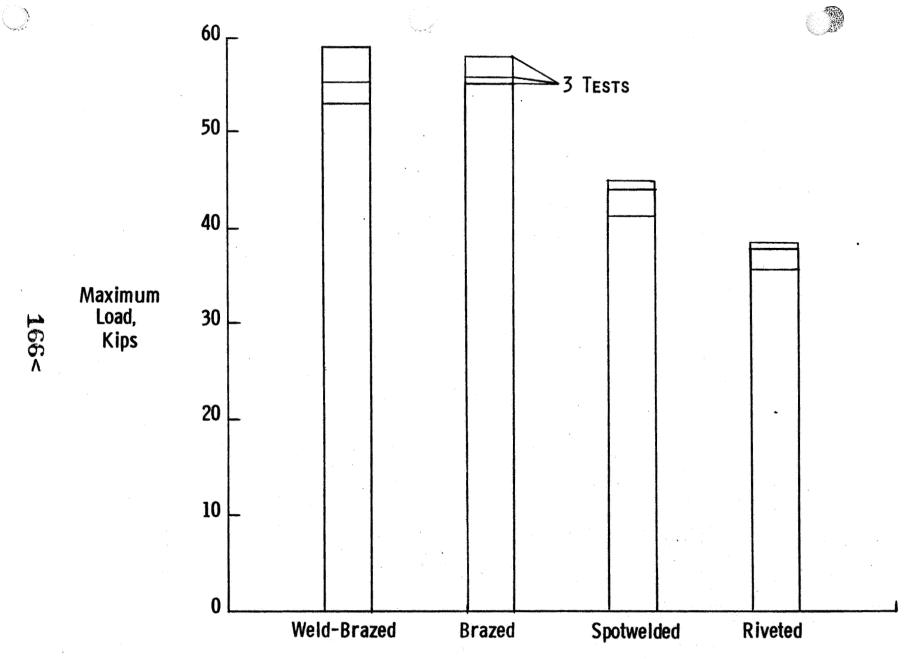
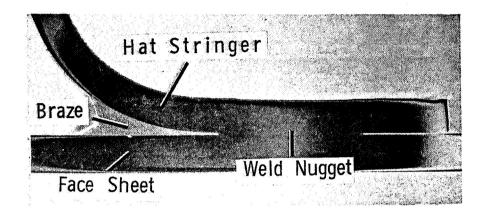
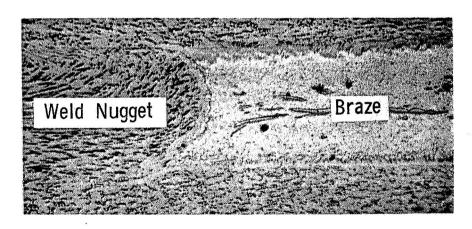


FIGURE 8. - MAXIMUM LOAD TO FAILURE FOR COMPRESSION PANEL TESTS.



(A) WELD-BRAZED JOINT (10X)



(B) WELD NUGGET-BRAZE INTERFACE (400X)

FIGURE 9. - CROSS-SECTIONS OF A WELD-BRAZED JOINT

N74 30930

Thin-Film Diffusion Brazing of Titanium Alloys

E. B. Mikus

A thin-film diffusion-brazing technique for joining titanium alloys by use of a Cu intermediate is described. The manufacturing method employed to fabricate aerospace structures uses integrally heated ceramic platens for the fabrication of flat, tapered, or curved honeycomb panels complete with edgemembers, inserts, and supporting straps.

The method has been characterized in terms of static and dynamic mechanical properties on Ti-6Al-4V alloy. These include tensile, fracture toughness, stress corrosion, shear, corrosion fatigue, mechanical fatigue and acoustic fatigue. Most of the properties of titanium joints formed by thin-film diffusion-brazing are equal or exceed base metal properties. One property, $K_{\rm Ic}$, is lower for joints, but the threshold stress intensity factor for stress corrosion, $K_{\rm Iscc}$, is greater for joints than annealed Ti-6Al-4V base metal.

The advantages of thin-film diffusion-brazing over solid state diffusion bonding and brazing with conventional braze alloys are discussed. The producibility advantages of this process over others provide the potential for producing high efficiency joints in structural components of titanium alloys for the minimum cost. Because of its high performance characteristics and relatively low cost, thin-film diffusion-brazing should find extensive use in aerospace vehicles of the future.

The author is associated with the Materials Research Laboratory of Northrop Corporation, Aircraft Division, Hawthorne, California

Thin-Film Diffusion Brazing of Titanium Alloys

A thin-film diffusion brazing process has been developed for joining titanium structural components such as thin skin honeycomb panels. The process has been termed NOR-Ti-BOND, and it relies on a combination of solid state diffusion and brazing techniques to effect aircraft quality joints in titanium structures.

In this paper, data that characterizes the NOR-Ti-BOND process since its development $\mbox{\ensuremath{^{(1)}}}$ will be reviewed.

METALLURGICAL PROCESS REQUIREMENTS

The NOR-Ti-BOND process utilizes a thin film of Cu to aid in the diffusion bonding of titanium to itself. When copper is placed in intimate contact with titanium and heated to 1635F, solid state diffusion takes place between the two elements until the eutectic composition, 66% Cu - 34% Ti, is reached according to the equilibrium diagram shown in Figure 1. At this point, a liquid forms and flows like a conventional braze alloy. Continued holding at temperature causes additional diffusion to take place between the liquid and the parent metal so that very quickly the liquid is no longer stable at 1635F and solidification occurs. Further thermal exposure is employed to adjust the final composition of the joint by solid state diffusion to the eutectoid composition of 5.5% Cu + 94.5% Ti. The resulting microstructure, shown in the insert of Figure 1, contains a Widenstatten structure of pro-eutectoid alpha and eutectoid/phases of alpha + Ti₂Cu.

The kinetics of the solid state/liquid state diffusion processes involved at the bonding temperature of 1700F are very rapid. The resulting changes in microstructure and extent of diffusion occurring at the joint interface is shown in Figure 2 for 1, 10, and 60-minute intervals. Within one minute, the joint strength achieves 50% maximum and at 60 minutes, full strength is achieved with a diffused zone of about 0.004 inches.

Copper As An Intermediate

The amount of copper used for joining ranges from 8 to 50 mg/in² of the joint area and depends upon the geometry of the joint. For joining honeycomb core or resistance seam bonding of shapes, only 8 mg of Cu/in is used; for honeycomb panels, from 8 to 50 mg of Cu/in of skin area is used, depending upon the core height; for large faying surface joining, properties have been optimized at 50 mg of Cu/in of joint area.

There are several approaches for applying the copper filler material used in the NOR-Ti-BOND process. These approaches include (1) placement of foil, (2) electroplating copper on the edges of the honeycomb core, and (3) electroplating copper on the facesheets and faying surfaces.

Copper foil of the required thickness (0.0002 to 0.0003-inch) is available, but the material is fragile and very difficult to handle dur-

(1) Wells, R. R. and Mikus, E. B., "Thin-Film Diffusion-Brazing of Titanium Members Utilizing Copper Intermediates," U.S. Patent No.3,417,461.

ing assembly of panel components, particularly where a shearing action is encountered during the assembly operation. However, honeycomb panels have been successfully brazed using copper foil.

With the electroplated honeycomb core edges approach, the Ti-Cu eutectic liquid is formed by reaction with the foil, and severe erosion of the foil may take place. In addition, the determination of the amount of deposit on each edge is difficult.

Electroplating of copper on facesheets is the simplest and most reproducible method for placement. The quantity of copper can be varied and controlled accurately, and it can be easily measured in a nondestructive manner with a beta-ray thickness gage. In addition, the adhesion of the electroplate to the substrate is good so that assembly of panel details is simplified. Erosion is minimized, since the skin or edgemember provides a large diffusion sink for the eutectic reaction.

Liquid Flow

The amount of copper used for joining titanium structures is governed also by the propensity of the liquid Ti-Cu phase to "drain." Since in honeycomb panels both horizontal or vertical planes exist, it is necessary to characterize the eutectic liquid flow characteristics.

The worst possible "draining" condition would occur on a vertical facesheet in an area where a large gap between skin and core exists. In such a case, no capillary forces would be present to direct the liquid into the nodes. To simulate this worst condition, flow tests were conducted on Ti-6A1-4V sheets coated with various amounts of copper and exposed to the braze cycle while oriented in a vertical position. Figure 3 shows that "draining" occurs at copper loading rates of between 40 to 50 mg of Cu/in. In addition, the eutectic liquid did not flow beyond the original plated area.

The optimum copper loading rate for various honeycomb core heights is shown in Figure 4. In none of the work performed to date on the fabrication of titanium structure by the NOR-Ti-BOND process has "draining" or eutectic flow been a problem.

NOR-Ti-BOND PROPERTIES

The properties obtainable with the NOR-Ti-BOND process can be classified into two categories; namely, those describing the basic properties of the joint itself and those that describe the properties of a structural configuration.

Joint Properties

Tensile Strength. Basic tensile properties have been determined for Ti-6Al-4V alloy obtained from sheet and l-inch thick plate and compared with butt joints fabricated using 100 psi pressure, 4 hrs. @ 1700F, and 50 mg Cu/in.

After exposure to the fabrication cycle, the plate material retained better than 90% of its original strength; tensile strength decreased approximately 5,000 psi to 138,000 psi, and yield strength decreased approximately 10,000 psi to 124,000 psi, with a corresponding increase in elongation and reduction in area. These mild changes were probably caused by some grain growth during the exposure at 1700F.

Tensile properties of the annealed sheet were similar to those of the plate. Exposure of the sheet to the fabrication cycle decreased the tensile strength approximately 8,500 psi to 132,000 psi and the yield strength approximately 12,000 psi to 125,000 psi, with an increase in elongation and reduction in area. Thus, the effects of the fabrication cycle on tensile properties of the sheet and plate were similar.

Tensile properties of butt joints were determined at temperatures from -150F to 900F, Figure 5. To obtain some measure of the thermal stability of the joints, room temperature tests were also conducted after a thermal exposure of 100 hours at 800F in air. This thermal exposure approximated the same amount of T_i -6Al-4V/Cu diffusion as a thermal exposure of 30,000 hours at 650F, a typical Mach 3 service life. Specimens from both bonding runs exhibited similar tensile strengths. No reduction in properties resulted from this thermal exposure.

Several specimens representing different bonding runs failed in the joints when tested at room temperature and -150F. However, the tensilestrength values were equivalent to strength values for specimens which failed in parent material. In addition, these values were very close to the tensile-strength values obtained for parent material exposed to the fabrication cycle. Visual examination indicated that the joint fractures were relatively flat; whereas, the parent material exhibited the more ductile "cup and cone" type of fracture.

Thus, the tensile strength of a NOR-Ti-BOND butt joint is at least as high as the tensile strength of parent material at temperature in the range of -150F to 900F.

Shear Strength of NOR-Ti-BONDED Joints. Shear strength of lap joints was determined at temperatures from -150F to 900F, Figure 5. With only 1-T overlap joints, all shear type failures were experienced.

The shear strengths of these NOR-Ti-BONDED lap joints are considerably higher than that associated with conventional brazing processes.

Fatigue Properties of Parent Ti-6A1-4V and Butt Joints. Results of sinusoidal, tension-tension fatigue tests at 1200 cpm and a stress-ratio of 0.1 are recorded in Figure 6 for as-received (annealed) Ti-6A1-4V, Ti-6A1-4V exposed to the fabrication cycle and NOR-Ti-BOND butt joints. The data were obtained on coupons taken from three separate bonding runs. No major differences were noted in the fatigue behavior of specimens from different bonding runs.

Of the 14 NOR-Ti-BOND joints tested, ten failed in the parent material and four failed in the joints. One specimen tested at a maximum

stress of 892 ksi failed in the joint outside the scatter band, and the joint may have been defective. Another, tested at a maximum stress of 103.3 ksi, failed in the joint after 792,000 cycles, which represented the low end of the fatigue scatter band. The remaining two joint failures occurred at maximum stress levels above 120 ksi.

Two of the as-received (annealed) parent material specimens tested above a maximum stress of 120 ksi exhibited better fatigue life than the joints or parent material exposed to the fabrication cycle. This was probably related to the slightly higher strength of the annealed parent material. Below 120 ksi, the fatigue behavior of NOR-Ti-BOND joints, parent material exposed to the fabrication cycle, and annealed parent material fell within the same scatter band, and no significant differences could be detected between the fatigue behavior of joints and parent material. At 10^6 cycles, the fatigue strength was approximately 100 ksi to 115 ksi.

These tests indicate that the fatigue strength of smooth, NOR-Ti-BOND butt joints is excellent and essentially equal to the fatigue strength of parent Ti-6Al-4V, particularly at stresses below 120 ksi. In addition, the results also show that the fabrication cycle does not reduce the fatigue strength of the parent Ti-6Al-4V to any significant degree.

Fracture Toughness. Fracture toughness of NOR-Ti-BOND joints containing 50~mg Cu/in² was measured after different fabrication cycles to determine the relationships between processing parameters and joint toughness. All of the specimens were fabricated so that the load was perpendicular to the rolling direction and the crack grew parallel to the rolling direction. The results are shown in Figure 7.

A bonding cycle of one hour at 1700F resulted in a maximum residual copper content of 9.5% at the center of the joint, based upon electron microprobe analysis. Fracture toughness of the joint was comparatively low. Four hours at 1700F resulted in a maximum residual copper content of 7.1%, while specimens held 12 hours at 1700F contained 5.9% and 5.4% copper, respectively. The fracture toughness of the NOR-Ti-BOND joints produced using the chosen processing cycle (4 hours at 1700F) was approximately 60% of the fracture toughness of the as-received material. However, by varying the maximum residual-copper content between 5.4% and 9.5% in the joints, the fracture toughness may range from approximately 40% to 90% of the fracture toughness of as-received (annealed) Ti-6A1-4V.

These results permit us to establish quantitatively the relationships between time at 1700F, maximum residual copper content, and fracture toughness of NOR-Ti-BOND joints.

The fracture toughness of a NOR-Ti-BOND joint does not appear to be highly sensitive to cooling rate. Tests were conducted over a range of cooling rates from $4^{\circ}/\text{min}$ to $40^{\circ}/\text{min}$ from 1700F to 1000F.

Fracture toughness tests on specimens exposed to the fabrication cycle show an increase in toughness over the as-received annealed parent material from 75 to 93 ksi $\sqrt{\text{in}}$. This increase was large enough that the

specimen thickness of l-inch no longer met the ASTM recommendation for insuring plane-strain conditions. Thus, the values found are somewhat higher than would result from a thicker specimen, and they are not true K_{Ic} values.

Stress Corrosion Behavior. Tests were conducted to determine threshold stress-intensity factors ($K_{\rm Iscc}$) for stress corrosion in 3.5% NaCl at room temperature. All of the $K_{\rm Iscc}$ tests were conducted by periodically increasing the load on pre-cracked WOL specimens in small increments until stress-corrosion crack growth occurred when the $K_{\rm Iscc}$ was exceeded. It was observed that stress-intensity factors as little as 10% above $K_{\rm Iscc}$ produced rapid crack growth and specimens failed within one to two hours. These failure times corresponded to crack-growth rates of approximately 1/8-inch to 3/4-inch per hour.

It was found that the $K_{\rm Iscc}$ values for the NOR-Ti-BOND joints are essentially equal to or slightly better than the $K_{\rm Iscc}$ values for ascecived (annealed) parent material and for parent material exposed to the fabrication cycle. The ratio $K_{\rm Iscc}/K_{\rm Ic}$ provides a measure of the degree of stress-corrosion susceptibility produced by the salt water. The ratio for the joints is 0.77, which is substantially higher than the values of 0.42 and approximately 0.37 obtained for as-received parent material and parent material exposed to the fabrication cycle. Thus, the parent material is more susceptible to stress corrosion than the joints. In addition, the data show that the fabrication cycle had no major effect on the $K_{\rm Iscc}$ for parent material.

In general, smooth specimens of titanium alloys are not susceptible to stress-corrosion in salt water. Several tests were conducted to determine stress-corrosion susceptibility of NOR-Ti-BOND butt joints in smooth specimens. In addition, one smooth specimen of parent material was tested after exposure to the fabrication cycle. After 1000 hours immersion in 3.5% NaCl at room temperature and under a tensile stress of 102,000 psi, the specimens showed no evidence of corrosion or stress corrosion. The specimens were then tensile tested at room temperature without any reduction in joint properties. Tensile properties were basically the same as those obtained on specimens which were not exposed to a stress corrosion test, Figure 5. Thus, smooth NOR-Ti-BOND joints and parent material exposed to the fabrication cycle are essentially immune to stress corrosion in 3.5% NaCl at room temperature.

Fatigue and Corrosion Fatigue of WOL Specimens. The fatigue behavior of parent material and NOR-Ti-BOND WOL specimens tested in air and in 3.5% NaCl is summarized in Figure 8. The parent material exposed to the fabrication cycle exhibited the largest crack length at failure, followed by annealed parent material and then NOR-Ti-BOND joints when tested in air. The crack lengths at failure were reasonably consistent with the fracture toughness values for the specimens. In 3.5% NaCl, the cracks grew approximately twice as fast as in air for the parent material.

For the NOR-Ti-BOND joints fatigued in air, the crack started in the joint but propagated into parent material and ran parallel to the joint but approximately 1/8-inch from it. This problem was solved by side notches of 1/16-inch radius and 0.025-inch depth along the joint. For a NOR-Ti-BOND joint in 3.5% NaCl, the crack grew approximately three times as rapidly as in air.



On the basis of tests on WOL specimens, the fatigue and corrosion fatigue behavior of parent material was somewhat superior to the behavior of the NOR-Ti-BOND joints. It is noteworthy that fatigue tests in air on smooth butt joints indicated comparable fatigue behavior for joints and parent material. Perhaps the presence of a sharp notch in the WOL specimen has influenced the results.

Several WOL specimens were examined by scanning electron fractography to determine fracture modes in fatigue and corrosion fatigue. As-received (annealed) parent material and parent material exposed to the fabrication cycle exhibited similar fracture modes. Figure 9 shows that the annealed parent material fatigued in air exhibited a normal, transgranular, fatigue failure with a small amount of secondary cracking. The fracture mode under corrosion fatigue, Figure 10, was transgranular quasi-cleavage with some secondary cracking. However, as the crack extended and the stress-intensity factor increased, the failure mode changed to transgranular cleavage with much less secondary cracking.

Under fatigue in air, the NOR-Ti-BOND joint exhibited a normal transgranular fatigue fracture with a small amount of secondary cracking, Figure 11. Under corrosion fatigue, the failure mode, Figure 12, was transgranular quasi-cleavage with secondary cracking along interfaces between alpha needles and eutectoid as well as in the eutectoid. Some areas of transgranular cleavage through the alpha needles were also evident. Thus, the NOR-Ti-BOND joints and parent material exhibited the same basic fracture modes.

It is interesting to note that the corrosion-fatigue failure modes for joints and parent materials were basically the same as failure modes under stress corrosion. Thus, stress corrosion is apparently the dominant part of the failure mechanism operating in corrosion fatigue.

Configuration Controlled Properties

The second category of properties that are used to characterize airframe structures are those influenced by the structural design.

NOR-Ti-BOND Honeycomb Panels. Preliminary design data on honeycomb panels fabricated with the NOR-Ti-BOND process are shown in Figures 13 to 17. The data are limited to flat wall, 1/4-inch square cell, Ti-75A core fabricated by the NOR-Ti-BOND process. Foil gages ranged from 0.0015-inch to 0.003-inch with a density range from 3.4 lb/ft³ to 6.7 lb/ft³. Core heights ranged from 0.5-inch to 1.5-inch. A limited amount of test data indicate that these equations are equally valid for Ti-3Al-2.5V alloy core. Ti-6Al-4V alloy skins were employed in thicknesses ranging from 0.012-inch to 0.060-inch.

Acoustical Fatigue Resistance. One of the most effective structural constructions for high acoustic environments is honeycomb panel configurations. This statement is based upon experience gained with adhesively bonded honeycomb panels or brazed metallic panels. In both cases, a considerable fillet is created at the core/skin interface to provide dampening characteristics and lower stress concentrations. Since the NOR-Ti-BOND process relies on a thin-film approach, the fillet formation is limited to only 0.004-inch to 0.005-inch radius. To determine the effect of these small fillets on acoustic fatigue response of NOR-Ti-BONDED panels, a series of beams were run in a progressive wave chamber generating a maximum power level of 167 db.

These beams were 18.5-inches long, 6-inches wide, with a core thickness of 0.5-inch or 0.6-inch. The skins were Ti-6Al-4V alloy. The side exposed to the acoustic pressure was 0.040-inch thick. The other skin was 0.012-inch thick. The core was NOR-Ti-BONDED core made of Ti-75A, non-perforated, flat wall, 1/4-inch square cells, with a foil thickness of 0.003-inch and a core density of 6.7 lb/ft³.

The beams were open at the sides; i.e., no edgemembers. But at the ends where the support attachment was made, some were sealed with bonded edgemembers.

Each beam was subjected to a series of parallel incidence, progressive wave acoustic exposures. The series consisted of 3-hour exposures at overall sound pressure levels starting at 155 db and increasing by 3 db every 3 hours until failure occurred. Failure was detected by noting changes in the response natural frequency, resonant amplitude, and skin strain as measured by strain gages. The results of these tests are shown in Figure 18.

Beams AB-15 and AB-19 failed in the center of the 0.012-inch skin side at an approximate rms stress of 16 ksi. Beam AB-20 failed at a defective edgemember to 0.040-inch thick skin. Without edgemembers, failure always occurred at the honeycomb-to-skin joint in a peeling mode at lower energy levels. It should be noted that these results, even for the open ended beams, are very acceptable considering the severity of the test.

Thermal Conductivity of Titanium Honeycomb Panels. In airframe design, honeycomb panels are often associated with areas where it is desirable to limit the heat transfer from the aerodynamic boundary layer; i.e., into integral fuel tanks of the wing or interior cabin of a spacecraft.

Titanium has an inherent low thermal conductivity and, when fabricated into honeycomb panels by the NOR-Ti-BOND process, relatively low heat transfer results. If, however, the heat path from the outside skin to the inner skin is increased by the addition of braze alloy in the cell nodes and cell wall/skin interface, a considerable increase in thermal conductivity may result that imposes severe weight penalties due to insulation requirements on the design of the final structure. In Figure 19, the thermal conductivity of a NOR-Ti-BONDED honeycomb panel is compared with a titanium honeycomb panel brazed with an aluminum alloy. The increased conductivity of aluminum plus the increased heat path cross-

section of the core has resulted in an order of magnitude rise in the thermal conductivity of the aluminum brazed panel.

MANUFACTURING PROCESSES

Thin-film diffusion brazing by the NOR-Ti-BOND process is a versatile approach to the fabrication of a variety of titanium honeycomb panel configurations. The technique developed utilizes hot ceramic platens as the basic tools.

Fabrication of Honeycomb Panels

Preparation of Panel Materials. Facesheet materials are first trimmed to the approximate size, degreased, and washed. They are lightly cleaned chemically with a nitric-hydrofluoric acid mixture. The sheets are electroplated with copper in a copper sulfate plating bath. Copper thickness on the facesheets and any other plated components is determined with a beta gage. This device uses a beta-ray emitting source and a Geiger counter for determining the thickness of the copper plate in a nondestructive manner.

The honeycomb core comes from two sources; if it is purchased, the foil ribbons are formed and resistance—welded into an expanded honeycomb configuration. This honeycomb must then be rigidized for machining. Machining is performed using a Blanchard grinder to achieve flat surfaces. Contoured surfaces present additional machining or grinding problems. The honeycomb is removed from the rigidizing surface plate, turned over, repotted, and machined on the other surface. Finally, the rigidizer is removed. At this time, the core is inspected for thickness and tolerance; then it is trimmed to the proper shape of the honeycomb panel. If the honeycomb is fabricated using the NOR-Ti-BOND process, it is fabricated and ground in the unexpanded condition. Thus, rigidizers are not required. After machining, the core material is expanded, trimmed to final size, and cleaned.

Edgemember and insert components are normally machined, stress-relieved, and then cleaned in a nitric-hydrofluoric acid solution. In most cases, the surfaces to be brazed are electroplated with copper in a copper sulfate solution. However, in some cases, it is desirable to apply the copper as a foil.

Tolerances used for the various components that are assembled into a honeycomb panel are as follows: facesheet material is normally as-received material from the rolling mills. Expanded honeycomb core is ground to \pm 0.001-inch if it is ground in the unexpanded condition. The height of edgemembers and other inserts must be within $\frac{+0.000}{-0.004}$ -inch of the honeycomb height in order to achieve the proper tolerance control in the panel.

Tooling and Retorts. The tooling material most commonly used in the fabrication of the titanium honeycomb panels is 321 stainless steel. The surfaces of the stainless steel which contact the titanium are flame-sprayed with zirconium oxide. Titanium surfaces, which were in contact

with the zirconium oxide—coated stainless steel, have been examined microstructurally and with the electron microprobe for possible contamination. No contamination has been noted. Stainless steel is used for slip sheets and tooling members to support edgemembers and perform positioning operations. With external Tees or other attachments, machined stainless steel honeycomb is used to fill in large areas rather than massive blocks which create heat sinks.

The panel details are encapsulated in a stainless steel brazing retort made with a stainless steel picture frame covered with thin facesheets used to achieve a diaphragming effect such that a dynamic clamping pressure can be applied to the honeycomb panel. A second matching stainless steel retort (pressure pillow) is used to apply the bonding pressure to the honeycomb panel, forcing good fitup between component parts. The brazing retort and pressure pillow are placed between a fused-silica brazing tool and evacuated using a mechanical roughing pump. Back-filling of the brazing retort is done with ultrahigh-purity argon which is passed through a heated titanium chip-getter. Five purging cycles and a leak check are normally conducted.

Fused-silica tools are heated by resistance wires placed approximately 3/8-inch below the flat surfaces. The surfaces of both tools have a TIR of 0.006-inch across the 2-foot by 3-foot working surface. A system of guard heaters around the sides of the retort has been used to provide good temperature uniformity during the fabrication cycle. Temperature across the panel are held within 50F during heating and within 30F during the one-hour diffusion cycle.

The present technique places the honeycomb panel retort on the bottom and the pressure-pillow retort on the top, Figure 20. During the brazing cycle, the panel to be brazed is pressed against, and tends to duplicate, the surface of the lower brazing tool. Therefore, the aerodynamic surface of the panel is placed down in the retort and the inside or internal structure surface is on the top during the brazing cycle.

For certain applications, the pressure pillow is omitted and the panel is clamped between the two flat silica-tool surfaces. This technique allows very accurate control of the final panel dimensions and good control of the panel configuration. The disadvantages of this system are that a controlled amount of core cell-wall deformation occurs in order to insure complete fit-up between the core and the facesheets. Thus, some portions of the panel have essentially perfect fitup, while others have a honeycomb core which is deformed up to 0.005-inch. In most cases, this amount of cell-wall deformation is irrelevant to the total performance of the structure.

The pressure-pillow technique has the capability of brazing panels without requiring matched tools. One tool controls the configuration of the aerodynamic surface; whereas, the other tool merely backs up the pressure pillow and provides heat for brazing. The pressure pillow then expands and applies the pressure, assures fitup, and presses the panel against the aerodynamic configuration surface.

With proper control of either the matched-tool concept or the pressure-pillow concept, honeycomb panels can be made with little or no deformation of the honeycomb core.

Two techniques are used to apply pressure to the faying surface joints of either edgemembers or inserts during brazing. Both methods require a close-fitting stainless steel tooling bar to be placed within an edgemember or overhanging insert. Since stainless steel expands about twice as much as titanium, the tooling is made to fit at 1600F and is therefore loose at room temperature.

When the edgemember is being brazed with the clamped fused-silica tool technique, the edgemember tooling-bar arrangement acts as a gage block. That is, the silica tools are forced in until they rest on the edgemember. When this happens, the honeycomb core is forced against the facesheet and the necessary compressive load is applied to the faying surface.

The pressure-pillow technique uses a similar concept, except that tooling bars must now be located in the pillow to transmit the force from the silica tool to the brazing retort. These tooling bars are attached to the perimeter of the pillow and not the pillow face, which would impair the diaphraming action.

Brazing Cycle. Present practice of controlling temperature and pressure during a typical brazing cycle follows: the panel-containing retort is purged five times with high-purity, gettered argon and finally backfilled with argon to approximately one-third of an atmosphere. The fused-silica tools are heated at a rate of 500F to 550F per hour to the brazing temperature and held at 1700F.

As the argon within the brazing retort expands on heatup, the internal pressure eventually reaches one atmosphere at 1200F. At this time, the pressure within the retort is allowed to exceed the clamping pressure in order to equalize the argon pressure throughout all of the honeycomb cells. This step insures an even argon pressure and reduces the possibility of having air trapped in a cell which might contaminate the cell prior to brazing. As the temperature increases over 1200F, the argon pressure in the retort exceeds one atmosphere.

With the matched-tool concept, this internal pressure is counteracted by use of the two fused-silica tools pressed against the surface of the retort and panel. Tool pressures are controlled in order to provide a clamping force. The retort edgemembers act like gage blocks in order to prevent excess tool movement from crushing the panel.

With the pressure-pillow technique, the clamping pressure is provided above 1200F by pressurizing the pillow. This pillow then presses against the brazing retort and the fused-silica tools. The fused-silica tool pressure is high enough to overcome the pillow pressure. To prevent collapse of the titanium honeycomb with the pressure-pillow technique, only a small pressure is maintained from 1200F to 1550F. Then, as the brazing or reaction temperature of 1635F is approached, the pressure differential is

increased to 1 psi. This clamping force of 1 psi across the honeycomb panel is held until a temperature of 1650F is reached. The pressure is then lowered until, at 1700F, a pressure of 3/8 psi is held to control the configuration of the honeycomb panel. The panel is held at 1700F for one hour to allow the copper to diffuse into the titanium and the titanium to diffuse into the joint.

The cooling rate is controlled by the natural cooling of the silica tools and the honeycomb-panel package. During cooling, a small, positive pressure is maintained against the panel to maintain alignment.

Quality Control and Nondestructive Testing. As previously mentioned, copper thickness is measured nondestructively prior to assembly and brazing. The panels are brazed in an inert atmosphere to assure cleanliness, and the brazing tools assure good fit and dimensional accuracy. The tools are checked for flatness after every run. No change in flatness has been observed after 29 runs, thereby providing good assurance of panel flatness.

After brazing, the panels are checked for flatness and for thickness which provides an indication of quality. Subsequent inspection by X-radiography provides detailed information on the internal structure of the core and the uniformity of node flow. Anomalies such as core-shifting, core-node separation, and cell damage can be detected by this method.

Inspection by ultrasonic pulse-echo and through-transmission C-scanning is conducted with highly reliable results. These techniques are being used primarily to detect facesheet-to-core and facesheet-to-edgemember unbonds.

Indications of unbonds have been verified by destructive tests. The advantage of these X-ray and ultrasonic techniques is that permanent full-size recordings are obtained. Thus, defects can be easily related to their actual location and size in the structure.

SUMMARY

In the case of honeycomb panels, the NOR-Ti-BOND process utilizes only a very small amount of added material, 0.02 lb of Cu/ft² of panel, to effect a strong bond equivalent to base metal in almost all properties. The copper, moreover, is placed on the entire sheet, which permits easy electrolytic deposition control of thickness and uniformity. The deposition is strongly adherent and can be quantitatively verified as to the proper quantities prior to bonding.

The core is completely bonded at the nodes. Therefore, the core is easily cleaned and much less susceptible to contaminant entrapment at node points. In addition, the core can be machined to the required height. Typical machining tolerance of \pm 0.003-inch is adequate in an unexpanded condition. This feature is desirable for low core preparation costs and easy handling qualities.

Another important feature of the NOR-Ti-BOND process is the option to bond "in situ" panel inserts, edgemembers, and straps while the panel

is being bonded. This feature precludes the use of subsequent fabrication processes to obtain a complete panel. Honeycomb panels, moreover, can be made to any desired shape with the appropriate tooling and fabrication process.

The producibility advantages, coupled with high performance characteristics at relatively low cost, makes the thin-film diffusion brazing of titanium process a leading contender for the fabrication of aerospace vehicles of the future.

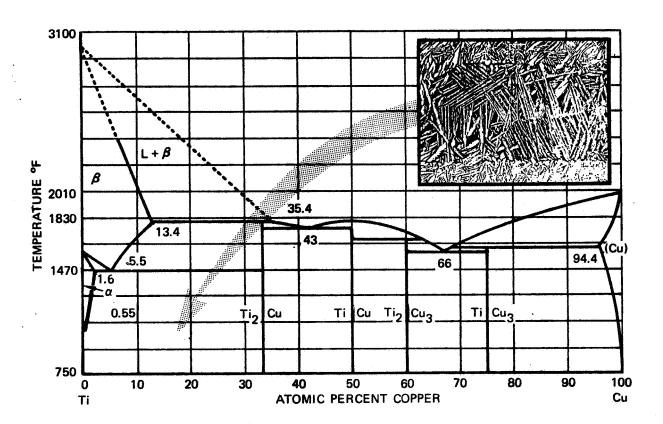
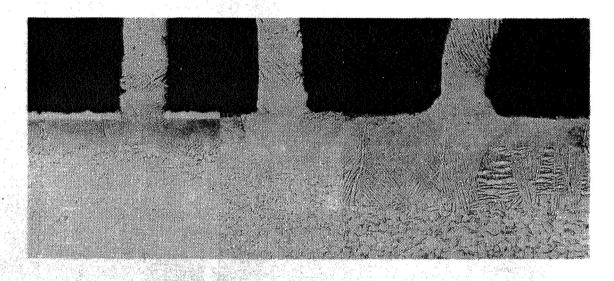


FIGURE 1. Ti/Cu PHASE DIAGRAM

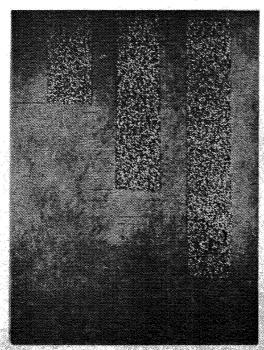


1 MIN

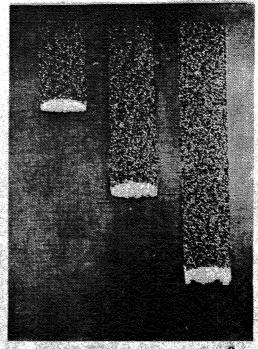
10 MIN

60 MIN

FIGURE 2. DIFFUSION OF Cu IN TI AT JOINT INTERFACE DURING BONDING AT 1700°F



COPPER QUANTITY: 40 MG/IN²
NO "DRAINING"



COPPER QUANTITY: 50 MG/IN²
"DRAINING" OCCURRED

HEATING RATE: 400F/HR

FIGURE 3. VERTICAL DRAIN BEHAVIOR OF NOR-TI-BOND LIQUID ON TI-6AI-4V

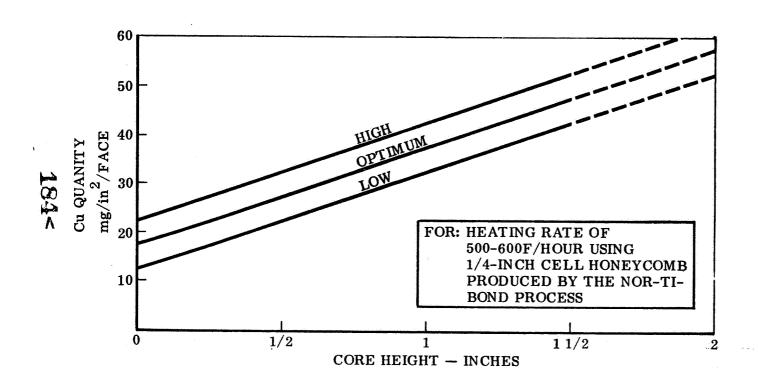


FIGURE 4. COPPER QUANTITY REQUIRED TO FABRICATE TITANIUM HONEYCOMB PANELS



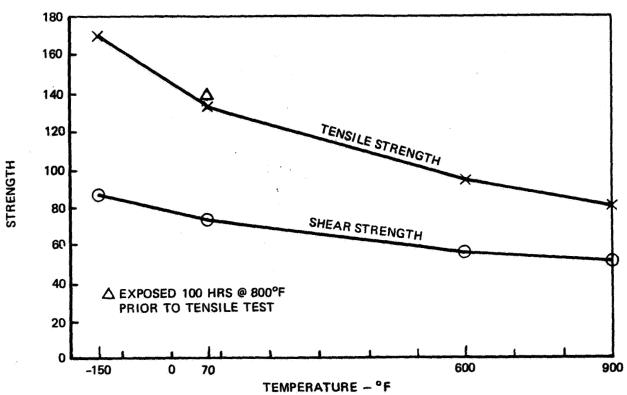


FIGURE 5. TENSILE AND SHEAR PROPERTIES OF NOR-TI-BONDED JOINTS

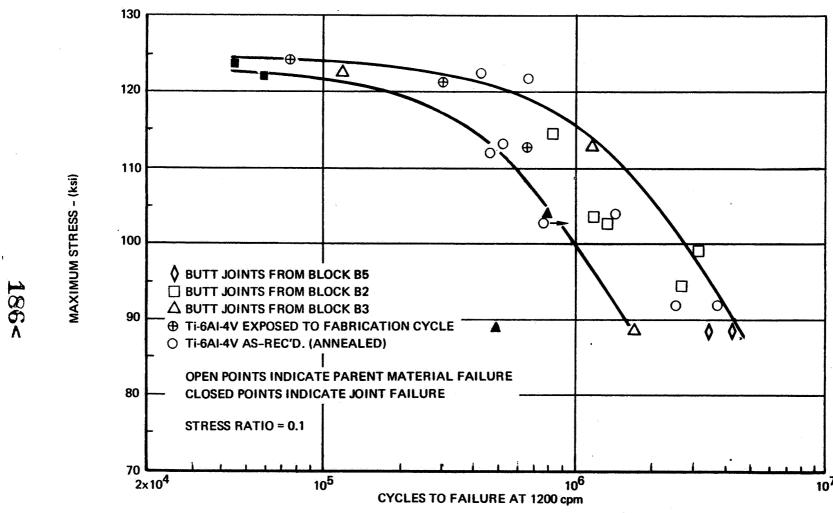


FIGURE 6. SINUSOIDAL, TENSION-TENSION FATIGUE PROPERTIES OF PARENT Ti-6AI-4V AND NOR-Ti-BOND BUTT JOINTS

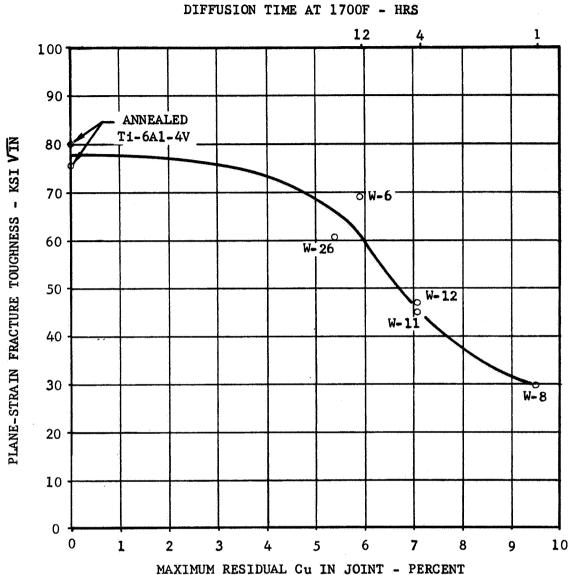


FIGURE 7. EFFECT OF RESIDUAL COPPER CONTENT AND DIFFUSION TIME AT 1700F (FOR 50 mg/in² Cu) ON FRACTURE TOUGHNESS OF NOR-TI-BOND JOINTS

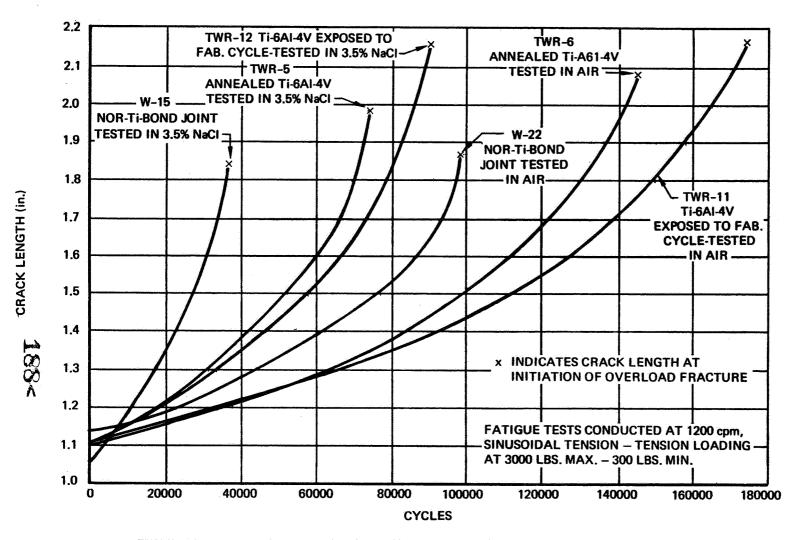


FIGURE 8. FATIGUE BEHAVIOR OF WOL SPECIMENS IN AIR AND 3.5% NaCI

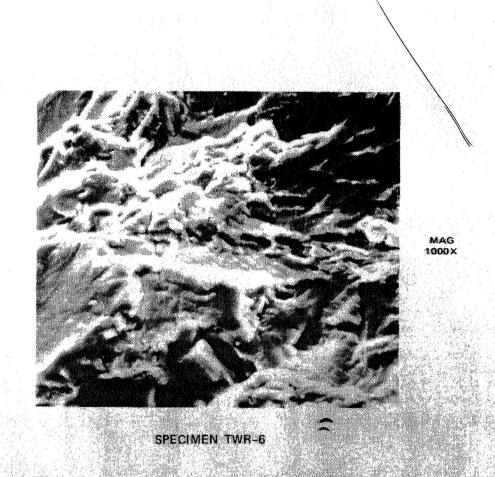
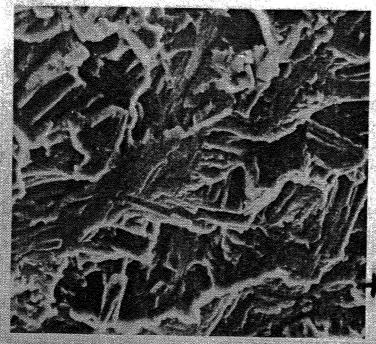
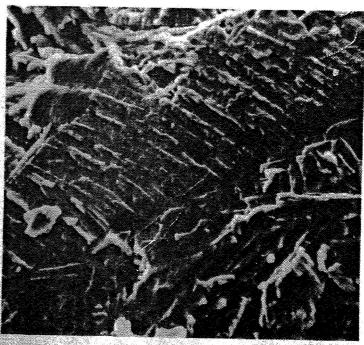


FIGURE 9. FRACTURE SURFACE OF ANNEALED TI-6AI-4V FATIGUED IN AIR





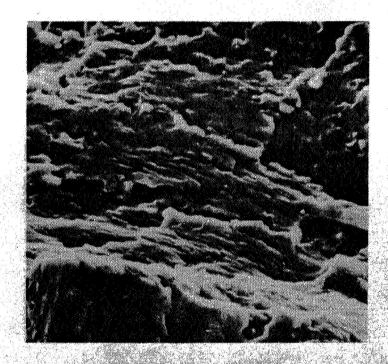


MAG 1000X

QUASI-CLEAVAGE REGION

CLEAVAGE REGION
SPECIMEN TWR-5

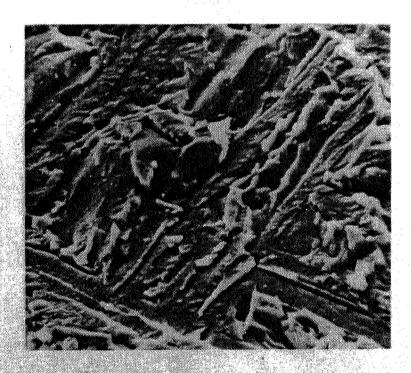
FIGURE 10. FRACTURE SURFACE OF ANNEALED TI-6AI-4V FATIGUED IN 3.5% Na CI



MAG 2000X

SPECIMEN W-22

FIGURE 11. FRACTURE SURFACE OF NOR-TI-BOND JOINT FATIGUED IN AIR



MAG 1000X

SPECIMEN W-15

FIGURE 12. FRACTURE SURFACE OF NOR-TI-BOND JOINT FATIGUED IN 3.5% Na CI

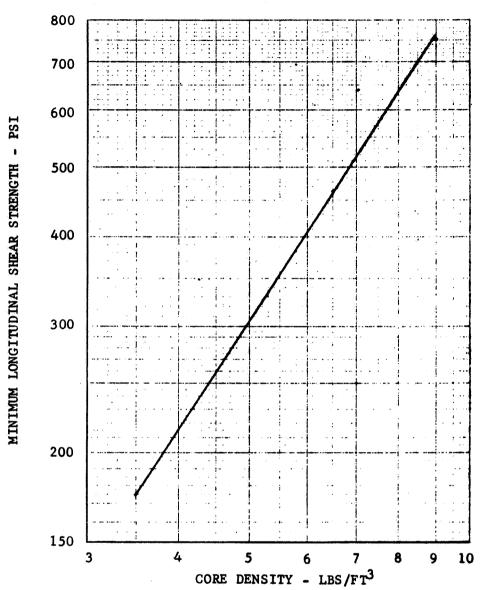


FIGURE 13. ANNEALED Ti-75A TITANIUM NOR-TI-BOND HONEYCOMB SQUARE CELL — FLAT WALL MINIMUM LONGITUDINAL SHEAR STRENGTH

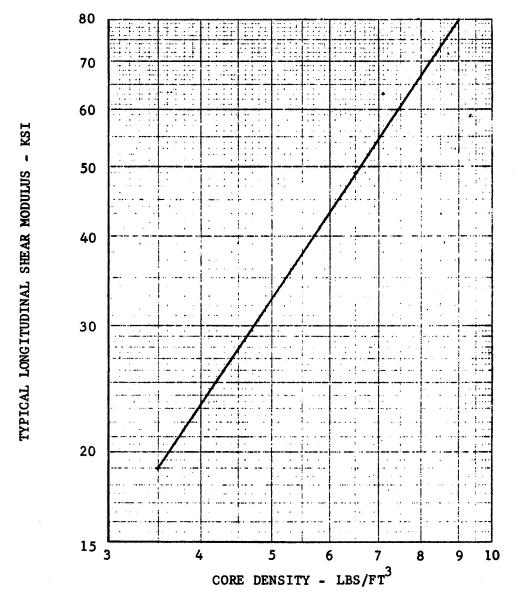


FIGURE 14. ANNEALED Ti-75A TITANIUM NOR-Ti-BOND HONEYCOMB SQUARE CELL — FLAT WALL TYPICAL LONGITUDINAL SHEAR MODULUS

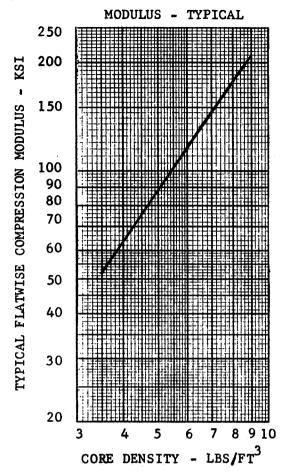


FIGURE 15. ANNEALED Ti-75A TITANIUM NOR-Ti-BOND HONEYCOMB SQUARE CELLS — FLAT WALL FLATWISE COMPRESSION

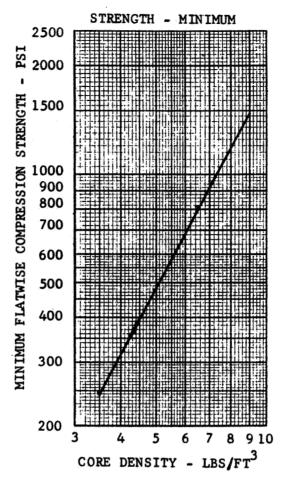


FIGURE 16. ANNEALED Ti-75A TITANIUM NOR-Ti-BOND HONEYCOMB SQUARE CELLS — FLAT WALL FLATWISE COMPRESSION

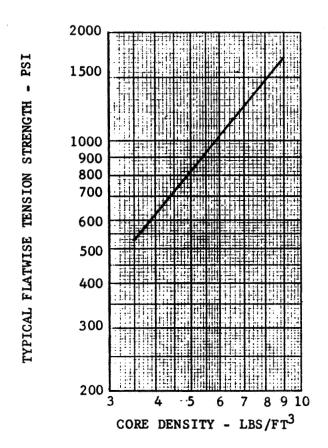


FIGURE 17. ANNEALED Ti-75A TITANIUM NOR-Ti-BOND HONEYCOMB SQUARE CELLS — FLAT WALL TYPICAL FLATWISE TENSION STRENGTH

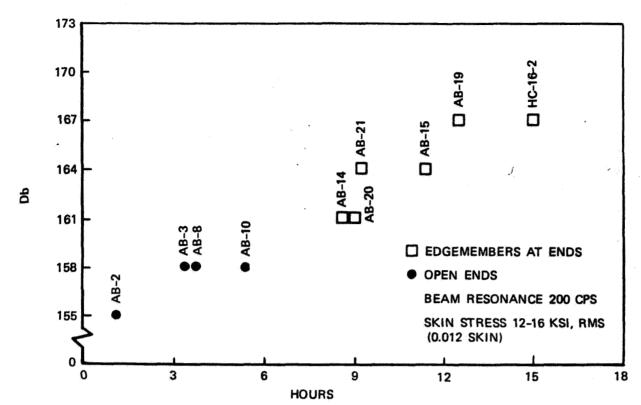
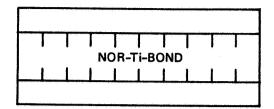


FIGURE 18. ACOUSTIC FATIGUE RESPONSE OF NOR-TI-BONDED HONEYCOMB BEAMS





5.0 BTU/HR/FT/°F



½" SKIN 6.2 #/FT³ CORE ½" HIGH

0.050" SKIN 4.9 #/FT³ CORE 0.90" HIGH

SKINS — Ti-6AI-4V CORE — Ti-75A

FIGURE 19. THERMAL CONDUCTIVITY OF TITANIUM HONEYCOMB PANELS

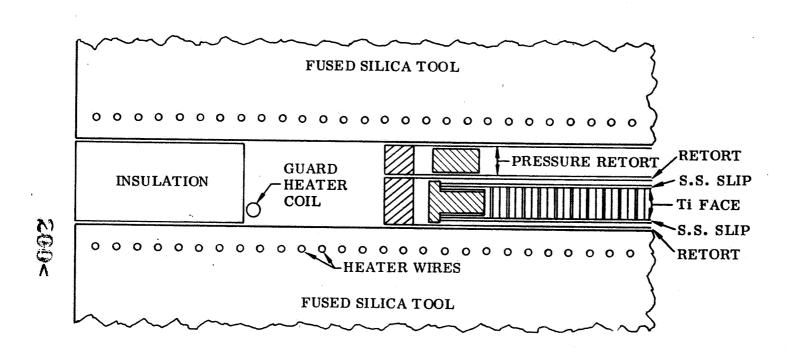


FIGURE 20. BONDING TOOL RELATIONSHIP

N74 30931

ASM/NASA/GWU SYMPOSIUM ON

WELDING, BONDING AND FASTENING

Williamsburg, Virginia

May 30 - June 1, 1972

HIGH POWER LASER WELDING

Conrad M. Banas Senior Research Engineer United Aircraft Research Laboratories East Hartford, Connecticut 06108

ABSTRACT

A review of recent developments in high-power, carbon-dixoide laser welding is presented. Deep-penetration welding in stainless steel to 0.5-in. thick, high-speed welding in thin gage rimmed steel and gas-shielded welding in Ti-6Al-4V alloy are described.

The effects of laser power, power density, focusing optics, gas-shielding techniques, material properties and weld speed on weld quality and penetration are discussed. It is shown that laser welding performance in thin materials is comparable to that of electron beams. It is further shown that high quality welds, as evidenced by NDT, mechanical and metallographic tests, can be achieved. The potential of the laser for industrial welding applications is indicated.

201<

INTRODUCTION

From its initial development, the laser has been hailed as a pontentially useful welding tool for a variety of applications. Until recently, however, laser welding has been restricted to relatively thin materials and low speeds by the limited power available on a continuous basis. With the development of multikilowatt, continuously-operating, CO₂ laser systems (Refs. 1-3 and Fig. 1), this limitation has been obviated and the scope of technically-feasible laser welding applications has been correspondingly broadened.

The laser's capability for generating a power density greater than 10^6 watt/in.² is a primary factor in establishing its potential for welding. A power density of this magnitude can only be duplicated with electron-beam welding equipment and provides the laser with the ability to produce deep-penetration welds. As may be noted from Fig. 2, which was obtained with electron-beam equipment, a deep-penetration threshold exists at a power density of the order of 10^6 watt-in.². At low power densities, characteristic of typical gas and arc-welding equipment, a shallow, roughly-hemispherical weld zone is formed. At somewhat higher power densities, characteristic of modern plasma-arc welding equipment, a wine-glass-shaped weld zone is generated. At still higher power densities, deep penetration is achieved. By way of illustration it is noted that a power density of 10^6 watt/in.² is equivalent to that provided by a thermal source at 23,000°R.

The deep-penetration capability of electron beams extends only a short distance out of vacuum. By contrast, CO2 laser beams can be transmitted for appreciable distances through the atmosphere without serious attenuation or optical degradation. In addition, laser beams may be readily directed and shaped with front-surface mirrors and they do not generate x-rays on interaction with a metallic workpiece. For these reasons the laser appears potentially more versatile for many production welding applications.

Several disadvantages of the laser relative to the electron beam may also be noted. The focused beam spot diameter is limited by diffraction to a size that is directly proportional to the radiation wavelength, λ , and the focal length of the optics and is inversely proportional to the effective aperture or beam diameter (Fig. 3). The ratio of focal length to aperture diameter is referred to as the f/number. Since the equivalent wavelength of a high-voltage electron beam is much shorter than the 10.6 micron wavelength of $\rm CO_2$ laser radiation, a higher f/number, and a correspondingly longer depth of field, may be utilized to provide a given power density. As a result, surface positioning is less critical than with laser beams and penetration into thick workpieces is facilitated.

Other factors which detract from the potential of lasers for welding

are that room temperature metal surface reflectivity for CO₂ laser radiation is quite high and that focused laser radiation can result in generation of a beam-absorbing plasma in the vicinity of a workpiece. Plasma formation stems from gas breakdown induced by the electric field due to the focused electromagnetic radiation (laser beam). In dry air the breakdown threshold for CO₂ laser radiation is of the order of 10⁹ watt/in.². Evolution of particles and metal vapor from the workpiece during the welding process, however, can reduce this threshold to a level of the order of 10⁹ watt/in.² (Fig. 4). If adequate provision is not taken to eliminate breakdown, beam absorption occurs in the generated plasma and inefficient welding performance is obtained. Since breakdown parameters depend on gas type, shield gas composition for laser welding must be selected on the basis of gas-breakdown characteristics as well as on weld zone metallurgical requirements.

Investigation of the effects of the above noted factors on laser welding performance has constituted a portion of the laser materials processing program at the United Aircraft Research Laboratories. This paper has been prepared to present a review of some of the more recent developments in high-power laser welding and to provide an insight into possible near-term industrial welding applications.

EXPERIMENTAL APPARATUS AND PROCEDURE

The laser welding tests described herein were conducted with a convectively-cooled, multikilowatt, continuous, CO2 laser. This unit, shown in Fig. 1, operates as an amplifier for a low power input beam from a stable laser oscillator. In this manner high optical output power is achieved in the fundamental (TEMOO) mode of laser oscillation; this facilitates focusing and thereby enhances metal working capability. The laser amplifier consists of twelve separate discharge tubes connected electrically in parallel and optically in series. High specific power per unit volume is achieved by the expedient of rapid flow of the gases through the tubes such that convective cooling of the discharge medium is achieved. The gases from the discharge tubes pass through a heat exchanger in which the waste energy from the electric discharge is removed, through a circulating pump, through a second heat exchanger which removes the heat of compression and then back through the laser channel. Recirculation of the gases permits reduction in pumping power requirements and operating cost. It is, however, necessary to continuously remove and replenish a small fraction of the circulating gas to maintain a constant composition. This requirement stems from the fact that CO2 dissociation and formation of oxides of nitrogen are induced by the high-voltage electric discharge.

A plane mirror mounted on a solenoid-actuated slide was used to deflect the high-power beam from the amplifier into a calorimeter which served to monitor power as well as to provide an energy sink for the beam between weld passes. As shown in Fig. 5, the beam was directed toward, and focused upon, the workpiece by an 18-degree-off-axis parabolic mirror. The workpiece was placed on a variable speed table which could be moved under the focused beam at speeds ranging from 5 to 500 ipm. A modified, gas-tungsten-arc welding fixture was used to provide a protective atmosphere for reactive materials; the trailer shield of this fixture was oriented such that the laser beam passed through the opening provided for the tungsten electrode.

During a welding test, the deflecting mirror was withdrawn and the workpiece was translated beneath the focused beam at a controlled speed. Most tests were conducted with the beam focused at the workpiece surface. Inert gas shielding was provided for reactive metals; for other materials a low-velocity crossflow of inert gas was used to prevent plasma formation. Workpiece travel (and hence weld length) was limited by the fixturing to approximately 6 inches. Since laser output can readily be held constant at the multikilowatt level for hours at a time, this limitation should not be construed as a limitation of laser welding capability.

DISCUSSION OF EXPERIMENTAL WELDING RESULTS

The high power laser equipment described in the foregoing section was utilized for investigations of welding in a number of materials. The first welds were effected in 300 series stainless steel with results represented by the butt weld cross section shown in Fig. 6. The 1/4-in., deep-penetration weld shown exhibits a depth-to-width ratio of about 7:1 and was formed in atmosphere at a speed of 50 ipm and a laser power of 3.5 kW. The edges of the butt weld configuration were machined to provide close fit up so that filler material was not required. Radiographic inspection of selected stainless steel welds has shown that sound, nonporous welds can be formed. Further, tensile tests have shown that welds exhibiting a strength equivalent to that of the parent material can be generated.

A parametric representation of laser welding performance in stainless steel is shown in Fig. 7. It may be seen from Fig. 7 that penetration increases essentially in proportion to the laser power level. Also to be noted is that the maximum penetration achieved was 0.5 in. at a laser power level of 5.5 kW and a welding speed of 10 ipm. Attempts to increase penetration by decrease in welding speed resulted in collapse of the deep-penetration mode and a decrease in penetration. Figure 7 further illustrates that the depth of penetration decreases slowly with increase in welding speed. Increasing the welding speed, however, does significantly decrease the width of the weld zone such that thermal energy input and distortion are minimized. The reduction in weld zone cross section with increase in welding speed is treated in more detail in the subsequent discussion of titanium alloy welding results.

Parametric curves similar to those for stainless steel have also been generated for low-carbon, rimmed steel and are presented in Fig. 8. Once again it is noted that the depth of penetration for laser welding decreases slowly with increase in welding speed and that penetration is approximately proportional to the laser power level. The absolute level of penetration obtained is somewhat less than that for stainless steel; this may be due to the higher thermal diffusivity of rimmed steel. Of particular note is that welding speeds greater than 200 ipm were achieved in 0.1-in. thick material at power levels of the order of 4 kW. High quality welds, which exhibited a tensile strength higher than that of the parent material, were obtained provided that the mating surfaces were appropriately treated with a deoxidant. Inert gas shielding also led to a significant improvement in rimmed steel weld quality. As may be seen in Fig. 9, gas shielding completely eliminated blowhole generation in rimmed steel without use of a deoxidant at the weld zone.

Helium shielding was also utilized on the top and bottom surfaces of the Ti-6Al-4V penetrations shown in Fig. 10. The material was machined prior to test to remove surface scale, then cleaned in an acid solution, subsequently rinsed with alcohol and dried with Freon-12. Material of 0.2 in. thickness was used and a copper chill bar was positioned approximately 0.02 in. beneath the lower weld surface. It is noted from Fig. 10 that a thin, high depth-to-width ratio melt zone is formed at high welding speeds. As welding speed is decreased, conduction into the surrounding material leads to a broader melted zone and to a characteristic hourglass shape. With further decrease in welding speed the fused zone becomes still broader and nearly uniform in width throughout the entire penetration. At very low welding speeds the deep-penetration mode collapses and an extremely shallow fused zone is obtained. The faster heating and cooling rates encountered at high welding speed also tend to reduce grain growth in the weld zone as may be seen in the magnified cross sections shown in Fig. 11.

The dependence of Ti-6Al-4V penetration on welding speed and laser power is shown in Figs. 12 and 13. It is noted that the general characteristics of the relationship in Fig. 12 are similar to those for stainless and rimmed steels shown previously in Figs. 7 and 8. The somewhat lower rate of decrease in penetration with speed may be caused by the lower thermal diffusivity of titanium alloy which facilitates the generation and maintenance of a stable deep-penetration welding mode.

Initial radiographic inspection of laser welds in Ti-6Al-4V alloy has shown evidence of pinhole porosity of the type encountered in electron beam welding. Such porosity may be due to the intermittent collapse of the deep-penetration cavity and underscores the requirement for precise definition and control of welding parameters in high-beam-power-density welding of titanium alloys. Post-weld heat treating, improved gas shielding and limited fatigue endurance tests are planned for future studies.

In order to place the above described laser welding performance in proper perspective, it is useful to compare the results with electron beam data. A convenient vehicle for this comparison is the nondimensional representation formulated in Ref. 4 and utilized in Fig. 14. The nondimensional parameter on the ordinate contains the depth of penetration, b, the laser power level, P, the thermal conductivity of the material, K, and a characteristic melting temperature, $T_{\rm M}$, which includes the heat of fusion divided by the specific heat. The parameter on the abscissa contains the thermal diffusivity of the material, α , the welding speed, V, and the incident spot size of the focused beam, d. With other parameters held constant, this representation can be considered as a curve of depth of penetration as a function of welding speed. Thus the characteristic should be, and is, similar to that for the parametric data presented for stainless steel, rimmed steel and titanium alloy in Figs. 7, 8 and 12.

Laser welding performance in aluminum, titanium, stainless steel and rimmed steel obtained to date is seen to be comparable to that for electron beams. In view of the relatively high initial surface reflectivity of metallic surfaces at 10.6 microns, it must be concluded that this reflectivity decreases essentially to zero during the deep-penetration process. It is postulated that the deep-penetration cavity serves as a black body radiation trap for the laser radiation and thus facilitates efficient laser welding. A corollary to the above conclusion relative to high welding efficiency is that plasma generation was effectively prevented in the tests reported. It should be emphasized, however, that performance comparable to electron beams may not necessarily pertain in thicker materials for which higher power levels (with attendant increased probability of breakdown) and higher f/numbers (to promote penetration) will be required.

CONCLUDING REMARKS

The welding performance which has been demonstrated, together with the unparalleled adaptability of laser welding to automation, indicates a high-potential for cost-effective, near-term industrial applications. Exploitation of this potential presently awaits the development of durable, high-power, production-oriented laser welding equipment. Recent attainment of significantly higher continuous laser power than that reported herein (Ref. 3), has substantially improved the prospects for such development.

ACKNOWLEDGEMENT

The work reported herein was performed at the United Aircraft Research Laboratories (UARL) under Corporate sponsorship. The author gratefully

acknowledges the contributions of personnel of the Electric Discharge Laser Technology Section of UARL to the development of the laser used in the tests and to the performance of portions of the experimental laser welding program.

REFERENCES

- 1. BROWN, C. O.: High-Power, CO₂ Electric-Discharge Mixing Laser. Applied Physics Letters, Vol. 17, No. 9, November, 1970.
- 2. BROWN, C. O. and J. W. Davis: Electric Discharge Convection Lasers.

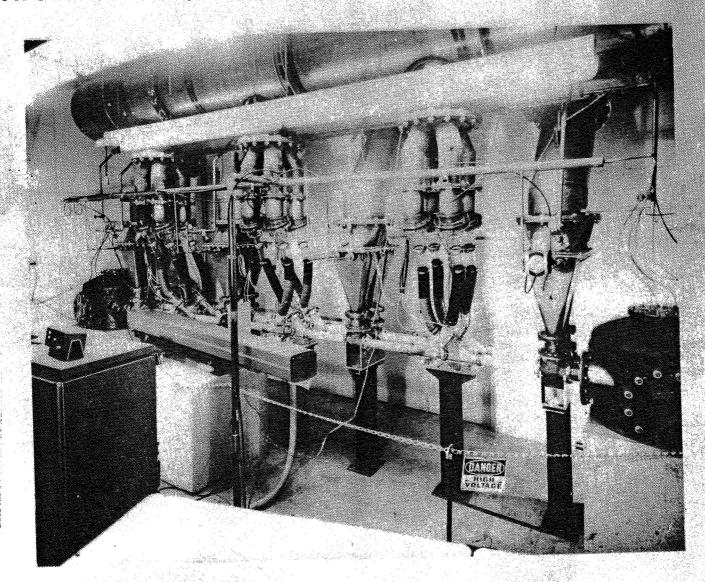
 Paper presented at the IEEE International Electron Devices

 Meeting, Washington, D. C., October, 1970.
- 3. DAVIS, J. W. and C. O. Brown: Electric-Discharge Convection Lasers: Paper 72-722, AIAA 5th Fluid and Plasma Dynamics Conference, June 26-28, 1972, Boston, Mass.
- 4. HABIANIAN, M. H.: A Correlation of Welding Variables, Proceedings of the 5th Symposium on Electron Beam Technology, 1963.

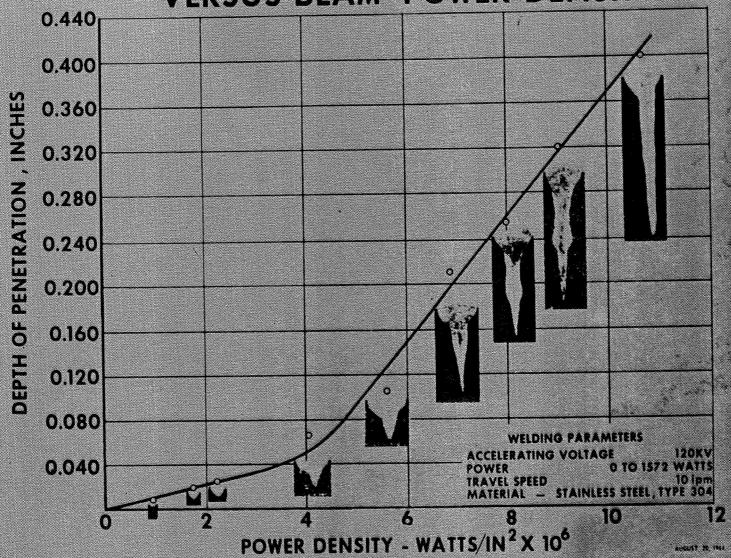
LIST OF FIGURES

- 1. High-Power, Closed-Cycle Laser Test Facility
- 2. Depth of Fusion versus Beam Power Density
- 3. Beam Focusing Parameters
- 4. Laser Induced Optical Breakdown
- 5. Deep-Penetration Welding Apparatus
- 6. Laser Butt Weld
- 7. Effect of Laser Welding Speed on Penetration (stainless steel)
- 8. Effect of Laser Welding Speed on Penetration (rimmed steel)
- 9. Effect of Inert Gas Shield on Rimmed Steel Welds
- 10. Effect of Speed on Weld Cross Sections (Ti-6Al-4V)
- 11. Effect of Speed on Weld Zone Grain Structure (Ti-6Al-4V)
- 12. Effect of Laser Welding Speed on Penetration (Ti-6A1-4V)
- 13. Effect of Laser Power on Penetration (Ti-6Al-4V)
- 14. Comparison of Laser and Electron Beam Welding Performance

HIGH-POWER, CLOSED-CYCLE LASER TEST FACILITY

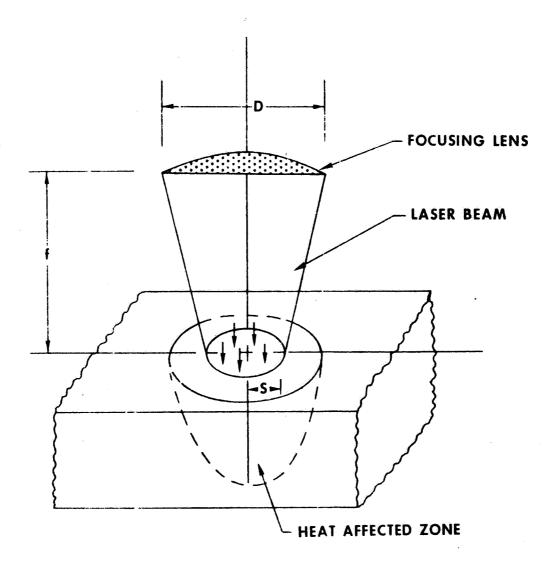


人のいなく



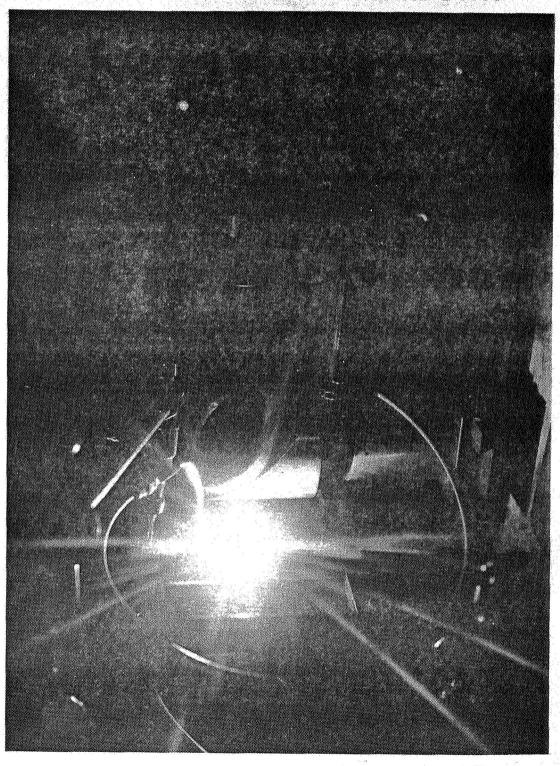
わだった

BEAM FOCUSING PARAMETERS

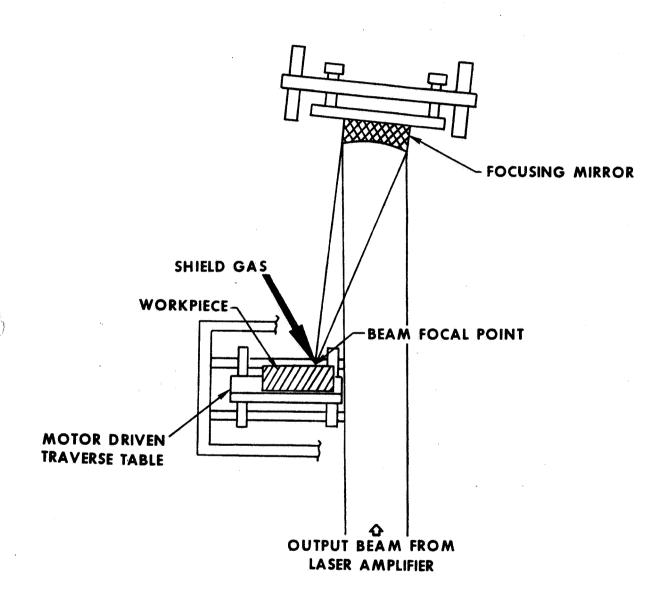


POWER DENSITY =
$$K \cdot \frac{P_0}{\lambda^2} \cdot \frac{D^2}{f^2}$$

LASER INDUCED GAS BREAKDOWN



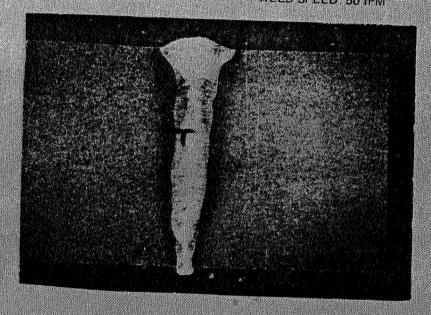
PLAN VIEW OF DEEP PENETRATION WELDING APPARATUS



LASER BUTT WELD

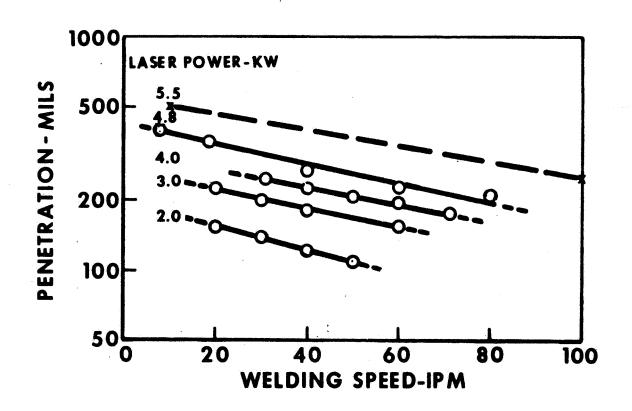
LASER POWER: 3.5 KW THICKNESS: 0.25 IN

MATERIAL: STAINLESS STEEL
WELD SPEED: 50 IPM

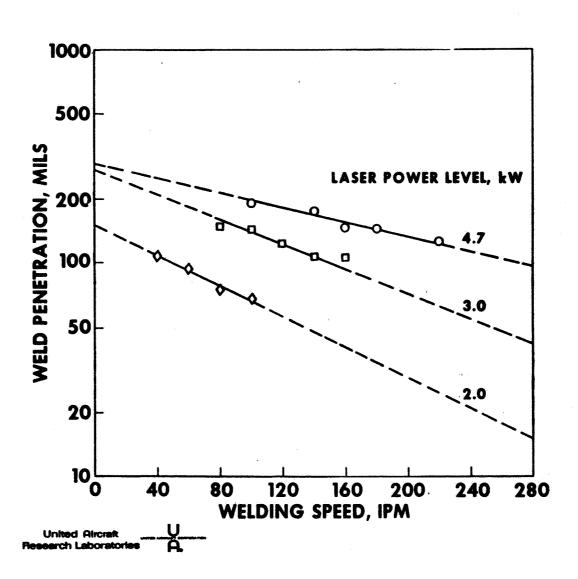


EFFECT OF LASER WELDING SPEED ON PENETRATION

STAINLESS STEEL



EFFECT OF LASER WELDING SPEED ON PENETRATION



EFFECT OF INERT GAS SHIELD ON RIMMED STEEL WELDS

4kW 200 IPM 0.5 IN



a. WITHOUT SHIELD



b. WITH SHIELD

EFFECT OF SPEED ON WELD CROSS SECTIONS

Ti-6Al-4V 3kW 10X

D.T IN



150 IPM



100 IPM



80 IPM



60 IPM

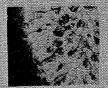


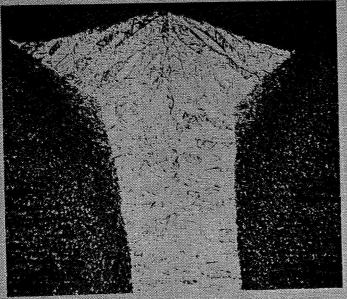
40 IPM

EFFECT OF SPEED ON WELD ZONE GRAIN STRUCTURE

3kW Ti-6Al-4V









50× 0.02 IN

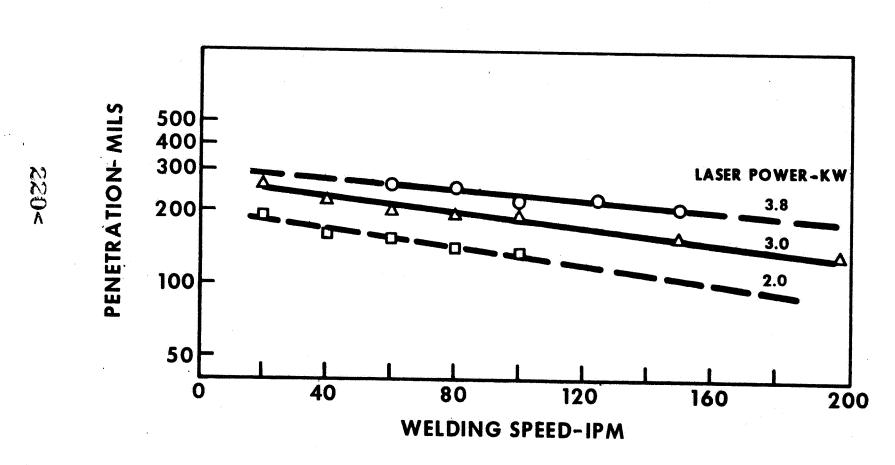
b. 40 IPM

a. 200 IPM

United Aircraft
Research Laboratories A

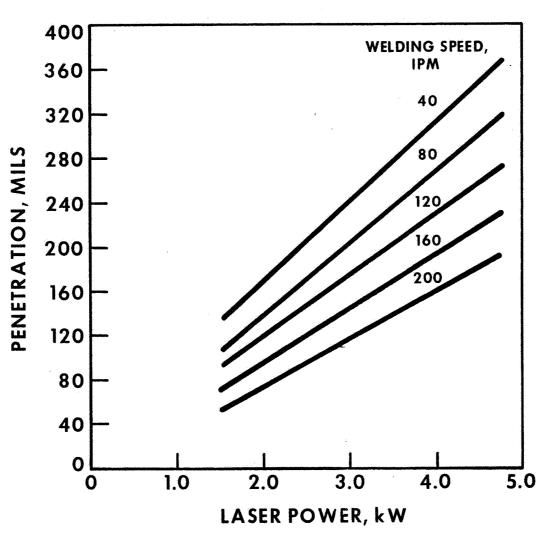
EFFECT OF LASER WELDING SPEED ON PENETRATION

Ti-6Al-4V



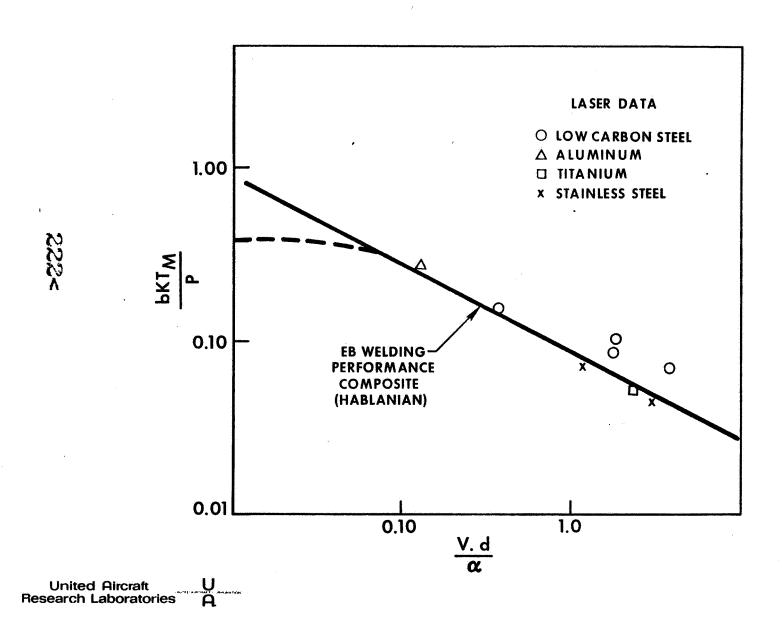
United Aircraft
Research Laboratories A





2211

COMPARISON OF LASER AND ELECTRON BEAM WELDING PERFORMANCE



COMMERCIAL AIRPLANE GROUP

September 6, 1972 6-8733-ASD-106

Dr. John D. Buckley Head, Heat Shield Section MS 206 NASA Langley Research Center Hampton, Virginia 23365

Dear Dr. Buckley:

Enclosed is the introduction to the "Adhesive Bonding Session" you requested. I hope that this is the type of introduction you had in mind.

Thank you for asking me to be Chairman of the Adhesive Bonding Session.

Very truly yours,

THE BOEING COMPANY Commercial Airplane Group

J. E. McCarty

Enclosure

ADHESIVE BONDING SESSION

J. E. McCarty , Chairman

The capability of adhesives to meet the rigorous satellite requirements of temperature and space outgassing is but one illustration of adhesive bonding versatility. The many functional components of a satellite system requires that several types of adhesive be available to meet both environmental and functional requirements. The extensive application of adhesive on the Application Technology Satellite (ATS) demonstrates that material systems are available today for a wide range of usage.

In Space Shuttle the unique requirements to reliable attach the Reusable Surface Insulation (RSI) called for development of a specific adhesive system. A low density foam system has been developed and tailored to these unique requirements. This system provides strain isolation for the RSI from the support structure and remains structurally stable in the Space Shuttle thermal environment. These unique applications continue to expose adhesive bonding as a valuable tool which is available to solve both common place and unique design problems.

Corrosion of the metal adherend in an adhesive bonded component is an environmental effect common to almost all of the aerospace bonded systems. The effect of the surface preparation and its stabilization by the adhesive primer system are the most important factors in preventing corrosion from reducing the reliability and durability of an adhesive bonding component. The development and application of corrosion resistant adhesive primer has given adhesive bonding a very significant step up in its capability to resist the corrosion induced by exposure to a humid environment.

These improved and unique material characteristics have given bonding the ability to be used in a wide spectrum of applications. However, before these adhesive systems can be used to effectively join various components,

there is the continuing need to expand the engineering understanding of bonded joint design. As the design/analysis discipline for bonded joints is expanded by application of more discriminating analysis techniques the joint strength reliability and fatigue durability will correspondingly be improved. This improvement will open up bonded joint applications which are not presently available to bonding.

One of these potential new applications is in combination with advanced composites. The characteristics of composites makes adhesive bonding the first choice of all possible joining techniques for composites. When applying advanced composites as a reinforcement to metal structures adverse residual stresses are established during the adhesive bonding elevated temperature cure cycle. Development of manufacturing techniques to remove this residual stress, can offer the composite reinforced metals structure concept an opportunity to be applied in a cost effective manner to airframe structures.

The progress in expanding the use of adhesive bonding as a reliable, durable and cost effective joining technique continues in both specialized and general application areas of space and aircraft systems. The specific development refered to above and expanded on in these papers, shows that there is an across the board development and application of adhesive bonding occurring today.

COMPANY

VALLEY FORGE SPACE CENTER, P.O. BOX 8555, PHILADELPHIA, PENNA. 19101

RE-ENTRY AND ENVIRONMENTAL SYSTEMS DIVISION

N74 30933

June 28, 1972

Dr. John Buckley Heatshield Section NASA-Langley Research Center Mail Stop 206 Hampton, Virginia 23365

Dear Dr. Buckley:

Enclosed are two (2) copies each of papers presented during

Session #2 of the "Welding, Bonding and Joining" Symposium.

Sincerely yours,

Ralph R. Hockridge, Supv. Engineer Plastics & Advanced Composites Lab

Room U7026 - VFSC-100

/am

Enclosure



1.0 INTRODUCTION

Most metallic, and non-metallic surfaces which are to be adhesively bonded are heavily contaminated with oxides, oils, shop soils, fingerprints, etc., and require some cleaning treatment prior to the bonding process. The importance of surface preparation and cleanliness cannot be overemphasized, therefore, and many investigators have shown convincingly that the performance and durability of the adhesive bond is to a large extent governed by the thoroughness of surface preparation.

Surface contamination in the form of rust, scale, oil, grease, and dirt is usually obvious. Nearly invisible contamination, on the other hand, may also be present, and represents a much greater potential hazard for premature bond failure. Examples of the latter are soldering flux residuals, perspiration in the form of hand and finger marks, chlorides from marine atmospheres, and sulfates from industrial atmospheres. Greases and oils, which lead to poor bond adhesion, are generally easily noticed and removed from the surface. Oxide and oxide-promoting agents, on the other hand, are much more insidious, and the reactions leading to premature adhesive failure may not take place until the article has been in service for some time and exposed to a severe environment, for example, high humidity or water immersion.

2.0 ALUMINUM

Recognizing that contaminants on the surface to be bonded can result in premature failure, considerable emphasis has been placed in recent years in the techniques of surface preparation. For example, in the use of aluminum, techniques have varied from the original concepts of solvent wipe, or sand and solvent wipe, to vapor degreasing, to chemical treatments which provide complex chromates as a surface layer, to acid paste treatments, to the most commonly utilized method today, of a dichromate-sulfric acid dip treatment.

However, in spite of the rather extensive data available from materials suppliers on adhesives as bonded to metallic surfaces, little information is generally available on the performance or bond strength of adhesively bonded joints when exposed to the weather. In Reference 1, it was stated: "It is commonly recognized that adhesive bonded joints are subject to deterioration under adverse environmental conditions. Weather can have a deleterious effect on the polymeric adhesive itself or on the adherend. In the latter case a weak surface layer is formed (as in corrosion) and the overall strength of the joint is reduced. The bond between the adherend and the metal itself may be seriously affected, especially if the joint is stressed during the time of exposure".



In the study referenced above, fourteen different adhesives were applied to 2024-T3 grade aluminum in the form of lapped bonded specimens which were exposed to the weather at Picatinny Arsenal, New Jersey; Yuma, Arizona; and the Panama Canal Zone; and also exposed to MIL-STD-304 temperature and humidity cycling test. A typical lap shear specimen generally utilized is shown in Figure 1, and represents the type utilized at GE-RESD. After a one year exposure at the Picatinny site, it was shown that the bonded joints prepared by sandblasting, as well as those joints prepared with the commercial acid paste treatment, showed a considerable loss in strength, while those joints prepared with sodium dichromatesulfuric acid treatment showed greater retention of strength. It was concluded that the acid paste and sandblast treatments resulted in a surface more susceptible to humidity attack than did the acid-dip treated surface.

Other studies conducted on aluminum (2) have examined filiform corrosion on aircraft aluminum alloys, both clad and unclad, overcoated with various protective paint coatings.

Another recent investigation (3) was conducted to study corrosive delamination of test panels representative of typical aircraft construction. In particular, the relative corrosive performance of clad vs bare aluminum alloys was evaluated. Failures observed on clad alloys were considered to be the resultant of galvanic corrosion in the bond line due to differences in electro-chemical potential between the cladding and the base alloys. Table I lists the potential of some commercial aluminum alloys.

ALLOY	TEMPER	POTENTIAL, VOLTS
2024	Т3	-0.68
2024	T81	-0.80
1230		-0.84
7075	T 6	-0.81
7072		-0.96
5052	H34	-0.85

TABLE 1. ELECTRODE POTENTIAL OF SOME COMMERCIAL ALUMINUM ALLOYS (3)

Figure 2 shows the progressive pitting action observed in bare and clad alloys, and shows that pitting is less likely to take place on clad alloys, and where pits do form that penetrate to the base alloy, lateral growth is initiated. This lateral corrosion growth results in more severe degradation of the bonded interface than does the pit growth characteristic of the bare alloy, and initiates a bond delamination failure.

An investigation had been conducted in-house (4) to evaluate the effects of humidity on epoxy bonded lap joints exposed to an environment more severe than the MIL-A-5090 requirements. The exceptions to the environment are shown in Table 2.

MIL-A-5090

120°F (322°K)

Exposed area 2 lineal inches (50.8 mm)

Panel suspended vertically for drainage.

TEST CONDITIONS

 160° F (344.3°K)

Exposed area 3 lineal inches (76.2 mm)

Panel laid flat to allow moisture condensation.

TABLE 2. TEST CONDITIONS (4)

The evaluation was conducted on 2024-T3 bare aluminum. Aluminum treatments prior to bonding included solvent degreasing for all panels with one set receiving a dichromate-sulfuric acid dip treatment, and the other set a commercial acid paste treatment. Lap shear ultimate strength data were obtained in the temperature range $-75^{\circ}F$ (213.7°K) to $+400^{\circ}F$ (477.6°K) prior to, and after a fourteen (14) day exposure to a relative humidity of 95 + 5 - 0%, and a temperature of $165 \pm 5^{\circ}F$ (347 \pm 2.8°K) in an automatically controlled chamber. The data, shown in Figure 3, indicated that although an approximate 25% decrease in lap shear strength was realized as a result of the humidity exposure on the acid paste treated surface, no adhesive failures were noted and the degraded property values were adequate for the particular design. Although slightly higher in value, the acid dip values decreased in a similar manner, and as indicated above (1), the acid dip treated surface retained a greater percentage of



strength. Test specimens were of the configuration shown in Figure 1. It must be emphasized that this data was obtained on non-porous adherends. It will be shown that in the case of one non-porous and one porous adherend, the environmental degradation is more severe.

3.0 CORK - ALUMINUM

In the case of one porous adherend, the effects of humidity exposure may be considerably more severe as is evidenced by a recent bonding problem on an in-house project. An insulative material, reconstituted cork in a resin matrix in sheet form, is bonded in a brick pattern to the exterior surface of an aluminum conical shape as typified by Figure 4. A typical cross-section of the insulated structure is shown in Figure 5.

Preparation of the outer surface of the aluminum faced aluminum honeycomb structure included solvent cleaning, application of a commercial acid paste treatment, pressure rinsing with water until the drippings from the structure were neutral, and an air dry period.

The cork insulation, pre-cut (lofted) to size, was placed on the structure by placing the edge of the sheet in contact first, to sweep any air entrappment to the edge of the sheet. Prior to contact, each sheet received a thin, ~ .005" (.13 mm) layer of an unfilled epoxy-polyamide adhesive, as did the faying surface of the aluminum. Each sheet, applied in a brick pattern, was taped to its adjoining sheet, and after completion of the lay-up, the entire assembly was vacuum-bagged and cured at an elevated temperature of 135°F (330.4°K) for four (4) hours at 29" Hg (97.929 x 10° N/M²). Subsequently, as a portion of the required testing of an aerospace assembly, the cork insulated structure was exposed to a series of cumulative tests:

- 1. Three day cyclic humidity per Figure 6.
- 2. Seven day cyclic humidity per Figure 6.
- 3. A temperature/altitude test to expose the bonded assembly to rapid depressurization to one torr and 0°F (255.4°K), representative of an altitude and temperature of 150,000 feet (45.7 kilometer).

230<

Upon removal from the temperature/altitude chamber, large areas of unbond were observed at the edges of the cork "brick work", and also "bubbled" lifted areas in the centers of some of the cork insulative panels. Sectioning of the failure areas indicated the presence of a few pit areas such as shown in Figure 2A, but more importantly, gross delamination of the cork and entire epoxy bond system from the aluminum substrate. A second assembly was then tested with similar results, as were test panels especially prepared to evaluate the corrosive delimination problem. To determine whether the delamination was initiated by moisture permeation from the cork seams, or was moisture penetration through the cork, test assemblies were prepared in the normal fashion, except with all cork seams sealed with various generic sealers. It became quickly obvious that seam sealing offered no advantage, moisture permeation of the cork matrix was undoubtedly the culprit, and that the acid paste treated surface was more susceptible to delamination than an aluminum oxide paper sanded and solvent cleaned surface.

Test assemblies were then fabricated utilizing several primers, including standard adhesion promoting types, and several anti-corrosive primers. In all cases where the anti-corrosive types of primers were utilized, no lifting or delamination of the cork was observed, and in subsequent panel teardowns, no corrosion was evident on the aluminum surface. Subsequently, an epoxy-polyamide primer was selected as the most compatible with the existing epoxy adhesive. The primer is green in color and contains strontium chromate pigment. The general application procedure is:

- 1. Solvent clean the aluminum with acetone or Methyl Ethyl Ketone (MEK).
- 2. Uniformly sand with 240 grit aluminum oxide paper.
- 3. Vacuum to remove sanding residue.
- 4. Solvent clean with acetone, followed by a low residual denatured alcohol.
- 5. Oven dry one (1) hour at 125°F (324.8°K).
- 6. Spray apply the epoxy primer to a dry film thickness of 0.002 inch (0.05 mm).
- 7. Air dry fifteen (15) minutes, and oven cure at 200°F (366.5°K) for two (2) hours.



Once primed, the assemblies may be stored at ambient conditions for periods up to six (6) months prior to cork insulation adhesive bonding. Prior to adhesive application and vacuum-bag bonding as described above, the primed assembly is:

- 1. Solvent cleaned with low residual denatured alcohol.
- 2. Uniformly sanded using 240 grit aluminum oxide paper to remove all surface gloss.
- 3. Vacuum cleaned to remove sanding residue.
- 4. Solvent cleaned with MEK and allowed to air dry for one (1) hour.

NOTE: Step 1 may be omitted if the primed assembly has not been stored after primer cure.

Since incorporation of the anti-corrosive primer into the bonding system, no humidity failures have been encountered on that assembly in a two (2) year manufacturing period.

4.0 CORK - TITANIUM

Mindful of the prior environmental problems associated with corrosive delamination, when a recent program required adhesive bonding of cork to titanium alloy 6-Aluminum -4 Vanadium, a test program was immediately established to verify the need for an anti-corrosive primer in the bond system.

Since the assembly precluded the use of dip treatments, or those requiring a rinse after treatment, panels nominally 12 inch \times 12 inch \times 0.060 inch (304.8 \times 304.8 \times 1.52 mm) were prepared as follows:

- 1. Solvent clean with MEK.
- 2. Sand with 240 grit aluminum oxide paper.
- 3. Solvent clean with MEK.

One-half of the test panels were then primed with the chromate/epoxy primer utilized for the aluminum bond efforts described above, and all panels were bonded with 0.25 inch (6.35 mm) cork utilizing a filled, flexibilized, epoxyamine cured adhesive.

After the cure, the panels were exposed to three (3) cycles of temperature-humidity per Figure 6 and inspected for unbonds. After inspection, the panels received seven (7) more cycles per Figure 6, and were again inspected. Upon conclusion of the ten cycles of temperature-humidity, the panels were exposed to a twelve (12) hour salt-fog test, and again inspected. The salt-fog conditions were as noted in Table 3.

CHAMBER CONDITIONING

16 Hours Prior to Test $95^{\circ}F + 20^{\circ} - 5^{\circ}$ (308.2°K + 11.1 - 2.8)

TEST CONDITION

12 Hour Cycle 95°F + 2° - 4° (308.2°K + 1.1 - 2.3) Salt Conc. = 3.6 ± 0.1%

TABLE 3. SALT FOG CONDITIONS

The test results are tabulated in Table 4 and show that only the panels primed with anti-corrosive primer can successfully pass the vehicle preflight test environment. Use of the anti-corrosive primer has, therefore, been incorporated into this system as pre-bond requirement.

5.0 SUMMARY

The use of an anti-corrosive primer has been shown to be essential to assure survival of a bonded structure in a hostile environment, particularly if a stress is to be applied to the adhesively bonded joint during the environmental exposure.

For example, the Lockheed L-1011 TriStar assembly, after exhaustive evaluation tests specifies use of chromate filled inhibitive polysulfide sealants, and use of corrosion inhibiting adhesive primers prior to structural bonding with film adhesive (5).

The day of corrosion-resistant primers is just beginning to dawn, and no bonded assembly subject to a humid environment should be designed without consideration of corrosive delamination, and its catastrophic effects.



- "How Weathering and Aging Affect Bonded Aluminum", R. W. Wegman, W. M. Bodnar, E. S. Duda, and M. J. Bodnar, <u>Adhesive Age</u>, October 1967, pp 22-26.
- "Filiform Corrosion of Aluminum", W. L. Slabaugh, W. DeJager,
 S. E. Hoover, and L. L. Hutchinson, <u>Journal of Paint Technology</u>,
 Vol. 44, No. 566, March 1972.
- 3. "Corrosive Delamination", Dr. F. J. Riel, <u>SAMPE Journal</u>, August/September 1971.
- 4. "Effect of Environmental Exposure on Bonded Aluminum Treated with Organic Conversion Coatings", R. R. Cerankowski, 10/5/64, Internal General Electric Document 8158-4004.
- 5. "L-1011 TriStar Places New Demands on Aircraft Sealants and Adhesives", D. A. Petrino, Adhesives Age, February 1972, pp 15 19.

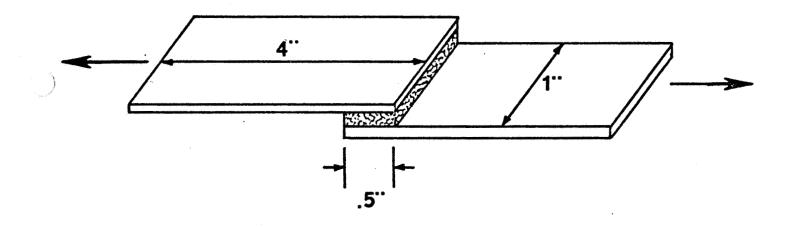


FIGURE 1
TYPICAL LAP SHEAR SPECIMEN

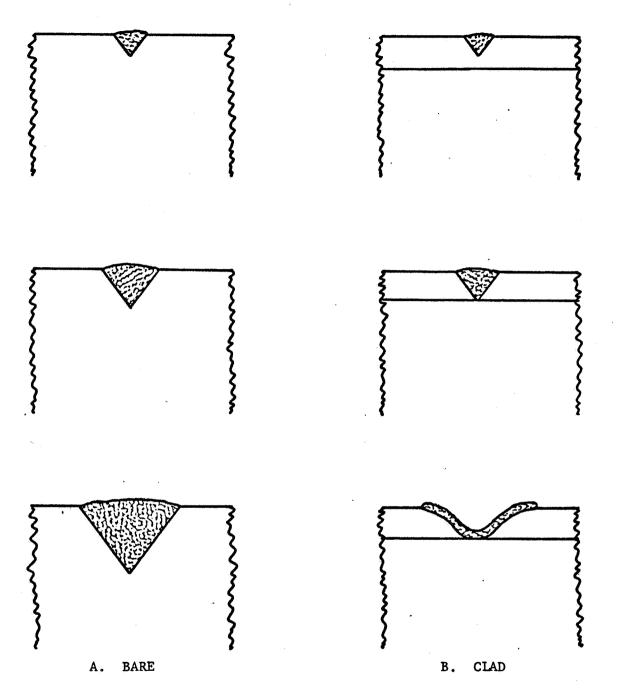


FIGURE 2.

PROGRESSIVE PITTING OF BARE AND CLAD ALUMINUM IN A CORROSIVE ENVIRONMENT (3)

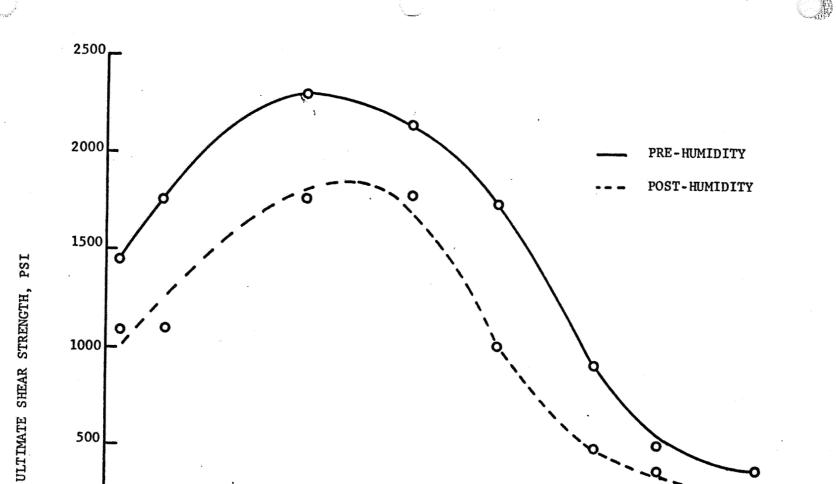


FIGURE 3 LAP SHEAR STRENGTH - HUMIDITY ENVIRONMENT

150

TEMPERATURE OF

225

300

375

__ 425

500

-75

0

75

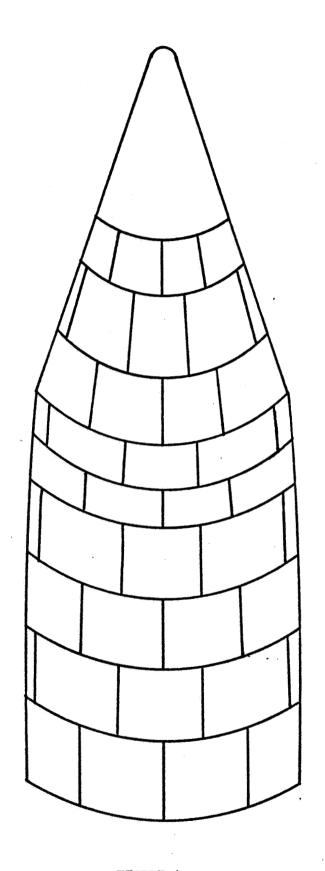


FIGURE 4

CORK INSULATED STRUCTURE

- 12 - 238<

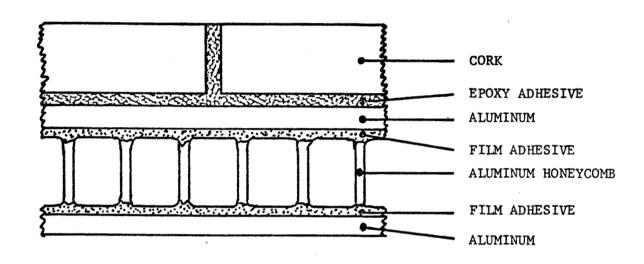


FIGURE 5

TYPICAL STRUCTURE CROSS-SECTION

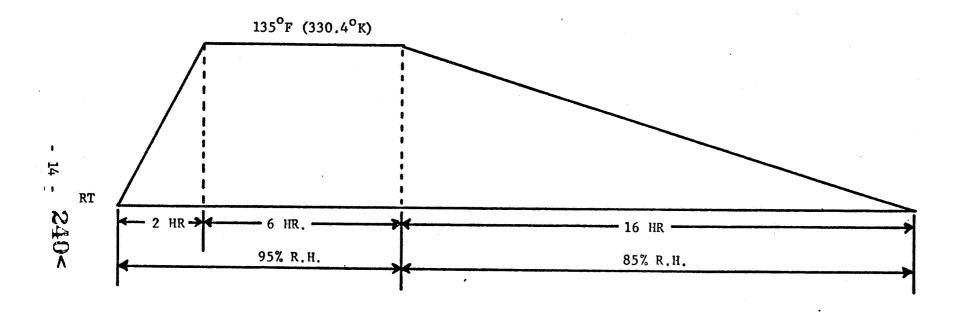


FIGURE 6

CYCLIC TEMPERATURE-HUMIDITY

SUMMARY OF CORK-TITANIUM BONDED SPECIMENS IN ENVIRONMENTAL TESTING

	SPECIMEN NUMBER	TYPE	POST 3 DAY T/H EVALUATION	POST 10 DAY T/H EVALUATION	POST 10 DAY T/H + 12 HR S/F EVALUATION
	75	Unprimed	ок	as and and and	2. 3 m (m. m. ∞
	76		OK	Side A 1.1" Unbond 1.5-2.0" Unbond Side D 0.8" Unbond 2" Unbond	
)	77	. ↓	ОК	Side A 1.1" Unbond 1.0" Unbond 4-5" Unbond	Side A - open and unbonded most of way
				Side B 0.4" Unbond 1.7" Unbond Side C	Side B 2" Unbond ½" Additional Unbond Side C
				3.9" Unbond 0.9" Unbond	4.5" Unbond 1.0" Unbond Side D 0.35" Unbond
	78 79 80	Primed	OK OK OK	ок ок	 ок

RESIDUAL THERMAL STRESS CONTROL IN COMPOSITE REINFORCED METAL STRUCTURES*

J. B. Kelly and R. R. June The Boeing Company Seattle, Washington

INTRODUCTION

Advanced composite materials, composed of boron or graphite fibers and a supporting matrix, make significant structural efficiency improvements available to aircraft and aerospace designers. Numerous developmental programs are being conducted throughout the industry to utilize this potential. Some of these programs are described in Reference 1.

Two distinct design philosophies have been developed as a result of various study programs: all composite construction and composite reinforced metal construction. The approach selection may be made on the basis of cost effectiveness, as determined through consideration of weight saving, the value of saving weight, and the raw material and fabrication costs. The inter-relationship of these factors is shown in Figure 1. Composite effectiveness factor (CEF) is defined as the ratio of weight saved to weight of composite used. Typically, all composite construction has a CEF of one while reinforced structures achieve two and higher. From Figure 1 it can be seen that high CEF values of reinforced construction translate to cost effective applications at an earlier date than all composite construction, especially at low values of weight saving.

*This work was sponsored by NASA Langley Research Center, under Contract No. NAS1-8858.



The weight saving potential of several reinforcing concepts was explored during Phases I, II, and III of NASA Contract NAS1-8858, and the results are reported in References 2, 3, and 4. Boron-epoxy composite was employed to reinforce metallic elements of aluminum and titanium. The reinforcement was joined to the metallic elements by adhesive bonding. During Phase I of this program the occurance of thermally induced residual stresses in the bonded assemblies was demonstrated.

Residual stresses occur when conventional elevated temperature adhesive bonding procedures are employed and the materials being joined have unequal coefficients of thermal expansion. Adhesive systems which cure at elevated temperatures are commonly employed to produce structurally adequate joints. Typical cure cycles are shown in Figure 2. The residual stresses occur because components of the assembly are brought together at room temperature, enclosed in a vacuum bag, and heated to the curing temperature in an oven or autoclave. During the heating process, thermal growth of each component proceeds without restriction. If the coefficients of linear thermal expansion are different, differing amounts of thermal growth occur. The bond between the components is established near the curing temperature and any subsequent temperature change, such as cooling to room temperature, will induct thermal stress, since the components are mutually restrained from expanding or contracting at their individual rates.

The residual stress level produced in composite reinforced metal structures is a function of cross-sectional area, modulus of elasticity, and coefficient of thermal expansion of the components and the temperature change from the temperature at which the components were stress free. The expansion coefficients of aluminum and composite materials are such that residual tension stresses are produced in the aluminum constituent after conventional adhesive bonding. The resulting stress levels are depicted in Figure 3. These residual tension stresses could adversely affect structural static strength and fatigue life.

Investigation, suggested by NASA, indicated that the residual stress level could be reduced through suitable modification to the manufacturing procedures employed during the adhesive bonding process. This program was initiated to evaluate the capability to reduce these residual stresses and to explore several approaches to achieve this control. A portion of the results of this program are discussed in this paper. Additional information may be found in Reference 5.

STRESS ALLEVIATION METHODS AND SPECIMENS

If composite reinforced metal assemblies are to be free of residual stresses at room temperature then they must be stressed when heated or cooled to any other temperature. This includes the temperature at which the adhesive bond between components of the assembly is established. It follows that bonded assemblies which are produced at elevated temperature will be stress free at room temperature if, during bonding, the components of the assembly are stressed to the appropriate level. These stress levels are predictable utilizing the relationships developed in Reference 6. During this program nine assembly methods, listed in Table 1, were employed to produce the desired stress distributions during the adhesive bonding process to control the residual stress level.

Assembly methods 1 and 2 (method designation taken from Table 1) utilized the self equilibrating nature of thermal stresses in bimaterial assemblies to achieve mechanical constraint. The metal and composite components of the assembly were joined at the desired stress free temperature with mechanical fasteners. The adhesive bonding material, uncured, was placed between the components prior to the installation of the fasteners. As the mechanically joined components were heated to cure the adhesive, each component attempted to expand at its own rate. This free expansion was prevented by the strain continuity imposed by the mechanical fasteners and equal but opposite forces were established within the components.

Subsequent cooling to room temperature was then accomplished with the same strain compatibility imposed by both the established adhesive bond and the mechanical fasteners. Since the components of the assembly were unstressed when they were mechanically joined and relative thermal growth was prevented during the bonding cycle, the resulting assembly is free of residual stress when it is returned to room temperature.

For assemblies which are not symmetric, the equal and opposite forces which occur during the cure cycle will produce an internal bending moment. In the absence of suitable constraint this bending moment will produce deflection so that equilibrium is maintained. This was the case with assembly method 1. The assembled components were enclosed in a vacuum bag, called an "envelope bag", which surrounded the assembly, permitting bending deflection to occur freely.

In contrast, assembly method 2 utilized a supporting tool to prevent deflection due to internal bending moment. The components were assembled, using mechanical fasteners, as described above. This assembly was then placed on a supporting tool and the vacuum bag was installed over the parts and sealed to the tool. Autoclave pressure over the vacuum bag surface provided the forces required to hold the component parts flat against the tool surface.

The stress levels which occur within the components when assembled by methods 1 or 2 are determined by the physical properties of the components and the relative cross sectional areas.

If a large piece of composite is to be joined to a relatively small section of aluminum, the stress level in the aluminum will be high. Since this stress occurs at elevated temperature where yield strength is reduced, failure in the metal might result. This potential limitation is overcome by mechanically fastening both the composite



and the metal component to a relatively stiff tool made of a material having a coefficient of thermal expansion about midway between the expansion coefficients of the assembly constituents. This approach was designated method 3. The expansion coefficients of aluminum and either boron or graphite composite are such that steel is a reasonable choice for tooling material. By fastening both assembly components to the steel tool, both components are forced to expand with the tool. Also, the stress level in the components during cure becomes a fixed value for all cross-sectional areas as long as the steel tool is substantially stiffer than either component.

The degree of control of stress levels which occur during the curing cycle is maximized through the use of preloading. This capability was explored through assembly methods 4, 5, and 6. At the curing temperature, the stress state of the components which is required to achieve a residual stress free assembly may be translated into a strain difference between the components. The stress level in either the composite or the metal component during the cure cycle may be arbitrarily selected, subject only to the requirement that inelastic deformation does not occur. By maintaining the correct strain difference between the components through adjustment of the applied load on the second component the completed assembly can be produced with no residual stress.

Assembly method 4 utilized the above approach to maintain the composite detail stress-free at all times. The metal component of the assembly was preloaded and constrained in this state by the tool. The required preload level, which determined strain, was computed based upon the required strain difference and the thermal expansion characteristics of the tool and the aluminum component. The preloaded aluminum was constrained to the tool by mechanical fasteners or by confining the metal component in a cavity within the tool. The cavity confinement approach was very convenient for assemblies which required the aluminum component to be preloaded in compression.

The preloading technique also makes it possible to produce assemblies which are free of residual stress at temperatures other than room temperature. This condition may be desirable for certain combinations of vehicle loads and temperatures. Adjusting the strain difference between the components of the assembly achieves the desired result. This can be done by method 4, which eliminates stress on the composite component, but this may induce prohibitively high stress levels in the metal component. Assembly methods 5 and 6 caused both components to be stressed. With assembly method 5, the metal component was preloaded and then both components were fastened to the tool. For assembly method 6 both components were preloaded (each to a different strain level) and then restrained by the tool. These techniques produced lower metal stress levels and higher composite stress levels during the cure cycle than would have occurred using assembly method 4.

Assembly method 7 was another technique employed to produce assemblies free of residual stress at a preselected temperature between the assembly temperature and the cure temperature. Both components were fastened to a steel tool but provision was made for a limited amount of free thermal expansion of one component prior to the introduction of mechanical constraint by the tool. This was accomplished by using oversize bolt holes in the metal detail.

Assembly method 8 utilized the thermal growth behavior of the aluminum component to accomplish the preloading. The metal details were cooled, causing contraction, and then placed in a cavity type tool. The length of the cavity was accurately controlled so that upon reheating to room temperature the desired amount of preload had been established. As with assembly method 4, the preload was selected so that the composite detail was unstressed during the adhesive bonding operation.

The final assembly method employed during this study was designed to control the thermal growth of the aluminum detail through continuous support on the tool rather than at the end of the part as was done with mechanical fasteners. The tool was made of fiberglass reinforced polyester. This material was selected because its coefficient of thermal expansion $(2.3 \times 10^6)^{-6}$ is close to the expansion coefficients of the composite materials. The aluminum component was bonded to the tool using a room temperature curing adhesive. Then the composite details were mechanically fastened to the aluminum and bonded. The fiberglass tool was then removed from the assembly by peeling the tool laminations.

The specimen configurations for this program were selected to be representative of potential aircraft structural applications. These included reinforced flat sheets, simulating fuselage and wing skins; hat stiffeners, which are employed in the fuselage; and zee section stiffeners, as are found in wing construction. The flat sheets and hat stiffeners were made of 7075 alloy aluminum and the zee stiffeners were 7178 alloy aluminum extrusions. All metal components were heat treated to the T6 condition. Figures 4 through 6 show representative specimens used in the study.

Composite materials used in this program were SP-272* boron-epoxy and SP-286* graphite-epoxy employing Modmor Type II graphite. Unidirectional laminates five and four plies thick (respectively) were fabricated, cured, and slit to the required width. These strips were stacked and bonded to produce the desired amount of reinforcement. In this way the ratio of composite area to total area (see Figure 3) was varied during the program.

*Available from Minnesota Mining and Manufacturing Company.

Adhesive systems employed for both the second stage composite bonding and for composite to metal bonding were AF-126* and AF 30*. These adhesive systems cure at 250°F and 350°F respectively, producing the two levels of residual stress shown in Figure 3 when conventional bonding practices are employed. Secondary bonding of composite elements was achieved using the same adhesive system and cure temperature which was used for the composite to metal bond.

The reduction in residual stress which was achieved with the various specimens and assembly methods was determined by measuring the strain induced in the components during fabrication. Strain was determined by measuring the distance between two scribed lines spaced approximately ten inches along the length of the specimen. Each component of an assembly was clamped flat and the initial distance between the marks was determined on an optical bench as shown in Figure 7. Following the adhesive bonding cure cycle these distances were remeasured, and from the change in length, strain and stress level were computed. Strain due to preload was also verified in this manner by measuring the distance between the marks before and after load application.

RESULTS

Representative results are shown in Figures 8, 9, 10, and 11, where the achieved residual stress levels in the aluminum components are shown as a function of the geometry parameter composite area/total test area. Figures 8 and 9 show results obtained with those specimens bonded with the adhesive system which cured at 250°F. The results shown in Figures 10 and 11 are for those specimens bonded at 350°F. All specimens in these groups were designed to be stress free at 70°F, resulting in stress producing temperature differences of 180°F and 280°F. For comparison, predicted residual stress levels which occur due to conventional bonding techniques are also shown.

*Available from Minnesota Mining and Manufacturing Company.

As can be seen in Figures 8 through 11, residual stress level was significantly reduced for both adhesive curing temperatures and for both boron and graphite reinforcement. The amount of residual stress reduction achieved was independent of the composite to metal ratio.

The results obtained with the individual assembly methods are compared in Figure 12. For each assembly method the average reduction in residual stress, expressed as a percent of the objective reduction, is shown. Assembly method 4, which employed preloading the metal component such that the composite reinforcement was not loaded, was the most successful. The average reduction of residual stress was slightly in excess of 100 percent, indicating that in some cases the preload level was more than desired. This was also the case with method 8, which employed cooling and confinement rather than mechanical means to achieve preloading.

Assembly method number 7 was not successful. This method required a limited amount of free thermal growth before constraint was applied, and this free growth did not occur. It is suspected the growth was prohibited by frictional forces.

All other methods, while not as successful as method 4, demonstrated significant potential with results within ± 30 percent of the objective.

Potentially significant creep deformation was consistently observed in the aluminum components of the assemblies cured at 350°F. This deformation, shown in Figure 13, was found to be a function of the stress level in the metal component at the cure temperature. The 7178-T6 aluminum alloy experienced larger creep deformation than 7075-T6 aluminum at comparable stress levels. Since these deformations were determined from bonded assemblies, two verification tests were performed. In these tests an aluminum component was confined in a tool and subjected to a cure cycle as had been used to fabricate the bonded assemblies. These results, also shown in Figure 13, substantiated the previous results. Creep deformation was not consistently observed in the assemblies bonded at 250°F.



CONCLUSIONS AND RECOMMENDATIONS

The results obtained during this study indicate that residual stress induced during bonding of composite reinforcement to metal structural elements can be reduced or eliminated through suitable modification to the manufacturing processes. The most successful method employed during this program used a steel tool capable of mechanically loading the metal component in compression prior to the adhesive bonding cycle.

Compression loading combined with heating to 350°F during the bond cycle can result in creep deformation in aluminum components. The magnitude of the deformation increased with increasing stress level during exposure to 350°F.

Additional developmental work is desirable to refine and scale-up the assembly methods of this study for production. Creep behavior and the effects of creep deformation upon other parameters such as fatigue life should be defined. The extension of these concepts for residual stress alleviation should be accomplished for multidirectionally oriented composite reinforcement.

REFERENCES

- 1. June, R. R., and Kelly, J. B.: Applications of Advanced Composites for Aircraft. SAMPE Quarterly; Volume 3, Number 2; January 1972.
- 2. Oken, S. and June, R. R.: Analytical and Experimental Investigation of Aircraft Metal Structures Reinforced with Filamentary Composites; Phase I: Concept Development and Feasibility. NASA CR 1859, December 1971.
- 3. Blichfeldt, B. and McCarty, J. E.: Analytical and Experimental Investigation of Aircraft Metal Structures Reinforced with Filamentary Composites; Phase II: Structural Fatigue, Thermal Cycling, Creep, and Residual Strength. NASA CR 2039, June 1972.
- 4. Bryson, L. L. and McCarty, J. E.: Analytical and Experimental Investigation of Aircraft Metal Structures Reinforced with Filamentary Composites; Phase III: Major Component Development. NASA CR to be assigned.
- 5. Kelly, J. B. and June, R. R.: Residual Stress Alleviation of Aircraft Metal Structures Reinforced with Filamentary Composites. NASA CR to be assigned.
- 6. Timoshenko, S.: Analysis of Bi-Metal Thermostats. Journal of The Optical Society of America, Volume II, 1925, pp 233-255.

LIST OF ILLUSTRATIONS



TABLE

1 ASSEMBLY METHODS

FIGURE

13

1	COMPOSITE EFFECTIVENESS
2	TYPICAL ADHESIVE CURE CYCLES
3	RESIDUAL STRESS WITH NO ALLEVIATION
4	REINFORCED SHEET SPECIMEN
5	REINFORCED HAT STIFFENER SPECIMEN
6	REINFORCED ZEE STIFFENER SPECIMEN
7	OPTICAL BENCH FOR LENGTH MEASUREMENTS
8	RESULTS - BORON REINFORCEMENT CURED AT 250°F
9	RESULTS - GRAPHITE REINFORCEMENT CURED AT 250° F
10	RESULTS - BORON REINFORCEMENT CURED AT 350° F
11	RESULTS - GRAPHITE REINFORCEMENT CURED AT 350° F
12	COMPARISON OF ASSEMBLY METHOD RESULTS

CREEP DEFORMATION OF ALUMINUM

·	1	MECHANICALLY JOIN COMPONENTS NO SUPPORTING TOOL
	2	MECHANICALLY JOIN COMPONENTS SUPPORT ON TOOL OR CAUL PLATE
א	3	MECHANICALLY JOIN COMPONENTS TO TOOL
YI A	4	PRELOAD METAL DETAIL AND CONSTRAIN BY TOOL COMPOSITE COMPONENT NOT RESTRAINED
	5	PRELOAD METAL DETAIL AND MECHANICALLY FASTEN ALL COMPONENTS TO TOOL
	6	PRELOAD ALL COMPONENTS AND MECHANICALLY FASTEN ALL COMPONENTS TO TOOL
	7	MECHANICALLY FASTEN COMPONENTS TO TOOL BUT ALLOW FOR LIMITED FREE THERMAL GROWTH OF METAL COMPONENT
	8	PRELOAD METAL DETAIL BY COOLING AND RETAINING IN TOOL
	9	BOND METAL DETAIL TO TOOL HAVING LOW COEFFICIENT OF EXPANSION MECHANICALLY FASTEN COMPOSITE DETAIL TO METAL DETAIL

TABLE 1 ASSEMBLY METHODS

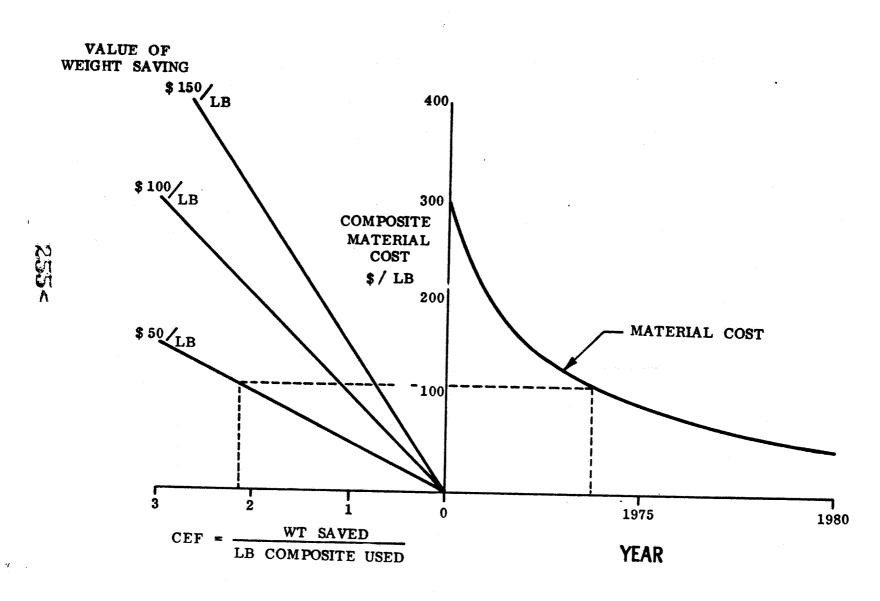


FIGURE 1 COMPOSITE EFFECTIVENESS

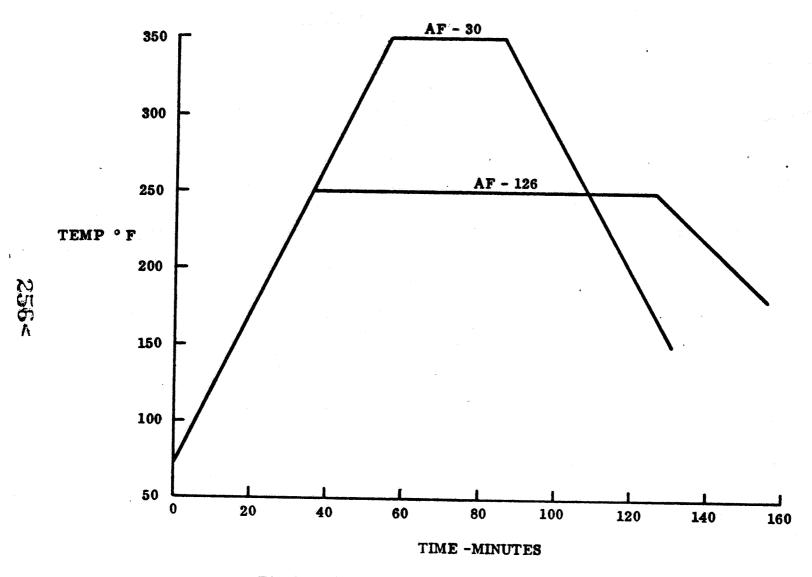


FIGURE 2 TYPICAL ADHESIVE CURE CYCLES



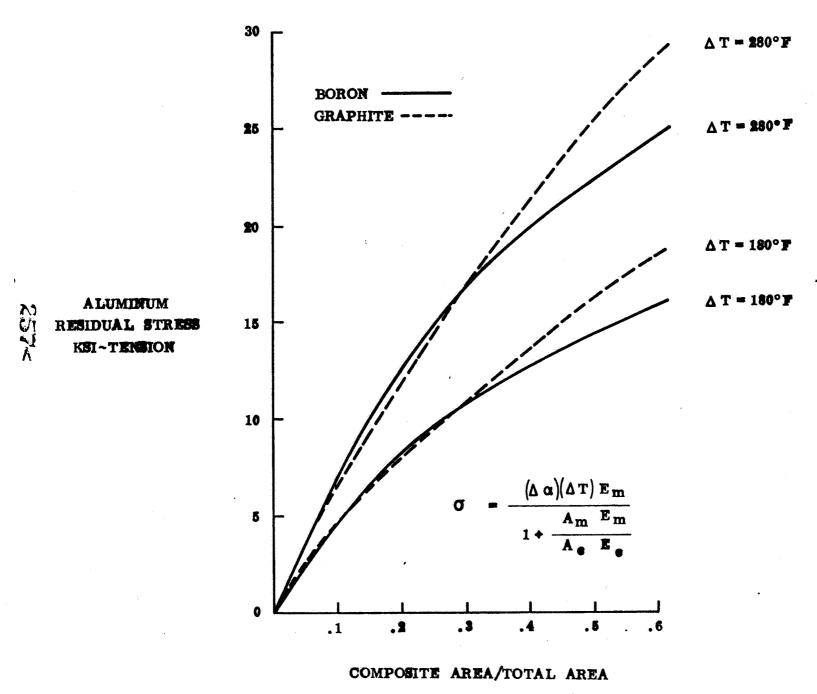
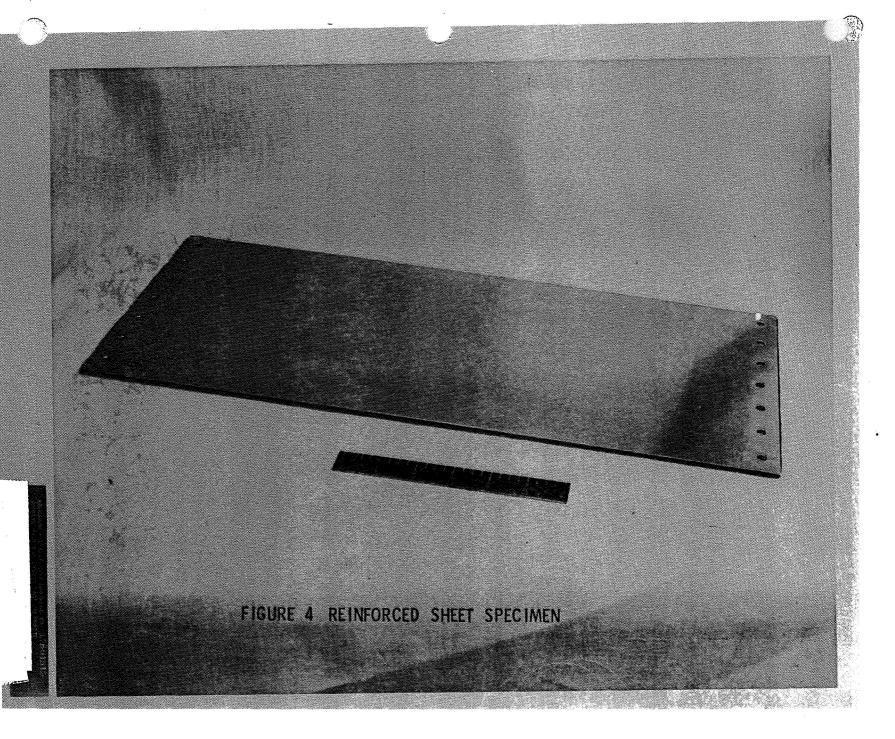
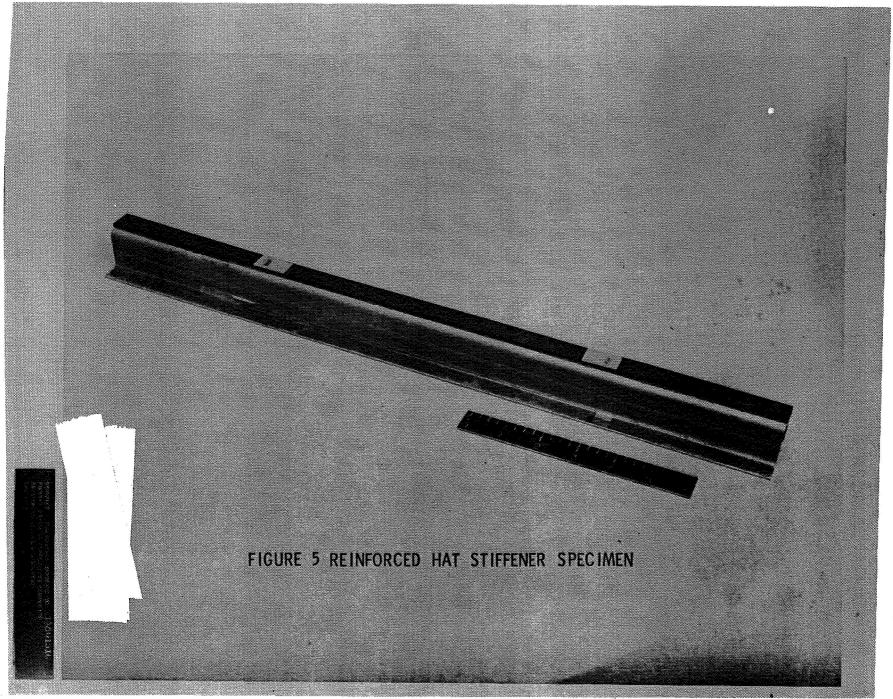
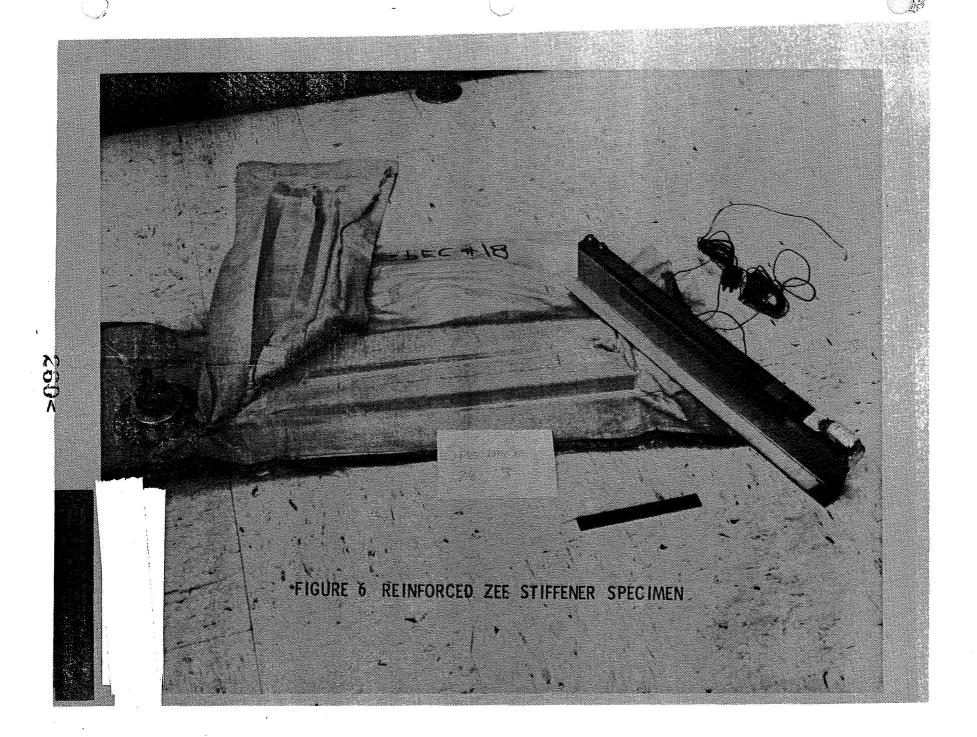
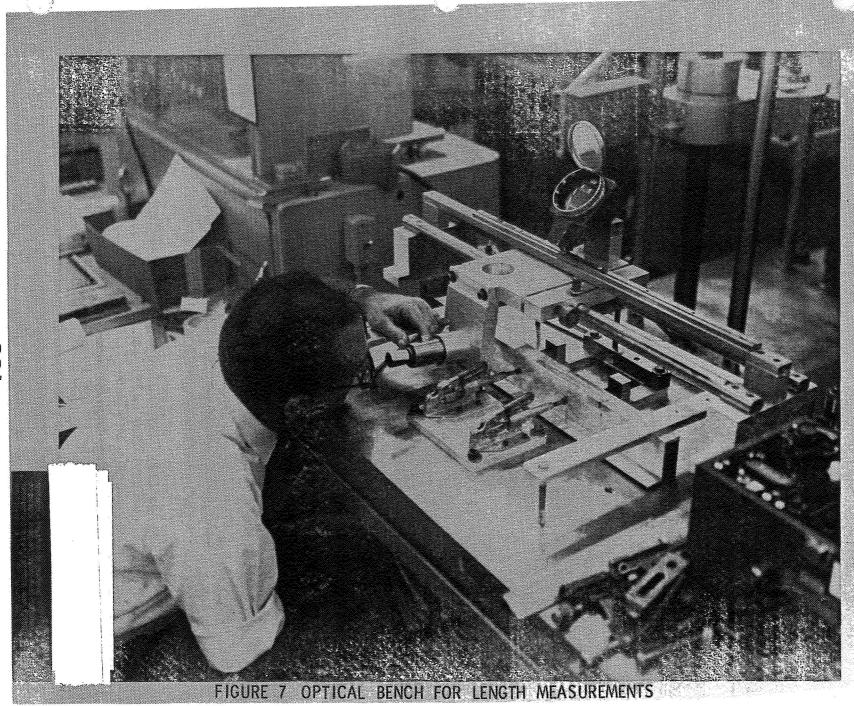


FIGURE 3 RESIDUAL STRESS WITH NO ALLEVIATION









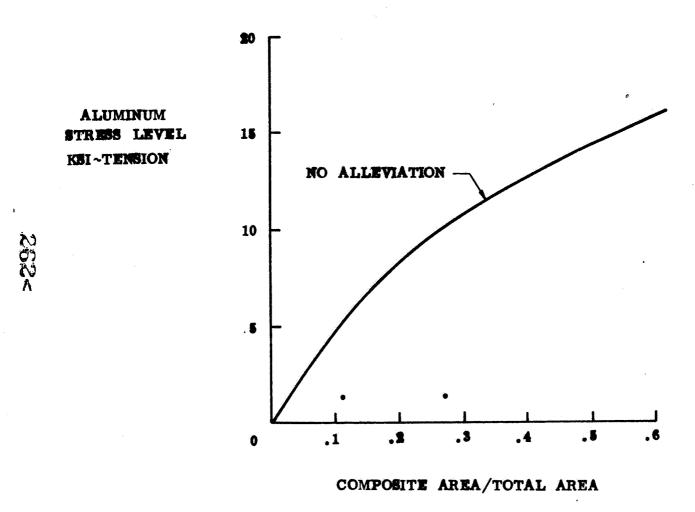


FIGURE 8 RESULTS - BORON REINFORCEMENT CURED AT 250°F

GRAPHITE REINFORCEMENT T = 180°F

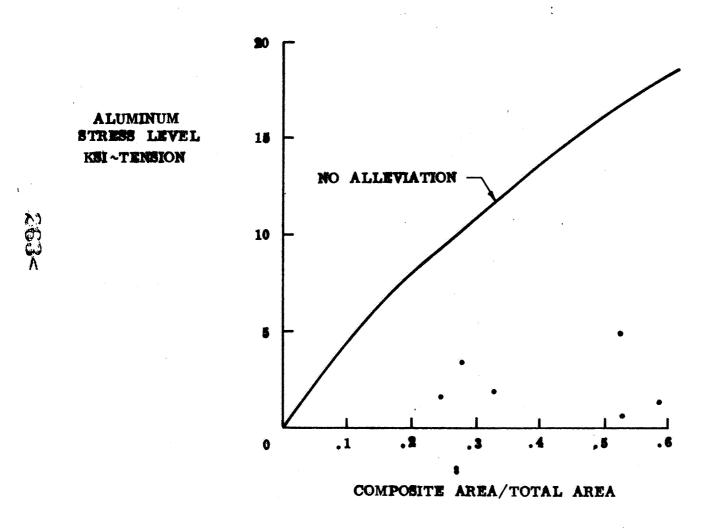


FIGURE 9 RESULTS - GRAPHITE REINFORCEMENT CURED AT 250 F

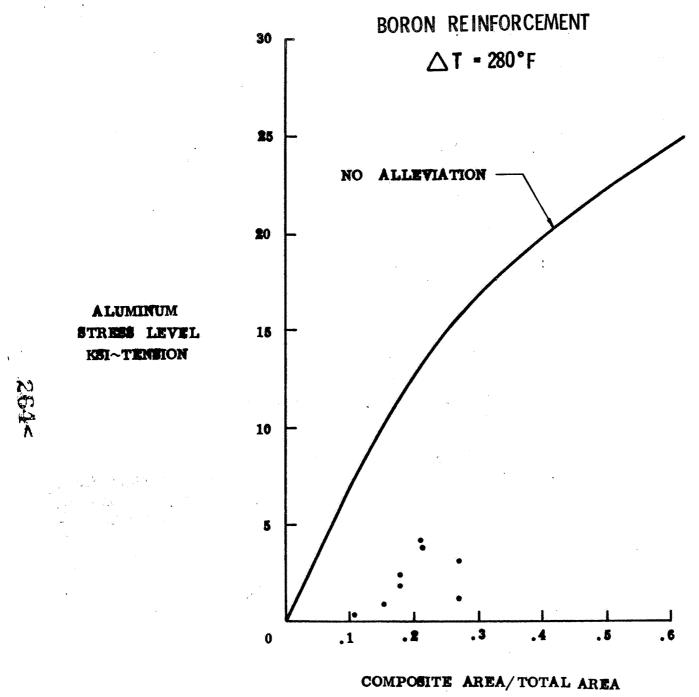


FIGURE 10 RESULTS - BORON REINFORCEMENT CURED AT 350°F

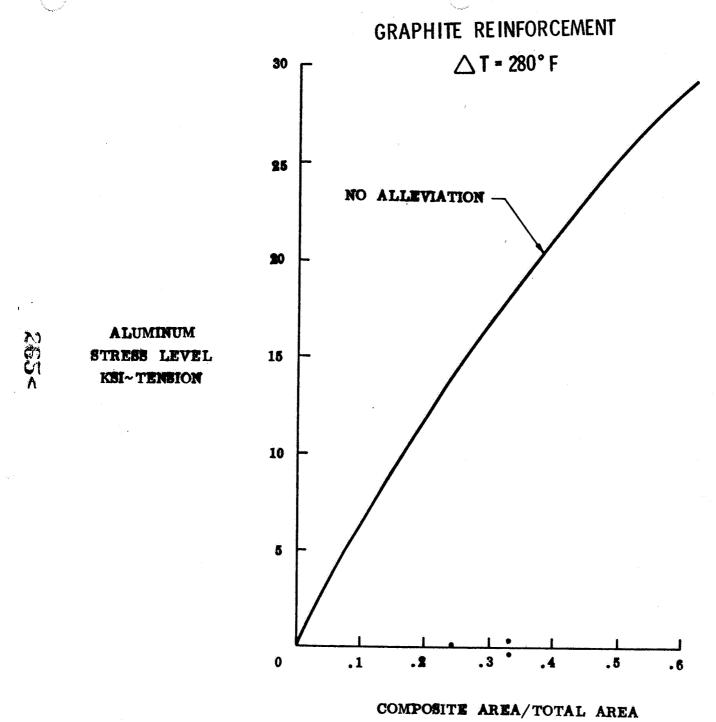


FIGURE 11 RESULTS - GRAPHITE REINFORCEMENT CURED AT 350°F

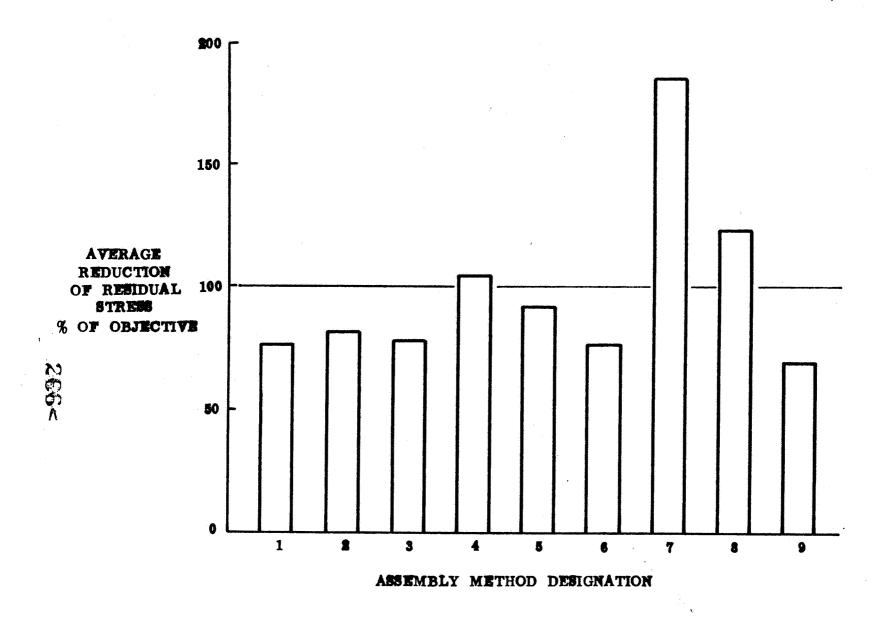


FIGURE 12 COMPARISON OF ASSEMBLY METHOD RESULTS

Salah Barangan Barangan

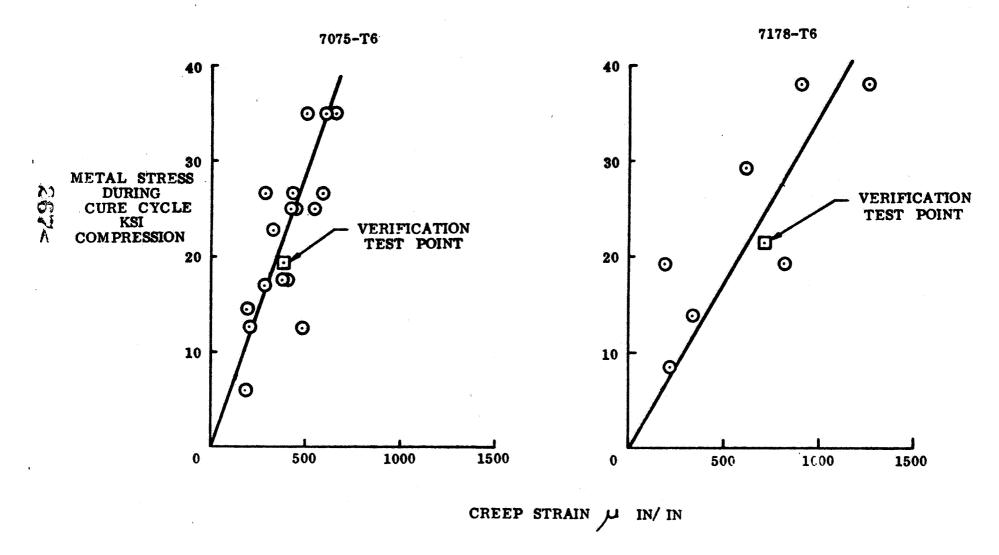


FIGURE 13 CREEP DEFORMATION OF ALUUMINUM

IN74 30935

BONDING OF REUSABLE SURFACE INSULATION WITH LOW DENSITY SILICONE FOAMS

BY

Dr. Arnold A. Hiltz; Ralph R. Hockridge; and Fred P. Curtis

Plastics and Advanced Composites Laboratory Re-Entry and Environmental Systems Division General Electric Company P. O. Box 8555 Philadelphia, Pa. 19101

Although the use of mechanical attachment and partial bond systems offer certain structural advantages in attaching Reusable Surface Insulation (RSI) to the Space Shuttle Structure, continuous bonding is regarded as the most reliable system. This is primarily due to the limited strength and strain capability of the high temperature ceramic materials requiring a soft foam pad material for strain isolation as part of the attachment system.

The foam bond attachment systems most likely to meet all the requirements, including both low and high temperature extremes are based on the Room Temperature Vulcanizing (RTV) silicone elastomers.

This paper describes approaches taken by GE-RESD to develop and evaluate reduced density, high reliable foamed bond strain isolation attachment systems for RSI. Included are data on virgin as well as on material that received 100 cycles of exposure to $650^{\rm OF}$ for approximately 20 minutes per cycle.

1.0 INTRODUCTION

1.1 Design

Typical areas of the space shuttle vehicle that may be covered with reusable ceramic insulation include leading edges, nose caps; windward body sections, wings, fins, and control surfaces. The maximum surface temperature requirements for each of these areas will define the applicable insulative material system to be used. Allowable primary structure or mounting panel temperatures will establish required insulation thicknesses.

The primary structure arrangements for these various regions of the vehicle include monocoque and semi-monocoque constructions with the RSI integrally attached.

In the integral panel concept (Figure 1), the insulation is bonded directly to the primary air frame structure, and all of the air loads are transmitted directly to this structure. Adhesive bonding makes direct attachment to the primary structure the most efficient approach.

The insulation may be bonded to standard structural materials such as aluminum, titanium, phenolic glass honeycomb, or super alloys such as Inconel. In the subject discussion, aluminum and titanium are considered as representative structural materials. The maximum operating temperature, including safety factors, is 350°F for aluminum and 650°F for titanium.

1.2 Requirements

1.2.1 Mechanical

Use of essentially continuous attachment is deemed necessary for RSI due to the limited strength and strain capability of these high temperature ceramic materials. This negates the use of individual mechanical attachments and requires the use of a soft foam pad material for strain isolation as part of the attachment system.

Typical tensile stresses that will develop in the foam bond material system, due to the thermal gradients resulting from entry heating, are shown in Figure 2 as a function of time for several heating rates representative of a typical cross range orbiter. It may be noted from Figure 2, that the required strength is relatively low. However, the maximum stresses occur at a time period in the mission when the temperature has peaked (Figure 3).

Several material properties are critical in the design of an RSI thermal protection system. They are 1) ultimate strength in tension and shear, 2) modulus of elasticity, and 3) thermal expansion.

Orbital soak-out, particularly at the -250°F temperature, develops high shear and tensile stresses in the bond system, since it is below its glass transition temperature.

Post-entry also imposes stresses on the bond since the RSI has become relatively cool but the bond has soaked out to the 400-600°F temperature range where strength properties are strongly influenced and reduced by temperature.

1.2.2 Weight

The manufacturing tolerances on the RSI and the airframe skin, and the requirements for low shear stiffness dictate a bondline thickness of at least 0.070". The densities of typical candidate adhesive systems range from about 66 to 90 lb/ft³ which at a bondline thickness of 0.070" translate into a bond weight of 0.385 to 0.525 lb/ft². Reduction of the bond weight, since the bondline thickness is relatively fixed, can best be achieved by reducing its density. Fortunately, this is also the direction desired for reducing the shear stiffness of the bond. However, a decrease in density will also decrease the strength of the bond. Accordingly, a trade-off is required between bond strength and bond density.

1.2.3 Thermal

The adhesive system must be capable of performing its intended function for 100 missions at the maximum normal entry design bondline temperatures without excessive thermal degradation or change in properties. These temperatures are $\sim 350^{\rm o}{\rm F}$ for an aluminum structure and $\sim 650^{\rm o}{\rm F}$ for titanium with a factor of safety. In addition, the system must be compatible with the -250°F temperature experienced during orbital stay. Figures 3 and 4 show typical area 1 and 2P temperature histories for various combinations of REI tile and bond thicknesses.

Area 1 and area 2P are NASA/MSC point design designations representing two extremes of shuttle heating for RSI applications. Area 1 is representative of heating which produces surface temperatures of 1400° F, and in area 2P surface temperatures of 2300° are reached.

1.2.4 Space Environment

Since the space shuttle will be subjected to a hard vacuum, care must be taken to remove materials which may volatilize and recondense on colder or more polar portions of the vehicle. In the open cell silicone foam system here discussed, volatiles are removed during the post-cure cycle. In addition, the bond system must be stable to the space environment radiation.

1.2.5 Ground Environment

The bond system must be stable to the effects of humidity, moisture and salt spray. It must not support the growth of fungus. It must also withstand aircraft ground handling, and be compatible with rocket and jet fuels as well as with common cleaning solvents.

2.0 ADHESIVE MATERIALS

Analysis of the established requirements for the RSI attachment indicate the most probable application method to be by adhesive bonding. As indicated, the use of a high shear stiffness adhesive induces high shear stress concentrations at the interface between the surface insulation and the structure, and, as a result, imposes unnecessarily high strength requirements on the bond and RSI. The use of a finite thickness flexible adhesive, on the other hand, results in the attenuation of stress concentrations and in a reduction of the shear stress requirements for both the adhesive and the insulation.

Careful evaluation of the available commercial materials with capability of meeting all the requirements led to the selection of the room temperature vulcanizing silicone rubbers (RTV). The following were selected for consideration and evaluation from the prime candidate systems indicated in Table I.

2.1 PD-200 (Base)

PD-200 (Base) is a solid methyl-phenyl silicone which can be cured to a strong rubbery state at room temperature with tin soap catalysts such as $T-12^1$ or Nuocure 28^2 . It cures by a condensation mechanism with the elimination of volatile by-products. Venting is necessary to achieve cure in the inner portions of large bonded areas of non-porous materials.

¹ Dibutyl Tin Dilaurate, M&T Chemical Corporation.

² Tin Octoate, Tenneco Chemicals, Inc., Nuodex Division

2.2 PD-200

PD-200 is an open cell, methyl-phenyl silicone foam exhibiting an extremely fine cell structure which is uniformly distributed. It is formulated and chemically blown at ambient temperature and pressure utilizing open pan type molds. Initial foaming and cure requires one hour. At this point the foamed bun is slit to remove the surface skins, then step wise post-cured to 350°F over a 26 hour period to stabilize weight and dimensions. Upon completion of post cure, the foam is slit to design thickness using commercial rubber slitting equipment.

2.3 PD-200 (Mod)

PD-200 (Mod) is an open cell, methyl-phenyl silicone foam. In contrast to the standard PD-200, by means of proper selection of catalyst concentration and process parameters pressure, reproducible foam materials having a density range of 15 to 25 lbs/ft³ have been produced. The PD-200 (Mod) is further processed (post-cured and slit) in the same manner as the standard PD-200 foam. This results in a foam system that can effect a large system weight saving over the standard PD-200.

3.0 BASIC ELASTOMER CHARACTERISTICS

3.1 PD-200 (Base)

PD-200 (Base) has been characterized by GE-RESD for use as an adhesive for re-entry vehicle application. It has also been used extensively in the production of GE Elastomeric Shield Materials (ESM).

It has excellent low temperature (\sim -180°F) flexural properties and high thermal stability. The ultimate strength of PD-200 (Base) as a function of temperature is shown in Figure 5. Tensile and shear moduli values as a function of temperature are shown in Figure 6, where it is seen that the modulus is relatively constant over a temperature range from 0 to +400°F.

Below -150°F, the modulus increases rapidly to the glass transition temperature of approximately -180°F. The thermal stability of the cured elastomer is shown by the thermogravimetric analysis curve of Figure 7. It is seen that PD-00 (Base) does not begin to lose weight at a significant rate until around 1100° F, and is quite stable at 600 to 650° F, the maximum bondline temperature for a titanium structure.

The coefficient of thermal expansion of PD-200 (Base) is 150×10^{-6} in/in/°F from -100°F to 600° F. Its specific heat is 0.4 BTU/lb°F from -100°F to 600° F. The thermal conductivity is shown in Figure 8.

Long term stability of the material at 600° F has been demonstrated under the SNAP-27* Program where greater than 200 psi tensile shear strength was exhibited at 655° F on specimens aged for eight weeks at 600° F.

Cure in deep sections has been achieved by strip bonding, i.e, by leaving gaps in the bond for air entry and volatiles removal. Removal of volatiles, however has not been a problem in the bonding of porous, low density insulation materials.

3.2 PD-200

PD-200 has been characterized by GE-RESD for use as a strain isolation. foam system for space shuttle environment application. Its low temperature flexibility and high temperature stability are similar to the PD-200 (Base). Typical tensile and shear properties of PD-200 as a function of temperature before and after cycling are shown in Figures 9 and 10. The tensile and shear moduli values as a function of temperature are shown in Figures 11 and 12. The low temperature modulus data is shown in Figure 13. The thermal stability of the cured foam is indicated by the thermogravimetric (TGA) analysis curve of Figure 14.

The specific heat of PD-200 is shown in Figure 15, the thermal conductivity is 2×10^{-5} BTU/Ft-Sec-OF (Figure 16), and the thermal expansion data is shown in Figure 17. Elevated temperature stability of the PD-200 foam has been demonstrated, and is indicated by the data presented in Table II. As indicated above, the long term stability of the base material has been demonstrated in the SNAP-27 Program.

In contrast to PD-200 (Base) where cure in deep section requires the strip bonding approach, bonding of the PD-200 foam has not been a problem due to its porous nature.

3.3 PD-200 (Mod)

PD-200 (Mod), a recent modification of the well characterized PD-200 foam system, is currently being extensively evaluated. The PD-200 (Mod), in a density range less than 20 lb/ft³, can offer considerable advantage in weight reduction and in strain isolation. As can be seen in Figure 18, 1.0 inch of foam at 28 PCF results in a tile thickness of 1.7 inch and a weight of 4.4 lb/fc (Curve A), while use of a 15 PCF foam (Curve B) results in a weight of 3.9 lb/ft a weight reduction of 0.5 lb/ft².

Space Nuclear Auxiliary Power Unit



4.0 ADHESIVE APPLICATION TO RSI SYSTEMS

During the development of the GE Reusable External Insulations (REI), it was necessary to bond samples to substrates (mostly aluminum) for evaluation against the Space Shuttle Orbiter environments of:

- a) Moisture
- b) Re-entry thermal simulation at representative local pressures
- c) Orbital cold soak exposure
- d) Airframe load strain compatibility

The specimen geometry consisted of a 4" \times 8" \times 1" REI panel bonded to an aluminum plate. Four inches of exposed aluminum on each end served for gripping the panel in a Universal Testing Machine. Each specimen was exposed to a thermal test cycle, and some specimens were also exposed to a -170° F cold soak prior to the heat exposure. Design of the specimens was such that the stress at the center of the REI face was equivalent to the maximum that would occur on an infinite size end. Earlier tests of this nature utilized solid PD-200 (Base). These tests indicated that the bond modulus (shear stiffness) of the solid adhesive was unacceptable for REI Mullite materials.

Consequently, the adhesive was changed from a solid bond to a foam bond system utilizing PD-200 and PD-200 (Base). Subsequent testing indicated the bond modulus to be acceptable for REI Mullite as a result of the strain isolation properties of the PD-200.

The PD-200 foam bond system was applied in two stages. The foam sheet was first bonded to the REI panel with PD-200 (Base), cured, then bonded to the precleaned, primed structure. Such an assembly has successfully survived exposure to a $-250^{\circ}F$ thermal cycle environment.

6.0 SUMMARY AND CONCLUSIONS

The room temperature vulcanizing silicone elastomers meet all the requirements for the attachment of reusable external insulation to the space shuttle vehicle. Of these flexible silicones, PD-200 (Base), especially when used in a reduced density configuration, such as PD-200 or PD-200 (Mod), could fulfill all the requirements. The adhesive systems based on PD-200 are usable up to approximately 650°F. Reduction of the density by chemical foaming provides a reduced weight and a lower modulus strain isolation bond system offering considerable advantage for the shuttle reusable surface insulation TPS.

ACKNOWLEDGEMENT

The authors are indebted to Jim Brazel for the thermal property data, to Dave Lowe for the mechanical property measurements, and to Jim Kreitz, Jr., for his bonding development contributions.

Portions of the work reported in this paper were sponsored by NASA Contracts NAS 1-10533 and NAS 9-12084.

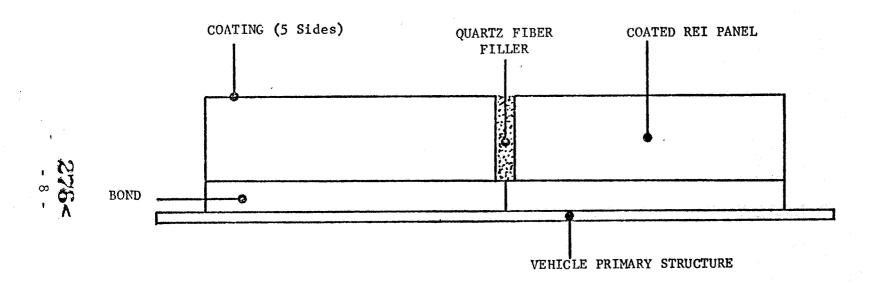
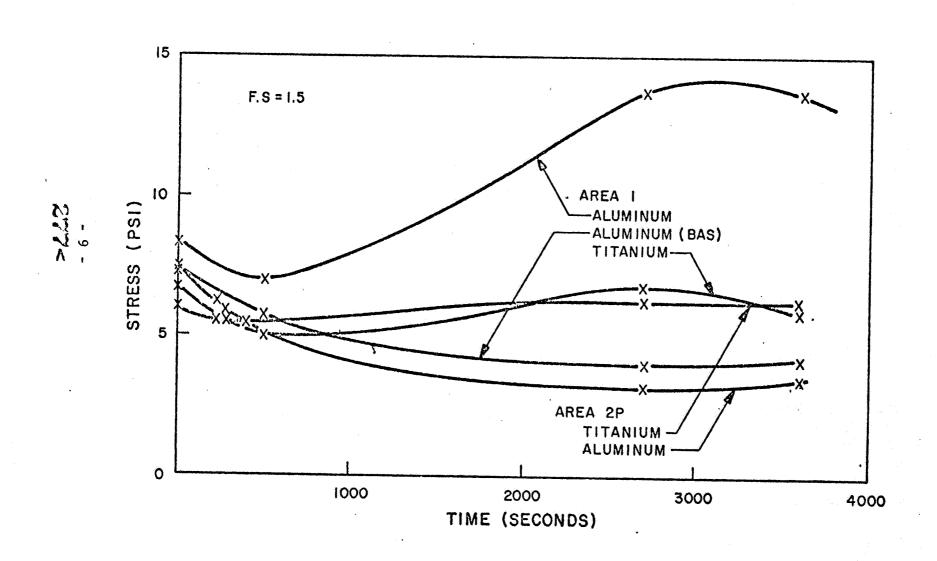


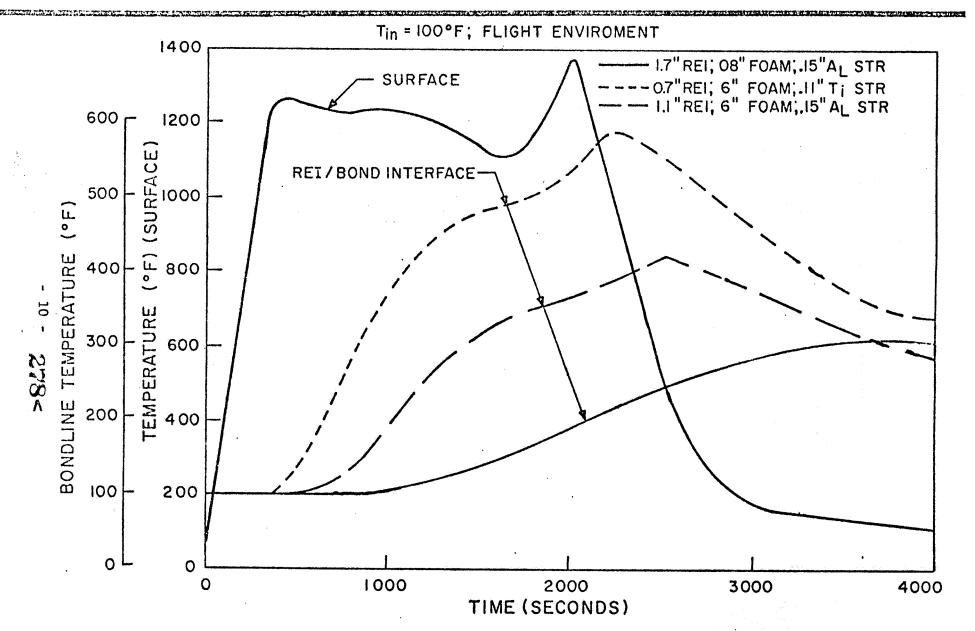
FIGURE 1
TPS INSTALLATION



BOND TENSILE STRESS HISTORIES



AREA I PROTOTYPE PANEL TEMPERATURE HISTORIES FIG. 3







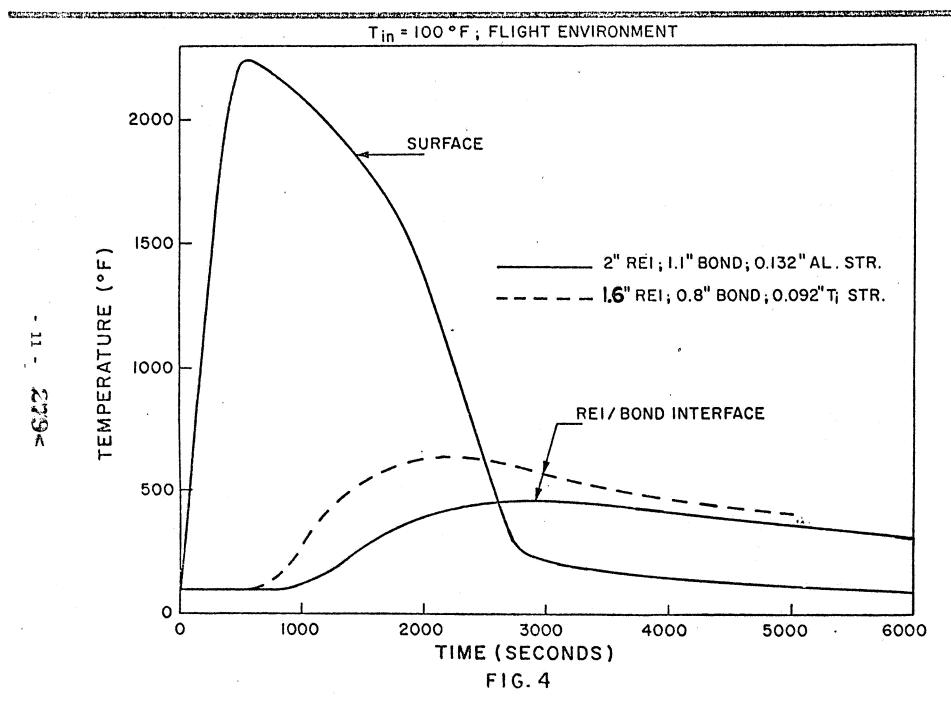


FIGURE 5

ULTIMATE STRENGTH OF PD-200 (BASE)

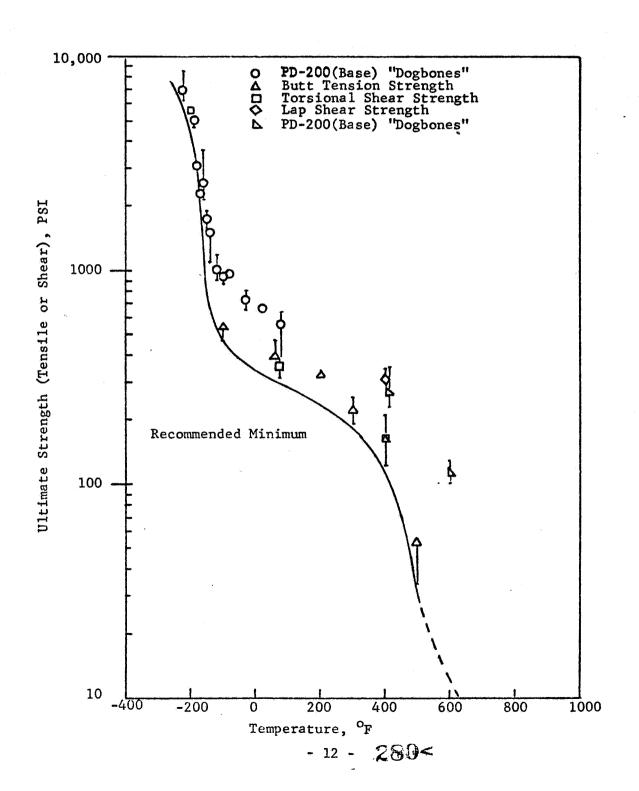


FIGURE 6

ELASTIC MODULI OF PD-200 (BASE)

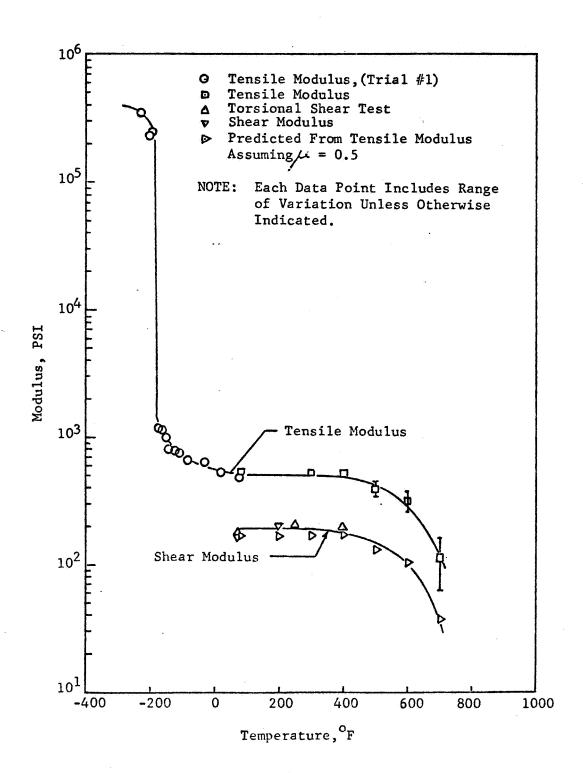


FIGURE 7

TGA ANALYSIS OF PD-200 (BASE)



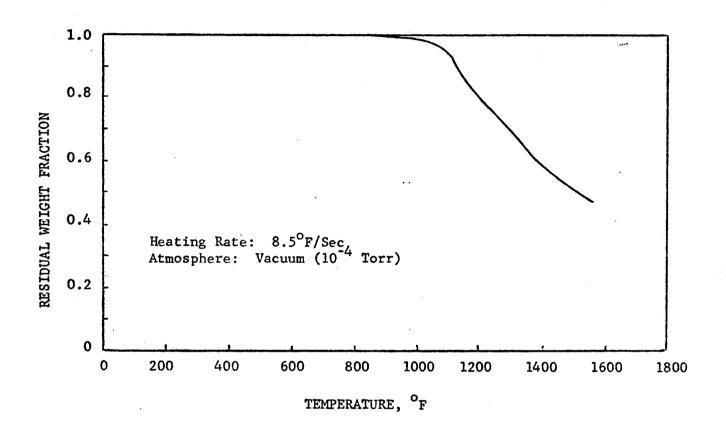
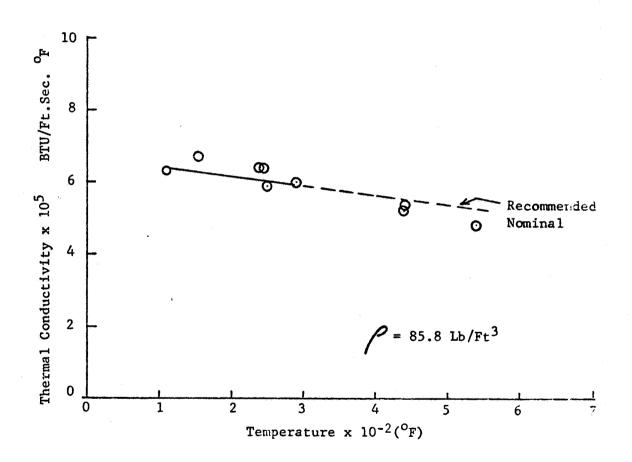
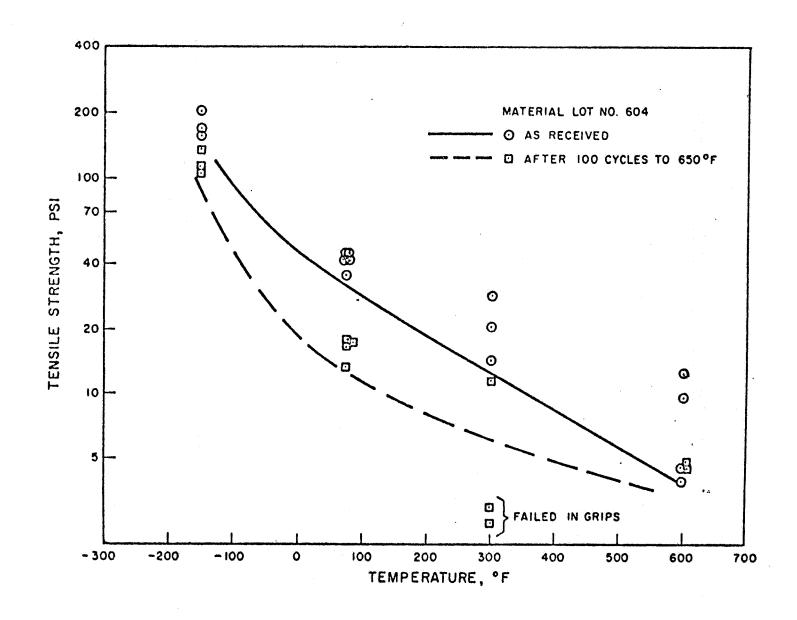


FIGURE 8

THERMAL CONDUCTIVITY OF PD-200 (BASE)



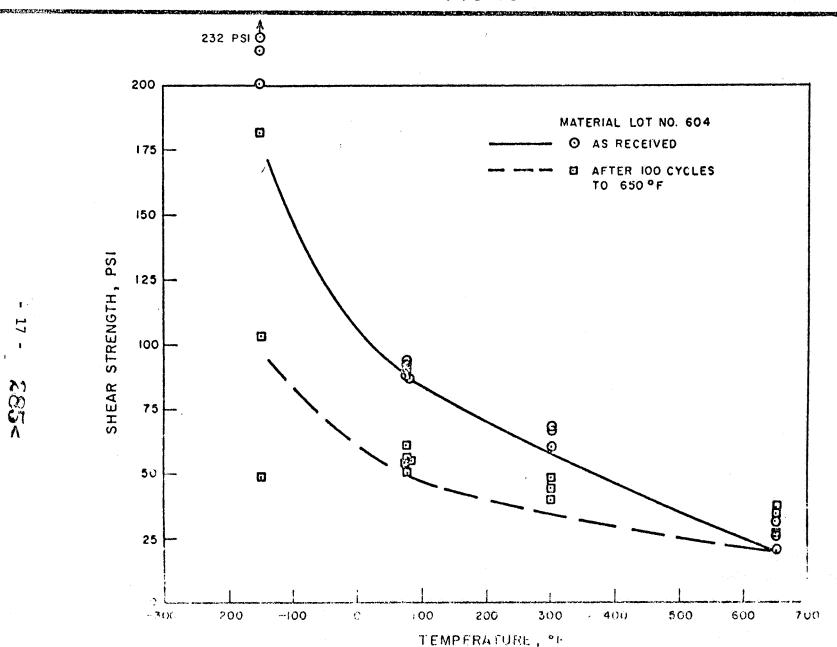
TENSILE STRENGTH OF PD200



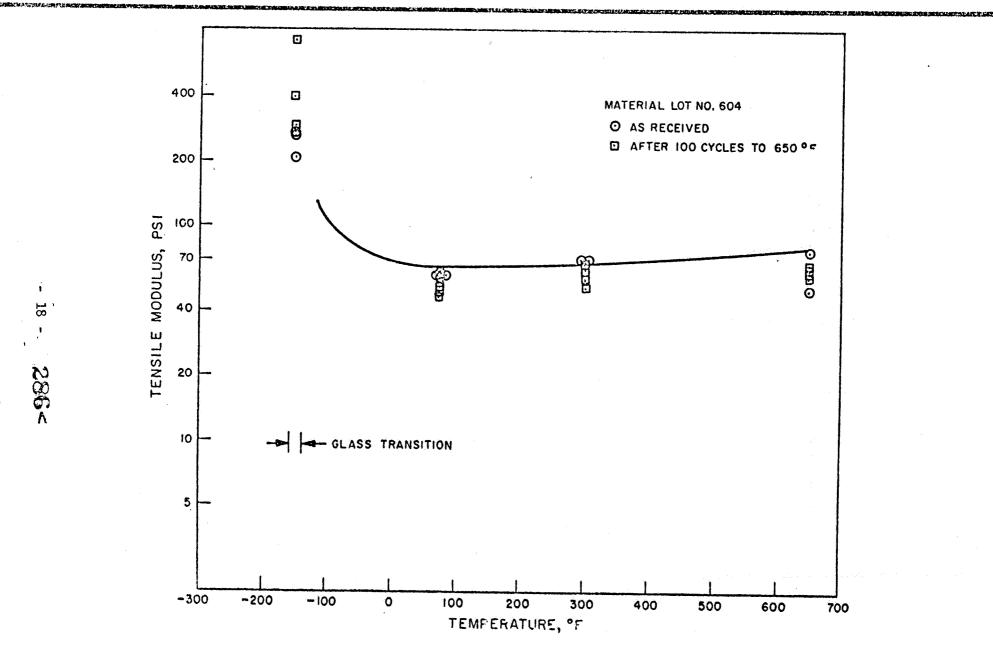




SHEAR STRENGTH OF PD200



TENSILE MODULUS OF PD200





SHEAR MODULUS OF PD200

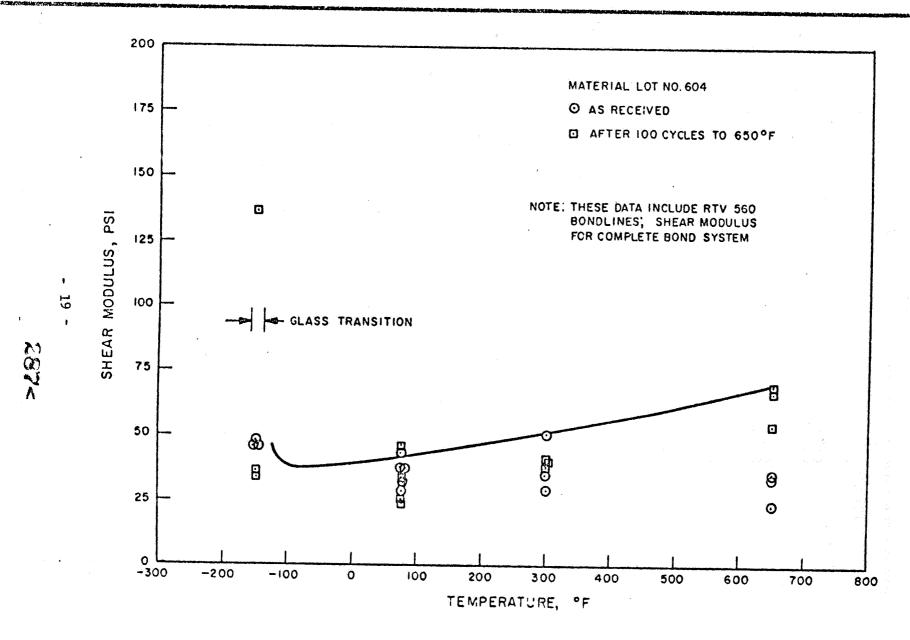
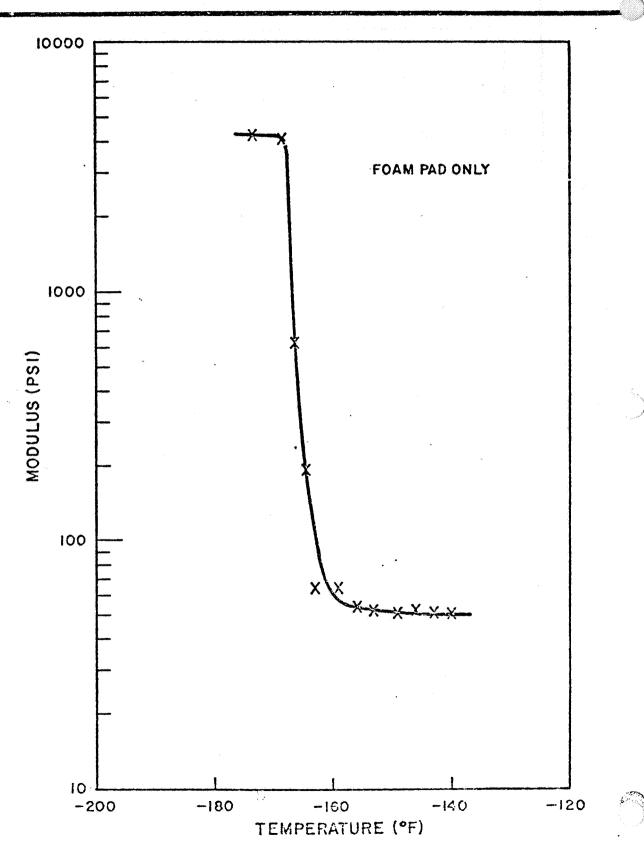
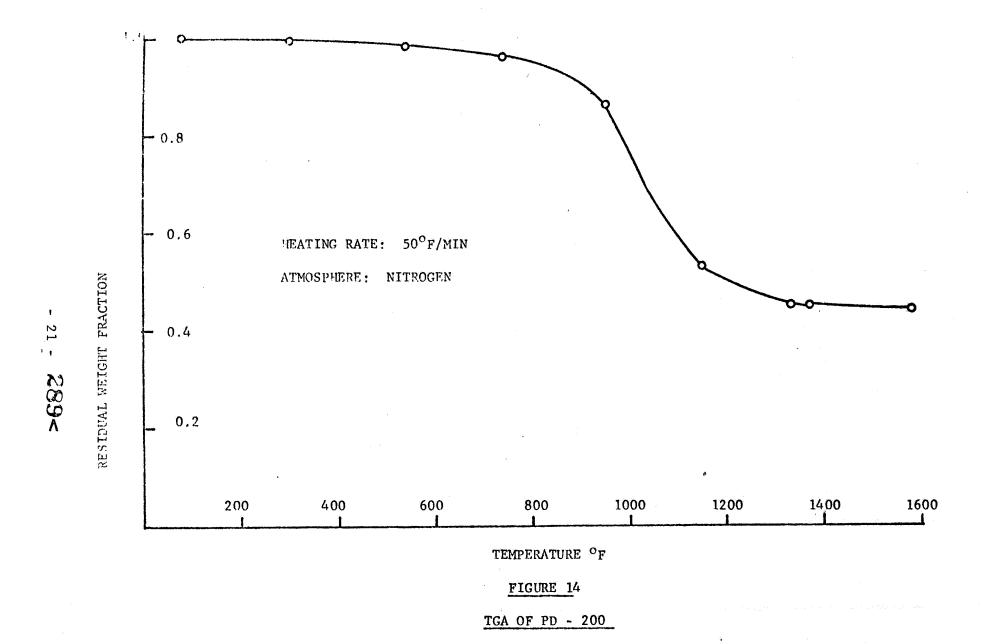


FIG. 13 LOW TEMPERATURE MODULUS OF PD200



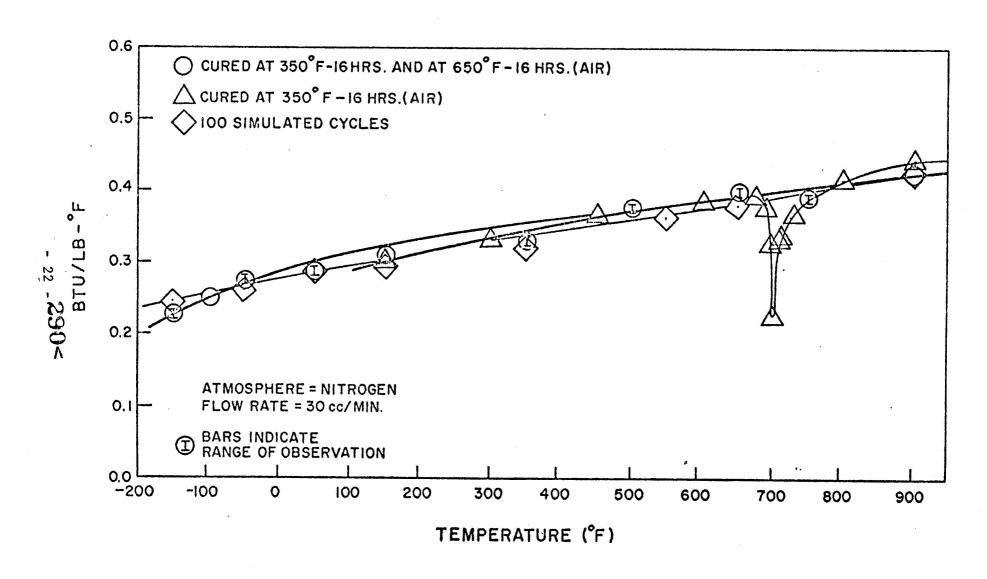
^{- 20 -}288<





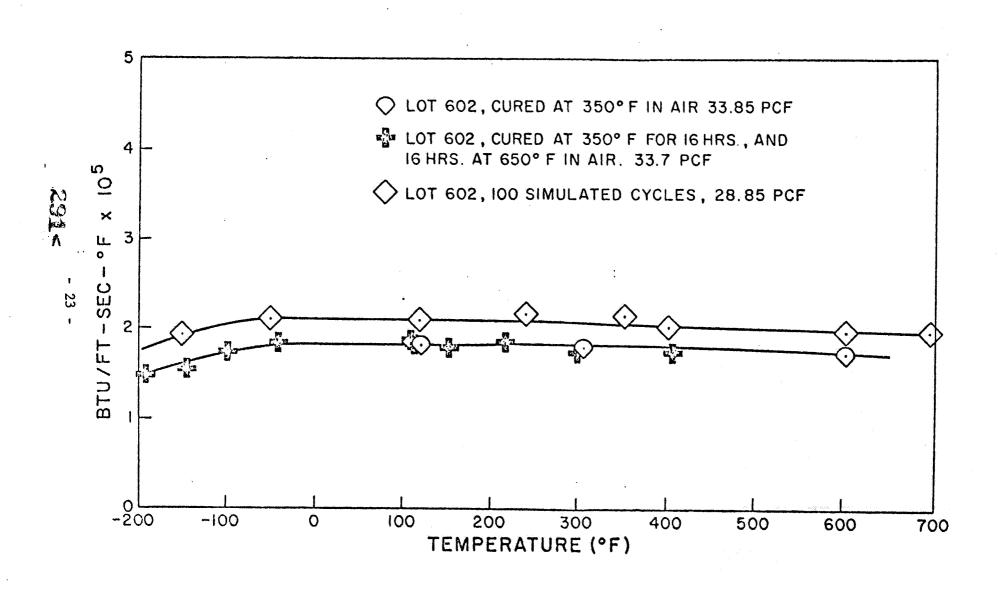
SPECIFIC HEAT OF PD-200(LOT#602).

FIG. 15





THERMAL CONDUCTIVITY OF PD-200 FIG. 16



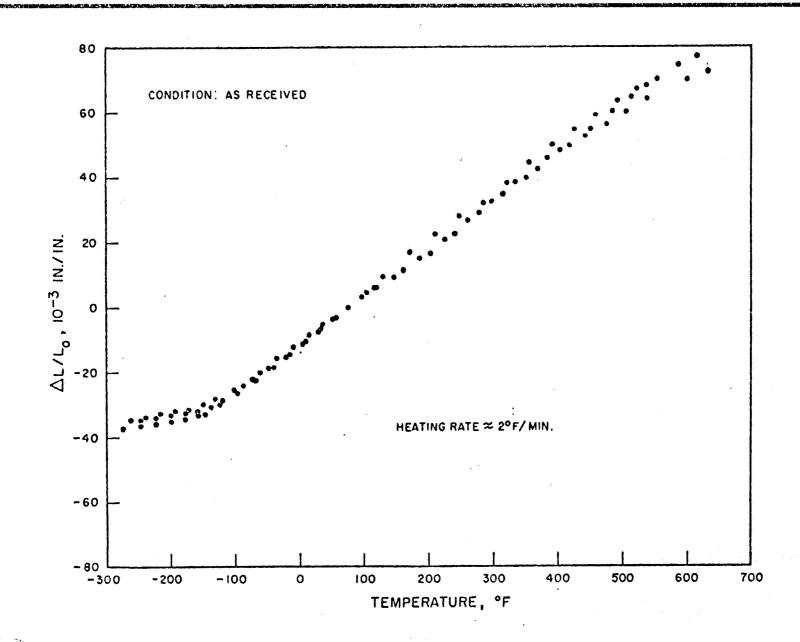


FIG. 18

EFFECT OF VARYING PD 200-F28 THICKNESS AREA 2-PERTURBED

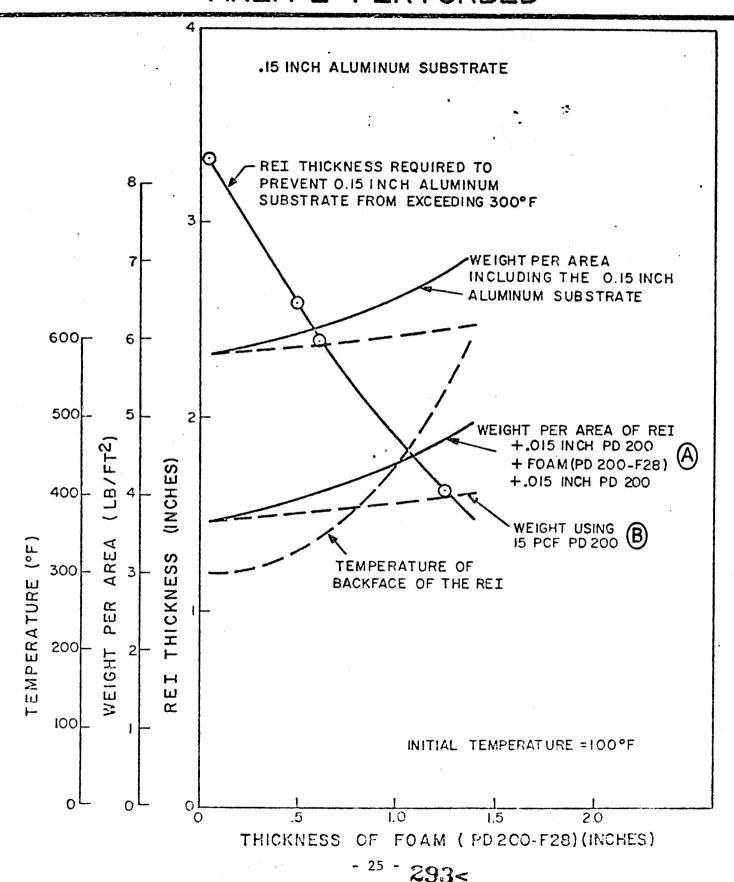


TABLE I RTV SILICONE ADHESIVE CANDIDATES

	COMPOUND	CHEMICAL TYPE	POLYMERIZATION MECHANISM	GLASS TRANS. TEMP.	STRENGTH	DECOMPOSITION TEMPERATURE
	RTV 630	Methyl Vinyl Silicone	Addition	-80 ^o F	High	High
- 26 ' 294	PD-195	Methyl Phenyl Vinyl Silicone	Addition	-180°F	High	High
	PD-200 (Base)	Methyl Phenyl Silicone	Condensation	-180 ⁰ F	Lower	Lower
	RTV 511	Methyl Phenyl Silicone	Condensation	-180 ^o F	Lower	Lower
	RTV 602	Methyl Phenyl Silicone	Condensation	-80°F	Lower	Lower
••	DC 93-046			-85 ^o F	Lower	Lower

TABLE II

ROOM TEMPERATURE LAP SHEAR STRENGTH OF PD-200 ADHESIVE

AFTER 16 HOUR THERMAL SOAK EXPOSURES

Exposure	Temperature,	$^{\circ}\mathbf{F}$
----------	--------------	----------------------

Test Number	75	450	550	625
1	94.5	67.1	49.3	33.7
2	83.3	58.6	46.3	31.3
3	82.6	70.0	52.5	31.8
4	84.2	63.5	56.4	32.0
5	83.2	62.2	41.8	32.6
$\overline{\mathbf{x}}$	85.6	64.3	49.3	32.3
S.D.	5.0	4.4	5.6	0.9
Failure Mode	All Cohesive	All Cohesive	All Cohesive	All Cohesive

Specimens:

 1.0×1.0 inch lap joint

.063 aluminum adherents .090 inch thick PD-200

RTV 560 bond ~ .005 inch thick (both sides)

SESSION 3 - UNIQUE JOINING TECHNIQUES

INTRODUCTION

R. E. Monroe - Chairman

Frequently the label unique is an invitation to argument on misinterpretation. The papers that comprise this session may stir such motives, but each represents a worthwhile contribution to our knowledge of various joining techniques. The diversity of subject matter confounds a meaningful summary. I prefer to recommend that each paper be studied for its novelty and provocative suggestions of applications as yet untried. Collectively, the papers illustrate the usefulness of the various approaches open to the researcher; theoretical study to assist in conception, explanation, and process improvement and the empirical approach to develop specific data.

N. Corvelli, Structural Mechanics Engineer Grumman Aerospace Corporation Bethpage, New York 11714

N74 30936

Abstract

The primary form of joining high strength advanced composite materials is adhesive bonded joints. The stepped bonded joint is an efficient configuration where the adhesive and composite matrix are co-cured. A design procedure for this type of joint is described along with the analysis technique upon which it is based. A modified elastic analysis accounts for the nonlinear behavior of the adhesive. A computer program with minimum running time and simplified input is utilized for analysis and becomes an efficient link in an iterative design procedure. Comparisons between analytical results and test results are shown. Material properties which are needed for design and methods of measuring these properties are discussed.

Introduction

In recent years advanced composite materials have been developed to the production level. At Grumman. this capability has been developed through a series of successful composite development programs, supported by both in-house and contract funding. The F14-A boron/epoxy horizontal stabilizer confirms this production capability.

A major problem with these high-strength, highstiffness materials is that of load introduction. This problem is a result of the highly anisotropic properties of the material. Bonded joints are used quite extensively and efficiently to introduce load into composite materials. Bonded joint technology, including design, analysis and fabrication, is essential for the successful utilization of composite materials. This technology must include design and analysis procedures which are simplified enough to be utilized in successive design iterations and reliable enough to eliminate overly conservative design requirements and minimize element testing. A design and analysis procedure which satisfies these requirements is discussed in this paper.

Bonded Joint Utilization

The boron/epoxy F14-A horizontal stabilizer, shown in Figure 1, is the first production utilization of advanced composite materials for primary structure. The construction is of full-depth aluminum honeycomb with boron/epoxy skins. All load is introduced into these skins through bonded joints. Each skin is framed by a stepped titanium splice member which is integrally molded into the laminate. The skins are bonded to the honeycomb core and mechanically fastened to the substructures (i.e. the pivot fitting and ribs) through these splice plates. Leading edge, trailing edge and tip structures are also mechanically attached through the splice plates. The loading on these splices vary around the periphery of the stabilizer to a maximum of 17,000 pounds/inch at the pivot fitting.

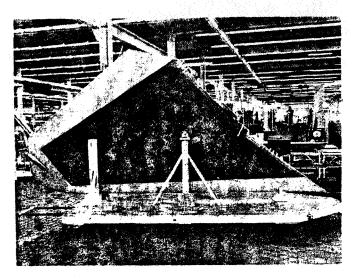


Fig. 1 F-14A Boron/Epoxy Horizontal Stabilizer

The configuration of a typical multi-stepped bonded splice such as those used on the F14-A horizontal stabilizer is shown in Figure 2. The bonded joint effects the transfer of load from the composite laminate to a metal splice plate. Just prior to the stepped region, the composite laminate thickness is increased to further strengthen the joint and to allow for a design with 15% margin of safety (a fitting factor). A fiberglass shim is also included to allow for introduction of a finite thickness of metal at the first step. Each step has a layer of adhesive between the adherends. The composite adherend may vary as to number of plies, ply orientation and step length on every step.

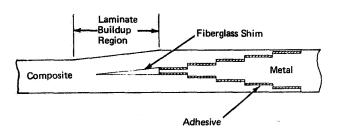


Fig. 2 Stepped Bonded Joint Configuration

Pictures of two typical splices utilizing this concept are shown in Figure 3. These splices are hybrid bonded to titanium with a double splice plate and boron aluminum brazed to titanium. They were tested to 45,000 pounds per inch in tension and 20,000 pounds per inch in compression, respectively, at 350°F. The ease of fabrication and efficient load transfer are the major reasons for the success of this joining method. The joint approximates a scarf and is co-cured to eliminate any

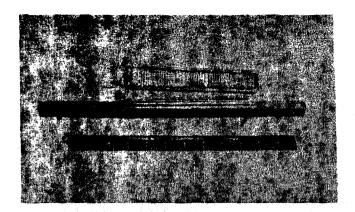


Fig. 3 Typical Stepped Joint Specimens

fit problem. That is, the adhesive layer is cured during the same cycle as the composite matrix and therefore the composite adherend conforms its shape to the metal splice plate.

Single Overlap Joint Analysis

Finite Element Analyses (FEA) were originally used to analyse the stepped bonded joints. Because of the extensive input required for a single analysis, use of this analysis in an iterative design procedure was very time consuming. A simplified analysis was thus sought.

Initially, a single overlap joint analysis was developed. The configuration and loading of a typical single overlap joint is shown in Figure 4. Each adherend is loaded at the ends of the overlap with bending moments, axial loads and shear loads. The adhesive exhibits both shear and normal streses. The assumptions made for this analysis are:

- All materials are linearly elastic
- Adhesive stresses are uniform through its thickness
- Axial stiffness of the adhesive is negligible
- Adherends bend with plane sections remaining plane (shear defection is neglected)

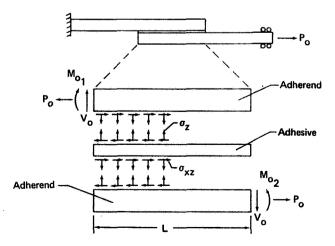


Fig. 4 Configuration And Loading-Single Overlap Bonded Joint

The adhesive stress distributions are then given by the solution of a set of simultaneous differential equations which are presented in Reference 1 along with a closed form solution. The results of this analysis are compared with that of a FEA in Figure 5 for a one-inch overlap of boron/epoxy bonded to titanium. The stresses at each end of the overlap are different due to the unsymmetric configuration of this particular joint. Good correlation is shown and the simplified continuous analysis gives essentially the same solution as the FEA.

Any solution for adhesive stress distributions which is useful for failure analyses must include the nonlinear behavior of the adhesive. Here this effect is included as a modification of the elastic solution. The relation between the elastic and plastic stress concentration factors is assumed to be:

$$K_p = 1 + (Ke - 1) \frac{G_{sec}}{G_{tan}}$$

where:

 K_e = elastic stress concentration factor K_p = plastic stress concentration factor $G_{\rm SeC}$ = second shear modulus at failure $G_{\rm tan}$ = initial tangent shear modulus

A similar relation was used by Hardrath and Ohman (Reference 2) for notched plate test data showing good correlation. This relation was based on theoretical analysis of Stowell (Reference 3).

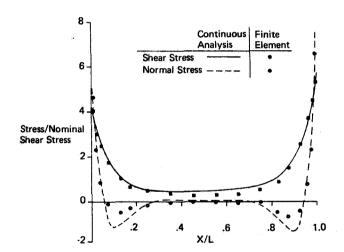


Fig. 5 Adhesive Stress Distributions-Single Overlap Bonded Joint

A nonlinear analysis was performed to test the validity of this modification. A single overlap joint was analyzed neglecting bending. The results of the nonlinear and elastic analyses are shown in Figure 6. For a failure analysis, only the peak stress from the nonlinear analysis is required and this is sought with the modification of the elastic solution. Comparison of the nonlinear and modified elastic solutions is shown in Figure 7. Stress concentration factors are shown for the peak adhesive stress equal to the shear ultimate stress of the adhesive, i.e. at the failure load for the overlap joint. Good correlation is demonstrated over the entire range of the joint length parameter, α L.

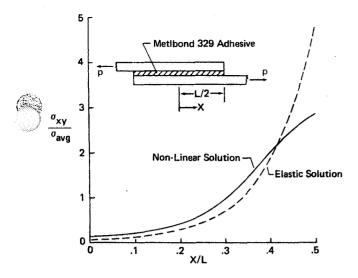


Fig. 6 Non-Linear and Elastic Shear Stress Distiributions

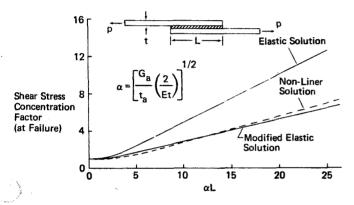


Fig. 7 Comparison of Non-Linear and Modified Elastic Solutions

Using this analysis for predicted strengths a comparison with test results for single overlap joints at room temperature is shown in Figure 8. Separate calculations were required for determination of the loadings at the ends of the overlap (see Figure 4) from an analysis of the entire test specimen and fixture configuration. Stress strain data of the adhesive was required along with the

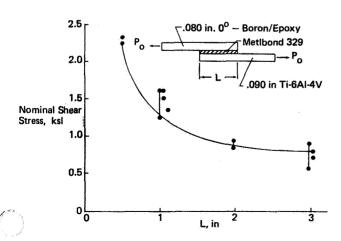


Fig. 8 Correlation With Test Results

properties of the adherends. The best method available for the determination of the adhesive stress strain behavior is the testing of specimens sketched in Figure 9. The tests involve torsion testing of a thin wall cylindrical specimen and tension testing of a round specimen. Both specimens contain a butt joint of the adhesive of interest. These are tests on adhesive bondlines of thicknesses representative of those in an actual joint. Extremely accurate displacement measuring equipment is required to perform these tests and measure the entire stressstrain relation of the adhesive. Accuracy of the order of 10⁻⁶ inches is required in this equipment. This test

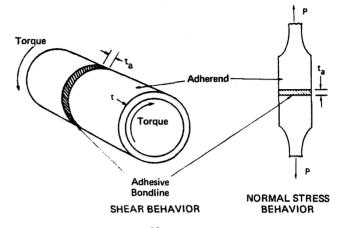


Fig. 9 Adhesive Material Property Tests

technique has been developed at Singer General Precision by Dr. John Rutherford (Reference 4) and successfully used to characterize some adhesives. Tests performed there on Metlbond 329 adhesive were used to determine the adhesive properties, Table 1, which were used for the predicted strengths.

Table 1. Methbond 329 adhesive properties at room temperature

Shear Ultimate Stress, F _{su}	9400 psi
Tension Ultimate Stress, Ftu	7700 psi
Shear Modulus, G _{tan}	0.34×10^{6} psi 1.43×10^{6} psi
Tension Modulus, Etan	1.43 x 10 ⁶ psi
Good/Gton	0.29
Eggs/Etan	0.64
G _{sec} /G _{tan} E _{sec} /E _{tan} Bondline thickness, t	0.008

Stepped Joint Analysis

This modified elastic solution is now used for the analysis of synmetric stepped bonded joints. The single overlap analysis is applied separately to half of each step as shown in Figure 10. Adherend bending is neglected and therefore the adhesive normal stresses assumed to be negligible. This assumption was verified by examination of early FEA results which showed the maximum adhesive normal stress to be less than 10% of the corresponding maximum shear stress. These low normal stresses are due to the symmetry of the joint configuration and the relatively small offset of load lines.

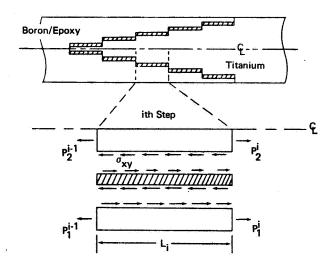


Fig. 10 Symmetric Stepped Bonded Joint

In a typical single overlap joint the normal stresses are greater than the shear stresses. The separate analyses of each step are combined by satisfying compatibility and equilibrium conditions at the internal discontinuities.

The stepped joint analysis is written into a computer program to facilitate the design procedure. The original program, STEP*, as presented in Reference 1 was used for boron/epoxy to titanium bonded joints. The most recent program, STPS4 (Reference 5), has revisions which include thermal stress calculations and provisions for application to various composite materials. This program was utilized for the prediction of joint strengths in the correlation with test data which is to follow.

The procedure used to design a stepped bonded joint in composite materials is outlined in Figure 11. The closed loop in the cycle is repeated by the designer in an interative design procedure. The operation is performed quickly at a remote terminal of the computer with complete interaction between the designer and computer. The input data required are the material properties and concise joint configuration parameters (i.e. number of steps, orientation and number of plies on each step, length of each step, and homogeneous adherend thicknesses). The program output includes the overall joint failure loads for many varied failure modes. The designer generally searches for a design with sufficient strength which is relatively balanced in strength.

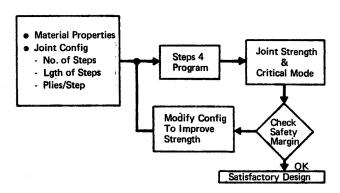


Fig. 11 Stepped Bonded Joints Design Procedure

Correlation with test data for joints designed in this manner is shown in Figure 12. The solid line would represent a one-to-one relation between predicted and test values. The test points shown are averages of test data representing a total of 23 tests. Joints have been tested in both tension and compression for temperatures varying from room temperature to 350°F. Tests have included joint loading as high as 48,000 pounds per inch. The dashed line represents a design value for each joint with the reduction due in part to the use of a 15 percent fitting factor and to the reduction of average material properties for design allowables. Correlation with test data is good with predicted values generally being conservative.

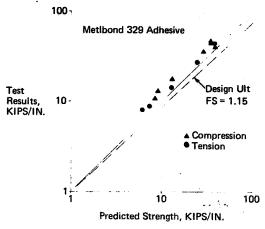


Fig. 12 Comparison of Predicted & Test Strengths of Stepped Bonded Joints

Conclusions

An analysis and design procedure has been described for stepped bonded joints in composite materials. The analysis utilizing a modified elastic solution is relatively easy to perform with a quick-running computer program. The simplified input required facilitates its use in a iterative design procedure. The predicted strengths are relatively accurate in comparison with test data and consistently conservative.

References

- Corvelli, M. and Saleme, E. "Analysis of Bonded Joints," Grumman Aerospace Corporation, Advanced Development Report No. ADR-02-01-70.1, July 1970.
- Hardrath, H.F. and Ohman, L., "A Study of Elastic and Plastic Stress Concentration Factors Due to Notches and Fillets in Flat Plates," NACA Report No. 117, 1953.
- Stowell, E.Z., "Stress and Strain Concentration at a Circular Hole in an Infinite Plate," NACA Technical Note TN 2073, April 1950.
- 4. Rutherford, J.L., Bossler, F.C., and Hughes, E.J., "Capacitance Methods for Measuring Properties of Adhesives in Bonded Joints," Rev. Sci. Inst. 39, No. 5, 666-671, May 1968.
- Torczyner, R. D., "STPS4, The Analysis of Advanced Composite Stepped Bonded Joints,"
 Grumman Aerospace Corporation, Composites
 Technical Note No. CTN-466-39, September 1971.



ADHESIVES AND THE ATS SATELLITE MAY 1972

N74 30937

Advanced Manufacturing Technology Martin Marietta Corporation Orlando, Florida 32805

ADHESIVES AND THE ATS SATELLITE

This paper describes six types of adhesives used in the Applications Technology Satellite (ATS).

The ATS will act as a relay for television and aircraft communications and will provide data on a series of experiments. These functions are expected to continue while the satellite is on station for 3 to 5 years over remote areas of the continental United States and, later, over India. The prolonged, exact station-keeping is maintained by sensors aimed at Polaris, the Sun and the Earth. These sensors must remain clean during the life of the satellite to avoid interference with this delicate station-keeping function.

The external surfaces and finishes on the satellite are selected to provide thermal control. These surfaces are less sensitive to contaminants than the sensor lenses, but gross localized discolorations can produce "hot spots" which can jeopardize satellite functions.

Selection of all materials was therefore limited to those which were known or proven to be "space compatible". The criteria for space compatibility was based on the Jet Propulsion Lab standards; less than one percent volatile and less than one-tenth of one percent condensable when exposed to 125°C + vacuum of 10-5 Torr for 24 hours.

Adhesives present a special problem when tested against this criteria. To be an adhesive, a material must flow enough to thoroughly wet the surfaces to be bonded. Materials which flow, even after high temperature cures, invariably contain volatile constituents in excess of the acceptance criteria. Adhesives discussed herein are limited to those which passed this space compatibility test and were selected for use on the satellite.

The satellite was constructed of honeycomb panels held together with aluminum fittings and beams. The fixed focus of the antenna is held rigid in spite of the thermal extremes of space by an epoxy-graphite composite truss assembly. The solar arrays and the module structures are lightweight honeycomb panels. A few of these panels provide most of the structure which holds the black boxes in place.

These structural panels consist of 2024-T3 aluminum foil skins, 0.012 or 0.025 inches thick and bonded to light-weight aluminum honeycomb core, specifically: 3.1-3/16 10P(5056)E per MIL-C-7438. This means that the core is 3.1 pounds per cubic foot, 3/16 inch cell size, perforated, 10 ten-thousands of an inch thick, expanded and made from 5056 aluminum alloy. Certain of the more heavily stressed panels use the thicker skin (0.025" instead of 0.012" thick).

Solar array panels are similar except that one of the two skins is a laminate of 0.005" (5 mil) aluminum foil bonded to 0.002" (2 mil) Tedlar film. (Adhesive for this laminate is Riegel Paper Co., No. E-463).

These flimsy components are bonded together to form strong rigid panels which comprise all of the solar array and most of the module structures. The adhesive which performs this feat is HYSOL EA 9601. This adhesive covers all internal surfaces of the honeycomb panels. Perforations in the core permit the panels to "breathe" so that volatiles from this adhesive are free to migrate thru the satellite. Tests at Goddard Space Flight Center showed 0.37%



volatile content and a condensible content of less than 0.03% for cured Hysol EA-9601.

Selection of this adhesive followed a detailed review of available adhesives and comparison of their properties, especially space compatibility, strength, temperature resistance and processing requirements. HYSOL-EA-9601 appeared to be the most desirable of the available materials and was selected when the Goddard tests showed adequate resistance to thermal vacuum.

Hysol EA 9601 is a beige tacky paste which is shipped and stored at 0°F or colder, and has a storage life of only two months. The adhesive is packaged in rolls up to 36 inches wide and 200 feet long. Both sides are protected by polyethylene separator sheets. It is hard and brittle while cold and becomes soft and tacky as it thaws. After thawing, it is cut to shape with a sharp knife or shears. The polyethylene separator sheet is then removed from one side and the bare adhesive is then pressed against one of the clean surfaces to be bonded. The other separator sheet is then removed carefully to avoid disturbing the adhesive and the second clean surface to be bonded is then positioned. The assembly is placed under pressure of 10 PSI or more. Vacuum bag pressurization was used for the ATS panels. The cure is effected by 1 hour at 250°F or 1 1/2 hours at 225°F.

Cleaning of the panels requires particular care. Where possible, aluminum panels are degreased, alkaline cleaned and acid etched before bonding. The Tedlar-aluminum foil laminate used in the solar panels is "spot cleaned" with MEK where necessary. These panels are previously cleaned during the Tedlar laminating process. Honeycomb usually requires only vapor degreasing and warm air dry.

Cure rate and temperature are critical. Optimum cure requires a heat-up rate from room temperature to cure temperature (225°F) in one hour or less. Prolonged heating at lower temperatures will allow the adhesive to sag and pull away from the core. Too rapid a heat-up rate can cause excessive bubbling and loss of strength.

Heat pipes are bonded into several of the module structural panels to carry heat from or to components and heat sinks as required. These heat pipes are sealed aluminum tubes, serrated or grooved internally similar to longitudinal gun barrel riflings. They are filled with anhydrous ammonia which boils at the heat source, condenses at the cold spot(s) and is carried back to the heat source through the serrations or grooves which act as capillaries. These heat pipes are filled with anhydrous ammonia and sealed with a weld before they are bonded into the honeycomb panels. Stress analyses showed that worse possible tolerance accumulation plus slight over-fill of a heat pipe could lead to a rupture at temperatures as low as 275°F. A test program confirmed the vendor's suggested alternate cure temperature of 225°F and all panels containing heat pipes were restricted to 230°F maximum temperature. Other panels were continued at 250°F to avoid the longer time required for the 225°F cure.

Test panels made to MIL-SPEC requirements (of MIL-C-7438) showed low peel strength after production was well underway. Investigation revealed that MIL-SPEC panels are made from heavier skins and larger, coarser core. Tests



with production core and light weight skins produced peel strength of 5 to 11 pounds per inch which is enough to cause some core failures on the light honeycomb. The adhesive used is only 0.030 pounds per square foot, approximately 2 mils thick when cured. HYSOL EA-9601 is usually obtained in a film weighing 0.060 pounds per square foot and may contain a supporting scrim cloth. The thin film adhesive is more than adequate for the lightweight satellite panels, but should be used in the heavier versions for more conventional hardware.

Peel strength of skin-to-core bonds does vary with adhesive film thickness as the thicker films have larger bond area in the core. Lap-shear strength, measured by skin-to-skin bonds, tends to follow vendor and specification data. Excess adhesive is squeezed out of lap shear panels to produce a thin glue line regardless of adhesive thickness at lay-up.

HYSOL-EA 9601 will produce lap shear strength of about 5,000 PSI at room temperature. Low temperature has no affect, but lap-shear strength drops to 4,300 psi at 180°F and 2,200 PSI at 250°F. Fortunately the ATS thermal control systems will prevent overheating of these panels. The <u>largest</u> structural loads are experienced during launch while the satellite is protected by its shroud cover.

Panel inserts are sometimes bonded during the panel initial lay-up using the same EA-9601 adhesive. Conductive epoxies or general purpose room temperature curing epoxies are used for inserts added after the panel is fabricated.

Another HYSOL product; EA 934 found numerous applications as a general purpose adhesive. HYSOL EA-934 (formerly shell-EPON 934) is a gray, thixotropic paste with amber, liquid, amine curing agent. This adhesive provides up to 3000 psi of lap shear strength, cures at room temperatures and has compressive strength of more than 10,000 psi at room temperature and 2,600 psi at 350°F. The high strength is derived from the hardness of this relatively brittle adhesive and care must be taken to avoid designs which impose severe peel strength on bonded areas.

EA-934 is used in the ATS to bond stand-offs in place, to fill gaps as a "liquid shim" and to bond doublers and other parts which must be installed without pressure-temperature cure cycles. It is often used to fill core void areas, especially where required to lock inserts into honeycomb panels.

EA-956 is similar to EA-934 except that it is an amber liquid with amber, liquid amine curing agent. The low viscosity of EA 956 permits it to be used in tight-fitting joints as in the graphite-epoxy truss to aluminum fitting joints. These joints are designed to keep stresses well below the 2,400 psi which may be expected at room temperature from the cured EA-956.

Electronic components in the ATS are vulnerable to temperature excursions and numerous measures have been incorporated into the design for thermal control. Louvers on the module faces are opened by bimetallic springs, as the temperature increases. A 25 degree rise in temperature will actuate the louvers. Closed, they retain heat and protect the electronics from over-cooling. When the louvers are open they allow heat to radiate out from the electronic assemblies of the earth viewing module. When facing the sun, they may reach temperatures as high as 500°F. Each louver is made from two thin polished aluminum skins bonded to



the hinge along their center line and to each other along their outer edges. Bond lines are about 1/8 inch wide and only a few mils thick. The adhesive is the Bloomingdale Rubber Company Primer BR-34. This material is a polyamide dispersed in a solvent. This is applied to the small glue line areas by a hypodermic needle. The adhesive is applied sparingly to both of the surfaces to be bonded. It is then allowed to air dry 30 minutes followed by an oven dry for 30 minutes at 220°F before the surfaces are joined. The parts are then clamped together in a jig and cured for 30 minutes at 270°F followed by 90 minutes at 550°F. The jig is designed to maintain 40 PSI pressure on the bond area during cure. The bonding procedure is tedious and exacting. Excess adhesive will interfere with the louver function while too little will result in bond failure and loss of the louver. The cure staging is time consuming. Results have been very good.

Velcro tapes permit easy installation or removal of thermal insulation blankets. The Velcro tapes are bonded to the structure and to the thermal insulation with CREST 7343/7139. This adhesive provides good flexibility and peel strength. This adhesive is supplied in two parts. The 7139 component must be melted to permit it to be added to the 7343 component. The material is sensitive to humidity which may cause it to become cloudy. The prepared adhesive is applied to both surfaces to be bonded, clamped in place and allowed to cure for 24 hours at room temperature or 4 hours at 160°F. Optimum room temperature cure requires 3 days.

Specialized adhesives are used to provide thermal and electrical conductivity. These materials are two-part epoxy pastes, filled with a conductive powder such as silver. Tecnit 72-08116 and Eccobond 57 are both used on the ATS.

Pressure sensitive tapes are used in several places on the ATS Satellite. The rigorous outgassing requirement eliminates most of the silicone adhesives which are commonly used for high temperature tapes. Kapton tape, backed with an acrylic adhesive is used to hold thermal blanket assemblies together. The Kapton tape has nearly the same optical properties as the Kapton outer covering of the thermal blanket. Acrylic adhesives are also used with teflon tapes. Silicone backed tapes are usually cured in place or overcoated to prevent their outgassing.

Ironically, the acrylic adhesives which are acceptable on pressure sensitive tapes are not acceptable when tested by themselves. The inert tape provides enough fron-volatile bulk to permit the qualification of the tape.

The above discussion covers the six principal ATS adhesives. The general classes may be summarized as follows:

- 1. Structural (honeycomb) adhesive EA-9601
- 2. General purpose (rigid) paste EA 934 and liquid EA-956
- 3. High temperature resistant BR-34
- 4. Flexible liquid-paste Crest 7343/7139
- 5. Conductive Eccobond 57 and Technit
- 6. Acrylic pressure sensitive adhesives (Restricted to tape only).



ATS STRUCTURAL ADHESIVE

- STRUCTURAL ADHESIVE: HYSOL EA-9601

Form: Unsupported, Beige Tacky Tape or Film, 0.030 lbs./sq. ft., nominally 0.003" thick

Applications: Honeycomb to core bonding

Packaging: 36 inch (max.) wide rolls, 200 ft. long. Both sides protected by polyethylene separator sheets

SHELF LIFE: Two months at 0°F (Maximum)

Applying: Warm to room temperature, cut to shape with knife or scissors, strip separator sheet from one side and lay the bare tape on one of the clean surfaces to be bonded. Remove the other separator sheet and close the assembly. Hold in close contact until cured.

Curing: One hour at 250°F or one and one-half hours at 225°F.

Minimum Pressure: 10 PSI

Properties Te	emp °F	-65°	75°	180°	_250°
Lap Shear St	. PSI	5,000	5,000	4,300	2,200
* Peel Strength; i	in lbs/in width	30	25	25	15

^{*} Full weight 0.060 lbs/sq. ft. adhesive

FOREWORD

The Applications Technology Satellite (ATS) was developed by Fairchild Industries at Germantown, Maryland, under contract to NASA's Goddard Space Flight Center, Greenbelt, Maryland.

The writer gratefully acknowledges the support of the Martin-Marietta Corporation in the completion and publication of this paper.

SUMMARY



Adhesives in the ATS Satellite allow the designers to save weight, simplify design and fabrication and provide thermal and electrical conductivity or resistivity as required. The selections of adhesives are restricted to those few which can pass the rigorous NASA outgassing tests in order to avoid contaminating lenses and thermal control surfaces in space.

An epoxy adhesive is used to construct the honeycomb panels which constitute most of the satellite's structure. General purpose epoxy adhesives hold doublers and standoffs in place and bond the truss to its fittings.

Specialized adhesives include a high temperature resistant polyamide, a flexible polyurethane and filled epoxies which conduct heat or electricity.

STRESS WAVE RIVETING

by

Basil P. Leftheris

N74 30938

Research Department Grumman Aerospace Corporation Bethpage, New York 11714

Introduction

Whenever a metal joint undergoes cyclic loads of constant or variable amplitude, the problem of fatigue becomes prominent in aircraft design considerations. Optimization of aircraft designs for long fatigue life is the goal of every design engineer in the aircraft industry. Despite the recognition of this goal, fatigue failures are still the most unpredictable and feared failures in aircraft structures. We can all appreciate, therefore, the continuous efforts of government and industry to understand fatigue and to improve the fatigue life of metal joints.

There are many possible combinations of material defects and applied loads that can cause fatigue failures. It is not the purpose of this paper to analyze details of such failures. To understand the motivation for our work, however, we state three conditions that must coexist in fatigue failures: 1

Madayago, Angel F., Metal Fatigue Theory and Design, John Wiley & Sons, New York, 1969.

- 1) Cyclic stress,
- 2) Tensile stress, and
- 3) Plastic strain.

In our efforts to improve fatigue life, therefore, we must prevent tensile stress or plastic strain or both of these conditions.

The Grumman Stress Wave Riveter (SWR) is a semiportable tool that can improve fatigue life in aluminum, steel, and titanium joints in aircraft structures, because it can eliminate one or two of the above conditions.

In addition, instead of the precisely machined holes and fasteners that are usually required with existing fastener systems, the SWR can be used with inexpensive rivets (8¢ per rivet) in holes with clearances varying from 0.002" to 0.020" in aluminum, and from 0.002 to 0.012 in titanium structures.

Description of the Stress Wave Riveter

Unlike the conventional concept of metal deformation under static forces that exceed the elastic limit, deformation may also take place under large rates of energy change that occur in high amplitude stress waves. The difference between the two types of deformation is the time duration of the applied force. In the static load, the duration is long as the force builds up from zero. In the stress wave, it can be very short (400-800 millionths of a second).

310<

In static loads the supporting structures must withstand the large forces applied to the rivet. When a stress wave is used, its wavelength, or time duration, is so short that the supporting structures do not have enough time to react. The result is a smaller device that can upset a rivet in a very short time. The other advantages of the stress wave type deformation of the rivet will be discussed later.

Once we establish the feasibility of deforming rivets with a powerful stress wave, we need a convenient method to generate the wave. We use electromagnetic repulsion. Figure 1 shows the main aspects of the tool. Although electromagnetic repulsion has been used for metal forming in many applications, it has not been used to deform metal directly by generating a stress wave. The amplitude of the stress wave generation by electromagnetic repulsion is not high enough to deform the rivet without an amplifier that changes both the wave's amplitude and its shape.

The stress wave propagates through the rivet at the speed of sound in steels (i.e., 2×10^5 in./sec). If its energy density (ft ~ lb/in.³) is high enough, it will bring the rivet material to its plastic state. When the rivet becomes plastic, however, the speed of sound drops drastically because the modulus of elasticity is small. (Speed of sound $C = \sqrt{E/\rho}$, where E = modulus of elasticity, $\rho = \text{density.}$) The elastic stress wave then becomes

a plastic stress wave trapped between two elastic-plastic interfaces, deforming the rivet in about 800×10^{-6} seconds.

Interference Fasteners

Holes drilled in structures that undergo cyclic loadings weaken the structure and reduce its fatigue life. This effect is shown in Fig. 2 where the similar fatigue specimens with and without holes were tested. The best fatigue life is for a specimen without holes $(K_T=1 \text{ where } K_T=\text{stress concentration factor})$. A good joint, therefore, will approach the curve $K_T=1$. Of course, no joint can achieve this monolithic state. Figure 3 shows the fatigue life of various joints. It is apparent that most of the methods give a joint with life considerably below the $K_T=1 \text{ curve}$. This is especially true in the low stress region.

Two methods have been used successfully during the last several years to improve fatigue life: a) interference fasteners; and b) plastic deformation of the surface of the hole. With interference fasteners, the hole is prepared several thousands smaller than the fastener. The fastener, either tapered or straight, is then driven through the hole and a nut is normally attached on the other side and tightened. With this method an interface pressure

²Speakman, E. R., <u>Fatigue Life Improvement Through Stress Coining</u>
<u>Methods</u>, 12th Annual Meeting ASTM, June 1969.

between the fastener and the hole wall leaves a radial compressive and a hoop tensile stress around the hole that reduce the stress concentration factor and improve fatigue life (see Fig. 4 — this is called propping). Since everything depends on the difference in size between the hole and the fastener, this method requires both precision-made fasteners and holes. The finish of the hole surface must be good enough to avoid surface cracks and to provide uniform interference. The result is shown in the increase in cost per hole.

In the second method, the hole surface is plastically deformed so that a relatively large compression residual hoop stress will remain after the operation (see Fig. 5). It can be achieved by passing an oversized hard ball or an oversized hard pin through the hole.

Deforming the hole surface is especially attractive because it could partially remove two of the three conditions that cause fatigue failure: a) tensile stress; and b) plastic strain.

In general, it is axiomatic that cracks will not propagate in a compressive stress field. In addition to the compressive residual stresses, this method also conditions the surface and eliminates surface defects that can cause cracks. Since most fatigue failures are caused by crack propagation, plastic deformation of the hole is a very effective way to increase fatigue life. We conclude, therefore, that while interference fasteners in general can improve fatigue life, they are expensive and in many aircraft applications inadequate. Deforming the surface of the hole plastically on the other hand gives greater improvement in fatigue life, with less expensive slug type rivets. A good example of the residual stresses is given in Fig. 6.

<u>Interference Rivet Joints</u>

The same reasons that were discussed above for interference fasteners apply to rivets. To establish interference, however, the rivet must be "oversqueezed" or deformed with high force to set up the interference. The force to oversqueeze a $\frac{1}{\mu}$ -inch rivet is approximately 30,000 pounds. Such high force can only be applied by large hydraulic squeezers. Ordinary pneumatic portable riveting tools cannot set up interference rivets without cracking the tails.

The large forces, however, start forming the tail at the same time they squeeze the rivet shank. The result is large interferences (expansion of the hole) near the tail (0.006" - 0.008") while the shank near the head is hardly expanded (0.000 to 0.001"). This nonuniformity of interference causes distortion in the skins. The nonuniformity in interference is even greater in aluminum skins. Furthermore, oversqueezed rivets can only be used in new aircraft because existing aircraft cannot be put under a squeezer to replace

³H. Armen, Grumman Research Department, Private Communication.

a bad rivet, or to do any repairs that require the replacement of a large number of rivets. Oversqueezed rivets can be used effectively to improve fatigue life in aircraft using titanium skins.

It is not acceptable, however, to use oversqueezed rivets in aluminum skins, because of the large uneven deformation near the tail of the rivet.

Stress Wave Riveting

The Stress Wave Riveter deforms the rivet material by a high amplitude stress wave. Thus, the entire rivet is set in motion radially. The rivet expands rapidly and impacts the hole surface before the rivet tail begins to form. Unlike the oversqueezed rivets, therefore, it sets up uniform interference without distortion in the skins (see Fig. 7).

Furthermore, the radial velocity is so high (over 200 in./sec) that upon impact with the hole surface it deforms the surface plastically. This is especially effective in aluminum skins using A-286 type rivets.

Thus the SWR combines the advantages of plastically deforming the hole and the economic advantage of a relatively nonprecision hole and inexpensive rivets like those used in oversqueezing. The additional advantage SWR offers is that it is a portable tool.

The fatigue life of joints riveted with the SWR is shown in Fig. 2. These results were established with 7076-T6 specimens, A-286 rivets and 0.006-inch interference.

An additional advantage is the large initial clearances between the rivet and the hole. In one typical example, $\frac{1}{4}$ -inch rivets were upset in 7076-T6 skins. The holes were larger than the rivet by 0.020-inch. The interference achieved was 0.002-inch.

The advantages of the SWR can be summarized as follows:

- 1) Portability. The tool weights 55 pounds (smaller tools are also available). It can be used with counterbalances. It can also rivet in any direction without precise line-up or initial pressure.
- 2) Uniform Interference. It provides uniform interference for better fatigue life.
- 3) Compressive Residual Stress Near the Hole Surface as in Shot Peening. The hole eliminates any surface defects in aluminum skins and provides compressive residual stresses that can arrest the propagation of small cracks.
- 4) Inexpensive. Standard rivets are utilized in holes drilled to relatively open tolerances.

CAPTIONS

Fig.	1	Stress Wave Riveter Schematic
Fig.	2	Constant Amplitude Fatigue of 7075-76 Specimens
Fig.	3	Constant Amplitude Fatigue of Various Types Joints
Fig.	4	Cyclic Stress in Riveted Joints with Propping
Fig.	5	Cyclic Stress in Riveted Joints with Plastic
		Deformations
Fig.	6	Radial and Circumferential Residual Stresses in
		Sheet with Rigid Oversize Fasteners $(z = \pm b)$
Fig.	7	Comparison of Riveted Specimens. a) Oversqueezed;

Stress Wave Riveted

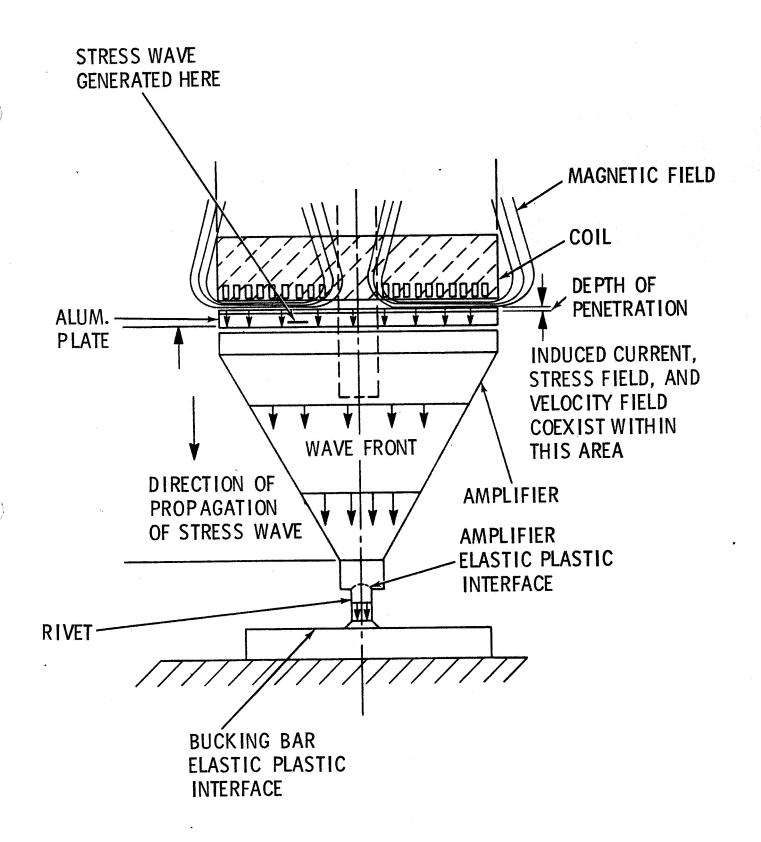
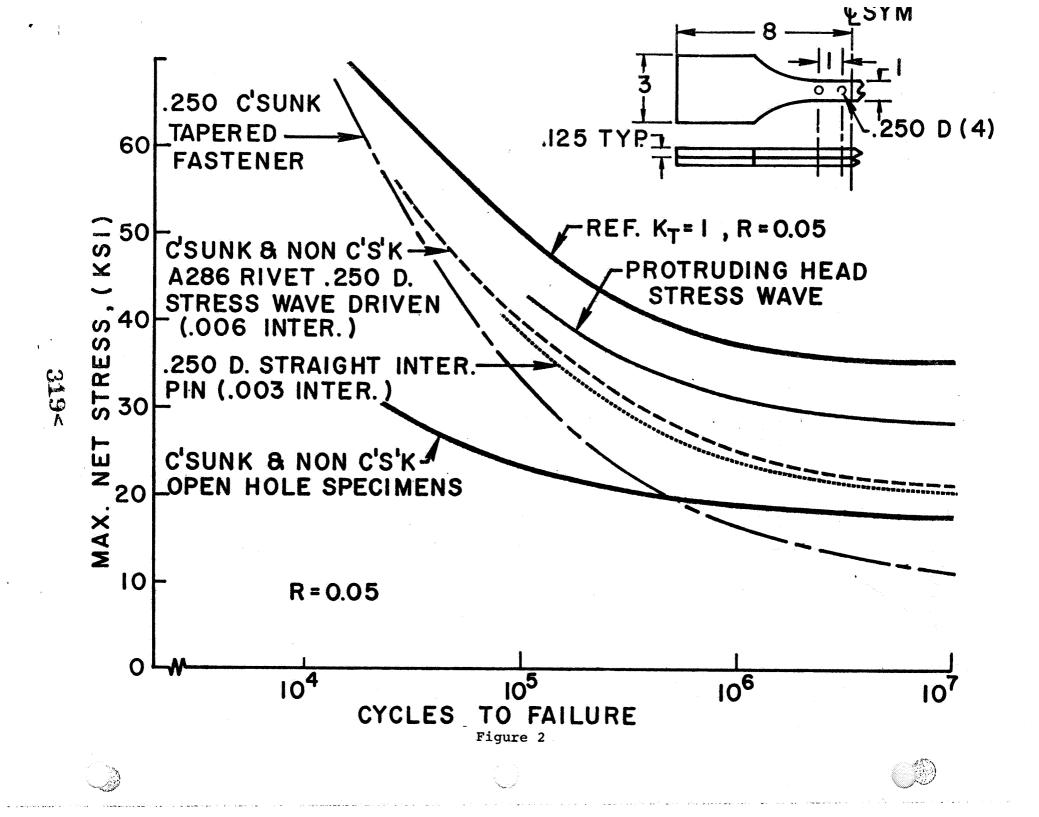


Figure 1. - Schematic diagram of basic shock wave riveter.



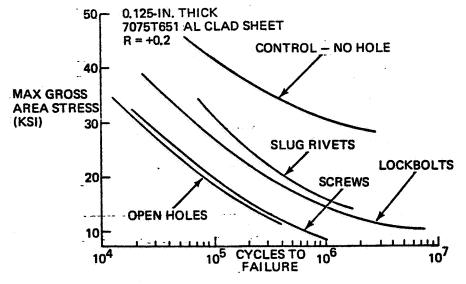


Figure 3

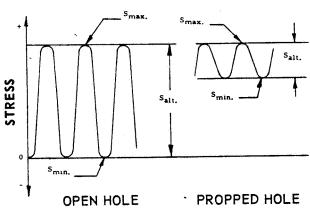


Figure 4

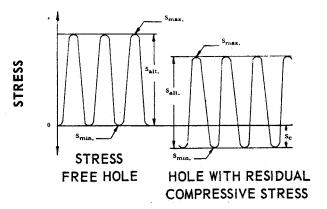


Figure 5



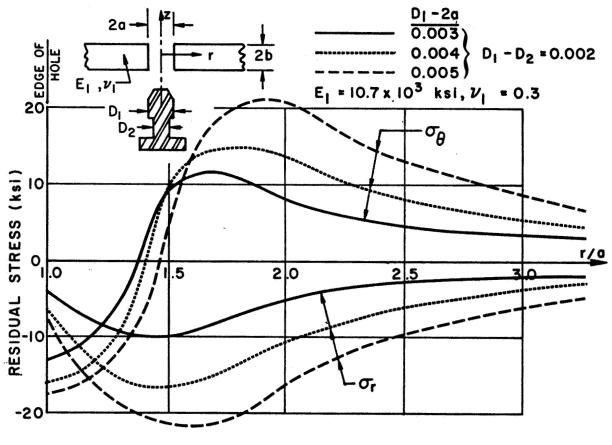
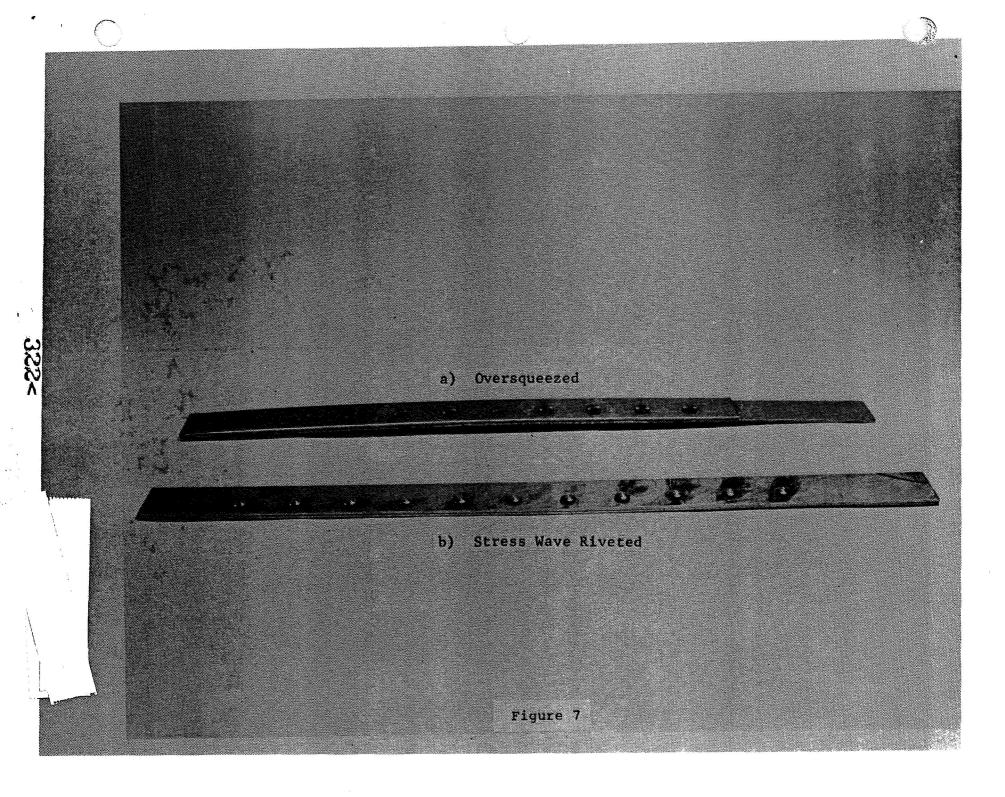


Figure 6



N74 30939

THE BI-COMPOSITE TRANSITION JOINT SD 72-SH-0051

K. C. DULLEA, JR.
MAY 26, 1972



323<



THE BI-COMPOSITE TRANSITION JOINT By K. C. Dullea, Jr.

The application of advanced composite materials to high performance structure frequently results in the desire to fabricate a structure from more than one composite system in order to tailor the composite material capabilities to the design requirements. The bi-composite transition provides a means of joining two different composite structural systems without the weight and complexity of mechanical attachments. The monolayer plies or combinations of plies of one composite system are interleaved with and bonded to the plies of the adjacent composite system, thereby providing a direct load transfer between the two composite structures. The bi-composite transition joint is suitable to general applications of composite materials and is not constrained to specific unique applications.



BI-COMPOSITE JOINT DEFINITION

The term "advanced composite" is used to represent material combinations such as boron/aluminum, boron/epoxy or graphite/epoxy which are composed of high strength and high stiffness fibrous material integrated into a matrix to produce high performance structure. A significant feature of advanced composite laminates is that they can be tailored to the required design loads by lamina quantitive and cross plying build up.

The several available advanced composite material systems provide the composite designer with many different choices concerning design allowables and mechanical properties. There is a considerable variance in design allowables such as tension, compression and shear strength as a function of fiber volume percent as well as between material systems. Table 1 shows the variance between material systems for boron based composites of 50 percent fiber volumes and for graphite based composites with 55 percent fiber volume. This data shows a compression strength allowable for boron/epoxy of 250 ks1, for graphite/epoxy of 140 ksi and for boron/aluminum of 157 ksi. Further investigation of the data reveals difference in tensile strength, tensile modulus, compression modulus and temperature effects for the noted composite material systems.

There are also choices from the mechanical properties such as density, thermal expansion coefficient, thermal conductivity, minimum form radius, machineability, ply thickness and cost as shown in Table 2. This mechanical properties data is based on the same fiber volume percent as the design allowable data. It can be seen that graphite based composites are less dense than boron based composites. The boron composites design allowables are generally higher than those for graphite composites, however because of the density difference the specific strengths are very close. The tensile strength factor for graphite epoxy is 3.04 and for boron/epoxy is 2.44. The minimum form radius for boron composite is 0.50 inches while for the graphite composite it is only 0.06 inches. Many other differences can be observed among the referenced mechanical properties.

Table 1. Recommended Composite Design Allowables

Composite System Fiber Volume \$ Density lb/in.3		B/Al 50 0.096		B/E 50 0.072		B/PI 50 0.074		G/E, HS 55 0.056		G/E, HM 55 0.058		G/PI, HS 55 0.058		G/PI, HM 55 0.050	
Temperature, F		RT	350	RT	350	RT	600	RT	350	RT	350	RT	600	RT	600
Tensile Strength, ksi	00	157	157	178	138	170	130	170	165	105	95	150	140	80	80
	90°	11.5	11.5	8.6	5.4	8.6	5.4	5.0	3.5	4.8	3.0	5.2	0.85	2.2	0.85
Modulus, msi	00	32	29	30	29	30	29	21.0	19.6	29.0	29.0	19.0	19.0	27	27
	900	19.6	14.4	2.7	1.1	2.7	1.1	1.1	1.0	1.1	0.8	1.3	0.8	1.1	0.8
Compression Strength, ksi	00	157	157	250	134	225	125	140	70 :	100	80	125	54	90	48
•	90°	11.5	11.5	36	15	36	15	35	25	35	25	14	11.5	14	11.5
Modulus, mei	o°	32	29	28	28	28	28	21.0	19.6	27	25	17	17	55	55
	90°	19.6	14.4	2.8	1.5	2.8	1.5	1.5	1.0	1.5	1.0	1.1	0.85	1.1	0.85
In-Plane Shear Strength, ksi	00	10.	10.	8.5	3.0	5.0	2.5	7.0	2.0	5.0	2.5	3.0	1.5	3.0	1.5
Modulus, msi	00	6.4	6.4	1.0	0.6	1.0	0.6	0.81	0.64	0.81	0.64	0.81	0.64	0.81	0.64
Major Poisson's Ratio 11 in./in.		0.22	0.24	0.20	0.24	0.20	0.24	0.25	0.3	0.24	0.3	0.37	0.51	0.37	0.51

Space Division

North American Rockwell

Table 2. Advanced Composite Mechanical Properties

×.		B/Al	B/E	В/РІ	G	/E	G/PI		
			5,5	<i>D</i> /11	нѕ	нм	HS	HM	
Density	lb/cu in.	0.096	0.072	0.074	0.056	0.058	0.058	0.060	
Specific Tensile Strength, R.T.	10 ⁶ inch	1.64	2.44	2.30	3.04	1.82	2.58	1.33	
Specific Modulus,	10 ⁸ inch	3.33	4.16	4.04	3.76	5.00	3.27	4.50	
Maximum Operating Temperature	F	650	350	600	350	350	600	600	
Thermal Expansion Coefficient	in./in./F	3.0	2.5	2.5	0	,o	o	0	
Thermal Conductivity	Btu/in. hr/sq ft/F	565	. 14	14	100	100	100	100	
Machinability		Poor ·	Medium	Fair	Very Good	Very Good	Very Good	Very Goo	
Bend Radius	in.	Large	.50	.50	.06	.06	.06	.06	
Minimum Ply Thickness	in.	.0053	.0053	.0053	.003	.003	.003	. 0ó3	
Cost	\$/1b	260* 454*	300* 524*	667 * 775 *	247	270	278	301	



Space Division
North American Rockwell





Because of the large selection of design allowables and mechanical properties available, in some design applications, it may become desireable to change from one advanced composite material system to a different one, i.e., boron/epoxy to graphite/epoxy. This approach is a continuation of the design flexibility already being used in aerospace structure advanced composite material system design applications. The bi-composite joint provides a means of joining two different advanced composite structural systems to tailor the unique design allowable and mechanical properties of each system to the design requirements of interest.

The bi-composite joint therefore is an interface between two dissimilar materials. Advanced composite structures are normally fabricated by means of tape layup where the plies of material are stacked in a predetermined pattern to provide the desired structural properties. In using bi-composite joint concept, a portion of the structure is fabricated from one composite material to take advantage of its properties while the remainder of the structure is fabricated of a different composite material to take advantage of other material properties. The bi-composite joint is the joining of these two composite systems as shown in Figure 1. Plies of one composite system are interleaved with plies of the second composite system and the voids are filled with epoxy resin. The bi-composite joint provides a smooth transition and transfer of loads across the joint.

The structural requirement in designing the bi-composite joint is to bond each layer of the first composite system to the corresponding layers in the adjacent composite system. This is required because of the cross plying used with composites. For example, with the layer orientation used in the illustration $[0/0-/\pm45/\pm45/90/0]$, the boron/epoxy outermost layers are arranged with the fibers oriented in the longitudinal direction. Therefore, the graphite/epoxy material must also be arranged with the outermost layers in the longitudinal direction. This approach provides an ordered load transfer across the joint, i.e., tension to tension, shear to shear, etc.

328<

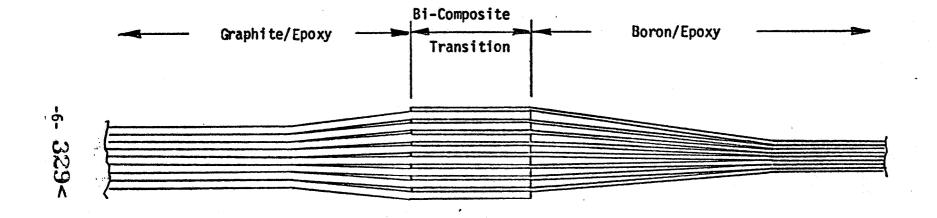


Figure 1. The Bi-Composite Transition Joint







REQUIREMENTS FOR BI-COMPOSITE JOINTS

One requirement for bi-composite joints involves the forming of a boron/epoxy stringer. The boron/epoxy composite system requires a 0.50 inch form radius which is difficult to layup and impractical to interface with the end fittings. One solution to the problem is to use a bi-composite transition joint and fabricate the end of the stringer from graphite/epoxy which has a 0.06 inch form radius as shown in Figure 2. This approach permits forming the end of the stringer into a closeout fitting that accepts mechanical attachments.

Another bi-composite joint requirement involves the efficiency of composite structures loaded in compression. Boron/epoxy has a twenty percent greater specific compressive strength than graphite/epoxy. However, as in the previous example, the boron/epoxy 0.50 inch form radius causes difficulty in fabricating hat section stiffeners for a skin stringer panel. The bi-composite joint can be applied by using graphite/epoxy layers arranged in [+45] orientation draped over the entire hat surface with boron/epoxy layers used on the caps only in the [0] orientation as shown in Figure 3. The resulting stringer has the advantage of the higher specific compressive strength of boron/epoxy and the smaller form radii available by using graphite/epoxy.

Thermal isolation requirements provide a use for the bi-composite joint. In the case of reentry vehicle with external thermal protection and advanced composite primary structure, the structure could be fabricated from graphite/epoxy or boron/aluminum to take advantage of lower material and fabrication costs with the thermal stand-offs fabricated from boron/polyimide to provide thermal isolation and higher temperature capability as shown in Figure 4. This requirement for the bi-composite joint permits the design of an all composite structure where the only mechanical joints are the attaching of the thermal protection panels.





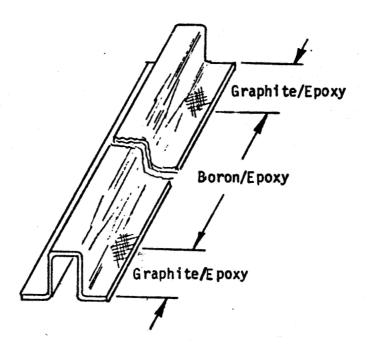


Figure 2. Bi-Composite Structural Reinforcement

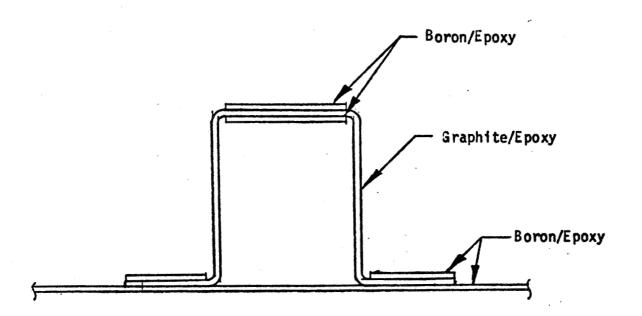
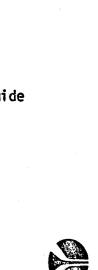
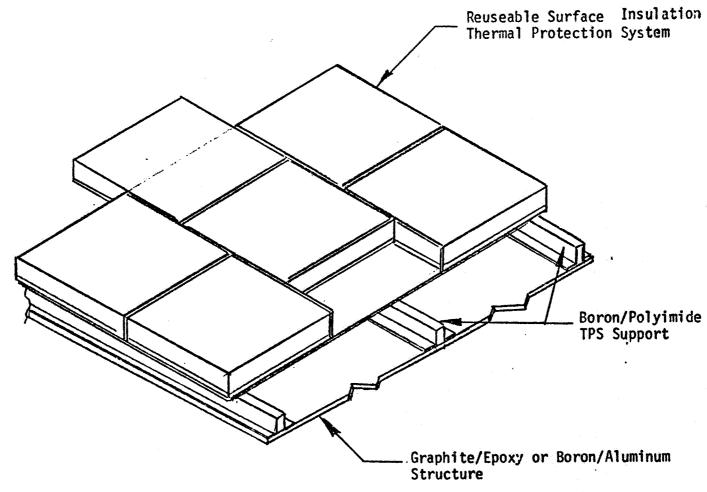


Figure 3. Bi-Composite Thermal Isolation



Space Division
North American Pross







Thermal distortion requirements also provide for application of the bi-composite joint. In designing advanced composite structures such as antenna disks, solar panel structures and thrust structures which are subjected to large thermal gradients, but where thermal deflection must be minimized, graphite based advanced composite systems should be used to take advantage of the very low, approximately zero, coefficient of thermal expansion. However graphite composites have a fairly high thermal conduction for non-metallics, therefore the supports for these items should be fabricated from boron composite materials to provide thermal isolation from the vehicle structure as shown in Figure 5.

One difficulty in applying boron fiber composite materials to aerospace structures is the drilling of holes for mechanical attachments. Successful use of mechanical attachments in composites has been demonstrated by interleaving metal shims for local reinforcement. However, drilling holes through a boron/epoxy laminate interleaved with metal shims is a very difficult operation. Again the bi-composite joint provides a means for designing around this difficulty by making a transition from boron/epoxy to graphite epoxy interleaved with titanium shims thereby providing a graphite/epoxy and titanium structure for drilling as shown in Figure 6. This joint permits a boron/epoxy composite structure with the resulting high compressive strength without the penalty in drilling and machining the boron material.

Combined stiffness and thermal warp requirements present another use for the bi-composite joint. On large manipulator arms such as those proposed for orbital payload handling, stiffness is a driving function. However, form radius and thermal warp make graphite composite necessary for the $[\pm 45]$ layer. The longitudinal layers of the structure could be made from a boron composite and significantly increase manipulator arm stiffness with a resulting small increase in thermal warp.

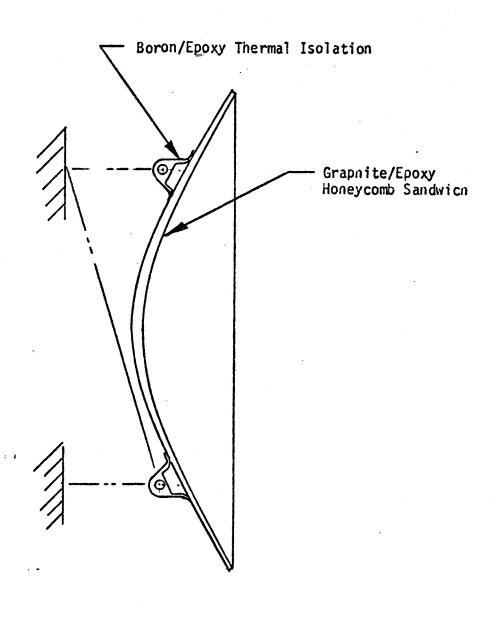


Figure 5. Bi-Composite Thermal Expansion 334<

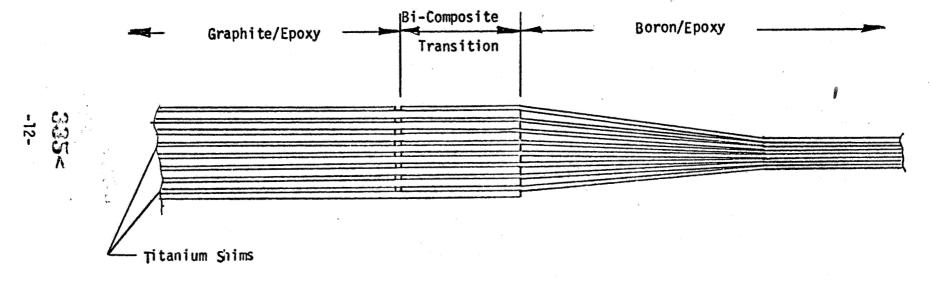


Figure 6. Bolted Joint Bi-Composite Requirements





TYPICAL BI-COMPOSITE JOINT APPLICATION

Several Saturn S-II stage unpressurized structures were considered for application of advanced composite materials in a recent NASA Contract NAS8-27278 with Marshall Space Flight Center. These structures, shown in Figure 7 include the forward skirt, aft skirt, thrust cone structure, interstage structure and the engine support longeron with the aft skirt being selected for advanced composite materials design application study. The composite applications included boron/epoxy and graphite/epoxy skin stringer structures as well as boron/epoxy and graphite/epoxy honeycomb sandwich as shown in Figure 8.

The aft skirt is a 33 foot diameter cylinder at the mold line, located by the inner surface of the skin, approximately 7 feet in length and stiffened by three ring frames. There are 216 extruded hat-section stiffeners, two inches high and two inches across the crown, equally spaced around the shell perimeter, resulting in a stringer center to center spacing of 5.76 inches.

The aft skirt is a load carrying shell structure, which transmits loads from the interstage during Saturn I/C boost and from the thrust cone during Saturn II boost to the aft flange of the LOX tank bolting ring. Two of the ring frames are dual purpose members providing shell stability for the aft skirt during Saturn I/C boost and thrust cone structural integrity during Saturn II boost. The maximum external body limit loads and associated distributed loads critical for aft skirt design are 5265 pounds per inch compression and 1250 pounds per inch tension. The aft skirt differential pressure is 3 psi and occurs at max $q\infty$. The temperature extremes are 200 F on the interstage end and -280 F at the LO2 tank interface.

336<

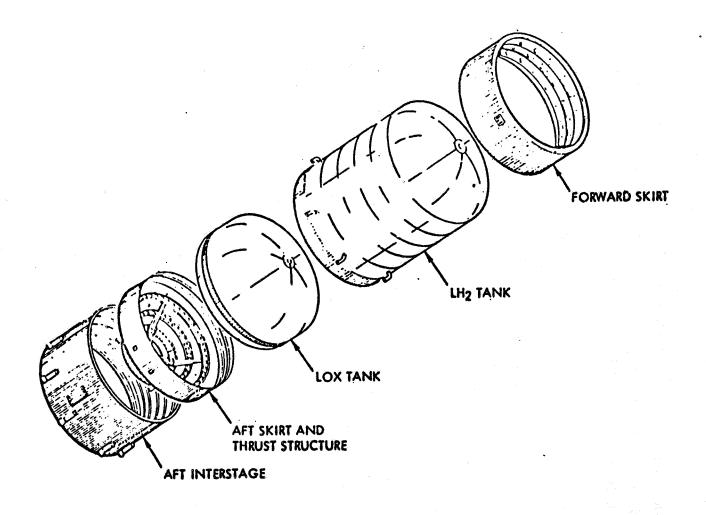
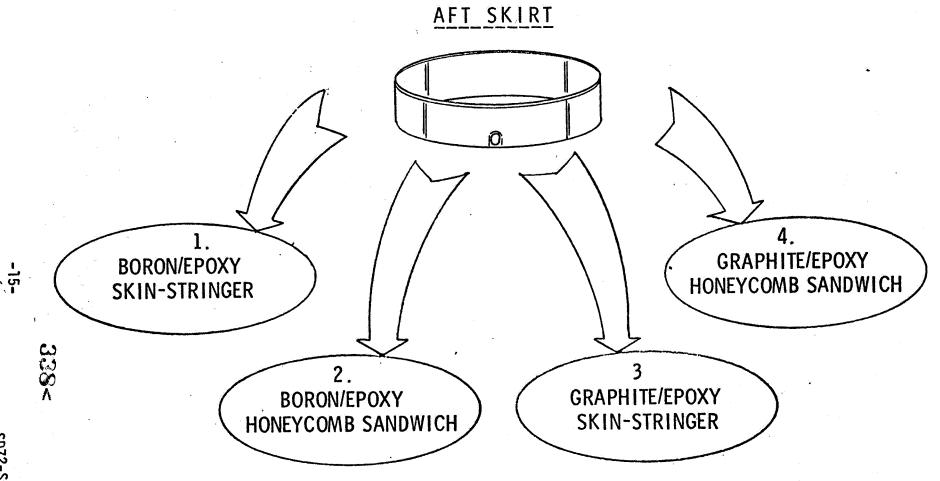


Figure 7. S-II Subassemblies











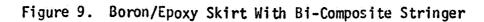


One of the composite application point designs, boron/epoxy skin-stringer, used the bi-composite joint concept. Composites of boron/epoxy are viable structural candidates, especially where stiffness to weight properties are desireable. Boron/epoxy has the advantage of a higher thermal coefficient of expansion than graphite/epoxy and is therefore more compatible for bonding to metal structures and also provides better thermal isolation properties than graphite/epoxy. Boron composites however, are more difficult to machine and the prepreg requires a 1/2 inch form radius and is difficult to drape. The boron/epoxy stringer reinforced skin concept given in Figure 9 is based on a laminate consisting of nine plies .007 thick with a laminate configuration of $[0/\pm 45/0/90/0/\pm 45/0]$. Titanium reinforcement is interleaved with the composite layers at the edges to provide for attachments.

The minimum weight boron/epoxy stringer has a dimension across the foot of 4.00 inches, a width across the crown of 2.09 inches and a height from crown to foot of 2.09 inches. The stringer spacing is 6.50 inches which results in 48 stringers per quarter panel. The boron/epoxy stringer has eight plies of composite with a laminate configuration of $[\pm 45_2]s$. The form radius is of course 1/2 inch.

A bi-composite joint was used in this study to counteract the 1/2 inch form radius at the stringer termination. Each end of the aft skirt boron/epoxy stringer interfaces with a three bolt attachment to adjacent stage hardware. One of the bolts is located on the stringer center line and one each on either side of the stringer through a bonded fitting as shown in Figure 10. A bi-composite transition was used to change from boron/epoxy to graphite/epoxy and the resulting 1/16 form radius. With the added layup flexibility a closeout type fitting could be designed into the end of the stringer. The smaller form radius also provided a more efficient bond for the adjacent molded chopped fiber fitting.

339<







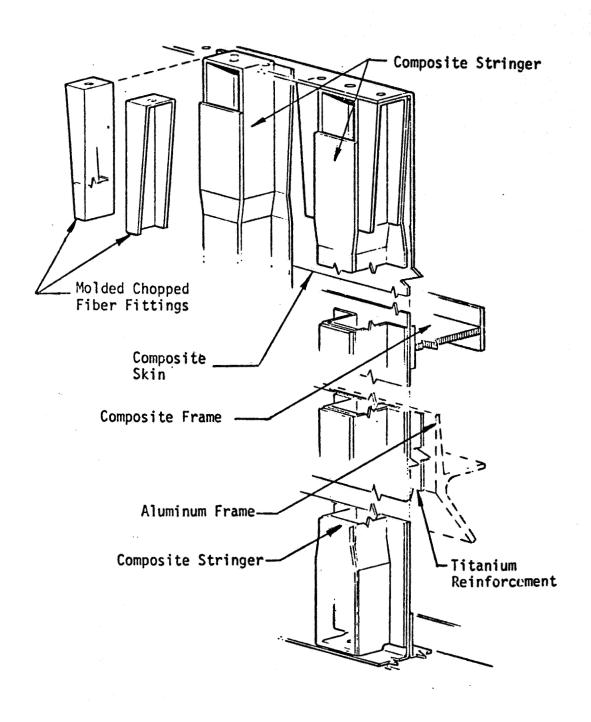


Figure 10. Boron/Epoxy Stringer



CONCLUSION

The bi-composite joint is applicable to a wide variety of design applications as illustrated in the preceding discussion. It is an effective solution to many design problem areas such as thermal expansion and/or isolation and to satisfy requirements for varying structural load/strength requirements within a given structural component. It also provides an effective way to alleviate manufacturing producibility constraints such as forming radius and machining operations associated with the boron fiber materials.

The inherent flexibility in fabrication operations associated with the laminar ply lay-up technique of composite materials permits the inclusion of a bi-composite material transition section with very little impact on the fabrication operation. This fact in conjunction with the potential benefits to be gained make the bi-composite joint a very attractive concept for satisfying specific design requirements in composite material structures.

APPROVAL FOR SCIENTIFIC AND TECHNICAL PRESENTATIONS AND PUBLICATIONS

TO : Jules M. Miller, M/S 105, 3251	DATE May 25, 1972
FROM : Aero-space Technologist,	AGENCY CODE 113-32-01-21
SUBJECT: Material enclosed consist of Abstract Rough draft, L-	∑ Final paper for ☐ Article
Small Scale Explosive Seam Welding	
Authors (if not all Langley authors, indicate affiliation and describe	nature of collaboration in par. 9):
L. J. Bement	827-
1. Paper will be presented by: L. J. Bement Respective authors' tel.	
2. Meeting Name: Symposium on Welding, Bonding, an	d Fastening
3. Date and place of meeting: May 30-31, June 1, 1972 - Willi	amsburg, VA
4. Sponsor: NASA, George Washington University, & The	
5. Status of material: 💢 Data are in hand 🔲 Data will be available by Classification of material: 🛣 Unclassified 🔲 Confidential 🔘 Sec	cret 🛛
Previous approvals: None X Rough draft	Langley X Sponsor
Abstract D	Headquarters 🛛
6. Previous or future publication(s) of essentially same material (if no NASA re Author(s) Title	Status
1 1 Demant Could Could Supressive Head	(If presented, state where, when
L. J. Bement Small Scale Explosive Weld of Aluminum	ling The Franklin Institute Philadelphia, PA Sept. 1971
7. Send present material to: Mr. Bland Stein	
8. Deadline date of action: June 30, 1972	
9. Additional comments (include statement regarding in-house review of paper	for external publication:
·	
10. Z References were checked by Technical Editing Section.	
11. Name of technical reviewer or chairman of editing committee:	Tel. n .
12. Mr. Samos 3281, of Technology Utilization No new technology involved.	Office advised of new technology involved
13. The undersigned, all divisions involved, concur in the above statements (sign	names):
Section Head Branch He Section Head Branch He	ead Division C.A.
 If "call for papers" or journal publication information is not in General Files 	s, attach to indicate what is required.
Copies of all correspondence received direct by authors regarding this n	natter were sent to Mr. Miller.
Submit original and one copy of this form with or	ach action.

N74 80940

SMALL-SCALE EXPLOSIVE SEAM WELDING

Laurence J. Bement

NASA Langley Research Center Hampton, Virginia

Presented at the Symposium on Welding, Bonding, and Fastening

Williamsburg, Virginia May 30 - June 1, 1972

SMALL-SCALE EXPLOSIVE SEAM WELDING

Laurence J. Bement

NASA Langley Research Center Hampton, Virginia

SUMMARY

This report describes a unique small-scale explosive seam welding technique that offers improvements over conventional explosive welding techniques. This technique has successfully joined a variety of aluminum alloys and alloy combinations in thicknesses to 0.125 inch, as well as titanium in thicknesses to 0.056 inch. The explosively welded joints are less than one-half inch in width and apparently have no long-length limitation. The "ribbon explosive" developed in this study contains very small quantities of explosive encased in a flexible thin lead sheath.

The evaluation and demonstration of this welding technique was accomplished in three phases: evaluation and optimization of ten major explosive welding variables, the development of four weld joints, and an applicational analysis which included photomicrographs, pressure integrity tests, vacuum effects, and fabrication of some potentially useful structures in aluminum and titanium.

This joining technique can complement existing fabrication techniques through its simplicity and the ability of producing low-cost joints with strengths up to that of the parent metal. A major disadvantage of this welding technique presently is the reservation in using explosives. Other disadvantages are the destructive mechanical shock produced by the welding operation, and sharp notches at joint interfaces creating stress concentrations.

INTRODUCTION

Explosive welding, which was first demonstrated in the early 1950's, can accomplish metallurgical bonds that are impossible to achieve by any other joining process, while maintaining material properties. Research in this area is presently being conducted by a variety of organizations: The Denver Research Institute (University of Denver and Martin-Marietta), Battelle Memorial Institute, Dupont, E. F. Industries, Pratt and Whitney, Aerojet General, United States Government institutions----Frankford Arsenal, and NASA (Marshall Space Flight Center and Langley Research Center)----and foreign governments, such as Great Britain, France and Japan.

The actual explosive welding process is accomplished by a collision of two metal plates explosively driven together. The basic mechanism of the metallurgical bonding/jetting process has not been exactly determined. To quote from the generally accepted theory, Reference 1, "A jetting collision is defined as an oblique collision in which the plate velocity, pressure, collision angle and collision point velocity are controlled such that a jet or spray of metal is formed at the apex of the collision and is forced outward from between the colliding plates at very high velocities. A jet is pictured in the oblique

345<

collision shown in Figure 1." The explosive welding process strips off both surfaces due to the collision of the plates, and the high pressures produced by the impact forces the now clean surfaces into intimate contact to achieve metallurgical, intermolecular bonding. The technique that is most closely analogous to this process is vacuum welding; two surfaces cleaned under a hard vacuum and pressed together mechanically can produce intermolecular bonding.



Explosive welding operations have generally been oriented toward area bonding, the cladding of metals. Relatively large quantities of "bulk" explosives, such as TNT (trinitrotulene), nitroguanidine and dynamite are hand-spread over the area to be welded. It is then initiated along one edge, and the detonation front sweeps across the area. A prerequisite for stable explosive welding is that the velocity of the collision point be less than the metal's sonic velocity.

Difficulty has been experienced by investigators in the explosive welding field in producing long, continuous seam welds in small area bonds, such as below one-half inch in width. Reference 2 describes a technique utilizing "primacord", a commercial name given to a cylindrically shaped, fabric-wrapped explosive cord. This joining technique relies on shaping at least one of the materials to be joined into a non-coplanar setup to achieve a joint that has a "width to length ratio of at least 1:10 or greater." Also, a caution is given that the detonation velocity of the primacord should not exceed 120% of the higher sonic velocity of the metal to be joined. As noted in Reference 2, "When the detonation velocity does exceed this amount, oblique shock waves often ensue that prevent formation of a strong metal-to-metal bond between the metal layers."

This report describes a novel small-scale explosive seam welding technique (small explosive quantities and plate thicknesses) developed and demonstrated in lengths to twelve feet at NASA Langley Research Center; the preliminary work is described in Reference 3. The joining mechanisms of this welding concept are shown in Figure 2 in the sketches. The plates to be welded are first separated and placed in parallel. The ribbon explosive which was developed for this technique is then placed on the plate to be welded and initiated. pressure drives the top plate downward, causing it to bend so that the center of the area under the explosive is the first to contact the lower plate. As the plate continues its descent, symmetrical critical oblique collision angles, producing the required jetting actions, are established to the sides. No joining occurs in the center area of initial plate contact. Jetting cannot be established in the direction of detonation, since the explosives' detonation velocity is about 150% of the sonic velocity in most metals. The actual jetting vectors produced are at 60° to 75° from the direction of detonation propagation. The photograph in Figure 2 shows the jetting streaks and bond area (the buffedappearing area) produced in an explosive weld in aluminum.

This explosive welding technique was demonstrated by joining 0.040 to 0.125 inch thick aluminum to similar thicknesses or to 0.25 inch thicknesses in a variety of aluminum alloys and combinations of alloys tempered to maximum hardness and strength. Also, titanium was joined in a thickness of 0.056 inch. Four lap-type joints were constructed with these materials, producing strengths up to that of the parent metal. The joints were examined photomicrographically,



and tested for pressure sealing capability. The effect of vacuum on the welding process was investigated. Some structures were constructed that represent potential fabrication applications.

APPARATUS

The ribbon explosive developed under this study is shown in cross section in Table 1. The explosive, RDX (cyclotrimethylenetrinitramine) is encased in a lead sheath that has been shaped into a thin rectangular cross section. The explosive quantity is commonly designated in grains/running foot of length. The detonation propagation velocity of this explosive is 26,000 feet/second. A localized pressure of several million psi is achieved in less than one microsecond, and has a duration of less than five microseconds. The flexibility of the explosive, due to its lead sheath, allows it to conform to as little as a 0.125 inch radius. This explosive ribbon is manufactured to aerospace standards with less than ten percent variations in explosive quantity down its length. The cost for manufacture of the material for this study was about one dollar per running foot in quantities of several thousand feet, plus shipping costs.

Commercial blasting caps, Dupont Model E-106, containing approximately two grains of high explosive, were used in this study to initiate the ribbon explosive.

Very little tooling is required to accomplish this welding technique: masking tape, aluminum shims to separate the plates, aluminum bars for anvils, and "C" -clamps to hold the anvils in place during the welding operation.

PROCEDURE

The approach for this study was divided into three major phases: optimize the major explosive welding variables, develop explosively welded joints, and conduct analyses and demonstrations for potential fabrication applications.

Explosive Welding Variables -- The following ten major variables were studied to determine and optimize their influence in explosive welding:

- 1. plate materials
- 2. plate thickness
- 3. explosive quantity
- 4. standoff (plate separation)
- 5. plate surface

- 6. plate deformation
- 7. mechanical shock
- 8. metal grain orientation
- 9. weld length
- 10. explosive residue
- l. Plate materials --- A variety of aluminum alloys, exhibiting a wide range of hardness and malleability, were studied: 2024, 2024 ALCLAD (1200 series clad), 2219, 6061, and 7075. Titanium, Ti-6Al-4V, was welded in the fully annealed condition. As received mill stock was used in all tests.
- 2. Plate thickness---Plate thicknesses from 0.040 to 0.125 inch were studied; the most influential performance factor in plate thickness is the required bending of the plate during the welding mechanism.
- 3. Explosive quantity --- The objective in this area was to optimize the explosive quantity to maximize the bond area, but minimize the damage to plates.

Also, a minimum quantity of explosive would decrease the mechanical shock in the plates during the welding operation and the sound and fragment shielding requirements.



- 4. Standoff (plate separation)---Plate separation distance and separation techniques were investigated. Separation distances were varied from zero to 0.125 inch. A variety of separation techniques, shown in Figure 3, were evaluated. Techniques "a" through "d" used a 0.063-inch 2024-T3 ALCLAD plate welded to a 0.25-inch 6061-T6 base plate for comparison. Techniques "e" and "f" used pre-bent plates of titanium, Ti-6Al-4V, of equal thickness with the ribbon explosive placed on both sides of the plate combination.
- 5. Plate surface---The effects of surface oxides, cleanliness, and smoothness were evaluated. Due to the markedly different hardness/malleability properties of oxides and the difficulty in determining oxide thicknesses, all aluminum and titanium alloy samples were chemically cleaned. This cleaning also removed oils and other surface contamination. Observations were made on the effects of surface scratches on weld performance.
- 6. Plate deformation---Techniques were investigated to minimize the undesirable indentations in the plates produced immediately beneath the ribbon explosive during the welding operation. Figure 4 shows the experimental setup using 0.063 to 0.125 inch 2024-T3 ALCLAD plates. The following "buffer" materials were placed between the ribbon explosive and the 0.063-inch plate: three layers (approximately 0.015 inch) of masking tape, 0.015 inch layer of epoxy (Ecco Bond) a 0.040-inch 2024-T3 ALCLAD plate, and a 0.040-inch 2024-T3 ALCLAD plate epoxied with a 0.010-inch thickness to the 0.063-inch plate.
- 7. Mechanical shock---An analysis and tests were made to determine and limit the effects of internal pressure shock waves created in the metal plates by the explosive pressure and the impacting of the plates during the welding operation.
- 8. Metal grain orientation---To determine the effect of the metals' internal grain orientation on the explosive welding operation, or the strength of the welded joint, welds were made across and with the grain.
- 9. Weld length---The shortest possible weld lengths were determined by observation of welds at their starting and ending points. To determine long-length limitations a 12-foot weld was made in 0.063 to 0.25 inch 2024-T3 ALCLAD. Thirty one-inch samples were made down its length to determine the uniformity of the joint.
- 10. Explosive residue---The explosive residue (materials, quantities, and location) was observed during and after the welding operation.

Weld Joint Development --- Several explosively welded joints were developed that are representative of current fabricational materials and requirements. Materials were selected for their strength in the most useful conditions of maximum hardness and temper. An effort was made to maximize the simplicity of the welding operation in terms of material preparation, weld setup, and necessary tooling.

Each joint was fabricated in a 12-inch length, using the optimum set of variables developed for each particular material or combination of materials. The joints were evaluated by cutting them into 1-inch-wide samples which were pull-tested along the plate axes. No effort was made to provide jigs or fix-tures which could place the joint in absolute shear during evaluation. The ultimate strength of each sample was recorded and compared to the tensile strength of the plates in pounds per running inch.

Applicational Analyses---To evaluate potential applications of this joining technique, several investigations were conducted: 1. Photomicrographs of joint interfaces, 2. pressure integrity of joints, 3. the effect of vacuum on the welding operation, 4. explosive contamination and safety, and 5. fabrication of some useful structures.

- 1. Photomicrographs---To evaluate and predict more fully the properties of explosively welded joints, representative joint samples were examined photomicrographically.
- 2. Pressure Integrity Tests---To determine if this weld joint was airtight, 0.040 and 0.063 by 3 by 3 inches 2024-T3 ALCLAD plates were welded to 0.5 by 3 by 3 inches 6061-0 plates, as shown in Figure 5, and pressurized with dry nitrogen.
- 3. Vacuum Effects---The effect of vacuum on the explosive welding operation was evaluated by comparing the performance of two similar joints: one welded in the atmosphere, and the other welded in a vacuum of 1×10^{-5} torr (a simulated altitude of approximately 400,000 feet).
- 4. Explosive Contamination and Safety---An effort was made to observe the effects of explosively created products on contamination to localized areas, and the requirements for shielding for personnel, as well as the safety requirements for personnel in handling and initiating the explosive.

A technique was developed to confine all explosive products, shown in cross section in Figure 6. The explosive is placed in a 347 stainless-steel tube. Properly designed end fittings provide total confinement. To demonstrate the performance of this technique, several tests were conducted by welding 0.040 to 0.25 inch 2024-T3 ALCLAD plates as follows:

- 1. An unconfined length of 15 grains/foot explosive was compared to the same 15 grains/foot in a totally sealed tube, 2. a 20 grains/foot length inside a tube with no end fittings was compared to the same 20 grains in a totally sealed tube, and 3. a length of 25 grains/foot explosive in a tube with no end fittings was used to weld 0.063 to 0.25 inch 2024-T3 ALCLAD plates.
- 5. Structural Fabrication Demonstrations---Several potentially useful structures were fabricated in this study: 1. A half-inch plug was welded into a 1-inch-diameter tube using a setup shown in Figure 7. The assembly was pressure-checked and pull-tested through the plugs along the tube axis.

 2. A 0.056-inch-thick (1 by 1 inch) titanium rib was welded to a flat plate, as shown in Figure 8. The strength of the joint was determined by comparison

to standoff technique "f" in Figure 3. 3. A 1/12-scale model of a space station-type structure was constructed (see Ref. 3), measuring 18 inches high and 18 inches in diameter. The 0.040-inch 2024-T3 ALCLAD skin, bulkheads, and deck were welded to 6061-0 0.25 by 0.5 by 18-inch-diameter rings and 0.125 thick, 0.75 by 0.75 by 18-inch angle. Two 2-inch-diameter plexiglass portholes were installed between the skin and 0.125-inch 6061-0 plates.

RESULTS

The results for this study will be presented in the three major phases previously outlined: Optimize the major explosive welding variables, develop explosively welded joints, and conduct analyses for potential fabrication applications.

Explosive Welding Variables---These variables at first appear to be independent, but during the welding operation actually become dependent. Due to the rapidity and violence of this operation, it is often difficult to determine which variable, or variables, predominated in producing success or failure.

- l. Plate Materials---The hardness and malleability of the materials affect its bending in producing the weld mechanisms; in general, the high-strength alloys require considerably more explosive energy. The harder materials create and efficiently transfer high-pressure shock levels, which are detrimental to the welding operation.
- 2. Plate Thickness---As the plate thickness increases, the explosive quantity must be increased, nonlinearly, to achieve the welding mechanism. Due to the pressure shock waves created during the welding operation, heavier plates produce beneficial attenuations and delay shock-wave reflections from influencing the weld operation.
- 3. Explosive Quantity---The optimum explosive quantities used to maximize joint strength and minimize plate damage are listed in tables described in the weld-joint development section.
- 4. Standoff---Plate separation distance prior to explosive welding does affect joining performance. A finite distance is required to allow the plates to be accelerated to the high velocities required to achieve welding. Again, this response is associated with another variable thickness and mass of the plates. In the joints created in this study using 0.040 to 0.125-inch-thick materials, standoff distances were set from 0.010 to 0.040 inch. Standoff distances to 0.125 inch were evaluated but unless these distances are held to less than half the plate thickness or fully annealed materials are used, fracturing and shearing can be expected.

The results of the standoff comparison test series, which used the setup shown in Figure 3, are tabulated below. The parent metal strength of the 0-063-inch plate in techniques "a" and "d" was 4300 pounds/running inch, and for the 0.056 titanium "e" and "f," 7320 pounds/running inch.

Technique	Average strength, pounds/inch	Std. dev.
a	3410	640
Ъ	3870	1000
c	4300	450
đ	4010	430
e	7320	110
f	5550	1540

The standoff in technique "a" can be accomplished with any convenient material; this study utilized both masking tape and aluminum shims. Standoff "b" allows the plates to be in full contact, simplifying the required setup. The scattered performance in technique "b" was partially caused by difficulty in bending the metal into the narrow groove while producing the welding mechanisms. Some mechanical locking was achieved at the groove's edge in both techniques "b" and "c." However, in "c" and "d" no plate bending was required to initiate the weld mechanism. The critical jetting angle is already present and jetting is immediately established. Both techniques "c" and "d" produced a central unbonded area that was approximately 0.030 inch, the width of the peak of the inverted "V."

Since the parallel plate process, standoff technique "a," was not effective in the welding of titanium, techniques "e" and "f" were developed. In both techniques, the plates were initially separated to allow for the develment of high impact velocities. On impact the critical collision angle is already established, producing the required jetting mechanism. Except for the first and last one-half inch of the joint welded in technique "e" the joint had a higher strength than did the parent metal; all the samples failed in the parent metal of the coupon, one-half inch away from the joint. The joint in technique "f," however, lacked both the high strength and uniformity.

- 5. Plate Surface---The effects of surface oxides on aluminum and titanium alloys were not evaluated due to the difficulty of determining the amount and type of oxides. However, no substantial change in joint performance was noted in specimens chemically cleaned and held at laboratory ambient for 4 weeks. Only aluminum alloys had sensitivities to oxides; commercially pure aluminum (1100, 1200, and the AICLAD series) required no oxide removal. Also, surface contamination such as oils and lubricants inhibited welding operations. Again, the degree of contamination is difficult to evaluate. This aspect is beneficial in preventing welding in selective regions, such as spot-welding. Narrow surface scratches deeper than 0.003 inch prevented joining in that particular area. However, the jetting mechanism was apparently unaffected continuing in the area surrounding the scratch.
- 6. Plate Deformation---The results of the "buffer" tests (Fig. 4) to limit the detrimental explosive pressure-induced indentations are shown below. The 0.063-inch material has a strength of 4300 pounds/inch.

Buffer material	Thickness, inch	Joint strength, pounds/inch	Std. dev., pounds
Masking tape	0.015	3800	320
Epoxy (Ecco Bond)	0.015	3980	300
2024-T3 ALCLAD	0.040	3767	510
2024-T3 ALCLAD Epoxy (Ecco Bond)	0.040	4200	400

The masking tape buffer alone increased the indent radius to 0.030 inch, and the epoxied plate increased it to 0.125 inch. A second benefit in using buffers is the diffusing of the explosive pressure, producing larger area, higher strength bonds. The inefficiency of the single-plate buffer is caused by pressure-reflective losses at the plate interface. A third benefit of buffers is the protection of plate surfaces from explosive contamination. The masking tape leaves only an imprint of the tape's texture after the firing.

7. Mechanical Shock---High-pressure shock waves are generated in the metal plates during the explosive welding process in several ways. Figure 9 shows the shock waves created when one plate is explosively driven against a second plate. The explosive pressure first induces a pressure to accelerate the plate, followed by a second shock produced when the plates impact. The magnitude of these shock waves is significantly increased by the hardness and lack of malleability of the materials. The shock waves created on impact propagate through the top and the base plates, and are reflected from outer surfaces. If these plates are of the same thickness and material and have the same sonic velocity, the reflected shock waves will arrive simultaneously. The rarefaction wave which is 90° out of phase with the compression wave, then places the weld in tension, causing the joint to fail. The resultant shock-wave vectors of each plate are reflected from the ends of the plates, compounding the destructive influence.

A final shock wave problem is the influence on structure or systems in the immediate vicinity of continued explosive welding operations. The shock waves can propagate through structure (attenuated by material, distance, and mechanical interfaces) and destroy already established welds or delicate components attached to the structure.

The "end effect," which can cause destruction of the entire joint, can be minimized by not welding the whole length of the joint — stopping the welding about 1 inch from the end. All reflected shock waves can be reduced by adding "anvils" of the same materials that are being welded. An example of one technique is shown in Figure 10. This added mass reflects less of the shock waves into the plates, as described in Reference 1. Further aids in absorbing and dissipating shock waves are provided by metal shims to accomplish plate standoff and silicone grease which responds like an incompressible fluid under dynamic loading.

Although shock-absorbing anvils are always beneficial, not all materials and setups require them to achieve success. Such was the case of aluminum

alloys in the fully annealed condition, the ALCLAD series, and the joining of thin plates to heavy plates (6061-T6 was demonstrated to have this ability). However, anvils were necessary in joining thin-to-thick setups of 2024-T4, 7075-T6, and 2219-T31 to 6061-T6. Also, anvils were required in welding equal thickness plates of 6061-T6, 2219-T31, and Ti-6A1-4V. So much shock energy was created in the weld attempts with 2024-T4 and 7075-T6 to like materials, anvils could not prevent the destruction of the joint immediately after it was established.

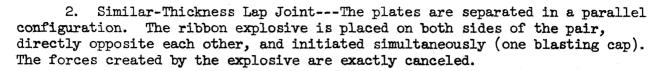
- 8. Metal Grain Orientation---The grain orientation of the metal had an appreciable effect on the materials ability to be bent to establish explosive welding. The metal plates respond in a near-fluid manner to the several million psi explosive loading; this allows the plates to be bent as much as its own thickness when worked across the grain. However, a bend of only half the plate thickness could be tolerated when worked with the grain, due to shearing along grain boundaries. Once welded with minimal bending, no appreciable change in joint strength was noted due to grain orientation.
- 9. Weld Length---The smallest weld length must be controlled by the individual materials efficiency in initiating the welding mechanisms: the finite distance required to achieve stable welding. For aluminum, this length is approximately 0.25 inch, and for titanium, 0.5 inch. A second length-limiting factor is the end effects mentioned in the section under mechanical shock, producing weakened joints in the last 0.5 inch. To achieve the strongest possible properties for any selected bond length, the welding operation would have to be initiated before, and carried beyond, the desired bond area.

In determining the long-length ability of this explosive welding mechanism, a 12-foot weld was made in 0.063 to 0.25-inch aluminum. The average strength of the 30 one-inch samples was 2660 pounds per running inch, with a standard deviation of 320. No indication of changes in the explosive welding mechanism was observed down the entire length.

10. Explosive Residue---The residue that is produced on functioning of the ribbon explosive in a weld setup consists of particles of lead (broken and melted into small particles), dustlike particles of unreacted carbon (the smoke produced), and the masking tape that was used to hold the explosive in place. Due to the explosive dynamics, this residue can be driven between the plates before they impact in the welding operation, causing surface contamination and low-strength joints. To inhibit this movement of residue, the access areas to plate interfaces are taped over. Also, the residue is prevented from contaminating plates by using buffer materials, as described in the section on plate deformation.

Weld Joint Development---The four explosively welded joints that were developed and demonstrated in this study are shown in Figure 11. The operational setups and mechanics follow:

1. Dissimilar-Thickness Lap Joint---The plates are separated in a parallel configuration. The ribbon explosive is placed over the desired weld area and initiated.





- 3. Sandwiched-Butt Joint---The two plates sandwiching the main structural plate are separated in parallel. The ribbon explosive is placed on both sides of the sandwich, directly opposing, and initiated simultaneously (one blasting cap). Each joint pair was accomplished separately.
- 4. Scarf Joint---The plates are separated in parallel. The ribbon explosive is placed on both sides of the pair, but the ribbon explosives' longitudinal axes are displaced relative to each other by one-half the width of the explosive. On simultaneous initiation the explosive pressure produced is not equally opposed over half its area, causing both the horizontal axes of the plates to bend into alinement, and the welding of the plates.

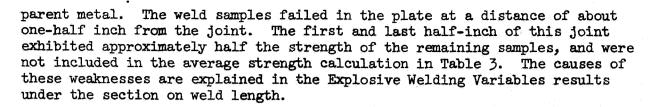
The detailed results of the four explosively welded joints are compiled in Tables 2 through 5, showing the materials welded, the explosive quantity used, the thin-plate material strength, and the average strength and standard deviation of each 10-sample group.

1. Dissimilar-Thickness Lap Joint, Table 2---The excellent malleability properties of 6061-T6 permitted the formation of many different alloy combinations; many of these combinations produced bond areas in the joint that could support the strength of the parent material. The lower strengths of some combinations can be attributed to the welding inefficiency (note the larger standard deviations) caused by both lower strength and malleability of the 0.25-inch materials. The joint strength is controlled by the weaker material. Noteworthy exceptions of the low-strength 0.25-inch materials are 2024-T3 ALCLAD and 6061-0. The high malleability of these materials appreciably increased the effective bond areas of the joint.

All of the possible combinations were not attempted. However, any combination using a 0.25-inch 7075-T6 or 2024-T4 base plate failed to join, again due to the hardness and low malleability.

2. Similar-Thickness Lap Joint, Table 3---The strength of the 2024-T3 ALCLAD joints again are limited by the soft commercially pure cladding material. However, a large percentage of the samples of the 6061-T6 and 2219-T31 joints exhibited strengths superior to the forces required to break the joint. These samples broke in the metal adjacent to the welded area. Since these joints were not placed in shear, but allowed a bending moment that was the thickness of the plate, plus the standoff distance, breakage at the weld edge was predictable.

The titanium joint exhibited markedly different characteristics. Due to the angular standoff setup, technique "e" of Figure 3, and the high degree of local rigidity of this material, the axes of the plates were driven into nearly perfect alinement and only minimal localized bending occurred. This combination of attributes produced a joint that exceeded the properties of the



- 3. Sandwiched-Butt Joint, Table 4---The 6061-T6 joints exhibited nearly parent metal strengths. It was not possible to predict which joint or member would fail. Considerable difficulty was encountered in the titanium joint, primarily due to alinement. Any misalinement caused an uneven distribution of the load within the members and a resultant failure in only one member.
- 4. Scarf Joint, Table 5---This welding technique produces highly efficient, high-strength joints primarily through two attributes: a larger bond area than that created in a straight lap joint, and part of this bond area is placed in tension. Also, the bending at the joint to produce plate alinement, a radius of approximately 0.25 inch, is accomplished without appreciable metal fracturing. This technique is so efficient that the joint of 0.040 inch 2024-T3 ALCLAD exhibited parent metal strength, despite the fact that the actual bond is achieved only in the soft cladding material.

In comparison to the similar-thickness lap joint, the 2024-T3 ALCLAD performance was considerably improved: for the 0.063-inch-thickness, the lap joint had an average strength of 2670 pounds/inch, and for the scarf, 3920 pounds/inch; for the 0.090 thickness, the lap was 3500 pounds/inch, and for the scarf, 5290 pounds/inch.

The 6061-T6 material did not respond as well in the heavier thicknesses to this joining technique. The 0.090-inch joint had a decrease in strength, as compared to the lap joint; the lap joint's strength was 4330 pounds/inch, and the scarf, 3830 pounds/inch. The 0.125-inch-thickness failed both to bend into alinement or bond.

APPLICATION ANALYSES

The results of the investigations in this area will be detailed in five divisions: photomicrographs, pressure integrity tests, vacuum effects, explosive contamination and safety, and structural fabrication demonstrations.

l. Photomicrographs---A representative example of a complete cross section of an explosive joint is shown in Figure 12, which was divided into four sections to permit printing on a single page. The joint is 0.063-inch 7075-T6 bonded to 0.250-inch 6061-T6. The central unbonded area, approximately 0.2 inch in length, is flanked by two symmetrical 0.050-inch bond areas. This ratio of bonded to unbonded areas is not necessarily representative of all weld joints. This ratio is affected by many explosive welding variables such as material, thickness, explosive quantity, and standoff technique. The largest gap in the central area is approximately 0.001 inch. The bond areas exhibit the classical "wavy" interface of all explosive welding.

The unbonded area, which runs the longitudinal length of the weld represents a possible chemical path for corrosion. However, properly selected weld patterns could seal it.



Since no material is added in this joining process, sharp notches are created at the joint interfaces. This could be a potential stress point for fatigue failure. Tiny internal fractures have been observed in heavier plates in the areas of maximum deformation caused by explosive pressure (the joint edges), again producing stress concentrations. However, as described in the section on plate deformation, this damaging effect can be reduced by the proper selection of buffer materials.

A series of photomicrographs of dissimilar-thickness lap joints are shown in Figure 14. The higher magnifications show the "wavy" interfaces. The peak-to-peak dimensions of these waves are in no case larger than 0.002 inch, showing that this bonding technique is only "skin deep." The parent metal grain structure near the bond areas is virtually unaffected.

The 0.063-inch 2024-T3 ALCLAD to 0.250-inch 6061-T6 joint shows that the 1200 series cladding is essentially undamaged, following the contours of the plate, immediately below the explosive and in the bond area. The "inverted V" standoff technique produced a nearly complete bond across the interface, reducing the unbonded area to only the peak of the "V." The pronounced wavy interface associated with the parallel plate setups is nearly absent.

A series of photomicrographs of similar-thickness joints are shown in Figure 14. The bond area of the 6061-T6 joint required severe etching to differentiate between the two plates. The titanium joint has a large central unbonded area, but the bond itself is excellent. The same bond under higher magnification shows a 0.001-inch peak-to-peak wavy interface, but emanating from these peaks are rays of apparent crystal reorientations, exhibiting peak-to-peak dimensions of 0.0045 inch.

These photomicrographs reveal that each interface is unique to materials and physical setup; so unique that each configuration can be identified by the "signature" of its explosively welded interface. There are no fusion or diffusion zones in these bonds, only grain boundary-width lines separating one metal from another.

- 2. Pressure Integrity Tests---After welding the plates in the configuration shown in Figure 5, the assembly was pressurized with dry nitrogen to 1000 psi and held for 5 minutes with no appreciable leakage. The 0.040-inch plate burst at 1300 psi, and the 0.063-inch plate burst at 1900 psi. The complete weld did not fail; the rupture occurred in the plate, breaking through the middle of the bond area.
- 3. Vacuum Effects---No appreciable change in strength was observed in the fabrication of a 0.090-inch 2024-T3 ALCLAD scarf joint under vacuum. A joint strength fabricated under atmosphere had an average of 5290 pounds, inch with a standard deviation of 510; a second joint fabricated under vacuum had a strength of 5420 pounds/inch with a standard deviation of 490. Air is simply a compressible fluid between the plates to be welded, resisting their movement

during the welding operation. However, air is beneficial in inhibiting the movement of explosive residue, helping to prevent contamination of areas to be welded, prior to the actual welding mechanism.

4. Explosive Contamination and Safety---The explosive residue, fragments of lead, carbon, and tape, as described in item 10 of the explosive welding variables, can damage and contaminate surrounding surfaces and are potentially hazardous to personnel. The bulk of this residue is emitted within ±10° of a plane on the center line of the explosive and perpendicular to the plate; no explosively driven residue is deposited on the plate surface, only the fallout from the surrounding volume.

Due to the very small explosive quantities used by this technique, only minimal shielding is necessary to capture or redirect this residue. A 0.040-inch aluminum structure placed 18 inches from the explosive source will stop these fragments. The very high pressure created by these minute amounts of explosive dissipates rapidly with distance; at 18 inches, the actual pressures are estimated to be less than one psi.

A second potential hazard to personnel is the explosive sound. The sound created by the ribbon explosive at 10 feet is comparable to the sound produced by a shotgun at 1 foot from its muzzle. This sound can be effectively muffled by using separate welding rooms, properly equipped with acoustical materials.

All explosive products, including lead, smoke, and sound can be totally confined by the apparatus shown in Figure 6. The only observable effects are the expansion of the tube and the rattling of metal. The ribbon explosive is placed in the bottom of the tube adjacent to the plate to be welded. On initiation, the explosive pressure transfers through the tube and accelerates the plate to be welded producing the normal explosive welding operation. The pressure transfer is facilitated by the use of silicone grease, which acts like an incompressible fluid under dynamic loading, at the tube-to-plate interface. The silicone rubber attenuates and diffuses the explosive pressure, preventing tube rupture. Flexible end fittings must be provided to achieve total confinement.

In determining the performance of this confinement technique, welds were made in 0.040-inch to 0.25-inch aluminum. The performance of a joint created with 15 grains/foot ribbon explosive directly applied to the plate (no tube) was 2300 pounds/inch with a standard deviation of 200: 15 grains/foot in a totally confined tube produced a weld of 1780 pounds/inch with a standard deviation of 240, a strength loss of 23%. A joint created by a 20 grains/foot ribbon explosive in an open-ended tube had a strength of 2300 pounds/inch with a standard deviation of 230; a totally confined 20 grains/foot ribbon explosive produced a joint strength of 2300 pounds/inch with a standard deviation of 240, no appreciable change.

To evaluate the maximum confinement ability of the tube, a 25 grains/foot ribbon was tested in an open-ended tube on 0.063 to 0.25-inch aluminum plates. The tube did not rupture and produced a joint with a strength of 2900 pounds/inch with a standard deviation of 170.

This explosive material, RDX, is not sensitive to inadvertent initiation during handling, cutting, or setup. Deliberate attempts would have to be made to expose the explosive itself and impact it sharply between hard surfaces to initiate it. The possibility of initiating the explosive inside its sheathing by deliberate hammering is remote. The ribbon explosive may be cut with sharp instruments, such as scissors, knives, or razor blades. However, the explosive is sensitive to heat; it will sublime slowly at approximately 200° F and burn at approximately 300° F. This burning is not detonation and the several million psi pressure is not generated. This material has not been tested to determine the unlikely possibility of the burning being accelerated to detonation.

Explosive materials such as HNS (hexanitrostilbene) and Dipam (dipicramide) are available that are completely insensitive to any shock stimulus other than that delivered by another explosive. Also, these materials can withstand 500° F for at least 5 minutes without burning.

The inexpensive electrically initiated blasting cap used to initiate the ribbon explosive is the major potential hazard in this operation. Special care must be taken in its handling to prevent impacts and static electricity, or the application of stray energy through the firing leads. Proper handling by personnel and adequate electrical grounding and firing systems can virtually eliminate this problem.

5. Structural Fabrication Demonstrations---To demonstrate the potential of this welding technique, several structures were fabricated and evaluated: an aluminum plug was welded into an aluminum tube, a titanium rib was welded to a flat titanium plate, and a 1/12 aluminum scale model of a space station-type structure was constructed.

Two plugs were welded into the tube, as shown in Figure 7. The assembly was pressurized with dry nitrogen to 1500 psi through a fitting mounted in one plug with no appreciable leakage. A pull-test on the aluminum plugs produced a tube failure at 8300 pounds force which is equivalent to a 38,100 psi tensile load. The weld joint was not pulled off either plug.

The titanium rib, fabricated in the setup shown in Figure 8, is shown in Figure 15. The first, and last inch of these joints failed to weld. This result was supported by similar tests conducted in Figure 3, technique "f." The average strength of this joint was 5550 with a standard deviation of 1540. This joint appears to be extremely sensitive to setup variables of explosive locations and standoff uniformity.

The space station-type structure fabrication, joining 0.040-inch skin, bulkheads, and deck to 18-inch-diameter rings and 0.125-inch-thick 0.75-inch angle was highly successful. The average weld strength was approximately 1000 pounds/inch. See Figure 16.



CONCLUSIONS

The general efforts in explosive welding since the 1950's have been directed toward relatively large-area bonding of metal combinations that are difficult to join by other techniques. Considerable difficulty has been experienced in the production of narrow, long-length weld joints with this areabond technique. This report describes a novel small-scale explosive seamwelding technique developed and demonstrated at NASA-LRC, which overcomes these difficulties. This technique can join a variety of aluminum alloys (2024, 2024 ALCLAD, 2219, 6061, and 7075) and aluminum alloy combinations (2024, 2219, 2024 ALCLAD, and 7075 to 6061) to 0.125 inch thickness, and titanium (Ti-6Al-4V) to 0.056 inch in seam welds less than one-half an inch in width with no apparent long-length limitation. Aluminum welds to 12 feet have been demonstrated.

The evaluation and demonstration of this explosive welding technique was accomplished in three major phases: evaluation of welding variables, joint development, and applicational analyses.

Ten major explosive welding variables were studied to determine their effects on welding performance. They are plate materials, plate thicknesses, explosive quantity, standoff-plate separation, plate surface, plate deformation, mechanical shock, metal grain orientation, weld length, and explosive residue. Adequate limitations or controls were demonstrated for all the variables except mechanical shock induced by the explosive and plate impact.

Four different explosively welded joints were fabricated and demonstrated in a variety of aluminum alloys tempered to maximum strength in a range of thickness and titanium. These joints are: dissimilar-thickness lap, similar-thickness lap, sandwiched-butt and scarf. These joints exhibited strengths up to that of the parent metal.

A series of applicational analyses were conducted. Photomicrographs revealed the classical "skin-deep" wavy interface (less than 0.002 inch) with no fusion or diffusion zones of conventional explosive welding. Since no metal is added in this joining technique, sharp notches exist at the outer edges of the bonded area between the plates, which could produce possible stress concentrations. In pressure tests, the explosively welded joints were demonstrated to be airtight. Also, this explosive welding technique is slightly more efficient under vacuum conditions.

The handling, cutting, and installation of the ribbon explosive is no more hazardous than many machining and fabricating processes. Very little shielding is required for containment of explosive products, and sound protection can be provided by conducting welding operations in acoustically shielded rooms. Furthermore, a technique was developed and demonstrated that can contain all explosive products, including fragments and sound, during explosive welding.

Several potentially useful structures were fabricated. An aluminum plug was welded into a thin-walled aluminum tube, achieving 85% of the tube's ultimate strength. A thin-walled titanium rib was welded to a flat titanium

plate of the same thickness. A 1/12-scale model of a space station-type structure was fabricated, using thin aluminum welded to aluminum rings and angle.



Recognizing the highly complex requirements in today's fabrication field, this small-scale explosive seam-welding technique can complement existing fabrication techniques through many of the advantages of conventional explosive welding techniques, as well as its unique advantages. This technique can join metals and alloys that are difficult, if not impossible, to achieve with nonexplosive approaches. It does not affect the temper/strength characteristics of these alloys. It can join thin materials to heavy stock, and is insensitive The unique advantages of this technique include the ability to produce narrow, long-length joints with a high degree of efficiency and low cost. Eight ounces of this explosive, excluding the lead sheathing, can produce a weld joint 140 feet long in 0.125-inch aluminum at a cost of \$131 in materials. The reproducibility of this technique is shown by the small standard deviations of the 41 weld joints in this study, averaging 10% of their respective mean values. This technique is very simple, requiring few tools and only minimal personnel skill and training. Finally, weld joints can be made in setups that produce no unbalanced reactionary forces.

REFERENCES

- 1. Carpenter, S. H.; and Wittman, R. H.: "The Theory and Application of Explosive Welding," The University of Denver.
- 2. Blank, G. F.; and Bothe, B. A.: United States Patent 3,543,388, "Controlled Area Explosive Bonding," issued December 1, 1970.
- 3. Bement, L. J.: "Welding of Aluminum With Linear Ribbon Explosives," Presented at the Seventh Symposium on Explosives and Pyrotechnics, Philadelphia, Pennsylvania, September 8-9, 1971.

TABLE 1
Cross-sectional Dimensions of Linear Ribbon RDX Explosive

Explosive Load grains/foot	Thickness inch	Width inch
7	0.020	0.220
10	0.020	0.300
15	0.025	0.315
20	0.030	0.365
25	0.035	0.370

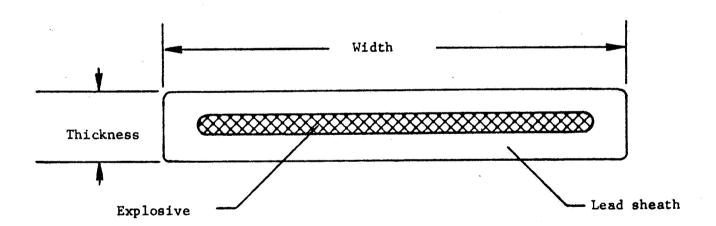


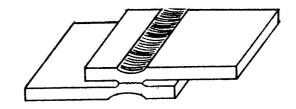
TABLE 2
DISSIMILAR-THICKNESS LAP JOINT STRENGTHS



	MATERIAL 0.063 to 0.250 INCH	EXP. QTY. GRAINS/FOOT	MAT. STRENGTH POUNDS/INCH	JOINT STRENGTH POUNDS/INCH	STD. DEV. POUNDS
t .	6061-T6 to 2024-0	20	3000	2500	430
<u>ငှာ</u> တ	6061-T6 to 7075-0	20	3000	2600	430
N	6061-T6 to 6061-0	20	3000	3300	240
n	6061-T6 to 6061-T6	20	3000	3400	30
	6061-T6 to 2024-T3A	20	3000	3000	200
	2024-T3A to 2024-T3A	20	4300	2700	360
	7075-T6 to 2024-T3A	20	5500	3400	200
	7075-T6 to 6061-T6	20	5500	3400	830
	0.070 to 0.250 Inch 2024-T4 to 6061-T6	20	4890	4380	830
	0.100 to 0.250 Inch 2219-T31 to 6061-T6	25	6370	3120	740

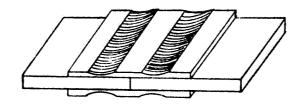


TABLE 3
SIMILAR THICKNESS LAP JOINT STRENGTHS



୍ଦ୍ର ବ୍ରଣ	THICKNESS INCH	MATERIAL	EXP. QTY. GRAINS/FOOT	MAT. STRENGTH POUNDS/INCH	JOINT STRENGTH POUNDS/INCH	STD. DEV. POUNDS
•	0.063	2024-T3A	15	4300	2670	260
	0.090	2024-T3A	20	6100	3500	220
	0.125	2024-T3A	25	8600	3520	380
	0.063	6061-T6	15	3000	2890	320
	0.090	6061-T6	20	4300	4330	190
	0.125	6061-T6	25	6000	4540	670
	0.100	2219-T31	25	6370	5040	130
	0.056	Ti-6A1-4V	25	7320	7320	112

TABLE 4 SANDWICHED-BUTT JOINT STRENGTHS

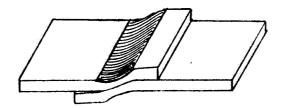


	THICKNESS INCH	MATERIAL	EXP. QTY. GRAINS/FOOT	MAT. STRENGTH POUNDS/INCH	JOINT STRENGTH POUNDS/INCH	POUNDS
, 63	0.040 to 0.063	6061-T6	15	3000	2880	310
364	0.063 to 0.090	6061-T6	25	4300	4100	580
Ä	0.063 to 0.125	6061-T6	20	6000	5720	720
	0.025 to 0.056	Ti-6A1-4V	25	7300	6240	1140





TABLE 5
SCARF JOINT STRENGTHS



THICKNESS INCH	MATERIAL	EXP. QTY. GRAINS/FOOT	MAT. STRENGTH POUNDS/INCH	JOINT STRENGTH POUNDS/INCH	STD. DEV. POUNDS
0.040	2024-T3A	7	2300	2490	100
0.063	2024-T3A	15	4300	3920	280
0.090	2024-T3A	20	6100	5290	510
0.125	2024-T3A	25	8600	4410	170
0.063	6061-T6	15	3000	2880	110
0.090	6061-T6	20	4300	3830	400

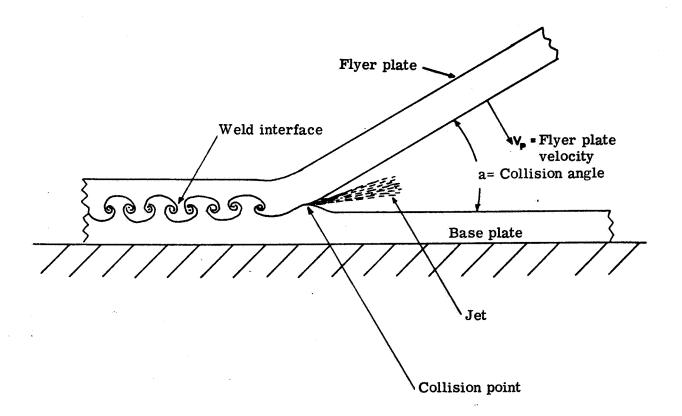
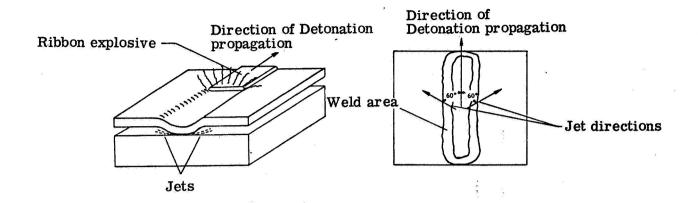
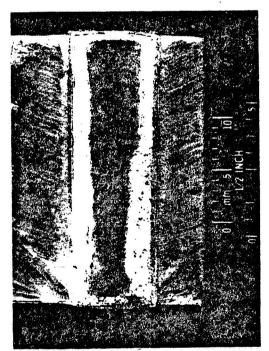


Figure 1. - Oblique collision of metal plates in an explosion welding operation.





Photograph of actual explosive weld, showing streaks produced by jetting action.

Figure 2. - Mechanisms of NASA-LRC explosive welding



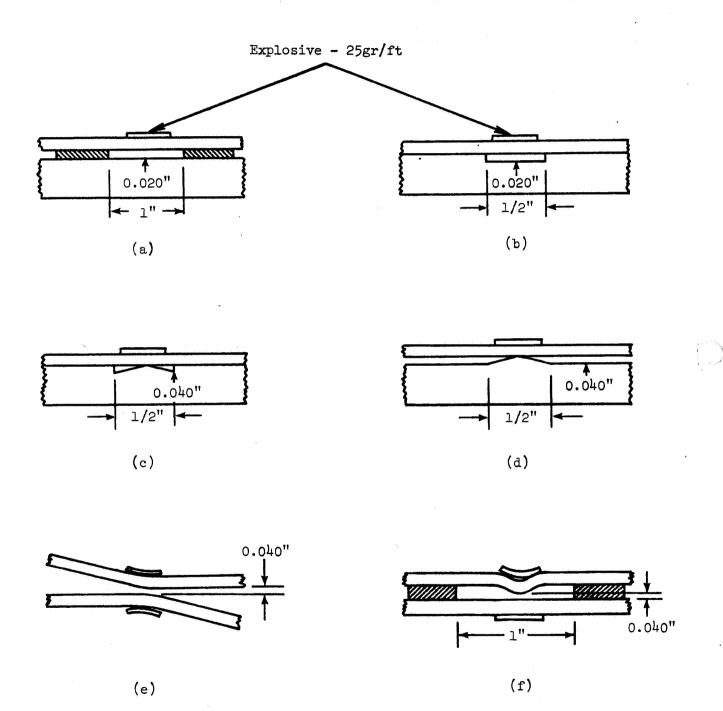


Figure 3.- Explosive welding standoff techniques. 368<

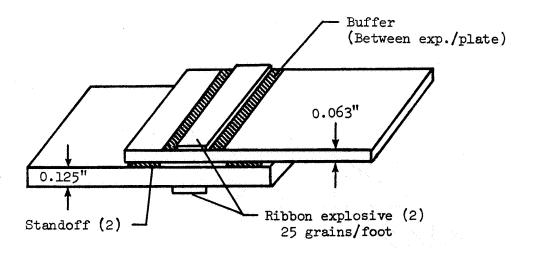


Figure 4.- Setup for buffer material evaluation.

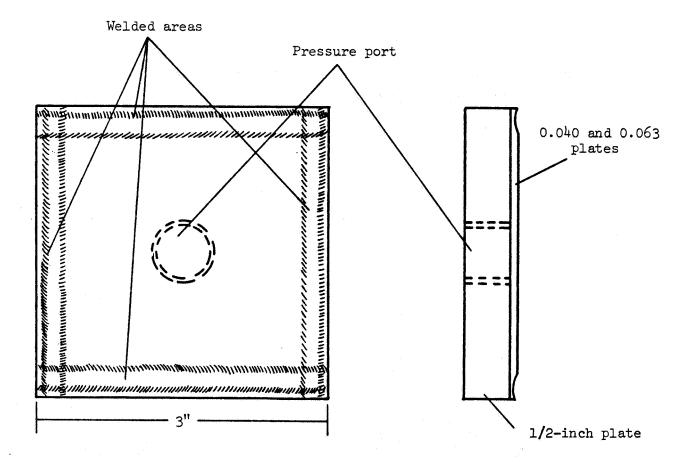


Figure 5.- Setup for pressure integrity tests.

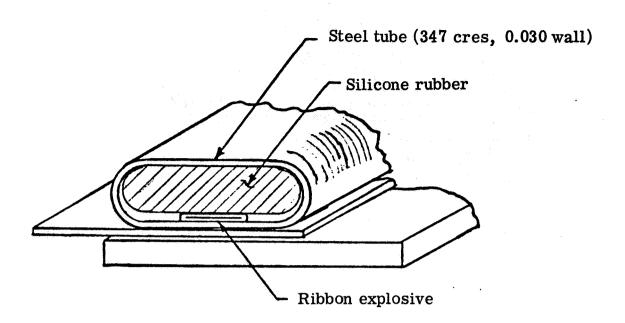


Figure 6. - Setup for explosive weld to achieve confinement of explosive detonation products.

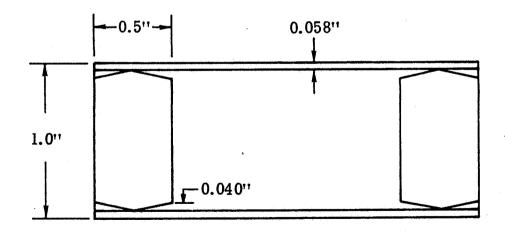


Figure 7. - Setup for explosive welding of 1/2" 6061-T6 plug in 1" 6061-T6 tube

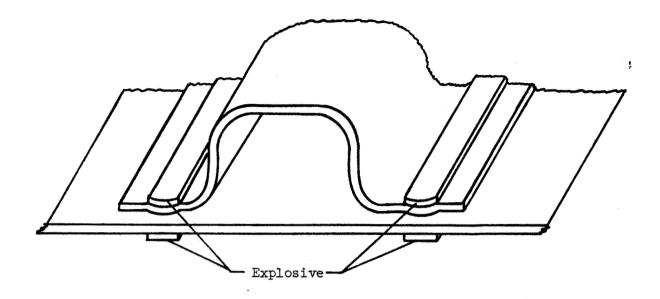


Figure 8.- Setup for explosive welding of titanium rib (without anvils).

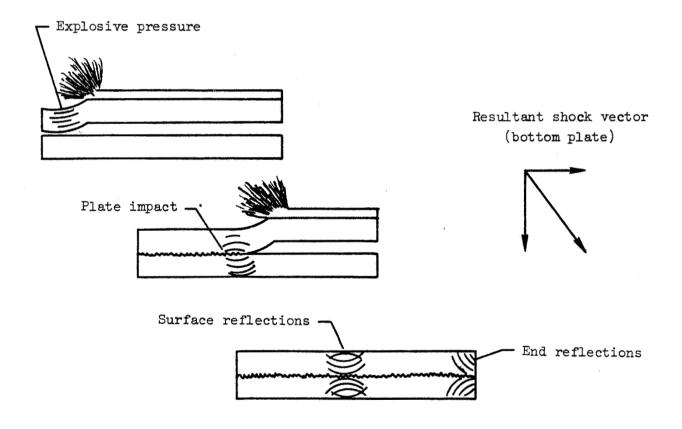


Figure 9.- Mechanical shock wave interference

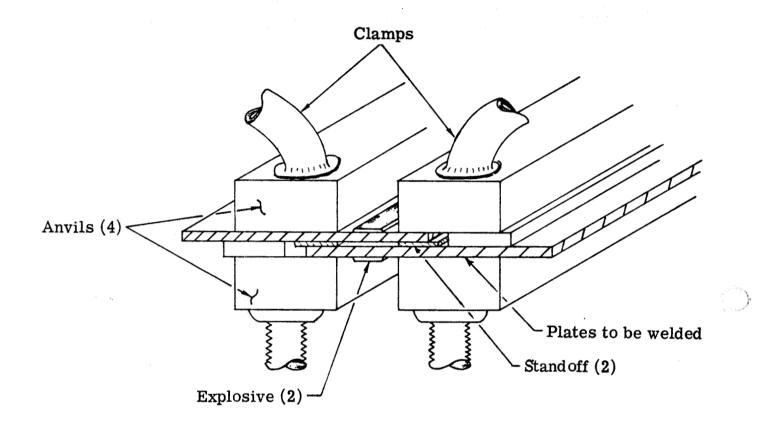
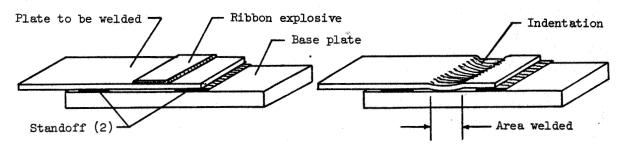
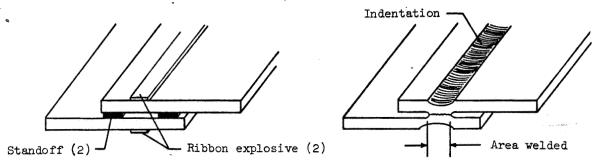


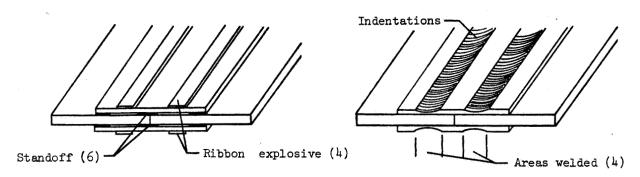
Figure 10. - Mechanical shock attenuation technique



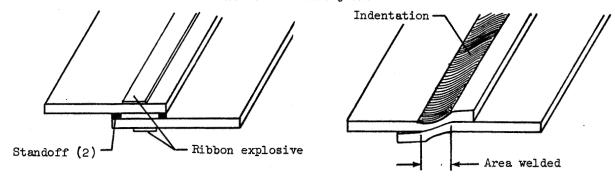
Dissimilar - thickness lap joint



Similar - thickness lap joint



Sandwiched - butt joint



Scarf joint

Figure 11.- NASA - LRC explosively welded joints.

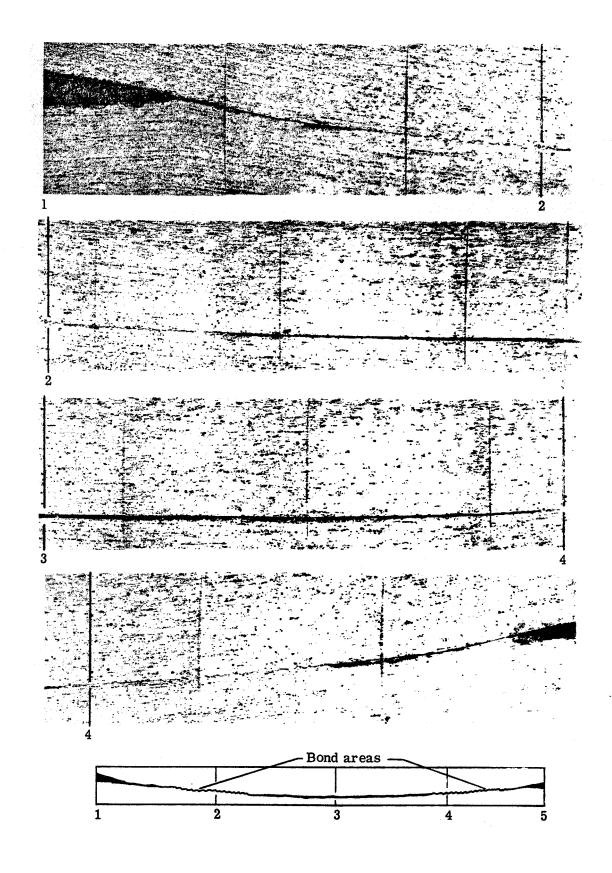
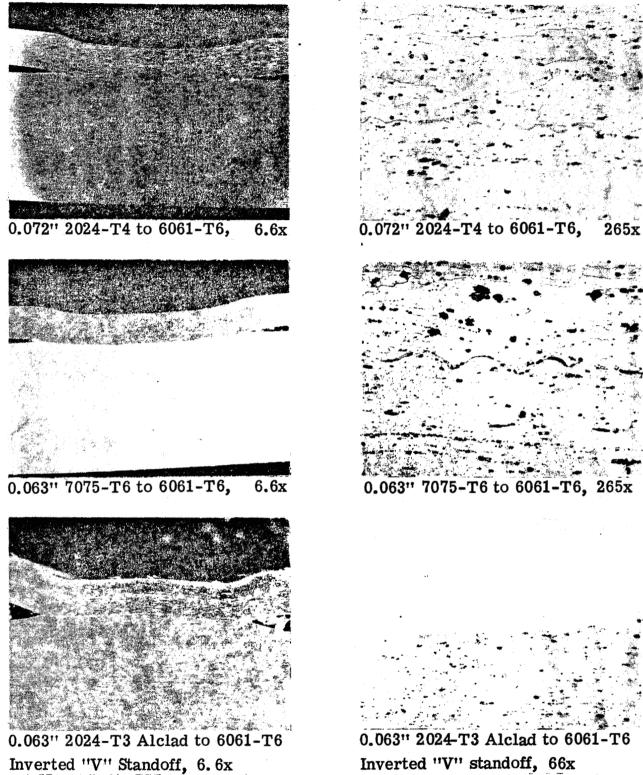


Figure 12. - Cross-section of a lap joint of 0.063" 7075-T6 to 0.25" 6061-T6, 54x



Inverted "V" Standoff, 6.6x Inverted "V" standoff, 66x
Figure 13. - Typical photomicrographic cross sections of dissimilar-thickness
lap joints.

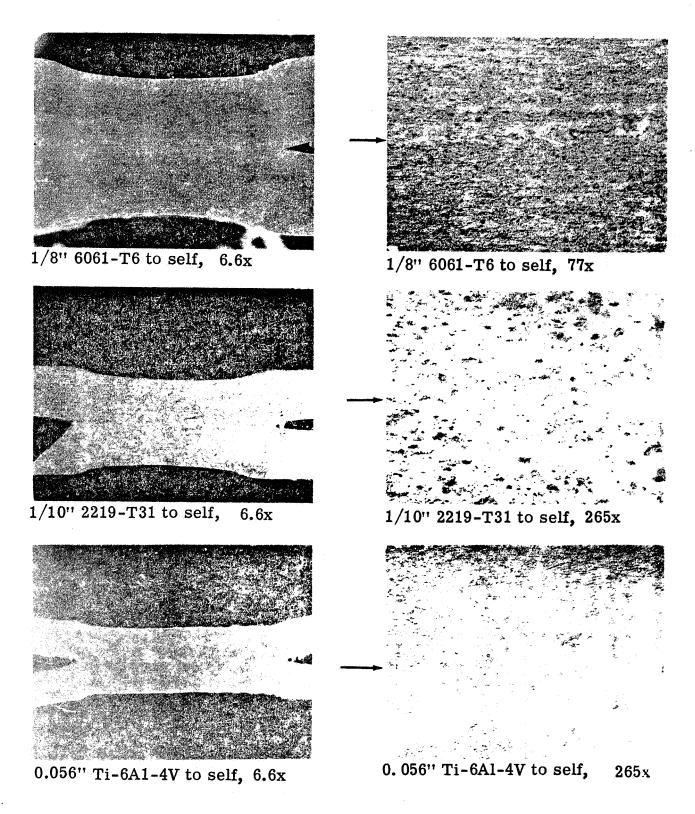


Figure 14. - Typical photomicrographic cross-sections of similar-thickness lap joints.

NASA L-72-3550

Figure 15.- Photograph of titanium rib section.

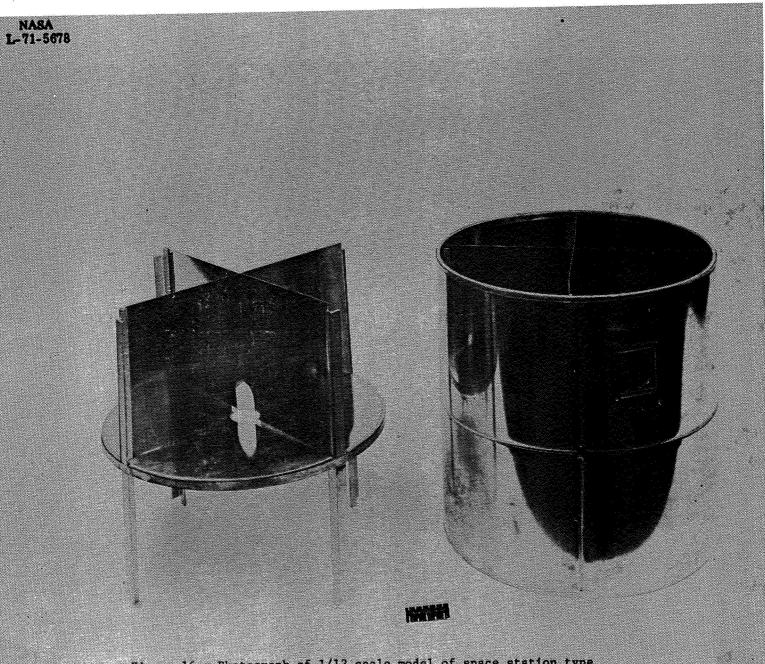


Figure 16.- Photograph of 1/12 scale model of space station type structure; the internal structure of the model is shown on the left.

WORCESTER POLYTECHNIC INSTITUTE WORCESTER, MASSACHUSETTS

#N74 30941

DIFFUSION BONDING OF IN 718 TO VM 350 GRADE MARAGING STEEL MAY 1972

STEPHEN R. CROSBY RONALD R. BIEDERMAN CHARLES C. REYNOLDS

ABSTRACT

Diffusion bonding studies utilizing a "Gleeble" have been conducted on IN 718, VM 350 and the dissimilar alloy couple, IN 718 to maraging steel. The experimental processing parameters critical to obtaining consistently good diffusion bonds between IN 718 and VM 350 are determined. Interrelationships between temperature, pressure and surface preparation were explored for snort bending intervals (< 15 min) under vacuum conditions. Successful joining was achieved for a range of bonding cycle temperatures, pressures and surface preparations.

The quality of the bond was evaluated by several test methods. Metallographic investigation of the joint for grain growth across the original interface and for growth of the diffusion zone was considered an important criterion of bond quality. Tensile testing for a simple butt weld configuration of both heat treated and as bonded samples was also used as a basis for this judgment.

Both annealed and heat treated diffusion couples were studied. A compatible heat treatment for both alloys was found to be possible. This simultaneous heat treatment resulted in bond tensile properties that were comparable to those obtained in the weaker parent material. The drastic yield strength differences and work hardening characteristics in the two alloys when heat treated insures the creation of a notch effect near the bond interface, with failure in this region likely. Therefore, the strength of the weaker parent material is used as a criterion for a successful tensile test of the heat treated bond. Studies of VM-350/VM-350 couples in the as-bonded condition showed a greater yielding and failure outside the bond region. This characteristic of failing outside the bond region is not necessarily a useful criterion for dissimilar alloy couples.



The desire to obtain quality joints in materials has long been of prime interest. The diffusion bond is capable of providing that superior joint [1, 2, 3] for many alloy systems. The process of diffusion bonding is best described as the formation of a metallurgically sound joint by causing interdiffusion of the surface atoms of either similar or dissimilar materials [4]. This bonding is usually performed at conditions below the melting point of any of the phases present, but high enough to assure fast diffusion rates. However, it is possible and often desirable to diffusion bond in the presence of a liquid phase which is transient [5]. Of the many types of diffusion bonding, the one considered in this research program is "yield strength controlled". This process uses a pressure during the formation of the joint that is higher than the yield strength of the weaker parent material [4].

Diffusion bonding is an attractive process as it virtually eliminates the inhomogeneity associated with recast structure and its attendant problems of segregation and varied grain size which are found in fusion welds. Diffusion bond properties approaching those of the parent material can be obtained. This results in engineering designs which require no increase in section size at the joint [2].

Many applications which require the superior metallurgical characteristics of the diffusion bond are also involved with extensive use of special high strength alloys [2]. Interest in diffusion bonding is often the result of finding that this technique is the only possible

method of joining high strength materials without producing highly inferior mechanical properties in the joint region. The successful joining of superalloys and specialty alloys often necessitates avoiding the formation of recast structures (fusion weld zone) making diffusion bonding the most attractive joining process [3].

Kaarlela and Margolis [3] describe some of the requirements for achieving good diffusion bonds in many of the superalloy systems. In their study, it was pointed out that acceptable bonds in iron base and nickel base alloys strengthened by aluminum and titanium were difficult to achieve. These alloys were bondable only at the highest temperatures and pressures ordinarily employed for the process, or by drastically increasing bonding time. Bartlett [6] indicates the need for very high temperatures (2000 to 2200°F) for bonding either iron base or nickel base alloys, due to low solubility of interstitials in these elements.

The problems associated with a jet engine shaft have suggested the possibility of a superalloy-iron base diffusion couple for overall superior fatigue properties. In this case, there are different requirements along the shaft for temperature and strength. The use of dissimilar materials along the shaft could meet these requirements offering considerable savings in terms of weight and elimination of complex cooling schemes. The purpose of this research was to determine the feasibility of diffusion bonding an 18% nickel maraging steel to a precipitation hardenable nickel base alloy and to determine a simultaneous heat treatment after bonding to obtain maximum mechanical properties of the two materials. Parameters which influenced the bonding process were studied with respect to the ease of sound joint formation. The bonding conditions which gave the most satisfactory results in terms of tensile strength and good microstructure were determined.

EXPERIMENTAL PROCEDURE

SURFACE PREPARATION

The samples used were 1-1/8 to 1-1/4 inches long and 1/4 of an inch in diameter. A flat steel block, drilled to hold the samples, was used to obtain different controlled surface roughnesses. Set screws held the longitudinal axes of the samples perpendicular to the faces which were polished or lapped. G. V. Alm [4] has indicated advisable surface finishes of 16 rms or better for bonding superalloys. The surface conditions obtained by using the polishing papers and lapping wheels were calibrated using both steel and glass, as material hardness affects the surface finish. Table 1 shows that surfaces equal to or better than the 16 rms were used. The ends not prepared for bonding were chamfered to fit the specimen holders in order to provide good electrical contact in the "Gleeble".

Two cylindrically ground bars 5/8 of an inch in diameter were used to hold the specimens. One end of each bar was clamped in the "Gleeble". The free ends of the bars were drilled to hold the specimens with three centering set screws placed 120 degrees apart. The bars themselves were kept aligned by two collars spaced by insulated plates. These support devices are shown assembled in Figure 1.

ATMOSPHERE

The entire specimen support apparatus is shown in Figure 1 as assembled. The vacuum chamber as prepared for bonding is shown in Figure 2.

TABLE 1
CALIBRATION OF POLISHING PAPERS AND LAPPING WHEELS

WHEEL OR LAP	SURFACE FINISH, MICROINCHES (ARITHMETRIC AVERAGE)
With Steel:	
400 grit	4.0 - 6.0
600 grit	2.0 - 4.0
5.0 micron alumina	1.0 - 1.4
0.3 micron alumina	* ·
With Glass:	
220 grit	10.0 - 15.0
320 grit	8.0 - 12.0
400 grit	2.8 - 3.2
600 grit	2.0 - 2.4
5.0 micron alumina	*

^{*}Profilometer scratches were noticed at these values of surface finish.

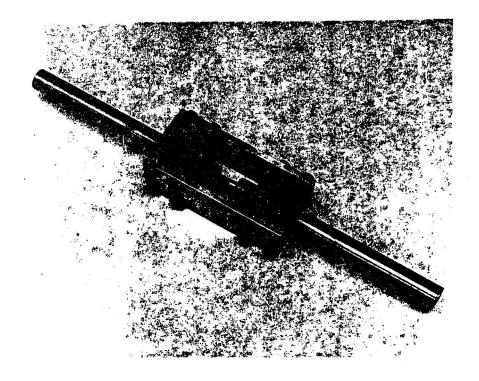


Fig. 1. — Specimen support device

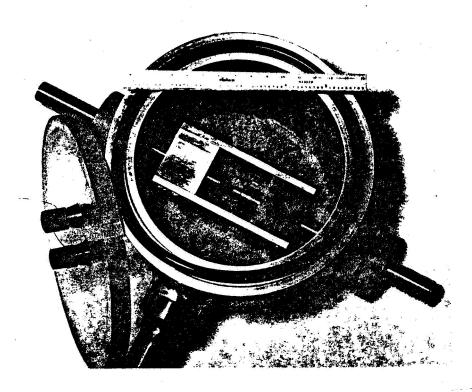


Fig. 2. — Vacuum chamber

Mechanical and diffusion vacuum pumps were used in series to evacuate the chambers and a vacuum of 10⁻⁴torr (0.1 microns of mercury) was consistently achieved. The samples were held apart in vacuum for at least ten minutes in order to remove molecular oxygen from the surfaces to be bonded. All samples were preloaded to prevent arcing at the bond surfaces.

"GLEEBLE" CONTROL

The "Gleeble", shown in Figure 3, was programmed to control several of the bonding parameters. The program generator on the "Gleeble". Figure 4, was set up to trigger the compressive load on the samples before heating. The value of this load is controllable and can be varied manually during the bonding process. Cline [2] indicates the pressure ranges necessary for bonding to be near 10,000 psi, and these values were used as a first approximation. The program generator also controls the rate of heating, the maximum temperature, and the time at temperature. Feedback for temperature control was provided by a chromel-alumel thermocouple percussion welded to the sample 1/16th of an inch or closer to the bond surface. The temperature range used was 1/2 to 2/3 the melting point of the lower melting temperature alloy, a rule of thumb suggested by Alm [4]. A multichannel recorder was used to obtain the simultaneous readout of temperature, load, and deformation as a function of time. Complete monitoring of the bonding variables was maintained throughout the bonding cvcle.

METALLOGRAPHY

Immediately after bonding, the samples were prepared for metallographic examination. Metallographic polishing and etching procedures used are standard. The entire metallographic processing procedure is presented in reference [7]. Some of the samples were mechanically tested in the

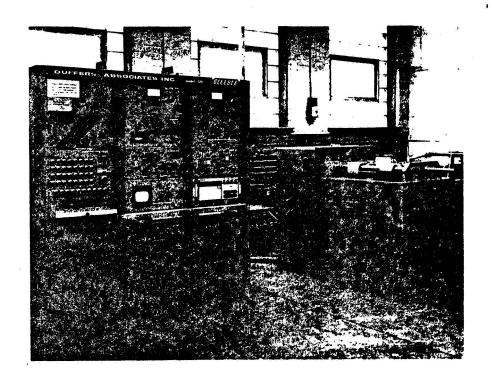


Fig. 3.—The "Gleeble"

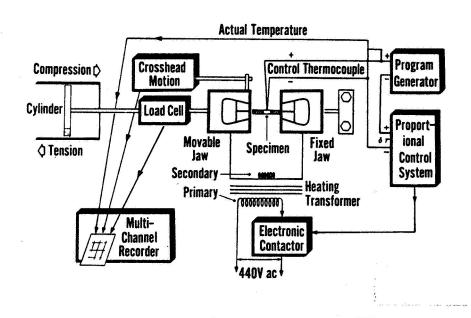
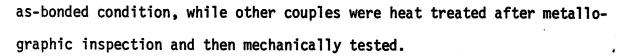


Fig. 4.—Schematic of "Gleeble" control system



HEAT TREATMENT

The heat treatment of the dissimilar alloy couple consisted of several steps, shown diagrammatically in Figure 5. The first sequence in the heat treatment was to solutionize the IN-718 at 1750°F for one hour. This was followed immediately by an air quench. The IN-718/VM-350 couple was reheated to 1325°F and held for 8 hours, then cooled at 100°F per hour to 1150°F and held for 8 hours, and finally air quenched. This treatment resulted in precipitation hardening of the IN-718 alloy and solutionizing of the VM-350 alloy. The VM-350 was then age-hardened for 3 hours at 930°F in an air atmosphere. Since the heat-treatment prescribed for IN-718 includes in its cycle the solutionizing treatment required for VM-350, the entire cycle for IN-718 is used as a solutionizing treatment for the VM-350.

TENSILE SPECIMEN PREPARATION

Preparation for the mechanical testing was done using a tool post grinder, because of the specimen size and difficulty in conventional machining of the alloys. The grinding wheel was contoured to create a tensile shape directly. The specimens were tested in a universal testing machine, using a strain rate of 0.2 inches per minute. Control samples were tested for both the as-received and the as-bonded conditions.

389<

Fig. 5. IN-718 and VM-350 Heat-treatment Cycles.

RESULTS



VM 350/VM350 Couple

Early trials indicated that diffusion bonding of VM 350 to VM 350 was feasible utilizing controlled resistance heating in the "Gleeble". This couple was used to evaluate the bond quality produced by the "Gleeble". Failure was expected to occur outside the bond region for properly bonded VM 350/VM 350. Table 2 shows the bonding parameters used and the resultant tensile properties for VM 350 to VM 350 trials. Early attempts showed incomplete bonding with voids present in the joint, as typified in Figure 6. However, with increased load, rougher surface finish, and the same temperature, improved bonding was obtained as shown in Figure 7.

IN 718/MM 350 COUPLE

The bonding parameters and resultant tensile properties for the IN 718/VM 350 couple are presented in Table 3. These results indicate that the surface finish, produced by a 5µ lap produces the best diffusion bonding tensile properties for the IN 718/VM 350 couple for constant pressure and temperature conditions. Photomicrographs showing the size of the diffusion zone for three temperatures are presented in Figure 8. The temperature dependence of the diffusion bonding process is evident from the thickness change of the bonding zone with temperature. A quantitative relationship between diffusion zone size and temperature is presented in Figure 9. From the slope of this plot an activation energy for the process was determined to be 33,000 CAL/MOLE. Also evident in Figure 8 is a variation in the rate of grain growth for the two materials. This is shown in Figure 10. IN 718, while initially finer in grain size than VM 350, undergoes a more rapid rate of grain coarsening than the VM 350.

TABLE 2

BONDING PARAMETERS AND TENSILE PROPERTIES FOR VM 350VM 350 COUPLES

BONDING TEMPERATURE	SURFACE PREPARATION	TIME MIN	MAXIMUM ² BONDING PRESSURE PSI	EQUILIBRIUM ² BONDING PRESSURE PSI	PERCENT REDUCTION IN AREA	S _{ult} PSI
. 2161	Electron Polish	- 5	26300	14,600		122,000
2161	5 Min Lap	5	23800	10,900	39.3	157,500
2161	600 grit	5	25400	10,900	55.9	163,000
2161	400 grit	5	21900	10,200	59.0	163,500
1800³	the same of the same time.	5			72.6	171,800

- 1. Maximum value is due to thermal expansion
- 2. Equilibrium value, controlled by cylinder on "Gleeble"
- 3. As received stock subjected to bonding cycle for comparison



Fig. 6 Undesirable microstructure in joint region (voids) for VM 350/VM 350 couple 375X

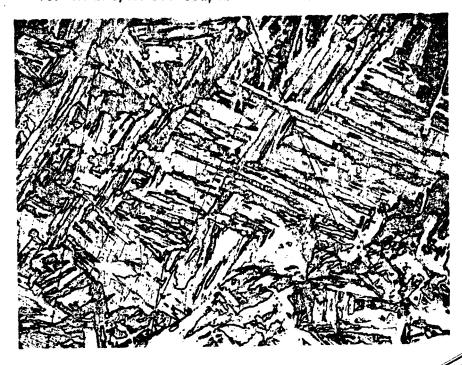


Fig. 7. Desirable microstructure in Joint region for VM 350/VM 350 couple 375X

TABLE 3
BONDING PARAMETERS AND TENSILE PROPERTIES FOR THE IN 718/VM 350 COUPLES

Bonding Temperature, °F	Surface Preparation	Time, Min.	Maximum¹ Bonding Pressure, psi	Equilibrium ² Bonding Pressure, psi	Per Cen Reducti in Area IN 718	on	Ultimate Strength, psi	Rockwel "C" Hardnes IN 718	S)
As Bonded: 1800 1800 1900 2000	5.0μ lap 0.05μ lap 600 grit 400 grit	5 10 5 5	23,400 26,000 18,200 23,800	13,300 20,800 10,900 12,800	11.1 46.7 7.9 11.3	6.6 22.1 2.2 3.3	105,200 ³ 136,800 ³ 76,100 91,720	23.4 22.7 (Too low (for R _c	26.4 32.3 25.5 21.9	
1700 1800 1900 1900 1900 2000 2000	0.5µ lap 5.0µ lap 600 grit 5.0µ lap 0.5µ lap 600 grit 5.0µ lap	5 5 5 5 5 5	10,000 10,800 14,180 13,300 15,000 12,500 12,500	6,670 4,160 10,000 7,200 9,160 8,340 7,500	5.7 5.6 1.7 6.7 5.0 2.0	4.0 2.1 1.4 2.2 3.5 1.3	196,000 205,000 76,000 ³ 201,800 ³ 173,000 178,700 ³	39.1 39.5 41.5 40.6 38.3 38.8	52.0 53.2 50.0 51.6 48.7 48.7	-13-

CONTROL SAMPLES

As-Bonded IN 718)1800°F " " VM 350) Heat Treated IN 718' " " VM 350'	5 5 			58.6 13.6 	72.6 50.3	151,800 171,800 184,000 358,000	21.0 42.0	29.0 59.0
--	------------	--	--	----------------------	------------------	--	------------------	------------------

- 1. Maximum value, due to thermal expansion
- 2. Equilibrium value, controlled by cylinder on "Gleeble"
- 3. These specimens polished to remove grinding scratches
- 4. Manufacturers' data

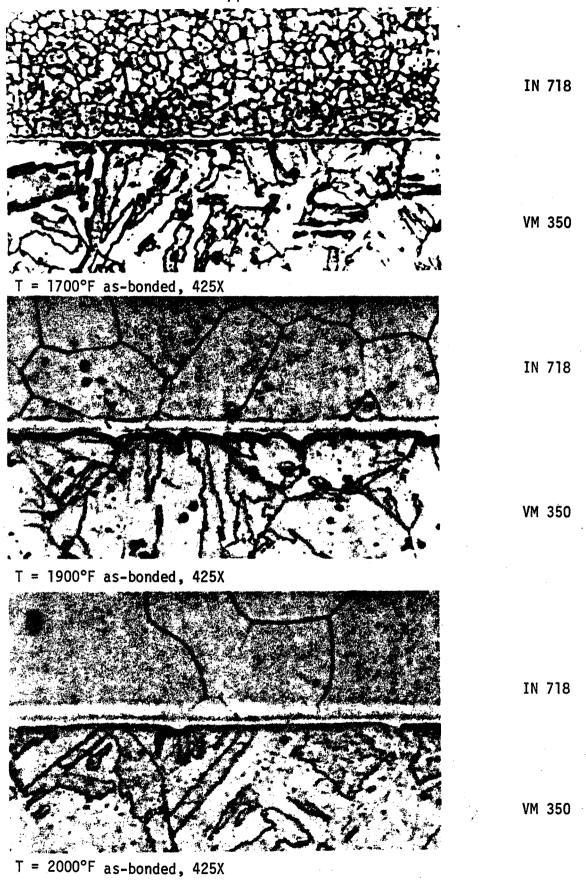


Figure 8 IN 718/VM 350 Diffusion Zone Thickness for 1700°F, 1900°F, and 2000°F

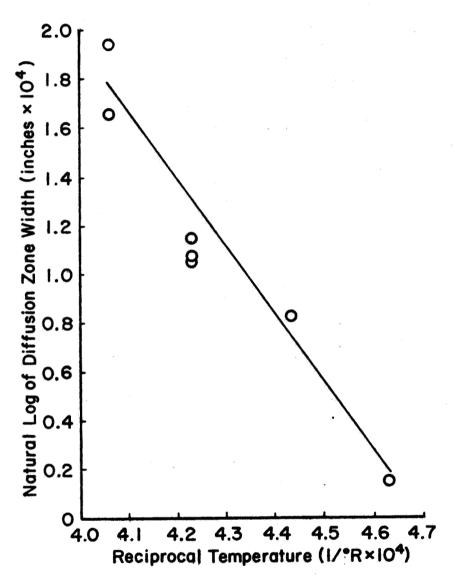


Fig. 9. Temperature Dependence of Diffusion Zone Width for IN-718 / VM-350 Couple.

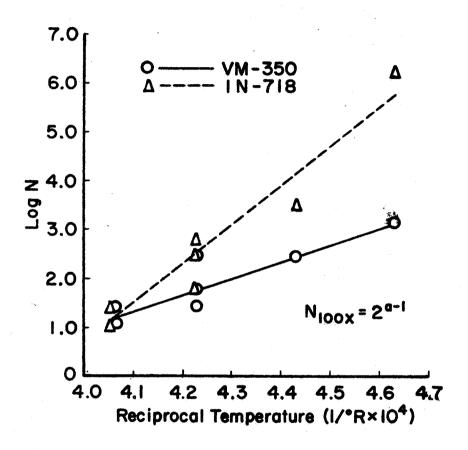


Fig. 10. Temperature Dependence for Grain Growth in VM-350 and IN-718.

PROPERTIES IN 718/VM 350 COUPLE

The results of tensile testing several as-bonded samples are presented in Table 3. The control tensile data for IN 718 and VM 350 which have experienced a similar bonding temperature-time cycle are also listed. As-bonded IN 718/VM 350 specimens exhibit ultimate strengths approaching that of the weaker parent material, IN 718. Rockwell C hardnesses for the simultaneously heat treated materials are in good agreement with expected values as shown in Table 3.

Chemical analyses of the major solid solution elements and hardening elements necessary for precipitation hardening in the diffusion zone region are presented in Figures 11 and 12. These profiles were obtained using an electron beam microprobe with a spot size of 4μ . The traverse across the interface was indexed in 2μ steps until constant base alloy composition was achieved. Profiles for iron, nickel, cobalt, molybdenum, chromium, aluminum and columbium were determined. The width of the diffusion zone from a chemical analysis standpoint was considered the distance over which a gradient in any element occurred.

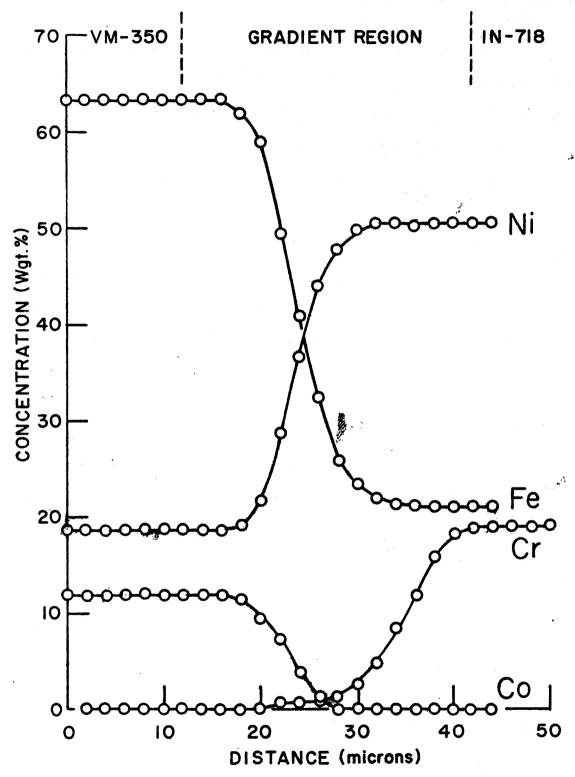


Fig. II. IN-718 / VM-350 Diffusion Bond Major Element Profiles

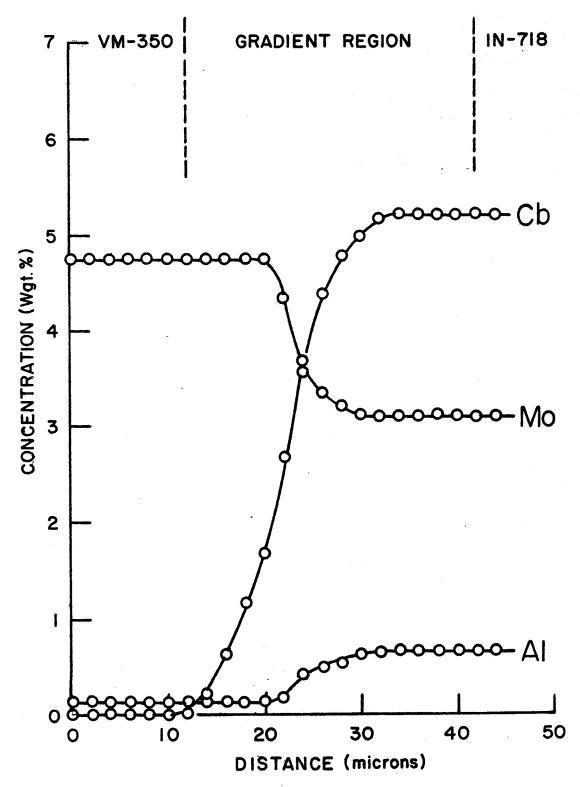


Fig. 12. IN-718 / VM-350 Diffusion Bond Hardening Element Profiles

399<

ANALYSIS OF RESULTS



VM-350/VM - 350 Couple

For diffusion bonding like materials, Owczarski, King, and O'Connor [8] have pointed out that ductility as measured by reduction in area is sensitive to the void content of the joint. They further state that void content decreases with time for a given temperature and pressure, until no trace of the original interface remains. If joint properties matching the parent material are to be obtained, grain boundary movement, which is rapid at higher temperatures, is considered essential to the bonding process [8].

For a 5 minute time interval, the VM-350 to VM-350 couple required a relatively high bonding temperature, in the neighborhood of 2150°F. The bonding pressure was approximately 10,000 psi after relaxation of stresses induced by thermal expansion. This stress was high enough to cause plastic flow of the material throughout the bonding cycle. Rough surface finishes provided for better plastic flow in the joint region, and therefore enhanced the rate of elimination of voids. Excellent bonding was achieved with failure in tension occurring outside the joint region. This clearly indicates that bond properties equal to or better than those of the base material can be achieved for this couple.

IN 718/VM350 COUPLE

Bonding of IN 718 to VM 350 showed that the width of the diffusion zone and grain size can be controlled by temperature. Figure 9 shows the temperature-width relationship to be exponential while Figure 10 indicates that the grain size of each alloy is exponentially related to the temperature, although the two alloys have significantly different grain growth rates. An

upper bonding temperature limit of 2100°F has been established for the IN 718/VM 350 couple due to the onset of intergranular melting in the IN 718 alloy. The void content of the joint also decreases with time [9] which is likely due to interdiffusion effects in the mixed alloy couple.

PROPERTIES IN 718/VM 350 COUPLE

In this dissimilar couple there is a yield and ultimate strength differential for these two alloys. In the as-bonded condition the yield strengths differ by about 20,000 psi. However, in the heat treated condition, the difference is approximately 200,000 psi. Differences in the slopes of the stress-strain curves after plastic deformation begins shows that the IN—718 will flow plastically an appreciable amount more than the VM—350 for a given load. This behavior leads to the formation of a notch effect in the joint region. The only plastic flow which can occur in this couple is limited to deformation in the weaker material before stress concentration due to the notch effect causes the sample to fail in the joint.

The long heat treatment process of approximately 24 hours results in significant strengthening of both alloys. This heat treatment in air also provides a measure of good bond integrity as oxides formed during this process did not invade the joint and split the couple apart. The ultimate strengths attained for both the as-bonded and heat treated couples indicate joint strengths comparable to the ultimate strength of IN—718 in the as-bonded and heat treated conditions respectively. The ultimate strength of the diffusion zone is also increased with heat treatment, as it is capable of supporting the high tensile loads after heat treatment.

ELEMENT DISTRIBUTION IN DIFFUSION ZONE

The width of the diffusion zone observed metallographically was approximately 13 microns. When diffusion profiles are used to establish zone width, a value of about 30 microns is determined. This approach for

determining width includes the depletion or relative immobility of certain alloying elements. However, considering the more mobile elements, agreement with the 13 micron width is observed. By fixing an arbitrary center for the joint, dependent upon the diffusion profiles, the relative degree of diffusion of the various elements can be compared. On this basis, it is noted that nickel diffuses more rapidly into the VM 350 than iron into the IN 718. Although chromium and cobalt are present throughout most of the joint, they do not diffuse considerably into the VM 350 or IN 718 respectively. The strengthening elements, columbium and aluminum, diffuse appreciably through the joint in conjunction with nickel, making strengthening of the interdiffusion zone possible by a precipitation process similar to that for IN 718. This is in good agreement with observed strengthening effects noted in heat treated couples that were tensile tested.



CONCLUSIONS

- The 'Gleeble' can be used for modeling the diffusion bonding process. This was demonstrated by successfully bonding the VM 350 to VM 350 couple.
- 2. Tensile testing and metallographic examination demonstrate that it is feasible to diffusion bond IN 718 to VM 350.
- 3. Deformation in the joint region assists bonding and is necessary for achieving consistently good bonds.
- 4. For a given time interval, the width of the diffusion zone and grain growth of both materials can be controlled during bonding primarily by variation in the temperature. An exponential relationship with an activation energy of 33,000 CAL/MOLE exists between temperature and the diffusion zone width. Separate exponential relationships exist between temperature and the grain size of the two materials.
- 5. The IN 718/ VM 350 couple fails in the joint region for room temperature tensile tests due to drastic yield strength and work-hardening differences between the two alloys.
- 6. The simultaneous heat treatment of IN 718 and VM 350 is possible and results in joints with ultimate strengths equaling the heat treated ultimate strength of the weaker alloy, IN 718.

FURTHER WORK

- Cyclic loading in tension and compression concurrently with cyclic heating and cooling should be investigated for their effects on grain growth.
- 2. The relationships between surface texture, intermediate foils, and inert or reducing atmospheres should be determined.
- 3. Shear, fatigue, and impact testing of the joint would supply important additional engineering design information.
- 4. Analysis for the presence of a strengthening mechanism in the diffusion zone is suggested.
- 5. The diffusion gradients present in the diffusion zone and base materials near the joint should be analyzed.

BIBLIOGRAPHY

- Metcalfe, A. G. "Basics of Diffusion Bonding." <u>American</u>
 <u>Machinist/Metalworking Manufacturing</u>. Vol. 114 (Oct., 1970), 97-99
- Cline, C. L. "An Analytical and Experimental Study of Diffusion Bonding." <u>Welding Journal</u>. Vol. 43 (Nov., 1966), 481s-489s.
- 3. Kaarlela, W. T. and Margolis, W. S. "Alloy Effects in the Low-Pressure Diffusion Bonding of Superalloys." Welding Journal. Vol. 46 (June, 1967), 283s-288s.
- 4. Alm, G. V. "Guide to Diffusion Bonding." <u>Materials Engineer</u>ing. Vol. 70 (Sept., 1969), 24-29.
- 5. Blank, G. F. "A Practical Guide to Diffusion Bonding."

 Materials in Design Engineering. Vol. 45 (Oct., 1966),

 481s-489s.
- 6. Bartlett, E. S. "Roll Diffusion Bonding of Titanium, Nickel and Iron-Base Alloys." New York: TMS Paper Selection No. F69-3, Metallurgical Society of AIME, 1969 (Pamphlet)
- 7. Crosby, S. R. "Diffusion Bonding of IN 718 to VM 350", M.S. Thesis, WPI, May 1972.
- 8. Owczarski, W. A., King, W. H., and O'Connor, "The Tensile

 Properties and Fracture Characteristics of Titanium Diffusion

 Welds." Welding Journal. Vol. 48 (Sept., 1969), 377s-383s.
- 9. Hirschhorn, J. S. <u>Introduction to Powder Metallurgy</u>. New York:
 American Powder Metallurgy Institute, 1969.

Summarizing Statement for Session on Modern Automotive Joining Techniques

Papers in this session dealt exclusively with metal joining techniques. One important trend that emerged from the papers presented was the increasing application of processes where practically no liquid phase forms during the joining operation and in which the presence of such a phase is not essential to the success of the process.

Perhaps the most striking feature to come out of the presentations was the tremendous diversity of production problems which find elegant solutions, in this branch of industry, through inventive and original applications of joining techniques. Finally, it was clearly established that large scale vacuum processing is no longer the exclusive preserve of the aerospace and nuclear technologies and that such processing can achieve high cost effectiveness when coupled with traditional mass production techniques.

W. M. Spurgeon Bendix Research Laboratories Southfield, Michigan 48076

N74 30942

One of the most important problems in manufacturing is how to join metal parts. In this presentation we discuss a joining process, diffusion bonding, that is receiving increasing attention from design and manufacturing engineers because of its advantages over more traditional joining methods. These advantages and its relatively few disadvantages will be outlined, along with some applications and the theory behind the process.

Let's start with the definition of diffusion bonding and the principles involved. The joining methods for metals can be classified as mechanical fastening, chemical or adhesive joining, and metallurgical joining, which in turn can be subdivided under the headings of soldering, brazing, welding and diffusion bonding. We define diffusion bonding as the unit operation of joining two pieces of the same or different alloys by making clean smooth surfaces on the metal parts, bringing them together in an inert or reducing atmosphere at a pressure and temperature high enough to exceed the yield point of the metal at the surface asperities, and holding them under these conditions until a bond of the desired strength is formed.

A bonding aid may or may not be used. If a solid bonding aid is used its functions are to increase the contact areas at the faying surfaces, to prevent oxidation of the surfaces to be joined, to provide a driving force for diffusion, and in some cases to prevent formation of intermetallic compounds. If a liquid bonding aid is used, its functions are to fill voids at the interface, to displace oxide films, to provide a driving force for diffusion and to accelerate diffusion.

Figure 1 illustrates coalescence by diffusion. Consider the problem of bonding two dissimilar alloys. In the surface of each alloy we have grains or small crystals in which the atoms are arranged in a regular fashion. When the surfaces of these grains are brought together under pressure and are heated, the atoms from one grain diffuse into the lattice of the other grain, and vice versa. We then have a situation as shown on the right side of the figure.

Figure 2 shows the pressure-temperature-time relationship for diffusion bonding. The upper limit on the temperature axis is, of course, the melting point of the lower melting of the two alloys. We can obtain sound joints so long as our pressure-temperature-time conditions are such that we are on or above the curved plane shown in this diagram.

Three stages can be discerned in diffusion bonding. Figure 3 shows the three stages for aluminum alloy 5052. In all three cases the workpiece has been heated at 1080°F. The photomicrograph on the left shows Stage 1, after heating for half an hour. Here we see that diffusion bonding has occurred only at the asperities. In Stage 2, obtained after heating for an hour, we see that half of the apparent surface area has become bonded. In Stage 3, after heating for two hours, the two parts are completely bonded.

Figure 4 shows six laminates of aluminum alloy diffusion bonded together, approaching Stage 3. The arrows indicate the original bond line.

Figure 5, taken from the literature on the subject, shows what happens when titanium parts are heated in contact under a pressure of 1000 pounds per square inch. On heating at 1400°F, only 75 percent of the contact area is bonded after 30 minutes. At 1500°F we reach 75 percent bonded condition in about 8 minutes but have not yet reached complete bonding after 30 minutes. On heating at 1600°F we obtain complete bonding after only 15 minutes. Here again, we see the relationship among time, temperature, and pressure, as they affect bond formation.

Many terms have been used to describe diffusion bonding. These include solid state bonding, cold welding, deformation bonding, thermocompression bonding, gas pressure welding, explosive bonding, extrusion bonding, friction welding, ultrasonic welding, crimping, and roll bonding.

Let's consider some typical applications of diffusion bonding. Figure 6 shows various types of hardware that have been made in our Laboratories by diffusion bonding. In some cases we bond below the yield point of the metal and in other cases above the yield point. We bond below the yield point in cases where we want to maintain accurate dimensions and tolerances, e.g., in making flueric elements and integrated circuits, miniature heaters, gas handling devices for space experiments, hydraulic devices, and heat exchangers. We can bond above the yield point in such cases as connecting cable wires to connectors, or in making shells for transpiration-cooled turbine blades.

In most cases, diffusion bonding is used as one unit operation of a multi-step manufacturing process. We have used one such process in making the various kinds of hardware described earlier. We call it the photoetched bonded laminate process and at this point I would like to describe the steps involved in it. We start by cutting an artmaster on a mechanized drafting machine. The artmaster is prepared from the engineering drawing of the part to be made and is cut on a two-part laminated plastic sheet. One part of the sheet is clear and water-white, the other part being clear and red in color. The artmaster is inspected for dimensional accuracy and then is reduced photographically on an engineering camera. If many images of the same pattern are desired they can be made on a special step and repeat machine. The end product of these operations is the tooling of the work, called an envelope transparency. It consists of two photographic films bearing the image of the pattern to be made, fastened together in registry.

While the tooling is being prepared, sheet metal strips are also being made ready. In fact, they are made into photographic plates by applying a photosensitive lacquer. Application may be by spraying, roller coating, or dip coating. The lacquer is dried, the metal sheets are sandwiched between two parts of the envelope transparency, and the assembly is exposed on both sides to ultraviolet light. The light passing through the transparent parts of the envelope cause the lacquer to harden and become insoluble. The lacquer under the opaque parts of the transparency remains soluble in organic solvents. After exposure, therefore, the plate is developed by immersion in an organic solvent. After a period of time, parts of the metal sheet will be bare and other parts will be coated with lacquer in the desired pattern. The coated sheet is now placed in a spray etcher. The bare metal is attacked and removed by the etchant and the metal under the lacquer remains in place. The etched sheets come through a rinse chamber and proceed out the other end of the spray etcher. The lacquer is then removed with a stripping agent. Figure 7 shows a metal sheet after etching. It contains the pattern for a signal processing network of flueric elements.

In the next step the laminates are stacked and aligned in a laminar flow hood, using reasonable precautions to keep the parts clean. The assembly is then fastened together in a thermal expansion press. Finally, it is placed in a vacuum furnace or in a furnace with a hydrogen atmosphere and diffusion bonded. After removal from the furnace the parts are then tested.

The photoetched bonded laminate process has a number of advantages. First, we can make intricate, close-tolerance passages in single blocks of metal. Second, we can make structures with this process which can not be made in any other way. Third, we can use alloys selected for resistance to service environments rather than for ease of fabrication. Fourth, we can use low cost tooling. Fifth, we can provide quick delivery, since the tooling is relatively easy to make. Sixth, the process is capable of high quantity production. Seventh, it requires only a low capital equipment investment.

Summarizing the steps for the diffusion bonding operation in this process: we have only to smooth the faying surfaces, clean them, apply the bonding aid (if one is used), clean the sheets again, assemble the piece parts, and heat under pressure.

Figure 8 shows an array of identical patterns used in making flueric elements. With a stack-up of such laminations we can make forty-five or more elements at a time.

Figure 9 shows a radiograph of a flueric integrated circuit, an adder for an air data computer. This is a single block of metal measuring about 4 by 5 inches and about 1/8 of an inch in thickness, made from stainless steel sheets. It contains extremely intricate passages in which close tolerances must be maintained. It is difficult to think of any other process by which this device can be made from metal.

Figure 10 shows a cross-section through the adder, which was made of diffusion bonded stainless steel. The arrows indicate the original bond lines. Note how the grain boundaries have crossed these original lines.

Figure 11 shows an integrated circuit for a bleed control used as part of an aircraft engine fuel control. It shows the various types of laminates used and what the final stack-up looks like. Figure 12 shows the bleed control or fluidic computer in place.

Figures 13, 14, and 15 show photomicrographs of some other alloys which have been diffusion bonded in our Laboratories. They include Inconel 600, diffusion-bonded TD-Nichrome, and diffusion-bonded chromium. In the case of diffusion-bonded TD-Nichrome we see one of the advantages of diffusion bonding, namely, that we do not destroy the dispersed oxide structure in making the bond. In the case of diffusion-bonded chromium, the black spots are particles of magnesium oxide added to the alloy to enhance its ductility.

We have also made heaters and heat exchangers by this process. Figure 16 shows on the right side how we make heater elements by etching Nichrome sheets. The arrow on the left illustrates how the elements are coated with aluminum oxide insulation, sandwiched into a frame, and then covered with base and cover plates which are bonded together to make the complete heater. Figure 17 shows the reaction bed for an oxygen generator made by essentially the same process. Figure 18 shows six aluminum tubes diffusion bonded together in a heat exchanger configuration.

We have used miniature heaters in making devices for space experiments. Figure 19 shows laminations that have been used for making diffusion bonded gas handling columns. Tracing through the arrow you can see the various steps used in making the final column which is shown in the upper right hand corner. The tabs extending from the sides are the contacts for the heaters built into the column. Figure 20 shows a gas chromatograph designed and built for space experiments. The lower part shows the various laminates used in making it. The first and fourth laminates have spiral half-cylinders etched into them. The second laminate is a frame for one of the heating elements which is the third item shown on the lower part. The complete assembly is shown on the upper part of the figure. Compare the size of this chromatograph with that of a laboratory gas chromatograph (Figure 21). The comparable part is the oven shown in the middle.

Now let us turn to some parts made by diffusion bonding above the yield point. The first example is cable wire-connector joining. In assembling an electrical cable one of the main problems is how to join the wires to the contacts. Normally this is done by soldering or crimping. With the experimental yield point bonder shown in Figure 22 we have demonstrated that these joints can also be made successfully by diffusion bonding. When we operate above the yield point of the

metal only half a second is required to make one of these joints. Figure 23 shows a photomicrograph of a joint prepared by yield point bonding of copper wire to a gold-plated brass contact.

We have also made shells for transpiration-cooled turbine blades by diffusion bonding. Figure 24 shows an example of one of our materials called PoroloyR. It is made by winding flattened wire on a mandrel according to a predetermined pattern and then bonding the wires together. The conical or cylindrical structures so obtained can be cut open and made into sheet metal; from this, porous shells, such as are shown on the right in Figure 25, can be made in air foil form, ready for fitting onto the structure shown on the left. Figure 26 shows a photomicrograph of the bonds in Poroloy made from an alloy called GE 1541. These are in the as-fabricated condition and illustrate both the nature of the bond and the nature of the pores. Figure 27 shows bonds in Poroloy made from the same alloy after it has been oxidized in air at 2000°F. As you can see, the pores are still open, the oxide is adherent, the bonds are sound. One of the virtues of the alloy selected is that the oxide film is protective and adherent. It does not spall or flake off and thus plug the pores of the material. Figure 28 shows the air flow in Poroloy before and after oxidation, and as you can see the permeability drops initially to about 80 percent of its initial value and then stays constant for as long as 600 hours of exposure at 1800 to 2000°F. This work has been described in a recent NASA report.

Figure 29 shows some of the alloys that have been bonded in our Laboratories. Note that they include heat-resistant alloys and aluminum alloys, both of which form adherent, refractory, stable, high-melting oxides. The problem in joining these alloys, of course, is to remove the oxide film and to keep it off until the bond is formed.

Now let's consider the advantages of diffusion bonding. First of all there are advantages insofar as mechanical properties are concerned. We can join most types of alloys. The joint is as strong as the parent metal. The final part has uniform response to heat treatment, and in general we can obtain better properties in the joint with active metals such as titanium.

There are also advantages from a chemical standpoint. There are no dissimilar metals introduced into the joint as is done in brazing. The joint is stress-free. Both of these are advantages if the part is exposed to a corrosive environment.

There are advantages for the designer in using diffusion bonding. He can join dissimilar metals. He can make thick sections by building up laminations, or he can join thick sections. The process is ideally suited to joining many thin sheets together and can also be used to join tubes and make various complex shapes. No weight is added as is the case when fasteners are added. Diffusion bonded joints are compatible with coatings, an important consideration particularly when the use of heat-resistant coatings is contemplated. Tolerances, of course, can be readily maintained.

The manufacturing engineer, too, finds many advantages in use of this process. He gets stress-free, ductile joints. He can make many joints at one time. Unlike brazing, he can recycle if he uses diffusion bonding. No finishing operations are required, such as flash removal. The process lends itself to mechanization.

Here we present some guidelines for design and manufacturing engineers. Diffusion bonding should be considered if we have workhardened, solution-strengthened, precipitation-hardened, dispersionstrengthened, or fiber-strengthened alloys to be joined and the properties of the alloys must be retained. It should be considered when structures with large cross sections must be made, having fine grains throughout, or when active metals such as titanium must be joined, or when dissimilar metals must be joined without forming intermetallic compounds. Diffusion bonding should be used when dissimilar metal combinations such as brazed joints can not be used because of the danger of corrosion, or when the joints must be coated, especially for high temperature service. It should be used when stressfree joints are required, or when reduced assembly weight is desired. Diffusion bonding is a good method to use when many lap joints are required in the assembly, especially laminations, or when structures must be made with intricate, close-tolerance channels or cavities. It should be used when weld structure spatters are not permissible, or when close tolerances must be held in the joint region.

Summarizing then, in its simplest form diffusion bonding is accomplished by placing clean metal surfaces together under a sufficient load and heating. The natural interatomic attractive force between atoms transforms the interface into a natural grain boundary. Therefore, in principle, the properties of the bond area are identical to those of the parent metal. Other advantages of diffusion bonding over conventional methods of bonding include freedom from residual stresses, excessive deformation, foreign metals, or changed crystal structures. Theoretically, any metal or metal combinations can be bonded. In our Laboratories, stainless steels, nickel-base superalloys, and aluminum alloys have all been successfully joined. Complex hardware, including integrated flueric devices, jet engine servovalves, and porous woven structures have been fabricated. The processing involved has been discussed, along with such theoretical considerations as the role of metal surfaces, the formation of metal contact junctions, and the mechanisms of material transport in diffusion bonding. Guidelines for utilizing the theoretical principles in joining operations were also presented.

COALESCENCE BY DIFFUSION

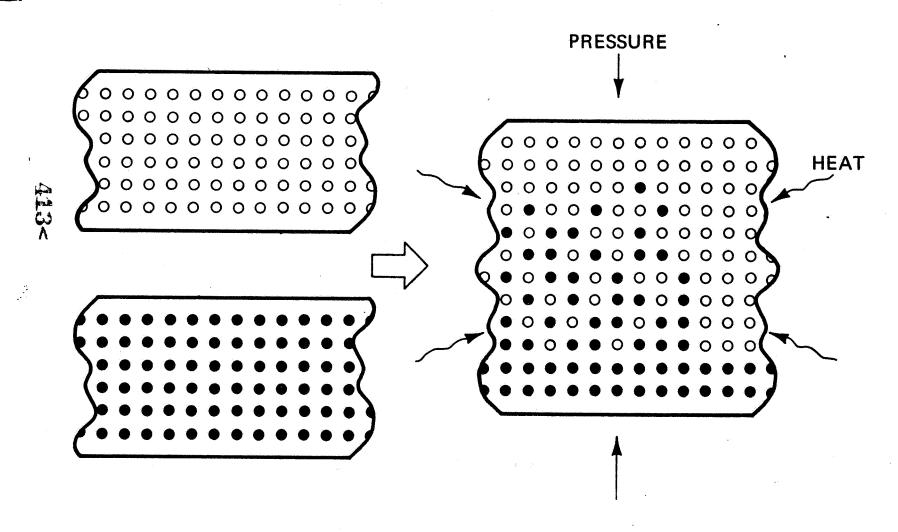


Figure 1.

PRESSURE-TEMPERATURE-TIME RELATIONSHIP FOR DIFFUSION BONDING

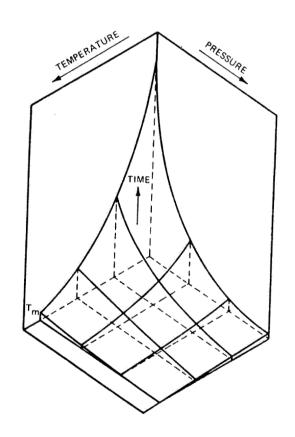
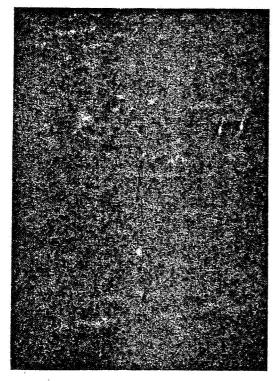
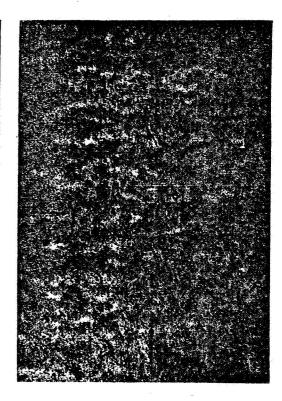


Figure 2.

THREE STAGES OF DIFFUSION BONDING (Aluminum Alloy 5052)





STAGE I 1/2 HR. AT 1080°F (500 X)

STAGE II 1 HR. AT 1080°F (500 X)

STAGE III 2 HRS. AT 1080°F (500 X)

Figure 3.

DIFFUSION-BONDED ALUMINUM ALLOY

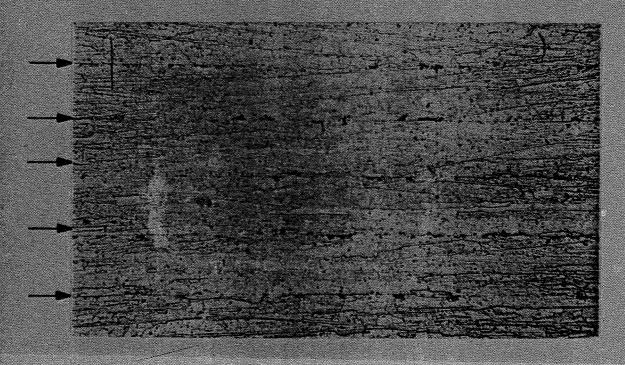


Figure 4. - Diffusion-bonded aluminum alloy (arrows indicate bonding interface).

BONDING TITANIUM

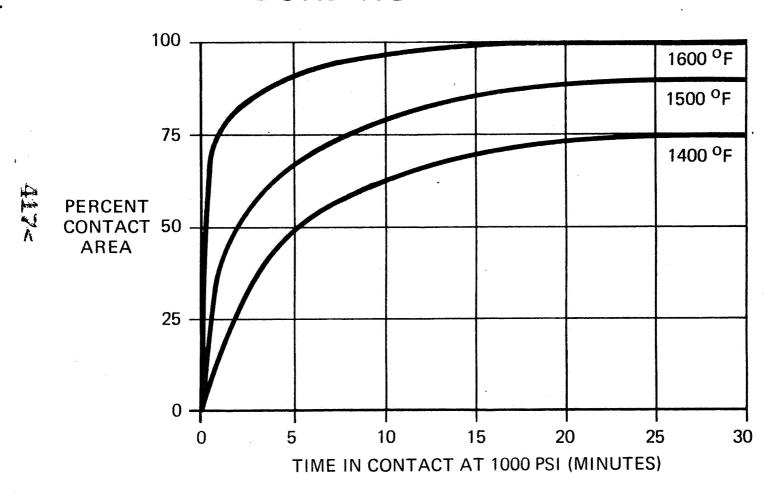


Figure 5.

HARDWARE MADE BY DIFFUSION BONDING

BELOW THE YIELD POINT

FLUERIC ELEMENTS AND INTEGRATED CIRCUITS
MINIATURE HEATERS
GAS HANDLING DEVICES FOR SPACE EXPERIMENTS
HYDRAULIC DEVICES

HEAT EXCHANGERS

ABOVE THE YIELD POINT

CABLE WIRE CONNECTOR JOINING
SHELLS FOR TRANSPIRATION-COOLED TURBINE BLADES

SIGNAL PROCESSING NETWORK ETCHED PROFILE

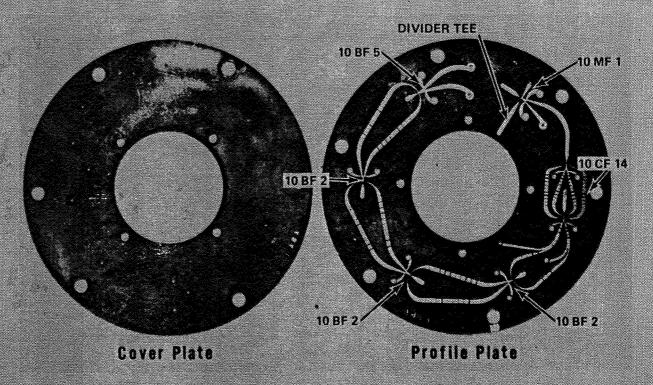


Figure 7.

ARRAY OF IDENTICAL PATTERNS

-									
	X				**************************************			**************************************	
100 E	X	STATE OF THE PROPERTY OF THE P	₩ inta	***	\$\frac{1}{2}\$	944 ***	349	\mathbb{X}	\mathbb{X}
	X		inch.	;ii4		$\frac{1}{2}$	$\frac{1}{2}$	*	*
		X			\$14F	SIG **	9848 ***********************************	ig W	

Figure 8.

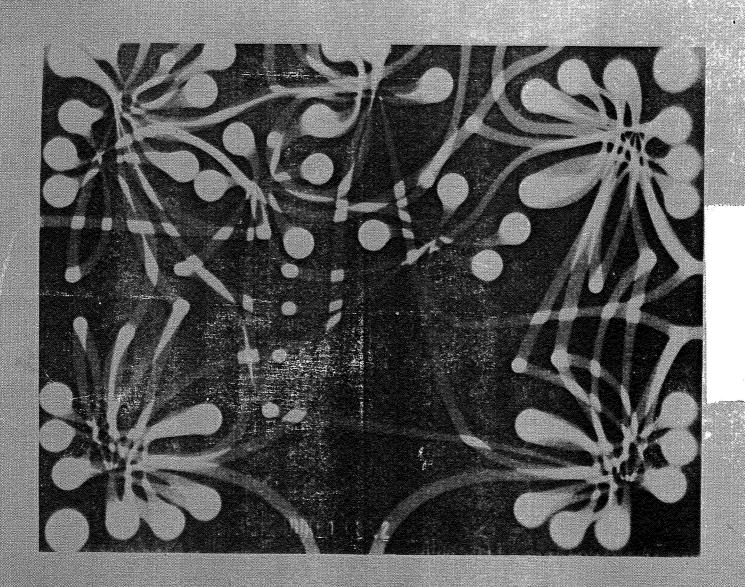


Figure 9. - Radiograph of Flueric integrated circuit.

4222

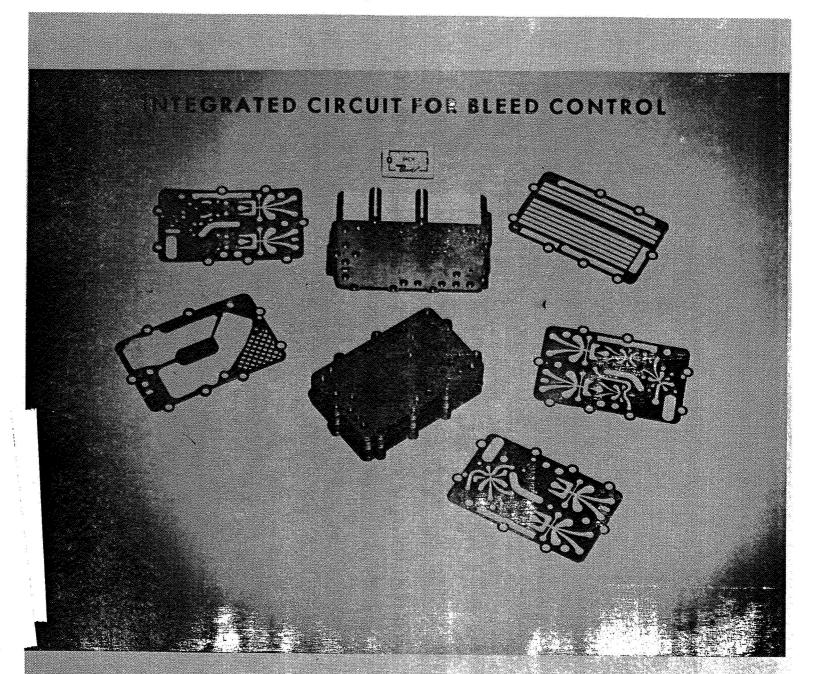


Figure 11.

COMPRESSOR BLEED CONTROL

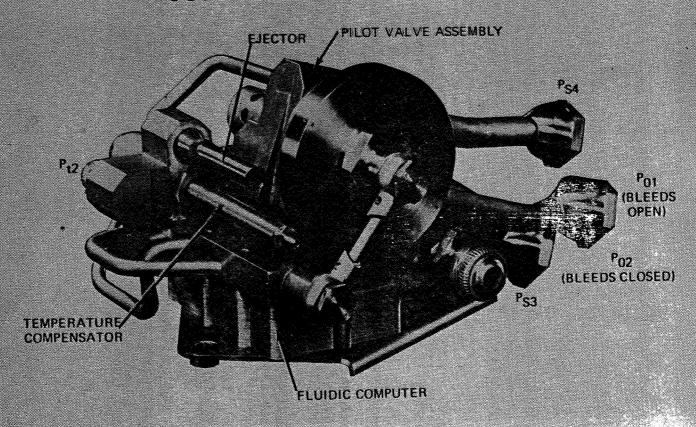


Figure 12.

INCONEL 600

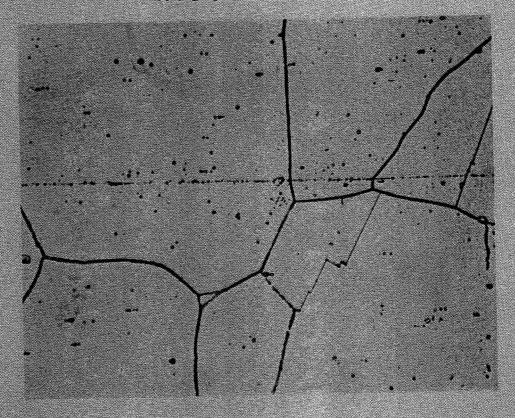
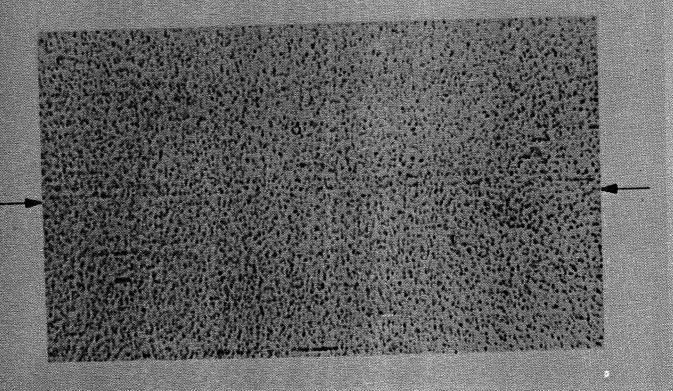
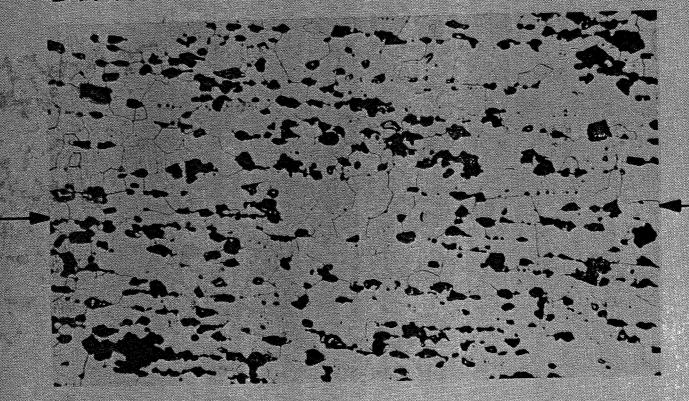


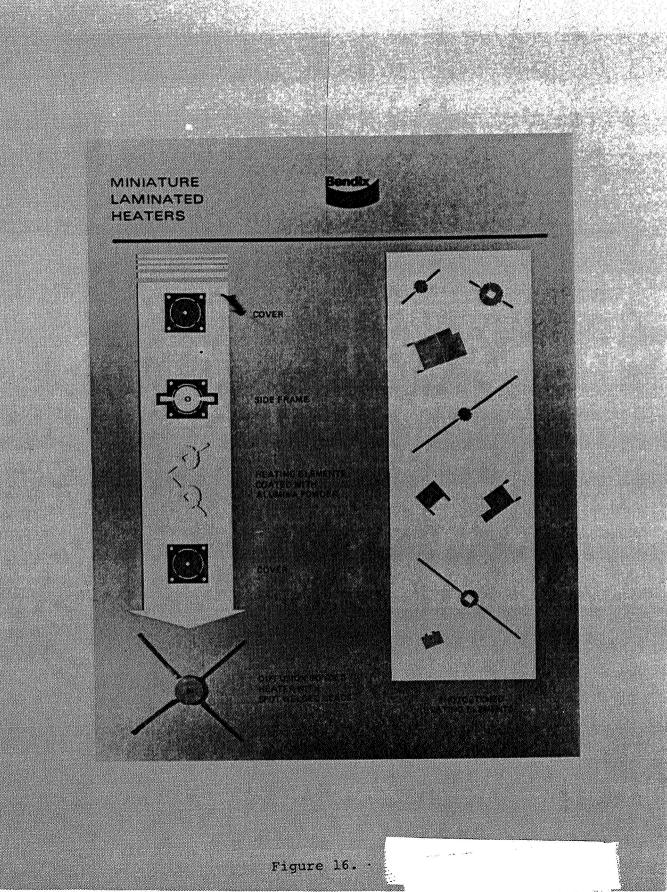
Figure 13. - Diffusion-bonded Incomel 600.

DIFFUSION—BONDED TD NICHROME



DIFFUSION-BONDED CHROMIUM





428<

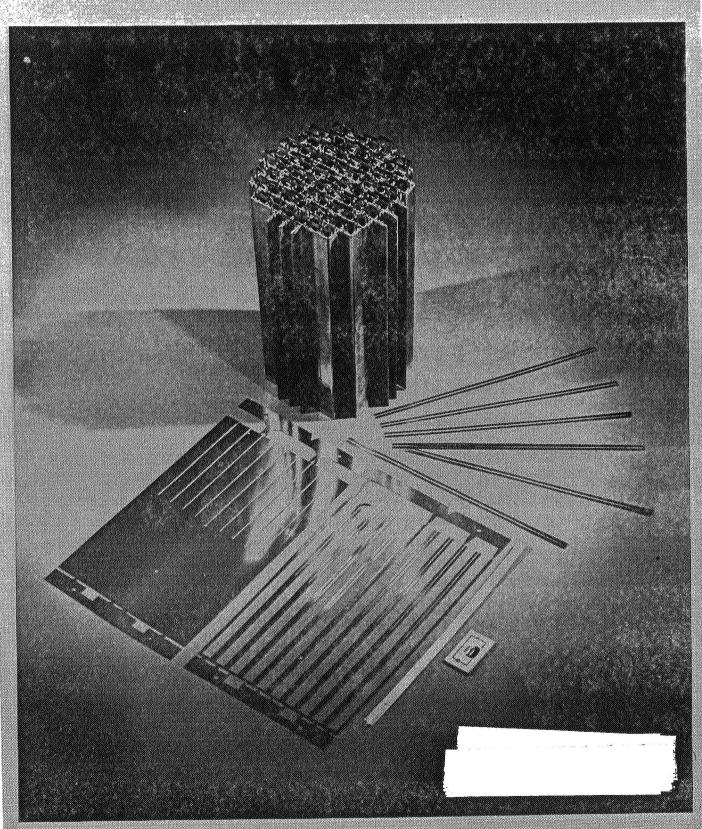


Figure 17. - Reaction bed for oxygen generator.

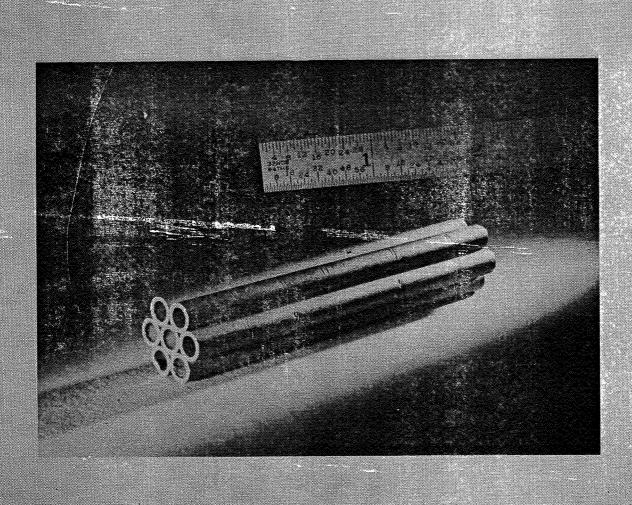


Figure 18. - Diffusion-bonded aluminum tubes.

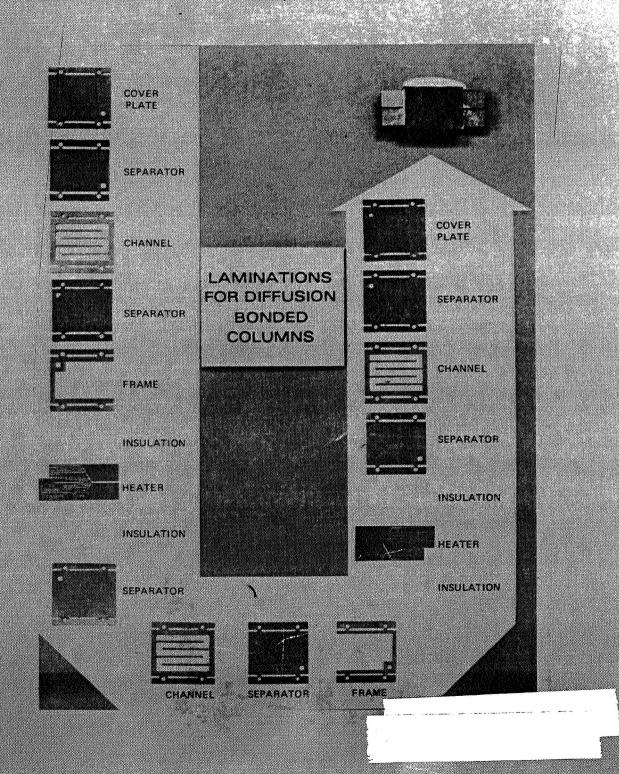


Figure 19. - Laminations for diffusion-bonded gas-handling columns.

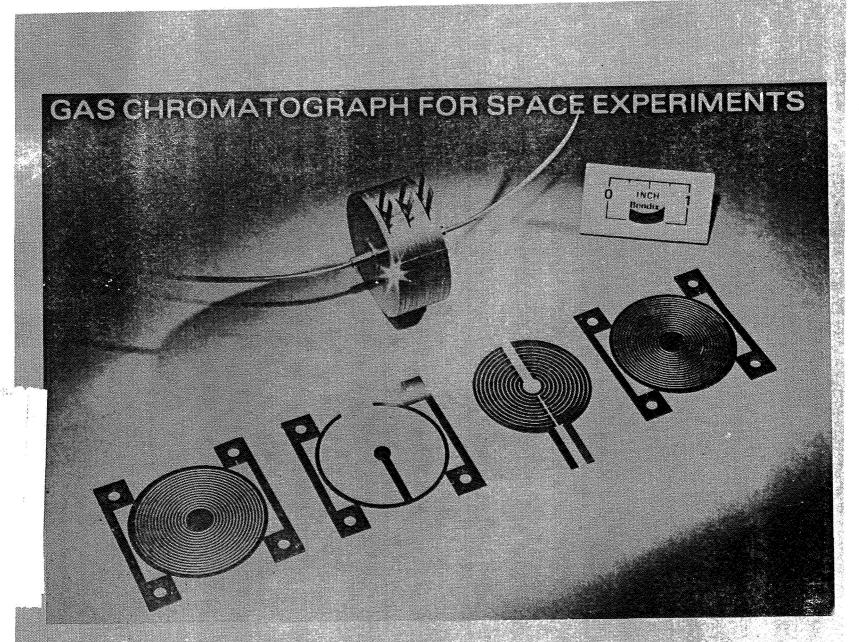


Figure 20.

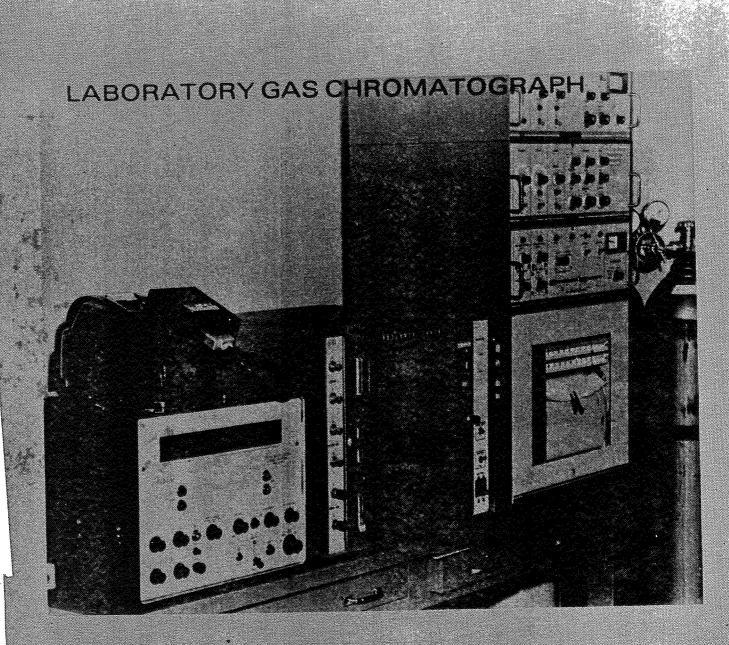


Figure 21.

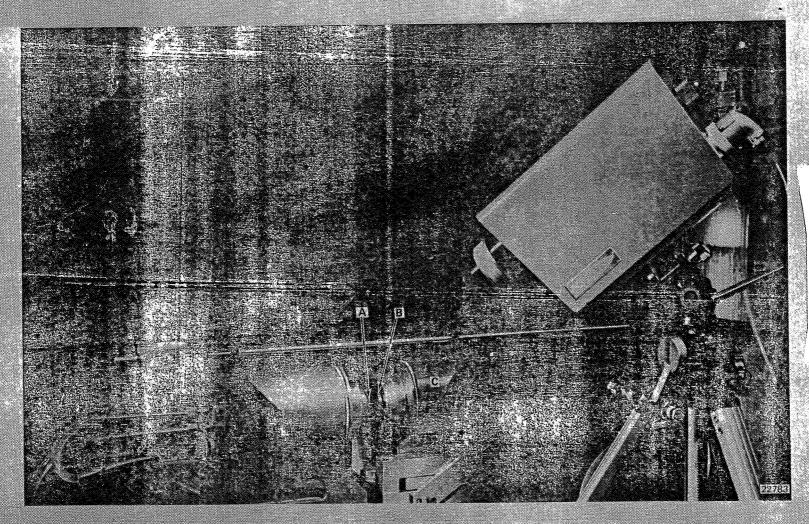
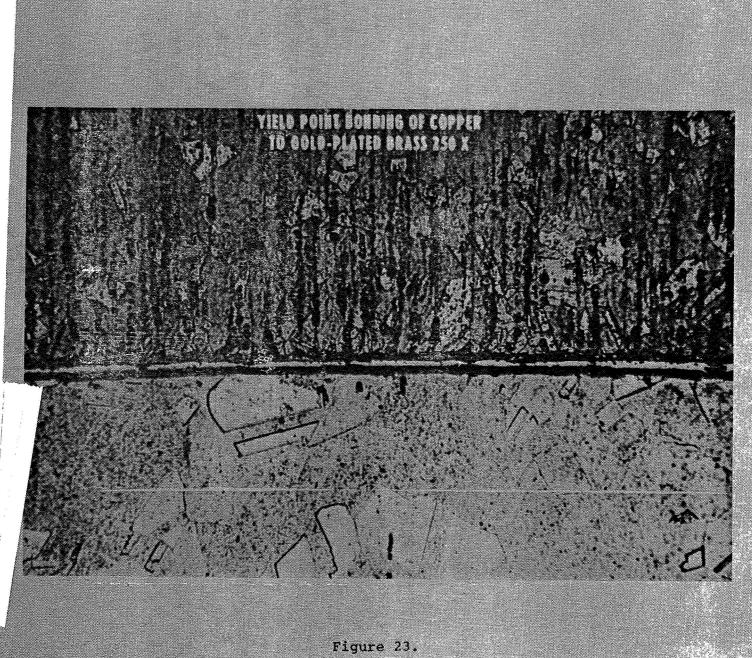


Figure 22. - Experimental Yield-Point Bonder
A - Workpiece
B - Chuck
C - Sliding quartz sleeve for atmosphere control



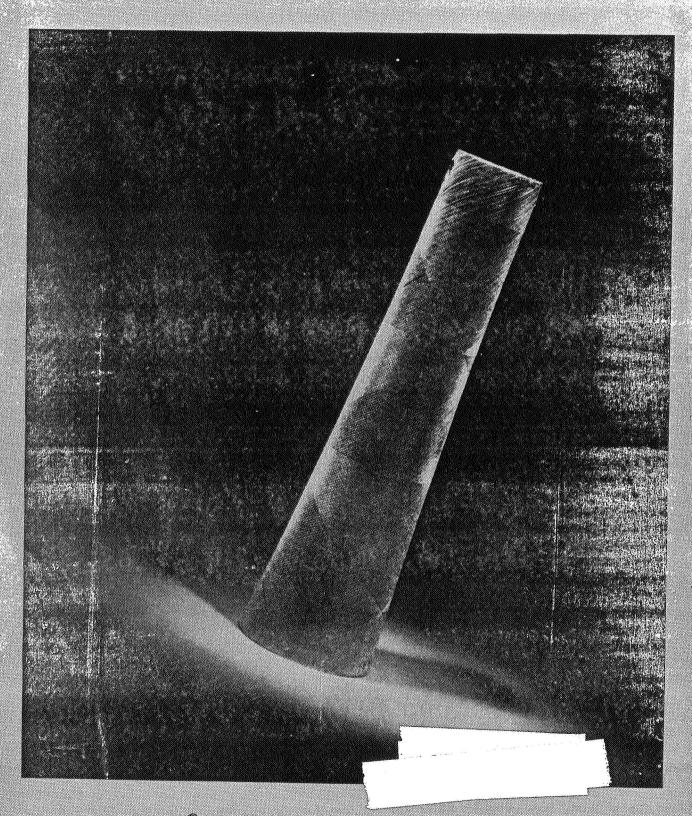


Figure 24. - Poroloy ® - flattened wire wound on mandrel and diffusion-bonded.

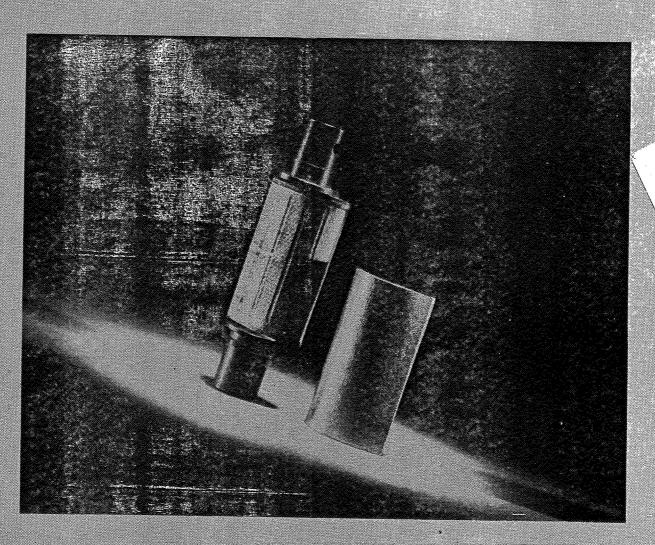
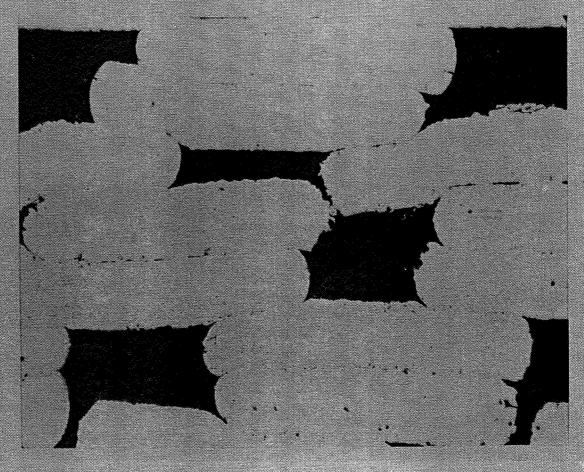
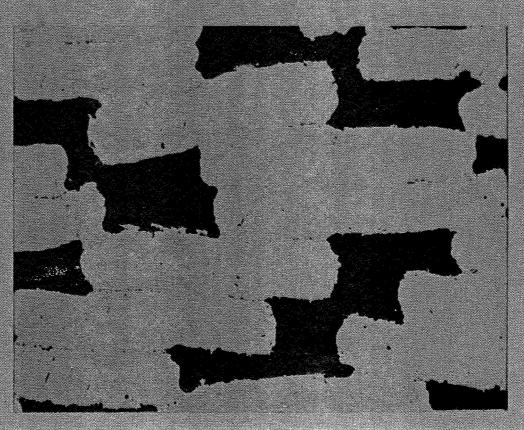


Figure 25. - Turbine Engine parts made from Poroloy $^{\circledR}$.

BONDS IN POROLOY MADE FROM GE-1541 AS FABRICATED



BONDS IN POROLOY MADE FROM GE-1541 AFTER OXIDATION, 600 hr, 2,000° F



AIR FLOW THROUGH POROLOY BEFORE AND AFTER OXIDATION

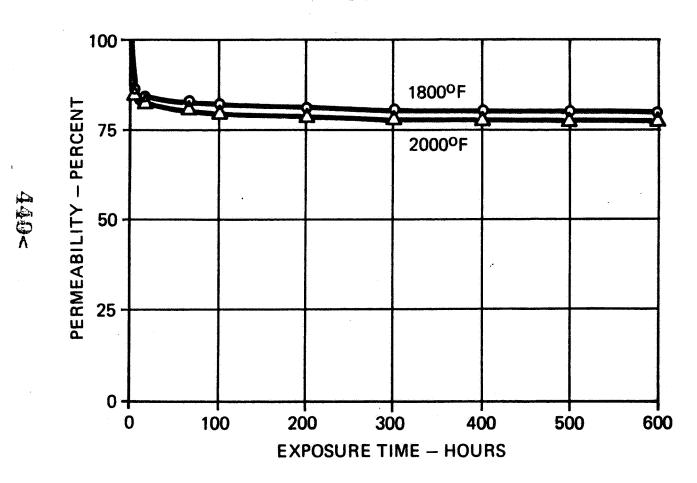


Figure 28.

ALLOYS BONDED

HIGH TEMPERATURE ALLOYS		COPPER ALLOYS
hair pair pauri	INCONEL 600	COPPER
	GE 1541	BRASS
	RENÉ 41	MONEL
	HAYNES 25	
	HOSKINS 875	
	UDIMET 500	
	STAINLESS STEELS	•
DISSIMILAR METALS		ALUMINUM ALLOYS
	NICKEL - 304 SS	2024
	COPPER - BRASS	5052
	COPPER - CAST IRON	6061

Figure 29. - Alloys bonded at Bendix Research Laboratories.

N74 30943

ULTRAPULSE WELDING: A NEW

JOINING TECHNIQUE

David G. Anderson
Director of Research and Development
The Quanta Welding Company
Troy, Michigan

June, 1972

ULTRAPULSE WELDING: A NEW JOINING TECHNIQUE

The Ultrapulse* welding (UPW) process is a relatively new form of resistance welding. UPW can be used for spot welding but most applications have been in the projection and butt welding areas. The purpose of this paper is to describe the UPW process as it applies to the automotive industry. The principles of UPW will be discussed, followed by a description of a number of automotive applications and finally by some UPW advantages and its limitations.

PRINCIPLES OF ULTRAPULSE WELDING

The Ultrapulse process is a resistance welding process that utilizes unidirectional current of high magnitude for a very short time with a precisely controlled dynamic force pulse. Peak currents of up to 220,000 amperes for two to ten milliseconds are used with synchronized force pulses of up to nine thousand pounds. Welding force and current pulses for a typical UP weld are shown on Fig. 1. The welding current passing through the relatively high resistance of the interface between the parts that are being joined results in highly localized heating. The

combination of localized heating at the mating surfaces and the force application results in the parts being forged together into a solid-state weld.



The short duration of the welding current and accurate control of all process elements limit heat generation to the immediate area of the interface being welded. The weld time is not long enough to cause the metal surrounding the welded interface or the electrodes to be heated to a high enough temperature for significant metallurgical changes to take place. The solid-state weld nearly eliminates the melting and mixing of the parts being joined at the weld interface. The unique localized heating at the interface also lessens the extensive grain size and phase changes normally encountered in resistance and arc welding. This makes it possible to join a variety of heat-treated and heat-sensitive alloys and dissimilar ferrous metals, with no deleterious effects on their physical properties. Dissimilar metal thicknesses are also welded with relative ease compared to other processes.

Conventional resistance welding is accomplished at lower welding current, but requires weld times on the order of fifty to one hundred times as long as Ultrapulse. These longer times result in greater heat losses, melting at the interface, metallurgical

transformations in the area surrounding the weld, distortion of the weldment as a result of extensive heating and rapid cooling, and heating of the electrodes.

AUTOMOTIVE APPLICATIONS OF UPW

UPW has been applied successfully to a variety of automotive parts. These applications have involved a number of materials, material combinations and joint designs. Examples which are cited here are typical of this family of parts.

Valve Lifter

This part consists of a cylindrical body (approximately one inch in diameter and two inches long) and a tip (approximately one inch in diameter and 0.1 inches thick). The body is made by conventional powder metallurgy techniques, using iron powder and graphite. An annular projection on the as-sintered body provides the necessary concentration of welding force and current for UP welding. The tip is a white cast iron disc; both planar surfaces are ground to assure parallelism and to provide a flat surface for welding.

Each weld pulse produces a welded part; weld time is approximately 0.010 seconds. The weld is angularly continuous (leak-tight) and is about 0.080 inches wide. The shear strength of the weld is 8,000 pounds. A photograph of the weld interface is shown on Fig. 2.

Automatic Choke Thermostat

One car manufacturer uses an automatic choke thermostat which includes a die-cast aluminum base and a machined thermostat shaft of aluminum alloy. The shaft is presently welded to the base by the manual gas tungsten-arc ("TIG") welding process. Shortcomings of this method are: (1) the gas tungsten-arc process is slow, (2) considerable operator skill is required, (3) a prior crimping operation is required to locate the shaft and to prevent its motion during welding, (4) expulsion occasionally is ejected into the coiled thermostat and produces a reject-part, (5) arc shielding and exhaust of fumes are necessary, and (6) the heat from the arc may be sufficient to move the thermostat from its calibrated position.

Ultrapulse welding has been used successfully for this application.

Both ends of the shaft were UP welded in one weld pulse, without
the need for prior crimping. A photograph of thermostats made
by the two methods is shown on Fig. 3. The left part was crimped
and then GTA welded; the right part was UP welded.

Distributor Cam

This part consists of two low carbon steel components: a machined tubular shaft and a flat stamping with a bored hole.

The relative angular position of the stamping on the shaft is critical. The manufacturer presently uses interference dimensions to produce a press-fit. The mechanically-fastened parts are then brazed.

The alternate assembly method employs UPW. The weld tooling locates the parts, eliminating the press-fit requirement. Gross production rate is estimated to be 1,500 parts per hour. A photograph of a UP welded distributor cam is shown on Fig. 4.

Connector

Connectors for fluid lines are conventionally made by three methods: (1) machining in one piece, (2) brazing two component parts, or (3) resistance welding two component parts. The first method permits the use of free-machining steels, but costs may be relatively high, due to the larger volume of metal that must be removed by machining. Connector components made from free-machining steels are difficult to resistance weld, so machining costs are higher for resistance welded connectors.

UP-welded connectors can be made from free-machining steel (e.g. AISI-1108). This permits the use of lower cost components and a high production rate joining technique. A typical UP-welded connector is shown on Fig. 5.

Attachment to Glass Plate

Attachments of metal parts to glass has been achieved with UPW. This is done by inserting a rivet-shaped stud into a hole in the glass and UP welding the stud end to a metallic part, thus securing the metallic part to the glass. The welds are achieved with these effects: (1) the glass is not damaged by the low "weld heat", (2) the stud remains at near-room temperature except in the immediate region of the weld (i.e. the stud diameter is unchanged), and (3) the shortening of the stud during welding is slight and repeatable (0.005 to 0.006 inches is typical). See Fig. 6 for a photograph of a window hinge attached to tempered glass plate by the UPW process.

Chrome-Plated Steel

Chrome-plated steel parts have been UP welded without damaging the plating. This permits the twin economies of lower plating costs (e.g. plate only one part) and high speed welding capability. Fig. 7 shows two coupons that have been UP welded. Both coupons are SAE-950 steel approximately 0.12 inches thick. The upper coupon was plated before welding; the lower one was not plated. A projection was formed in the non-plated coupon prior to UP welding. The shear strength of the weld was over 3,000 pounds.

Attachment to Vinyl-Coated Steel

UPW has been used to weld to vinyl-coated steel sheet without damaging the decorative vinyl. Such a weld is shown on Fig. 8. An annular projection was machined on the nut prior to welding. In this example, the weld diameter was 0.35 inches and the thickness of the steel sheet was 0.040 inches.

Exhaust Valve Tip

The requirement is to produce an exhaust valve with a hardened $R_{\rm C}$ 50 tip on the stem. The exhaust valve is an austenitic steel; the tip is AISI-8740 alloy steel. The conventional method employs a resistance welder to projection weld an annealed tip to the end of the exhaust valve stem. The tip is subsequently induction hardened, prior to the final machining operations.

Ultrapulse welding has been used to weld pre-hardened tips to these exhaust valve stems, without tempering the wear surface of the tip. Fig. 9 shows a UP-welded exhaust valve in the as-welded condition. Weld microstructure is shown on Fig. 10. The lighter region is the valve stem material; the darker region is the tip. The extremely narrow heat affected zone is indicated by the width of the tempered zone in the tip (less than 0.008 inches).

ADVANTAGES OF ULTRAPULSE WELDING

The UP-welded products which have been described in this paper embody several of the product advantages of UP welding. These advantages are summarized here, as well as the characteristic advantages of UP equipment.

Weld Finished or Semi-Finished Parts

The high thermal efficiency and low heat input of UPW permits finished (e.g. ground surface) parts to be welded. This is in contrast with other welding processes which may require weld flash or upset weld metal to be removed. The welding of finished parts permits substantial reduction of machining costs. In many instances, parts can be case-hardened and finish-ground prior to UP welding. This permits selective hardening without the use of stop-offs and more efficient use of available furnace space.

Dimensional Accuracy of As-welded Parts

The very rapid heating rate and the subsequent localized heating zone produce dimensional changes only in the immediate area of the weld. The width of a typical dimension-affected zone (DAZ) is 0.020 inches. The narrow and reproducible DAZ enables high-tolerance parts to be UP welded to a high degree of accuracy.

This accuracy includes both the location of the weld and the overall length (or thickness) of the welded assembly.

As an example of the dimensional capabilities of the UPW process, consider the following example. Two parts are finish-ground before UP welding. In a sampling of 100 parts, the as-welded parts were concentric within 0.0055 inches total indicator reading. Axial shortening of the parts during welding varied from a minimum of 0.0057 inches to a maximum of 0.0069 inches, a range of 0.0012 inches. The parts were also measured for perpendicularity. The total indicator reading at a diameter of one inch ranged from a minimum of 0.0002 inches to a maximum of 0.0012 inches.

Unusual Metal Combinations

Some metal combinations which are non-weldable or difficult to weld with most other processes can be UP welded. Some of these unusual combinations are listed below.

- 1. Carbonitrided low carbon steel to "hardenable" cast iron.
- 2. Sintered iron powder to white cast iron.
- 3. Carburized low carbon steel to low carbon steel.
- 4. A "Stellite" alloy to gray cast iron.
- 5. Low carbon steel to gray cast iron.
- 6. Chrome-plated SAE-950 steel to bare SAE-950 steel.

- 7. Re-sulfurized free-machining steels.
- 8. Porous low-density nickel structure to stainless steel.
- 9. Austempered AISI-8620 to cold-drawn low-carbon steel.

Weld Near Heat-Sensitive Materials

Various thermally-sensitive assemblies have been successfully welded by the UP process. Five of the parts which were described earlier in this paper are examples of UP-welded parts which are heat sensitive (see Figs. 3,6,7,8,9, and 10).

High Production Rates Possible

The UP weld is accomplished so quickly (e.g. 0.010 seconds) that welding time is not a significant portion of the cycle time of the welding system. The handling of parts (loading and unloading) is usually the most significant time element. The use of production aids, such as parts' feeders and dial index tables, can permit welding rates of 1,500 parts per hour.

Little Need For Water Cooling

Conventional resistance welding equipment requires water cooling of at least three components: the welding electrodes, the secondary windings of the welding transformer, and the switching devices, whether they be ignitron tubes or silicon-controlled rectifiers.

UPW equipment does not require water cooling of any component for most applications.

Low Input Power Demand

The UPW power supply is the stored-energy type. The system capacitors are charged to the desired voltage and the switch-gear turns "on" at the appropriate time to deliver the stored energy to the pulse welding transformer. The procedure is then repeated. This technique permits the capacitors to be re-charged during the parts' unloading and re-loading portions of the welding cycle. The demand placed on the power system by the UP welder is thus much lower than a conventional direct-energy resistance welder. Five KVA is a typical power demand for a UPW system; 150 KVA is typical for a conventional resistance welder.

Power Line Voltage Not Critical

The power line voltage has an important effect on the quality of welds made with conventional resistance welders. For example, a decrease of 10 percent in primary voltage will produce a 19 percent decrease in weld heat. This is not the case in UPW, however. The UPW power supplies charge to the same final welding voltage, even though the power line voltage may vary by 20 percent from its nominal value.

No Power Line Voltage Transients Caused by UPW

Other resistance welding processes may cause substantial "dips" in line voltage or put "spikes" back onto the power lines. UPW causes neither effect. The relatively slow capacitor-charging time of UPW (two seconds minimum) allows the line voltage to remain quite stable. Also, the UPW system is isolated from the power line during the duration of the weld pulse.

Good Power Factor

In conventional resistance welding, the impedance of the secondary (welding) circuit determines the power factor. Such power factors are usually quite unfavorable (e.g. 20 percent lagging) due to the relatively large value of inductive reactance in the secondary circuit. Power factor correction capacitors or synchronous motors may then be necessary to raise the power factor level of the power system to a more favorable level.

UPW equipment does not produce such a problem. The load that the power line "sees" is the capacitor-charging circuit. A typical UPW power factor is 90 percent lagging, so no power factor correction is required.

Weld Area

UPW requires a certain current density to produce a satisfactory weld in a given application. The UPW system has an upper limit of welding current. For ferrous materials the maximum area that can be welded with one pulse is approximately 0.25 square inches. This value cannot be attained in some applications, where part resistance or welding circuit inductance lowers the maximum current that can be produced.

Good Fit-Up Required

"Fit-up" is a measure of the quality and consistency of the two surfaces which are to be welded. Good fit-up is required for UPW, since the degree of melting and upsetting that occurs is slight. An as-cast surface on a sand casting is too rough to produce good quality UP welds. Surface finishes whose roughness exceeds 120 micro-inches RMS is also too rough for many applications.

Part Design

The design of the parts which are to be welded must permit the application of the necessary force and current magnitudes to the weld joint. The resistance of the parts determines the maximum current that can be produced. The structural properties of the

parts determine the maximum force that can be applied to the parts without excessive permanent deformation occurring.



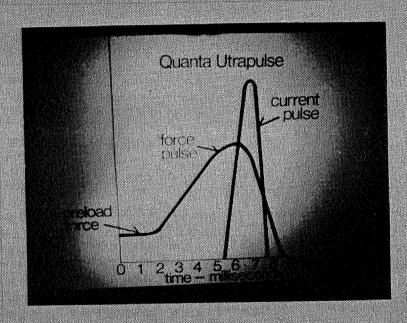
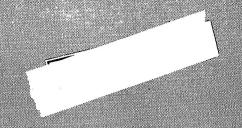


Fig. 1. Welding force and current pulses for a typical Ultrapulse weld. Note that the abscissa units are in milli-seconds.



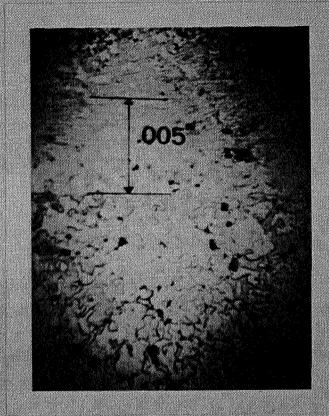


Fig. 2. Photomicrograph of an Ultrapulse-welded valve lifter. The lower material is the sintered iron body; the upper material is a white cast iron tip. Magnification is approximately 200x.

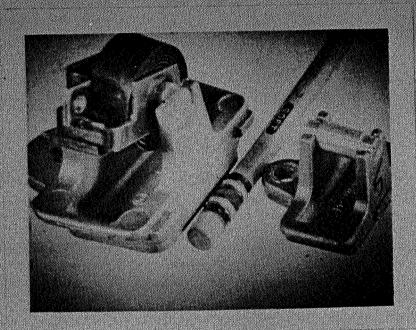


Fig. 3. Similar automatic choke thermostat components that were joined by different methods. The shaft was held in place in the left assembly by crimping; manual gas tungsten—arc welding was then used to weld one end of the aluminum shaft to the die—cast aluminum body. Both ends of the shaft were Ultrapulse welded in one pulse to the body on the right.

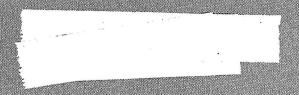




Fig. 4. An as-welded distributor cam that was welded by the Ultrapulse welding process.

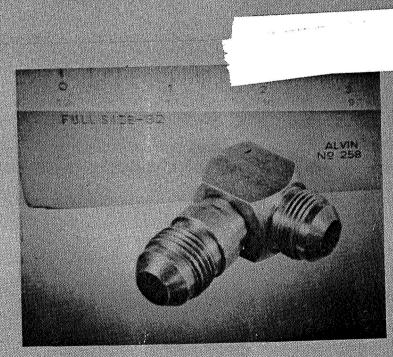


Fig. 5. An Ultrapulse-welded connector. Both parts are free-machining steel.

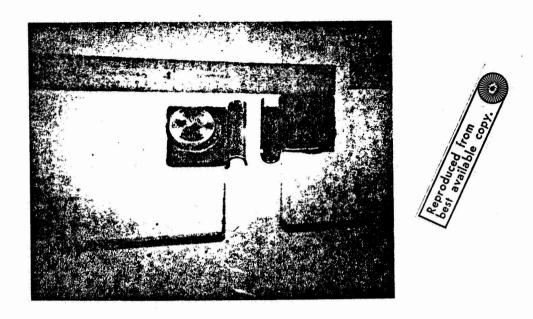


Fig. 6. Two window hinges attached to glass plates by Ultrapulse welding.

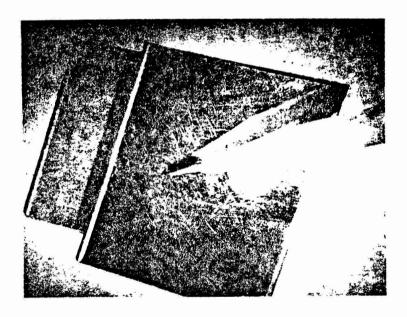


Fig. 7. Chrome-plated steel Ultrapulse-welded to bare steel. The weld location is beneath the pencil tip.

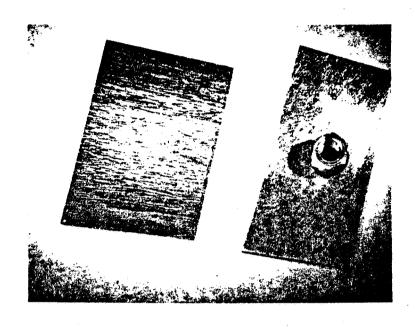


Fig. 8. Photograph of two identical samples showing the ability of Ultrapulse to weld a part (a nut in this case) to the back of vinyl-coated steel sheet.

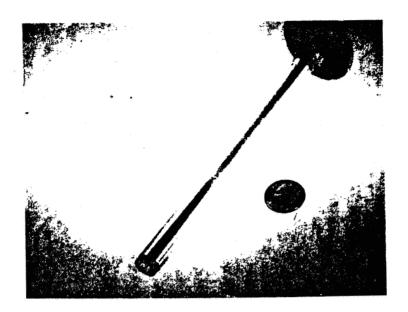


Fig. 9. Photograph of an Ultrapulse-welded exhaust valve. A previously-hardened tip ($R_{\rm C}$ 50) is welded without tempering the tip wear surface.



Fig. 10. A photomicrograph of the exhaust valve weld above. Magnification is 200X.

WELDING TECHNIQUES

Charles R. Manning, Jr., Chairman

This session consisted of six papers on existing and new welding processes, primarily for medium to heavy section joints.

N74 30944

FACTORS AFFECTING THE STRENGTH OF MULTIPASS LOW-ALLOY STEEL WELD METAL

Ву

Boris M. Krantz

MANAGER, METALLURGICAL DEVELOPMENT FILLER METALS RESEARCH AND DEVELOPMENT DEPARTMENT AIRCO WELDING PRODUCTS & MURRAY HILL, NEW JERSEY

ABSTRACT

The mechanical properties of multipass high-strength steel weld metals depend upon several factors, among the most important being 1) the interaction between the alloy composition and weld metal cooling rate which determines the as-deposited micro-structure, and 2) the thermal effects of subsequent passes on each underlying pass which alter the original microstructure. The bulk properties of a multipass weld are therefore governed by both the initial microstructure of each weld pass and its subsequent thermal history. Data obtained for a high-strength low-alloy steel weld metal have confirmed that a simple correlation exists between mechanical properties and welding conditions if the latter are in turn correlated as weld cooling rate.

This report summarizes the results of both metallographic analysis and tensile tests of weld metal synthetically subjected to the thermal history occurring in 2-in. GMA weldments made at both the lower- and upper-limit of the practical range of energy input-plate temperature conditions. The yield strength of the weld metal deposited at 40 kj/in-200°F and after subsequent austenitizing is approximately 175 ksi. Further exposure of this fully martensitic weld metal to peak temperatures in the intercritical range formed significant amounts of ferrite which reduced the yield strength to 140 ksi. Further thermal treatments at several sub-critical tempering temperatures produced marked carbide spheroidization and agglomeration but no change in yield strength. The resultant final microstructure was therefore a mixture of ferrite and tempered martensite having a yield strength of approximately 140 ksi. 455<

The weld metal deposited at 60 kj/in-300°F was cooled at rates slow enough to cause transformation to proeutectoid ferfite and possibly upper bainite, the combination of which produced a yield strength of 152 ksi. Reaustenitizing this as-deposited structure lowers the yield strength to 144 ksi due to the additional formation of ferrite and bainite. Subsequent cycling within the intercritical region produced more ferrite and a decrease in yield strength to 137 ksi. The structure of multipass AX-140 weld metal deposited at 60 kj/in-300°F is thus comprised of tempered martensite, ferrite and tempered bainite, the latter two constituents accounting for the lower strength of weld metal deposited at relatively high energy inputs.



INTRODUCTION

The mechanical properties of high-strength low-alloy steel weld metals are influenced by many factors. Probably the most significant factors with alloys designed to produce yield strengths in the range of 100-150 ksi are the composition, the solidification substructure, and the solid state transformations occurring during both the initial cooling and the multiple thermal cycles resulting from subsequent passes in a multipass Although the importance of the first two parameters cannot be ignored, the latter two are of special interest since they can be controlled readily by proper selection of welding parameters. Several studies (1,2) have shown that the yield strengths of such weld metals are decreased markedly when relatively high levels of welding energy-input and/or plate preheat temperature are used. As a result of these investigations, recommended ranges of welding conditions have been specified for each composition of weld metal in order to achieve satisfactory mechanical properties.

An analysis of data generated in a series of AX-140 welds has shown that a simple correlation exists between weld-metal strength and welding conditions if these conditions are expressed as the corresponding weld cooling rates (1). When interpreted in this fashion, it is clear that rapid losses in strength occur when the weld metal is deposited with conditions causing cooling rates slower than a certain critical level. The mechanism

commonly postulated to explain this pronounced softening has been the formation of non-martensitic microconstituents. Knowledge of the continuous-cooling transformation characteristics have thus enabled the minimum-allowable cooling rate to be defined. This, in turn, allows one to define the combination of welding energy input and preheat temperature for a given plate thickness to avoid the formation of a weak phase during the initial cooling of each weld pass. However, this information is incomplete since every pass in a multipass weldment is "heat-treated" by the thermal cycles caused by subsequently-deposited passes. Thus the resultant mechanical properties of a multipass weld must be governed as much by the microstructural changes produced by repetitive thermal treatments of the initially-deposited structures as they are by the characteristics of the initial sturucture. The real question to be answered is whether the strength-limiting factor is predominantly the initially-formed structure or the heat-treating effect of subsequent thermal cycles.

The purposes of this program have been (a) to determine the microstructures of as-deposited GMA weld metal made at typical low- and high-energy inputs and to define their effect on mechanical properties, and (b) to determine the changes occurring in these microstructures and the final mechanical properties as a result of the thermal cycling in multipass weldments. The latter effects were studied with miniature weld metal specimens each of which contained only that microstructure characterizing a particular set of weld thermal cycles, and which were used to

469<

determine the sequential changes in the properties of a specific region of a multipass weld metal.

EXPERIMENTAL PROCEDURE

Experiments were designed to reproduce synthetically the metallurgical and mechanical property changes occurring in as-deposited weld metal as the result of multipass welding. Microstructural changes were studied using conventional optical and electron microscopy techniques. Tensile properties were determined using miniature tensile specimens initially machined from actual weld passes deposited at specific welding conditions Aand then subjected to thermal cycles typical of 2-in. thick multipass welds. To insure an essentially identical composition in all specimens, they were taken from an AX-140 weld pad as shown in Fig. 1, to avoid dilution with the base plate. Table 2 shows the chemical analysis of both sets of specimens and confirms that identical analyses were obtained. The AX-140 weld pad was deposited on 2-in. thick HY-130(T) plate to insure that heavy plate cooling conditions existed. The weld deposits were spaced sufficiently far apart to insure that the thermal effects caused by one weld deposit would not affect those already made. To insure that the specimens consisted entirely of as-deposited beads, transverse sections of the rough-machined blanks were ground and etched to locate the specimen center for final machining.

The finish-machined specimens were heat-treated in the Duffers' Gleeble (3) and subjected to the thermal cycles recorded when depositing multipass welds at 40 kj/in-200°F and 60 kj/in-300°F. The specific sets of peak temperatures to which the specimens were exposed are presented below:

PEAK TEMPERATURE OF THERMAL CYCLES PRODUCED WITHIN A TYPICAL PASS DURING MULTIPASS WELDING

Energy Input	Preheat Temperature	Peak Temperature OF		
40 kj/in.	200°F	1890 - 1365 - 895 - 415 - 380		
60 kj/in.	300°F	1900 - 1400 - 995 - 975 - 780 - 770		

It should be noted that although thermal cycles having similar peak temperatures were observed at each set of welding conditions, the measured cooling rates are significantly slower at the 60 kj/in-300°F conditions. Therefore, significantly different microstructures were produced, as will be described in a following section of this paper. The heat-treated specimens were machined to the miniature tensile specimen configuration shown in Fig. 1. The reduced section, 0.092-in. length and 0.045-in.dia., was machined so that the prior position of the control thermocouple (percussion-welded on the specimen during Gleeble heat treatment) was centered within the reduced gage length. Tensile tests were made with a standard Instron testing machine at a cross-heat travel speed of 0.02-in/min.

The tensile strengths reported were calculated from the maximum sustained load and the initial sample cross-section area. The reported 0.2% offset yield strengths were estimated from the load-crosshead extension data by assuming that the crosshead travel causes uniform strain only within the reduced gage length. Analyses of the experimental errors in load measurement and of

one standard deviation in measuring cross-section area indicated a maximum error of \pm 3% in the resulting tensile strength data.



Prior metallographic studies and mechanical tests of thermally-cycled specimens showed that significant decreases in strength should be expected when the as-deposited welds are reheat-treated. This softening could not be explained by the formation of bainite rather than martensite as indicated by the accepted continuous cooling diagram for AX-140. Accordingly, the transformation characteristics were rechecked with the rapid response, high-resolution dialatometer of the Duffers' Gleeble. The net resolution of this system in combination with the instrumentation of temperature and specimen dilation permitted volume changes of 0.05% to be detected in the 0.250-in.diam. specimens used. Additional evidence of transformation was also obtained by the inverse cooling rate method described in a subsequent section of this paper.

RESULTS AND DISCUSSION

CONTINUOUS-COOLING DIAGRAM FOR AX-140 WELD METAL

The AX-140 continuous cooling transformation diagram obtained in this investigation is shown in Fig. 2. The significant difference in comparison to the previously-accepted diagram is the addition of a ferrite-start (Fs) transformation line. The remainder of the diagram, i.e., the occurrence of a martensitestart (Ms) line at 780°F and an upper bainite-start (Bs) line, is essentially identical to the published CCT diagram. imposed on this figure are bands of initial cooling cycles measured at 40 kj/in.-200°F and 60 kj/in.-300°F welding conditions. According to these data, a martensitic microstructure will form during cooling to room temperature when AX-140 weld metal is cooled at rates equal to or faster than those characterizing the 40 kj/in.- 200° F welding conditions. However, when this weld metal is deposited at the slower-cooling rates characterizing the 60 kj/in.-300°F welding conditions, the diagram predicts the formation of proeutectoid ferrite prior to the martensite transformation assumed to predominate. Upper bainite is an additional transformation product probably formed during these cooling con-The net result at room temperature is a mixture of ditions. ferrite and upper bainite in a predominantly-martensitic matrix. The influence of these cooling conditions upon the weld metal

morphology and tensile properties was revealed by conventional replica electron microscopy and mechanical tests of heat-treated weld metals.



METALLOGRAPHIC AND MECHANICAL PROPERTIES OF AS-DEPOSITED AND THERMALLY-CYCLED WELD METALS

The tensile and yield strengths of the as-deposited and thermally-cycled welds are plotted in Fig. 3 as a function of their cumulative thermal history shown schematically at the bottom of the figure. Both the metallographic observations and the strength measurements of each weld metal were made in the as-deposited condition, again after the as-deposited specimens were reaustenitized by a weld thermal cycle having a peak temperature of 1900°F, and after each of the subsequent weld thermal cycles. The data thus indicate the sequential changes in microstructure and mechanical properties occurring in typical underlying passes in 2-in. multipass weldments made at both 40 kj/in.-200°F and 60 kj/in.-300°F welding conditions.

<u>Influence of 40 kj/in. Energy Input and 200°F Preheat</u> <u>Temperature</u>

As shown at the left of Fig. 3, the tensile and yield strengths of weld metal deposited at 40 kj/in.- 200° F are 182 and 177 ksi, respectively. Similar strengths were observed after the sample was reaustenitized at 1890°F. Examination of

the CCT diagram in Fig. 2 indicates that a fully martensitic microstructure is produced during the initial cooling cycle from the fused state. The sample heated to an 1890° peak temperature cools at virtually the identical rate. The conclusion is logically drawn that both the initial as-deposited and the reaustenitized weld metals are completely martensitic, and that the strengths in both conditions should be similar. The high strength levels observed also serve as indirect proof that martensite is present since the tensile strength of a 0.1%C steel fully quenched to martensite is reported to be approximately 180 ksi (4). Electron micrographs of replicas at magnifications of 3000X (Figs. 4 and 5) show the 40 kj/in. weld metal specimens in both the as-deposited and as-deposited plus 1890°F reaustenitized conditions to have an extremely fine acicular morphology arrayed in the pseudo- (111) geometry indicative of the low-carbon martensite (5).

The presence of a completely martensitic structure after both the as-deposited cooling cycle and the 1890°F peak temperature thermal cycle also is evident in Fig. 6a, an inverse cooling rate plot of the cooling cycle of the 1890°F thermal cycle. This classic technique (6) enables the detection of exothermic phase changes otherwise undetectable by observation of conventional cooling curves. The 1100° - 800°F range of temperature experiences a continuous decrease in cooling rate shown by a gradual increase in the length of time to cool a fixed number of degrees. The marked change occurring between 800 and 780° indicates the occurrence

of an exothermic phase transformation, this being the formation of martensite. The further perturbation at 740°F is probably due to the continued formation of martensite and not to any new phase formation. Therefore, the as-deposited cooling cycles must behave similarly to the austenitizing cycle just described since their cooling rates are essentially identical.

Exposure of the reaustenitized weld metal to a weld thermal cycle with a peak temperature of 1365°F results in large decreases in both the tensile and yield strength to levels of 156 and 138 ksi, respectively. This is due to the formation of ferrite during the partially austenitizing heat treatment, a phenomenon also reported (7) to occur in low-carbon low-alloy steel weld heat-affected zones. The ferrite formed during the intercritical thermal cycle appears as relatively large, featureless microconstituents shown in Figs. 7a and 7b, electron micrographs taken at magnifications of 3000X and 5500X, respectively. Note that the overall acicularity is retained and that the prior structure (shown in Fig. 5) displayed none of these constituents believed to be ferrite. A lineal analysis of the area fraction of ferrite indicated this phase to comprise approximately 55% of the microstructure. This amount is much lower than the 75 - 80% predicted from the conventional Fe-C metastable phase diagram. But when the eutectoid composition and the A_1 - and A_3 -phase boundaries are modified (8) for the AX-140 composition, the presence of ferrite in these quantities can be predicted by conventional lever-law calculations.

Figs. 8a and 8b are electron micrographs taken at magnifications of 5375% and 12,000%, respectively, after the partially-ferritic weld metal was exposed to an additional weld thermal cycle with a peak temperature of 895°F. Clearly visible in both these micrographs is the tempering effect of the 895°F peak temperature thermal cycle and the resultant precipitation of carbides. Similar structures were observed in specimens subsequently subjected to the 415 and 380°F peak temperature thermal cycles. Tempering of the martensite and aging of the supersaturated ferrite formed during the rapid intercritical treatment are the principal phenomena occurring in this series of specimens, i.e., the 895, 415, and 380°F peak temperature thermal cycles. The tensile and yield strengths observed showed some variability, however, no significant decreases were observed.

Influence of 60 kj/in-300°F Weld Thermal Cycles

The mechanical properties of various regions of multipass welds made at 60 kj/in. with 300°F preheat are also shown in Fig. 3. These are significantly weaker than equivalent AX-140 welds deposited at 40 kj/in. and 200°F. The as-deposited tensile and yield strengths are 169- and 152-ksi for the 60 kj/in-200°F weld metal as compared to 182- and 177-ksi for the faster-cooled 40 kj/in-300°F weldment. Based upon the continuous-cooling diagram, the decrease in strength in the 60 kj/in-300°F is due to the formation of ferrite at 950 - 1000°F, upper bainite at 800°F, and martensite at 780°F. Thus, the final room temperature

microstructure is comprised of ferrite, upper bainite and martensite. This microstructure is shown in Figs. 9a and 9b. Both of these electron micrographs were taken at magnifications of 5500X and 12,000X, respectively. The relative proportion of these phases was not determined due to the extensive and difficult metallographic effort required. However, it seems reasonable to assume the presence of more martensite than bainite in these structures since the diffusion-controlled bainite transformation occurs for only 2 to 3 seconds prior to the beginning of the martensite transformation. Thus it is unlikely that any large amounts of upper bainite could form.

Reaustenitizing the as-deposited microstructure at 1900°F significantly decreased the tensile- and yield-strength to 159and 144-ksi, respectively. The cooling cycle from the 1900^{0} F peak temperature is slower than the initial cooling, thus permitting longer times to form both ferrite and bainite. Therefore, when compared to the as-deposited microstructure, it is reasonable to assume a larger volume fraction of ferrite and bainite in the overall structure, and, thus a lower strength. Typical electron micrographs of this structure are shown in Figs. 10a and 10b at magnifications of 5500 and 13,000X, respectively. Somewhat coarser, but nevertheless similar features to those of the as-deposited structure are visible in both micrographs since no major differences in structure would be predicted from the weld metal's transformation characteristics. The presence of ferrite also was independently confirmed with the inverse-coolingrate analysis of the 1900°F peak temperature thermal cycle as

shown in Fig. 6b. More scatter is evident than in the 40 kj/in-200°F curve, but a major transformation is clearly apparent at approximately 950°F as is the martensite formation at approximately 780°F. These data verify the ferrite formation detected by means of dilatometry.

The sample treated at 1900°F was partially reaustenitized with an additional weld thermal cycle having a peak temperature of 1400°F. This resulted in a continued loss in both tensile and yield strength to levels of 145- and 132-ksi, respectively. As was the case with the 40 kj/in-200°F weld metal, the resulting microstructure consisted of a partially-transformed ferrite-bainite and/or martensite aggregate as shown in Figs. 11a and 11b. Clearly evident in these electromicrographs are ferritic-microconstituents dispersed in a bainite-martensite matrix. The area fraction ferrite was approximately 63% compared to the 72% level predicted on the basis of a modified equilibrium diagram.

Continued exposure of the mixed ferrite-bainite microstructure to three more weld thermal cycles having peak temperatures of 995, 780 and 770°F caused no significant change in tensile and yield strengths, the final levels being 146- and 132-ksi, respectively. The microstructures produced after each of these heat treatments show the anticipated precipitation of carbides resulting from the combined effects of tempering the martensite and/or bainite and aging the supersaturated ferrite. Typical microstructures are shown in Figs. 12a and 12b, electron

micrographs taken at magnifications of 5375X and 12,000X, respectively. Again, in similar fashion to the behavior observed after tempering the lower energy-input weld metals, clear evidence of precipitation is present within both microconstituents, although no change in tensile properties occurs. The resultant microstructure is, therefore, comprised of a mixture of tempered martensite and bainite together with aged ferrite.

Summary of Weld Metal Reheat-Treatment Studies

The results of mechanical tests of both series of weld metals indicate the marked influence of both the initial weld cooling rates and the subsequent heating cycles which affect the formation of ferrite in the microstructure and properties of individual weld deposits. These data have shown that AX-140, and by inference, any metallurgically-similar high-strength low-alloy steel weld metal when initially deposited at cooling rates sufficiently fast to form martensite possesses a very high strength and is weakened significantly after exposure to a series of weld thermal cycles having peak temperatures between the upper and lower critical temperatures.

Confirmation that conventionally-measured tensile properties of multipass welds are controlled by thermal effects as described in the results of this study is shown in Table 3. These data compare typical ultimate tensile strengths of multipass 2-in. GMA weldments (9) with those of the miniature weld metal specimens subjected to the entire series of weld thermal cycles. Although

the data for the multipass and thermally-cycled specimens differ by approximately 6%, a discrepancy of this magnitude is considered small considering the type of comparison being made. It was concluded that the approach used in this investigation to synthesize the microstructural and mechanical property changes occurring in underlying passes was valid and represents with good accuracy the phenomena occurring within an actual weldment. multiplicity of thermal cycles cannot be avoided in a multipass weldment with the ensuing formation of ferrite, the only strengthlimiting factor left to the control of the welding engineer or metallurgist is the formation of proeutectoid ferrite during initial cooling of each weld pass, i.e., by maintaining a maximum practical weld cooling rate. In the AX-140 system, or in any other high-strength low-alloy steel weld metal, this is accomplished by specifying maximum levels of both energy input and plate temperature, the adherence to which will insure minimum weld metal strength levels.

<u>ACKNOWLEDGEMENT</u>

now of Electrotherm (

The author wishes to acknowledge with thanks, K. Dorschu and A. Lesnewich of Airco for the contribution of their experience. gained in the initial studies of process effects on weld metal properties and J. Devine for performing with precision and accuracy the dilatometry studies which provided key technical information in this investigation. In addition, appreciation must also go to the Naval Ship Systems Command of the U.S. Navy for its sponsorship under Contract NObs - 94535 (FBM).

REFERENCES

- (1) DORSCHU, •K.E.

 Control of Cooling Rates in Steel Weld Metal.

 Welding Journal, 48(2) (1969).
- (2) CONNOR, L.P. et al
 Development of Procedures for Welding HY-130(T) Steel.
 Welding Journal, 46(7): 309s -321s (1967).
- (3) NIPPES, E.F. and SAVAGE, W.F.
 Development of Specimen Simulating Weld Heat-Affected-Zones
 Welding Journal, 28(11): 534s 546s (1949).
- (4) BAIN, E.C. and PAXTON, H.W.
 Alloying Elements in Steel.
 ASM, Metals Park, Ohio (1966).
- (5) WAYMAN, C.M.
 Introduction to the Crystallography of Martensitic Transformations.
 N.Y. MacMillan Company, 1964.
- (6) KEHL, G.L.
 Principles of Metallographic Laboratory Practice.
 N.Y., McGraw Hill, 1949.
- (7) SAVAGE, W.F. and OWCZARSKI, W.A.
 The Microstructure and Notch Impact Behavior of a Welded Structural Steel.
 Welding Journal, 45(2): 55s 65s (1966).
- (8) ANDREWS, K.W.
 Empirical Formulae for the Calculation of Some Transformation Temperatures.

 JISI, July 1965. pp. 721 727.
- (9) DORSCHU, K.E.
 HY-130/150 weldments: Summary report on the development
 of filler metals and joining procedures.
 Air Reduction Co, Inc., Murray Hill, N.J.
 Report to Bureau of Ships, Contract No. NObs 88540, SR007-01-01,
 Task 853.
 RE-66-014-CRE-34 (January 26, 1966).

TABLE 1

GAS-METAL-ARC WELDING CONDITIONS FOR 2-IN.
THICK HY-130(T) WELDMENTS

Airco Weld No.	2444-17	2444-25	
Energy input (kj/in.)	40	60	
Preheat/interpass (^O F)	200/225	300/325	
Current (amp)	270	285	
Voltage (DCRP)	25	25	
Travel Speed (ipm)	10	7	
Electrode Extension (in.)	3/4	3/4	
Shield Gas	A-2% 0 ₂ at 50 cfh A-2% 0 ₂ at 50 cfh		
Wire Diameter (in.)*	1/16	1/16	
Wire Feed Speed (ipm)	140	195	

^{*}Wire from heat 1P0047 of AX-140 welding wire.



TABLE 2

CHEMICAL ANALYSIS OF HEAT-TREATED AX-140
GMA WELD METAL SPECIMENS

	40 kj/in-200 ⁰ F Welding Conditions	60 kj/in-300 ⁰ F Welding Conditions
С	0.092	0.090
P	0.008	0.007
S	0.007	0.007
Si	0.24	0.22
Mn	1.62	1.58
Ni	2.25	2.24
Cr	0.88	0.87
Мо	0.57	0.56
W	0.017	0.013
Nb	0.004	0.004
v	0.013	0.013
Cu	0.088	0.088
Co	0.017	0.015
A1	0.009	0.005
Zr	••	
Ti	0.008	0.006
В	0.0007	0.0008
Sn	0.011	0.011

Note: Above analyses obtained by vacuum spectrographic analysis of samples of chips from each weld metal.



TABLE 3

COMPARATIVE ULTIMATE TENSILE STRENGTHS OF CONVENTIONAL AND THERMALLY-CYCLED WELD METAL TENSILE SPECIMENS

	Ultimate Tensile Strength (ksi)	
	40 KJ/IN-200°F	60 KJ/IN-300°F
Conventional Bulk		
Weld Metal Specimens	159	157
Thermally-cycled Specimens	150	144

40 KJ/IN - 200°F OR 60 KJ/IN - 300°F **DEPOSITS** LOW DILUTION WELD PAD 2 - INCH HY-130 (T) PLATE 0.125 DIA. 0.092 GAGE LENGTH

Figure 1. - Schematic representation of specimen preparation. 488



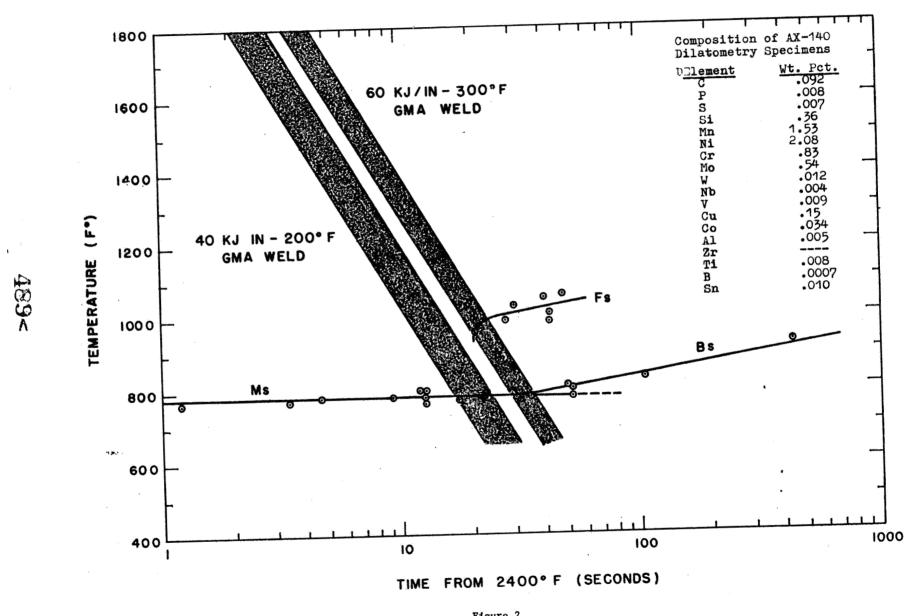


Figure 2

782-Krant

GAS METAL ARC WELDING CONDITIONS

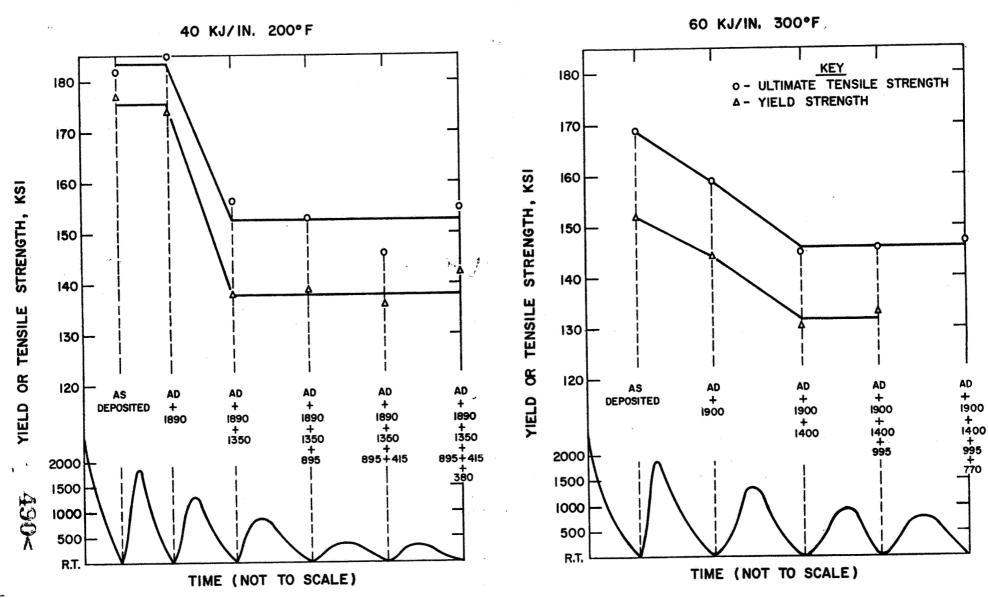
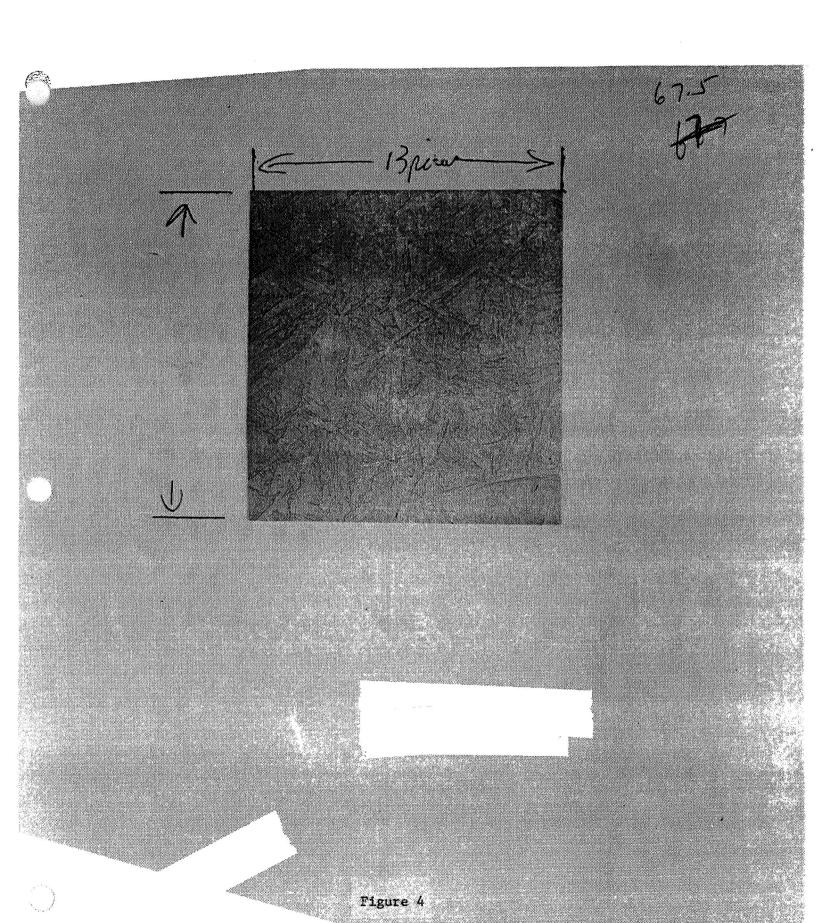


Figure 3

Fig 3 - Krantz



491<

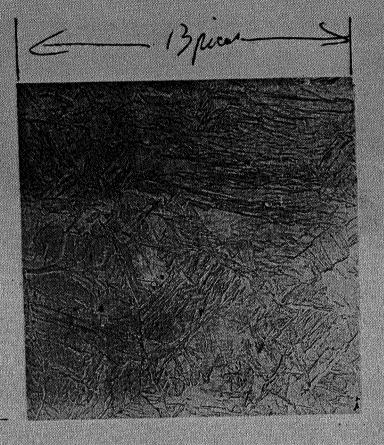




Figure 5

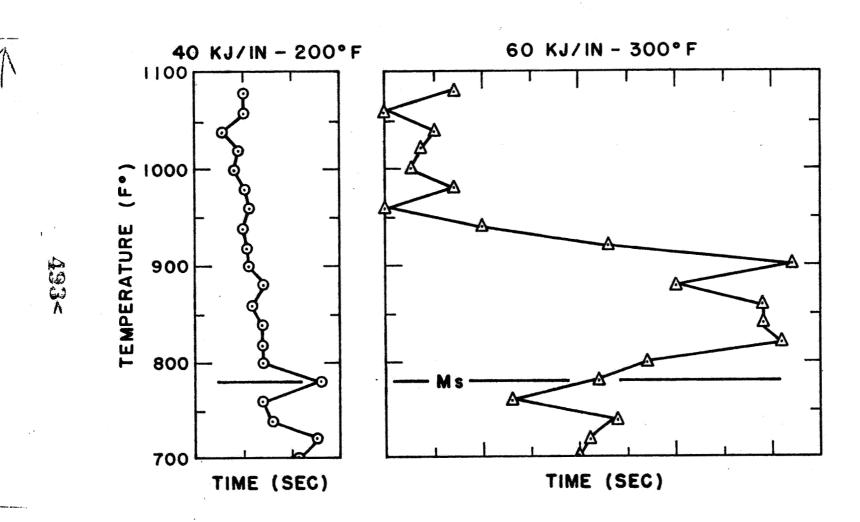
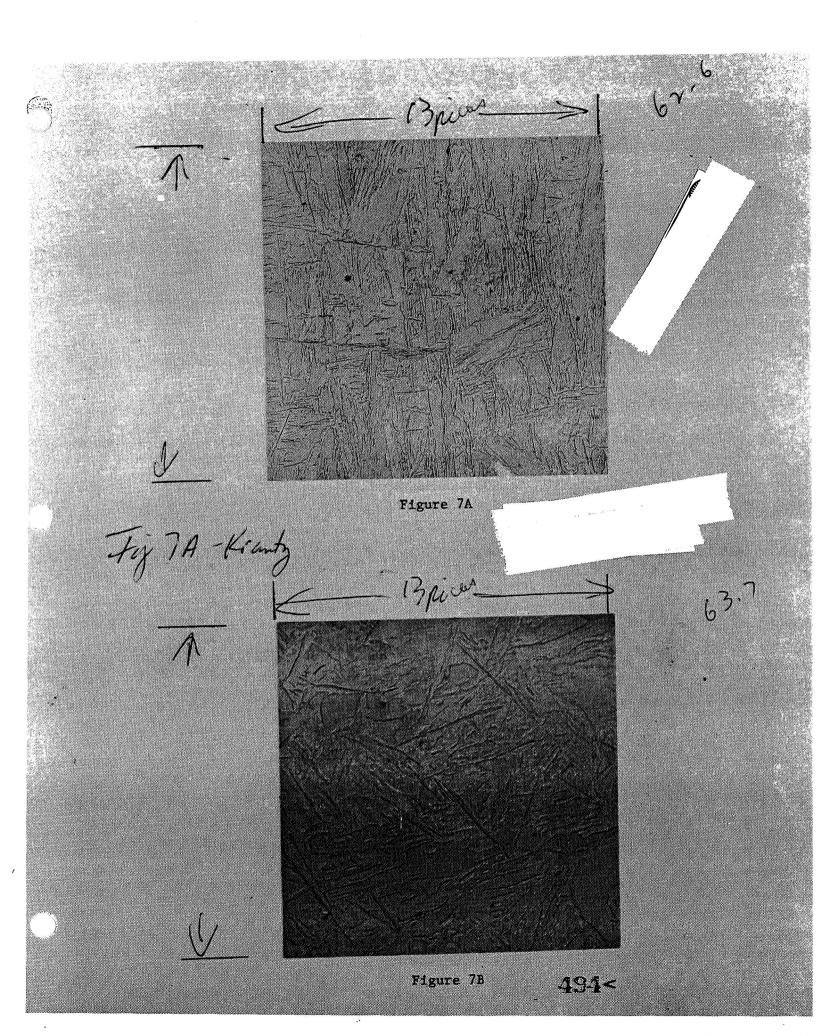


Fig. 6. INVERSE COOLING RATE ANALYSIS of 1900°F AUSTENITIZATION WELD THERMAL CYCLES OCCURRING at 40 KJ/IN.-200°F and 60 KJ/IN.-300°F WELDING CONDITIONS.



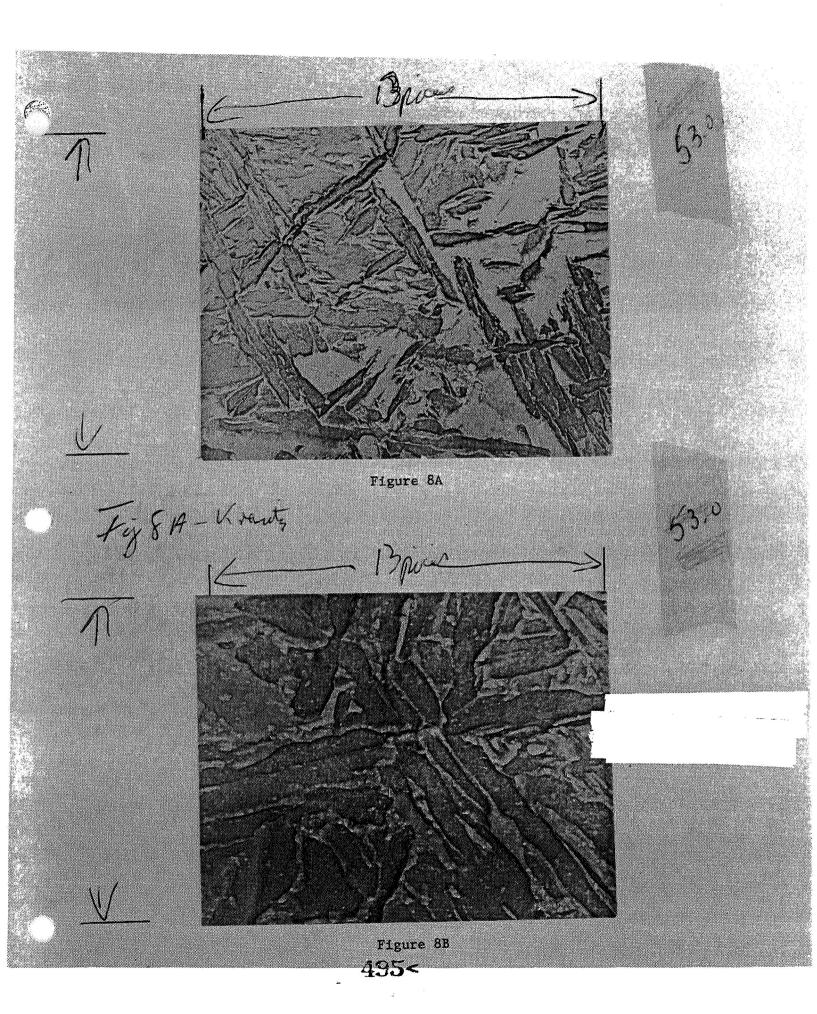
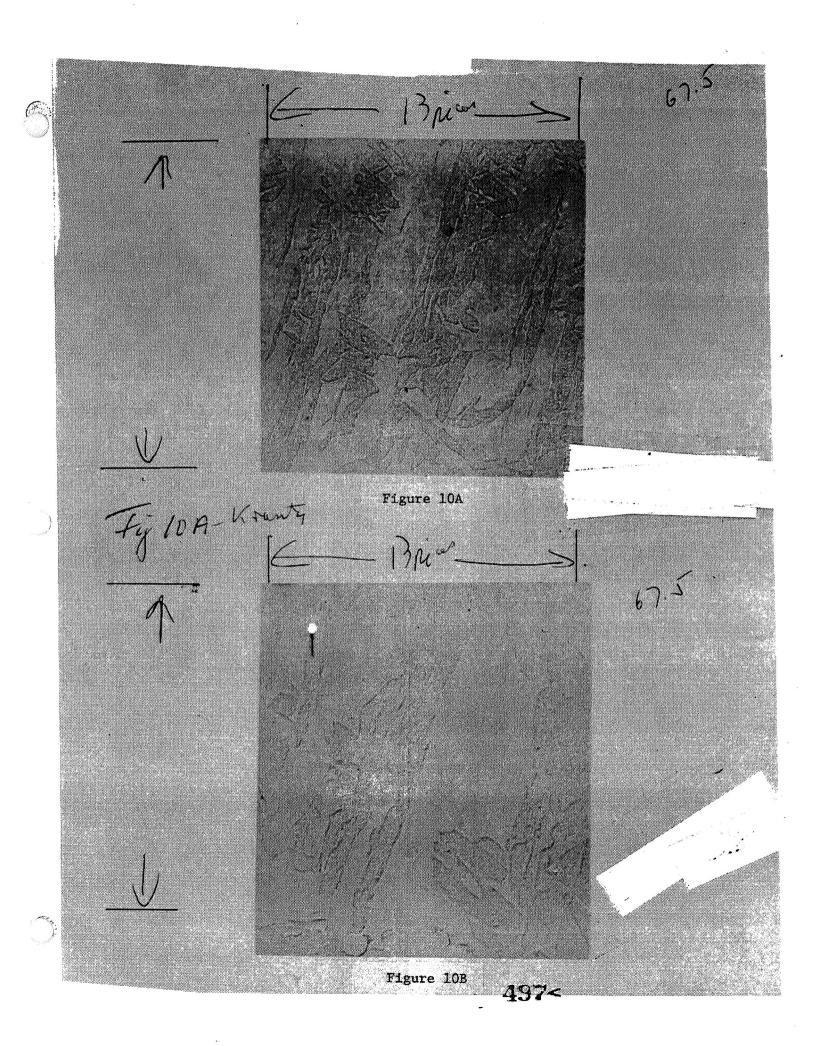
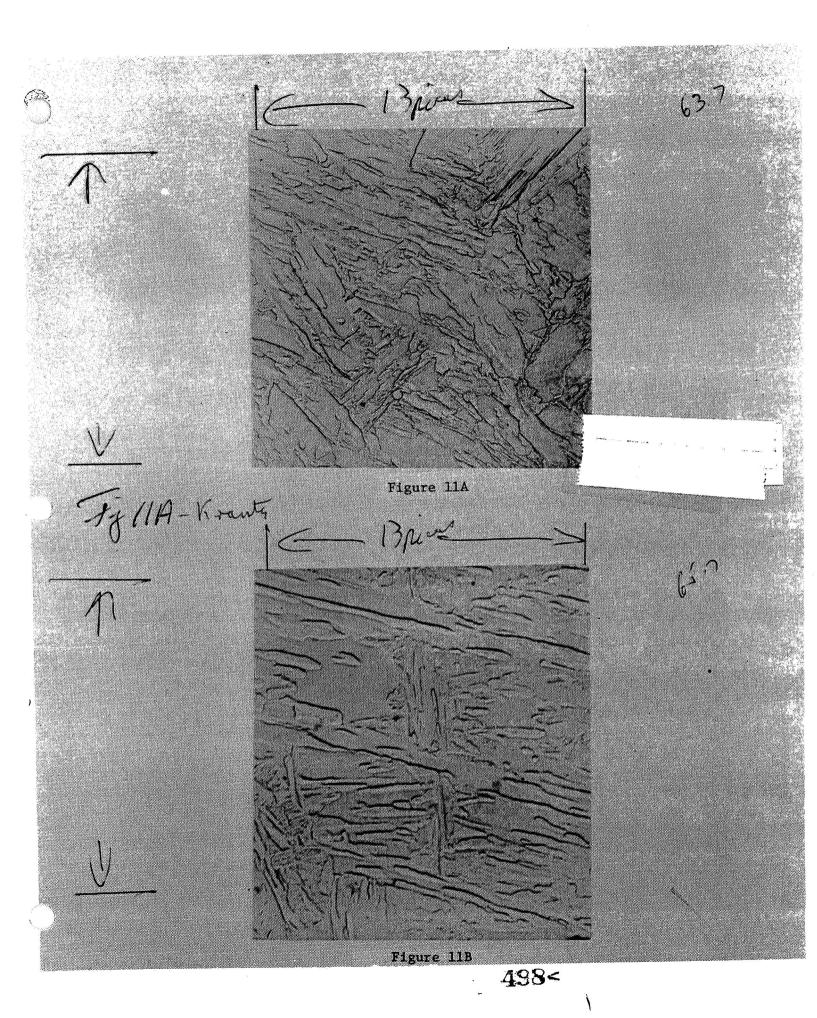


Figure 9A Fy GA-Kranty 496< Figure 9B





Fij DA-Kranty Figure 12A Figure 12B

N74 30945

I. BACKGROUND

Butt welding of thick plates is usually accomplished by such welding systems as shielded metal arc welding (SMAW), gas-metal-arc welding (GMAW) or gas tungsten arc welding (GTAW). As indicated in Fig. 1a, a major portion of welding in each of these processes involves the replacement of base metal which has been removed to provide appropriate access for shielding or slag removal. For example, in the case of a 2-inch-thick plate employing a 60° double-vee joint, the amount of sound base metal removed and subsequently replaced by weld metal approximates 1.1 square inches in cross-sectional area; a square butt joint could produce an equivalent joint with less than 0.5 square inches of weld deposit.

As indicated in Fig. 1b, the primary need for a double-vee joint in inert gas arc welding of thick plate is to provide access for the shielding cup in the root area. Welding is accomplished with the wire extended approximately 1/2 inch from the nozzle. A preferable approach to welding would be to use square butt joints with a minimum gap between the edges, such as can be achieved with electron beam welding. Other processes used for square butt joint welding of heavy sections are high density GTAW, submerged arc, electroslag, electrogas and automated narrow-gap GMAW. The narrow-gap welding process is a unique GMAW process which is under development by the Naval Ship Systems Command. The above mentioned automated processes are limited in the repair of defects and welding of inaccessible areas which have to be accomplished by other manual methods.

Due to rising labor and materials costs, a need has arisen for investigating new systems which can more economically fabricate structural components of naval ships. The Extended Electrode Technique (EET) is a

unique welding process which offers promise of reducing welding time, welding costs, and quantity of weld metal deposited by 50%. Work performed to date has demonstrated the feasibility of the process for joining quenched and tempered steels under laboratory conditions using manual methods and under shipyard conditions using an automated method. Mechanical tests on weldments indicate that satisfactory large-scale EET weldments can be produced.

The Extended Electrode Technique described in the next section was developed to achieve the advantages of close butt welding and to complement the automated narrow-gap process.

II. EXTENDED ELECTRODE TECHNIQUE

The Extended Electrode Technique illustrated in Fig. 2 utilizes square butt joints with a nominal 1/4- to 3/8-inch gap opening. Wire and gas are fed through standard GMAW semi-automatic welding equipment into the center of the gap. The technique can be used in either the manual or automated mode with wire extensions beyond the contact tube of as much as 2 inches The major differences between the Extended Electrode Technique and the previously mentioned automated narrow-gap welding process are noted in Table I. Gas Shielding

The purpose of the gas mixtures in EET welding is to protect the molten filler wire tip from atmospheric contamination and to produce an arc that is controllable at 2-inch depths with optimum penetration. Shielding gas used in the process is directed down the center of the groove and also over the surface of the surrounding plate by the two separate shielding systems illustrated in Fig. 2. The inner shielding gas protects the bare wire and the molten puddle in the bottom of the groove; the external shielding device

prevents air aspiration into the inner shield column by flooding the plate surface with an inert gas.

The external gas shielding mixture which was used throughout the investigation is a mixture of 98% argon and 2% oxygen. When this mixture, which is normally used to weld ferrous materials, is employed as an inner shielding gas deep in the groove in EET welding, an erratic semispray arc is produced. This arc plays against the sidewalls without reaching the bottom of the weldment, resulting in a porous honeycomb-type weld. The addition of helium (He) to the Ar+2% O₂ gas tends to transform the arc characteristic from an erratic semispray mode to an unstable globular mode. This arc is hotter, due to the higher ionization potential of He, but like the Ar+2% O₂, it also fails to produce a stable arc at the bottom of the groove. Addition of carbon dioxide (CO₂) to the Ar+O₂+He gas in moderate amounts (5% to 15%) tends to stabilize the arc in a globular-type transfer mode which permits welding of up to 2-inch depths. The CO₂ addition reduces the surface tension and gives good wetting characteristics.

Due to the oxidizing potential of CO₂ gas (normally equivalent to Ar+10% O₂), a mixture devoid of O₂ gas was attempted in a further effort to optimize the shielding gas. Mixtures with 3:1 and 1:1 ratios of helium to argon with 5% to 8% CO₂ were prepared. The arc produced by these gas mixtures was similar in characteristics to those obtained with the Ar+He+CO₂+O₂ gas noted above but appeared narrower in width. This narrowing of the arc can cause lack of fusion problems in EET welding if the joint opening is too large. It is therefore considered that the elimination of oxygen from the shielding gas mixture makes a narrower joint opening (3/8-inch) more practical, especially if the process is automated without oscillation of the welding torch.

Arc Characteristics

Stable arcs with good deposition characteristics are obtained without the use of superimposed travel guides or electrical controls, other than what would normally be used in conventional manual GMAW welding. The arc transfer at the root, which is shown in Fig. 3, is of the globular type. The tendency for spray transfer increases as the length of the electrode extension decreases. In the case of 2-inch-thick material, the globular transfer changes to a spray transfer mode at approximately mid-thickness due to the I²R heating of the electrode.

III. EET Welding of HY-80 Steel

The quenched and tempered HY-80 steel which was chosen as the base plate material has mechanical properties and composition as shown in Table II.

Small scale mechanical tests performed on the weldments consisted of the following:

- 1. All-weld tensile properties.
- Transverse-weld tensile properties.
- 3. Charpy V-notch properties (Transverse weld).
- 4. Side bends for ductility.

Nondestructive tests which were performed include:

- 1. Radiography
- 2. Ultrasonic
- 3. Macro examination.

Five different diameter electrodes were tested, the smallest being 0.035-inch and the largest 0.092-inch. Attempts to weld with the 0.035- and 0.045-inch-diameter electrodes (specimens V-1 and V-2) were unsuccessful due to excessive heat buildup in the extended portion of the wire. When the

small diameter wires (0.035- and 0.045-inch) made contact with the plate the wire would glow and burn off. Attempts to lower the wire feed rates and amperages did not produce desired welding conditions, and further tests using the small diameter wires in the flat position were discontinued.

The 0.062-inch-diameter wire has performed in a satisfactory manner. The parameters developed for all wires are shown in Table III. The parameters developed with the 0.078- and 0.092-inch-diameter electrodes were considerably different from those for the 0.062-inch wire. Higher currents, in the range of 350 to 450 amperes, were generally necessary to obtain the same arc conditions with the larger wires (0.078- and 0.092-inch) as were obtained with the smaller 0.062-inch wire.

Table IV gives results of the mechanical tests performed on welds with parameters described in Table III. With only a very minor exception (CVN 46 ft/lbs at -60° F) in specimen V-5, both types of filler wires, AX90 and MI88, performed satisfactorily with respect to usability and mechanical properties. The effect of filler wire diameter on Charpy V-notch values while holding the other parameters, such as travel speed, amperage and voltage, almost constant is shown in Fig. 4. The 0.062-inch-diameter wire yielded the highest room temperature Charpy V-notch (CVN) values. Travel speeds noted in Tables III and Fig. 5 appear to significantly affect the CVN values; the slower speed giving higher CVN values than the faster speed. However, the yield strength of these weldments were not significantly affected. Little difference was observed between the yield strengths of the welds using higher travel speeds with the same type and diameter filler wire. Deposition Rate Affected by I²R Heating

Electrode extension to a 2-inch depth is very pronounced on the amount of metal deposited in the weldment. As the length of electrode from the con-

tact tip to the work piece is increased, the rate of metal deposition increases. This phenomenon occurs because of resistance heating (I²R) of the extended portion of the electrode, i.e., the I²R effect preheats the electrode, facilitating melting and thereby increasing the deposition rate. Fig. 6 shows the effect of the electrode extension on melting rate for various conditions of welding current, shielding gas and gas temperature¹. Heating the shielding gas increases the melting (and deposition) rate, while changing the shielding gas has relatively little effect on melting rate.

To determine whether I²R heating had any effects on the properties of weldments, a standard double-vee, explosion-bulge weldment was fabricated with an electrode extension maintained equal to that used for the root pass of a square butt EET weldment.

The all-weld yield strength and Charpy V-notch properties (Table V) of the standard double-vee EET weldment were generally 10% to 30% higher than those of the square butt EET weldment. Bend test, yield strength, and toughness (Charpy V-notch at 0° F) results from both weldments were satisfactory. The transverse weld tensile properties were the same for both weldments. The explosion bulge performance of both weldments was considered satisfactory in accordance with specifications. Both weldments sustained a reduction in thickness greater than 16%. In comparing the results of the two test plates, the square butt EET weldment had a greater reduction in thickness and a lesser degree of cracking on the fifth shot than did the standard double-vee EET weldment. Results of this test and other explosion bulge tests previously reported 3 indicate that the high reduction in thickness attained in narrow, square butt weldments may be due to the type of joint configuration used in welding. However, it is apparent that the I²R heating of the extended electrode does not have a direct effect on the explosion bulge

performance of EET weldments.

· EET Under Shipyard Conditions.

To establish the feasibility of making EET welds under field conditions, a production facility was contracted to produce an automated EET weldment under field conditions. Preparation procedures are shown in Table VI. Conventional GMAW semi-automatic spray welding equipment was used with a Linde CM-37 automated carriage for positioning the GMAW gum. After the initial side was welded, the backing strap beneath the weld was are gouged and ground to a 1/8-inch depth below the surface of the plate and manually rewelded with a 5/32-inch-diameter E11018 SMAW electrode. The parameters and bead sequence used for the EET welding of the 72-inch-long plate are shown in Table VII. Fig. 7 shows the satisfactory results of the explosion bulge test and other mechanical properties of the weldment prepared under shipyard conditions.

It is concluded that satisfactory EET welds can be made in large sections under shippard conditions by the automated EET procedure.

IV. COMPARISON OF EET AND CONVENTIONAL GMAW TECHNIQUES

Direct comparison was also made between weldments using EET and conventional GMAW processes using the material shown previously in Table II.

Results of tensile, Charpy V-notch and side bend tests are shown in Table VIII along with values for comparable conventional GMAW welds made with the same type wire and plate. Typical hardness values for EET welds are shown in Fig. 8. EET weld yield and tensile strengths obtained were approximately 15% higher and Charpy values lower than those using the same type filler wire and conventional GMAW processes.

Explosion bulge tests of conventional GMAW weldments with HY-80 steel normally attain 16% to 20% reduction in thickness. Explosion bulge tests

of EET weldments have achieved reduction in thickness of over 20%. These results have been consistently obtained with weldments prepared by the Extended Electrode Technique and are considered to be the upper quality scale of explosion bulge performance for materials of this type. Soundness of the EET weldments determined by nondestructive testing was comparable to welds produced by manual GMAW processes.

V. ADVANTAGES OF EET

In summary, the more significant advantages of the Extended Electrode Technique over other conventional GMAW techniques are shown in Table IX.

These include:

- Decreased Distortion Weldment distortion is reduced by the minimal amount of weld metal deposited.
- Reduced Plate Preparation In a double-vee joint normally used in thick sections, five flame cutting operations are required. One cut to square the edges and the remaining four to prepare the desired bevels. In addition, each beveled side has to be ground clean to permit a sound weld. In using the EET technique only one flame cutting and two grinding operations are necessary.
- Minimum Amount of Arc Time and Weld Metal Due to the reduced
 number of passes, the amount of weld metal and arc time is reduced by 50%.
- Versatility The technique can be used manually, where it offers the advantages of conventional GMAW systems; and can be useful for short runs or in confined spaces. It also can be readily automated.
- When used as a manual system the EET technique becomes a useful repair tool. Comparative repairs with other techniques require the removal and redeposition of substantially large quantities of weld metal in a "Vee" or "U" type joint configuration.

VI. LIMITATIONS OF EET

- It should be recognized that the Extended Electrode Technique is in a state of development and not a completed production tool. Limited field tests under production conditions have been promising; however, the results indicate that additional field tests will be required for modifications that will transform the technique from a laboratory development to a useful production tool.
- At the present state of development, the Extended Electrode Technique has only been used for thicknesses of 2 inches or less. Applicability to greater thicknesses has not been explored. Accordingly, it is hoped that further work will enable the process to be utilized in thicker sections.
- Work to date has been limited to ferrous materials. It is anticipated that applications relative to nonferrous materials such as aluminum, copper nickel and titanium alloys may be feasible.

ACKNOWLEDGMENT

The authors gratefully acknowledge the Naval Ship Systems Command, Mr. B. B. Rosenbaum (SHIPS 03422), for sponsorship of the program on which this paper was based.

REFERENCES

- C. E. Jackson and J. S. Clark, "Study of the Extended Electrode Technique for Welding Ship Structures," Ohio State University Report (Department of Welding Engineering), in progress
- NAVSHIPS 0900-005-5000, "Standard Procedures for Preproduction Testing Materials by the Explosion Bulge Test," November 1965.
- 3. A. Pollack, "Narrow-Gap Welds in 2-Inch HY-80 Steel," NASL Project 9300-1, Technical Memorandum No. 12, 7 August 1964.

Table I
DIFFERENCES IN TECHNIQUES

	Criteria	Extended Electrode Technique	Narrow Gap Process
1.	Extended Contact Tube	Not Required	Required
2.	Wire Straightner	Optional	Required
3.	Special Equipment	Not Required	Required
4.	Wire Diameter Range	0.062" to 0.092"	0.035" to 0.045"
5.	Non-automated (Manual) Feasi- bility	Yes	No

Table II
HY-80 BASE PLATE PROPERTIES

Chemical	Analysis	Mechanical Properties					
Element	Porcent	Longitudinal/Transver	rse				
C Mn Si P S Ni Mo Cr V	0.16 0.34 0.30 0.006 0.012 2.40 1.25 1.47 0.006 0.006	Yield Strength, ksi Tensile Strength, ksi Elongation, % Reduction in Area % Charpy V-notch (Average ft-lb) -60° F	83/83 99/100 30/26 79/73 96/117				

Table III Parameters for EET Welding



Joint Design - Square Butt Edge Preparation - Ground (after flame cutting) Position - Flat

Polarity - Direct Current, Reverse Preheat Temperature 200° - 300° F

					Specime	n Code				
	ν-1	ν-2	ν-3	v-4	ν-5	v-6	v-7	ν-8	v-9	v-11
Filler Wire Type	AX90	AX90	AX90	MI88	AX90	MI88	MI 88	MI 88	MI 88	AX90
Filler Wire Size (inches)	0.035	0.045	0.062	0.092	0.092	0.062	0.062	0.092	0.078	0.062
Gas Mixture (internal shielding)	(1)	(1)	(1)	(1)	(1)	(2)	(2)	(2)	(2)	(4)
Gas Mixture (external shielding)	(5)	(5)	(5)	(5)	(5)	(5)	(5)	(5)	(5)	
Gas Flow, cfh (internal/external)	110/ 100	110/ 100	100/ 100	120/ 100	120/ 100	100/ 100	100/ 100	100/ 100	100/ 100	150
Wire Feed, ipm	150- 300	150- 300	350	145	160	300	300	300	300	350
Travel Speed, ipm	(6)	(6)	14	12	12	14	16	13	15	13 .
Range, amperes	200	250	280- 360	400- 460	360- 450	280- 330	290- 310	350- 410	330- 360	280- 380
Range, volts	22	24	30- 39	32 - 39	34- 40	27- 32	27- 28	24- 32	24 - 32	28- 35
Interpass Temperature Maximum, ° F	200	200	250	260	240	250	250	250	250	260
Number of Passes	(6)	(6) [.]	15	12	12	10	10	10	12	11

^{(1)&}lt;sub>46%</sub> (Argon+2% Oxygen) +46% Helium + 8% Carbon Dioxide

cfh - cubic feet per hour ipm - inches per minute

^{(2) 25%} Argon+70% Helium + 5% Carbon Dioxide

^{(3) 46%} Argon+46% Helium + 8% Carbon Dioxide

^{(4)98%} Helium+2% Oxygen

^{(5)98%} Argon+2% Oxygen (6)Weldments aborted

Table IV Mechanical Properties of EET Weldments

		Yield	Tensile		Reduction		Side	Chavera	arpy V	-Notch	l) • F	
Code	Tensile Type	Strength ksi	Strength ksi	Elonga- tion, %	in Area %	Fracture	Bend Test	-60°	0°	+30°	Room Temp	Wire Types
V-3	Trans- verse weld .505	80.9/ 81.6	96.8/ 97.7	18.0,′ 18.5	66.2/ 68. 7	Base/ Base	(3)	53	80	93	104	0.062 AX90
v-3	All weld .252	110.1/ 113.6	129.8/ 126.3	20.0/	63.5/ 63.0	-	-	-	-	- ≪	-	0.062 AX 90
V-4	Trans- verse weld .505	82.7/ 84.1	99.0/ 100.8	18.0/ 17.0	63.1/ 65.9	Base/ Base	(3)	62	84	102	102	0.092 MI88
v-4	All weld .252	108.4/ 107.6	123.3/ 118.7	19.0/ 17.0	70.2/ 65.2	-		-	-	-	-	0.092 MI88
V-5	Trans- verse weld .505	84.3/ 82.4	99.9/ 98.7	18.0/ 17.0	68.5/ 63.6	Base/ Base	(3)	46(2)	71	82	93	0.092 AX90
V-5	All weld .252	107.2/ 110.5	121.2/ 124.2	20.0/ 15.0	62.8/ 29.4	-	-	-		-	-	0.092 AX90
v -6	Trans- verse weld .505	82.6/ 89.0	99.0/ 99.0	20.0/	67.6/ 66.5	Base/ Base	(3)	64	76	97	97	0.062 MI88
v-6	All weld .252	107.9/ 115.7	116.5/ 122.7	16.0/ 17.0	56.0/ 57.7	-	-	-	-	-	-	0.062 MISS
V-7	Trans- verse weld .505	82.5/ 86.3	99.0/ 102.5	18.0/ 18.0	65.7/ 66.3	Base/ Base	(3)	52	75	78	83	0.062 MISS
V-7	All weld .252	106.0/	119.2/	15.1/ 15.6(2	51.5/ 56.5	-	-	-	-	-	-	0.062 MI88
v-8	Trans- verse weld .505	81.2/ 80.4	98.4/ 97.9	19.0/ 19.0	63.4/ 67.9	Base/ Base	(3)	54	77	77	77	0.092 MISS
v-8	All weld .252	101.5/	114.8/ 118.8	18.0/	54.1/ 68.9	•	-	-	-	-	-	0.092 MI88
v-9	Trans- verse weld .505	86.4/ 84.7	105.8/	13.8/ 19.5	67.3/ 64.9	Base/ Base	(3)	55	62	63	64	0.073 MISS
v-9	All weld .252	118.5/	136.5/ 131.4	16.0/ 17.0	40.0/ 56.0	-	-	-	-	-	-	0.078 MISS
V-11	All weld .252	87.7/· 103.0	100.7/ 113.1	22.0/	68.5/ 64.5	-	(4)	56	79	80	84	0.069 AX90

⁽¹⁾ Average of four specimens through thickness.
(2) Lower than required by MIL-E-23765/2 (100S).
(3) Two of two specimens passed 2T bend test.
(4) Not tested due to lack of material.

Table V
Results of Mechanical Property Tests
Square Butt EET Weldment vs Standard Double Vee Weldment

						ونت ورانون	
Plate Code	Tensile Type	YS, ksi	TS, ksi	Elonga- tion, %	RA,%	Frac	70
		Tensile	Test Re	sults			
466	0.505 Transverse Weld			18.0/ 17.0			Metal/ Metal
(Square Butt EET)	0.252 All Weld	102.5		21.0	55.0/ 65.5	-	
541	0.505 Transverse Weld			16.5/ 16.5	67.5/ 65.5		Metal/ Metal
	d 0.252 All V Weld		121.0/ 132.5		65.5/ 67.5	-	-
	(Average			est Resul		kness)
	Temperatur	re (° F)	Plat	e 466	Plate	e 541	
	-60		4	5(1)		67	-
	0 +30 RT		7 8	71 81 .		86 90 90	
		Side B	_	Results	3		
		. j	No. of S	pecimens	Passin	g 2T	
	Plate Coo			of 2			

⁽¹⁾ Lower than the 50 ft-lb required by specification MIL-E-23715/2 (SHIPS).

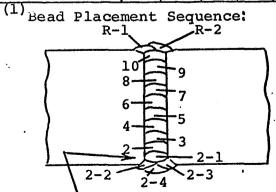
YS = yield strength, TS = tensile strength; RA = reduction in area

Table VI
PREPARATION PROCEDURES FOR EET WELDING

	the state of the s
Size of Plate (in.)	- 72x30x2
Joint Design	- Square Butt
Edge Preparation	- Ground (After Flame Cut)
Welding Position	- Flat
Polarity	- Direct Current, Reverse
Filler Wire Diameter	- 0.062-Inch Airco AX90 (Passes 1 to 9, Rl and R2) - 0.157-Inch Airco 11018 (Passes 2-1 to 2-4)
Preheat Temperature °F	- 150 Minimum
Interpass Temperature °F	- 300 Maximum
Welding Equipment	- Linde CM-37 Carriage
	 Linde SEH-3 Wire Feed Motor and Control
	- Linde ST-5 Gun

Table VII
BEAD SEQUENCE AND PARAMETERS

Bead No. (1)	1	2	3	4	5	6	7	8	9	10	R-1	R-2	2-1	2-2	2-3	2-4
Amperes, Avg.	285	290	320	340	360	360	370	380	370	370	300	300	185	185	185	185
Volts, Avg.	40	37	37	35	34	33	32	32	31	30	29	29	24	24	24	24
Travel Speed, inch per min.	13	13	13	13	13	13	13	13	13	13	13	13	5.9	9.1	7.6	10.3
Gas Mixture CODE	(2)	(2)	(2)	(3)	(3)	(4)	(4)	(4)	(4)	(4)	(4)	(4)	-	-	-	-
Joules (K joules per inch)	49	50	55	55	53	55	54	55	53	51	39	39	48	30	35	26 ⁻



- $(2)_{46\%}$ (Ar+2% O_2) + 46% (He)+ 8% CO_2 at 130
- (3) cu-ft. per hr. $(Ar+2 + O_2) + 50$ (He) at 120 cu-ft.
- per hr.

 (4) 50 cu-ft. per hr. (Ar + 2% 0₂), no external shield

Bead No. 1 removed by carbon arc back gouging

MECHANICAL PROPERTIES OF CONVENTIONAL GMAN WELDMENTS VS WELDMENTS PREPARED USING EXTENDED ELECTRODE TECHNIQUE

		ELECTRODE NIQUES	CONVENTIONAL GMA			
	0.062'' DIA: WIRE	0.092'' DIA, WIRE	0.062'' DIA. WIRE	0.092'' DIA. WIRE		
YIELD STRENGTH, KSI	113.6	107.2	99	96		
TENSILE STRENGTH, KSI	126.3	121.2	108	107		
ELONGATION, %	20.0	20.0	23	21		
REDUCTION IN AREA, %	63.0	62.8	68	65		
CHARPY 'V' NOTCH (FT-LBS)						
-60°	52	54	17	73		
0°	80	71	110	101		
-30°	92	82	130 .	110		
RT	104	93	130	121		
SIDE BEND TEST	ACCEPTABLE	ACCEPTABLE	ACCEPTABLE	* ACCEPTABLE		

Table VIII

NSRDC

CUMPAKATIVE DAT	A: CONVENTIONAL vs	EET WELDING
CRITERION	CONVENTIONAL	EET
DISTORTION	APPRECIABLE	MINIMAL
PLAME CULS PER JOINT GROUND SURFACES PER JOINT	133	1.00
ARC TIME,* min. (per ft. weldment) VOLUME OF WELD MEIAL,* in (per ft.)	30 24	12 12
YIELD STRENGTH, ksi CVN at 30° F, ft.—Ib. HY 80	100 100	110 93



FIGURE CAPTIONS

- Double-Vee Joint Required to Provide Access for Shielding Cup in Root
 Area in Inert Gas Arc Welding of Thick Plate.
- 2. Arrangement for Extended Electrode Technique Welding of Thick Plate.
- 3. Globule Formation of EET Welding
 - a. Globule Has Fallen and Formation Beginning
 - b. Globule Half grown
 - c. Globule Grown Almost Ready to Fall
 - d. Globule Has Fallen and in Contact with Plate.
- 4. Effect of Diameter of Filler Wire on Charpy V-Notch Tests with Other
 Parameters Held Approximately Constant (MI88 Wire, 25% Ar+70% He+5% CO₂
 Internal Shielding gas).
- 5. Effect of Travel Speed on Charpy V-Notch Tests with Other Parameters
 Held Approximately Constant (MI88, 0.062-Inch Diameter Wire,
 25% Ar+70% He 5%+CO₂ Internal Shielding Gas).
- 6. Melting Rate Versus Electrode Extension.
- 7. Results of Shipyard Implementation of EET Welding.
- 8. Typical Hardness Values of EET Welds (Values in R_c).

a.

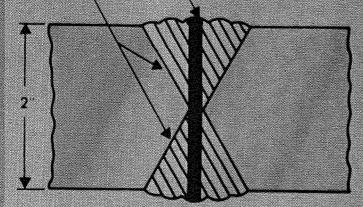
519<

BASE METAL TO BE REMOVED

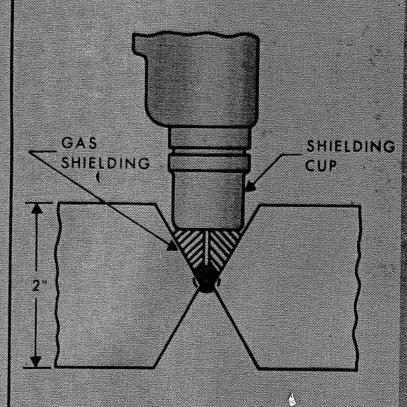
— AND REPLACED BY WELD METAL

USING 60° DOUBLE-VEE JOINT

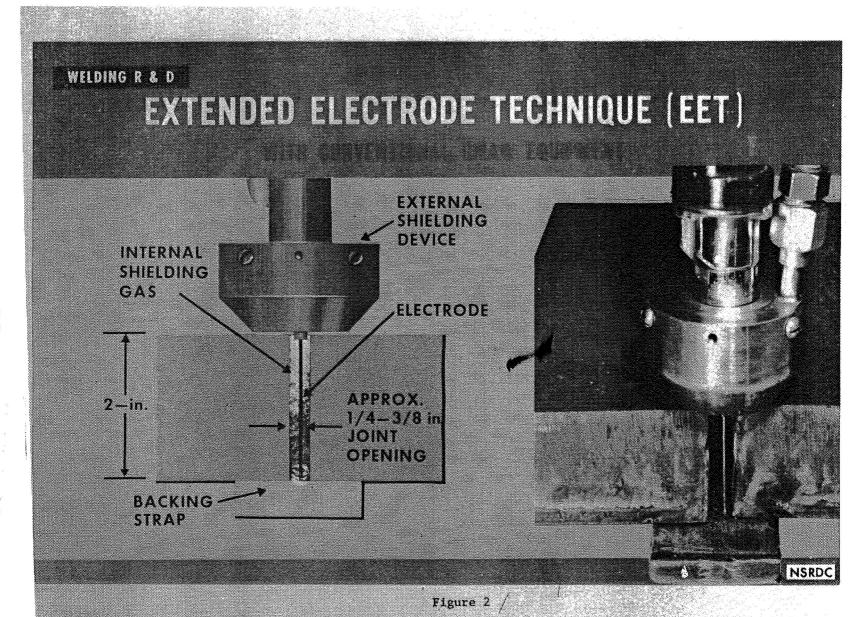
AREA TO BE FUSED USING SQUARE BUTT JOINT CONFIGURATION

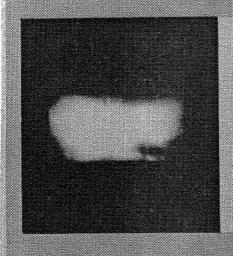


Ь.



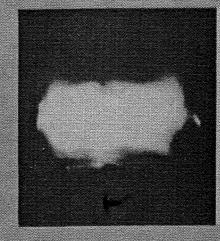
NSRDC





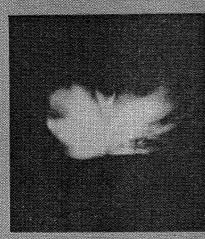


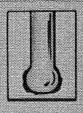
a. GLOBULE HAS FALLEN AND FORMATION BEGINNING



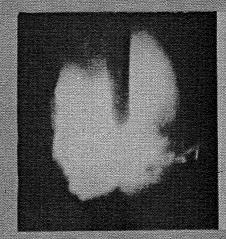


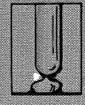
b. GLOBULE
HALF GROWN





c. GLOBULE GROWN ALMOST READY TO FALL





d. GLOBULE HAS
FALLEN AND IN
CONTACT WITH
PLATE

Figure 3

NSRDC

EFFECT OF FILLER WIRE DIAMETER ON CHARPY VINOTCH PROPERTIES

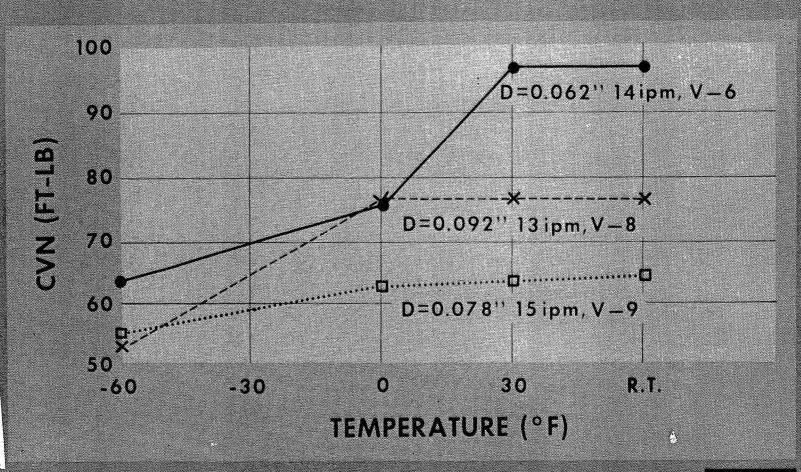


Figure 4

° NSRDC

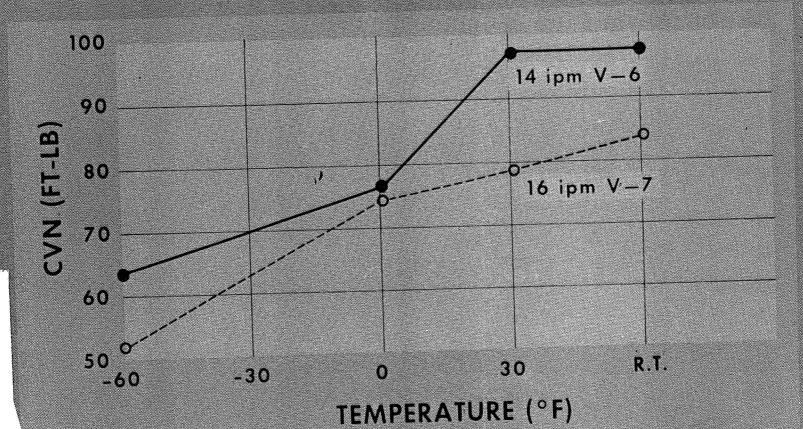


Figure 5

NSRD61

EFFECT OF MELTING RATE VERSUS WIRE EXTENSION

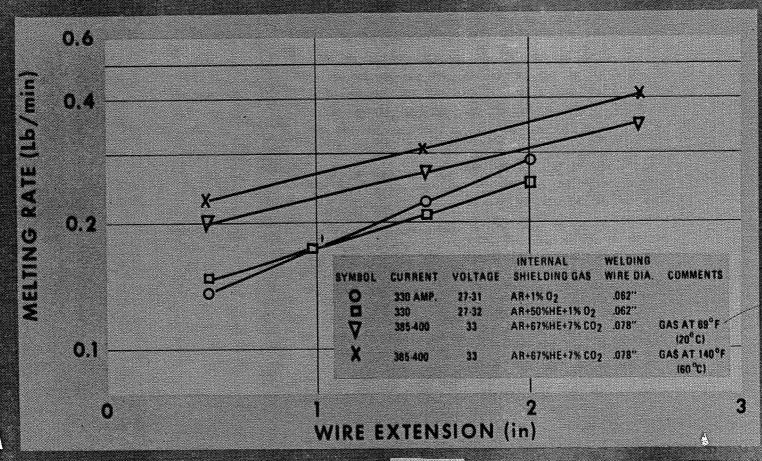
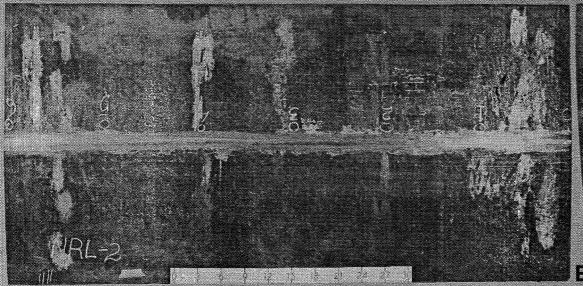
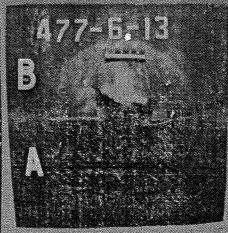


Figure 6

NSRDC

WELDING R & D SHIPYARD IMPLEMENTATION OF EET WELDING



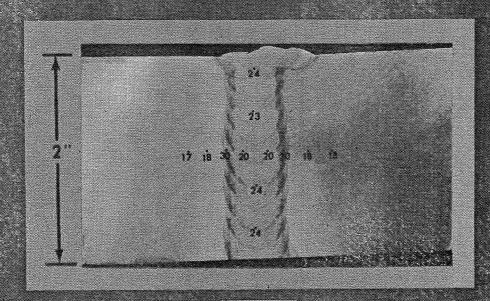


72—in. LONG - 2—in. THICK HY 80 STEEL YIELD STRENGTH 115 ksi
TENSILE STRENGTH 126 ksi
ELONGATION 22%
REDUCTION IN AREA 67%
CVN @ 30°F 110—ft.-lbs.

EXPLOSION BULGE RESULTS

NUMBER OF SHOTS 6
PENTOLITE CHARGE 24—lbs.
REDUCTION IN
THICKNESS 26%
DEPTH OF BULGE 6—in.
INSRDC

(VALUES IN R_c)



NASA/ASM George Washington Symposium
"WELDING, BONDING, AND FASTENING"
Williamsburg, Virginia

May 31, 1972

N74 30946

Session 6, Welding Techniques

3. "ELECTROSLAG AND ELECTROGAS WELDING", By Hallock C. Campbell
Director of Research and Technology, Arcos Corporation, Phila., Pa.

The structures described in this paper won't fly,...but electroslag and electrogas welding could well have been used to build the transporter that carries the Apollo/Saturn rocket along its first mile toward the moon; and these processes are used to weld the presses that form NASA vessels, and the storage tanks, ships, barges, bridges, and buildings involved in numerous NASA projects. Not everything NASA touches actually flies.

These two new joining methods perform welding in the vertical position, and therein lies the secret of their impressive advantages in material handling, in weld preparation, in welding speed, in freedom from distortion, and in weld soundness. Once the work has been set in the proper vertical position for welding, no further plate handling is required. Overhead cranes need not be recalled to turn the plates over, as would be required in multi-pass downhand welding. The molten filler metal is held in place by copper shoes or dams, and the weld is completed in one pass.

comparing a single pass weld in l1-inch plate with the laborious 1200 passes required in a manual weld, makes obvious how many advantages will accrue from single pass welding. Plate preparation requires no U-grooves or complicated bevels with root faces: merely a straight flame-cut edge, to give a 90° butt joint or recently a single-vee joint with open root. The gap to be filled is less than 1½ inches wide no matter how thick the plates, hence welding progresses rapidly. Commonly some 35 lbs. of metal are deposited per hour by each wire used; in electroslag welding with three wires the deposition rate is over 100 lbs. per hour. Not uncommonly electroslag and electrogas welds are completed in one-fifth the time required by other welding methods.

The great advantage of electroslag welding is weld quality, resulting from metallurgical refining of the filler metal by the slag, and from the directional solidification of the weld from below upwards, rejecting non-metallic impurities into the slag bath. The metal solidifies as a clean sound weld, remarkably free from distortion.

As mentioned already, a weld pool between vertical plates will have to be constrained by dams. For oil and water storage tanks, for structural steel beams, and for various small assemblies, it is sufficient to use thick copper bars on the side of the joint remote from the welding machine, or even on both sides (in consumable nozzle welding). On the working side (or on both sides), water-cooled sliding shoes are used, whose rise is coordinated with the upward solidification of the weld. Into the pocket so created the filler metal



is guided by a snorkel reaching over the top of the near shoe, or by a consumable guide centrally located within the joint gap.

Between plates 1½ to 5 inches thick or thicker, the process employs an electrically conductive molten slag pool, about 1½ inches deep, which melts the filler metal and the edges of the plates by its high temperature (3000°F), hence the name electroslag welding. In electroslag welding there is no arc once the slag pool has been established.

In welding plates 1/2 to 3 inches thick the process is electric arc welding, shielded with CO2 or argon gas, hence the name electrogas welding. A small amount of flux is frequently used to improve the surface of the weld, since it lubricates the moving shoe.

To feed wire through a consumable nozzle requires little equipment. Figure 1 shows a weld being set up for demonstration, before view of the nozzle becomes blocked by the copper shoes.

To use travelling shoes and a snorkel, controls are provided which can climb a mast or track placed beside the work. Mechanical controls used earlier for oscillation and dwell have since been replaced by solid state electronics. Figure 2 shows a portable slag/gas machine equipped with one water-cooled shoe, which climbs a standard track. In this case copper backing bars must be preplaced against the far side of the joint to contain the weld pool.

For welds more than 5 or 6 inches thick, two or more wires are fed into the slag by sophisticated equipment which reaches through the joint to hold the far shoe in place. Figure 3 shows a laboratory set-up from the far side. Water and gas connections to the shoe are evident. The arm is free-floating in two horizontal directions, and self-tracking along the joint. One of the first production applications of a 2-or 3-wire machine in this country was that shown in Figure 4, the preparation of plates of HY80 wider than any plates Lukens Steel Co. can roll, to make a blank from which to spin nose cones for submarines.

A typical application of electrogas welding is the welding of storage tanks, such as the group of surge towers at the Oahe

Dam in South Dakota. The vertical seams in these towers were all welded with electrogas welding machines which could be mounted on carriages hung from the top of the tank being constructed. Figure 5

shows a cage being swung into position. These tanks were welded with square butt preparation, but current practice for oil storage tanks, whose plates vary from ½ to 1½ in. thick, is a Vee grove preparation with root gap 3/16 in. backed by a single copper bar (typically 1 in. x ¼ in. x several feet long). The angle of vee differs for the several plate thicknesses, to give in each case a face opening 7/8 in. across, closed by the water-cooled shoe carried by the traveling machine. A single filler wire is fed into this pocket and protected by inert gas or CO₂ flowing from orifices in the shoe and the wire guide. The wire is oscillated by the equipment to distribute the arc heat uniformly over the weld pool.



A typical three wire application of electroslag welding is that shown in Figure 6, a structural frame destined for a mammoth hydraulic press. Figure 7 shows a 15 inch thick sub-assembly, ready to be joined along two 6-foot seams. Figure 8 will be recognized by ASM members as the cover picture on Metal Progress magazine in December 1967. At this stage one of the lower seams is being completed. Figure 9 shows the completion of the upper seam. Regularly four such seams are completed in five working days, including assembly and disassembly of the equipment. This job welded by submerged arc would take four to six weeks.

Another important application of electroslag welding is the assembly of stainless steel pump casings for nuclear power plants. The circumferential seam in Figure 10 is rotated downwards past the electroslag welder, which stands stationary until the tangent discharge pipe is reached, when rotation is halted and the welding equipment rises.

Repairs to shafts and spindles are commonly made by electroslag welding. Figure 11 shows the weld preparation for a 9 in. diameter shaft. Note the run-off tabs, which provide a rectangular weld area. The excess metal is cut off after the shaft has been welded. A large spindle is shown in Figure 12, a repair so thick that two 2-wire welding machines were brought to the joint, one on each side. Figure 13 shows the welding in progress.

To summarize this brief survey of an extensive subject, stressing in particular the ways in which electroslag and electrogas welding fit into the theme of this Symposium, these new joining methods

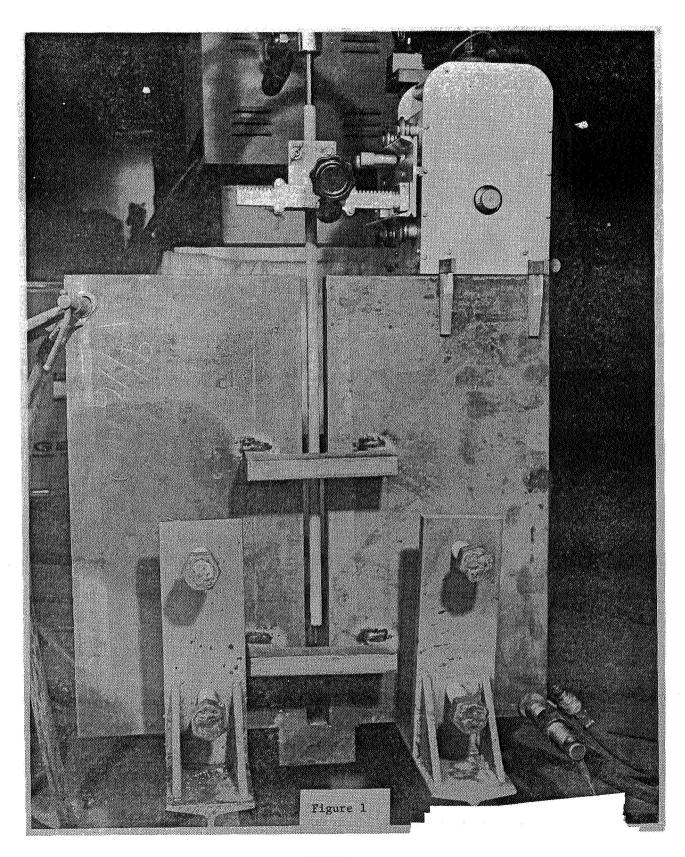


save weight, (of course—so does any welding method); they save time, in weld preparation;

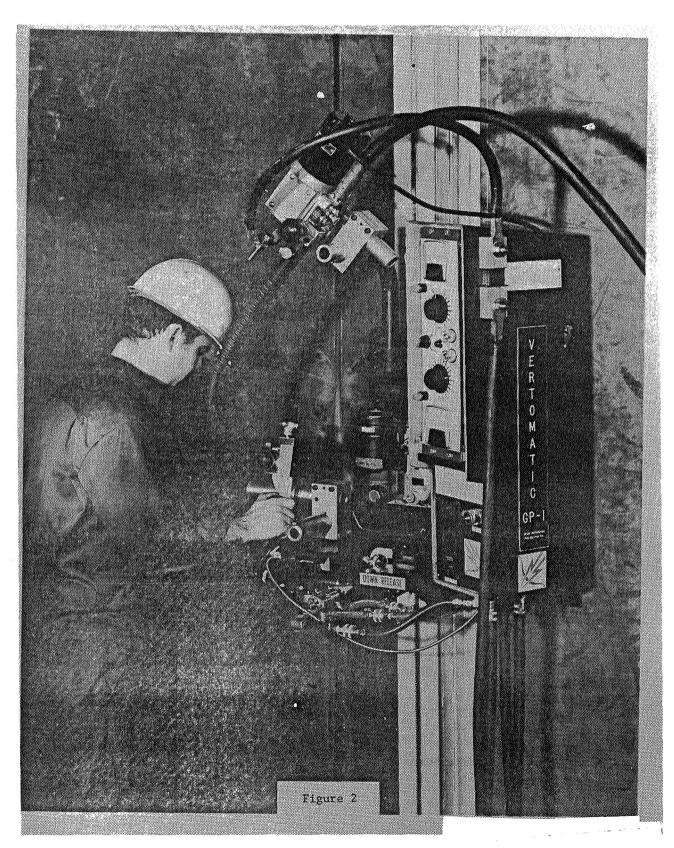
they save <u>labor</u>, in material handling;

they save <u>time</u>, <u>again</u>, in the welding operation itself;
they produce a <u>sound</u>, <u>undistorted weld</u>, because it is completed in one symmetrical pass and is solidified directionally with rejection of impurities into the discarded slag.

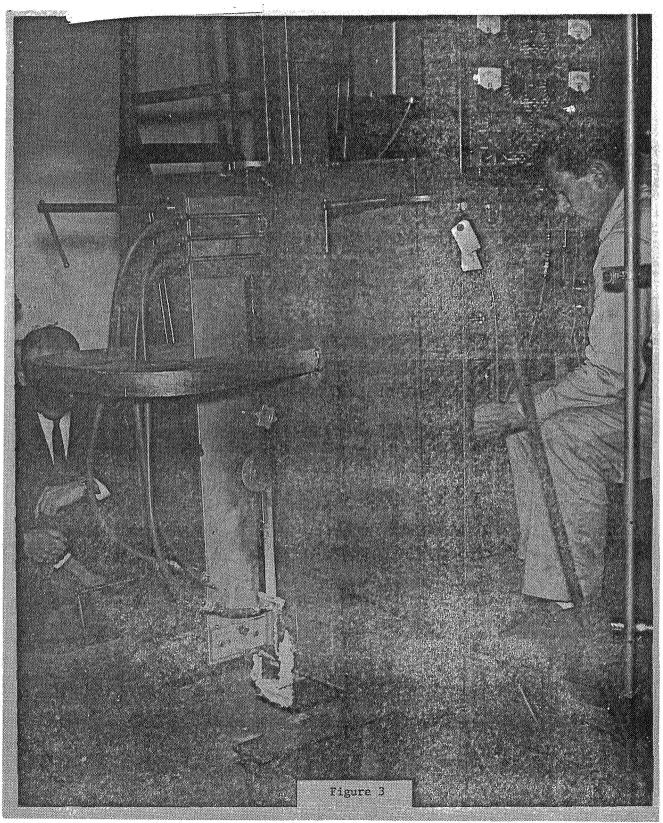
I think it will pay many of you to adapt these processes to your own joining applications.



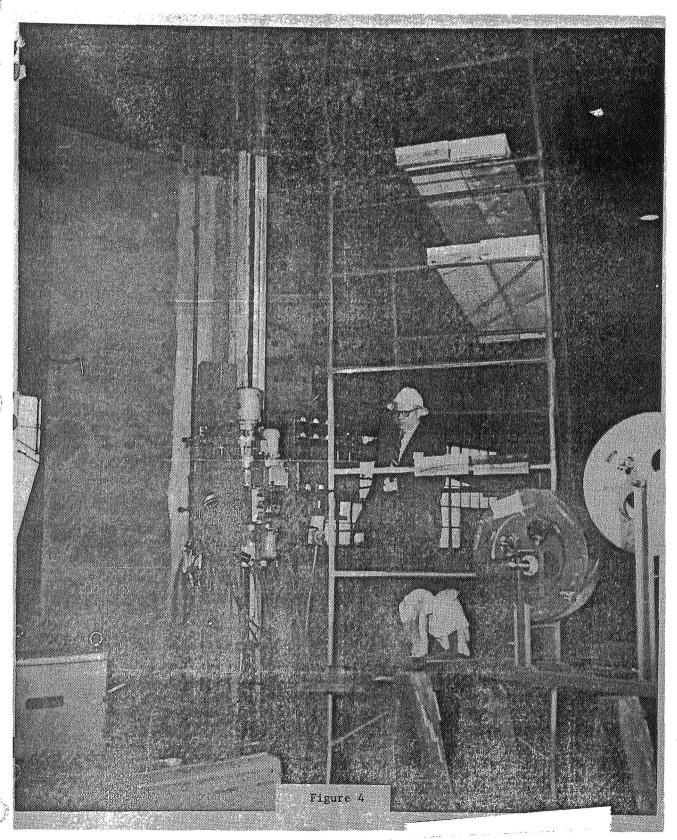
533<



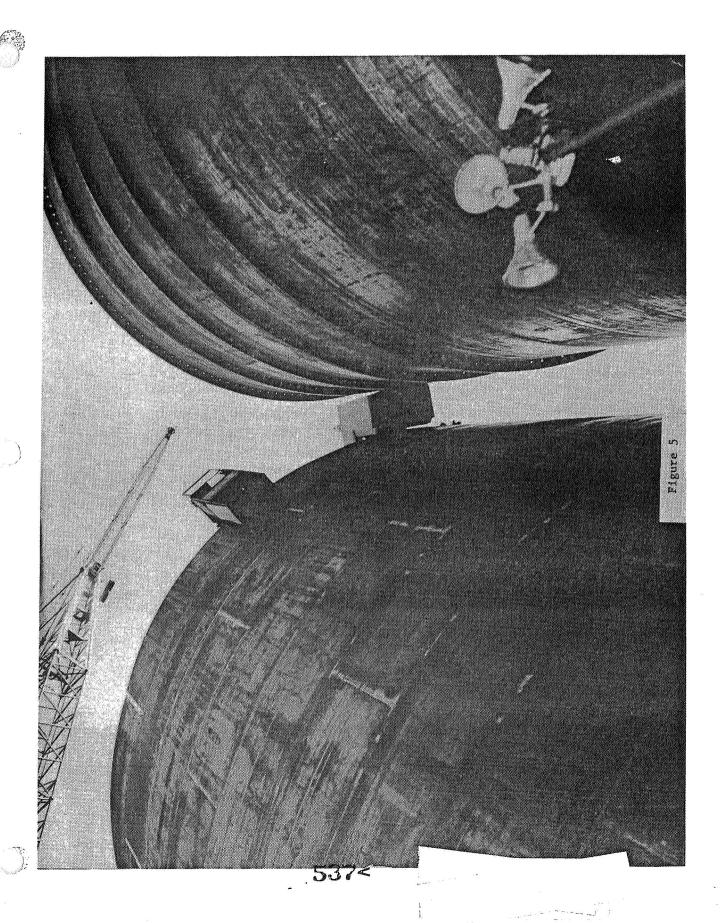
534<

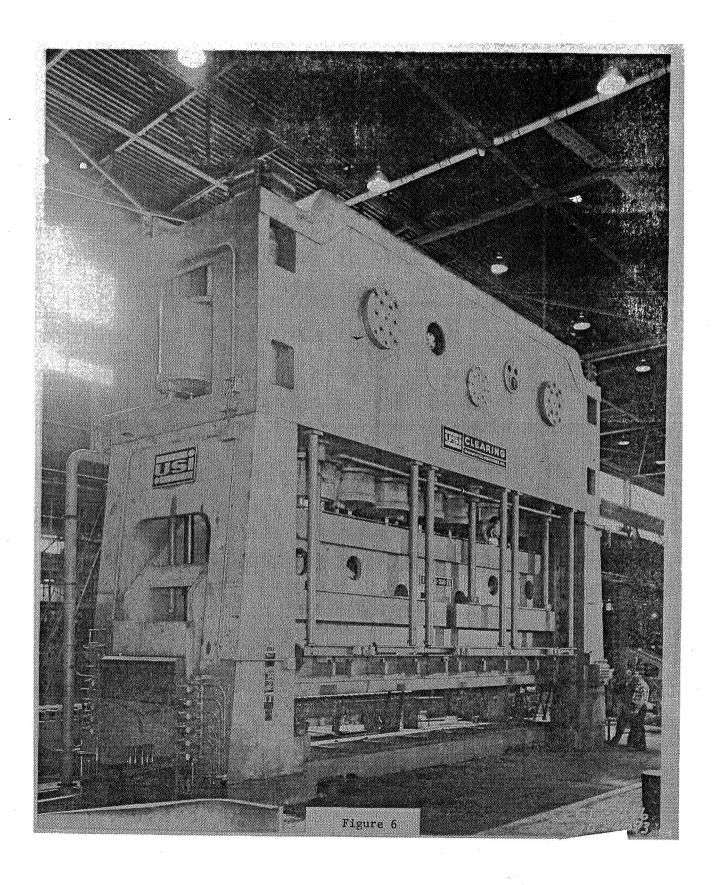


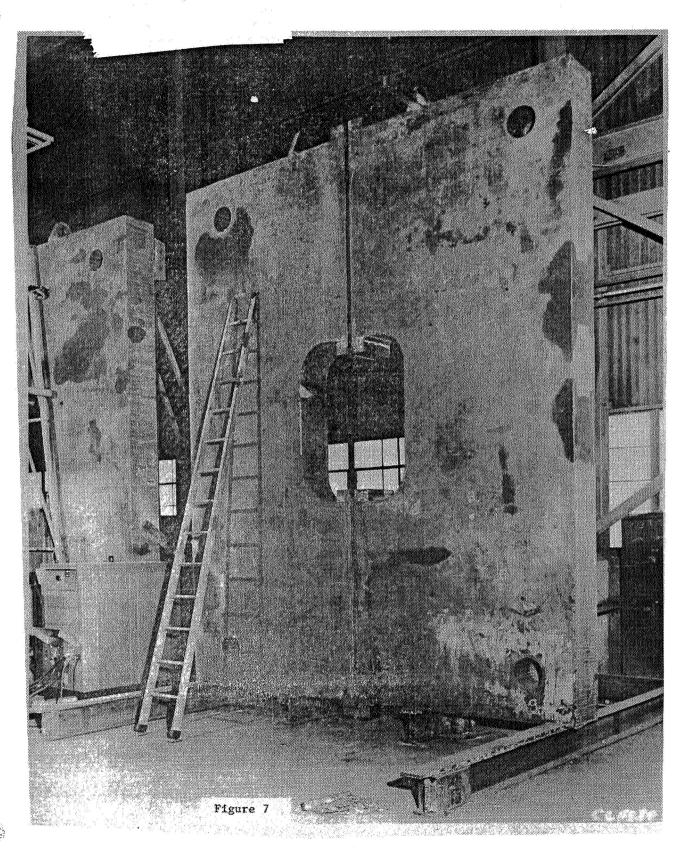
535<



536<







539<

The Next 40 Years in Materials

METAL PRO

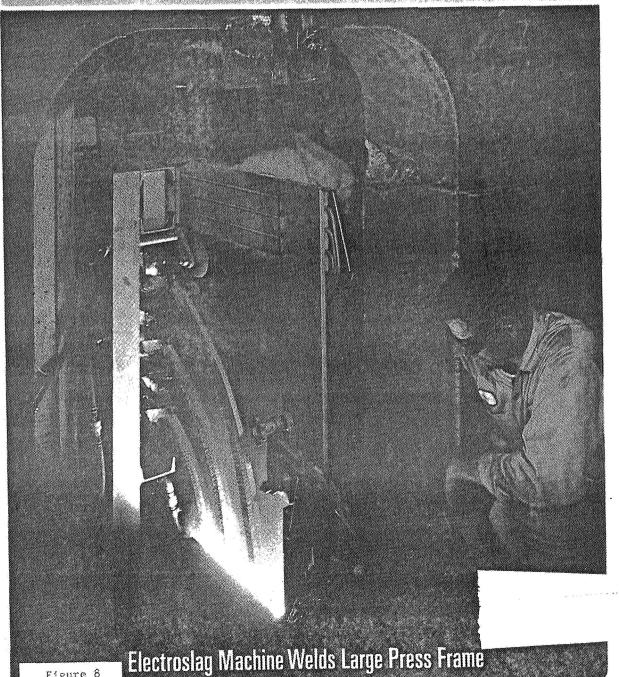
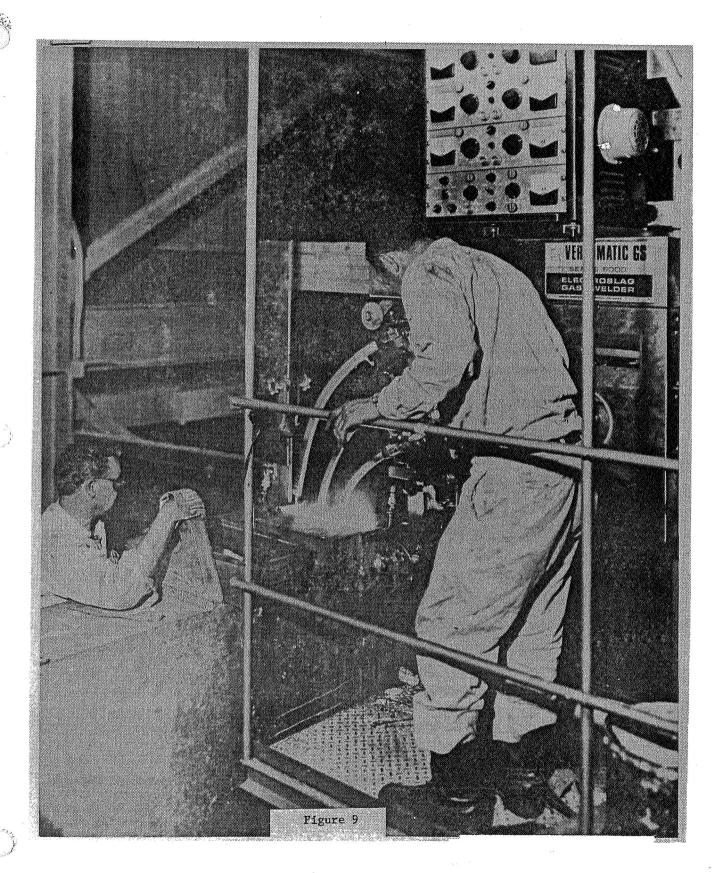
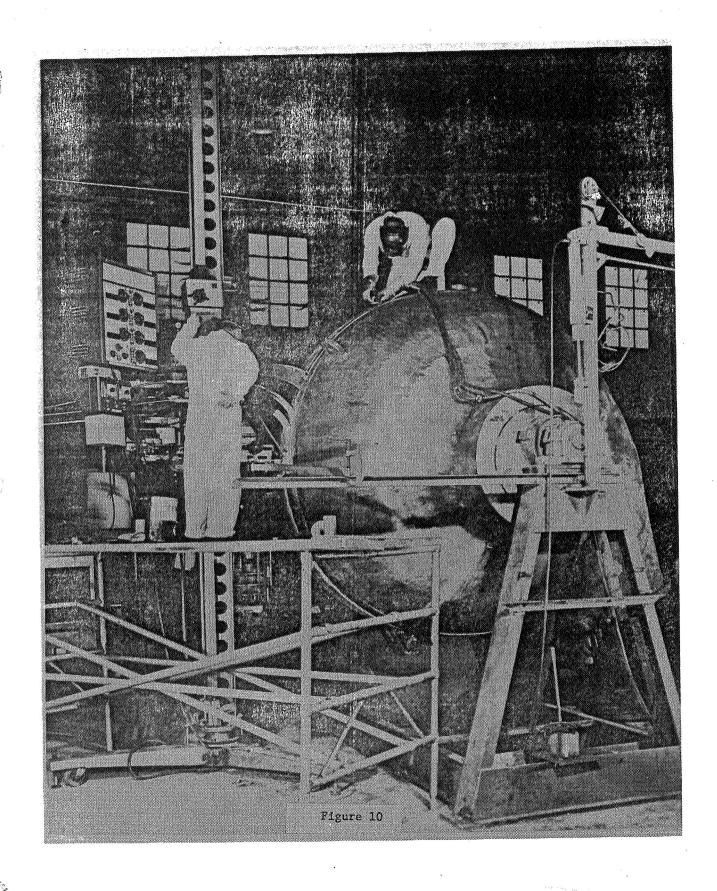
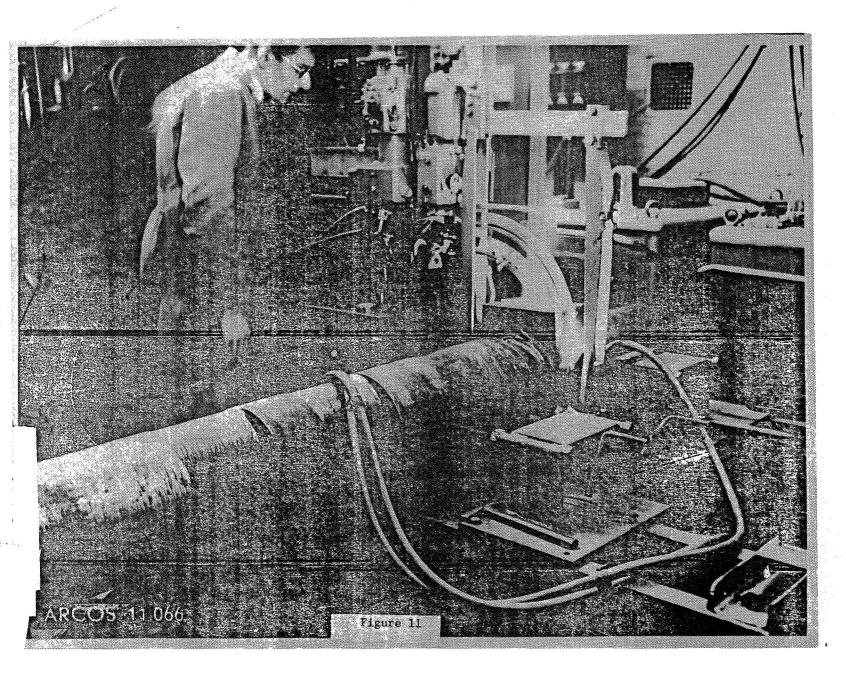
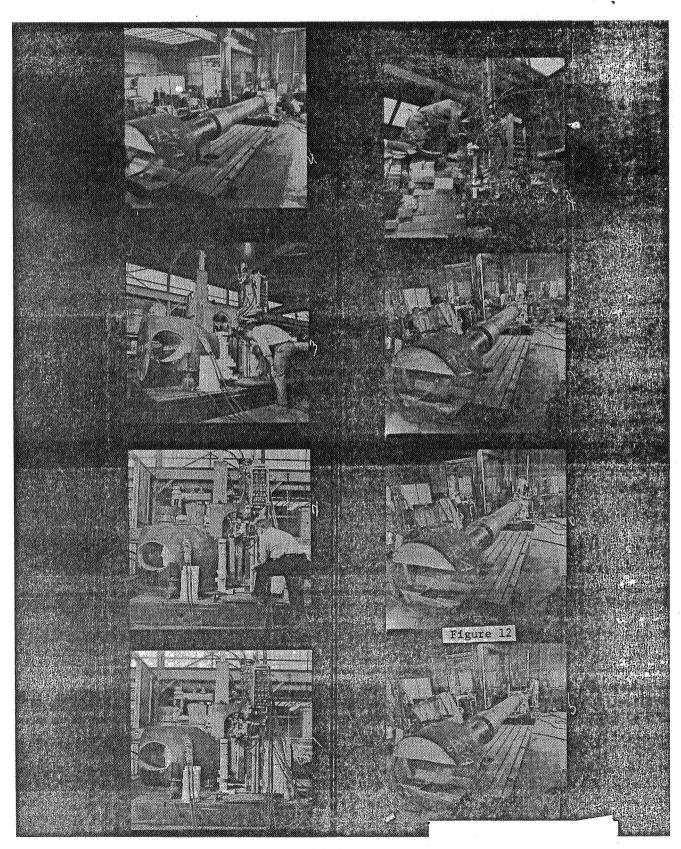


Figure 8

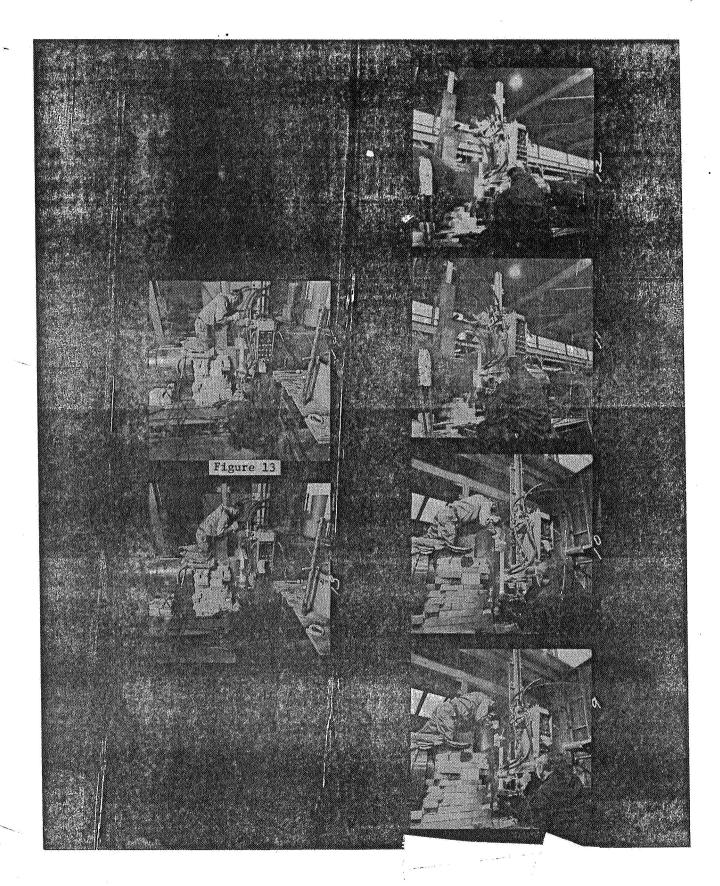








544<



545<

N74 30947

ADVANCED FUSION WELDING PROCESSES,

SOLID STATE JOINING AND A SUCCESSFUL MARRIAGE

Fred R. Miller
Senior Project Manager
Manufacturing Technology Division
Air Force Materials Laboratory
Wright-Patterson Air Force Base, Ohio

Historically, our technological progress has resulted from the challenging design requirements of advanced aerospace systems which have led to the evolvement of new materials, new applications, and a complementing family of joining processes. Mission profiles for advanced systems continually emphasize the need for the highest possible material strength to weight ratios at the higher speeds over a wide range of temperatures. As these new materials emerge for application their ability to be joined must be determined with processes and techniques developed to permit their practical use. Characterization of the material to be joined, the geometry of the component parts, their thickness and dimension, the required joint properties, and the environment which the assembly must withstand are essential to selecting the joining or fastening process. The technical area of metals joining is recognized as vital to the production of advanced Air Force systems since joints of high integrity with properties approaching those of the parent material are essential for maximum utilization of the required materials.

A sizeable number of joining processes exist some of which are relatively new and are gaining substantial application for meeting the joining requirements of current and future production. The processes are categorized as fusion welding, solid state joining and specialized

combinations an example of which is the weldbond process. This is a resistance spot weld-adhesive bond process working in combination to obtain the benefits of each process. The particular processes selected for discussion herein have gained significant government and industry development and have evolved for production use. These are electron beam welding, plasma arc welding, diffusion bonding, inertia welding, and weldbond.

ELECTRON BEAM WELDING

Electron beam welding is defined in the Welding Handbook as a fusion joining process in which the workpiece is bombarded with a dense stream of high velocity electrons, and virtually all of the kinetic energy of the electrons is transformed into heat on impact. (Reference 1) Electron Beam welding as a fusion process offers the advantages of high depth to width ratios, small heat affected zones, reduced residual stress and distortion. It is conducted in a single pass full penetration mode as opposed to the conventional multi-pass arc welding processes. Electron Beam welding is continually gaining new application for production and has been demonstrated for joining critical structures. North American Aviation made an electron beam close out weld on the wing to stub wing fuselage attachment in the B70 program. Solar Division of International Harvester electron beam welded the rotor hub from 2.250 inches thick Ti-6A1-4V for the Cheyenne Helicopter program. (Figure 1) Solar is also applying electron beam welding to wing flaps and slat tracks on the Lockheed L1011 airplane. Grumman Aerospace Corporation is currently electron beam welding the wing center box of the F-14 airplane from titanium 6A1-4V alloy. (Figure 2)

The Grumman commitment to electron beam weld the F-14 titanium center wing box structure represents the most advanced application of the electron beam welding process to primary critical aircraft structure. The commitment to electron beam weld titanium was based on a significant

والمنافعة المنافعة المنافعة

weight savings potential (estimated at 50% less than steel). The structure is fabricated from 45 machined parts and the completed assembly has approximately 70 welds all made in a vacuum environment by electron beam welding.

In primary critical aircraft structure, electron beam welding may be considered to offer a certain amount of risk since it is a relatively new process with no previous application to wing carry through structure. It should be noted that the F-111 wing carry through structure of D6ac steel was gas tungsten arc welded by using multi-pass welding techniques. Without belaboring the point, the welded F-111 carry through structure was never determined to be a problem area. The electron beam welding process offers significant advantages over the gas tungsten arc welding process. Electron beam welding advantages of high depth to width ratio, smaller heat affected zones, reduced residual stress and distortion are desirable. The ability to complete a weld in a single pass at reduced heat input, compared with a multi-pass gas tungsten arc weld is a desirable objective.

The electron beam process is not a utopian push button automated process. For successful application to complex structures during the course of fabrication, the process requires a cooperative effort between designers, welding engineers, metallurgists, quality assurance and stress engineers.

Large structures dictate a requirement for large electron beam welding equipment and accompanying large vacuum chambers. (Figures 3 and 4) This necessitates during the welding process that the tooling, fixturing, joint fit up, gun to workpiece alignment and seam tracking must be precise. Since the electron beam process produces a narrow weld (.020 to .060 approx.) joint, fit up must be precise. The possibility of the beam missing the joint exists. In the case of the F-14 Grumman uses what is referred to as a "witness line" technique to assure the desired weld width and penetration. This witness line tech-

nique involves the scribing of lines parallel to the weld joint on both the surface and underside of the joint. The weld is made along the joint in a full penetration pass. Subsequent to welding, the weld is visually inspected to determine if the witness lines are obliterated by the weld bead on both the surface and underbead side. If the lines are wiped out it provides assurance that the joint has been fully penetrated and width of weld is acceptable. This may appear to be a crude seam tracking approach to assure weld width and penetration, but it does work. Other EB seam tracking techniques such as probes riding in or parallel to the joint and depending on transducer correction thru servo controls have not established confidence levels equal to the "witness line" technique.

There are other concerns regarding precautionary measures with the EB process to avoid defects. As in any arc welding process defects can occur. Some of the more significant defects include arc outs, porosity, undercutting and lack of fusion. Arc out (electron beam is extinguished) usually occurs during a welding operation as a result of contamination of the electron beam welding gun components. A special glow discharge cleaning procedure is utilized regularly and is effective in keeping filaments clean for welding. Most arc outs occur when welding at high power inputs or when the beam is operated continuously for long periods of time. Defects caused by arc outs can be repaired in titanium by rewelding with precise control of slope out of the beam.

The foregoing types of defects that may occur in EB welding dictate a requirement for highly reliable nondestructive inspection techniques, for assured quality control. Grumman in their F-14 program has placed major emphasis on nondestructive inspection techniques, including dye penetrant, X-ray, C-Scan ultrasonic techniques and delta ultrasonics. A continued effort is in progress to develop more reliable standards to assist in the interpretation of ultrasonic scan patterns.

In the F-14 program Grumman generated mechanical properties data for the titanium 6A1-4V alloy and titanium 6A1-6V-2Sn. Grumman welded the titanium alloys by electron beam and gas tungsten arc in varying thicknesses. In general the tensile strengths, elongations, and joint efficiencies of the electron beam welds were better than the gas tungsten arc welds. Tension-tension fatigue properties of EB welds in 0.50 inch Ti 6A1-4V were better than gas tungsten arc welds of the same thickness made in 4 passes with filler wire. Grumman generated a substantial amount of surface flaw crack growth data under constant amplitude for one inch thick EB welded, annealed Titanium 6A1-4V plate. Grumman also conducted F-14 wing spectrum fatigue loading tests on one inch thick Ti-6A1-4V in order to be able to relate fracture toughness variations with flaw growth rate and establish realistic limit loads for structural designs.

An Air Force Materials Laboratory, Manufacturing Technology Division sponsored program is currently in progress at Grumman for evaluation of sliding seal electron beam welding system. (Figure 5) Aluminum 2014-T 651, Titanium 6A1-4V and HY 130 steel in plate thickness have been welded and the capabilities of the sliding seal electron beam_welding equipment to produce weldments with quality acceptable for aerospace structure have been determined. (Figure 6)

The sliding seal electron beam welding system was produced by Sciaky Bros. under a previous Air Force contract. It consists of a portable vacuum, moving electron beam welding head that is mounted on a ram manipulator, back up tooling and associated power supply and controls. The power capacity of this unit is 30 kilowatts (60 KV, 500 ma) with vacuum pressures ranging between 1 X 10⁻⁴ torr and 100 microns of Hg. This vacuum is obtained by pumping between two nonmetallic seals in the welding head.

Under a recently completed AFML contract at Bell Aerospace electron beam welding of HY 130 steel, D6ac low alloy high strength steel fully heat treated, 9 Ni-4Co-.30C steel, and titanium 6Al-6V-2Sn in a range of thicknesses from 0.125 through 1.0 inches was conducted. The mechanical properties of electron beam welds were comparable to base

metal properties and exceeded the properties of other competing fusion welding processes. (Figure 7)

Electron beam welding will continually gain new applications in large structures built up from smaller segments. The joining of plate materials, smaller forgings and the advantages of the single pass full penetration capability enhances consideration for using the process. The weight reduction realized by eliminating the penalty associated with mechanical fasteners and hole generation in thick plate stimulates consideration of the process for weight critical structures.

PLASMA ARC WELDING

Plasma arc welding is an arc welding process in which the heat is produced by a constricted arc between a nonconsumable electrode and a workpiece (transferred arc), or between a nonconsumable tungsten electrode and a constricting orifice, (nontransferred arc). (Reference 2) Plasma arc welding is closely related to gas tungsten arc welding. Plasma is present in all arcs. If a constriction containing an orifice is placed around the arc, the amount of ionization, or plasma, is greatly increased. This results in higher arc temperature, a more concentrated heat pattern, and higher arc voltage than can be obtained with a nonconstricted arc.

The plasma arc welding process has evolved in a manner typical of any new joining process considered for aerospace application. The equipment producing industry in recognizing the potentials of the plasma arc torch as an energy source for welding took the lead in designing and marketing plasma arc torches for mechanized welding. The Air Force Materials Laboratory, Manufacturing Technology Division realizing the potentials of the plasma arc process and the relative shortage of data and experience sponsored a program in July 1966 with the Aerojet-General Corporation for a comprehensive process development and evaluation for application to aerospace materials and structures. (Reference 3) Under this initial Air Force sponsored contract Aerojet developed substantial data describing the capabilities of the plasma arc welding process for

making straight-seam and circumferential butt welds in rocket motor cases and other weight-critical pressure vessels. The materials welded in this program were 18% Nickel maraging steel, 9 Nickel-4 Cobalt, and Titanium 6A1-4V over a range of thicknesses from 0.25 inches through 0.62 inches. Aerojet also demonstrated the capability of applying the plasma arc welding process by producing girth welds in six, 24 inch diameter spherical pressure vessels. Three of these spheres were 0.25 inch thick 6A1-4V titanium alloy, and three were 0.50 inch thick 18% Ni 200 KSI grade steel. The welded vessels were nondestructively inspected by visual, dye penetrant, X-ray and ultrasonic techniques. The vessels were heat treated, then hydrostatically pressurized to burst failure. Hydrostatic pressure and related strain gage data were recorded for all tests and acoustical wave emission corresponding to incremental flaw growth were monitored for two burst tests. (Figure 8) The results of this pressure vessel test program verified the plasma arc process potential for producing high quality butt welds reported in previously published literature.

Subsequent to the foregoing contract an AFML program was awarded to Allison Division, GMC, for development of the plasma needle arc process (0.1 to 10.0 amps) for selected thin gage engine materials and applications. (Reference 4) Several alloys were welded including titanium 6A1-4V. The needle arc process is limited to a maximum of approximately 0.030 inches in thickness. Under this contract thin gage engine components including exhaust collector inner cones for the T 63 engine, outer combusion case for the T 63 engine (Figure 9), anti-icing compressor vane for T 56 engine and a compressor arc discharge tube for the T 63 engine were welded. This program resulted in the conclusions that low amperage plasma arc welds are equal to gas tungsten arc welds in respect to weld bead contour and weld travel speed. Welding operators certified to MIL-T-5021 require no training for use of low amperage plasma arc except for brief equipment operation explanation. The pilot arc system enabled the welding operator to initiate the arc in exactly

the desired spot as he is able to see the pilot arc and weld seam through a weld lens before transfer to welding current. This prevented stray arc strikes and marks detrimental to thin material welding. This program resulted in the recommendations that plasma arc welding is an acceptable and advantageous process for joining foil materials up to 0.030 inches in edge, square butt, and flange melt down joints.

In sequel to the plasma needle arc (10 amp) process a program was conducted by the Allison Division, GMC, for a plasma arc process optimization of the Linde 100 ampere low current plasma arc welding process. (Reference 5) Five materials common to gas turbine engines were welded. These included 310 stainless steel, 410 stainless steel, Inco 718, Titanium 6A1-4V and 4130 steel alloys. Included were thicknesses of 0.015 through 0.125 inches. Test panels for manual and machine welding included square butt, edge, lap, and T joints. Single pass, keyhole mode machine welding with the addition of filler material for square butt joints was highly successful for gages of .048 through 0.125 inches. Keyhole mode welding provided assured penetration, significant reduction in weld bead width, lower amperage requirements and higher travel speed. Weld strength mechanical properties showed 100% joint efficiency by uniaxial tensile tests. Microstructures were essentially the same as seen in gas tungsten arc welds. Radiographic and fluorescent penetrant examinations revealed welds essentially free of porosity and completely free of tungsten inclusions. It was concluded from this program that in comparison with gas tungsten arc welding plasma arc offers increased flexibility of operation, assured penetration in the keyhole mode, greater thickness capacity at 100 amps, reduced need for operator skill, improved quality and potential cost savings. Application of this process will definitely render significant benefits in joint designs requiring square butt and edge welds.

With the industry development and the AFML sponsored development discussed above the plasma arc welding process became prioritized

in aerospace company funded joining development programs. The most impressive development and application of the plasma arc welding process for large aircraft structure was conducted by The Boeing Company for SST prototype application. (Reference 6) The inherent characteristics of the plasma arc process were proven to be particularly advantageous in the welding of titanium components for the supersonic transport. The significant advantages of plasma arc over gas tungsten arc and gas metal arc welding were found to be low weld bead width to depth ratio, narrow heat affected zone, less critical preweld cleaning required, considerably less porosity occurrence, less distortion due to lower total heat input, less critical torch to work distance and part fit up requirement, faster welding speed, elimination of tungsten inclusions and electrode deterioration problems. The advantages over the electron beam welding process were found to be substantially lower original equipment cost, better operator visibility, and lower detail part and fabrication costs. Boeing conducted an extensive plasma arc welding development program beginning with a survey and tests of existing welding equipment. Their methodical evaluation included preweld cleaning requirements; evaluation of orifice and tungsten electrode life; relationship of amperage, orifice gas, orifice diameter and electrode diameter to part thickness; orifice to work distance in inches; maximum allowable joint mismatch, root opening and misalignment; weld bead depth to width ratio for keyhole mode welding; maximum allowable torch lead, lag and work angles and the minimum and maximum thickness weldable in the keyhole mode. As a result of this process evaluation Boeing evolved a plasma arc welding technique for fabricating integrally stiffened wing panels from titanium 6A1-4V approximately twenty-eight (28) feet long. (Figures 10, 11, and 12) The set up involved machining a titanium 6A1-4V plate and leaving a stub where the "L" shaped stiffeners 0.050 to 0.125 inch thick were to be joined. The machined plate with stubs

plasma arc keyhole welded in the downhand position. During initial SST

was fixtured in the vertical position.

"L" shaped stiffeners were then

prototype part fabrication 7000 linear inches of plasma arc weld in 0.125 inch thick stiffeners were produced with no internal defects indicated by X-ray inspection with 2% of thickness definition. The commitment of plasma arc welding for the integrally stiffened panels on SST attests to the high confidence levels for the process.

DIFFUSION BONDING

Diffusion bonding is a solid state process for joining detail parts into integral configurations with a continuous metallurgical structure. (Reference 7) Bonding is accomplished by the application of pressure and heat for a predetermined period of time in an adequate environment. The pressure is applied to establish intimate contact between the detail parts and the heat to activate the migration of items across the interface for a sufficient time cycle to develop a bond. With the use of sufficient heat, pressure and time the bond interface and the zone near the bond become a single homogeneous microstructure. The material near and within the bond interface has mechanical properties equal to the base material with the result that a diffusion bond can be the optimum structural joint. There have been many approaches evaluated to perform the diffusion bonding cycle depending on the type of equipment used to apply the pressure. (Reference 8) These have included bar rolling mills, plate rolling mills, extrusion presses, hydraulic presses such as forging presses or sheet metal presses and resistance seam welding equipment using both spot and wheel electrodes.

Under a program at North American Rockwell an H53 helicopter rotor hub was selected for diffusion bonding. The rotor hub had been made from a forging of titanium 6A1-4V material. The forging weighs about 1000 pounds but the finish machined weight is about 230 pounds. This part has been successfully diffusion bonded. (Figure 13) Two rotor hubs were sectioned and evaluated by the contractor and a third hub was evaluated by the Air Force Materials Laboratory. A fourth hub was diffusion bonded and shipped to Sikorsky Aircraft where it was machined and dynamically fatigue tested. The test data compared to forged hub

data indicates that there is no significant difference between the diffusion bonded hub and production forged hubs.

Other Air Force Materials Laboratory, Manufacturing Technology Programs included two programs for roll bonding titanium alloy structural sections. McDonnell-Douglas made T-shapes and a complex shape using a bar rolling mill to apply the pressure. North American Rockwell conducted a program and made an airfoil shape, "J" sections, "Z" sections, "L" sections, and a "Hat" section. These parts were made on a plate rolling mill.

The potentials of diffusion bonding were recognized for fabrication of jet engine components. A program was conducted by General Electric for the development of a diffusion bonding process for assembling hollow titanium compressor blades. A comprehensive evaluation for acceptable bonding parameters was conducted. Most significant results of the bonding parameter studies was the determination that to obtain 100% bonding a controlled deformation of approximately 2 percent upset is required regardless of thickness. (Reference 9) Also significant was the surface finish evaluation which showed that for finishes rougher than 32 RMS, higher deformations were required to obtain 100 percent bonding. In this program hollow compressor blades were made from sheet plate, and bar stock rather than from forged halves (Figure 44) (Reference 10) Essentially the method consisted of

- a. Creep form airfoil shape
- b. Chem-Mill concave cavity
- c. Machine convex cavity
- d. Bond airfoil
- e. Bond dovetail blocks
- f. Finish machine

The diffusion bonded blades were tested to establish the integrity of a fabricated diffusion bonded airfoil by:

- 1. Ballistic impact
- 2. Bench fatigue

- 3. Whirligig fatigue
- 4. Stress deflection
- 5. Micro-examination

The test data from the diffusion bonded blades were compared with the GE4 (SST) hollow blades produced using forging procedures. Results on all the deflection tests indicate that finished blades produced by both methods have physically similar characteristics. On the GE4 (SST) engine a 175 pound per engine weight reduction was achieved by using hollow titanium compressor blades in stages through 4. (Reference 10) The use of sheet, plate and bar stock for manufacture of hollow blades enabled substantial cost savings up to 50% over previous methods for manufacturing large hollow blades.

A program is currently being conducted at Pratt & Whitney for a diffusion bonded titanium alloy hollow fan disk. This contract is establishing a manufacturing method to produce hollow diffusion bonded titanium alloy fan disks from titanium 6A1-2Sn-4Zr-6Mo. Under this program the hollow rim of the disk will be produced by diffusion bonding. The hub and spacer will be made integral with the disk by inertia bonding which is also a solid state joining process. The disk being fabricated and tested is the first stage fan disk of the TF-33P7 engine.

Another method of diffusion bonding is based on the concept of conventional resistance spot or seam welding using resistance welding equipment. Under an AFML program at Solar, San Diego, a continuous seam diffusion bonding machine was constructed. The machine is based on a resistance welder modified, and includes a closed loop control for pressure and temperature. (Reference 11) Bonding of titanium and its alloys was demonstrated with the manufacture of single and double web I beams, rib reinforced panels, box beams and other shapes. Joint quality of I beams were evaluated by tensile tests, end compression tests, four point loading bend tests and fatigue tests. This continuous seam bonding technique has advanced to the extent that it is currently being used in advanced systems application. A titanium vane is being

CSDB bonded for Pratt & Whitney and engine seals from Hastelloy X are being fabricated for the CF6 engine at General Electric. (Figures 15 and 16)

Diffusion bonding is intended for extensive use on the Bl program at North American-Rockwell. A large number of components have been identified and North American's press bonding capability will be utilized.

There is continued concern over the mondestructive inspection of diffusion bonded parts. The major concern is whether or not ultrasonic testing methods or any other nondestructive testing techniques are good enough to assure a sound product especially with reference to unbonded or partially bonded areas. This condition dictates that there must be precise control of the diffusion bonding process. Cleanliness of parts is critical and bears emphasis, control of the amount of deformation is critical during the bonding cycle. Metallographic sectioning and mechanical testing will continually be required over a sampling plan to assure reproducible acceptable quality.

INERTIA WELDING

Inertia welding is a process where one workpiece is fixed in a stationary holding device and the other workpiece is clamped in a spindle chuck with attached flywheel. The flywheel is accelerated to a predetermined speed, driving power is cut and the rotating part is thrust against the fixed piece. Friction between the parts decelerates the flywheel converting stored energy to frictional heat and a solid state joint results. Under a manufacturing technology contract at General Electric inertia welding was established as an improved method of jet engine compressor manufacture and demonstrated by the fabrication of TF39 stages 14-16 of the compressor rotor spool. One of the TF39 stages 14-16 compressor rotor was finish machined. Reduced machining costs and overall component weight reduction are significant benefits. Based on the mechanical properties data evolved in the TF39 stages 14-16 and the tolerances attainable for rotor spools General Electric has

committed the inertia welding process for use in fabrication of compressor rotors for the B1 engine.

In the contract at General Electric welding parameters were developed for Inconel 718 cross rolled plate. (Reference 12) With an established flywheel size there are only two parameters to control, namely, thrust and surface speed. Once correct weld conditions have been established based on mechanical property tests, microexamination and visual examination of the size and nature of the flash, and nondestructive inspections, the amount of weld upset by length reduction of the weldment can be the basic process control technique. The process being automatic is intrinsically very reproducible. A statistical test plan was used to arrive at welding parameters for the Incomel 718. One inch outside diameter by 0.100 and 0.200 inch wall cylinders were specimen sizes used. Statistical analysis of the test data showed that the flywheel moment of inertia had little influence on the amount of upset or weld quality. Rotors were experimentally fabricated from both Inconel 718 plate which had been cold flanged to provide outside edge preparation and from Inconel 718 forged disks. Rotors made from plate stock were found to contain cracks after machining. While the cause of the cracking was not conclusively determined, it is believed that the following were all contributing factors:

- 1. Excessive grain size of cross-rolled plate
- 2. Improper machining of weld flash
- 3. Improper acid etch cleaning

All of these factors can be controlled or modified, and, therefore, the cracking should be preventable.

Sound experimental rotors were made from forged disks. Since previous metallographic studies had shown the presence of liquated phases in Inconel 718 inertia welds made at high angular velocities, the flywheel moment of inertia was increased from 26,038 to 32,500 lb-sq ft, thereby allowing some reduction in welding speed. Three sets of 24-in. dia.test rings welded in the wall thickness-diameter study

were cut apart and remachined for additional test piece welds.

Welding of the three ring sets and test disks from two forgings showed no significant changes in the welding parameters, maximum input energy and welding pressure, from those used for cross-rolled plate. The two rotor welds were then made with good dimensional and upset results.

The rotor was machined and then aged in vacuum using controlled heating and cooling rates of 200 F/hr to reduce any possibility of warpage or distortion of the nearly finished machine rotor. The standard Inconel 718 aging cycle of 8 hr at 1325 F + 8 hr at 1150 F was used. Dimensional inspection after aging showed that no significant changes or distortion had occurred, and zyglo inspection showed no defect indications. The finished machined rotor is shown in Figure 17.

Inertia welding was one of several processes evaluated under an Air Force sponsored program at Pratt & Whitney Aircraft for joining of bimetal shafts. The ideal low pressure turbine shaft would be made from two joined materials using an alloy with high fatigue and high yield strength at the cold end, and a material with high fatigue strength, high creep strength, and corrosion resistance at the hot end. (Reference 13) Such a bimetal shaft would be lighter in weight, and, with no cooling requirement, the complexity of the cooling air system would be effectively reduced. In this particular program the coextrusion process was selected for joining the bimetal shafts. For the AMS 6304 steel to Inconel 718 bimetal combination it was determined that a value of 130 KSI in tension at room temperature was assigned as the acceptance level at the joint. This value was expected to provide a joint suitable for engine operating conditions. The results of test specimens in tension and shear showed that coextrusion was the best method for making bimetal shafts in the materials combination selected. coextrusion process produces a metallurgical bond between the two materials being joined by forcing the materials through an extrusion die at an elevated temperature and reducing the cross sectional area. (Figure 18)

The finished shaft was assembled into a TF30-P-3 engine which was run in a 150 hour endurance test. The test consisted of 25 six hour cycles. (Figure 19) Though test specimens in this program showed lower fatigue strength than the coextruded joints it is believed that the inertia welding process offers considerable potential for joining bimetal shafts. It is felt that by changing joint designs and material combinations the inertia weld can be shown to possess mechanical properties, including torsional fatigue strength equal to coextruded joints. It is expected that inertia welded shafts would be considerably more cost effective because of reduced steps in processing to the finished condition.

Cherrybuck (R) fasteners produced by the Cherry Rivet Division of Townsend, Santa Ana, California, produces bimetal solid titanium fasteners by inertia welding. The fastener is made from Ti 6A1-4V inertia bonded to a commercially pure ductile tail. (Reference 14) WELDBOND

This process represents the marriage suggested in the title of this paper. The process uses resistance welding in complement with adhesive bonding. Most of the work conducted thus far has been resistance spot welding through the adhesive. In process application the force of the electrodes moves the adhesive from the spot weld so a resistance weld nugget is formed with adhesive surrounding the nugget and covering the remainder of the faying surface.

Lockheed-Georgia began experimental process studies of resistance welding through high strength adhesives in the mid 1960's. Extensive static, axial load fatigue, and sonic testing produced weldbonded structures superior both in strength and in weight advantage to those joined by high strength tapered fasteners. Preliminary cost studies indicated that the automatic weldbonding process would result in a large cost savings in the total production process. In July 1969 the Air Force Materials Laboratory, Manufacturing Technology Division, awarded a contract to Lockheed-Georgia for fabrication of a full scale

fuselage barrel section by the resistance spot weld-adhesive bonding process. A full scale fuselage barrel section 85 inches in diameter by 120 inches long from 2024 and 7075 aluminum alloys, was fabricated during the program. (Reference 15 - Figure 22)

Actual joining of parts using a combination of resistance spot welds and adhesive is relatively straight forward. To begin with most of the processing steps involved in resistance spot welding are applicable to weldbonding. The parts are chemically cleaned as for spot welding, wrapped and stored up to 36 hours if required, and removed for welding.

The paste adhesive is applied to the parts. The parts are then brought together and temporarily clamped. The parts are then placed between the electrodes of a conventional three phase, variable pressure type spot welder and are welded together. After welding the structure is placed in a low temperature oven and the adhesive is cured for approximately one hour. Time and temperature is dependent on the type adhesive used and the alloy being weldbonded.

The fuselage barrel section was subjected to upbending, downbending, and torsional loads to the C140 test spectrum. These loads represented limit loads sustained by the fuselage. Figure 23 shows the fuselage at maximum torque. Note the shear buckles that were produced during this loading. Thick buckling demonstrated that the weldbond joints were highly stressed during the static loading sequence. Subsequent to the torque load the fuselage was subjected to pressure cycling with the pressure ranging from 1 PSI to 12 PSIG (1 cycle being equivalent to 1 flight pressurization). The fuselage was subjected to 48,000 cycles which is approximately 4 lifetimes of an aircraft before failure occurred. The failure was a three (3) foot long tear through mechanical fasteners. This test dramatically demonstrated the improved strength of the weldbonded structure when compared with the mechanically fastened joint.

Fabrication and test of the fuselage barrel section confirmed and substantiated data obtained during earlier development of the weldbonding process. Some of these data are as follows:

- Radiographically clear spot welds could be consistently obtained when welding through paste adhesive.
- 2. High quality welds could be made in high strength aluminum alloy up to 72 hours after layup of the parts with adhesives at the parts interface.
- 3. Axial load fatigue endurance had been increased
 many times over that of mechanical fasteners. (Figure 20)
- 4. Joint static strength of weldbond was superior to all other joints tested. (Figure 21)

The weldbond process offers the potential of significantly lower manufacturing costs. The work performed at Lockheed-Georgia Company indicates that the cost of a weldbonded fuselage structure is 25 to 50% of the cost of a riveted assembly. Similar cost savings are anticipated in other applications.

Currently in progress at Lockheed-Georgia is a weldbond program sponsored jointly by the Air Force Materials Laboratory and Air Force Flight Dynamics Laboratory. This program will optimize the weldbond process for aluminum, generate structural design and engineering data, fabricate test specimens and full scale flight "hardware" for the C-130 aircraft. The fabricated aluminum component will be static and fatigue tested prior to installation of a panel section on the C-130. (Figure 24) A service test will be conducted with continued surveillance of performance over an extended time period.

A relatively small contract was AFML sponsored at Lockheed-Georgia to establish weldbond parameters for titanium. Titanium 6A1-4V in the solution treated condition in thicknesses of 0.045 and 0.063 inches was used in one series of tests. Titanium 6A1-4V in the annealed condition in thicknesses of 0.020" and 0.025 inches was used in other tests. The two better adhesives from several evaluated were 3M Company EC 3419 and 3M Company EC 2214 Hi-Flex. Realistic evaluation of weldbonded

joints in titanium required that wherever possible weldbond joint strength would be compared directly to strength of other type joints. Joints were designed utilizing spot welds only, mechanical fasteners only, mechanical fasteners with adhesive, and structural adhesive bond only. Joint configurations, joint overlap, and joint thicknesses were kept identical in order to obtain a direct strength comparison at room and elevated temperatures. Weld schedules were established using MIL SPEC W-6858-C as a baseline reference. From the tensile tests conducted for each comparative process the weldbond joints show a superior strength at room temperature in all types tested. Weldbond joints were produced that were consistently stronger than those of either mechanical fasteners, structural adhesive bonds, or mechanical fasteners with adhesive at the ioint interface. The combined peel strength of spot welds and adhesive bond joints was approximately five times greater than that of a bond joint alone. Detailed test data are included in the paper entitled "Development of the Weldbond Process for Joining Titanium." (Reference 16) to be included in the publications from this symposium.

Lockheed Missiles & Space Company, Sunnyvale, California, has conducted extensive work with the weldbond process. Their work is covered in the paper entitled "Weldbonding Sheetmetal Structures" and will be included in the published articles from this symposium. (Reference 17) They have conducted work for evaluation of weldbond for large propellant tanks at cryogenic temperatures. Lockheed-Sunnyvale has also developed the process for spacecraft shroud applications using a resistance wheel electrode concept. This type of application is a corrugation to flat face sheet design. In the previous design the corrugated panel was attached to the face sheet by rivets. The use of weldbond in place of rivets will produce a panel which is far stronger and less costly to make.

NASA, Manned Spacecraft Center, Orbiter Procurement Center, Houston, recently awarded a contract to Lockheed-Sunnyvale entitled 'Weldbond Development Program for Space Shuttle Application." This program will lead to the application of weldbonding to cryogenic pressure vessels (LH₂ and LO₂, temperature range + 300°F to -423°F), atmospheric gas

containers (crew cabin), and in general to space structures.

Sikorsky Aircraft Division of United Aircraft Corporation has used a significant amount of weldbond on their S67-Blackhawk helicopter particulary in the tail cone section.

Weldbond is also being evaluated for use in rail car bodies, trailer truck bodies, and metal cabinets subject to high vibratory conditions.

The future of weldbond looms big. The improved properties of the process over competing processes and reduced manufacturing costs enhances its potential for extensive production application.

The foregoing discussion is but a summary of selected works with five specific joining processes. Since it is but a sampling of metals joining technology one can readily envision the interdisciplinary involvement, the magnitude of the metals joining area and the need for continued development of technology by industry and government.

LIST OF REFERENCES

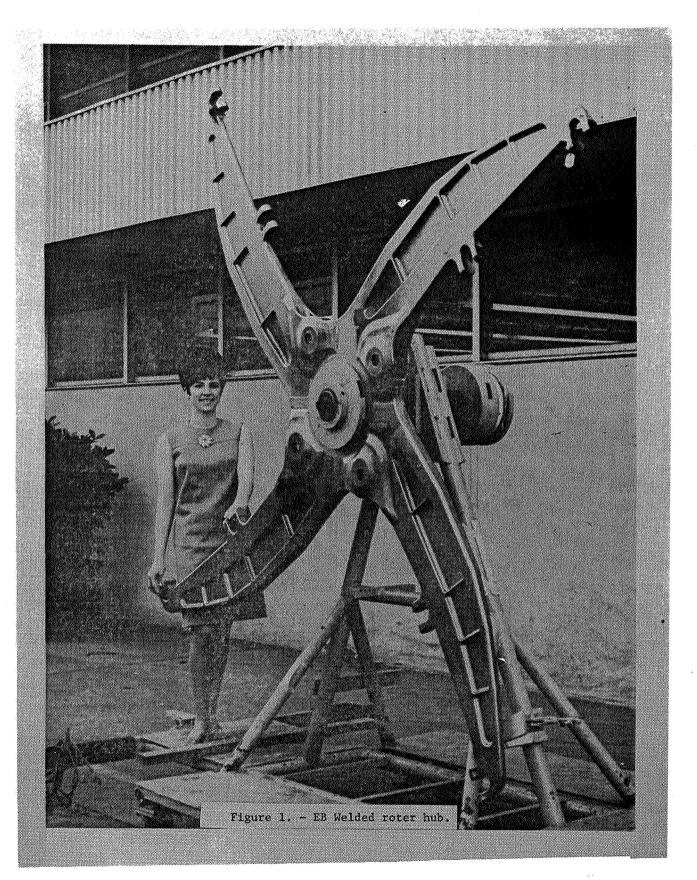
- Weld Characteristics, Materials Amenability, and Applications by Robert H. Witt, Grumman Aerospace Corp., presented at Electron Beam Metallurgical Processing Seminar, 8-11 Feb 1971, Oakland, California.
- 2. Welding and Brazing, Volume 6, Metals Handbook
- 3. Program Summar, Plasma Arc Weld Development, AF33(615)-5353, Project 9-800, Aerojet-General Corp., Fullerton, California, W. Gaw.
- Plasma Arc Welding of Thin Materials, Technical Report, AFML-TR-66-177, June 1967, AF Contract F33615-67-C-1159, Project 815-7, Allison Division, General Motors Corp.
- 5. Low Current Plasma Arc Welding, Technical Report, AFML-TR-70-131, July 1970, AF Contract F33615-69-C-1893, Project 821-9, Allison Division, General Motors Corporation.
- 6. Manufacturing Development Report, MDR 6-62045, Plasma Arc Welding Application of SST Prototype Titanium Components.
- 7. Diffusion Bonded Titanium Structures, Technical Report AFFDL-TR-71-51, June 1971, McDonnell-Aircraft Company, F33615-70-C-1121.
- 8. The Odyssey of Diffusion Bonding, by H. A. Johnson and G. W. Trickett, AFML/LTP, Wright-Patterson AFB, Ohio for Society of Manufacturing Engineers.
- 9. Using Solid State Joining in Gas Turbine Engines, D. C. Martin, Battelle Memorial Institute, and F. R. Miller, Air Force Materials Laboratory, Wright-Patterson AFB, Ohio. Presented at ASME Gas Turbine and Fluids Engineering Conference and Products Show, San Francisco, California, March 26-30, 1972.
- 10. Fabrication of Diffusion Bonded Hollow Titanium Blades, General Electric Company, Cincinnati, Ohio, Contract F33615-68-C-1215.
- 11. Production Tool for Diffusion Bonding, AF33(615)-2304, Technical Report AFML-TR-68-213, Volume I, Arthur G. Metcalfe and Fred K. Rose, Solar Division, International Harvester Company.

LIST OF REFERENCES

- 12. A Technical Briefing, Fabricated Compressor Rotors, Contract F33615-67-C-1884, General Electric Company, Cincinnati, Ohio.
- 13. Development and Demonstration of Manufacturing Techniques for Joining Bimetal Shafts, Contract AF33(615)-5380, Pratt & Whitney Aircraft Division, United Aircraft Corp., Robert A. Doak, Project Engineer.
- 14. Literature from the Cherry Rivet Division of Townsend Company, Santa Ana, California.
- 15. Resistance Spot Weld-Adhesive Bonding Process, Final Report AFML-TR-70-227, Lockheed-Georgia Company, Dallas Fields.
- 16. Development of Weldbond Process for Joining Titanium, Dallas Fields, Lockheed-Georgia Company, AF Contract F33615-71-C-1099.
- 17. Weldbonding Sheetmetal Structures, Lockheed Missiles and Space Company, Sunnyvale, California, Fletcher Sullivan.

LIST OF FIGURES

Figure No.	<u>Title</u>			
1	Cheyenne Helicopter Rotor HUB			
2	F14 Wing Center Box Section			
3	EB Rectangular Box Welding System at Grumman			
4	EB Chamber Welding System at Bosies			
5	Sliding Seal Electron Beam Welding System			
6	Sliding Seal EB Welds			
7	Welding Data Bell Aerospace - F33615-70-C-1131			
8	Titanium Pressure Vessel Staged for Burst Test with SWAT Accelerometers Attached.			
9	Outer combustion Case for T63 Engine, Plasma "Needle" Ar			
10	Integrally Stiffened Titanium 6A1-4V Plasma Arc Welded Panel			
11	Integrally Stiffened Titanium 6A1-4V Plasma Arc Welded Panel			
12	Schematic of the Plasma Arc Process used for Integrally Stiffened Panel			
13	H53 Rotor Hub Diffusion Bonded			
14	Processing Sequence for Diffusion Bonded Hollow Blades			
15	Continuous Seam Diffusion Bonded Vane			
16	Continuous Seam Diffusion Bonded Engine Seals			
17	View of a Finish Machined Rotor			
18	Schematic of Coextrusion Process			
19	Finished Coextruded Bimetal Shaft			
20	Axial Load Fatigue Strength of Weldbond as Compared to Rivets			
21	Static Joint Strength of Weldbond as Compared to Other Type Joints			
22	Fuselage Barrel Section 85" Diameter X 120" Long. Aluminum 2024 and 7075 Alloys			
23	Fuselage in Torsional Loading			
24	Weldhond Panel on C130 Aircraft			



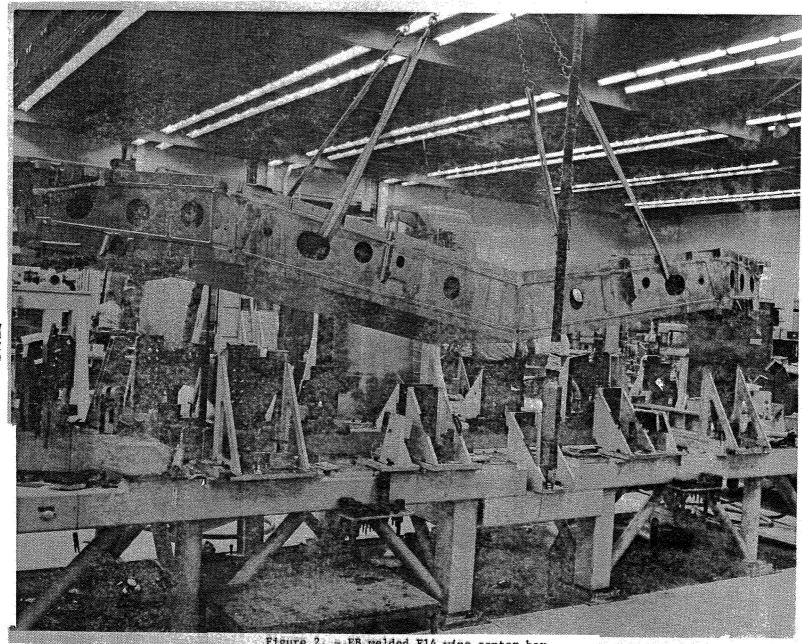
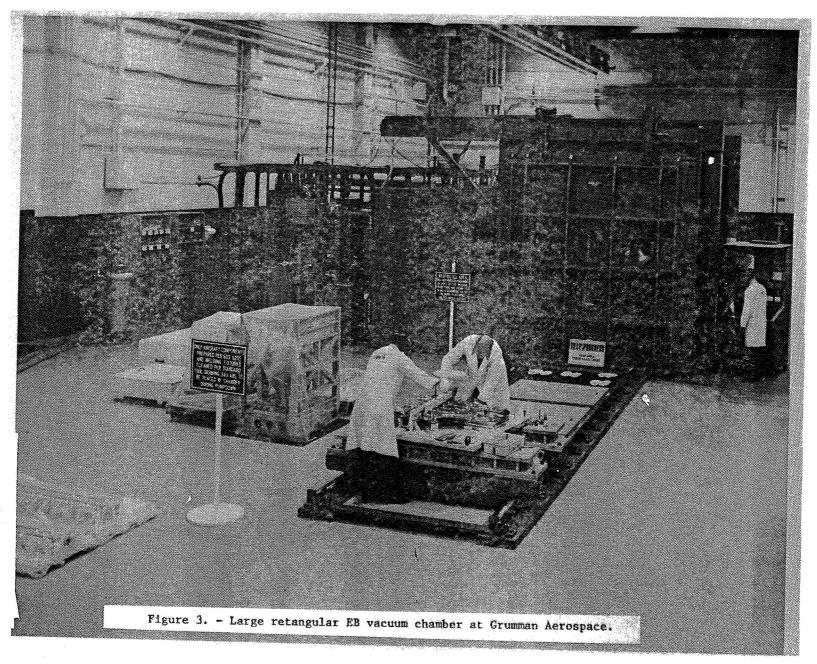
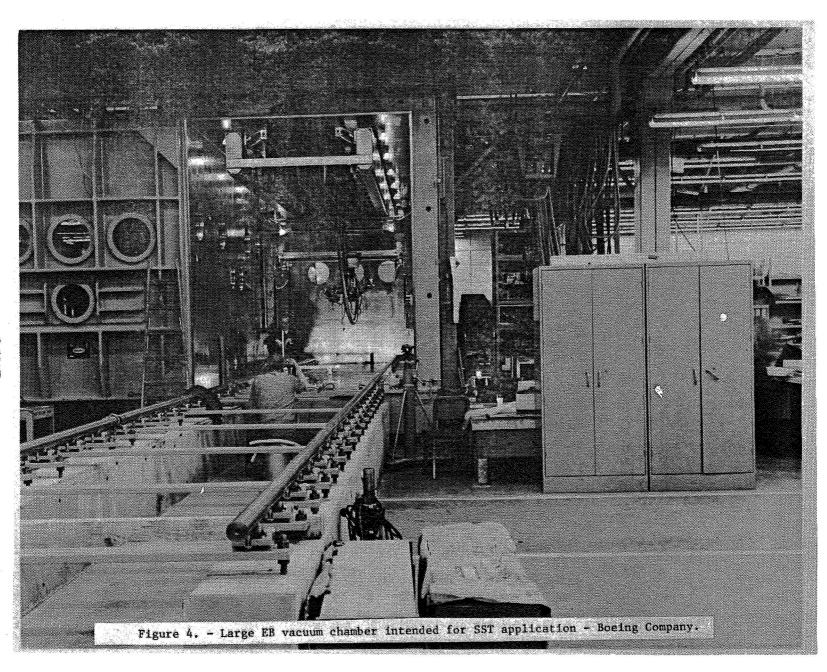


Figure 2. - EB welded F14 wing center box.





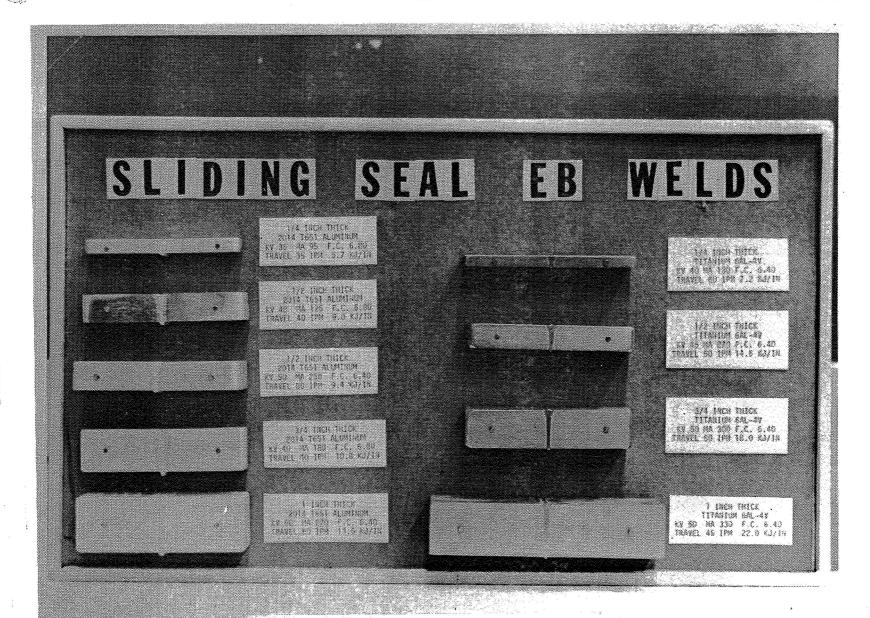


Figure 6. - Sliding seal electron beam welds.

	TOTAL WELD TIME	QUALITY OF WELD	COST OF JOINT PREPARATION	DISTORTION
BEST SELECTION	EB	EB	HOT WIRE	EB
57.55 ∧	PLASMA	PLASMA	PULSED	PLASMA
	HOT WIRE	PULSED	PLASMA	PULSED
LESS DESIRABLE	PULSED	HOT WIRE	EB	HOT WIRE

Figure 7. - Process selection based on welding several high strength alloys under AF contract at Bell Aerospace.

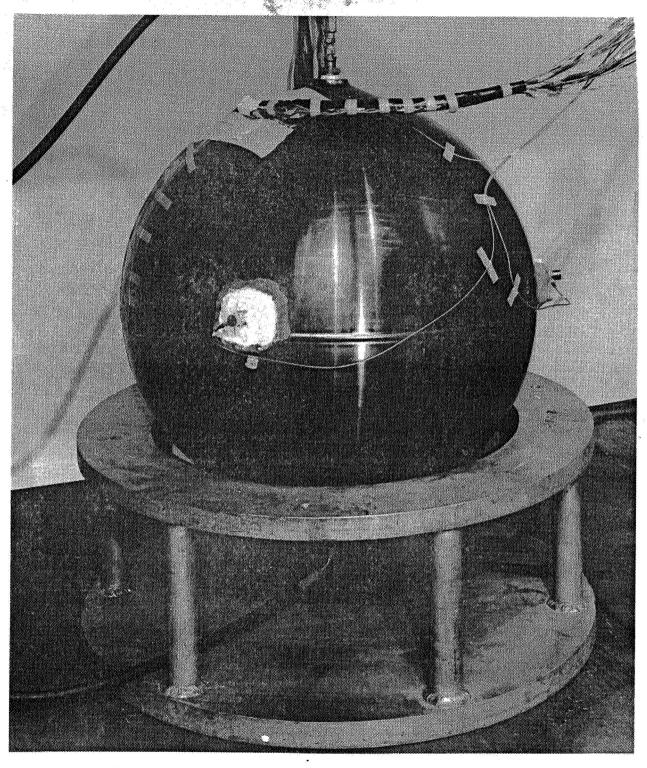
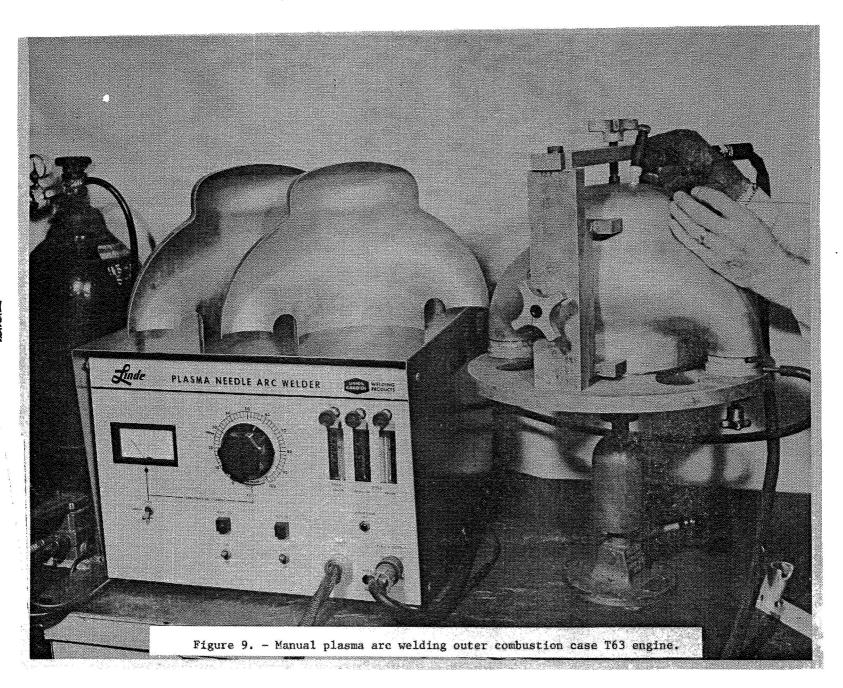
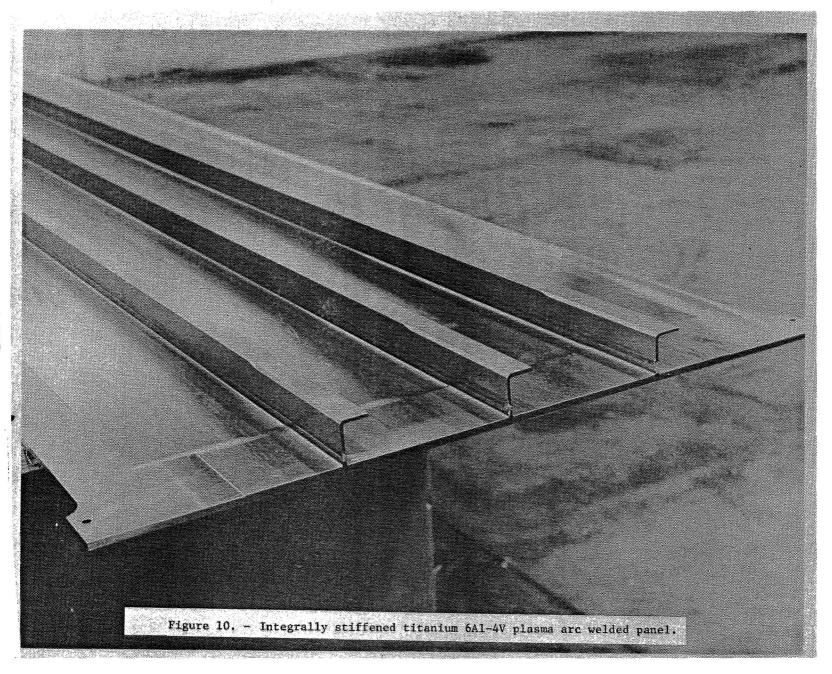


Figure 8. - Plasma arc welded titanium pressure vessel staged for burst test with stress wave attenuation accelerometers attached.





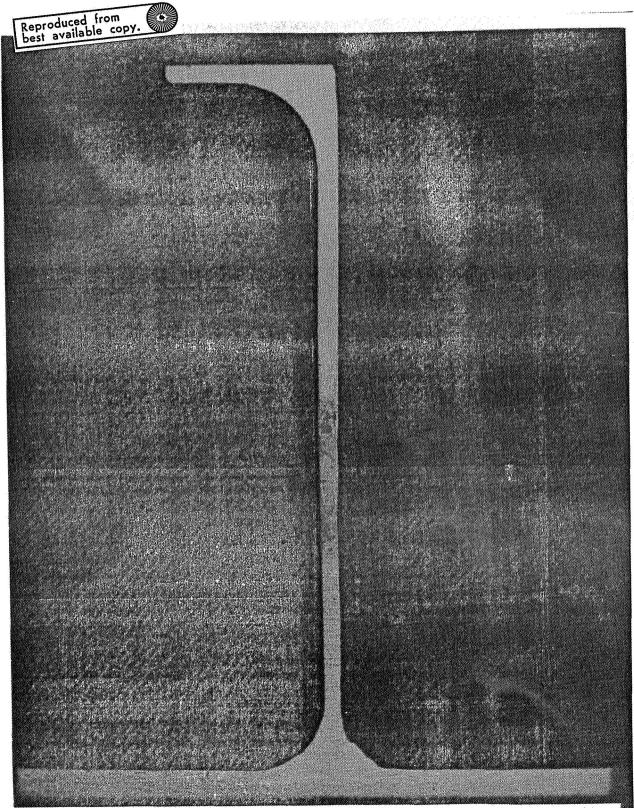


Figure 11. - Integrally stiffened titanium 6A1-4V cross section plasma arc weld microstructure.

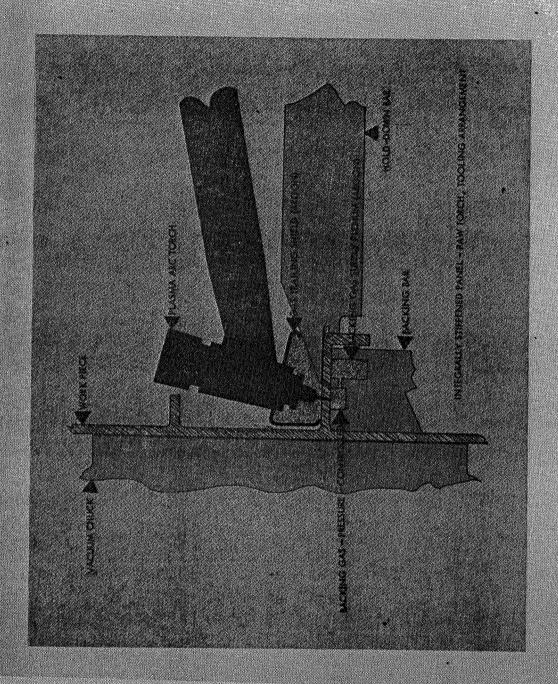
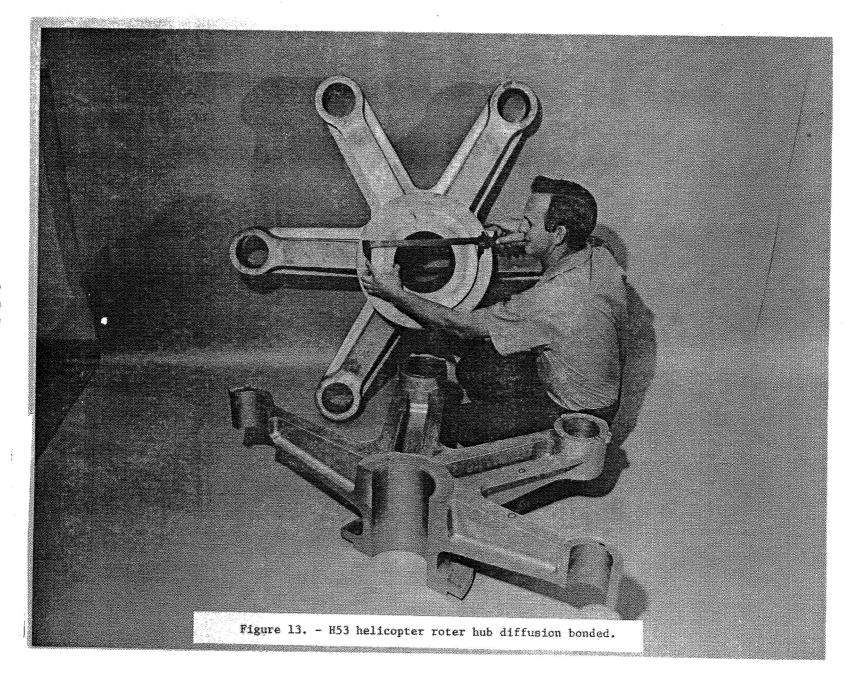
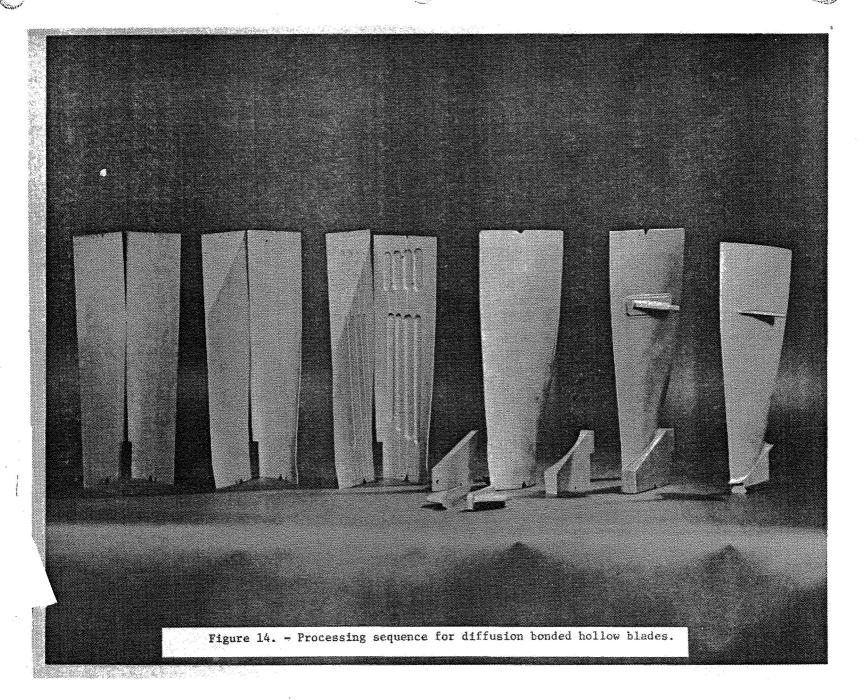


Figure 12. - Schematic cross section of general panel and stiffener support and holding system in conjunction with plasma arc welding torch position.

BUEING





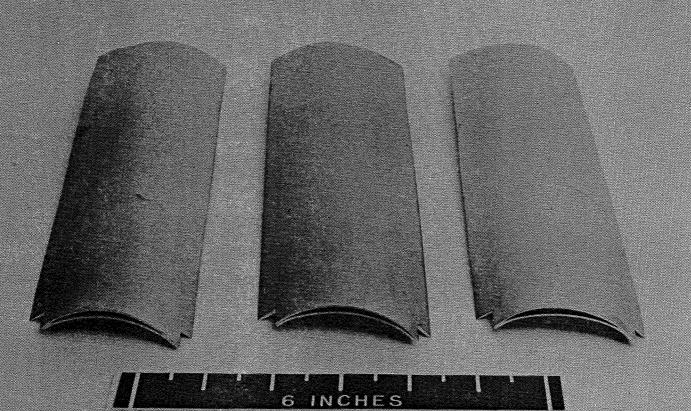
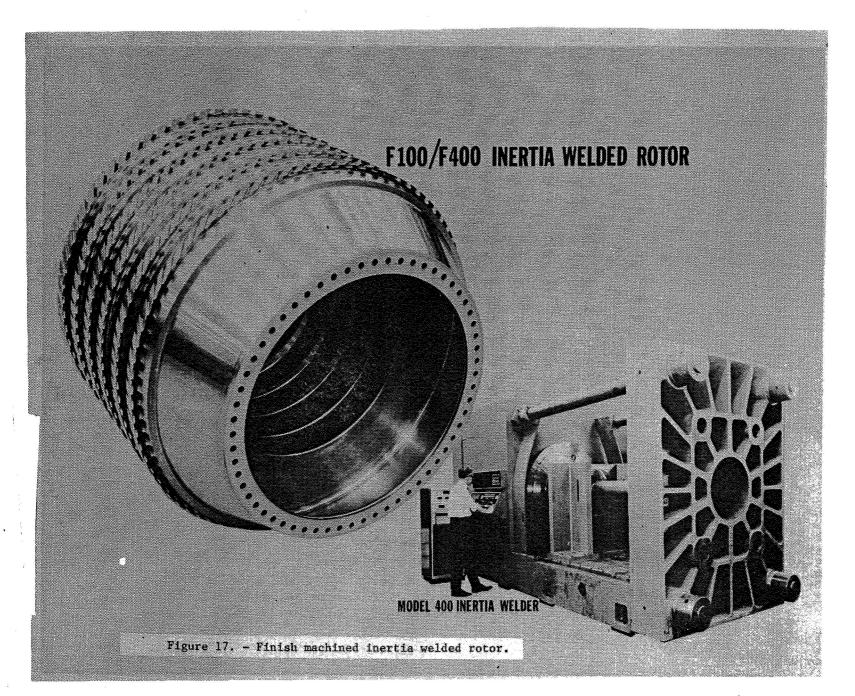


Figure 15. - Continuous seam diffusion bonded vane.



SCHEMATIC OF COEXTRUSION PROCESS

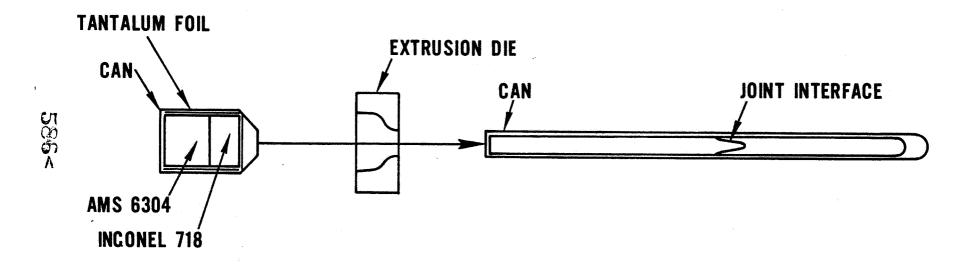


Figure 18. - Schematic of coextrusion process.

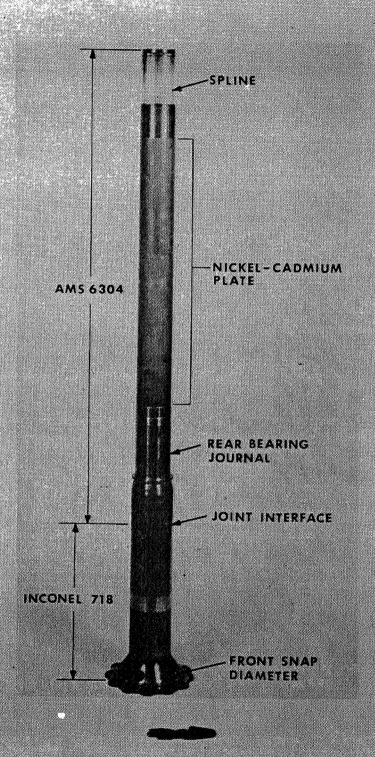


Figure 19. - First bimetal TR30-P-3 pressure shaft.

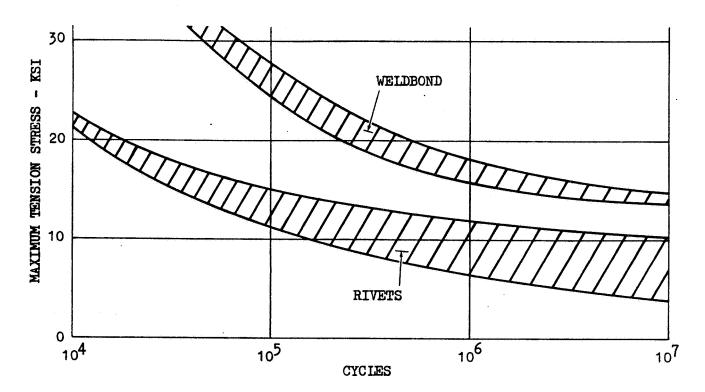


Figure 20. - Axial load fatigue strength of weld bond as compared to rivets.

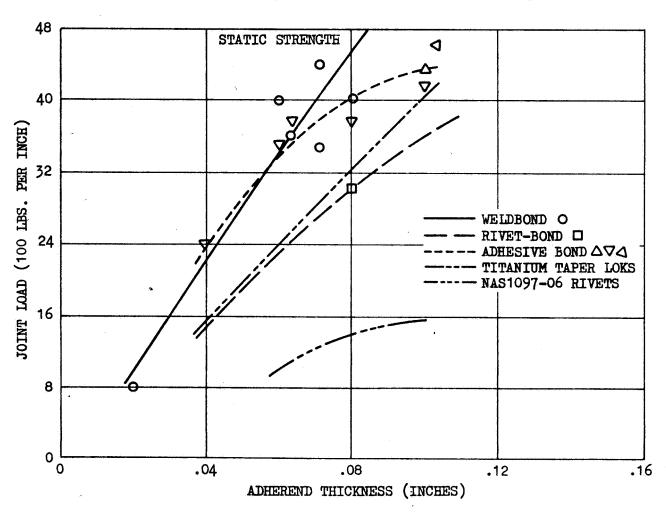
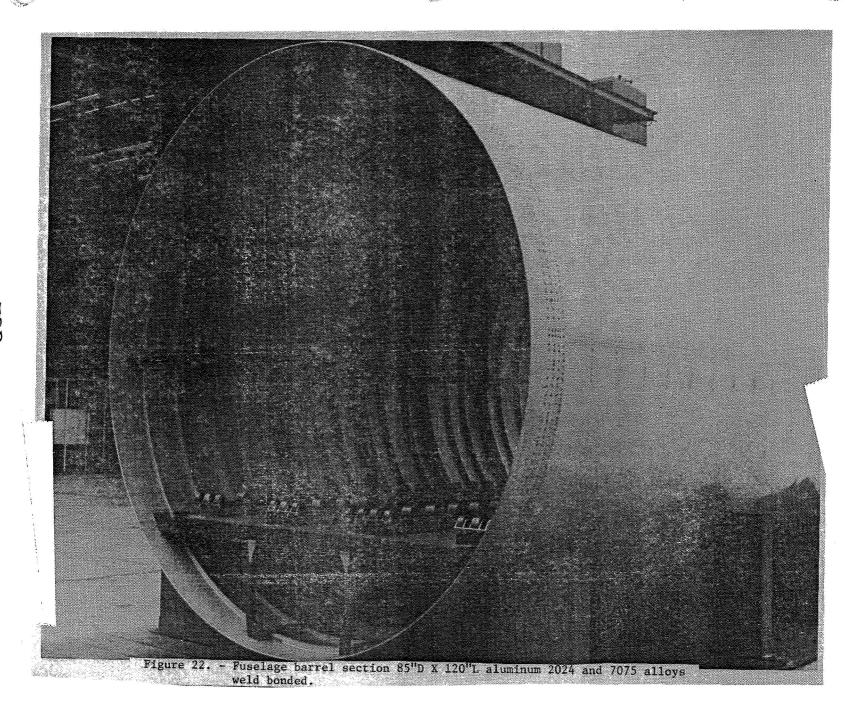
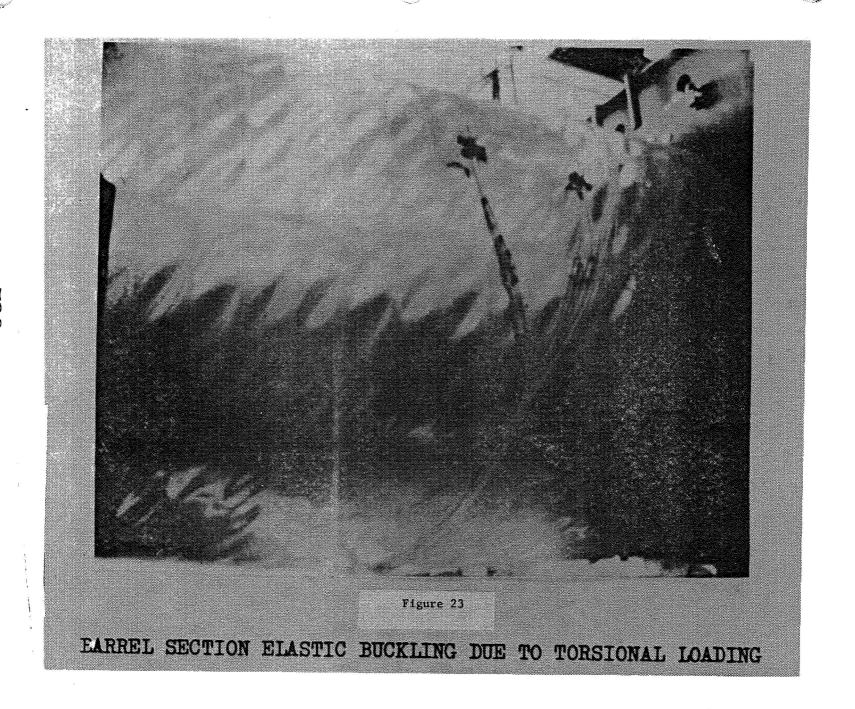


Figure 21. - Static joint strength of weld bond as compared to other type joints.







N74 30948

SUBMERGED ARC WELDING OF HEAVY PLATE

By: Robert A. Wilson
Vice President
The Lincoln Electric Company

It has become apparent that the size and complexity of weldments has increased in the last few years.

The list of these weldments is endless but include buildings, bridges, ships, steel mills and chemical processing equipment, as well as pressure vessels and piping of all kinds.

In almost every case this increase in weldment size has been accomplished by a common denominator -- heavier plate.

The submerged arc process is particularly suitable for heavy plate welding because of its ability to combine very high deposit rates along with excellent quality. It does these things without the smoke and spatter often accompanying other processes.

It is available today in several forms that are pointed to the fabricators of heavy sections with long, short or round about welds.

Tandem arc full automatic equipment is particularly suitable for those long heavy welds where speed and deposit rate are of the first order. An attachment called long stick-out which makes use of the IR drop on long electrode extensions can be included on this equipment to increase deposition rates 50% or more.

In addition, the long familiar DC single arc automatic head represents the least investment and greatest flexibility in full automatic equipment.

For the fabricator who has short heavy welds to make, semiautomatic submerged arc equipment is available to do a wide variety of jobs with great freedom of mobility. Attachments and travel mechanisms are sold for this equipment to extend its use even further into the full automatic range for the heavier plate thicknesses.

Although heavy plates have been welded in some industries for a long time, most of us are really neophytes when 2 inch, 4 inch, 6 inch and heavier plates start to appear on the drawing boards.

What are these differences that require such careful consideration with heavy plates even though the general specifications appear to be similar to those we have been welding successfully for years in lesser thicknesses?

The first and most serious mistake anyone can make is to assume that, since the chemistry and physicals are similar to material used before, the welding is also similar, and that the only difference is the time it will take to make larger welds. This is a serious underestimation and can lead to all kinds of problems including failure or at the least, costly repairs.

Let's take a look at the characteristics of heavy plates with respect to their effect on the welding process.

A. Thickness and Mass:

Just thickness or size alone can present special problems which have a direct bearing on the welding operations. These heavy plates are more difficult to:

1. handle

4. fit and tack

2. work on

5. position

3. bend or form

6. preheat

7. Cut and bevel accurately

Mistakes or lack of equipment in the above areas can add many problems that must be corrected later on. Let's take a good look at some of the possibilities.

Flame cutting and beveling accuracy are much more important in heavy plates since the volume of weld metal added has a direct bearing on shrinkage and cracking tendencies. On fillets for example, the amount of weld metal goes up as the square of the leg side and the potential for shrinkage increases proportionately.

In the case of butt welds the 60° included angle preparation so often seen on lighter plates is certainly out of the question since it requires excessively large quantities of weld metal with its attendant shrinkage. The type of plate preparation we would like to have on these heavy butt welds are U's or double U's. However this type of plate preparation is difficult and costly. The next best situation are joints with small included angles (9-11°) with sufficient width at the bottom to provide access for the first passes.

Since the heavier plates are harder to bend or form, designed joints are harder to realize for the fitters. This results in joints normally that have greater variations than we would normally like to see.

Tacking is extremely important on heavy plates. Days of work may be lost or costly straightening might be required when tacks break on heavy weldments. Occasionally it may be necessary to locally preheat the areas where tacking is required. In all cases these tacks must have sufficient throat to resist the shrinkage of the main welding operations until sufficient weld metal has been deposited to hold the parts in alignment. For submerged arc welding, these tacks may take the form of welds 4 to 5 inches long and three or more layers deep with tapered or cascaded ends. On heavy plate these tacks should always be made with low hydrogen electrode.

B. Thickness and Plate Chemistry:

In the steel mill, all steel plates and rolled sections undergo a rather slow rate of cooling after being rolled while red hot. The red hot thick sections, because of their greater mass, cool more slowly than thin sections. For a given carbon and alloy content, slower cooling from the critical temperature results in a slightly lower strength.

For the normal thicknesses, the mill has no difficulty in meeting the minimum yield strength required. However, in extremely thick mill sections, because of their slower cooling, the carbon or alloy content might have to be increased slightly in order to meet the required yield strength. Examples of how the mills correct for this problem are shown in the ASTM specifications shown here (Figure 1) for two common steels.

Figure 1 See page 4

Figure 1

B. Thickness and Plate Chemistry (Cont'd.)

How carbon changes with plate thickness:

A 516

Grade 55		
	C	Mn
1 /2"	.18	.60 to .90
1/2 to 2	20	
1/2 00 2	.20	
2 - 4	.22	.60 to .120
4 - 8	.24	
	0.5	
8 - 12"	. 26	
A 515		
Grade 55		
1 "	.20	•90
1 - 2	22	
1 - 2	.22	
2 - 4	.24	

.26

.28

Since a weld cools faster on a thick plate than on a thinner plate, and since the thicker plate will probably have a slightly higher carbon or alloy content, welds on thick plate, because of admixture and fast cooling, will have higher strengths, but lower ductility than those made on thinner plate. Special welding procedures may be required for joining thick plate (especially for the first or root pass), and preheating probably will be necessary. The object is to decrease the weld's rate of cooling so as to increase its ductility. More will be said about this later.

C. Shrinkage and Stress

4 - 8

8 - 12"

On thick plates with large welds, if there is metal-to-metal contact prior to welding, there is no possibility of plate movement. As the welds cool and contract, all the shrinkage stress must be taken up in the weld, (Figure 2(a). In cases of severe restraint, this may cause the weld to crack, especially in the first pass on either side of the plate.

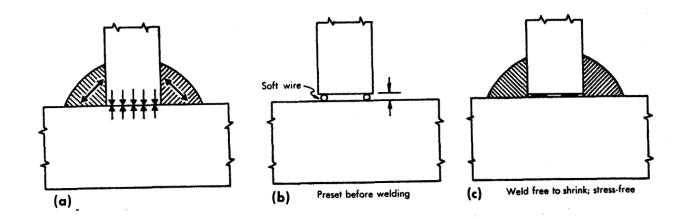
C. Shrinkage and Stress (Continued)

By allowing a small gap between the plates, the plates can "move in" slightly as the weld shrinks. This reduces the transverse stresses in the weld. See Figures 2(b) and 2(c). Heavy plates should always have a minimum of 1/32 inch gap between them and if possible 1/16 inch.

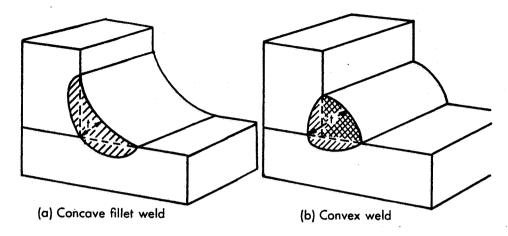
This small gap can be obtained by means of the following:

- 1. Insertion of spacers, made of soft steel wire between the plates. The soft wire will flatten out as the weld shrinks. If copper wire is used, care should be taken that it does not mix with the weld metal.
- 2. A deliberately rough flame-cut edge. The small peaks of the cut edge keeps the plates apart, yet can squash out as the weld shrinks.

Figure 2







D. Bead Shape and Cracking

Bead shape is another important factor that affects fillet weld cracking. Freezing of the molten weld due to the quenching effect of the plates commences along the sides of the joint where the cold mass of the heavy plate instantly draws the heat out of the molten weld metal and progresses uniformly inward until the weld is completely solid. Notice that the last material to freeze lies along the centerline of the weld.

To all external appearances, the concave weld (a) in Figure 3 would seem to be larger than the convex weld (b). However, a check of the cross section may show the concave weld to have less penetration and a smaller throat (t) than first thought; therefore, the convex weld may actually be stronger even though it may have less deposited metal(darker cross section).

Designers originally favored the concave fillet weld because it seemed to offer a smoother path for the flow of stress. However, experience has shown that single-pass fillet welds of this shape have a greater tendency to crack upon cooling, which unfortunately usually outweighs the effect of improved stress distribution. This is especially true with steels that require special welding procedures.

When a concave fillet weld cools and shrinks, its outer face is stressed in tension, Figure 4(a). if a

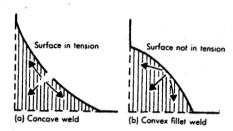


Figure 4

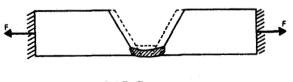
surface shrinkage crack should occur, it can usually be avoided by changing to a convex fillet (b). Here the weld can shrink, while cooling, without stressing the outer face in tension and should not crack. For multiple-pass fillet welds, the convex bead shape usually applied only to the first pass.

For this reason, when concave welds are desired for special design considerations, such as stress flow, they should be made in two or more passes — the first slightly convex, and the other passes built up to form a concave fillet weld.

Groove Welds

On heavy plate, it is usually the first (or root) pass of a groove weld that requires special precautions. This is especially true of the root weld on the back side of a double Vee joint because of the added restraint from the weld on the front side. The weld tends to shrink in all directions as it cools, but is restrained by the plate. Not only are tensile shrinkage stresses set up within the weld, but the weld frequently undergoes plastic yielding to accommodate this shrinkage.

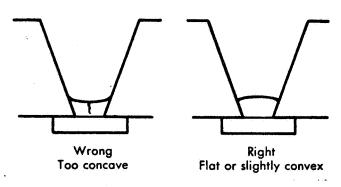
Figure 5



Some idea of the possible locked-in stress and plastic flow of the weld may be seen in Figure 5. Imagine the plate to be cut near the joint, allowing the weld to freely shrink (dotted lines). Then pull the plates back to the original rigid position that they would normally be in during and after welding (solid lines). This necessitates a stretching of the weld.

In actual practice all of this stretch or yielding can occur only in the weld, since the plate cannot move and the weld has the least thickness of the joint. Most of this yielding takes place while the weld is hot and has lower strength and ductility. If, at this time, the internal stress exceeds the physical properties of the weld, a crack occurs which is usually down the centerline of the weld.

Figure 6



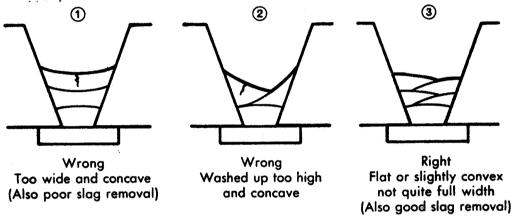
The problem is enhanced by the fact that the first (or root) bead usually picks up additional carbon or alloy by admixture with the base metal. The root bead thus is less ductile than subsequent beads.

A concave bead surface in a groove weld creates the same tendency for surface cracking as described for fillet welds, Figure 6. This tendency is further increased with lower ductility.

Increasing the throat dimension of the root pass will help to prevent cracking — use electrodes or procedures that develop a convex bead shape. Low hydrogen welding materials are useful and preheat can be specified.

Beach shape in submerged arc welding can be very "ropey" because of too high a flux pile which creates a damming action on the molten metal. Always keep the flux pile as low as possible without having the arc break out.

The problem of centerline cracking can even occur in the succeeding passes of a multiple pass weld if the passes are excessively wide or concave. Corrective measures call for a procedure that specifies a narrower slightly convex bead shape, making the completed weld two or more beads wide, side by side. Figure 7.



Internal Cracks and Weld Width to Depth of Fusion Ratio

Where a cracking problem exists due to joint restraint, material chemistry or both, the crack usually appears at the weld's face. In some situations, however, an internal crack can occur which won't reach the weld's face. This type of crack usually stems from the misuse of a welding process that can achieve deep penetration or poor joint design.

The freezing action for butt and groove welds is the same as that illustrated for fillet welds. Freezing starts along the weld surface adjacent to the cold base metal, and finishes the centerline of the weld. If, however, the weld depth of fusion is much greater than width of the face, the weld's surface may freeze in advance of its center. Now the shrinkage lorces will act on the still hot center or core of the bead which could cause a centerline crack along its length without this crack extending to the weld's face, Figure 8(a).

Internal cracks can also result with improper joint design or preparation. Figure 8(b) illustrates the results of combining thick plate, a deep penetrating welding process, and a 45° included angle.

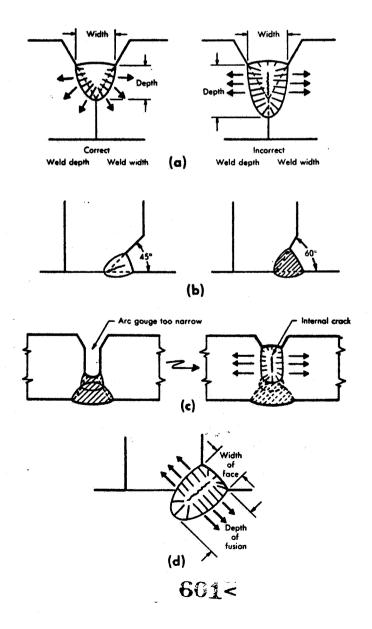
600<

A small bevel on the second pass side of the double-V-groove weld, Figure 8(c), and arc gouging a groove too deep for its width led to the internal crack illustrated.

Internal cracks can also occur on fillet welds if the depth of fusion is sufficiently greater than the face width of the bead, Figure 8(d).

Although internal cracks are most serious since they cannot be detected with visual inspection methods, a few preventative measures can assure their elimination. Limiting the penetration and the volume of weld metal deposited per pass through speed and amperage control and using a joint design which sets reasonable depth of fusion requirements are both steps in the right direction.

Figure 8



Underbead Cracking

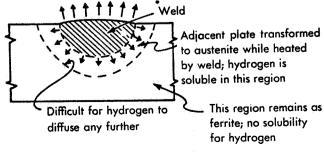
Underbead cracking is usually not a problem with the controlled analysis low carbon steels up to 1". This problem, if it occurs, is in the heat affected zone of the base metal. It can become a factor with thick plate as the carbon or alloy content of the steel increases. As an example, this can occur with the heat treatable very high strength, high carbon low alloy steels like 4140 or 6150. The construction alloy steels which have over 100,000 psi tensile strength and are heat treated before welding, also can experience underbead cracking in thick plates.

Low hydrogen processes, including submerged arc, should be used to join these materials since one cause of underbead cracking is hydrogen embrittlement in the heat affected zone. Hydrogen in the welding arc, either from the electrode coating or from wet or dirty plate surfaces and fluxes, will be carried by the droplets of weld metal being deposited and absorbed into the molten metal beneath the arc.

As the welding arc progresses along the plate, the deposited hot weld metal (which has now solidified) and the adjacent base metal heated by the weld above the transformation temperature are both austenitic at this elevated temperature, and have a high solubility for hydrogen. Fortunately, a considerable amount of hydrogen escapes through the weld's surface into the air; however, a small amount may diffuse back through the weld into the adjacent base metal. (The rate of diffusion decreases with decreasing temperature.)

Beyond the boundary of the heat affected zone, the base metal is in the form of ferrite, which has practically no solubility for hydrogen. This ferrite boundary becomes an imaginary fence, and the hydrogen tends to pile up here, going no farther. See Figure 9.

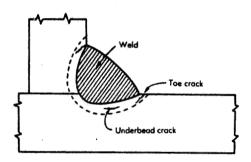
Figure 9



Upon further cooling, the heat affected area transforms back to ferrite with almost no solubility for hydrogen. Any hydrogen present tends to separate out between the crystal lattice and builds up pressure. This pressure, when combined with shrinkage stresses, any hardening effect of the steel's chemistry, and quench rate may cause tiny cracks. Since weld metal is usually of a lower carbon than the base plate, this trouble occurs mainly just beyond the weld along the austenite-ferrite boundary and is called "underbead cracking". See Figure 10. If some of these cracks appear on the plate surface adjacent to the weld, they are called "toe cracks". Slower cooling by welding slower and preheating allows hydrogen to escape and helps control this problem.

The use of low-hydrogen producing welding materials eliminates the major source of hydrogen and with proper preheat usually eliminates underbead cracking on heavy plates.

Figure 10



E. PREHEAT IS A PREREQUISITE TO SUCCESS

Thick plates always suggest greater restraint, higher quench rates and greater hardenability, all of which aggravate the tendency for weld or base metal cracking.

From a practical standpoint, preheating is the most effective single means of minimizing the inherent difficulties in welding thick plates. From a metal-lurgical standpoint it is generally recognized that the need for preheat increases with the plate thickness. But it is equally true that the difficulty and the cost of preheating also increases very rapidly with the thickness and the complexity of the weldment. The weldor also is made more uncomfortable by the use of high soaking preheats. The net result is that too often either the required preheat has not been ob-

E. Preheat is a Prerequisite to Success (Continued)

tained or the heating has been too localized and therefore ineffective. One experience with extensive field repairs usually teaches that preheating not only is a "must" but also is well worth the expense in lowering the total cost of a job.

WHY PREHEAT? WHAT'S ITS PURPOSE?

The basic purpose of preheating is seldom clearly understood by those who are required to do it. This in itself contributes to its being done improperly.

The main purpose of preheating is to slow down the cooling rate -- therefore it is the "volume" of heat as well as the temperature that is important. A thin surface area of high temperature is not enough if there is a mass of cold metal underneath.

Because of the heat absorption capacity of a thick plate, the heat affected zone and the weld metal may be in a highly quenched condition unless sufficient preheat is provided. It is time at temperature during the cooling period which really counts. Without adequate preheat intolerably high hardness and brittleness could occur in the weld or adjacent area.

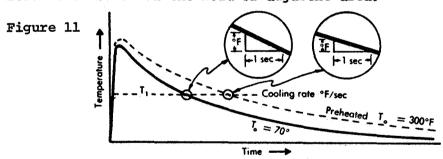


Figure 11 — This indicates the temperature in the heat affected zone as the weld arc passes by. The cooling rate (OF sec) is slower when preheat is used.

When the purpose for preheating is misunderstood, it is not likely to be done properly. For example, in one instance involving a series of cracked welds, the operator insisted he had preheated to the required temperature which seemed to rule out one possible explanation for the cracks. On further checking he was asked what he did after he preheated it. His reply was, "I went to lunch."

E. Preheat is a Prerequisite to Success (Continued)

Another popular misconception is that the only purpose of preheating is to "get any moisture out of the joint." These concepts are wrong and they accomplish little or nothing when applied to massive weldments.

Preheating is used for one of the following reasons:

- To reduce shrinkage stresses in the weld and adjacent base metal; especially important in highly restrained joints. Will eliminate tendency towards cracking and distortion.
- To provide a slower rate of cooling through the critical temperature range (about 1600°F to (1330°F) preventing excessive hardening and lowering of ductility in both weld and heat-affected area of the base plate.
- 3. To provide a slower rate of cooling through the 400°F range, allowing more time for any hydrogen that is present to diffuse away from the weld and adjacent plate to avoid underbead cracking. Underbead cracking normally presents no problem when welding the lower carbon steels except on heavier plates. Preheat may be necessary to prevent its occurrence with the higher carbon steels even when low hydrogen processes are used. More often, some other problem, such as a highly restrained joint between very thick plate or high alloy content steel, is the factor that demands a higher preheat temperature to prevent weld cracks.
- 4. The importance of the effect of the cooling rate in heavy plate welding cannot be overemphasized. For example, the cooling rate of a 6 inch plate is over four times that of a 3/4 inch plate and about twice that of a one and a half inch plate even though the interpass temperatures (300°F) and heat input (36,000 Joules) are held the same. This cooling rate can only be reduced to the same general level by increasing the preheat and interpass temperature of the six inch plate to 500°F. The specific degree of preheat required for any application can only be determined by taking into account such factors as base metal chemistry, plate thickness, restraint,

E. Preheat is a Prerequisite to Success (Continued)

and rigidity of the members, heat input of the process, etc. Some guide lines are available, but the best of these cannot be considered totally accurate if only because of the nebulous factor of rigidity and restraint in the assembly.

Any of these recommendations are represented as "minimum preheat recommendations" and they should be accepted as such.

The American Welding Society has set up minimum preheat and interpass temperature requirements as shown in Table 1.

TABLE 1 - MINIMUM PREHEAT AND INTERPASS TEMPERATURE!

This material has been compiled from the preheat data contained in the AWS Building Code D1.0-69 and AISC 1.23.6.

Thickness of Thickest Part at Point of Welding Inches	Welding Process					
	Shielded Metal-Arc Welding with other than Low Hydrogen Electrodes	Shielded Metal-Arc Welding with Low Hydrogen Electrodes: Submerged Arc Welding: Gas		Shielded Metal-Arc Welding with Low Hydrogen Electrodes: Submerged Arc Welding with Carbon or Alloy Steel Wire, Neutral Flux: Gas Metal-Arc Welding; or Flux Cored Arc Welding	Submerged Arc Welding with Carbon Steel Wire, Alloy Flux	
	ASTM A36; A53 Grade B; A375; A500; A501; A529; A570 Grades D and E	ASTM A36; A242 Weldable Grade; A375; A441; A529; A570 Grades D & E: A572 Grades 42, 45, and 50; A588	ASTM A572 Grades 55, 60 and 65	ASTM A514	ASTM A514	
To 3/4, incl.	None (2)(3)	None (2)(3)	70°F	50°F	50°F	
Over 3/4 to 1-1/2, incl.	150°F	70°F (4)	150°F	125°F	200°F	
Over 1-1/2 to 2-1/2, incl.	225°F	150°F	225°F	175°F	300°F	
Over 2-1/2	300°F	225°F	300°F	225°F	400°F	

1. Welding shall not be done when the ambient temperature is lower than 0°F. When the base metal is below the temperature listed for the welding process being used and the thickness of material being welded, it shall be preheated (except as otherwise provided) in such manner that the surface of the parts on which weld metal is being deposited are at or above the specified minimum temperature for a distance equal to the thickness of the part being welded, but not less than 3 inches, both laterally and in advance of the welding. Preheat and interpass temperatures must be sufficient to prevent crack formation. Temperature above the minimum shown may be required for highly restrained weld. For A514 steel the maximum preheat and interpass temperature shall not exceed 400°F for thicknesses up to 1-1/2 in., inclusive, and 450°F for greater thicknesses. Heat input when welding A514 steel shall not exceed the steel producer's recommendation.

When the base metal temperature is below 32°F, preheat the base metal to at least 70°F and maintain this minimum temperature during welding.

303 (g)Members do not have to be preheated for single pass tack welds which will later be remelted and incorporated into continuous submerged are welds.

403 welding heat input for A514 steel should not exceed the steel producers recommendations.

415 (g) For single pass fillet welds over 3/8" made with multiple electrode submerged arc, the preheat and interpass temperature may be such that result in a hardness in the heat affected zone of less than 225 VHN for steels not exceeding specified T.S. of 60 ksi and 280 VHN for steels not exceeding T.S. of 70 ksi.

EFFECTIVE PREHEATING

Because of the difficulty of getting massive members up to the required preheat, human patience often runs out before the job has been done properly. However, the requirements are clearly stated (Table 1) --- and restated on page 17 of this paper.

E. Preheat is a Prerequisite to Success (continued)

PREHEAT AND INTERPASS TEMPERATURE

Keep it hot until job is finished or else preheat again. This is a simple rule to apply when welding heavy plate. Since the purpose of preheating is to reduce the quench rate, it logically follows that the same slow cooling should be accorded all passes. This can only be accomplished by maintaining an interpass temperature which is at least equal to the preheat temperature. If this is not done each individual bead will be subjected to the same high quench rate as the first bead of a non-preheated assembly.

On a massive weldment it is not likely that the heat input of the welding process will be sufficient to maintain the required interpass temperature. Thus an additional source of heat will often be required as welding progresses.

When preheating large weldments, slow soaking or preheating in a uniform manner has a very desirable effect on the welding operations. It prevents cracking of tacks and welds caused by uneven local heating and shrinkage.

When is preheat needed?

- 1. When mass or plate size is sufficient to cause excessive cooling rates
- 2. When weldment is at a low temperature
- 3. When ambient surrounding temperature is low
- 4. When weldment has complex shape or large variation in size of adjacent parts
- 5. When carbon manganese or alloy contents have been increased to levels that indicate possible problems. HOW MUCH PREHEAT IS REQUIRED?

Welding in low ambient temperatures or shop welding on steel brought in from outside storage on cold winter days greatly increases the need for proper preheat. Footnote 1 of the AWS Table 1 shown on page 15 states as follows: E. Preheat is a Prerequisite to Success (continued) Footnote 1 -- Table 1

"Welding shall not be done when the ambient temperature is lower than OOF. When the base metal is below the temperature listed for the welding process being used and the thickness of material being welded, it shall be preheated (except as otherwise provided) in such manner that the surface of the parts on which weld metal is being deposited are at or above the specified minimum temperature for a distance equal to the thickness of the part being welded, but not less than three inches, both laterally and in advance of the welding. Preheat and interpass temperatures must be sufficient to prevent crack formation. Temperature above the minimum shown may be required for highly restrained weld. For A514 steel the maximum preheat and interpass temperature shall not exceed 400°F for thicknesses up to 1-1/2 in., inclusive, and 450°F for greater thicknesses. Heat input when welding A514 steel shall not exceed the steel producer's recommendation."

When the recommendations given in Table 1 are conscientiously applied to massive members it sometimes becomes apparent that the old concept of a man with a single preheating torch in his hand is not going to get the job done. Large weldments may require more heat and the application of heat over a wider area than a single torch can provide. Other methods which have been used are thermostatically controlled electric strip heaters, multiple jet and infra-red gas heaters built to fit the contour of the weldment; also, electrical resistance heating systems which are designed primarily for stress relieving have been used for this purpose.

When adequate preheat is not provided it may be an easy matter to give reasons (or excuses) why it was not done, but this will not remove the problem. Weld metal or base metal cracks are the inevitable result of inadequate preheat which in turn results in very expensive cut outs and repairs.

F. WELD CHEMISTRY

One area we have not mentioned is the tendency in submerged arc welding for the manganese and silicon contents
to build up in heavy multipass welds. This means that
proper procedures and wire-flux combinations should be
chosen not only for the plate chemistry but for the
thicknesses involved. There frequently is a tendency
in heavy plate welding to "over match" or make the weld
stronger than it should be. This should not be done since
it will reduce the ductility and increase shrinkage stresses
that may cause cracks in the plate itself.

Heavy plate welding with submerged arc or any other process presents additional problems to the fabricator which are critical if good welds are to be made. The following list of variables must be controlled:

A. Joint Design and Preparation

Design for minimum amount of weld to reduce shrinkage forces and retain accessability for welding equipment. If possible, design the joint and prepare the steel so that the lamellar pattern (direction of rolling) will be parallel with the weld shrinkage forces laminations are known to exist at the weld location (this can be determined ultrasonically), remove the questionable material and butter it with low hydrogen weld metal.

B. Fit-Up

Control fit-up as closely as possible to reduce weld time and shrinkage forces. Allow slight gaps for shrinkage of heavy sections.

C. Tacking

Tack with low hydrogen electrodes and make sure the tacks are of sufficient size to hold parts in alignment until sufficient weld has been deposited. Preheating may be necessary for tacking in some instances.

D. Positioning and accessability

Position job properly to make the most efficient use of the process.

E. Preheating and Interpass Temperatures

Uniform preheating and interpass temperatures are extremely important in heavy plate welding. Do not assume that the heat input from the arc will be sufficient to maintain interpass temperatures at the proper level after preheating. Outside heat may have to be applied even as welding progresses. Slow, uniform cooling is desirable especially in low ambient temperatures. This would be especially true if either the weld metal or the base metal is hardenable because of alloy or carbon content.

F. Welding Procedures and Sequence

Welding procedures should be carefully chosen beforehand to assure the quality required. Welding sequence is of great important in helping to control distortion. Bead shape and location in multipass welding should be anticipated to prevent cracking or slag inclusions. Do not over match base metal with weld metal as this can cause excessive shrinkage forces and cracking. The susceptibility to delayed cracking is proportional to the hydrogen content of the welding atmosphere and greater crack sensitivity is exhibited by high chemistry base metal and by heavier plate thicknesses.

In general, cracking will initiate in the heat affected zone of the base metal, except in cases where the weld metal is of higher hardness.

Do not make concave bead shapes or single pass beads that are deeper than they are wide.

Tandem and long stickout procedures can be extremely helpful in giving maximum deposit rates on heavy plate welding.

G. Choice of Submerged Arc Equipment

Highest Deposit Rate - Full automatic tandem arc DC-AC or DC-AC-AC for long, heavy welds.

Most Flexibility - Full automatic single arc DC.

Most versatile for short, heavy welds - Semiautomatic DC with and without travel mechanisms.

Long stick-out attachments - Suitable for all sub-arc equipment to increase deposition rates or decrease heat inputs on quenched and tempered steels.

N74 30949

Electroslag Welding of 75 to 100 Ton Ingots

bу

Charles R. Manning, Jr.
North Carolina State University
Raleigh, North Carolina

June 1972

The principle of electroslag welding is not new. For many years the techniques of heat generation by passing an electric current through a molten slag has been known. The general scheme includes some method of containing the molten slag pool between the components to be joined with the electrode tip immersed in the liquid slag. The current passing between the electrode and the base metal heats the melt to a very high temperature and increases the electrical conductivity of the slag. The slag pool temperature exceeds the melting point of the base and filler metal. The molten base metal and filler metal then collect below the slag pool and together make up the weld pool. As this metal solidifies it joins the previously mentioned components and is what we refer to as the weld area.

Much work has been done in ESW throughout the world during the past twenty years especially in the USSR. With the continuing advances in the state of the art in ESW has brought about a new remelting technique called Electroslag Remelting.

Work in the USA was carried on by Hopkins at Furth Sterling using a DC process. Work was also being carried out on a large scale a Paton Institute at Kiev under Drs. B. Paton and B. I. Medivar using both DC and AC. The material obtained by the ESR process showed improvement in elongation, reduction in area, impact strength and fatigue strength over conventionally melted material (open hearth and Electric Furnace). During the 1960's and the early 1970 people throughout the world were continually working on increasing the size of ESR ingots. By late 1971 ingots of 40 to 80 tons had been produced.

The question continuously arises, how big can you produce ESR ingots? At present two furnaces are nearly operational for large ingots. One is to produce 100 ton ingots and the second 150 ton ingots. When one considers large turbogenerators these values are small. To day companies are pouring 375 ton static cast ingots for turbogenerators. There are real problems associated with large ingots like these such as shrinkage and liquation which results in severe defects in ingots. These large ingots after processing produce finished shafts with a weight in the neighborhood of 175 to 200 tons or about 55 to 65% of ingot weight. It has been proved to date on ESR ingots of lesser weight that finished shafts can be obtained weighing 80% of ingot weight. Considering the microstructure and macrostructure control that can be obtained using the process ingots of larger weight should follow the same pattern.

Recent work at Paton Institute has shown it is possible to join large crossection components by ESW and obtain equal or better properties to the ingot itself in the following manner. Previously large sections were joined by welding using a rumber of wire electrodes in a consumable nozzle. It is very often possible to get improper feeding of these separate wires into the slag pool and leads to defects in the weld zone. Secondly, the wires are not of the same composition as the ingots and so the weld zone will differ in composition from the ingots. Thirdly, when welding large sections of air hardening, steels heating the components to 375 to 425°C are required. Using the above method it is very difficult if not impossible to weld without heating.

The principle of electroslag welding is not new. For many years the techniques of heat generation by passing an electric current through a molten slag has been known. The general scheme includes some method of containing the molten slag pool between the components to be joined with the electrode tip immersed in the liquid slag. The current passing between the electrode and the base metal heats the melt to a very high temperature and increases the electrical conductivity of the slag. The slag pool temperature exceeds the melting point of the base and filler metal. The molten base metal and filler metal then collect below the slag pool and together make up the weld pool. As this metal solidifies it joins the previously mentioned components and is what we refer to as the weld area.

Much work has been done in ESW throughout the world during the past twenty years especially in the USSR. With the continuing advances in the state of the art in ESW has brought about a new remelting technique called Electroslag Remelting.

Work in the USA was carried on by Hopkins at Furth Sterling using a DC process. Work was also being carried out on a large scale a Paton Institute at Kiev under Drs. B. Paton and B. I. Medivar using both DC and AC. The material obtained by the ESR process showed improvement in elongation, reduction in area, impact strength and fatigue strength over conventionally melted material (open hearth and Electric Furnace). During the 1960's and the early 1970 people throughout the world were continually working on increasing the size of ESR ingots. By late 1971 ingots of 40 to 80 tons had been produced.

The question continuously arises, how big can you produce ESR ingots? At present two furnaces are nearly operational for large ingots. One is to produce 100 ton ingots and the second 150 ton ingots. When one considers large turbogenerators these values are small. To day companies are pouring 375 ton static cast ingots for turbogenerators. There are real problems associated with large ingots like these such as shrinkage and liquation which results in severe defects in ingots. These large ingots after processing produce finished shafts with a weight in the neighborhood of 175 to 200 tons or about 55 to 65% of ingot weight. It has been proved to date on ESR ingots of lesser weight that finished shafts can be obtained weighing 80% of ingot weight. Considering the microstructure and macrostructure control that can be obtained using the process ingots of larger weight should follow the same pattern.

Recent work at Paton Institute has shown it is possible to join large crossection components by ESW and obtain equal or better properties to the ingot itself in the following manner. Previously large sections were joined by welding using a number of wire electrodes in a consumable nozzle. It is very often possible to get improper feeding of these separate wires into the slag pool and leads to defects in the weld zone. Secondly, the wires are not of the same composition as the ingots and so the weld zone will differ in composition from the ingots. Thirdly, when welding large sections of air hardening, steels heating the components to 375 to 425°C are required. Using the above method it is very difficult if not impossible to weld without heating.

To over come this a new method has been developed which utilizes four electrodes as shown in the same figure 1. To start, the electrodes are made of the same chemical composition as the ingots. All electrodes are consumable. The outer two electrodes are rectangular where as the inner two are of square cross-section. The current supply from the transformer to the electrodes is in a bifilar manner or to 3+5 and 4+6 as shown in figure 2.

The bifilar arrangement allows for a higher power factor and reduces inductive losses. Using this method a very large amount of energy imput (0.15 kwt/cm^2) to the consumable nozzle is obtained. This very high amount of energy imput provides the necessary heating of the ingots being welded and avoids the requirements of preheating the large ingots. The arrangement is shown in figure 3 for welding a 60 inch diameter ingot. The next figure shows two 60 inch diameter, 40 ton ingots welded together.

This process has a number of advantages over any previous method including, better and more homogeneous mechanical properties, better chemical composition and structure uniformity, no reason for prior or simultaneous heating of ingots during welding. Simpler equipment and much better realiability of welding and reduction of flaws in welded joints and finally cost is lowered.

Using this process it is now possible to produce medium size ingots (100 tons) and join as many as are required (3-6) to produce 500 or 600 ton ingots which could never be produced by static casting. Also it gives very good possibilities in producing large complicated shapes by joining in this manner.

Now let us look at some of the properties obtained.

Table I gives the elemental analysis and gas content in the electrodes, ingot and weld metal utilized in the investigation. The analysis shows a very consistent composition except for a large reduction in sulphur, hydrogen, oxygen and nitrogen. This reduction is very desirable and will aid in improving the mechanical properties and fracture toughness of the material. The ratio of deformation of a large ESR ingot after heat treatment which included quenching in oil at 840-860°C and tempering at 670-680°C is given in table 2. The mechanical properties at the various deformation ratio are given in figure 5. After a deformation of 1.5 (diameter reduced 44" to 35") all mechanical properties have improved. Only impact strength continues to improve on further forging although it is more than sufficient at 1.5.

Two rotor steel ingots (Cr-Ni-Mo-V, like HY 150) were welded together using this technique. Specimens were taken along the longitudinal axis of the ingot in the ingot and in the weld zone. Specimens were also cut perpendicular to this axis in the heat effected zone. Two sets of specimens were obtained one at the periphery and the second at the center.

Table 3 gives the following properties, yield and tensile strength, elongation, reduction in area and impact strength, after an oil quench and 620°C temper.

After

a 1.5 forging reduction the properties are greatly improved and the material would be very useful for rotor application with rotation speeds to 3000 rpm. This new technique will allow fabrication of very large rotors of extremely high quality and at a much lower cost.

CONCLUSIONS

The following conclusion were drawn from material presented in this paper:

- 1. The new process to weld large ingots is more reliable and reduces possible welding defects.
- 2. The large heat imput during welding alleviates preheating.
- 3. Chemical homogeneity of weld joints is improved.
- 4. Micro- and macrostructure of weld zone is similar to that of the ingot.
- 5. Mechanical properties of the weld metal are equal to those of the ingot.

The author would like to thank Dr. B. E. Paton and Dr. B. I. Medovar of Paton Institute, Kiev, USSR for the information and data presented in this paper.

TABLE 1.

ELEMENTAL ANALYSIS AND GAS CONTENT IN WELD METAL

selection C Si Mn S P Cr Ni Mo V A Open Hearth electrodes for ESW and ESR 0,25 0,28 0,44 0,017 0,015 1,57 3,2 0,41 0,16 - Metal of ESR ingots 0,23 0,25 0,50 0,007 0,012 1,60 3,5 0,50 0,160 0	Position of sample selection	Composition, %										
electrodes for ESW and ESR 0,25 0,28 0,44 0,017 0,015 1,57 3,2 0,41 0,16 - Metal of ESR ingots 0,23 0,25 0,50 0,007 0,012 1,60 3,5 0,50 0,160 0		С	Si	Mn	S	P	Cr	Ni	Мо	V	Al	Cu
ingots 0,23 0,25 0,50 0,007 0,012 1,60 3,5 0,50 0,160 0	electrodes for	0,25	0,28	0,44	0,017	0,015	1,57	, 3,2	0,41	0,16	- .	0,11
		0,23	0,25	0,50	0,007	0,012	1,60	3,5	0,50	0,160	020	0,10
ESW Weld Metal 0,24 0,22 0,50 0,009 0,012 1,60 3,2 0,49 0,160 0	ESW Weld Metal	0,24	0,22	0,50	0,009	0,012	1,60	3,2	0,49	0,160	016	0,09

Position of sample	(
selection	(H)	(0)	(N)	
		ė		
Open Hearth electrodes for ESW and ESR	0,00027	0,0041	0,0039	
Metal of ESR ingots	0,0001	0,0028	0,0025	
ESW Weld Metal	0,0001	0,0015	0,0020	

TABLE 2.

RATIO OF DEFORMATION

	Diameter (in.)	Forging Ratio		
As Cast	44	1		
Forged	35	1.5		
Forged	30	2.0		
Forged	26.8	2.5		
Forged	25	3.0		
Forged	19	5.0		

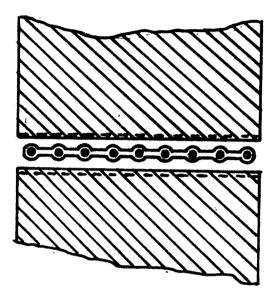
Length of Shaft 125" (10 feet) Steps at least 18" each

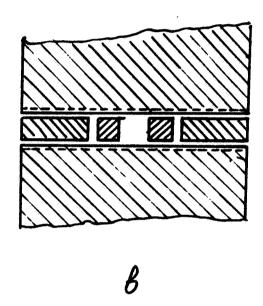
TABLE 3.

Mechanical properties of welded joint of a ESR rotor steel

				Mechanical pro		Input
Specimen taken from	Deformation ratio	KSI	KSI	Elongation %	Reduction %	ft.1b/in ²
	no	125	141	16,1	45,8	499
Weld metal (weld axis)	1.5	135	148	18,1	61,7	578
	2	138	152	18,4	62,8	569
Heat-affected zone (fusion line of weld with ingot metal)	no	128	144	15,8	65,4	606
₩.	1.5	138	151	16,9	62,5	676
	2	137	149	16,2	65,4	755
Parent metal	no	121	137	16,7	50,0	503
	1.5	135	146	19,2	66,0	746
	2	137	149	19,0	65,5	746

NOTE: Notch in impact specimens, in regions of coarse grain 1.5+2.5 mm from fusion line into direction of ingot.

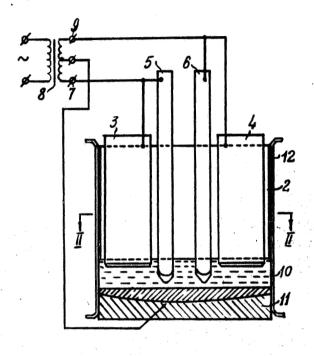




 α

Fig.1. Diagram of electrodes location in the gap

- a) in the old ESW method;
- b) in the new ESW method.



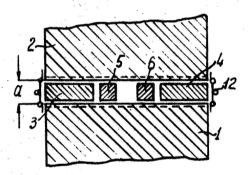


Fig. 2. Diagram of electroslag welding process of heavy sections according to the new method.

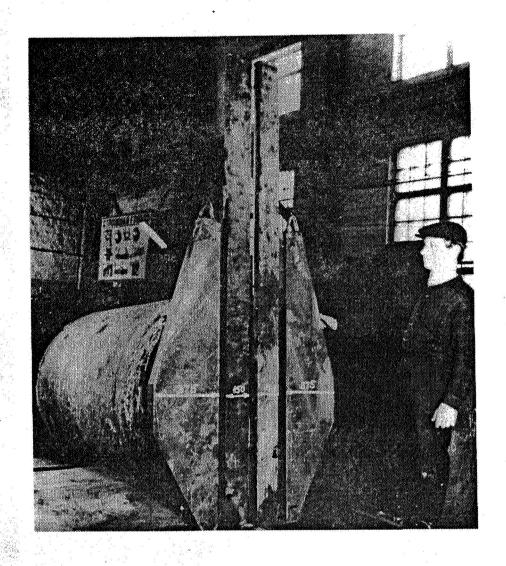


Fig. 3. Arrangement of fixed and movable electrodes in a welding gap during welding according to the new method.

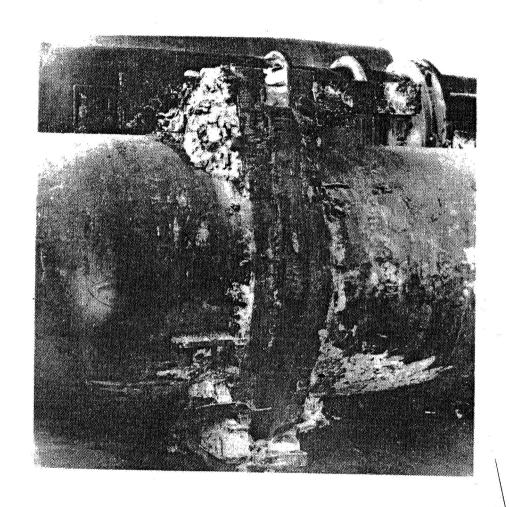


Fig. 4. Appearance of a welded joint formed by welding 40 ton Cr'- Ni ESR steel ingots of 1500 mm (60 in.) dia. according to the new technology.

Fig. 5. Effect of ratio of deformation on the mechanical properties of the heavy ESR ingots.

FN74 30950

SUMMARY OF THE NONDESTRUCTIVE EVALUATION SESSION OF THE SYMPOSIUM ON WELDING, BONDING AND FASTENING SYMPOSIUM

Advanced material systems and designs require improved nondestructive evaluation (NDE) techniques for quality control, failure analysis and properties monitoring. In this session, papers were presented that highlighted some advanced NDE techniques such as infrared scanning systems, laser holographic applications and the use of the mossbauer effect.

Applications of these techniques were discussed for evaluating the new space shuttle external insulation materials, aircraft structures and engine components and precursors to crack initiation and growth.

It was brought out that recent improvements in instrumentation have made the infrared scanning camera and laser holographic systems applicable to a wide range of materials and structures. At present the Mossbauer effect is in the research stage and considerable development and evaluation must be done to move this technique from the laboratory into general usage.

> R.C. Stinebring, Session Chairman Staff Consultant General Electric Company

(2)

*N74 30951

SPECIAL NONDESTRUCTIVE TECHNIQUES

FOR EVALUATING

SPACE SHUTTLE SURFACE INSULATION

R. C. STINEBRING
STAFF CONSULTANT-NONDESTRUCTIVE TESTING
GENERAL ELECTRIC RE-ENTRY AND ENVIRONMENTAL
SYSTEMS DIVISION

FOR PRESENTATION TO: NASA-ASM SYMPOSIUM WILLIAMSBURG, VIRGINIA JUNE 1, 1972

INTRODUCTION

Advanced materials systems generally require improved, unique and advanced nondestructive testing techniques.

These techniques often become the pacing or limiting item for the utilization of new material systems. Some agencies, such as the Nuclear Reactor Branch of the Bureau of Ships, do not permit new designs to be used in critical structures and components if they cannot be adequately inspected by NDT techniques.

The Space Shuttle vehicle will use new and advanced material systems and will require sensitive NDT techniques for assuring the initial quality of the materials and structures. In addition, this multi-use re-entry vehicle will have to be nondestructively evaluated periodically to assures its reuse capability.

At General Electric-Reentry and Environmental Systems Divisions, we are developing sensitive NDT techniques as we develope the thermal protection system materials. Primarily these materials consist of fibrous composites of mullite with a protective coating and appropriate attachment systems.

NDT techniques have been developed for performing in-process evaluations for material variability and for process control. Several of these techniques show considerable promise for evaluating the reusable surface insulation during the operational phase of the shuttle.

DISCUSSION OF NDT TECHNIQUES

A. Radiographic Densitometry

The mechanical and thermal properties of the mullite composite are greatly influenced by the variability in local density and it is therefore necessary to measure the variability and to control it during processing steps.

This is done, at GE-RESD, by obtaining an image of a step block of mullite composite, with known density steps on each x-ray of the billet. (Figure 1).

The x-ray film is then scanned with a photodensitometer and variations in photometric density are calibrated with the known density gradients of the x-ray image of the step block. The areas of greatest variability are recorded, as well as the average. This information is plotted and maintained on a Quality Control Chart to monitor the process variability and to assure that the process remains in control.

In addition, the density data from each billet is used for predicting the mechanical properties by means of the sonic modulus equation:

$$V_1^2 d = F_0$$
 where

 V_1 = longitudinal sonic velocity

d = density

 E_{n} = dynamic modulus

B. Sonic Velocity and Sonic Modulus

The sonic velocity of a material is a fundamental physical property and is related to the mechanical properties of stress and strain. In composites,

the velocity can often be empirically correlated with modulus and is useful in predicting and monitoring the directional mechanical properties. In materials having a very low strain value, the sonic velocity may permit good approximations to be made on the ultimate tensile properties.

The sonic velocity is obtained by means of a system shown schematically in Figure 2. The velocity is measured through the thickness of the billet in the same locations as we obtained the radiometric density reading. The velocity measurement, thus obtained, is used in the modulus equation to monitor the variability of this mechanical property (Figure 3). This measurement is also plotted graphically on a control chart as a means of monitoring the process variability.

C. Infrared Coating Evaluation

The external insulation material is covered by a ceramic coating to make it waterproof and also to give a proper emissivity and erosion resistance.

Small defects in the coating, which may result from processing variables or damage from handling and environmental cycling, are detected by a unique application of an infrared test.

In this test, the specimen or assembly is covered with a film of water which is applied by brushing or dipping. The water is wiped away from the surface after a few minutes and the part is warmed slightly by means of a heater unit.

When the specimen is viewed with the infrared scanning camera the damaged or defective areas stand-out markedly as dark regions on a light background (See Figure 4).

The water penetrates through pinholes or cracks and then spreads into the mullite material in the immediate vicinity of the defect. The zone which is formed is considerably larger than the defect and, as a result, is easily detectable. The whole process is similar to a standard dye penetrant technique but does not contaminate the material and serves as a truly functional test.

In addition to the waterproofness test, the infrared technique is sensitive to non-adhering coating areas. These areas also show up as darker (cooler) areas and can be seen by slightly warming the specimen and viewing it with infrared scanner as it cools.

D. Beta-Backscatter Coating Thickness

The coating thickness is a parameter which must be monitored to assure multi-mission erosion resistance.

At General Electric-RESD, we use a Betascope backscatter method which can readily measure discrete coating areas to a precision of about ±.001".

In this technique, a beta emitting isotope is placed in proximity to the coated surface and the beta energy backscattered onto a detector cell is measured over a 15 second interval. The integrated beta energy is directly proportional to the coating thickness (Figures 5, 6).

SUMMARY

In summary, several unique and sensitive NDT techniques have been successfully applied to the GE-RESD external insulation materials for inprocess monitoring and control.

Some of these techniques can be applied to large structures or are portable enough to be used for evaluating the material when it has been installed on the Space Shuttle vehicle. The infrared technique will be further investigated for evaluating the operational vehicle for coating defects and damage and the beta-backscatter may be applied to the operational vehicle to measure residual coating thickness.

/m1

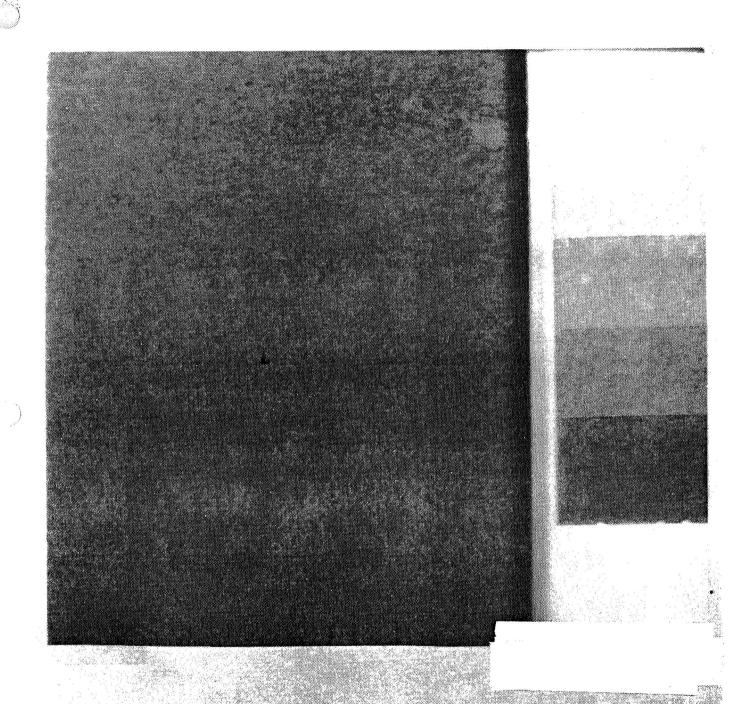


FIGURE 1 - X-RAY REVERSAL PRINT OF REUSABLE SURFACE
INSULATION PANEL SHOWING THE VARIABLE DENSITY
STEP BLOCK.

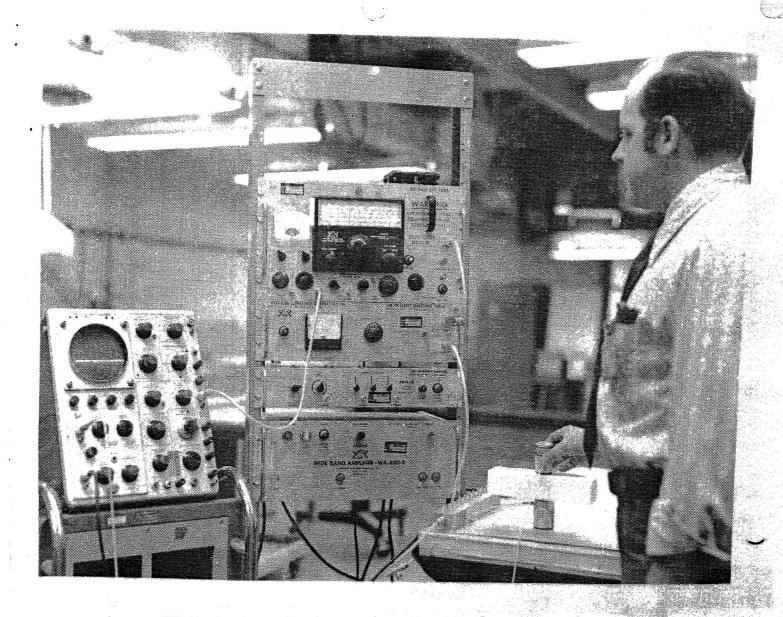


FIGURE 2- SONIC VELOCITY AND MODULUS MEASUREMENT EQUIPMENT.

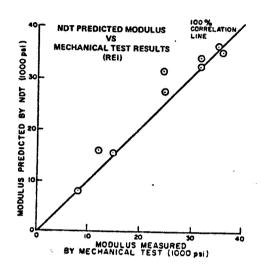


FIGURE 3 - CORRELATION OF NDT MEASURED SONIC MODULUS AND
TENSILE MODULUS OF REUSABLE EXTERNAL INSULATION

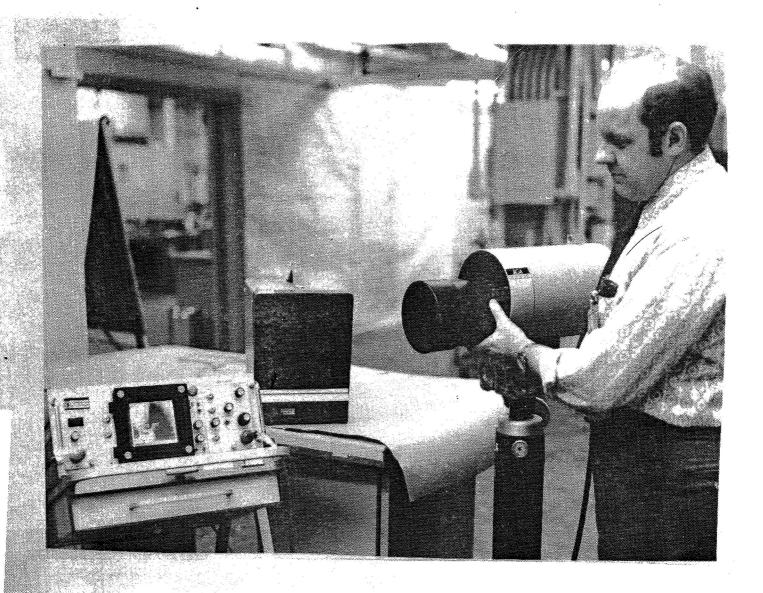


FIGURE 4 - G. E. INFRARED SCANNING CAMERA SYSTEM FOR EVALUATING REUSABLE EXTERNAL INSULATION FOR WATERPROOFNESS



FIGURE 5 - BETA-BACKSCATTER METHOD FOR MEASURING COATING THICKNESS ON REUSABLE EXTERNAL INSULATION.

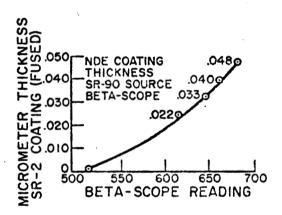


FIGURE 6 - CORRELATION OF BETA-BACKSCATTER MEASUREMENT

AND ACTUAL COATING THICKNESS ON REUSABLE EXTERNAL

INSULATION

N74 30952

MOSSBAUER EFFECT AND ITS APPLICATIONS

IN MATERIALS RESEARCH

Jag J. Singh Langley Research Center Hampton, Virginia

Presented at
Symposium on Welding, Bonding, and Fastening
Williamsburg, Virginia
May 30 - June 1, 1972

MOSSBAUER EFFECT AND ITS APPLICATIONS

IN MATERIALS RESEARCH

Jag J. Singh Langley Research Center

INTRODUCTION

Mossbauer effect spectroscopic measurements provide data for a selected atom and its environments in a given matrix. The Mossbauer spectrum of a given atom, in a certain chemical environment, is unique and its characteristic parameters can be measured with a great degree of accuracy. The presence of any chemical impurities, or changes in the atomic composition of its neighborhood, will cause changes in the Mossbauer parameters. The measurement of these changes can serve as the basis for analysis of matrix variations. (See Figure 1 for a summary of various factors that can affect Mossbauer parameters.)

It is generally recognized that in any well-behaved metal fatigue failure, the following sequence of events occurs: The application of stress (cyclic or static) causes the movement of defects already present in the specimen, besides producing new defects. These defects concentrate in the regions of stress concentration. (In otherwise unflawed materials, fatigue cracks always nucleate in these regions.) This defect concentration, which precedes crack nucleation and its eventual growth, actually amounts to environmental changes for Mossbauer atoms located in these regions.

These changes in the atomic composition of the Mossbauer absorber atom environment can be sensed by examining changes in the sensitive parameters

of the Mossbauer spectra. We have completed a preliminary study of changes in the isomer shift and line width of commercial nonmagnetic steel specimen. The results of this study will be discussed in this paper.

EXPERIMENTAL PROCEDURE

(a) Mossbauer Spectrometer. This study first involved the development of an efficient backscattering technique of Mossbauer spectroscopy, since the existing techniques (Refs. 1 and 2), shown in Figures 2 and 3, are either inefficient or require a specialized specimen geometry. The essential element of backscattering spectroscopy is the radiation detector. An annular detector, which would permit the collimated incident radiation to pass through to strike the test specimen located immediately behind it appears to meet the requirements of high detector-specimen solid angle as well as of in situ measurements. Such a detector has been developed and is shown in Figure 4. It consists of a 2" x 2" x 0.6" NaI(Tl) crystal, with a 0.6" diameter central hole, coupled to two matched photomultipliers. A schematic diagram of the electronic circuit for equalizing the gains and the time constants of the two multiplier channels is shown in Figure 5. This figure also shows the rest of the circuit - including the Mossbauer source motion transducer and the multichannel analyzer.

The incident beam has to be well-collimated in order to minimize the dispersion in the source-scatterer relative velocity and also to

avoid striking the radiation detector before striking the specimen (scatterer). A magnified view of the source collimator and the test specimen is shown in Figure 6. Using the dimensions given in this figure, it is easily seen that the collimator assembly keeps the incident photon beam divergence at the scatterer to an angle less than 2.5°. This low divergence reduces the source velocity dispersion at the scatterer to less than 0.1 percent.

The annular radiation counter, in combination with a stable electromechanical transducer and drive system producing motion of the source with constant acceleration through a range of velocities, can be used to study Mossbauer spectra in both the transmission and scattering geometries. Figures 7 and 8 show the transmission and the backscattering spectra, respectively, obtained with a $0.8~\text{mg/cm}^2$, Fe^{57} -enriched iron target. Figure 9 shows a typical backscattered Mossbauer spectrum obtained with a 0.030-inch thick nonmagnetic (SS-347) steel scatterer. The Mossbauer source in all these cases was a 10-mc Co⁵⁷ source in platinum matrix. The absorber/scatterer in each case was positioned to subtend an angle of π steradians at the detector. From Figures 7 and 8, it is clear that the present detector configuration is capable of producing equally good transmission and backscattering Mossbauer spectra. Figure 9 clearly shows that the present system is usable with scatterers of any arbitrary thickness (Ref. 3).

(b) Metal Fatigue Damage Study. As indicated in the introduction, when a metal specimen is progressively fatigued, dislocations start

piling up in the regions of stress concentration. In the absence of stress raisers, these dislocations will be randomly distributed throughout the test specimen and will not have a significant effect in modifying the absorber atom surroundings. Following these arguments, austenite steel specimen (SS-302, SS-321, and SS-347) with stress raisers were prepared in two different geometrical configurations shown in Figure 10. Experience has shown that test specimen with these configurations develop cracks at the notches or the sharp cuts, presumably due to dislocation concentration there. These specimen were subjected to tension-tension cyclic loading in the range 2 kgm/mm² \rightarrow 20 kgm/mm² at the rate of 1000 cpm and the backscattered spectra from them * measured at different levels of fatigue cycles. These spectra were analyzed and the values of isomer shift, peak width, and the Mossbauer resonant fraction were computed using a program described in Ref. 4. Typical results showing the dependence of two selected Mossbauer parameters on the number of fatigue cycles in (SS-347) specimen are shown in Figure 11.

DISCUSSION

The defect/dislocation pile up in the regions of stress concentration in the test specimen leads to the creation of several nonequivalent Mossbauer absorber atom sites in the area under observation. In the

^(*) The spectra were obtained from the regions where stress raisers were located, namely, the edges of the notches or the sides adjacent to the eloxed cut.

5

case of point defects, it can be argued (Ref. 5) that the net result is the superposition of several modified Mossbauer frequencies, w^{i} :

$$w' = w_0 + \sum_{\ell m} a_{\ell m} w_{\ell m} \tag{1}$$

where w = undisturbed Mossbauer frequency

 $a_{\ell m}$ = concentration of defects of type m at ℓ

 $w_{\ell m}$ = frequency shift caused by the defects of type m at ℓ = $\alpha_{ij}^{m} U_{ij} (-r_{\ell})$

where α_{ij}^m stands for the deformation tensor relating the frequency change and the deformation potential, U_{ij}^m (-r_k).

This statistical summation should result in widening the Mossbauer peak and also changing the isomer shift. The effects of point defects and dislocations on line widths - in limiting cases - are expected to be of the following form (Ref. 5):

where N_d = linear dislocation density

 N_d^0 = dislocation loop density

and R = characteristic dimension of the dislocation loop.

Thus, one expects the Mossbauer parameters to continue to change with the fatigue cycles till a nucleus of the crack has been formed. This change is expected to be of the "saturation" type since the later dislocation development will have reduced effect in creating additional nonequivalent sites or lattice distortion. The "saturation" change can be related to the critical stage of the specimen when crack nucleation is imminent.

An examination of Figure 11 shows that the peak width shows a distinct upward trend with the increasing number of fatigue cycles whereas the isomer shift is barely affected. This may be interpreted to indicate that quadrupole splitting is playing a role. However, the specimen were commercial, polycrystalline steels of ill-defined history and detailed measurements on single crystal specimen should be made before any firm conclusions can be drawn (Ref. 6). It does appear, however, that the changes in the Mossbauer parameters with fatigue are small and the use of W¹⁸¹ as the Mossbauer source may be more appropriate. (This stems from the long half life, Ref. 7, of Ta¹⁸¹ (6.25 keV) state, leading to a natural line width of 3.2 x 10⁻³ mm/sec compared with 0.197 mm/sec for Fe⁵⁷.) Ta¹⁸¹, which can be diffused into the material under study will have a tendency to go to the grain boundaries where dislocations also tend to concentrate.

REFERENCES

- 1. Mossbauer Effect Methodology, Vol. I, edited by I. J. Gruverman. Published by Plenum Press, 1965.
- 2. K. R. Swanson and J. J. Spijkerman: J. Appl. Phys. 41, 3155, 1970.
- 3. J. J. Singh: Nucl. Instr. & Meth. (to be published) and NASA TN D-6819, 1972.
- 4. L. M. Howser, J. J. Singh, and R. E. Smith, Jr.: NASA TM X-2522, 1972.
- 5. L. B. Kvashnina and M. A. Krivoglaz: Fiz. Metal. Metalloved, 23, 1967.
- 6. J. J. Singh: Bull. Am. Phys. Soc., 17, 547, 1972.

-12 * 41

7. Tables of Isotopes (6th Edition), edited by C. M. Lederer, J. M. Hollander, and I. Perlman. Published by John Wiley and Sons (1967).

Applications Of Mossbauer Spectroscopy To Physical Metallurgy Are Based On The Following Factors:

- (1) NEIGHBORING ATOM INTERACTIONS.
- (2) LOCAL CUBIC SYMMETRY.
- (3) ELECTROSTATIC (QUADRUPOLE) INTERACTIONS.
- (4) LATTICE DISTORTION (POLYCRYSTALLINE ALLOYS)

CHANGES IN THESE FACTORS, RESULTING FROM DISLOCATION MOVEMENTS AND PILE UP, AFFECT THE INTERNAL MAGNETIC FIELD, THE ISOMER SHIFT, THE ELECTRIC FIELD GRADIENT AND THE LATTICE PARAMETERS AT THE ABSORBER ATOM SITES. THESE CHANGES MAY BE MORE PRONOUNCED IN MATERIALS WITH LOW STACKING FAULT ENERGIES.

FIGURE 1

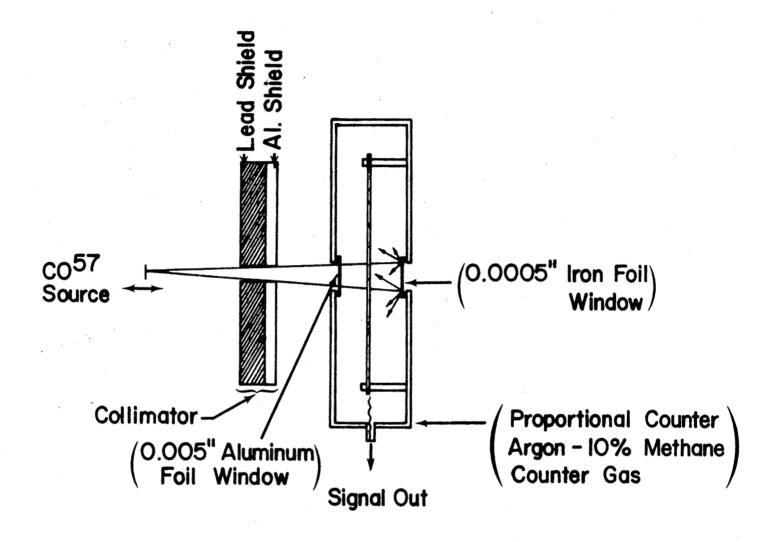


Figure -2. Schematic Arrangement for Scattering Geometry (E-Counting) in Mossbauer Spectroscopy.

FIGURE 2

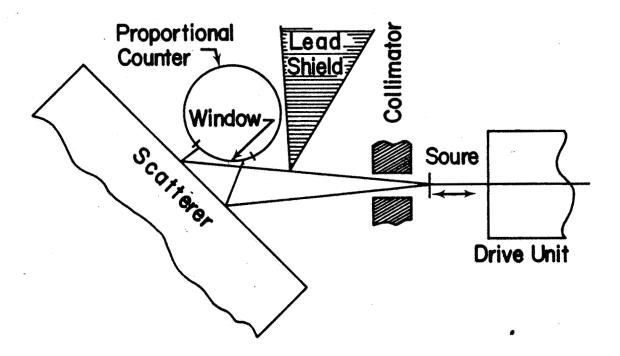
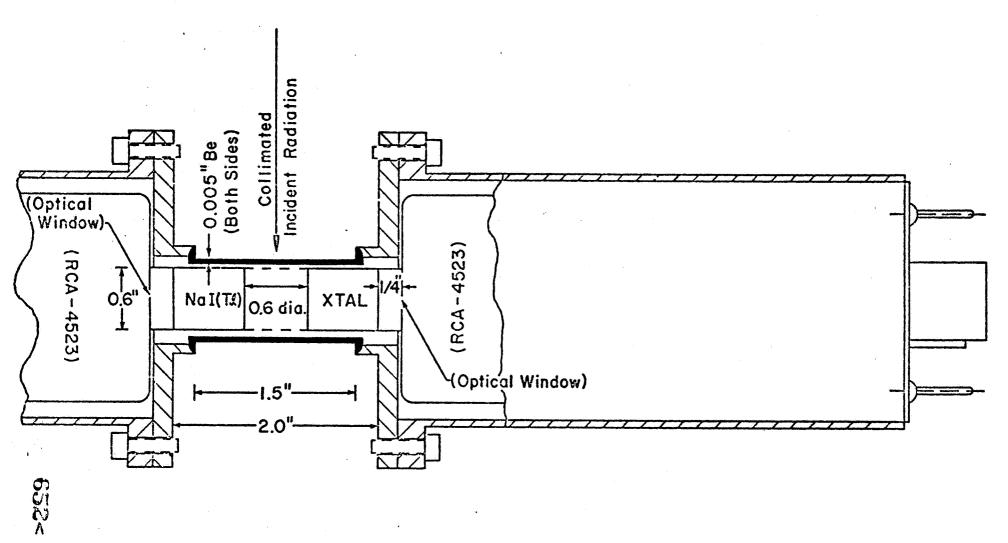
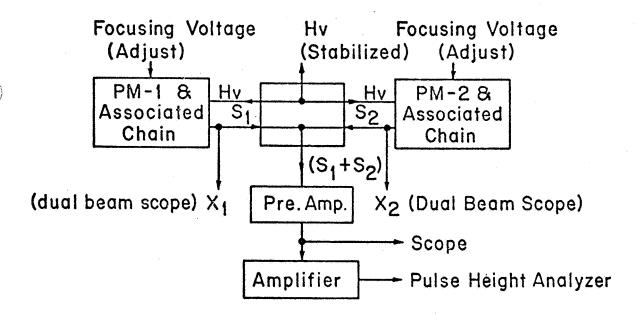


Figure -3. Schematic Arrangement for Scattering Geometry (Photon Counting) in Mossbauer Spectroscopy.

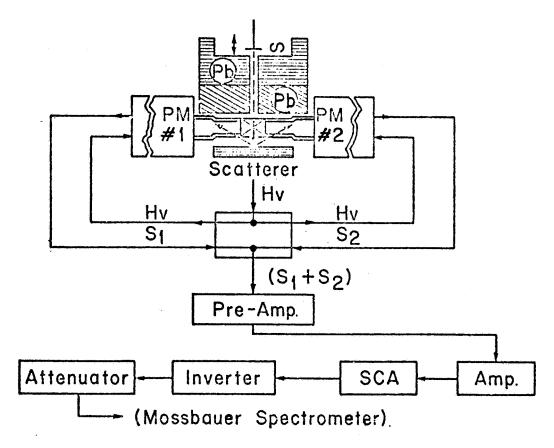
FIGURE 3 651<



Schematic Drawing of the (0.6" \times 2" \times 2") Annular Na I (TL) Detector Assembly. (Notice the 0.005" Beryllium Windows on Both Sides.)

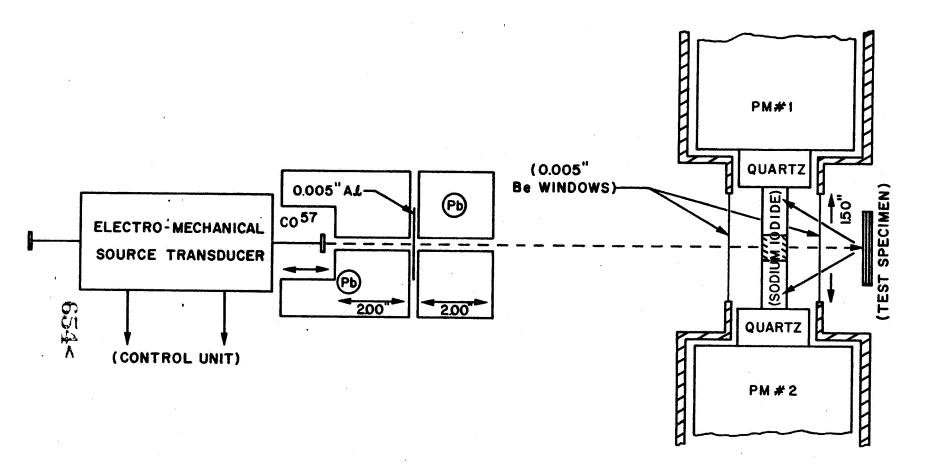


General Circuit for Equalizing Photomultiplier Gains and Pulse Arrival Times.



Schematic Diagram of the Signal Conditioning Circuit for Mossbauer Spectrometer.

FIGURE 5 653<

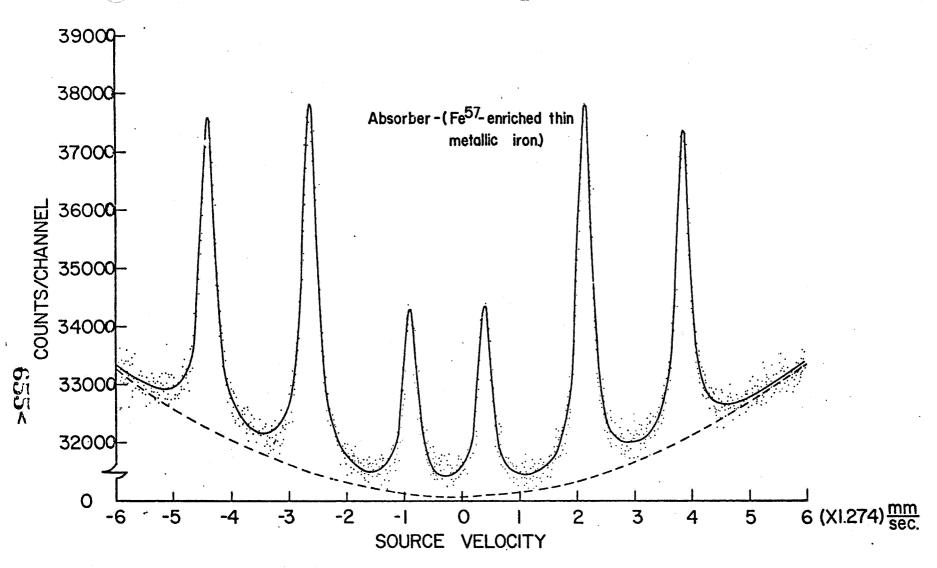


EXPERIMENTAL SET-UP FOR MES INSPECTION.

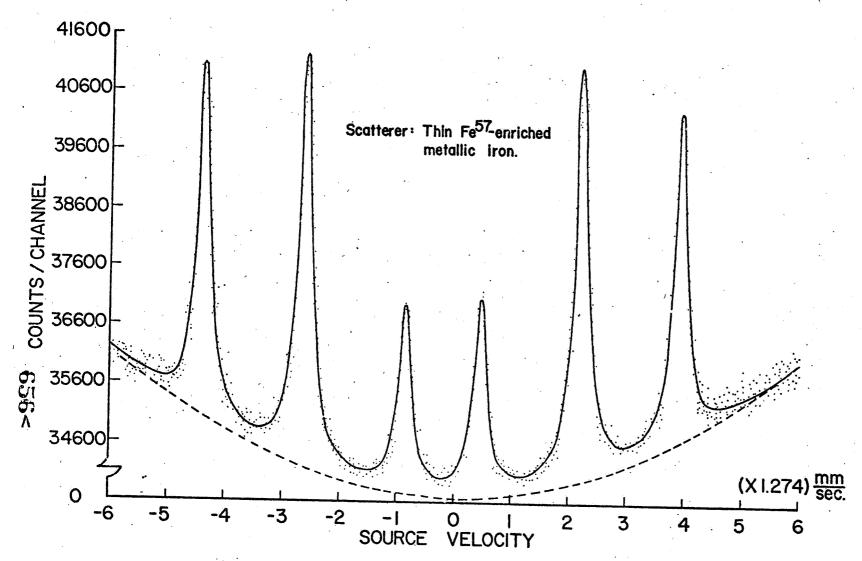
FIGURE 6



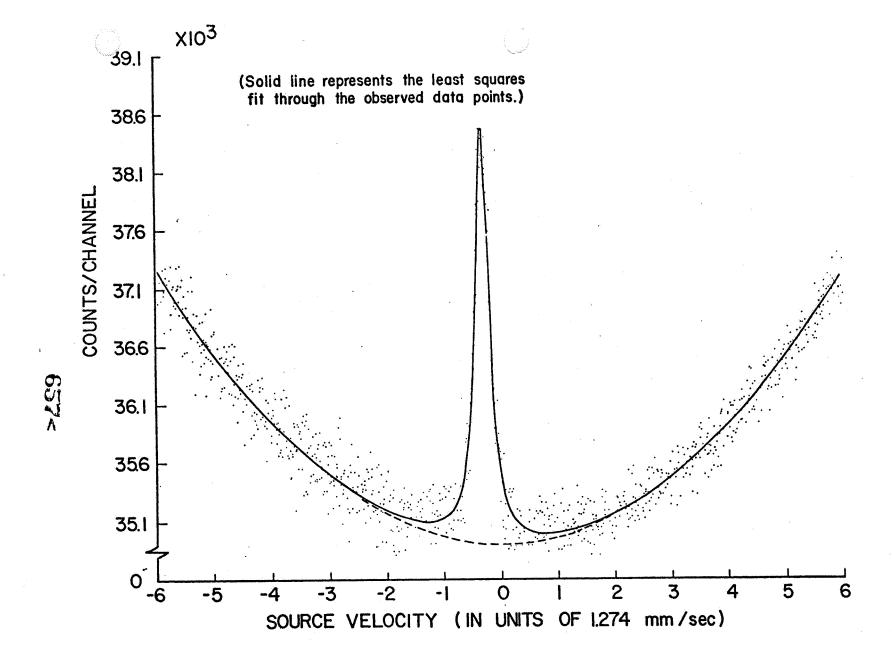




A Typical Transmission Spectrum from a Thin (0.8 mg/cm 2) Fe 57 -Enriched Iron Absorber with the Langley Detector. (Notice the Characteristic Scattering 'Peaks' Instead of the Transmission 'Dips'.)

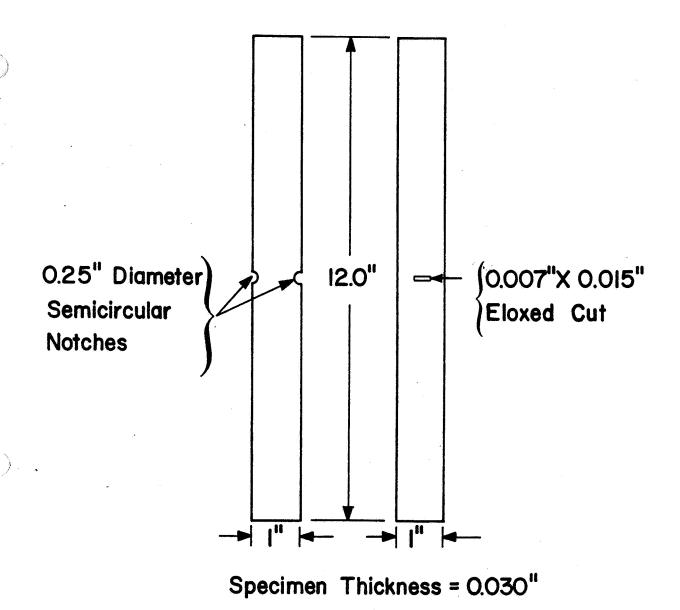


A Typical Backscattering Spectrum from a thin (0.8 mg/cm²) Fe⁵⁷-enriched Iron Scatterer with the Langley Detector. (Notice the pronounced Scattering Peaks Characteristic of Scattering Geometry.)

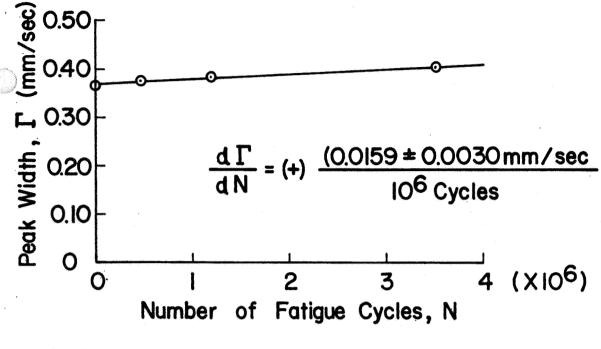


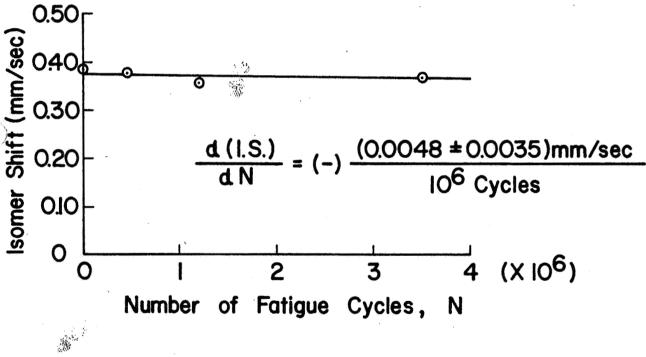
Backscattered Spectrum from a (SS-347) Steel Specimen Using the Radiation Detector Described in this Paper.

FIGURE 9



Geometrical Configurations of Steel Specimen used in the Study of Fatigue-induced changes in their Mossbauer Spectra.





Dependence of Mossbauer Peak Width (Γ) and Isomer Shift (I.S.) on Cyclic Stress in SS-347 Steel Specimen.

MY4 30953

TRENDS IN MECHANICAL FASTENERS

By:
Jack B. Levy
Engineering Materials and Processes
Information Operation (EMPIS)
General Electric Company
Schenectady, New York 12345

ASM Symposium on Welding, Bonding and Fastening The Williamsburg Colony Williamsburg, Virginia 23185

June 1, 1972

CONTENTS

	Page
INTRODUCTION	2
TRENDS IN THE BUSINESS WORLD	2
Safety and Reliability	2
Maintenance and Repair	2
Competition	2
TRENDS IN MECHANICAL FASTENERS	3
Specialty Fasteners	3
Thread Rolling Screw	3
Self Drilling and Tapping Screws	4
Locking Screws	4
Tamperproof Fasteners	4
Flanged Bolts and Nuts	4
METRICATION	4
CONCLUSION	5

APPENDIX I

First Progress Report on Work of ANSI Special Committee to Study Development of an Optimum Metric Fastener System

* * * * * *

INTRODUCTION

Fastener manufacturers are very creative. They continually develop new products and minor variations of old products. How do you separate those which have a future from those which are only a gimmick? In most instances it takes considerable experience and testing before judgement can be passed, and the results are usually controversial. For that reason, in this brief report, we will confine ourselves to only a few new variations which should be used in ever increasing volume over the forseeable future. This will then allow the maximum possible time to discuss the trend towards metrication.

Before discussing fastener trends, let us look at some of the trends in the business world which will influence the kinds of fasteners that we will use in the coming years.

BUSINESS TRENDS

Safety and Reliability

There is an ever increasing amount of pressure on producers to make reliable products, at a cost which will enable them to remain competitive. This need for reliability is absolutely necessary if the breakdown of a product could cause harm to people or damage to property. In addition, all new products are guaranteed for a fixed period of time. Consumer organizations and the government have been constantly demanding more liberal terms in favor of the consumer. It is profitable to have trouble free service during the warranty period to avoid repair costs which will be charged back to the parent company. This will generate a need for better quality fasteners which will incorporate many of the latest design innovations.

Maintenance and Repair

As products become more complex, it becomes increasingly more difficult and time consuming to locate individual problem areas when a breakdown occurs. When this is coupled with the rising cost of labor, it rapidly creates a condition where it is cheaper to replace than repair. By replace, it does not necessarily mean that an entire product must be discarded. There is a trend toward building products into subsections. Just that portion of the product in which the problem occurs needs to be detached and replaced. The consumer might replace the faulty section himself or if outside service is required the labor costs will be held to a minimum.

Since there will be less repairing of the small internal parts of a subassembly, there will be a trend toward permanently joining by rapid production methods such as welding. On the other hand, the larger subassemblies may still be joined by conventional threaded fasteners or quick release type of fasteners, such as spring clips, quarter turn, and push button designs.

Competition

The fastener industry is very competitive and the last 2 years were the toughest in recent times. The aerospace and defense business went

(Continued on Page 3)

Competition (Continued)

into a rapid decline. At the same time there was a big influx of imported fasteners. At present, imports have been limited almost exclusively to the lower quality standard fasteners. Some domestic fastener manufacturers recognize that they cannot compete in this category. They are beginning to import, rather than produce ordinary fasteners. At the same time they are giving ever increasing attention to specialty items.

TRENDS IN MECHANICAL FASTENERS

Specialty Fasteners

The vast majority of new ideas in fasteners will never enjoy wide usage. Usually the biggest handicap is cost. That is, most new developments cost more than the standard they are supposed to replace. This creates an initial resistance. Everyone is trying to cut costs. Buying a more expensive fastener subjects them to criticism from those who watch the pennies. However, there will be occasions when spending more money for fasteners is warranted:

- 1. Lower Assembly Cost No one will object to spending more for a purchased part if it is less costly to install and results in a lower overall cost.
- 2. <u>Improved Design</u> Higher initial cost can be justified if the change results in a safer and more reliable product.
- 3. Lower Maintenance Cost With increased attention being paid to the cost of servicing, a higher priced fastener can justify its existence if it will reduce the time required to disassemble and reassemble a product for normal maintenance and repair.

Some of the specialty fasteners which are enjoying ever increasing usage includes the following:

Thread Rolling Screws

There are several different thread rolling screw designs which are commercially available. Each type has several contact points around the starting threads. These points gradually form a thread through interrupted contact, rather than the continuous forming principle of conventional tapping screws. These contact points or tiny lobes are generally invisible to the eye. They form threads with comparatively low torsional effort. Therefore, they require less driving torque to seat the screw. There will be a wider margin for setting the driving gun to cut off before reaching the higher torque values that can strip a thread. These screws also provide a high degree of thread engagement which produces a tight fit. This minimizes the need for lock washers or other locking devices.

Self Drilling and Tapping Screws

This type of screw combines the characteristics of yesterday's tapping screw with the best features of a factory sharpened twist drill. They drill their own pilot hole and provide their own threads in one operation. They can be placed exactly where they are wanted without the time consuming effort to align holes in mating parts. This can sustantially reduce assembly cost in the factory.

Locking Screws

There is a trend toward the use of fasteners that offer some kind of locking feature to maintain preload and minimize fatigue problems. They also prevent loosening, rattles and squeaks. There are many ways to provide locking action, such as:

Plastic pellets or strips fused to the thread
Deformed thread
Resilient bulge on one side of a thread
Anaerobic adhesives (single component liquid that cures
only in the absence of air)
Two part epoxy adhesives
Precoat each ingredient separately on the fastener or
Micro-capsulation of the active ingredient

Tamperproof Fasteners

There is an increasing need for fasteners that are designed to prevent unauthorized removal. Tamperproof fasteners are needed on equipment located in public places to discourage vandalism and thievery. They are also needed on some consumer products as a safety measure to protect the amateur repairman from harming himself or causing serious damage to the equipment.

Flanged Bolts and Nuts

There is an ever increasing need for fasteners which provide a greater load-bearing area. This is especially true for bolting softer materials. A flanged bolt or nut will permit tightening to higher preloads and generally eliminate the need for washers.

Metrication

A few years ago almost everyone in the fastener industry was certain that United States would not convert to metric threaded products in their lifetime. Even today there is no great rush toward the usage of metric fasteners in this country. However, those USA companies which manufacture and market identical products in different parts of the world have three (3) choices:

1. They can standardize on inch fasteners because they are more easily purchased overseas than metric fasteners can be purchased domestically.

METRICATION (Continued)

- 2. They can use inch fasteners in USA production and metric fasteners in overseas production.
- 3. They can standardize on metric fasteners for all products, whether domestic or foreign production.

Most USA companies select either of the first two choices listed below. Nevertheless there will be a trend toward choice No. 3, as pressure is applied both from overseas customers and US proponents of the metric system.

We anticipate a very slow and gradual conversion from US customary units to metric S1 units. Those concerned with measurements in USA should develop the dual capability to think in both systems. The S1 system is not the old metric system with a new name. It does contain several major changes. The absolutely new units in the S1 system are the Newton and Pascal. The Newton is a measurement of force and the Pascal is a measurement of stress. Another unit which will be commonly used by the fastener industry is torque measured in Newton metres. (note the new official spelling of the word "Meter".) Temperature will be measured in centigrade or kelvin units. Kelvin is the same as centigrade except that absolute zero is zero degrees K and all values are offset by 273.15 degrees.

The American National Standards Institute (ANSI) recently organized a special committee to study the development of an optimum metric fastener system. This committee will make recommendations. They will not develop standards. However, it it anticipated that these recommendations will be given serious consideration by those fastener committees that are responsible for developing industry standards. This special ANSI committee will attempt to complete its study within the next two years. They will issue progress reports at periodic intervals. See Appendix I for the first report, dated March 30, 1972.

CONCLUSION

The future for mechanical fasteners is more than the few speciality fasteners and ever increasing usage of metric units previously discussed. The ideal fastener does not yet exist. The most important need is for a fastener that can be assembled automatically. The ultimate in the assembly of parts would be a fastener which automatically falls in position and locks without individual attention. Thus requires installation machinery that is compatible with the purchased fastener. In the future fastener manufacturers must develop and sell complete systems or work very closely with their customers manufacturing engineers to develop this kind of automated equipment.

Committee Correspondence

ANSI Special Committee to Study Development of an Optimum Metric Fastener System

ADDRESS WRITER AT: INDUSTRIAL FASTENERS INSTITUTE 1505 EAST OHIO BUILDING CLEVELAND, OHIO 44114 PHONE (216) 241-1482 March 30, 1972

FIRST PROGRESS REPORT ON WORK OF ANSI SPECIAL COMMITTEE TO STUDY DEVELOPMENT OF AN OPTIMUM METRIC FASTENER SYSTEM

In July, 1971, announcement was released to the technical press in USA and Canada of appointment by the American National Standards Institute of a Special Committee to Study Development of an Optimum Metric Fastener System.

The Committee's assignment is to re-examine the engineering of mechanical fasteners, thoroughly study all of their dimensional, mechanical and performance features, and to develop an entirely new system which would be as technically superior as the state-of-the-art permits, and which would reduce to the fewest possible the number of different fasteners to be recognized as standard. All dimensions and properties of the new system will be stated in metric (SI) units.

With the July, 1971 press release was a promise to periodically inform the press of the Committee's progress and accomplishments.

- The ANSI Committee has met 4 times, and its 5 working Subcommittees have held a total of 12 meetings.
- The Committee is using as the basis for all its studies the originally proposed series of 25 diameter/pitch combinations recommended in the January, 1971 IFI Engineering Report with the proviso that the series

would be re-examined periodically as new data is developed. The decision was influenced by a "Monte Carlo" computer program comparing the ISO series of preferred metric sizes of fasteners against the IFI series to learn the relative material wastage based on current usage by sizes and strength grades. The IFI series indicated a savings of nearly 4%.

- One of the biggest European concerns with the initial IFI recommendations was the indicated non-mating of new threads with existing ISO metric threads. An extensive analysis, involving statistical evaluation of actual thread measurements taken on over 5,000 nuts and screws as supplied by 9 producers, showed that the probability of interference between a screw with the new optimum metric high radiused root external thread and existing ISO internal threads (nuts and tapped holes) would be negligible.
- Design of the screw thread system is well advanced. The basic thread form is approved, the design form for an allowance and a non-allowance thread fit is close to completion, a technically innovative gaging practice has been designed and will be checked out with specially manufactured gages, the tolerance and allowance systems are being developed. The basics of a sophisticated technique for evaluating the merits of different diameter/pitch series have been defined and will be used to assist reaching final decisions on sizes and thread pitches.
- The advice of over 200 fastener engineers was sought on new ideas for improving the design of various fastener products. Based on this response, a comprehensive listing of criteria which must be satisfied in the design of new products has been established. A detailed computer

program is now under way to search out optimum configurations for bolt and screw heads and shanks. Dr. R. Kasuba, Professor Mechanical Engineering, Cleveland State University, has been retained as a consultant. Companion studies on nuts will start shortly.

- One of the principal goals of the study is to assure maximum utilization of material, to give designers full use of a product's inherent strength capabilities. Considerable work has been done to evaluate different concepts of approach, and an extensive fact finding research effort is now being shared by several fastener producers and users to gather data on actual mechanical properties of representative products now being manufactured and used.
- Work to establish inspection and quality assurance procedures has started,
 even though the need for quick accomplishment is not as urgent as other
 phases of the study.
- While the bulk of the work will be done analytically, physical testing of actual product will be necessary to cross check and verify. Arrangements have been made to collect quantities of inch and metric series fasteners from various countries of the world to be used in physical testing.
- A team of 6 members of the ANSI Committee will visit Europe in mid May to discuss the progress of the Committee's technical studies with representatives of European industry.

The Committee has approved and released two recommendations - OMFS-1 "Rules for the Use of SI Units Applicable to Mechanical Fasteners" and OMFS-2 "Basic Thread Form for Optimum Metric Fastener Screw Threads."

Copies of each are attached.

Single copies of these Recommendations are available without charge upon written request to Industrial Fasteners Institute, 1505 East Ohio Bldg., 1717 East 9th Street, Cleveland, Ohio 44114.

American National Standards Institute, Inc. — 1430 Broadway, New York, N. Y. 10018 U.S.A.

FOREWORD

The ANSI Special Committee to Study Development of an Optimum Metric Fastener System was appointed in April 1971. Its assignment is to develop a total system of metric module mechanical fasteners, taking advantage of every opportunity to improve fastener performance capability through product redesign and the most efficient use of materials, and to limit to the fewest possible the number of different sizes, series, grades, types and styles of fasteners necessary to adequately satisfy the engineering requirements of the majority of industrial applications. All dimensions and properties of the system will be stated in metric (SI) units.

The International System of Units (SI) is a rationalized and coherent system of measurement units based on the metric system. SI was developed by the General Conference of Weights and Measures. It was officially adopted by the Conference in 1960, and has since been accepted by the International Organization for Standardization (ISO) and the International Electrotechnical Commission (IEC). SI is in a continuing state of review and refinement, the most recent additions and modifications being accepted by the Conference in 1971. At the present time, SI consists of seven base units, two supplementary units, a series of derived units consistent with the base and supplementary units, and a series of prefixes for the formation of multiples and submultiples of the various units. Complete details of SI can be found in ISO R1000, NBS 330, or ASTM E380.

This Recommendation was prepared by the ANSI Special Committee to guide it in the units, prefixes, and editorial style to be used in the preparation of engineering documentation resulting from its studies.

1.0 SCOPE

- 1.1 This Recommendation abstracts from the International System of Units (SI) the units for those quantities most commonly used to define the characteristics, dimensions, and properties of mechanical fasteners. This document also outlines editorial style rules to be followed when using SI units.
- 1.2 Appendix A to this Recommendation gives information on conversion of U.S. customary units to SI units. Also as an assist to familiarize fastener producers and users with relationships between SI units and customary units, the appendix presents several approximate equivalencies.

2.0 REFERENCE DOCUMENTS

The material presented in this Recommendation is abstracted from the following sources:

ISO R1000 — Rules for the Use of Units of the International System of Units and a Selection of the Decimal Multiples and Submultiples of the SI Units

NBS Special Publication 330 — The International System of Units (SI), published by U.S. Department of Commerce, National Bureau of Standards

6'70<

Published and Issued by Industrial Fasteners Institute 1505 East Ohio Bldg. 1717 East 9th St. Cleveland, Ohio 44114 USA

RULES FOR THE USE OF SI UNITS

APPLICABLE TO MECHANICAL FASTENERS
IN THE OPTIMUM METRIC FASTENER SYSTEM

OMFS-1

Page 1 of 4

Issued: February, 1972 Revised:

All recommendations are advisory only. Their use by anyone is entirely voluntary. Reliance thereon for any purpose by anyone is at the sole risk of that person or the user of the product, and the ANSI Committee and the IFI are not responsible for any loss, claim or damage arising therefrom. In formulating and approving recommendations, the ANSI Committee and the IFI have not investigated and will not investigate patents which may apply to the subject matter. Prospective users of the recommendations are responsible for advising themselves of and protecting themselves against any patent infringement liability which may arise out of such use.

American National Standards Institute, Inc. - 1430 Broadway, New York, N. Y. 10018 U.S.A.

ASTM E380 (ANSI Z210.1) - Standard Metric Practice Guide (A Guide to the Use of SI - the International System of Units), published by the American Society for Testing and Materials

SAE Rules for the Use of SI (Metric) Units in SAE Reports, published by the Society of Automotive Engineers

3.0 QUANTITIES

3.1 LENGTH. The SI base unit for length is metre (m). [NOTE: The spelling "meter" should not be used.]

All linear dimensional characteristics of fasteners (diameters, heights, thicknesses, lengths, thread dimensions, etc.) shall be expressed in millimetres (mm). Tolerances shall be given in millimetres (mm), and surface roughness in micrometres (µm).

3.2 MASS. The SI base unit for mass is kilogram (kg).

The mass (commonly referred to as weight) of a fastener and masses related to fastener manufacturing and marketing shall be expressed in kilograms (kg). Alternatively, grams (g) may be used to express a small mass, and megagrams (Mg), which equals 1000 kg, may be used when expressing a large mass.

NOTE: Considerable confusion exists in use of the terms mass and weight. Mass is a property of matter to which it owes its inertia. If a body or particle of matter at rest on the earth's surface is released from the forces holding it at rest, it will experience the acceleration of free fall (acceleration of gravity). The force required to restrain it against free fall is commonly called weight. This force is proportional to the mass of the body and is often expressed in mass units (kg); but as it is a force, it should be expressed in force units (N). The acceleration of free fall varies in time and space; weight (which is proportional to it) does too, although mass does not. In common parlance the term "weight", as of a container of bolts, is used where the technically correct term is mass. Since this non-technical usage of the term "weight" is common, the term should be avoided in technical usage.

3.3 DENSITY. The SI unit for density is kilogram per cubic metre (kg/m³) and shall be used when expressing densities related to fasteners.

3.4 TIME. The SI base unit for time is second (s). When expressing time the following units are acceptable: second (s), minute (min), hour (h), day (d), week and year.

3.5 TEMPERATURE. The SI base unit for temperature is kelyin (K).

Because of the wide usage of the degree Celsius, particularly in engineering and non-scientific areas, the Celsius scale (formerly called the centigrade scale) shall be used when expressing temperature as related to fastener manufacturing processes and to fastener application practices. The Celsius scale is related directly to the kelvin scale as follows:

one degree Celsius (1°C) equals one degree kelvin (1K), exactly

and

a Celsius temperature (t) is related to a kelvin temperature (T), as follows:

T = 273.15 + t, exactly

3.6 PLANE ANGLE. The SI unit for plane angle is radian (rad), and is equal to $180^{\circ}/\pi$ (57.296°). For fasteners, plane angles shall be expressed in degrees (°) with decimal subdivisions instead of minutes and seconds.

3.7 AREA. The SI unit for area is square metre (m²). For fasteners, the recommended unit for expressing area is square millimetre (mm²).

3.8 VOLUME. The SI unit for volume is cubic metre (m^3) .

For fasteners, the recommended unit for expressing volume is cubic millimetre (mm³).

3.9 FORCE. The SI unit for force is newton (N). For fasteners, forces (loads) shall be expressed in newtons (N), kilonewtons (kN) or meganewtons (MN).

671<

Published and Issued by Industrial Fasteners Institute 1505 East Ohio Bldg. 1717 East 9th St. Cleveland, Ohio 44114 USA

RULES.FOR THE USE OF SI UNITS APPLICABLE TO MECHANICAL FASTENERS IN THE OPTIMUM METRIC FASTENER SYSTEM

OMFS-I

Page 2 of 4

Issued: February, 1972 Revised:

All recommendations are advisory only. Their use by anyone is entirely voluntary. Reliance thereso for any purpose by anyone is at the sole risk of that person of the user of the product, and the ANSI Committee and the IFI are not responsible for any loss, claim or damage arising therefrom, in formulating and approxing recommendations, the ANSI Committee and the IFI have not investigated and will not investigate patents which may apply to the subject matter. Prospective users of the renommendations are responsible for advising themselves of and protecting themselves ago into patents infringencial liability which may arise out of such him.

American National Standards Institute, Inc. - 1430 Broadway, New York, N. Y. 10018 U.S.A.

3.10 STRESS. The SI unit for pressure or stress is pascal (Pa), and equals one newton per square metre (N/m^2) .

For fasteners, stresses shall be expressed in megapascals (MPa).

3.11 TORQUE. The SI unit for torque is newton-metre (N-m) and shall be used for fasteners.

3.12 MULTIPLE AND SUBMULTIPLE PREFIXES. The multiple and submultiple prefixes used to quantify SI units as used for fasteners shall be as follows:

Multiplication Factor	Prefix	SI Symbol
1 000 000 = 106	mega	M
$1000 = 10^3$	kilo	k
$0.001 = 10^{-3}$	milli	m
$0.000001 = 10^{-6}$	micro	μ

4.0 RULES FOR STYLE AND USAGE

- 4.1 GENERAL. The units as noted for their applicability for fasteners in Section 3 should be used.
- 4.2 APPLICATION OF PREFIXES. The prefixes given in 3.12 should be used to indicate orders of magnitude, thus eliminating insignificant digits and decimals, and providing a convenient substitute for writing powers of 10 as generally preferred in computation. For example —

2 N x 10³ or 2000 N becomes 2 kN

7.2 mm x 10^{-3} or 0.0072 mm becomes 7.2 μ m

Prefixes should be applied to the numerator of compound units, except when using kilogram (kg) in the denominator. Since kilogram is a base unit of SI, this particular multiple is not a violation and should be used in preference to the gram.

With SI units of higher order such as m² or m³, the prefix is also raised to the same order; for example, mm² is 10⁻⁶m² not 10⁻²m².

4.3 SELECTION OF PREFIX. When expressing a quantity by a numerical value and a unit, a prefix should be chosen so that the numerical value prefer-

ably lies between 0.1 and 1000, except where certain multiples and submultiples have been agreed for particular use, for example MPa. The same unit, multiple, or submultiple should be used in tables even though the series may exceed the preferred range of 0.1 to 1000.

The decimal point shall be used to indicate decimal parts of a quantity. Whenever a numerical value is less than one, a zero should precede the decimal point.

- 4.4 CAPITALIZATION. Symbols for SI units are only capitalized when the unit is derived from a proper name; for example, N for Isaac Newton. Unabbreviated units are not capitalized, for example, kelvin and newton. Numerical prefixes given in 3.12 and their symbols are not capitalized; except for the symbol M (mega).
- 4.5 PLURALS. Unabbreviated SI units form their plurals in the usual manner. SI symbols are always written in singular form. For example,

50 newtons or 50 N

25 millimetres or 25 mm

- 4.6 PUNCTUATION. Periods are not used after any SI unit symbol, except at the end of a sentence.
- 4.7 NUMBER GROUPING. It is the practice in many metric countries to use a comma (instead of a decimal point) to indicate decimal parts of a quantity. Consequently, to avoid confusion, commas to separate multi-digit numbers into groupings of three shall be omitted, and digits shall be placed without spaces or other separators both to left and right of the decimal point. To facilitate convenient reading, effort should be made, through selection of appropriate prefixes, to limit the number of digits to the left of a decimal point to four or less.
- 4.8 DERIVED UNITS. In symbols for derived units, a center dot is used to indicate multiplication (for example, N·m), and a slash to indicate division (for example, kg/m³). Symbols to the left of the slash are in the numerator, and symbols to the right are in the denominator.

Published and Issued by Industrial Fasteners Institute 1505 East Ohio Bldg. 1717 East 9th St. Cleveland, Ohio 44114 USA

RULES FOR THE USE OF SI UNITS APPLICABLE TO MECHANICAL FASTENERS IN THE OPTIMUM METRIC FASTENER SYSTEM

OMFS-1

Page 3 of 4

Issued: February, 1972

All recommendations are advisory only. Their use by anyone is entirely voluntary. Reliance thereon for any purpose by anyone is at the sole risk of that person or the user of the product, and the ANSI Committee and the IFI are not responsible for any loss, claim or damage arising therefrom. In formulating and approving recommendations, the ANSI Committee and the IFI have not investigated and will not investigate patents which may apply to the subject matter. Prospective users of the recommendations are responsible for advising themselves of and protecting themselves against any patent infringement liability which may arise out of such use.

American National Standards Institute, Inc. - 1430 Broadway, New York, N. Y. 10018 U.S.A.

APPENDIX A – SI UNITS AND CONVERSIONS FOR QUANTITIES COMMONLY D IN DEFINING CHARACTERISTICS AND PROPERTIES OF MECHANICAL FASTENERS	ίLΥ	STENERS
APPENDIX A – SI UNITS AND CONVERSIONS FOR QUANTITIE IN DEFINING CHARACTERISTICS AND PROPERTIES OF MECH.	SCOMMO	ANICAL FA
APPENDIX A – SI UNITS AND CONVERSIONS FOR (DUANTITIE	OF MECH
APPENDIX A – SI UNITS AND CONVERS IN DEFINING CHARACTERISTICS AND PI	IONS FOR	ROPERTIES
APPENDIX A – SI UNITS AND IN DEFINING CHARACTERIST	CONVERS	ICS AND PI
APPENDIX A - SI U	NITS AND	ACTERIST
APPENDI IN DEFIN	X A - SI U	ING CHAR
	APPENDI	IN DEFIN

density cubic metre kilogram mass gram megagram density kilogram per cubic metre temperature dogree Celsius area square metre square milimetre					
Hure	SYMBOL	CONVERSIONS FROM CUSTOMARY UNITS	OM CUSTO	(1) OMARY UNITS	(2) APPROXIMATE EQUIVALENCIES BETWEEN
iture		TO CONVERT FROM	To	MULITPLY BY	SI AND U.S. CUSTOMARY UNITS
Iture	m mm 7F	inch foot foot	mm mm	2.540000° E+01 3.048000° E+02 3.048000° E-01	25 mm = 1 in. 300 mm = 1 ft 25 µm = .001 in.
ıture	kg g Mg	ounce pound ton (2000 lb) ton (2000 lb)	9 kg kg Mg	2.834952 E+01 4.535924 E-01 9.071847 E+02 9.071847 E-01	2.8 g = 1 oz 1 kg = 35 oz 1 kg = 2.2 lus 1 Mg = 2200 lbs
oerature .	kg/m ³	pounds per cubic foot	kg/m3	1.601846 E+01	16 kg/m³ = 1 lb /ft 3
	2 ₀ sr	degrees Fahrenheit	၁့	°C = 5/9 (°F-32)*	0°C = 32°F (exact) 20°C = 68°F (exact) 100°C = 212°F (exact) 480°C = 900°F
	netre mm ²	square inch square foot	mm ² m ²	6.451600" E+02 9.290304" E-02	645 mm ² = 1 in. ² 1 m ² = 11 ft ²
cubic metre cubic millimetre	etre mm ³	cubic inch cubic foot cubic yard	_m 3 _m 3	1.638706 E+04 2.831685 E-02 7.645549 E-01	16400 mm ³ = 1 in. ³ 1 m ³ = 35 ft ³ 1 m ³ = 1.3 yd ³
newton kilonewton force meganewton	M K N	ounce-force pound-force pound-force kip (1000 lbf)	N N N N N N N N N N N N N N N N N N N	2,780139 E-01 4,448222 E+00 4,448222 E+00 4,448222 E+00 4,448222 E-03	1 N = 3.6 oz 4.4 N = 1 lbf 1 kN = 225 lbf 1MN = 225 kips
stress megapascal	MPa	pound-force/inch ² (psi) kips/inch ² (ksi)	MPa MPa	6.894757 E-03 6.894757 E+00	1 MPa = 145 psi 7 MPa = 1000 psi 7 MPa = 1 ksi
torque newton-metre	E.Z	inch ounce inch pound foot pound	E E E	7.061552 E-03 1.129848 E-01 1.355818 E+00	1 N·m = 140 in, oz 1 N·m = 9 in, 1b 1.4 N·m = 1 ft lb 1 N·m = .75 ft lb

Cunversion factors that are exact are followed by an asterisk. Other conversion factors have been rounded in accordance with accepted rules, and conversions will be accurate

Curversion factors are presented for ready adaption to computer read-out and electronic data transmission. The factors are written as a number greater than one and less than ten with six decimal places. This number is followed by the letter E (for exponent), a plus or minus symbol, and two digits which indicate the power of 10 by which the number must be multiplied to obtain the correct conversion. For example: 6.894757 E-03 is 0.006894757. Similarly, 1.638706 E+04 is 16387.06. only to the sixth decimal place

The relationships given in this column are not exact, except for those noted. All others are rounded equivalencies and are presented strictly to give a quick appreciation of the maynitude of SI quantities in comparison with those expressed in U.S. customary units. None of these relationships should be used when making a conversion to SI units.

Published and Issued by Industrial Fasteners Institute 1505 East Ohio Bldg. 1717 East 9th St. Cleveland, Ohio 44114 USA

RULES FOR THE USE OF SI UNITS APPLICABLE TO MECHANICAL FASTENERS IN THE OPTIMUM METRIC FASTENER SYSTEM

OMFS-1

Page 4 of 4

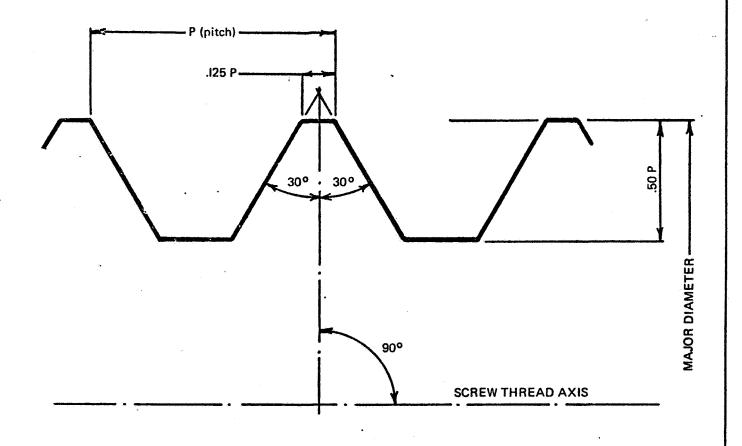
Issued: February, 1972 Revised:

All recommendations are advisory only. Their use by anyone is entirely voluntary, Reliance thereon for any purpose by anyone is at the sole risk of that person or the user of the product, and the ANSI Committee and the IFI are not responsible for any loss, claim or damage arising therefrom. In formulating and approving recommendations, the ANSI Committee and the IFI have not investigated and will not investigate patents which may apply to the subject matter. Prospective users—of the recommendations are responsible for advising themselves of and protecting themselves against any patent infringement liability which may arise out of such use.

American National Standards Institute, Inc. - 1430 Broadway, New York, N. Y. 10018 U.S.A.

1.0 SCOPE

- 1.1 This Recommendation defines the basic thread form for optimum metric fastener screw threads.
- 1.2 DEFINITION. The basic thread form of a thread standard is the cyclical outline, in an axial plane, of the permanently established boundary between the provinces of the external and internal threads. This boundary governs the conditions of assembleability and must be permanently respected in order to preserve the integrity of the standard. For normal fastening screw threads the basic thread form defines the theoretical maximum space which the internal thread is permitted to occupy within the basic major diameter of the externally threaded member.



674

Published and Issued by Industrial Fasteners Institute 1505 East Ohio Bldg. 1717 East 9th St. Cleveland. Ohio 44114 USA

BASIC THREAD FORM FOR OPTIMUM METRIC FASTENER SCREW THREADS OMFS-2

Page 1 of 1

Issued: MARCH 1972 Revised:

All recommendations are advisory only. Their use by anyone is entirely voluntary, Reliance thereon for any purpose by anyone is at the sole risk of that person or the user of the product, and the ANSI Committee and the IFI are not responsible for any loss, claim or damage arising therefrom. In formulating and approving recommendations, the ANSI Committee and the IFI have not investigated and will not investigate patents which may apply to the subject matter. Prospective users of the recommendations are responsible for advising themselves of and protecting themselves against any patent infringement liability which may arise out of such use.

* N74 30954

TITANIUM FASTENERS

JOSEPH L. PHILLIPS
MANUFACTURING RESEARCH & DEVELOPMENT
COMMERCIAL AIRPLANE GROUP
THE BOEING COMPANY

Titanium fasteners were first introduced to a Boeing product in the B-52 approximately twelve years ago. Today, titanium fasteners are used in large quantities throughout the aircraft industry. Most of this usage is in aluminum structure; where titanium structure exists, titanium fasteners are logically used as well.

What are the factors involved in selecting titanium as a fastener material and what are some of the special considerations involved? Answers to these questions plus some discussion of alloys, special fasteners and installation methods constitutes the content of this paper.

BASIC SELECTION CRITERIA

Mechanical fastening of aluminum structure most commonly employs aluminum rivets. To accommodate increases in shear loads, the rivet diameter is increased. This reaches a practical limit at 3/8 inch diameter with most existing driving methods; in addition, there is a trade off on maximum diameter versus weight of structure to accommodate it. At this point, a design selection of a smaller diameter, higher shear strength fastener is made. In the past, this was usually a cadmium plated steel bolt type of fastener of 180 ksi UTS.

This 180 ksi UTS steel has a shear allowable of 95 ksi; since the most commonly used titanium alloy (Ti-6A1-4V) also has a shear allowable of 95 ksi, a direct substitution is possible on the basis of strength alone. However, the cost of such a titanium fastener will run 2 to 2-1/2 times that of the steel fastener. If cost of the product alone is paramount, the choice is obvious. If weight is critical, then a trade-off may be justified. In a large airplane such as the Boeing 747, the use of titanium instead of steel for most of the non-aluminum fasteners saves approximately 4000 pounds of weight. The price for this saving is approximately \$30 per pound. The criteria for acceptability of this added cost will vary in accordance with the importance attached to weight reduction in the product. Generally, a figure of \$100 a pound is often used when weight reduction is required to meet guarantees in commercial aircraft; even higher figures may be justified to provide mission capability in military aircraft.

Since the direct substitution designated is for a 180 ksi UTS, 95 ksi shear alloy steel bolt, the question often arises about the justification for the use of titanium if higher strength steels are used - such as 260 ksi UTS, 156 ksi shear.

The titanium will still provide some weight saving in this case since the density of steel is approximately twice that of titanium, but the cost per pound saved increases to \$190 per pound. However, the 260 ksi steels have led to some difficulties with fastener reliability; in addition, to affect the weight reduction indicated produces a fastener referred to by some stress engineers as a spaghetti fastener - one with a poor L/D ratio. Such fasteners may not prove to be critical in static bearing allowables, but they will often degrade the design fatigue rating of a structure.

Where space becomes critical or high clamp forces are required, then a steel fastener of 220 ksi UTS, 125 shear may prove to be a better selection than titanium. This relates to both the fastener diameter and the head and nut portions of the fastener. The steel will allow a higher strength in a smaller diameter; providing high clamp up with the titanium will eat up the weight savings in thicker heads longer threads and thicker nuts to compensate for the lower strength.

Besides weight savings, titanium fasteners may also be selected for their corrosion resistance or their strength at elevated temperatures. The corrosion resistance referred to is for the titanium fastener itself - when fabricated from the proper alloy. Galvanic considerations when used with dissimilar metals is another matter that will be covered later. For instance, titanium fasteners in titanium fittings attached to a fiberglass, ocean racing sailboat would provide both weight reduction and excellent corrosion resistance.

Elevated temperature usage would be primarily related to usage in titanium structure - where the titanium structure was required to meet temperatures too high for aluminum. Such usage should generally be limited to 600°F; above this temperature, susceptibility to salt corrosion and degradation of mechanical properties makes other materials such as A-286 and Inconel 718 more attractive.

ALLOY SELECTION

The predominate alloy in use for titanium fasteners is Ti-6A1-4V, the "workhorse" titanium alloy. This is based on several reasons:

1. Until recently, most high strength titanium fasteners were bolt type fasteners that did not require deformation in installation;

- 2. The 6Al-4V alloy is one that users have the most experience with in general (introduced in 1954) and the most knowledge of with regard to thermal performance;
- 3. Its long term existence and extensive general usage has led to a consistency of mill product not always obtainable with other alloys;
- 4. There are very few titanium alloys with strengths better than 6A1-4V.

Besides strength, density, corrosion properties and thermal properties, the primary considerations in alloy selection are intended usage as either a bolt or rivet type of fastener. Generally, the higher strength alloys have been used as bolts; the commercially pure alloys and, recently, the beta alloys as rivets. Some specific alloys that have proven to be most successful are listed below:

- 1. <u>Ti-6Al-4V</u> as stated before, this is the workhorse alloy. Its density is 0.160 lbs/in³ and its shear strength is 95 ksi. It is readily available, its properties can be relied on, and it has good strength retention at temperature. Ti-6Al-4V can be used as a conventional rivet in titanium structure when heat treated to 90 ksi if the edges of the hole in the structure are chamfered and the rivet is upset by machine squeezing. It cannot be reliably upset by impact driving without cracking unless its shear strength is reduced to 82 ksi.
- 2. $\underline{\text{Ti-6Al-6V-2Sn-}}$ this alloy appears attractive as the best current substitute for $\overline{\text{Ti-6Al-4V}}$. It is slightly heavier (density = 0.164 lbs/in³), but it has a better shear strength (105 ksi). It is also a better choice for use at elevated temperatures since it retains its strength better than $\overline{\text{Ti-6Al-4V}}$.
- 3. <u>Ti-11-1/2Mo-6Zr-4-1/2Sn</u> this is the Beta III alloy. It was the first titanium alloy that proved reasonable to drive by impact means without cracking difficulties or a need to chamfer corners and still have a reasonably high strength (90 ksi shear). It is, however, somewhat heavier (.183 lb/in³) and could represent a significant weight difference in a large, all titanium aircraft such as the SST. All of the beta alloys also display some thermal stability problems and should not be used above 500°F.

- 4. <u>Ti-8Mo-8V-2Fe-3Al</u> this is another beta alloy with similar formability characteristics to Beta III. It is also somewhat lighter (.172 lbs/in³) and may prove to be lower in procurement price since it does not have the melt control problem experienced with the Beta III alloy.
- 5. Commercially Used Alloys the CP40 alloy is the most commonly used alloy where a lower strength titanium alloy rivet (35 ksi shear) will suffice. The CP55 alloy (50 ksi shear) can also be driven by impact means, but with more difficulty. The CP70 alloy is difficult to drive. All of the CP alloys also lose their strength rapidly at elevated temperature.
- 6. M172 this is a new alloy of 55% Columbium and 45% titanium with a shear strength of 50 ksi. It has proven to be an excellent substitute for the CP40 alloy since it can be driven as easily as an aluminum rivet and produces less distortion in thin titanium sheet structure. Another potential use in a bimetal fastener will be discussed later.

Some other alloys that have been considered, but have not been acceptable or worthwhile are:

- 1. <u>Ti-8A1-1Mo-1V</u> this alloy is stronger than Ti-6A1-4V and was strongly considered for both structure and fasteners in the SST until it was found to have serious stress corrosion problems under certain conditions.
- 2. <u>Ti-1Al-8V-5Fe</u> this is also a higher strength alloy than the Ti-6Al-4V, but has proven to be very brittle in installation and subject to stress embrittlement in service. The first has required use of 60° heads to prevent failures when installing bolts in interference fits; the latter has resulted in a high percentage of head failures in service.
- 3. <u>Ti-7Al-12Zr</u> looks as good as Ti-6Al-4V, but offers no significant advantages to justify its application.
- 4. <u>Ti-13V-11Cr-3A1</u> a difficult to machine, high strength titanium alloy that can be squeeze driven but exhibits brittleness after an elevated temperature soak.

5. <u>Ti-3Al-2-1/2V</u> - an 80 ksi shear alloy that appears to have good characteristics for a rivet on the basis of its mechanical properties and has been used in a crimp type of nut (Huckrimp); however, it has not proven usable in test driving as a rivet.

FABRICATION

The fabrication of titanium fasteners could achieve some importance in their comparative costs, but, generally, the techniques used are relatively universal for all alloys. Ti-6Al-4V titanium fasteners are "warm" headed whereby the end of the wire slug is heated to approximately 900°F with an induction coil immediately prior to heading. Some manufactures are cold heading the Beta III alloy. Including heading, a typical sequence of operations to produce a threaded, titanium fastener such as the Boeing PT bolt follows:

- 1. Metallurgical check of raw material for heat treat response
- 2. Warm head
- 3. Inspect for dimensions and laminations
- 4. Heat treat
- 5. Inspect mechanical properties
- 6. Shave flash from head
- 7. Profile grind shank and head
- 8. Roll head to shank fillet
- 9. Roll threads
- 10. Inspect for laminations
- 11. Roll entry radius
- 12. Inspect for dimensions
- 13. Phosphate flouride coat
- 14. Lubricate and package

Since the shanks and head on precision fasteners (0.0005 total tolerance) are ground and titanium is considered to be notch sensitive, the fillet rolling operation has been considered absolutely essential for fatigue performance. It should be noted that the grinding operation contributes significantly to the cost of a titanium fastener; if the shank tolerance can be increased to approximately 0.015 inch, the grinding operation can probably be eliminated and the fastener cost reduced.

Heat treatment is of some importance with regard to prevention of hydrogen embrittlement. It also presents some difficulties with regard to preventing distortion in fasteners such as lockbolts that have a large L/D ratio with the break off pintail added to the regular fastener length. Special precautions have proven necessary with the bimetal fastener to prevent hydrides at the bimetal interface. In this case, the parts per million of hydrogen in the two components are held well below normal requirements and are balanced to provide equilibrium at the interface (to prevent migration). These fasteners are heat treated in a "boat" in a vacuum furnace. When they are to be quenched, the boat is withdrawn into an inert atmosphere chamber. The boat is then inverted to dump the fasteners within a few seconds through the inert atmosphere directly into a rotating collecting basket in the water quench tank.

SPECIAL CONSIDERATIONS

Even though most titanium alloys are very resistant to corrosion, they can form galvanic couples when used with other metals. Such galvanic couples can lead to undesirable galvanic corrosion. The galvanic couple is of a relatively high order of magnitude with aluminum although the surface oxides tend to diminish its effects; nevertheless, it is sufficient to ultimately lead to problems. Thus, titanium fasteners used in aluminum structure must take this factor into account. Some of the methods utilized or considered to handle this problem are discussed below:

Wet Sealant or Primer

This method involves painting the hole or fastener with chromated polysulfide sealant or a chromated epoxy primer and installing the fastener while the sealant or primer is still wet. Some companies that use aluminum nuts on bare titanium fasteners coat the entire fastener; others that use cadmium plated steel nuts coat only the most critical exposed end grains in the countersink. At best, this is a costly, messy approach albeit one that appears to work.

Dry Sealant or Primer

In this approach, a controlled thickness of sealant or primer is precoated on the underside of the fastener head and cured. This operation is performed by the fastener manufacturer. The concept was pioneered by Boeing and is currently in use. Only the countersink zone is treated since a coating on the entire fastener would



create installation difficulty, would create electrical grounding problems and is not necessary since the material acts like a gasket to prevent the intrusion of electrolytic fluids to the rest of the fastener/structure interface. In addition, the dry coating assures the existence of more corrosion inhibiting chromates in the coated interface area since less of the material extrudes from the interface than occurs with wet materials. This method avoids the installation/housekeeping problems and costs associated with the wet methods.

<u>Cadmium Plating</u>

Cadmium plating has been used widely for years on steel fasteners as a sacrificial coating to prevent galvanic corrosion damage to aluminum structure. It has also been used on titanium fasteners for the same purpose. Much attention has been focused on the use of cadmium for this purpose as a result of some studies that indicate that cadmium causes cracking of titanium. Actually, this is a surface microcracking phenomena that requires high tensile stress, high bearing pressure (to cause intimate contact) and elevated temperature with increased incidence as the temperature increases. At ambient temperatures microcracking can only be produced in the laboratory at pressures exceeding the yield point of the titanium. It should be noted that the alloy steels used for cadmium plated fasteners for many years are even more susceptible to this microcracking than titanium under equivalent conditions. Many years of service with cadmium plated steel fasteners and several years of service with cadmium plated titanium fasteners used at ambient temperatures has disclosed no problems. Nevertheless, we believe that a cautious approach should be exercised and cadmium should not be used on any titanium fasteners that are exposed to temperatures above 150°F.

Aluminum Plating or Coating

From a viewpoint of galvanic corrosion in aluminum structure, aluminum plating has appeared to be an attractive alternative for a number of years. In fact, a field test conducted in an Air Force-Lockheed study in 1965 to 1967 showed aluminum plating to be superior in corrosion protection. Aluminum plating has not come into common usage for this purpose since then because aluminum cannot be plated with more conventional electroplating methods. The more exotic methods required presented high costs and volume limitations. In the interim, other methods that use organic or inorganic binders to paint on aluminum followed by a fusion or bake-out operation have been developed.

The use of aluminum is attractive to the aircraft industry for other reasons besides structural corrosion protection. These are:



- 1. <u>Color Matching</u> bare titanium is dark in color and presents a cosmetic appearance problem when used in unpainted, exterior aircraft skins of aluminum.
- Paint Adhesion bare titanium does not have good paint adhesion. Abrading will provide adhesion, but painting must follow abrading immediately. This is impractical. The best method of providing paint adhesion on titanium is a phosphate flouride conversion coating. Unfortunately, this is black in color and color matching is difficult in fuselage areas where both painted and unpainted zones exist and painted to unpainted belt lines vary from customer to customer.
- 3. <u>Compatibility with Aluminum Nuts</u> coating all over with aluminum avoids any necessity to provide auxiliary protection for aluminum nuts to guard against galvanic corrosion. Actually, this may not be a significant problem since the anodize coating on the nut alone may prevent any difficulty. Testing relative to this is in progress.

Even though successful, lower cost plating operations are now becoming available, there is a further problem that is currently unsolved. A high shear capacity fastener of titanium will normally be used in a slight interference fit to assure equal load transfer on all fasteners or even in an interference fit up to 0.006 inch (for a 1/4 inch diameter fastener) for fatigue applications. The aluminum coatings, as deposited, are too soft and tend to pile up on fastener installation causing either difficulty with fastener seating or random, premature fatigue failures. Use of further treatments such as hard anodizing add too much cost and become unattractive in that respect.

Phosphate Flouride

There is some evidence that a phosphate flouride conversion coating alone provides galvanic corrosion protection equivalent to the other methods mentioned. Where usage is definitely in a painted area and especially if there is an interference fit, the phosphate flouride coating is especially attractive since it provides good paint adhesion, provides a good base for holding insertion lubricants and will not permit pile-up problems on insertion.

Titanium Anodize

The proprietary titanium anodize process, Tiodize, is also of interest since it is non-conductive and integral with the surface. Color matching is a problem with the Tiodize conversion alone. Installation and corrosion tests of Tiodized fasteners with a thin flash coating of vapor deposited aluminum for cosmetic purposes are now in progress.

Lubrication

Titanium fasteners which are used in aluminum or titanium structures usually must be lubricated for nut torquing or installation in interference fits. Rivet type fasteners initially installed in clearance holes do not require lubricant. The most satisfactory lubricant for the fastener itself, when used in aluminum structure, is cetyl alcohol. This is a long chain alcohol that can be put on by dipping fasteners in a solution of cetyl alcohol and solvent or by barrel tumbling the fasteners in powdered cetyl alcohol. Use of this lubricant allows practical installation of up to 3/8 inch diameter fasteners using conventional rivet guns and with interference fits up to 0.006 inch. Any cetyl alcohol residue is easily removable with a water rinse or solvent wipe to prevent subsequent problems with paint or sealant adhesion.

When titanium fasteners are to be installed in titanium structure with interference fits or titanium nuts are to be used on titanium fasteners, the fastener or nut should be coated with a dry lubricant. Any of a number of these are used successfully by various manufacturers; tests at Boeing indicated that Lubeco 2123 produced the lowest installation and removal forces (after exposure to elevated temperature) and Esnalube 380 produced the lowest friction in nut torquing of those tested.

FASTENER SELECTION

Fastener selection should always be based on achieving the lowest installed cost while providing the required performance. In terms of lowest cost, a rivet type of fastener would normally be the best selection. There are, however, limitations. These are:

1. Structure Material - if the structure is aluminum or similar strength material, a conventional titanium rivet cannot be used without distortion problems and excessive expansion of the structure adjacent to the driven button. Special titanium rivets have been developed for use in aluminum. These will be discussed in the following section.

2. <u>Fastener Size</u> - the higher strength Beta III rivets can be practically driven with manual impact type rivet guns only up to 3/16 inch diameter. The lower strength CP40 rivets can be practically driven manually up to 1/4 inch diameter and the M172 alloy (55% Columbian) up to 3/8 inch diameter.

With rivet squeezing equipment, the force capabilities designate the limits. The squeeze requirements are:

•			,	Regular Upset (1bs)	Oversqueeze for Fatigue (lbs)
Beta III	· 😛	3/16		11,000	18,000
		1/4	-	20,000	32,000
		3/8	-	45,000	72,000
CP40	_	3/16	-	5,500	· · · · · · · · · · · · · · · · · · ·
		1/4	-	12,000	
		3/8	-	21,000	-
M172	-	3/16	_	3,000	
		1/4	-	6,500	
		3/8	<u>.</u>	12,000	

It should be noted here that Boeing has developed an electromagnetic riveting system that utilizes two, precisely synchronized, semi-portable guns to drive a rivet. With this equipment, a rivet is upset in 1/2000 of a second. Initially, this equipment was developed to drive aluminum slug rivets up to 3/8 inch diameter to a precision, repeatable interference profile. It has been demonstrated that this equipment can also be used to reliably upset pre-manufactured head Beta III rivets. Sizing up this equipment to handle larger forces and diameters is relatively easy in comparison to large, stationary squeeze machines. A manufactured head rivet is specified because it is not practical to use slug rivets of titanium. Flush shaving of an installed slug is excessively difficult and impractical.

3. Access - if open access does not exist, the electromagnetic equipment cannot be practically utilized; panel or part size will also limit practical application of portable or stationary squeeze equipment.

4. <u>Clamp-Up</u> - if a high clamp-up is required for a tension application or a high load transfer shear application, a titanium rivet type fastener cannot provide this degree of clamp-up. In fact, a squeezed titanium rivet, with the springback that occurs after upset, will provide very little preload in the joint.

In aircraft construction, non-specialized bolt type applications up to 3/8 inch diameter normally utilize either a Hi-Lok type or lockbolt type of fastener. The lockbolt can be installed quicker by manufacturing personnel and its break-tang pull-up load provides greater assurance of initial component clamp-up. The lockbolt type of fastener does have installation access limitations that the Hi-Lok type fastener does not. Thus, the lockbolt type fastener is usually specified as the preferred steel fastener with Hi-Lok types used in limited access locations. With titanium fasteners, however, the cost of the additional material in the break off tang of a lockbolt makes it more difficult to provide a competitive procurement price. Thus, a singular type of titanium fastener for the application under discussion is usually specified.

SPECIAL FASTENERS OR SYSTEMS

With some exceptions, most special fasteners or systems have been developed to improve the fatigue performance of joints in aluminum structure or to reduce the installed costs for such fatigue rated systems. Even though many of these fasteners were developed specifically in titanium this does not preclude the use of other alloys for the specific fastener concepts. However, in the aircraft industry, the continuing demand for improved performance and the associated weight reductions required will probably result in a continued and increasing use of titanium fasteners. Of the many special concepts that have evolved, only those we consider most significant or of most probable application will be discussed.

Taperlok- this fastener has a tapered shank and is inserted into an interference fit tapered hole. The prestressing caused by the interference improves fatigue performance. Until recently, it has been the primary non-aluminum fastener available for fatigue improvement and is normally considered the baseline for fatigue comparison of other systems. It should be noted that the interference that produces the best fatigue performance with the Taperlok system is not necessarily the best value for apparent interference with other systems. This is especially so when rivet type systems of titanium are used.

Another factor relative to flush head, titanium Taperloks is of importance. When used in aluminum structure the lack of any prestressing from shank interference in the countersink zone can be offset with a steel Taperlok via high torque preload. Examination of fatigue data indicates that a conventional 100° head titanium Taperlok is not capable of equivalent fatigue performance. This is probably the result of lessened pressure in the countersink extremities from the lower modulus of the titanium as evidenced by fatigue failure origins of all titanium Taperlok installations at the countersink/skin juncture. To offset this problem (if necessary), the titanium Taperlok would require a modified head design such as the Boeing 70° head driven into a mismatching 82° countersink or the interference fit 82°/10° Boeing wedge head design.

Boeing PT Bolt - this is a straight shank titanium fastener that was developed as a lower cost alternative to the tapered shank fastener system for use in aluminum structure. Its use is practically limited to 3/8 inch diameter, whereas the tapered shank system is not so limited. The degree of interference used with this fastener to achieve fatigue performance (0.003 to 0.006 inch) dictates that it must be bare (properly lubricated) or have a coating that will not strip on installation. As currently used, this is a phosphate flouride coating. The entry on this fastener is radiused to allow interference installation without hole damage; to assure this, it was found that a rolled finish was necessary on this radius. Another feature is a 70° included angle head with a generous head to shank fillet and a slight crown on top. The 70° head is manually impact driven into a mismatching 82° countersink. This deforms the countersink and provides the necessary prestressing in this zone as well. The crown serves to allow this driving without danger of contacting the surface of the structure. For added galvanic corrosion protection, the countersink is primed with a chromated epoxy primer and allowed to dry before fastener installation. The drying is necessary to retain the primer with the degree of "wiping" involved in fastener installation.

It is interesting to note that the concern shown over the years about the notch sensitivity of titanium and the chamfering provided in holes for the head to shank fillet may not have been necessary. That is, the titanium PT bolt has shown (at least with the 70° head design) to be capable of handling a significant interference in this area.

687<

Rivbolt - this is currently a Beta III titanium rivet type of fastener. It was originally developed for use in titanium structure, but its initial usage has been in aluminum structure as a lower cost alternative to the tapered shank fastener system. The rivet is installed with a small, square cross section collar adjacent to the structure on the driven button side. A pre-manufactured head with a slight crown is on the other end. During installation, the collar is restrained from excessive expansion by the installation tooling. If precise tooling and precise upset pressures are used, this fastener can be used for fatigue critical applications. The crown on the head serves to produce expansion in the shank adjacent to the head when driven with a flat tool. The tooling on the other end must prevent excessive expansion of the collar on one hand, but it must allow some on the other. If no expansion of the collar is allowed, the shank will treat the collar like an extrusion die and there will be no expansion immediately adjacent to the collar within the hole.

It is interesting to note that this fastener was originally developed with the Ti-6Al-4V alloy. This seemed to result in some variation in expansion results because the ductility of the Ti-6Al-4V varies in its allowed heat treat range. In addition, the Ti-6Al-4V required use of a directional collar that had a radius or chamfer on one side of its bore. This radius was required to prevent cracking of the button on upset and to enhance the flow of metal. A changeover to the Beta III alloy allowed use of a non-directional, square cross section, symmetrical collar.

This fastener can also be used to some advantage in titanium structure to prevent distortion via a more uniform expansion profile.

The apparent interference produced with this titanium fastener in aluminum structure is also of interest. Apparent interference (with regard to probable fatigue performance) is usually defined by calculating the difference between the original hole diameter and the final rivet diameter. With an aluminum rivet, the final result is a rivet with some remaining interference in a partially yielded hole. With the greater comparative springback of the titanium Rivbolt, the end result is a net fit fastener in a yielded hole. Such yielding is similar to that achieved with coldworking to produce a yielded compressive zone around the hole. In the higher yield strength 7000 series aluminum alloys and in titanium structure, this could prove to be especially beneficial.

Unfortunately, the Rivbolt requires relatively high installation forces to produce the required results. This currently limits the fastener diameters or the reach that can be used for this fastener. The electromagnetic riveting system appears to offer potential for eliminating this current restriction.

3

Wedgehead Lockbolt

This is a fastener developed at Boeing as a second generation alternative to the tapered shank fastener system and as a lower cost, manual installation alternative to the Boeing PT bolt. This is a titanium or steel lockbolt with an 82°/10° double angle head. The fastener is installed into a straight, interference fit hole with an 82°/8° interference fit countersink. The latter provides the necessary interference for fatigue performance in the countersink with a definite depth control not requiring skill to install. The fastener is held in place with an aluminum or titanium self-sealing, swaged on collar. The seal is provided with a small, integral, circular fin on the collar. The advantages for this fastener are use of a low cost collar versus an expensive seal nut, fluid-tightness on both ends of the fastener and easier installation.

Bimetal Rivet

This is a unique, new rivet type fastener of titanium that appears to have excellent potential for application. The fastener, as originally configured, has a Ti-6Al-4V titanium shank with a protruding or 100° flush head and a friction welded end of CP titanium. This provides a high strength shank with an easily driven end to hold the fastener in place. The friction welding process is one that lends itself to practical production of the bimetal joint and one that extrudes all impurities from the joint as it is produced. The resulting joint has no cast structure and has proven excellent in static and fatigue strength tests.

A recent evolution of this concept has been use of the M172 alloy for the welded on end to produce a high strength rivet type fastener that can be upset as easily as an aluminum rivet.

Since the upsetting of the softer end only serves to hold the fastener in place and does not produce any hole filling expansion of the shank, this fastener must be driven into an interference fit hole when the installation requires fatigue improvement. The lack of any threads allows the end of this fastener to be ideally tapered for such

interference installations. Additionally, the lack of any secondary components such as collars or nuts coupled with the lower upset forces makes this fastener ideally suited for installation on existing automatic riveting equipment.

For fatigue critical installations, it is our opinion that a fastener head design such as the wedgehead will have to be incorporated to provide the maximum fatigue performance.

Standard Fasteners with Mandrel/Sleeve Prestressing

Boeing has developed a system of prestressing a fastener hole in aluminum or titanium structure in such a way that fatigue performance can be achieved with standard bolt type titanium fasteners. This process can be used for any diameter although it is especially applicable above 3/8 inch diameter in aluminum structure as an alternative to the tapered shank fastener system not covered by the other alternative systems.

The prestressing is accomplished by pulling a tapered mandrel through a thin wall, split, disposable, pre-lubricated sleeve. The lack of direct contact with the highly reactive aluminum or titanium hole allows a high degree of expansion to be used to produce a large yielded, compressive zone around the hole. The process also allows use of a one-man, one-side operation.

In summary, titanium fasteners offer potential weight savings to the designer at a cost of approximately \$30 per pound of weight saved. Proper and least cost usage must take into consideration type of fastener per application, galvanic couples and installation characteristics of protective coatings, cosmetic appearance, paint adhesion, installation forces and methods available and fatigue performance required. It is hoped that the content of this paper has shed some light on these considerations.

FASTENING ON THE F-14A FOR COST EFFECTIVE FATIGUE RESISTANCE BERNARD H. BEAL GRUMMAN AEROSPACE CORPORATION

N74 30955

FASTENING ON THE F-14A FOR

COST EFFECTIVE FATIGUE RESISTANCE

BERNARD H. BEAL

GRUMMAN AEROSPACE CORPORATION

Introduction

Advancements in the state of the art continually challenge the airframe designer to cost effectively meet the requirements that arise with each new aircraft and its ever more demanding missions. The Grumman designed F-14A is a classic example of this fact, generated around the severest performance parameters.

To enumerate:

- o The Navy posture for the 1970's requires an air superiority aircraft second to none
- o Interchangeable multi-mission role capability was essential to broad spectrum cost effective carrier operations
- o Greatly increased fatigue life over previous models
- o Severely increased fatigue spectrums
- o Minimum practicable structural maintenance
- o Broad speed range variation from low subsonic to high supersonic

Preliminary design studies dictated a variable geometry wing to meet these design objectives. Experience with the F-lll Aircraft and the early study versions of the Boeing Supersonic Transport, made it clearly apparent that success in such a design would require weight optimization, maximum working stress levels and minimized fatigue concentration factors particularly in the moveable wing.

An extensive development program to guarantee these goals was conceived and activated at Grumman, and resulted in three major decisions.

- o Extensive use of titanium as a structural material was essential
- o Electron beam welding would be most effectively and selectively employed
- o Interference fit fastening techniques were to be the principal mechanical joining means for the structure

Mr. Robert Witt in his paper on Tuesday, discussed Electron Beam Welding accomplishments. This presentation will, therefore, be addressed to the development and use of the interference fit systems as they contribute to cost effectiveness and reliability for the F-14A.

Discussion

For historical perspective, designing for interference fit fastening in aircraft is not new. In 1961, tapered fasteners in interference fit were installed in limited quantities in the RA-5C Vigilante, to obtain some extended fatigue life. With the passage of years, use of these fasteners increased, but it was not until the present family of aircraft that the interference fit concept was adopted as a major overall approach to structural joining. This discussion will be limited to its application on the F-14A aircraft.

Properly used, interference fit fastening provides an effective means for accomplishing two very desirable airframe design objectives. It makes possible a structure which is both optimized for weight, and yet fatigue resistant beyond normal life expectancy. In the past, this was a contradiction, since increasing fatigue resistance usually meant adding mass to the structure to reduce the operating stresses.

But the secret of interference fit fasteners is their unique ability to reduce the stress concentrations inherent in and around fastener holes by the generation of residual circumferential tensile stresses at the edge of the hole and radial compressive stresses in the wall of the hole.

This stress concentration factor due to the fastener hole is the major contributing element in establishing the required thickness of a mechanically fastened structural joint. It therefore follows that the thickness can be reduced as the concentrations are minimized. The resulting weight reduction thus produced by interference fit fastening becomes obvious.

Today, many different fastening systems can produce variations of this end product with some degree of success. However, this paper offers no comparisons other than those affecting the selection of the F-14A fastening systems. Furthermore, theoretical analysis and critique of these systems is not included. Grumman has, from design to implementation, resolved the problem on the basis of function, performance, cost effectiveness and repairability, with cost effectiveness as the principal target for the development effort. Definite economic limits were the forcing constraints on any fastening system chosen.

With titanium wing structure to be joined by interference fit fastening, Grumman was in a difficult position. Despite some previous industry use of interference fastening in titanium structure, Grumman was breaking new ground with an entire wing design committed to such a combination, which emphasized the intense concentration required on cost. A mind open to new approaches was essential if a satisfactory

conclusion was to be reached.

This immediately opened the field for screening fastening systems beyond those commercially available at that time. Entirely new approaches had to be devised and considered to assure that the most cost effective end product would be found. All Engineering and Manufacturing disciplines concerned participated in the design, evaluation and ultimate selections.

After considerable research and development, two different interference fit fastening systems resulted for the F-14A to meet the high and low load transfer joint requirements. Although, in both types, the end product is similar, each system performs a specific function within the limits of its own unique application. Because of these differences each system will be presented separately. We will start with the case of medium to high load transfer applications, such as beam to wing cover attachments.

For this, a two piece straight shank interference fit fastening system is used. Initial ground rules required any satisfactory interference fit system to provide all of the mechanical and physical properties available in conventional fasteners, and in addition be capable of installation in titanium structure with thicknesses varying to triple the fastener diameter. Fastener Material galvanically compatible with the titanium structure was mandatory since normally acceptable protective finishes would not survive in this application.

The then generally accepted tapered fastener gave rise to serious concern over its ability to meet all these objectives within the required cost limits. Manufacturing capability required to produce

these sensitive tapered holes on a production basis to Grumman specification requirements was Concern #1. Because titanium is a much less forgiving material than alumimum, tapered holes on the F-14A demanded three coincident qualities for acceptance:

- o Taper
- o Roundness
- o Diameter

With no known proven quality control method available to inspect these requirements economically, no guarantee that the benefits displayed by tapered fasteners in laboratory tests could be substantiated for production. At this point, investigation of straight shank fastening became a mandatory alternative.

Conventional titanium HiLok fasteners from HiShear Corp. of Torrance, Calif., in early functional installation tests when coated with commonly used molybdendum disulfide (MoS₂) dry film lubricant, first indicated a possible successful path to pursue. With minor variations, this fastening system was baselined at the best available starting point for the formidable task ahead. The development of a finishing system to permit installation of titanium pins into titanium structure, without the characteristic material galling during the insertion of the fastener into the hole was clearly Task #1. Task #2 required effective use of standard portable impact tooling on installation for use where squeezing access to both faces is unattainable.

Early test soon established an achievable interference level of .0045 for 1/4 inch diameter pins. By combining the expected hole

tolerance of .0020 with normal ground shank fastener tolerance of .0005, the resultant interference spread for the fastening system was set at .0025. An empirical percentage of diameter concept for determining larger size interference levels was next derived. Figure 1 illustrates the interferences established for such a straight shank fastening system. The minimum interference level of .002 for 3/16 and 1/4 inch fasteners was confirmed by fastener fatigue tests to a minimum level of .0015 with the additional .0005 supplying the probability insurace for reliability in the system. Element fatigue testing of interferences below .0015 produced some inconsistencies making the absolute minimum guarantees essential. Figure 2 presents partial results of F-14A spectrum fatigue testing of this fastening system with both .0015" and .0040" interference levels in unloaded joint configuration. Note that the improvement in fatigue life provided by straight shank interference fit fastening techniques is clearly evident.

Completion of this early testing led into efforts to improve the dry film lubrication. With the wing structural materials of Ti6AL4V and Ti6AL6V 2 Sn alloys, the initial fastener materials investigated were A-286 stainless steel and 6AL 4V titanium for reasons of galvanic compatibility. Very shortly, the A-286 material was discarded for lack of a finishing system capable of meeting all installation parameters. With the full concentration centered on titanium fasteners, numerous lubrication systems were tried and found wanting. It became apparent, however, that the ultimate finish would consist of an anodic coating base for some molybdenum disulfide dry film lubricant.

A finishing system developed and produced by Tiodize Corp. of

Burbank, Calif. successfully permitted reliable nongalling installations for titanium fasteners ranging through 5/16 inch diameter in all anticipated conditions. Proper lubrication of these fasteners is vital for two obvious reasons:

- o Ease and repeatability in the installation of nondamaging fasteners
- o Removal of fasteners if necessary, without hole damage

 Structural repair or modification requiring removal of so called permanent
 fasteners had to be anticipated. The possibility always exists for an
 apparently properly installed fastener to gall the hole if inadequate
 finish is used, making normal removal impossible.

Accordingly, an acceptance requirement has been generated wherein sample test pins from each lubricated production run are installed in maximum interference and then removed from a titanium test plate. Lack of shop problems to date has validated this in-process lubrication control. Figure 3 compares the relative drive forces required to install a straight pin into three different materials. Also of interest is the obvious modulus ratio of 1:1 with use of titanium fasteners and structure, which demands maximum efficiency of the finishing system in the fastener/hole interface.

Interference fit fasteners in diameters as great as three quarters of an inch next appeared as a probable requirement raising new concern over the relationship between the compressive strength of the 6AL 4V titanium already selected as the fastener material, and the obviously high installation forces they would require. Another material was accordingly sought to meet the existing requirements and yet provide the added installation strength necessary to meet all conditions.

Maximum galvanic compatibility along with corrosion resistance became an essential requirement in choice to preclude any stress corrosion potential because of aircraft carrier environmental conditions.

The winner, one of the few candidate alloys was Multiphase 35N which might well have been conceived specifically for the F-14A. It is a quartenary base material (35Ni 35 Co 20 CR 10 Mo) exhibiting extremely high resistance to straight corrosion and unsusceptible to stress corrosion cracking when tested in a 3.5 percent Na Cl solution for 180 days. Strength levels in excess of 260 K.S.I. Ftu are achievable exceeding the F-14 requirement of 132 K.S.I. Fsu (228 K.S.I. Ftu). MP35N offers other advantages as a bolting material, giving further emphasis to its selection. After cold work and aging the material meets the following minimum properties:5

Tensile Strength	260,000 PSI
Yield Strength at .2% offset	230,000 PSI
Elongation in 4 diameters	8%
Reduction in Area	35%

This high yield and ductility is the basis for a fastener with the excellent bending and fatigue strength essential for inboard joints of a fighter type wing.

Standard Pressed Steel Co., of Jenkintown, Pa., the producer of these fasteners, supplied prompt resolution of the lubrication problem with a molybdenum disulfide coating of their own development.

All interference parameters for this two material fastening system, except materials, strengths and finishes were held constant. MP35N is utilized in 3/8 inch dia., through 5/8 inch dia. pins (representing

ten percent of the two system total), with 6AL 4V titanium used in all the smaller diameters.

Figure 4 shows the configuration of this fastener. Although it is commercially known as HiLok/HiTigue, observe that the bead commonly associated with this fastener type has been revised to a transition radius proven more adaptable for titanium use. There is also an enlarged shank, for installation in standard size holes, thus preventing thread damage to the hole during installation.

To fully guarantee minimum interference fit in production with total repeatability and reliability, the fastener shank grinding and the hole production in the structure are rigidly controlled.

Grumman's cost effectiveness for this straight shank fastening system can best be defined at this time in terms of the following comparison relative to other systems:

- o Standard Fastener configuration low unit cost
- o Conventional straight hole (one shot)
- o Standard off the shelf cutting tools
- o Completely simple hole inspection
- Conventional installation equipment(squeezing or impact driving)
- o Reduced installation forces
- o Minimum workforce indoctrination

Moving to the second fastening system, controlled squeeze force riveting, a brief resume of the F-14A wing design is in order. The titanium pivot fitting is electron beam welded to the wing cover. To compliment this configuration, and reduce machining operations, 'Z' and built up 'Y' section stringers are mechanically fastened to the wing

covers. This structural arrangement of the upper and lower wing cover assemblies is illustrated in Figures 5 and 6.

A fastening system selection for the low load transfer joint characteristics of skin/stringer attachments was again based on the most cost effective method achievable. After an in depth analysis of the wing geometry and loading, an upsetable fastener type inserted in a clearance hole appeared feasible if production installation techniques could be developed to produce a reliable, repeatable interference fit system. Only with the proper controls, however, could such an installation be accomplished while having most of the advantages of the conventionally riveted joint, such as a very inexpensive fastener in a drilled .005 tolerance hole.

The initial functional tests clearly showed the need for a rivet material with upset ductility, yet having a modulus sufficient to overcome titanium's elastic resistance and produce the necessary interference fit. Material galvanic compatibility with titanium was again mandatory. Review of the available alloys resulted in selection of fully aged A286 stainless steel. It offers the required mechanical properties, is notably low in strain rate sensitivity, is reasonably priced and has a well known usage history. Possible alternate use of titanium beta alloys was not pursued at the time because of a low confidence level in repeatability of the published properties, and the slight improvement in the strength to weight ratio did not justify the increased cost.

In the finally derived process, the rivet is installed under application of a controlled squeeze force of approximately 500 K.S.I.,

hence giving the system its name. A more commonly known title, however, is the oversqueezed riveting system because of the obviously high installation forces involved. Figure 7 shows the installation of these rivets on Grumman's automated riveting equipment. Repeated tests have shown that, with the allowable geometric condition limits, this force consistently produces a minimum interference fit of .0015 between rivet and hole. Unloaded joint configuration spectrum fatigue test results of this fastening system as shown in Figure 8 compares with open hole testing in a common type specimen. This direct comparison illustrates the fatigue life improvement offered by this concept. Testing of loaded joints, though also conducted, will not be discussed in this paper since any advantages in load transfer have not been incorporated in the F-14A design.

The intended goal, achieved in both of these systems, yields a structure statically rather than fatigue critical, derived through the stress concentration factor reduction at all fastener holes.

Installation of this rivet, as shown in Figure 9 obviously required floor mounted squeezing equipment to guarantee the necessary controls. Though desirable, a portable installation was not realized, however, until the Grumman developed stress wave riveter was introduced. The technical specifics of this remarkable device were the subject of a presentation on Tuesday by Mr. Basil Leftheris, another Grumman colleague. However, at the risk of duplication, discussion of its use in this application is pertinent. Although the apparent benefit from the stress wave riveter is portability, illustrated in Figure 10, resoundingly significant improvement in the end product resulted in two areas.

Against a trapezoidal fit of the installed oversqueezed rivet, (much greater interference fit at the upset tail than at the manufactured head), the stress wave riveter produces a more uniform fit from head to tail, because the speed at which the stress wave travels through the rivet to create interference fit and upset results in a rivet less sensitive to joint thickness. The stress wave riveter surpasses all other forms of upsetting because of their basic limitation in that they form the rivet tail before shank expansion. Therefore, since the energy produced is more efficiently used, the stress wave riveter can and does more consistently produce a greater and more evenly distributed interference fit.

Another fallout of this method is effective coining of the surface of the fastener hole by the inertia forces generated under the high speed stress wave mechanism. The cost effectiveness of this fastening system is best demonstrated by a comparison of riveted and bolted joints:

	Oversqueezed Rivet	Conventional Riveting	Conventional Bolting
Hole Tolerance	•005	.005	.002
Fastener Shank Tolerance	.001 (clearance .002/.008)	.005	.0005
Configuration	One Piece	One Piece	Two Pieces
Installation Method	Squeezing/ Stress Wave	Squeezing/ Bucking	Torque Wrenches

In summation, the benefits derived from interference fit fastening techniques produced under laboratory conditions for aerospace structures have been amply demonstrated many times. Grumman Aerospace, however, as all others, must build vehicles in the real world, not in laboratories.

For this reason, development of the F-14A systems was based on hard rate application in reality, the Production Shop. Only here can proven ultimate cost effectiveness and reliability of such systems be attained.

The high level of success achieved in reaching these much sought after goals has been most rewarding to this time. The few minor difficulties encountered to date in implementation indicate that the correct selections were made. Surely, the valuable, practical experience gained on the F-14A has provided the firm foundation to build the future advances in this state-of-the-art essential to the better, more complex and sophisticated vehicles of tomorrow.

BIBLIOGRAPHY

- 1. Smith, Clarence R., "Preventing Fatigue Failures", <u>Assembly</u>
 Engineering, April 1968.
- 2. Wolfman, A., "Effects of Salt Water Exposure and Relaxation of Installation Stresses of Interference Fasteners in Ti6AL 4V and Ti6AL 6V2Sn Annealed Alloys", August 1969.
- 3. Gill, Frank, "Recent Developments in Structural Airfram Fasteners", Hi Shear Corp., Torrance, Calif.
- 4. Montano, J.W., "A Mechanical Property and Stress Corrosion Evaluation of MP35N Multiphase Alloy", National Aeronautics and Space Administration, Washington, D.C., May 1971.
- 5. Aerospace Material Specification (AMS) 5758, Society of Automotive Engineers, New York, May 1971.
- 6. Wolfman

INTERFERENCE LEVELS US FASTENER DIAMETER

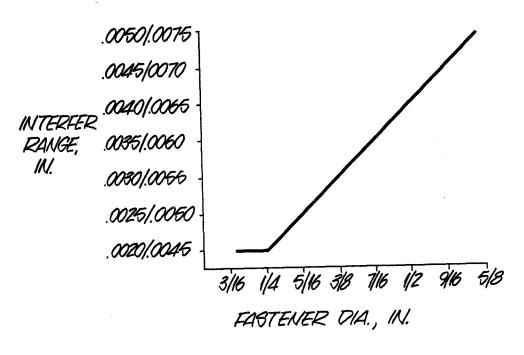


FIGURE 1

TWO PIECE STRAIGHT SHANK INTERFERENCE FIT FASTENER-SPECTRUM FATIGUE

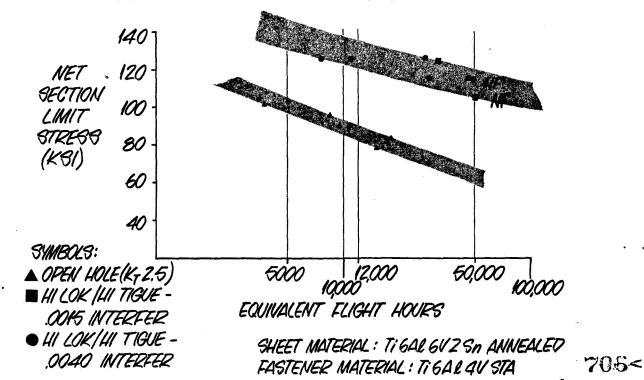


FIGURE 2

TYP ASSY PRESSURES OF 5/16 IN. HI LOK /HI TIGUE PINS IN AL & TE

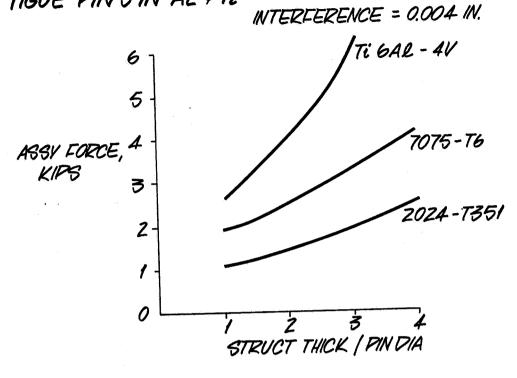
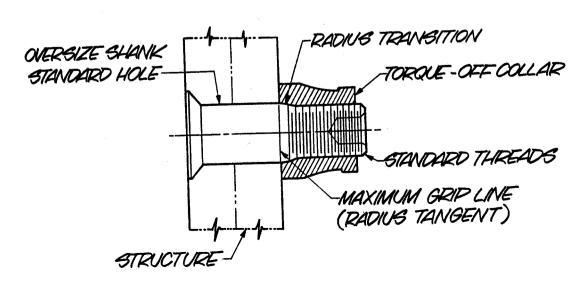


FIGURE 3

INSTALLED STRAIGHT SHANK INTERFERENCE FIT FASTENER



UPPER WING COVER ASSY

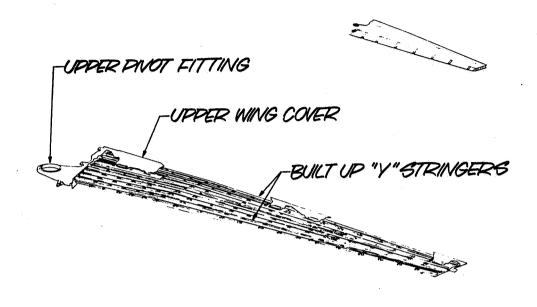
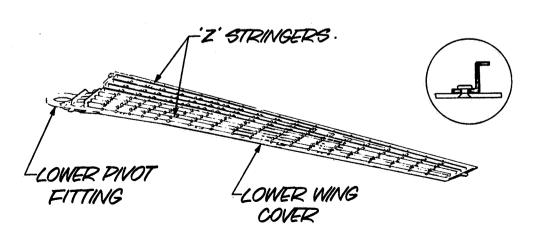


FIGURE 5

LOWER WING COVER ASSY



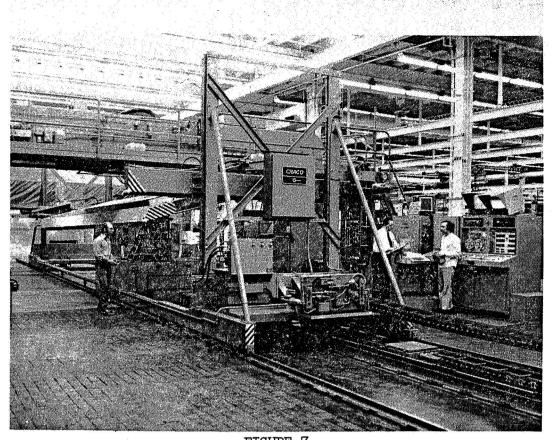
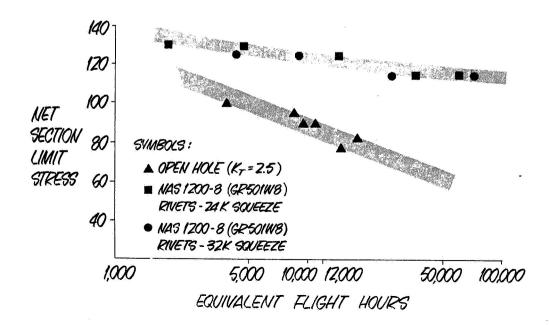


FIGURE 7
CRACO AUTOMATIC RIVETING MACHINE

OVERSQUEEZED RIVETS - SPECTRUM FATIGUE

SHEET MATERIAL: TIGAL GV 2 SN ANNEALED FASTENER MATERIAL: A286 CRES FULLY AGED



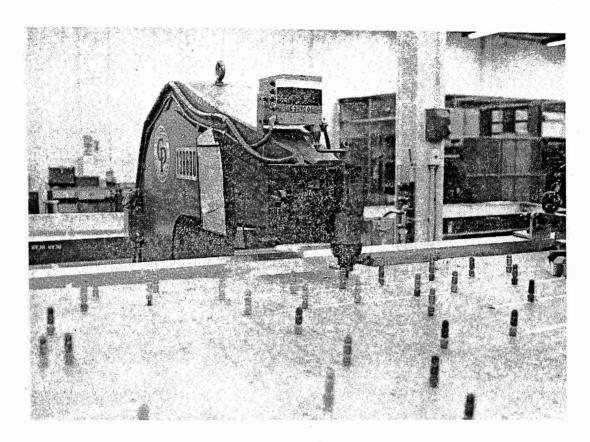


FIGURE 9

OVERSQUEEZED RIVETING ON
CHICAGO PNEUMATIC CP-4 MACHINE

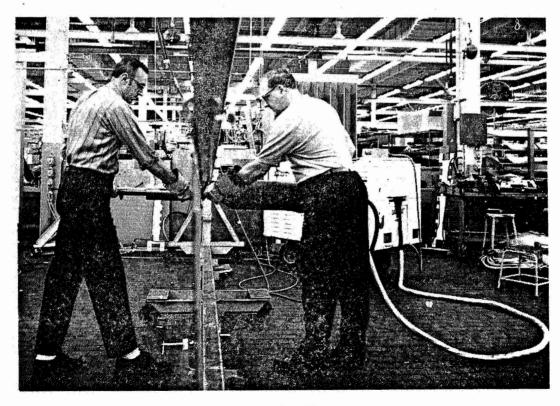


FIGURE 10
STRESS WAVE RIVETING

bу

W. J. Dewalt

174 30950

N74 30956

Presented at the Symposium on Welding, Bonding and Fastening at Williamsburg, Virginia, on May 30 - June 1, 1972

Alcoa Research Laboratories Aluminum Company of America New Kensington, Pennsylvania July 26, 1972

"THE ALCOA RAM FASTENER - A REUSABLE BLIND RIVE"

. ABSTRACT

Results of tensile, shear, fatigue and accelerated weathering tests are presented for the Alcoa Ram Fastener, a reusable, single-unit blind rivet. The effects of variations in hole size, grip length and sheet thickness on strength properties of the fastener were determined. The test results show these fasteners to have strength characteristics suitable for light structural applications. Exposure to accelerated weathering did not impair their performance.

Introduction

type of blind rivet consisting of a nylon plastic jacket and an aluminum alloy locking stem. One outstanding feature of this fastener is that, after being installed, it can be easily removed with simple tools. Another feature, which is unique, is that it can be used over and over again. The fastener, therefore, should be ideal for applications where frequent disassembly and reassembly of a unit are necessary, but where high structural strength is not a requirement.

This paper describes the Alcoa Ram Fastener and recommends installation procedures. It also provides engineering data to assist designers in the consideration and evaluation of this fastener. Results of tensile, shear and fatigue tests of joints are shown. Data are also presented on the effects of accelerated weathering tests on the performance of the fastener.

II. Description of Fastener

Figure 1 shows the two components of the Alcoa Ram Fastener: The aluminum locking stem and the nylon jacket. The stem is made of aluminum alloy 2024-T4, a high-strength alloy commonly used for threaded fasteners. The jacket is made of Dupont Zytel 71G, a 33% glass reinforced nylon. Figure 1 shows the Alcoa Ram Fastener in both the "open" and

"installed" positions. It is supplied to the user with the stem and jacket assembled, in the open position. At this point it is a single-unit blind rivet; the stem and jacket cannot be separated without destroying one or the other. In the open position the fastener is either ready for installation or, after it has been installed, ready for removal from the workpiece.

Figure 1 shows several additional features of the Alcoa Ram Fastener. The contours of the split or expansion end of the jacket, and the bulb machined on the end of the stem, are designed to facilitate insertion into the hole. After the fastener is placed in a hole, it is driven by pushing the stem with either thumb pressure or a hammer. In this position the disc on the head of the stem is seated in a recess molded in the head of the jacket, and the slotted end of the jacket has been expanded to form the blind head. The purpose of the disc on the stem is to remove the fastener from its installed position. The groove molded into the head of the jacket provides access for a plier-like tool (or even a small screwdriver) to grasp the disc and pull the stem until the fastener is in the open position. The fastener can now be removed, intact and ready for reuse, since with a slight time delay the nylon jacket recovers its initial shape.

Current production of the Alcoa Ram Fastener is confined to two diameters, 3/16 and 1/4-in., and, for both sizes, lengths to accommodate grips ranging from 0.100 to

0.600 in., in increments of 0.050-in. As indicated in Fig. 1, it is recommended that a fastener made to accommodate a nominal grip thickness to used in joint thicknesses within ± 0.025 in. of the nominal value. For the tests described herein, fasteners designed for grip thicknesses considered as short (0.150 in.), medium (0.350 in.) and long (0.600 in.) were used.

The suggested or "recommended" hole diameters for the Alcoa Ram Fasteners are: 0.187 to 0.192 in. for the 3/16-in. size and 0.250 to 0.255 in. for the 1/4-in. size. The initial development work and evaluations indicated that best overall performance, from the standpoints of clamping action and strength, was obtained when these hole sizes were used. To show the effect of hole diameter on tensile and shear strength, tests were made with "oversize" holes, nominally 0.010-in. larger than the fastener nominal diameter. Actual diameters of the oversize holes were from 0.197 to 0.202 in. for the 3/16-in. size and 0.260 to 0.265 in. for the 1/4-in. size.

III. Engineering Properties

Figure 2 illustrates some types of applications envisioned for the Alcoa Ram Fastener. Quite often there is a strength requirement attendant to such applications. The tests conducted at the Alcoa Research Laboratories were made to provide basic information that would be helpful to an engineer or designer.

The results of tests to determine the tensile load carrying capacity of 3/16 and 1/4-in. diameter Alcoa Ram Fasteners are summarized in Figs. 3, 4 and 5. At least five tests were made for each test condition plotted in these figures. In all of the tensile tests failure occurred in the nylon jacket, not in the aluminum stem. Two kinds of failures occurred. In some cases the expanded, slotted end of the nylon jacket was sheared off by the test fixture. In other cases the failure was at the juncture of the head and the body of the jacket.

The results plotted in Fig. 3 are for tensile tests made using recommended hole diameters. The average tensile breaking loads for the 3/16 and 1/4-in. diameter Alcoa Ram Fasteners were about 100 lb and 180 lb, respectively. For both diameters the fasteners with the shortest (0.150 in.) grip length gave the lowest tensile breaking loads. Included in the results shown in Fig. 4 are tests of fasteners that were reused fifty times before testing. No difference was observed in the strength of these fasteners and of those used only once.

Figures 4 and 5 compare the tensile strengths of fasteners tested with recommended and oversize holes. For both sizes the use of oversize holes tended to decrease tensile strength. The average loss, however, was much greater for the 3/16-in. size than for the 1/4-in. size, 43 1b or 43 per cent versus only 15 1b or 8 per cent, respectively.

Results of the shear tests made of Alcoa Ram Fasteners using steel fixtures are summarized in Figs. 6, 7, 8 and 9. Not less than five tests were made for each condition shown in these figures. All failures were by shearing of the nylon jacket. When this occurred, the compressive clamping action was released and the joined members spread apart. There were no shear failures of the aluminum stem.

The shear strength results shown in Figs. 6 and 7 were obtained using steel test fixtures prepared with recommended hole diameters. Average single-shear values obtained at the three grip lengths ranged from 185 lb to 370 lb for the 3/16-in. size and from 265 lb to 560 lb for the 1/4-in. size fastener. The wide variance in single-shear strengths for both sizes is the result of having to use different thicknesses of plate for the different fastener grip lengths. Figure 7 shows that the effect was not nearly so drastic in tests where the fastener was in double shear.

The data plotted in Figs. 9 and 10 show that oversize holes also tend to reduce shear strength of Alcoa Ram Fasteners. On the average, the loss from the shear strength values obtained using recommended hole sizes for both fastener diameters was about 10 per cent for the 0.150-in. grip length fasteners and about 20 per cent for the 0.600-in. grip length fasteners.

Fatigue strength data were obtained using single-lap specimens joined with 3/16-in. diameter Alcoa Ram Fasteners. The

specimens were made of 0.080-in. thick aluminum alloy 3003-H14 sheet and employed the recommended hole size. The fasteners were designed to accommodate a nominal 0.150-in. grip thickness. The test setup and joint dimensions are shown in Figs. 10 and 11. Fatigue tests were made of ten specimens, two of which were subjected to 500 hours of continuous salt spray prior to testing. The tests were made in a 5 kip Krouse fatigue testing machine. In these tests, a specimen was considered to have failed, even though still intact, when it could not maintain the initial test load because of wear of the nylon jacket. The results plotted in Fig. 11 show that the specimens loaded to half the static failure load gave fatigue lives on the order of 5 million cycles. This compares favorably with data obtained at Alcoa Research Laboratories for other types of fasteners under similar conditions of test. It should be noted that the exposure to salt spray prior to testing had no adverse effect on fatigue strength.

Both accelerated and long-time corrosion test programs are being employed to determine the effects of "weathering" on the performance of Alcoa Ram Fasteners. For the accelerated tests, two kinds of exposures were used. One was a Weather-O-Meter and the other a Salt Spray Test. For the long-time tests, exposures will be outdoors for several years at two locations:

New Kensington, Pa. (industrial atmosphere) and Point Judith, R. I. (seacoast atmosphere).

The Weather-O-Meter test consists of ten two-hour exposure cycles per 24-hour period. In each cycle the specimens are exposed to ultraviolet light for the two-hour period, with a de-ionized water spray during the last 18 minutes. The test temperature is a constant 145°F. In this test individual fasteners (in both the open and installed positions) and fasteners installed in lap joints of aluminum alloy 3003-H14 sheet were exposed for total periods of 100 and 500 hours. After exposure for up to 500 hours, the individual fasteners were installed and removed 50 times without any indication of failure. Only a slight whitening of the black nylon plastic indicated some mild surface degradation, but this had no adverse effect on performance.

The salt spray test consists of a continuous spray of 5 per cent NaCl solution at 95°F for 500 or 1000 hours. In this test the fasteners were installed in lap joints of either aluminum alloy 3003-H14 or painted steel sheet. Examination of specimens after 500 and 1000 hours exposure revealed only mild corrosive attack on the 2024-T4 locking stems inside the nylon sleeves, which were unaffected. As mentioned previously, 500 hours exposure time had no adverse effect on the fatigue strength of lap joints made with alloy 3003-H14 sheet.

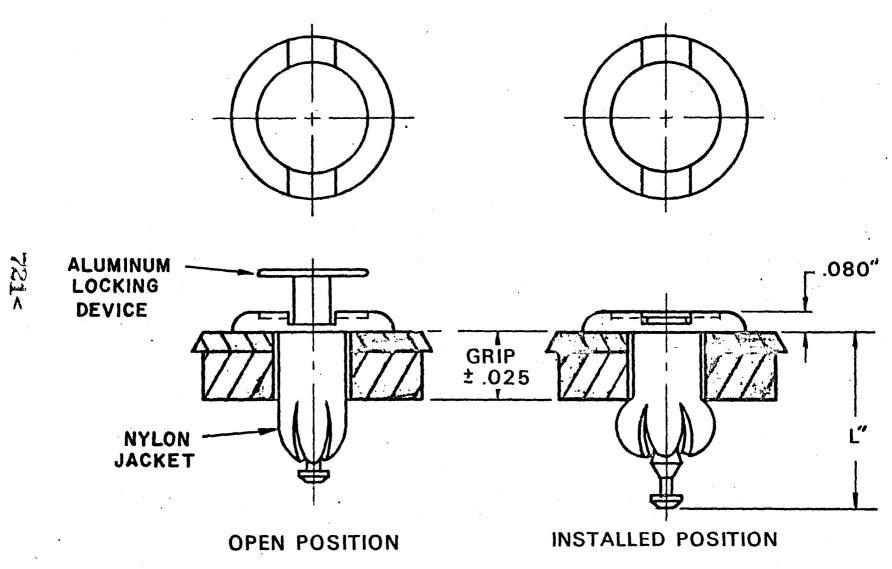
IV. Summary

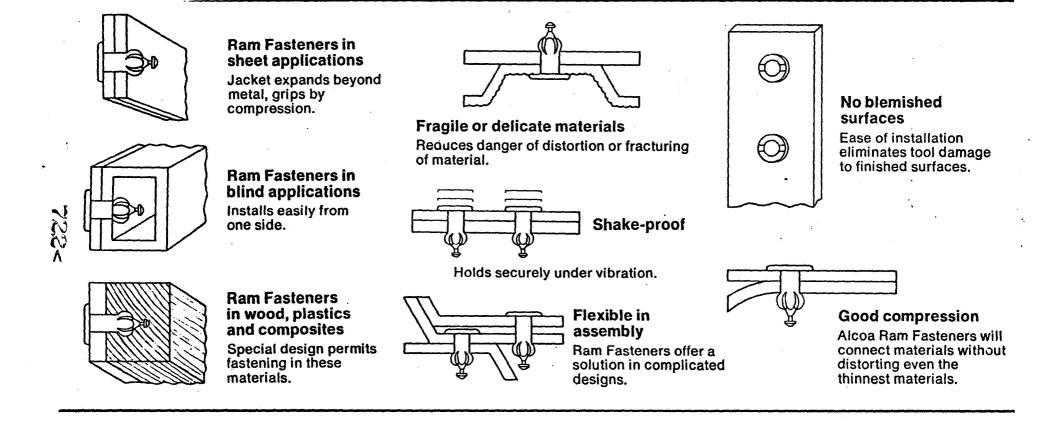
The information in this paper shows that the Alcoa Ram Fastener has strength characteristics suitable for

light structural applications. The tensile and shear strength values given should serve as a guide to the designer for his particular strength requirements. Cptimum strengths, as would be expected, are obtained when hole clearance is kept to a minimum and the ratio of the fastener diameter to the least thickness of sheet being joined is about 1. Excellent resistance to loosening by vibration was demonstrated by the long fatigue lives obtained in the lap joints tested at a maximum load equal to half the static strength. The accelerated corrosion test results confirmed the re-usability feature, even after exposure to rather severe environments.



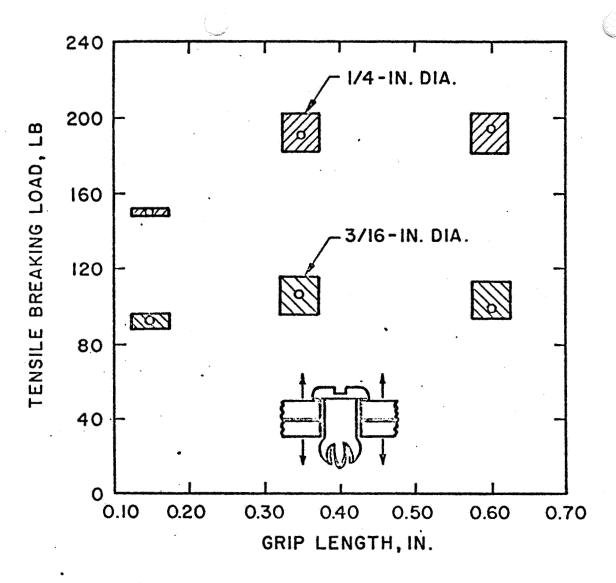
ALCOA RAM FASTENER ASSEMBLY



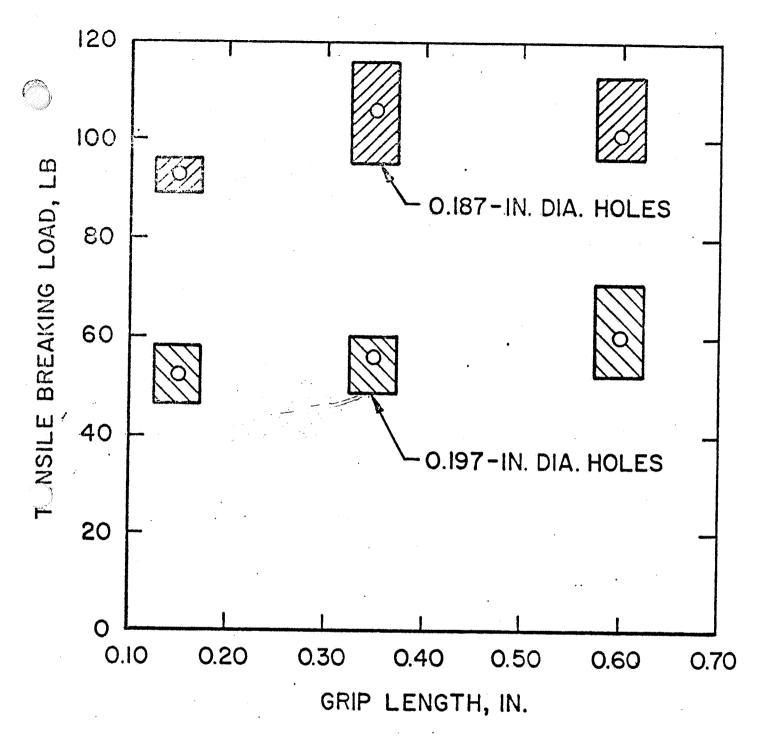


SOME TYPICAL APPLICATIONS FOR THE ALCOA RAM FASTENER



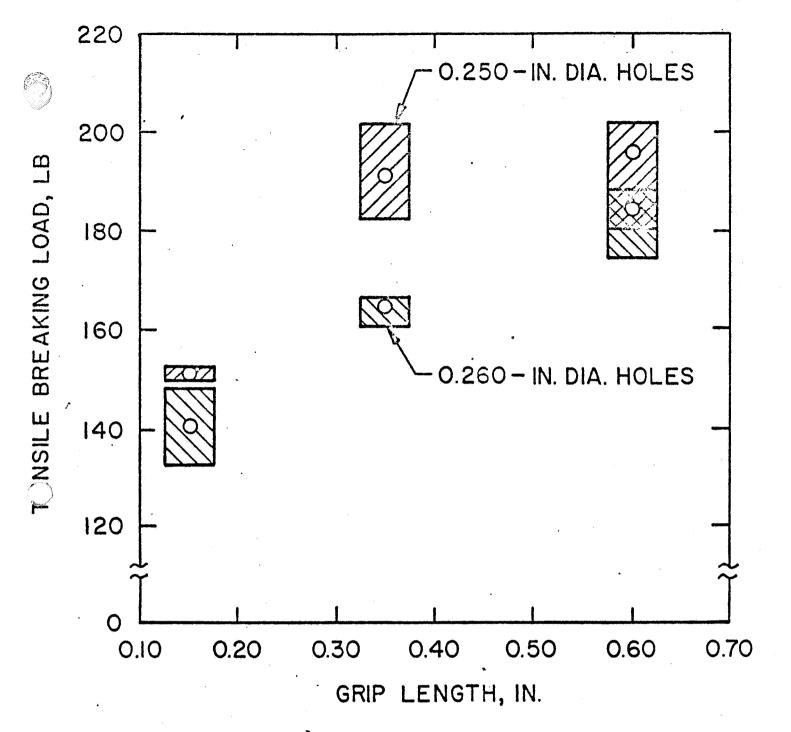


TENSILE STRENGTH OF ALCOA RAM FASTENERS



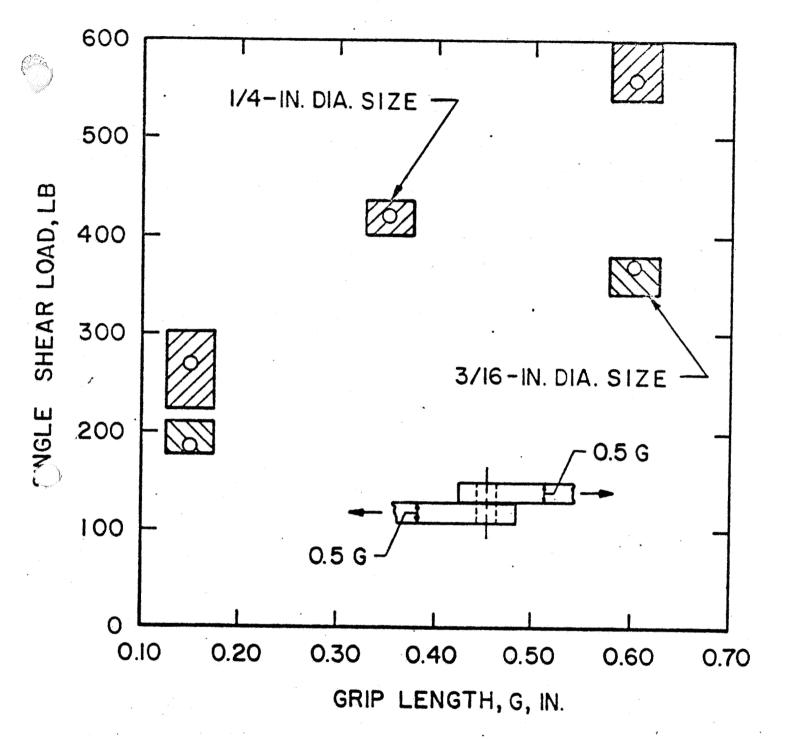
EFFECT OF HOLE SIZE ON TENSILE STRENGTH OF 3/16-IN. DIAMETER ALCOA RAM FASTENERS

724<

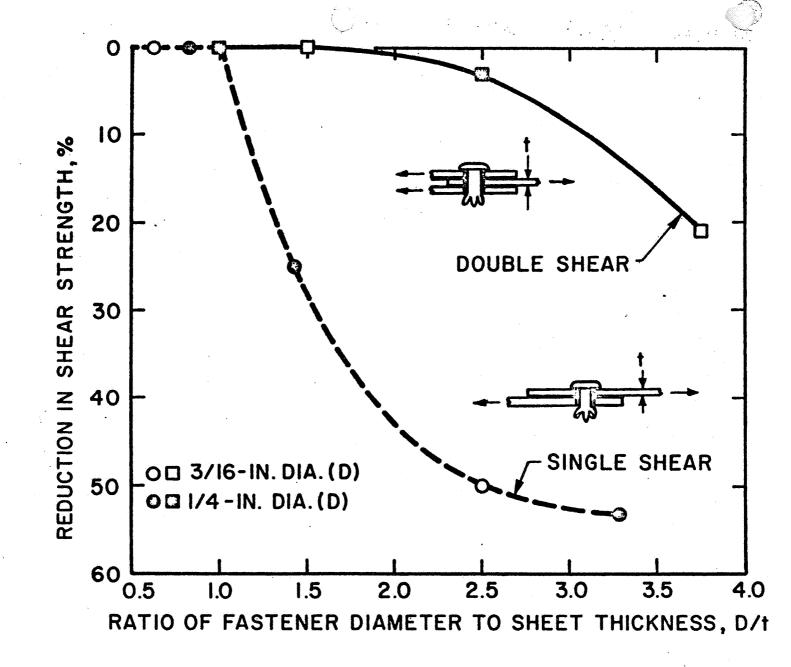


EFFECT OF HOLE SIZE ON TENSILE STRENGTH OF 1/4 - IN. DIAMETER ALCOA RAM FASTENERS

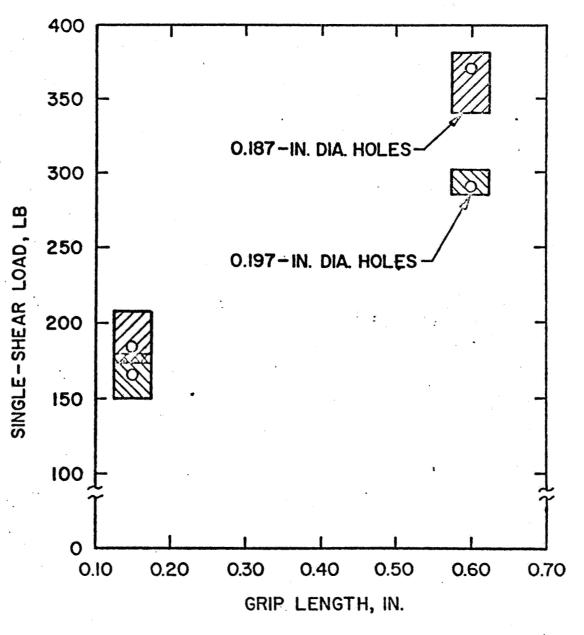
725<



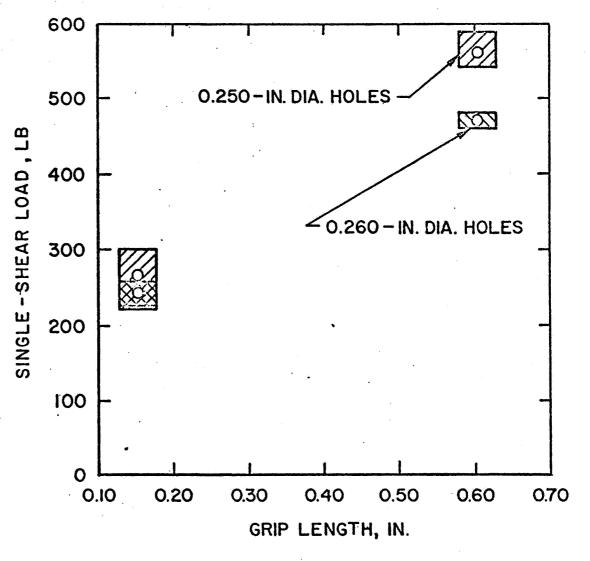
SINGLE - SHEAR STRENGTH OF ALCOA RAM FASTENERS



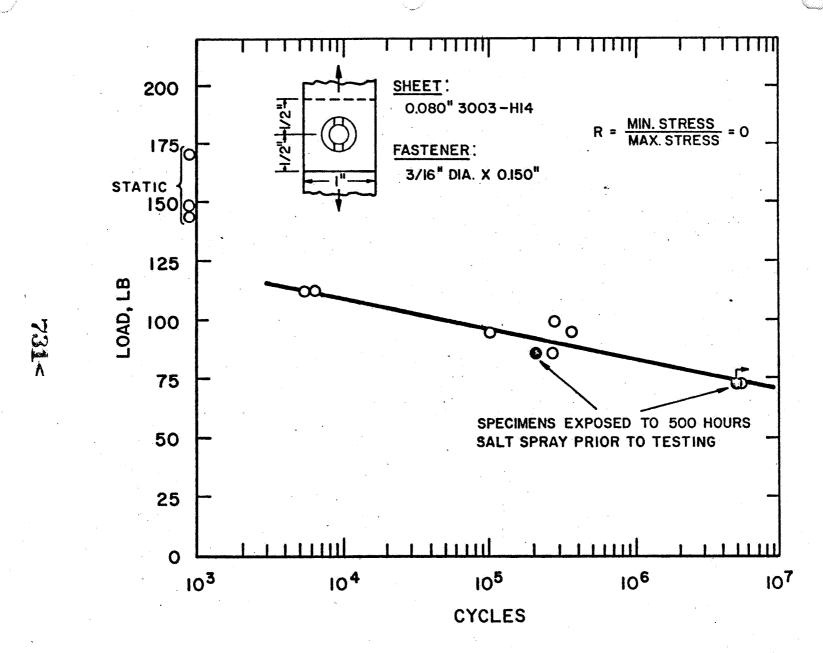
EFFECT OF SHEET THICKNESS ON SHEAR STRENGTH OF ALCOA RAM FASTENERS.



EFFECT OF HOLE SIZE ON SHEAR STRENGTH OF 3/16-IN. DIAMETER ALCOA RAM FASTENERS



EFFECT OF HOLE SIZE ON SINGLE-SHEAR STRENGTH OF I/4-IN. DIAMETER ALCOA RAM FASTENERS



FATIGUE TESTS OF LAP JOINTS CONTAINING ALCOA RAM FASTENERS

N74 30957

Mechanical Fasteners for 1800°F and Above

Ъy

Thomas A. Roach Manager of Materials Research SPS Laboratories

Standard Pressed Steel Co. Jenkintown, Pa. 19046

Presented at the Symposium on Welding, Bonding, and Fastening
May 30-31, June 1, 1972
Williamsburg, Virginia

INTRODUCTION

This presentation is intended to review the state-of-the-art of mechanical fasteners for 1800°F and above and to discuss some of the problems associated with the use of these fasteners.

Until recently the need for mechanical fasteners at 1800°F and above appeared urgent in view of the projected requirements of the space shuttle for metallic heat shields which would be reusable for 100 cycles of orbit and reentry. The present concept of the thermal protection system however has resulted in a deemphasis of the metallic systems and an emphasis on the reusable external insulation (REI) approach and on the ablative approach used so successfully on the Mercury, Gemini, and Apollo programs. Each of these approaches may require a compromise of the original goal of 100 reuses and quick turnaround. Work is therefore continuing on the metallic concept as a back-up system or possibly as the system which will ultimately permit the achievement of the original program guidelines.

MATERIALS UNDER CONSIDERATION

An all metallic space shuttle orbiter might well employ the following spectrum of materials:

Aluminum Alloys
Alloy Steels
Titanium Alloys
A-286
Inco 718
Rene' 41
Haynes Alloy No. 188
TD NiCr
Coated Refractory Alloys (Cb752-C129Y)

Up through the Rene' 41 the fastener technology is fairly well established and this discussion will therefore deal with only those alloys with a 1800°F or higher capability which will include HA188, TD NiCr and the refractory metal alloys such as Cb752 and C129Y.

HAYNES ALLOY NO. 188 (H.A. 188)

This alloy is a compromise between the high temperature strength of Haynes Alloy No. 25 and the oxidation resistance of Hastelloy "X". It possesses good fabricability and is an excellent fastener material in that the base metal properties are readily attainable in a finished fastener. Many different fastener configurations have been made in HA188 for heat shield development programs, primarily under Phase B funding. Included were flush head, pan head, hex head, and special head bolts in sizes primarily #10 (3/16") and 1/4". Also made were plate nuts, flanged and unflanged hex nuts and rivets.

TD NiCr (Ni - 20 Cr - 2 ThO2)

This material is the second of the usable high temperature dispersion strengthened materials to come into prominence. (The first being TD Ni.) The high temperature strength is dependent upon the presence of an ultrafine dispersion of ThO_2 particles throughout the Ni - 20 Cr matrix. At present the only source of material suitable for fastener manufacture is Fansteel Inc.

The properties of TD NiCr fasteners are sufficiently high at 2200°F to permit their consideration for use up to this temperature. A graph of 100 hour rupture stress for various temperatures is shown in Figure 1. This includes other materials for a comparison.

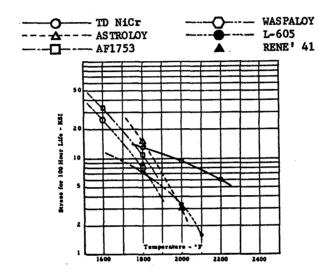
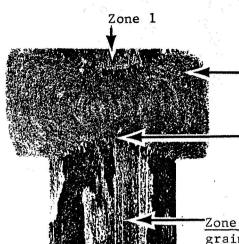


Figure 1. Effect of Temperature on Stress to Produce Rupture in 100 Hours.

These properties are not attainable in parts in which significant amounts of deformation are applied to generate a head. Herein lies the main obstacle in the path of the use of TD NiCr fasteners. The strength of the TD NiCr is so dependent on prior work and thermal history that the result of various amounts of work in the forming of most types of heads is to render the fastener head-critical with the failure strength usually being significantly less than optimum material properties or thread strength. This problem is the subject of work soon to be completed by Standard Pressed Steel Co.'s R & D Laboratories under Air Force Contract F-33615-67-C-1494. A typical microstructure of a forged head part is shown in Figure 2. In this figure three distinct structures can be seen with failure usually occurring through Zone 2.





<u>Zone 3</u>. Fully recrystallized to extremely fine grain structure - poor properties.

Zone 2. Fully recrystalled to intermediate grain structure - properties questionable.

Zone 1. Fully recrystallized to larger grain structure - optimum properties.

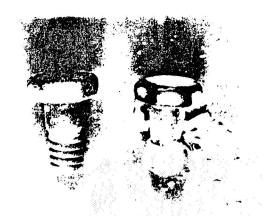
Figure 2. TD NiCr bolt head sectioned to show structure. Material was initially unrecrystallized, head forged at 2000°F, recrystallized at 2450°F.

REFRACTORY METAL ALLOYS

Beyond the temperature limit of TD NiCr it becomes apparent that the useful engineering materials must be those with melting temperatures significantly above those of nickel and cobalt base alloys. Thus the logical choices are columbium (melting point 4474°F) and tantalum (melting point 5425°F). The two other most common refractory metals, molybdenum and tungsten are not generally considered because of their low ductility and resulting poor fabricability.

The main problem associated with these materials is their poor oxidation resistance which makes a coating mandatory in an oxidizing environment.

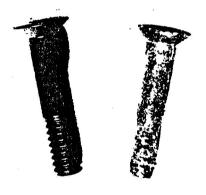
Examples of this need are shown in Figures 3, 4, and 5. Figures 3 and 4 show the drastic difference between coated and uncoated columbium and tantalum bolts. Note that both uncoated parts were exposed to only 1500°F for one hour whereas the coated parts were exposed near their maximum use temperatures. Figure 5 demonstrates that the coating process is at least as important as the coating chemistry. In this example the bolt in the rear of the test block is T-222 coated with WSi2 by Process "A". The oxide on the front edge of the block is the residue of three T-222 bolts coated with WSi2 by Process "B". These examples clearly indicate the need not only for a coating but also indicate the need for careful process selection, process control and quality assurance procedures to prevent catastrophic oxidation failures.



Coated-Sylvania R512E Exposed 2400°F 32 One Hour Cycles

Uncoated Exposed 1500°F 1 Hour

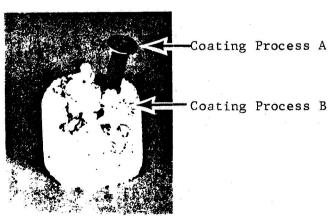
Figure 3. Cb752 bolts exposed as shown.



Coated Vitro WSi₂ Exposed 3000°F -10 minutes

Uncoated Exposed 1500°F -1 Hour

Figure 4. T-222 bolts exposed as shown.



WSi₂ Coated Exposed 3000°F - 10 minutes

Figure 5. T-222 bolts exposed as shown.

Beyond the coating problem, the properties of columbium and tantalum appear attractive enough to permit their use at 2500°F and 3000°F respectively.

In the case of columbium alloy fasteners, many have been made for Shuttle Phase B programs. These have all been made by hot forging heads, rolling threads and all other operations typical of a high performance aerospace fastener. The dimensions were adjusted to allow for coating.

EFFECT OF COATING ON USABILITY

It is logical to ask why, since good coatings are available, are these problems associated with the use of mechanical fasteners. The problems relating primarily to fasteners can be summarized as follows:

A. Difficulty in Coating Internal and External Threads

The presence of such things as sharp radii on various parts of fasteners creates difficulties for the coaters. It is extremely difficult to achieve a uniform coating over such abrupt changes in geometry. The accessibility of the threads in small diameter nuts makes coating application difficult and inspection virtually impossible.

Once the coating has been applied these same areas become those most subject to coating damage due to chipping during handling and use.

One partial remedy to this problem is the use of the thread form developed by SPS under Air Force Flight Dynamics Laboratory sponsorship. This thread form provides for closely controlled roots and crests with liberal radii. It can be adjusted for individual coatings over the range of thickness common to these materials. This Refractory Thread Form is shown in Figure 6.

B. Close Tolerances in Threads

As a corollary to "A", the normal tolerances on screw threads are significantly smaller than the differences which can be created by normal coating variation. In considering this one must keep in mind the fact that a .0001" variation in coating thickness effects the pitch diameter by $4 \times .0001$ " or .0004". This is illustrated in Figure 7.

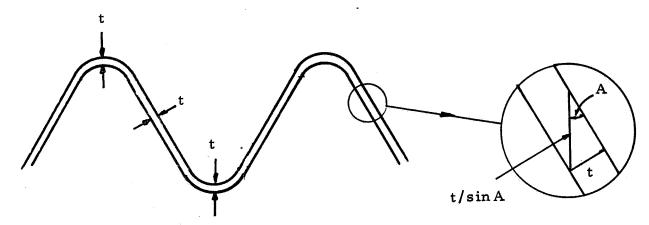
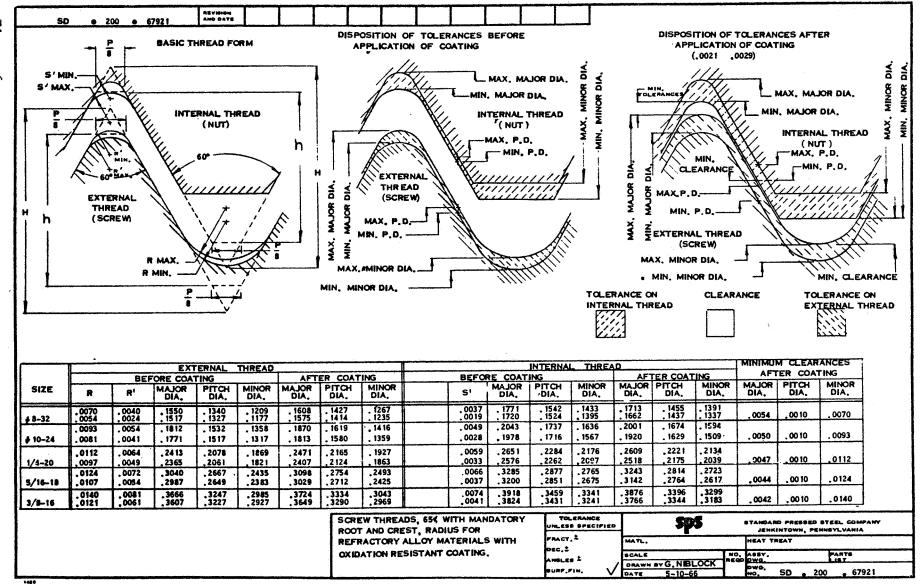


Figure 7. Factors involved in coating thickness allowance determinations.







Since the thread form has an angle A of 30°, t/Sin A = 2T, which is the effect on the pitch radius. This, of course, becomes 4T when considering the pitch diameter. Add to this the fact that both internal threads and external threads experience this 4T factor and it would be possible with a .0005" coating tolerance to cause a .004" variation in finished dimensions. In the small fasteners typically used thus far the .002 pitch diameter variation is approximately equal to the tolerance allowed on the pitch diameter uncoated parts. This could severely limit the interchangeability which is desirable in high volume fastener usage.

C. Need for Mechanical Drives for Tightening

If a fastener is to perform its function of holding a joint together under a defined preload, it must have this preload applied to it by some means. The normal way is to provide a driving configuration in the head so that the bolt can be torqued relative to the nut (or tapped hole). The presence of a drive of some sort creates another area of difficult coatability. In addition, and probably more important, the torque applied to tighten the fastener can cause chipping of sharp corners and in areas of high localized stresses.

The best available solution to this problem is to design drives which provide only the necessary torque and minimize the sharp corners and localized bearing areas.

D. Abrasion and Compression in Threads and Bearing Areas

Because of the fairly rough nature of the coatings (50 Mi-AA) installation causes somewhat higher torques than desired and this can cause the coating to chip. In addition the high local stresses in the contact areas of the threads and on the bearing areas under head and under nuts can and does cause compressive failure of the coatings.

E. Locking Features

A requirement for locking features in a bolt or nut creates a problem by further localizing stresses in the area of the locking feature.

F. "Welding" of Coated Components

The conditions existing in the use of coated refractory alloy fasteners creates the ideal diffusion bond that is:

- 1. High compressive stresses
- 2. High temperature
- 3. Semi-fluid coating components (SiO2)

Difficulties are often encountered in disassembly and even when fasteners can be removed it is common to create coating damage during removal.

One answer is the use of a barrier to prevent a bond from forming. One such barrier was developed by SPS. It is a proprietary formulation known as LF87-66-1. This provides lubrication for one installation and a barrier

for ease of removal. The residue is easily removed after one thermal cycle so that a fresh application can be made for the next thermal cycle. This material has a temperature use range up to 2600°F and is, therefore, also useful in the prevention of seizing on HA188, TD NiCr and other high temperature materials.



SUMMARY

I have attempted herein to discuss this area of technology with emphasis on some of the problems which need to be solved before a metallic heat shield can become a reliable item of hardware. I must point out that with the present reduced interest in this field the work necessary to solve the problems will not be pursued. Only active interest by N.A.S.A. or the Shuttle Contractor will generate the activity necessary to bring the technology of mechanical fasteners for 1800°F and above to the level it must be to fulfill the needs of a major program such as the Space Shuttle.

